Petro-chemical characterization and evolution of Permian coal deposits of South Karanpura coalfield, Jharkhand, India

Thesis submitted in partial fulfillment

for the Award of Degree

Doctor of Philosophy

by

MRITYUNJAY KUMAR JHA

RAJIV GANDHI INSTITUTE OF PETROLEUM TECHNOLOGY

JAIS – 229304

PGE14-001 *2020*

CERTIFICATE

It is certified that the work contained in the thesis titled ***"Petro-chemical characterization and evolution of Permian coal deposits of South Karanpura coalfield, Jharkhand, India"*** by ***"Mrityunjay Kumar Jha"*** has been carried out under my supervision and that this work has not been submitted elsewhere for a degree.

It is further certified that the student has fulfilled all the requirements of Comprehensive, Candidacy and SOTA.

Supervisor

Dr Alok Kumar Singh
Associate Professor,
Rajiv Gandhi Institute of Petroleum Technology,
Jais, Amethi, Uttar Pradesh, India

DECLARATION BY THE CANDIDATE

I, ***Mrityunjay Kumar Jha***, certify that the work embodied in this thesis is my own bona fide work and carried out by me under the supervision of *"**Dr Alok Kumar Singh**"* from *"2014"* to *"2020"*, at the Rajiv Gandhi Institute of Petroleum Technology, Jais. The matter embodied in this thesis has not been submitted for the award of any other degree. I declare that I have faithfully acknowledged and given credits to the research workers wherever their works have been cited in my work in this thesis. I further declare that I have not willfully copied any other's work, paragraphs, text, data, results, *etc*., reported in journals, books, magazines, reports dissertations, theses, *etc*., or available at websites and have not included them in this thesis and have not cited as my own work.

Date: (Mrityunjay Kumar Jha)
Place: Jais, Amethi

CERTIFICATE BY THE SUPERVISOR(S)

It is certified that the given declaration by the student is correct to the best of my/our knowledge.

Supervisor

Dr Alok Kumar Singh
(Associate Professor)
Rajiv Gandhi Institute of Petroleum Technology,
Jais, Amethi, Uttar Pradesh, India

Head of Department

Dr Satish Kumar Sinha
(Associate Professor)
Rajiv Gandhi Institute of Petroleum Technology,
Jais, Amethi, Uttar Pradesh, India

CERTIFICATE

CERTIFIED that the work contained in the thesis titled "**Petro-chemical characterization and evolution of Permian coal deposits of South Karanpura coalfield, Jharkhand, India**" by **Mr. Mrityunjay Kumar Jha** has been carried out under my supervision. It is also certified that he fulfilled the mandatory requirement of TWO quality publications arose out of his thesis work.

It is further certified that the two publications (copies enclosed) of the aforesaid **Mr. Mrityunjay Kumar Jha** have been published in the Journals indexed by –

(a) SCI
(b) SCI Extended
(c) SCOPUS
(d) *Non-indexed Journals – (only in special cases)
(*Please enclosed DPGC resolution in this regard)

(Dr Alok Kumar Singh)
Supervisor **Convener, DPGC**

N.B.: Please strike out the category (a, b, c, d) that is not applicable.

COPYRIGHT TRANSFER CERTIFICATE

Title of the Thesis: ***Petro-chemical characterization and evolution of Permian coal deposits of South Karanpura coalfield, Jharkhand, India***

Name of the Student: Mrityunjay Kumar Jha

Copyright Transfer

The undersigned hereby assigns to the Rajiv Gandhi Institute of Petroleum Technology Jais all rights under copyright that may exist in and for the above thesis submitted for the award of the *"Doctor of Philosophy"*.

Date: (MRITYUNJAY KUMAR JHA)

Place: Jais, Amethi

Note: However, the author may reproduce or authorize others to reproduce material extracted verbatim from the thesis or derivative of the thesis for author's personal use provided that the source and the Institute's copyright notice are indicated.

Acknowledgement

I owe all those who have helped me to complete this study, and the following words will never suffice to repay this debt, but still, I would like to record my heartfelt gratitude and thank everyone for their support, assistance, and encouragement.

I want to express a deep sense of gratitude and profound admiration for my thesis supervisor Dr Alok Kumar Singh. He guided me through this work and always stood by me in an extremely distressing time, and it is only because of his guidance, support, and encouragement that I could meet this challenge of completing my thesis successfully.

I am thankful to the present director Prof. A. S. K. Sinha and former directors Prof. P. K. Bhattacharya as well as Prof. J. P. Gupta of Rajiv Gandhi Institute of Petroleum Technology (RGIPT), Jais, Amethi for extending the research facility in Geology and Geochemistry Research lab and providing financial assistance to me, which enabled me to undertake my field trips and conduct experiments.

My sincere gratitude is towards Dr Satish Kumar Sinha, the Head of the Department, Petroleum Engineering and Geoengineering, for his constant encouragement and help. I am thankful to all the faculty members for their help and guidance. The gratitude is also extended to the other teaching and non-teaching staffs of the Institute for supporting me during this work. Many thanks to the teachers and professors from my previous schools and colleges especially faculties from Patna University and ISM, Dhanbad, who enhanced my knowledge and made me capable. I am also thankful to The Council of Scientific and Industrial Research (CSIR) for awarding me 'CSIR- Senior Research Fellowship (SRF) – Direct' for helping me financially during the last year of my work.

I want to thank the officials and staff of Central Coalfields Limited for their invaluable cooperation during the sampling and field visit.

Helpful resources were gathered from the library of Rajiv Gandhi Institute of Petroleum Technology, Amethi; Banaras Hindu University, Varanasi and numerous other public and private collections online and offline. I am thankful to the librarians and staff of these institutions.

I want to thank those people, who helped me regarding books, and journals from their collections, from the core of my heart for their valuable support. I sincerely acknowledge the help provided by several reviewers and editors of the various journals, who improved

the contents of my manuscripts that were part of this thesis. Special thanks to Dr James Hower, Dr Binoy Kumar Saikia, Dr Bhagwan Das Singh, Dr Atul Kumar Varma and Dr Prakash Kumar Singh for their help in improving my manuscripts.

I am sincerely thankful to the director of Central Drug Research Institute (CDRI), Lucknow to provide the ultimate analysis facility. Director, Keshava Deva Malaviya Institute of Petroleum Exploration (KDMIPE), Dehradun, Uttarakhand is thankfully acknowledged for providing a Rock-Eval Pyrolysis facility. I would also like to thank the officials of ONGC, Ahmedabad, Gujarat for providing the XRD facility and Prof. J. K. Tripathi, the Vice-Chancellor, Jawaharlal Nehru University, New Delhi for the XRF facility. I am also thankful to the Director, Birbal Sahni Institute of Paleosciences, Lucknow for providing a GC-MS facility.

I appreciate the help and cooperation of my lab mates Dr Aniruddha Kumar and Mr Alok Kumar. I am also thankful to the other scholars of RGIPT, including Dr Rewati Raman Ujjawal, Dr Tripti Rai, Dr Karunesh Kant, Miss Komal Shukla, Dr Amit Ghosh, Dr Shama Perveen, Mr Somendra Singh, Mr Praveen K Mourya, Ms Reena and Mr Sumon Debnath. Thanks are also due to my friends outside the institute.

My father, Sh. Jitendra Jha and mother Smt. Gita Rani deserves special mention. They had been a constant source of inspiration, and I would have never been able to accomplish this work without their blessings. I am thankful to my family members, including elder brother Mr Rajiv K. Jha, sister in law Mrs Ruma Jha and younger brother Mr Saurabh K. Jha for their moral support that has been of immense value to me. Lastly, I am thankful to my lovely wife, Shruti Kiran and my sons Raghav and Saumitr for being always by my side and making my mood happy during the distressful time. Last but not least, I am thanking the Almighty (Lord Shiva) for accompanying me.

(Mrityunjay Kumar Jha)

Table of Contents

CERTIFICATE ii
Acknowledgement vii
Table of Contents ix
List of Figures xiii
List of Tables xx
Symbols and Abbreviations xxiii
Preface xxv
CHAPTER 1. GENERAL INTRODUCTION 1
1.1 Introduction 1
1.2 The occurrence of coals in India 3
1.2.1 The geological occurrence of the Gondwana coal 5
1.2.2 The geological occurrence of the Cenozoic coal and lignite 7
1.3 Review work on Gondwana coals in general 8
1.4 Review work on South Karanpura coals 9
1.5 The objective and scope of the present work 11
1.6 Fieldwork 12
1.7 Laboratory work 13
CHAPTER 2. GEOLOGY 15
2.1 Introduction 15
2.2 Geology of the Gondwana basins of India 15
2.3 Geology of the Damodar Valley 18
2.4 Geology of Karanpura basin 21
2.5 About the South Karanpura 23
2.6 Regional geology of South Karanpura 23
2.6.1 Precambrian basement 24
2.6.2 Talchir Formation 24
2.6.3 Karharbari Formation 25
2.6.4 Barakar Formation 25
2.6.5 Barren Measure Formation 25
2.6.6 Raniganj Formation 26
2.6.7 Igneous intrusive 26
2.6.8 Structures 26
2.7 Location and communication of the study area 28
2.8 Topography and drainage 28

2.9 Climate 29
2.10 Vegetation 29
2.11 Mode of Occurrence of Coal Seams in South Karanpura coalfield 29
2.11.1 Introduction 29
2.11.2 The regional occurrence of coal seams 33
CHAPTER 3. SAMPLING AND METHODS OF STUDY 38
3.1 Introduction 38
3.2 Method of coal sampling 38
3.3 Preparation of Coal Samples 39
3.3.1 Sample preparation for petrographic studies 39
3.3.2 Sample preparation for geochemical analyses 41
3.4 Methods of study 42
3.4.1 Petrographic study 42
3.4.2 Chemical analyses of coal 46
CHAPTER 4. COAL PETROGRAPHY 52
4.1 Introduction 52
4.2 History of Coal Microscopy 53
4.3 History of Coal Petrography in India 56
4.4 Present Work 58
4.5 Megascopically recognizable constituents 58
4.5.1 Vitrain 60
4.5.2 Clarain 60
4.5.3 Durain 61
4.5.4 Fusain 61
4.6 Macroscopic Description of Coal Seams of South Karanpura Coalfield 62
4.6.1 Bright coal 62
4.6.2 Banded bright coal 63
4.6.3 Banded coal 63
4.6.4 Banded dull coal 63
4.6.5 Dull coal 63
4.7 Macroscopic Seam Profiles of South Karanpura Coalfield 64
4.7.1 Coal seams of Barka Sayal area 64
4.7.2 Coal seams of Argada area 67
4.8 Microscopically recognizable constituents in coal seams of South Karanpura 69
4.8.1 Maceral Analysis 71
4.9 Quantitative Occurrence of Microscopic constituents 109
4.9.1 Distribution of microscopic constituents in coal seams of the Barka Sayal Area 110

4.9.2 Distribution of microscopic constituents in Coal seams of the Argada Area 126
CHAPTER 5. GEOCHEMICAL CHARACTERISTICS 147
5.1 Introduction 147
5.2 Proximate analysis 148
5.2.1 Moisture 148
5.2.2 Ash Yield 149
5.2.3 Volatile Matter 149
5.2.4 Fixed Carbon 149
5.2.5 Distribution of Proximate constituents 150
5.3 Ultimate analysis 169
5.3.1 Introduction 169
5.3.2 Carbon 169
5.3.3 Hydrogen 170
5.3.4 Nitrogen 170
5.3.5 Sulphur 170
5.3.6 Oxygen 170
5.3.7 Distribution of Ultimate constituents 171
5.4 Determination of Major oxides in coals of South Karanpura coalfield 186
5.4.1 The occurrence of Major Oxides in the coals of the South Karanpura coalfield 187
5.4.2 Distribution of Major oxides in coals of South Karanpura coalfield 191
5.5 Distribution of Major Elements in coals of South Karanpura coalfield 194
5.5.1 Relation of Major Elements with Ash Yield 196
5.6 Trace Element in the coals of South Karanpura coalfield 202
5.6.1 The occurrence of Trace Elements in Coals of South Karanpura coalfield 203
5.7 X-ray Diffraction Study of Coals of South Karanpura 207
5.7.1 X-ray Diffraction Study of Coal seams of Barka Sayal area 208
5.7.2 X-ray Diffraction Study of Coal seams of Argada area 212
5.8 Fourier Transform Infrared Spectroscopy of Coals of South Karanpura 215
5.8.1 Fourier Transform Infrared (FTIR) Spectroscopy of Coals of Barka Sayal area 218
5.8.2 Fourier Transform Infrared (FTIR) Spectroscopy of Coals of Argada area 219
5.9 Organic Geochemistry of Coals of South Karanpura 220
5.9.1 Organic geochemical analysis of coal seams of Barka Sayal area 220
5.9.2 Organic geochemical analysis of coal seams of Argada area 223
CHAPTER 6. MATURATION (RANK) AND SOURCE ROCK POTENTIAL OF COALS OF SOUTH KARANPURA COALFIELD 225
6.1 Introduction 225
6.2 Rank based on Chemical and Petrological Parameters 226

6.3 Maturity assessed by Rock-Eval Pyrolysis Method 228
6.3.1 Maturity of coals of Barka Sayal area 232
6.3.2 Maturity of coals of Argada area 234
6.4 Coals of South Karanpura as a Hydrocarbon Source Rock 237
6.4.1 Type of Organic Matter 237
6.4.2 The quantity of Organic Matter 242
6.4.3 Source Rock Maturity 244
6.4.4 Oil yield 248
CHAPTER 7. DISCUSSION 255
7.1 Introduction 255
7.2 Petro-chemical characterization of coals of South Karanpura coalfield 255
7.3 Kerogen Type 283
7.4 Thermal Maturity and oil potential 286
7.5 Indication of Petroleum Generation 288
7.6 Relation of Major and Minor Element with Mineral Matter 289
7.7 Petro-chemical correlation 291
7.8 Occurrence and significance of major/minor and trace elements 295
7.9 Evolution of coals of South Karanpura 301
7.9.1 Development of Flora 303
7.9.2 Development of Coal Facies 304
7.9.3 Depositional Environment 319
7.10 Coalification Trend 320
CHAPTER 8. CLASSIFICATION AND POTENTIAL UTILIZATION 324
8.1 Introduction 324
8.2 South Karanpura Coals on the Seyler's Classification Chart 329
8.3 Classification according to West German and North American System 330
8.4 Classification of Coals according to Indian Standard (IS: 770- 1977) 332
8.5 South Karanpura Coals in the International Classification System 332
8.6 Potential Utilisation of Coals of South Karanpura coalfield 336
CHAPTER 9. SUMMARY AND CONCLUSION 341
References 345

List of Figures

Figure 1.1 Broad location map of the study area (South Karanpura Coalfield, India)..... 3

Figure 1.2 Coalfield-wise inventory of geological reserve of Indian coal. 4

Figure 1.3 Important Gondwana coalfields of India (Dutta *et al.* 2011a). 7

Figure 2.1 Gondwana basins of India (Mukhopadhyay *et al.* 2010). 17

Figure 2.2 Geological map of Damodar River Basin. 19

Figure 2.3 The geological map of South Karanpura Coalfield (after Raja Rao, 1987). 27

Figure 2.4 Field photographs 30

Figure 2.5 Field photographs 31

Figure 2.6 Geological map of South Karanpura coalfield showing sampling locations. 32

Figure 4.1 Different macroscopic bands present in banded humic coal 60

Figure 4.2 Macropetrographic seam profiles of coal seams of the Barka Sayal area. 66

Figure 4.3 Macropetrographic seam profiles of coal seams of the Argada area. 68

Figure 4.4 Representative photomicrographs..... 81

Figure 4.5 Representative photomicrographs..... 82

Figure 4.6 Representative photomicrographs..... 91

Figure 4.7 Representative photomicrographs..... 92

Figure 4.8 Representative photomicrographs..... 93

Figure 4.9 Representative photomicrographs..... 94

Figure 4.10 Representative photomicrographs..... 100

Figure 4.11 Representative photomicrographs..... 101

Figure 4.12 Representative photomicrographs..... 104

Figure 4.13 Distribution of group of macerals in South Karanpura coals. 109

Figure 4.14 Macro-petrographic section of Sayal Seam..... 111

Figure 4.15 Macro-petrographic section of Sayal Balkudra Seam 111

Figure 4.16 Macro-petrographic section of Upper Semana Seam 112

Figure 4.17 Macro-petrographic section of Lower Semana Seam..... 112

Figure 4.18 Macro-petrographic section of Hathidari Seam 113
Figure 4.19 Macro-petrographic section of Bansgarha Seam 113
Figure 4.20 Macro-petrographic section of Argada Seam 127
Figure 4.21 Macro-petrographic section of Argada-A Seam 127
Figure 4.22 Macro-petrographic section of Argada-B Seam 127
Figure 4.23 Macro-petrographic section of Argada-C Seam 127
Figure 4.24 Macro-petrographic section of Argada-D Seam 129
Figure 4.25 Macro-petrographic section of Argada-I Seam..... 129
Figure 4.26 Macro-petrographic section of Argada-J Seam..... 130
Figure 5.1 Variation of proximate constituents of Sayal seam..... 152
Figure 5.2 Variation of proximate constituents of Sayal Balkudra seam. 152
Figure 5.3 Variation of proximate constituents of Upper Semana seam. 153
Figure 5.4 Variation of proximate constituents of Lower Semana seam. 153
Figure 5.5 Variation of proximate constituents of Hathidari seam. 154
Figure 5.6 Variation of proximate constituents of Bansgarha seam..... 154
Figure 5.7 Variation of proximate constituents of Argada seam..... 159
Figure 5.8 Variation of proximate constituents of Argada-A seam. 159
Figure 5.9 Variation of proximate constituents of Argada-B seam..... 161
Figure 5.10 Variation of proximate constituents of Argada-C seam..... 161
Figure 5.11 Variation of proximate constituents of Argada-D seam. 162
Figure 5.12 Variation of proximate constituents of Argada-I seam. 163
Figure 5.13 Variation of proximate constituents of Argada-J seam. 163
Figure 5.14 Variation of ultimate constituents of Sayal seam. 174
Figure 5.15 Variation of ultimate constituents of Sayal Balkudra seam. 174
Figure 5.16 Variation of ultimate constituents of Upper Semana seam. 175
Figure 5.17 Variation of ultimate constituents of Lower Semana seam. 175
Figure 5.18 Variation of ultimate constituents of Hathidari seam. 176
Figure 5.19 Variation of ultimate constituents of Bansgarha seam..... 176

Figure 5.20 Variation of ultimate constituents of Argada seam. 181
Figure 5.21 Variation of ultimate constituents of Argada-A seam. 182
Figure 5.22 Variation of ultimate constituents of Argada-B seam. 182
Figure 5.23 Variation of ultimate constituents of Argada-C seam. 183
Figure 5.24 Variation of ultimate constituents of Argada-D seam. 183
Figure 5.25 Variation of ultimate constituents of Argada-I seam. 184
Figure 5.26 Variation of ultimate constituents of Argada-J seam..... 184
Figure 5.27 Variation of major oxides in coals of Barka Sayal area..... 193
Figure 5.28 Variation of major oxides in coals of Argada area 193
Figure 5.29 Variation of major elements in coals of Barka Sayal area..... 195
Figure 5.30 Variation of major elements in coals of Argada area 195
Figure 5.31 Scatter plot of major elements with ash yield for coals of Barka Sayal area..... 197
Figure 5.32 Scatter plot of major elements with ash yield for coals of Barka Sayal area..... 198
Figure 5.33 Scatter plot of major elements with ash yield for coals of Argada area 199
Figure 5.34 Scatter plot of major elements with ash yield for coals of Argada area 200
Figure 5.35 Variation of trace elements in coals of Barka Sayal area 204
Figure 5.36 Variation of trace elements in coals of Argada area..... 204
Figure 5.37 Pie chart showing main mineral components present in the Barka Sayal area..... 209
Figure 5.38 Pie chart showing main mineral components present in Argada area 214
Figure 5.39 FTIR spectra of the raw coal, Bansgarha Seam..... 216
Figure 5.40 FTIR Spectra of the ash of the coal obtained using low-temperature..... 216
Figure 5.41 Combined FTIR Spectra of the raw coal and ash. 217
Figure 5.42 Combined FTIR Spectra of the raw coal of the coals of Barka Sayal area..... 219
Figure 5.43 Combined FTIR Spectra of the raw coal of the coals of Argada area 219
Figure 6.1 Rank of coals based on Random Vitrinite reflectance and V.M..... 227
Figure 6.2 Rank of South Karanpura coals in the diagram proposed by Kotter (1960)..... 228
Figure 6.3 Type of kerogen in South Karanpura coals (after Cornford, 1979). 238
Figure 6.4 Plot of Hydrogen index (HI) versus oxygen index (OI) 239

Figure 6.5 Cross plot between vitrinite reflectance (VRo %) and Hydrogen Index (HI)..... 239
Figure 6.6 Plot of remaining hydrocarbon potential (S2) versus TOC 240
Figure 6.7 Kerogen types of the coals of Barka Sayal as well as the Argada area..... 241
Figure 6.8 Kerogen types present in South Karanpura coalfield based on A-factor (aliphatic/aromatic peak intensity) and C-factor (carbonyl/aromatic peak intensity). 242
Figure 6.9 Cross plot between total organic carbon and fixed hydrogen potential (S2) 243
Figure 6.10 Plot of genetic potential (S1+S2) versus total organic carbon (TOC) 244
Figure 6.11 The main stage of evolution (maturation) of the organic matter and their relation with the coal rank (coalification) (after Tissot & Welte 1984). 245
Figure 6.12 The plot of HI versus Tmax (°C) for Kerogen type and thermal maturity stages.. 246
Figure 6.13 Plot of Tmax versus Production Index showing the hydrocarbon-generation..... 247
Figure 6.14 Plot of Tmax versus Vitrinite Reflectance showing the maturity levels..... 247
Figure 6.15 Ternary diagram based on maceral composition indicating the hydrocarbon potential of South Karanpura coals (after Tissot & Welte, 1984). 248
Figure 6.16 Correlation of Oil yield (b) with microscopic constituents..... 250
Figure 6.17 Cross plot of Vitrinite reflectance and the values of H/C and O/C..... 251
Figure 6.18 Correlation plot of total reactive macerals (RM) (vol. %) with Oil yield (b) %, Oil wt. %, TOC, S2, and HI for coals of South Karanpura coalfield. 252
Figure 7.1 Macro-petrographic section, range of mean values of microscopic, vitrinite reflectance, proximate and ultimate constituents of Sayal seam, South Karanpura coalfield, India. 259
Figure 7.2Macro-petrographic section, range of mean values of microscopic, vitrinite reflectance, proximate and ultimate constituents of Sayal Balkudra seam, South Karanpura coalfield..... 260
Figure 7.3 Macro-petrographic section, range of mean values of microscopic, vitrinite reflectance, proximate and ultimate constituents of Upper Semana seam, South Karanpura coalfield..... 262
Figure 7.4 Macro-petrographic section, range of mean values of microscopic, vitrinite reflectance, proximate and ultimate constituents of Lower Semana seam, South Karanpura coalfield 263
Figure 7.5 Macro-petrographic section, range of mean values of microscopic, vitrinite reflectance, proximate and ultimate constituents of Hathidari seam, South Karanpura coalfield, India. 265

Figure 7.6 Macro-petrographic section, range of mean values of microscopic, vitrinite reflectance, proximate and ultimate constituents of Bansgarha seam, South Karanpura coalfield, India. ... 266
Figure 7.7 Macro-petrographic section, range of mean values of microscopic, vitrinite reflectance, proximate and ultimate constituents of Argada seam, South Karanpura coalfield, India. 268
Figure 7.8 Macro-petrographic section, range of mean values of microscopic, vitrinite reflectance, proximate and ultimate constituents of Argada-A seam, South Karanpura coalfield, India. 270
Figure 7.9 Macro-petrographic section, range of mean values of microscopic, vitrinite reflectance, proximate and ultimate constituents of Argada-B seam, South Karanpura coalfield, India. 271
Figure 7.10 Macro-petrographic section, range of mean values of microscopic, vitrinite reflectance, proximate and ultimate constituents of Argada-C seam, South Karanpura..... 273
Figure 7.11 Macro-petrographic section, range of mean values of microscopic, vitrinite reflectance, proximate and ultimate constituents of Argada-D seam, South Karanpura..... 274
Figure 7.12 Macro-petrographic section, range of mean values of microscopic, vitrinite reflectance, proximate and ultimate constituents of Argada-I seam, South Karanpura 276
Figure 7.13 Macro-petrographic section, range of mean values of microscopic, vitrinite reflectance, proximate and ultimate constituents of Argada-J seam, South Karanpura..... 277
Figure 7.14 Ternary plot exhibiting the distribution of group macerals 278
Figure 7.15 Ternary plot exhibiting the distribution of microlithotype 279
Figure 7.16 Interrelationship among micropetrographic (vitrinite, liptinite, inertinite and visible mineral matter) constituents for coals of South Karanpura coalfield..... 280
Figure 7.17 Interrelationship among micropetrographic (vitrinite, liptinite, and inertinite) and proximate (volatile matter, daf basis) constituents for coals of South Karanpura coalfield. 282
Figure 7.18 Interrelationship among vitrinite reflectance and proximate constituents (volatile matter and fixed carbon, daf basis) for coals of South Karanpura 282
Figure 7.19 Interrelationship of ash yield with the volatile matter, fixed carbon, visible mineral matter, and carbominerite concentration for coals of South Karanpura..... 283
Figure 7.20 The kerogen type in coals of South Karanpura coalfield..... 285
Figure 7.21 Type of kerogen present in coal seams of South Karanpura coalfield..... 285

Figure 7.22 Variation of group macerals and visible minerals in the coals of different seams of South Karanpura coalfield. 292
Figure 7.23 Variation of microlithotype along different coal seams of South Karanpura 292
Figure 7.24 Variation of minimum, maximum and mean vitrinite reflectance along different coal seams of South Karanpura coalfield. 293
Figure 7.25 Variation of proximate constituents along different coal seams 293
Figure 7.26 Variation of ultimate constituents along different coal seams 294
Figure 7.27 Plot of SiO2 versus (Al_2O_3+K_2O+Na_2O) showing paleoclimate condition 299
Figure 7.28 Plot of V and Ni concentration values showing depositional condition for samples of South Karanpura coalfield (after Galarraga et al., 2008). 299
Figure 7.29 Cross-plot between the ratio of V/(V+Ni) and Total Sulphur content (S_{total} wt.%), showing different paleoclimatic conditions (after Hail et al., 2017). 301
Figure 7.30 Cross-plot of Zr (ppm) and TiO_2 (wt.%), showing provenance source rock type for coal seams of Barka Sayal area (after Tao et al., 2017). 301
Figure 7.31 Coal facies deciphered from Gelification Index (GI) and Tissue Preservation Index (TPI) concerning depositional setting and type of mire for Coals of Barka Sayal area 307
Figure 7.32 Coal facies deciphered from Gelification Index (GI) and Tissue Preservation Index (TPI) concerning depositional setting and type of mire for Coals of Argada area 307
Figure 7.33 Correlation between tissue preservation index (TPI) and gelification index (GI) for different seams of Barka Sayal area, South Karanpura coalfield. 308
Figure 7.34 Correlation between tissue preservation index (TPI) and gelification index (GI) for different seams of Argada area, South Karanpura coalfield. 309
Figure 7.35 GWI vs VI Paleo-environment diagram of Barka Sayal area 312
Figure 7.36 GWI vs VI Paleo-environment diagram of coals of Argada area 312
Figure 7.37 Depositional conditions of Barka Sayal coals based on maceral and mineral matter content (after Singh & Singh, 1996) 313
Figure 7.38 Depositional conditions of coals of Argada area based on maceral and mineral matter content (after Singh & Singh, 1996) 313

Figure 7.39 Peat-forming environment based on maceral and mineral matter contents of Barka Sayal area, South Karanpura coalfield (after Singh et al., 2012). 314
Figure 7.40 Peat-forming environment based on maceral and mineral matter contents of coals of Argada area, South Karanpura coalfield (after Singh et al., 2012). 314
Figure 7.41 Coal facies based on the microlithotype of coals of Barka Sayal area 315
Figure 7.42 Coal facies based on the microlithotype composition of coals of Argada area 315
Figure 7.43 Pristane/n-C_{17} versus phytane/n-C_{18} cross-plot of the Lower Gondwana coal samples from South Karanpura coalfield, India (modified after Hunt, 1996) 318
Figure 7.44 Environments of coal deposition related to microlithotype composition of coals of South Karanpura coalfield (modified after Smyth 1979). 320
Figure 7.45 Relationship between vitrinite reflectance, depth and rock temperature for the coals of South Karanpura coalfield (A) Rm versus depth and (B) Rm versus temperature. 323
Figure 8.1 Plots of South Karanpura coals in Seyler's coal classification chart based on Carbon and Hydrogen contents. A) Barka Sayal area, B) Argada area. 330
Figure 8.2 Rank of coals of the South Karanpura Coalfield, Jharkhand, India, based on Random Vitrinite reflectance (VRo %) and V.M. (daf basis) 331
Figure 8.3 Classification and proposed potential utilisation of South Karanpura coals. A) Barka Sayal area, B) Argada area. 334
Figure 8.4 Plots of coals in ECE-UN Classification Scheme (UN-ECE classification, 1998). A) Barka Sayal area, B) Argada area. 335
Figure 8.5 Seyler diagram modified by Snyman (1989) further modified for coals of Barka Sayal area of South Karanpura Coalfield for showing their suitability for specialized fields of utilisation. A) Barka Sayal area, B) Argada area. 338

List of Tables

Table 1.1 Type-wise inventory of geological reserves of Indian coals 4

Table 1.2 State-wise distribution of Gondwana coalfields in India 6

Table 1.3 State-wise distribution of Cenozoic coal/lignite fields..... 8

Table 2.1 The stratigraphic succession of the Damodar Valley Basin 20

Table 2.2 Stratigraphic sequences of Formations in Karanpura Basin..... 22

Table 2.3 Generalized stratigraphy of South Karanpura Coalfield 24

Table 2.4 Location and name of the individual seam present in South Karanpura 29

Table 2.5 Collieries of Barka Sayal area with important coal seams 33

Table 2.6 Collieries of Argada area with important coal seams..... 35

Table 4.1 Comparison of coal lithotype nomenclature (modified after Rusnak 2017). 59

Table 4.2 The classification of Black coal lithotypes (after Diessel 1965). 62

Table 4.3 Macropetrogrphic seam characteristics of Coals seams of the Barka Sayal 65

Table 4.4 Macropetrogrphic seam characteristics of Coals seams of the Argada area. 69

Table 4.5 Subdivision of the maceral group vitrinite 70

Table 4.6 Comparison of key characteristics of group macerals (Osborne, 2013)..... 72

Table 4.7 Correlation of the huminite macerals of brown coals and lignite 74

Table 4.8 Correlation of the macerals of bituminous coals..... 75

Table 4.9 Classification of Liptinite Group of Macerals (Pickel *et al.* 2017). 84

Table 4.10 Macerals of the inertinite group 95

Table 4.11 Summary of the microlithotype of hard coal..... 106

Table 4.12 Summary of the carbominerite. 106

Table 4.13 Maceral and mineral matter content of Barka Sayal area..... 115

Table 4.14 Maceral content (mineral matter free) basis of Barka Sayal area..... 118

Table 4.15 Microlithotype and carbominerite content of Barka Sayal area 121

Table 4.16 Microlithotype content (carbominerite free) basis of Barka Sayal area 124

Table 4.17 Maceral and mineral matter content of Argada area 132

Table 4.18 Maceral content (vol.%) of different coal seams of Argada area, South Karanpura coalfield, Jharkhand, India 136

Table 4.19 Microlithotype and carbominerite content (vol.%) of coals seams of Argada area, South Karanpura Coalfield, India. 140

Table 4.20 Microlithotype content (carbominerite free) basis (vol.%) of different coals seams of Barka Sayal area, South Karanpura Coalfield, Jharkhand, India 144

Table 5.1 Proximate constituents (wt%) of coal seams of Barka Sayal area 155

Table 5.2 Proximate constituent (wt.%) of coal seams of Argada area 164

Table 5.3 Ultimate analysis of coals seams present in the Barka Sayal area 177

Table 5.4 Ultimate constituents (wt.%) of coal seams of the Argada area. 185

Table 5.5 The concentration of oxide of major elements in South Karanpura coals 190

Table 5.6 The concentration of major elements in coals of South Karanpura 194

Table 5.7 The concentration of selected trace elements in coals of South Karanpura 206

Table 5.8 XRD analysis of coal ash samples of South Karanpura coalfield, India. 210

Table 5.9 Prominent peaks identified in the FTIR Spectra 218

Table 5.10 Biomarker compounds identified in the samples of the Barka Sayal area. 221

Table 5.11 Biomarker parameters calculated for samples of the Barka Sayal area. 222

Table 5.12 *n*-alkanes and isoprenoids compounds identified in the Argada area. 223

Table 5.13 Biomarker compounds present in the samples of the Argada area 224

Table 5.14 Biomarker parameters calculated for the samples of the Argada area. 224

Table 6.1 Geochemical parameters describing source rock generative potential 231

Table 6.2 Total Organic Carbon and their Source Rock Implications 231

Table 6.3 Hydrogen index and their principal products (after, Peters 1986). 231

Table 6.4 Maturation based on Production Index (PI), Temperature (Tmax), and Vitrinite Reflectance (VRo %) (after, Peters 1986)..... 231

Table 6.5 Geochemical parameters describing the type of hydrocarbon generated..... 231

Table 6.6 Source Rock Evaluation Data of coals of Barka Sayal area, South Karanpura coalfield, Jharkhand, India. 234

Table 6.7 Source Rock Evaluation Data of coals of Argada area, South Karanpura coalfield, Jharkhand, India. 236
Table 6.8 Coal characteristics required for hydrogenation..... 249
Table 6.9 Values of Conversion, Oil yield, and Petrofactor Calculated for South Karanpura Coals Using Empirical Formula 253
Table 7.1 Environmental significance and mode of occurrence of selected trace elements present in the Coals of South Karanpura coalfield (Gluskoter 1975). 296
Table 7.2 Calculated chemical proxies to determine the paleo depositional settings and slagging behaviour of coals of the South Karanpura coalfield. 297
Table 8.1 Definition of broad rank categories: low, medium and high rank..... 326
Table 8.2 Subcategories of low-rank coals..... 326
Table 8.3 Sub-categories for medium-rank coals..... 327
Table 8.4 Sub-categories for high-rank coals (anthracites)..... 327
Table 8.5 Classification by the petrographic composition 327
Table 8.6 Ash yield classification 327
Table 8.7 Classification of the coals of South Karanpura coalfield (seam-wise) as per the International Organization for Standardization (ISO) classification scheme 328

Symbols and Abbreviations

Symbols & Abbreviations	Comments	Symbols & Abbreviations	Comments
%	Percentage	°C	Degree Celsius
µm	Micro meter	AG	Argada coal seam
Av	Average	ASTM	ASTM International/ American Society for Testing and Materials
BG	Bansgarha coal seam	BIS	Bureau of Indian Standards
C	Carbon	Ca	Calcium
Cd	Cadmium	cm	Centi meter
Co	Cobalt	cps	Count per second
Cr	Chromium	Cu	Copper
db	Dried basis	daf/dafb	Dry ash-free basis
dmf/dmmf	Dry mineral matter free basis	FC	Fixed carbon
Fe	Iron	FTIR	Fourier Transform Infrared Spectroscopy
GC-MS	Gas Chromatography-Mass Spectrometry	GI	Gelification Index
GSI	Geological Survey of India	GWI	Ground Water Index
H	Hydrogen	HI	Hydrogen Index
IBM	Indian Bureau of Mines	HD	Hathidari coal seam
Inert	Inertinite	ICCP	International Committee for Coal and Organic Petrology
K	Potassium	Km	Kilometer
Lipt	Liptinite	M	Meter
max	Maximum	min	Minimum

Symbols & Abbreviations	Comments	Symbols & Abbreviations	Comments
m.m.f./mmf	Mineral matter free basis	Mg	Magnesium
Mg	Magnesium		
Mn	Manganese	N	Nitrogen
Na	Sodium	Ni	Nickel
O	Oxygen	OI	Oxygen Index
ONGC	Oil and Natural Gas Corporation	OM	Organic Matter
Pb	Lead	ppm/ppb	Parts per million/parts per billion
S	Sulfur	SD	Standard deviation
SL	Sayal coal seam	SBK	Sayal Balkudra coal seam
T_{max}	Maximum Temperature	TOC	Total Organic Carbon
TPI	Tissue Preservation Index	Vitr	Vitrinite
VI	Vegetation Index	VM	Volatile Matter
vol/vol.	Volume	VRo	Vitrinite Reflectance
VRo	Vitrinite Reflectance	vol/vol.	Volume
VRomax	Maximum vitrinite reflectance	wt/wt.	Weight
XRD	X-ray diffraction	XRF	X-ray fluorescence
Zn	Zinc		

Preface

The previous studies of South Karanpura coals were made for mine development with the main emphasis on the maximum production of coal from mines. During these studies, aspects of the depositional environment of coal seams were not covered properly, which is a prime controlling factor in many aspects of coal utilization. Though some sporadic data on petrographic and geochemical components have been generated by some workers on South Karanpura coals in general, there has been no attempt made so far to characterize these coals on a regional scale to comment upon the depositional environment and hydrocarbon potential.

The present work undertakes a detailed petrographic and geochemical study of coals from South Karanpura coalfield, Jharkhand, India, to determine the lateral as well as vertical variations in megascopic (lithotype) and microscopic (maceral and microlithotype composition) constituents and in geochemical characteristics (proximate constituents, ultimate constituents, major oxides and trace elements). Research methodology has included standard tools, techniques and procedures in the field of study.

This study discusses the depositional environment, ancient ecosystem and peat-forming communities of South Karanpura coals. It will facilitate future researchers, mining operators in the area of South Karanpura coalfield to draw imperative insight into these coals. This study also focuses on the potential environmental contamination studies and effective utilization of these coals followed by the proper classification method. To tackle the energy crisis, an attempt has been made to find out the hydrocarbon potential of these coals. South Karanpura coalfield is a major Gondwana coalfield hence the studies done for this coalfield may also be valid for the other Gondwana coalfields of India.

The entire work has been documented in nine chapters. **The first chapter** introduces the necessity, scope, and objective of this work. A review of works done by several authors on Gondwana coals has also been mentioned with a detailed review of work done in the South Karanpura coalfield. **The second chapter** describes the geology of the Gondwana basins of India and Damodar valley, further confined to the Karanpura basin and geology of the South Karanpura coalfield, in detail. This chapter also introduces the mode of occurrence of different seams present in two main areas of South Karanpura Coalfield. **The third chapter** discusses the sampling techniques implemented and methods of different analyses carried out for the present work. **The fourth chapter** presents the megascopic as well as microscopic petrographic properties of the coals of the study area. **The fifth chapter** is devoted to the geochemical aspects identified for these coals and the geochemical analyses such as proximate, ultimate, XRD, XRF, FTIR and GC-MS of the coals have been described therein. **The sixth chapter** focuses on the maturity and the source rock characteristics of the coals of South Karanpura coalfield. **The seventh chapter** presents the discussions made for the identification of the paleodepositional environment, petroleum generation potential, and environmental aspects of major and trace elements present in these coals, based on the identified petrological and geochemical characteristics. **The eighth chapter** presents the classification of the coals of South Karanpura coalfield using international and national classification schemes and provides a suggestion for the potential utilization of these coals. **The ninth chapter** is the final chapter and presents a summary and conclusion of the complete work. At last, all the **references** cited in the thesis are mentioned.

1 CHAPTER 1. GENERAL INTRODUCTION

1.1 Introduction

The socio-economic development of a country depends on how well it fulfills its energy demand. For a big nation like India, energy demand is also enormous, which can be fulfilled by either non-renewable resources such as fossil fuels (oil, coal, and natural gas) that cannot be recovered in a human lifespan or with renewable resources such as solar, wind, hydropower, tidal power, etc., that can recover their potential in time significant by human needs. Due to existing technology and infrastructure to utilize fossil fuels, it is currently economical for decentralized energy use. Among fossil fuels, coal is the most important and conventional source of energy. Coal accounts for most of the Indian electricity production and acts as a raw material for several industries. It is found in the form of sedimentary rocks (organo-clastic sedimentary rock) and recognized as an inflammable organic substance, composed mainly of hydrocarbons, and capable of being used as fuel to supply heat, light, or both. The definition of coal may vary based on the area of utilization (Flores 2014). Coal contains volatile matter, moisture, and ash in varying proportions. On the elemental scale, it is mainly composed of carbon, hydrogen, nitrogen, sulfur, and oxygen. Besides, coal is also a storehouse of various minerals (Irdi *et al.* 1993; Ward and Taylor 1996; Singh *et al.* 2010, 2015b; Zhao *et al.* 2016; Finkelman *et al.* 2019; Jiang and Yu 2019; Li *et al.* 2019; Liu *et al.* 2019b) and trace elements (Mastalerz 2001; Sun *et al.* 2010; Jia *et al.* 2015; Karayiğit *et al.* 2017b; Zou *et al.* 2018; Arbuzov *et al.* 2019; Dai *et al.* 2020a).

Coal mining in India began in 1774 when John Sumner and Suetonius Grant Heatly of the East India Company commenced commercial exploitation in the Raniganj Coalfield along the western bank of Damodar River (Fox, 1931). As of April 1, 2018, India has

estimated coal reserves of 319.020 billion metric tonnes (Gt) (Geological Survey of India 2018), which is the fifth-largest coal reserves in the world. India is one of the largest coal producers in the world, producing more than 268 million tonnes (Mt) of coal currently (Wang *et al.* 2018).

Gondwana coal shares the major portion of the Indian coal inventory (>99%). Gondwana coals are deposited in the eastern and central parts of India. Few Gondwana coal deposits are reported in Assam and Sikkim in the northeastern part of the country in their Permian sequences. In contrast, Cenozoic coal occurs in the states of Assam, Arunachal Pradesh, Nagaland, Meghalaya, and Jammu and Kashmir (Pareek 1988). A total of about 8.91 Gt of the country's lignite resources are confined within a 150 m depth from the surface in the states of Tamilnadu, Rajasthan, Gujarat, Pondicherry, Jammu and Kashmir, Kerala and West Bengal. Sporadic occurrences of lignite are also reported in certain areas of Alleppey, Varkala, Cannanore, in Kerala and Ratnagiri in Maharastra.

The state of Jharkhand ranks first in Indian coal reserve (83.15 Gt) (Geological Survey of India 2018), whereas second in the case of coal production (Indian Bureau of Mines 2018). The main deposits of Jharkhand are the Jharia, East Bokaro, West Bokaro, North Karanpura, South Karanpura, Giridih, Rajmahal, Ramgarh and Deoghar coalfields. Most of these coalfields are situated along a narrow belt running in an east-west direction.

The South Karanpura Coalfield, one of the important coalfields of Jharkhand state, is a part of the Damodar valley and is located in Ramgarh district (Figure 1.1). It contains 809.63 Mt of medium coking coal and 6.822 Gt of non-coking coal to a depth of 1200 m, as of April 1, 2018 (Geological Survey of India 2018). This coalfield covers an area of 194 km^2 bounded by latitudes 23°38'–23°45'N and longitudes 85°05'–85°28'E (Raja Rao, 1987).

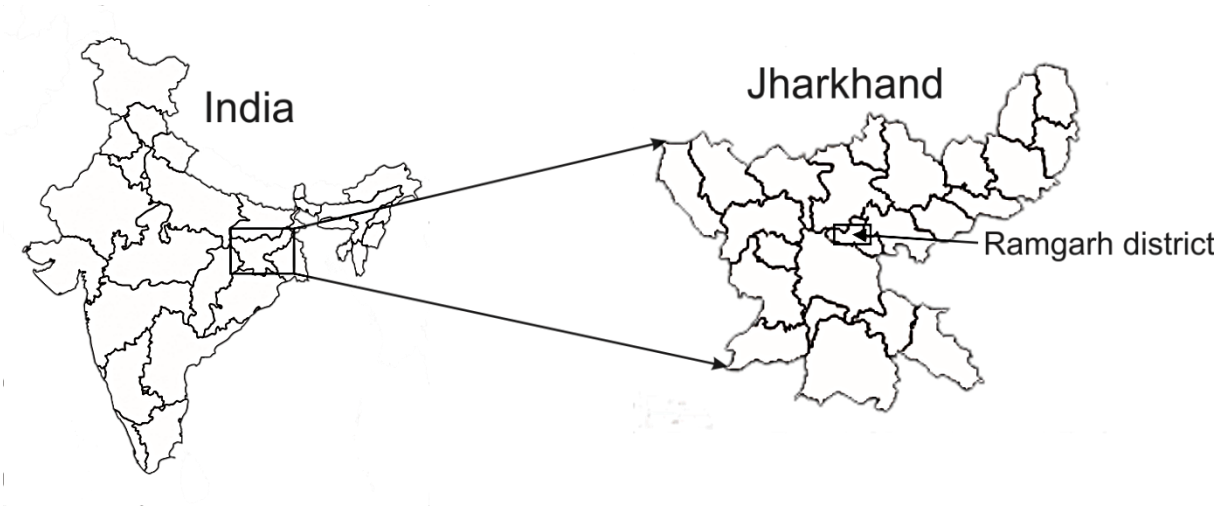


Figure 1.1 Broad location map of the study area (South Karanpura Coalfield, Jharkhand, India).

The present work was undertaken with a view of studying the coal deposits of the South Karanpura coalfield using systematic sampling and the modern approach of petrography and geochemistry. Although, many workers have studied the characteristics of the coals, shales, and other rocks of the area, the systematic sampling and regional approach were neglected in the previous studies.

1.2 The occurrence of coals in India

There are mainly two distinct stratigraphic horizons present in India, containing economic coal formations: Gondwana sediments (Upper Paleozoic to Mesozoic systems) and Cenozoic sediments. The exploration activities in India are carried out by government agencies such as the Geological Survey of India (GSI) and its subsidiaries, Central Mine Planning and Designing Institute (CMPDI), Coal India Limited (CIL), Mineral Exploration and Corporation Limited (MECL), etc. These agencies have established 319.020 Gt of coal reserves in the country up to a depth of 1200 m., considering the coal seams of 0.90 m or above thickness (Geological Survey of India 2018). A coalfield-wise inventory of the geological reserve of Indian coal is presented in Figure 1.2 (Indian Bureau of Mines 2018).

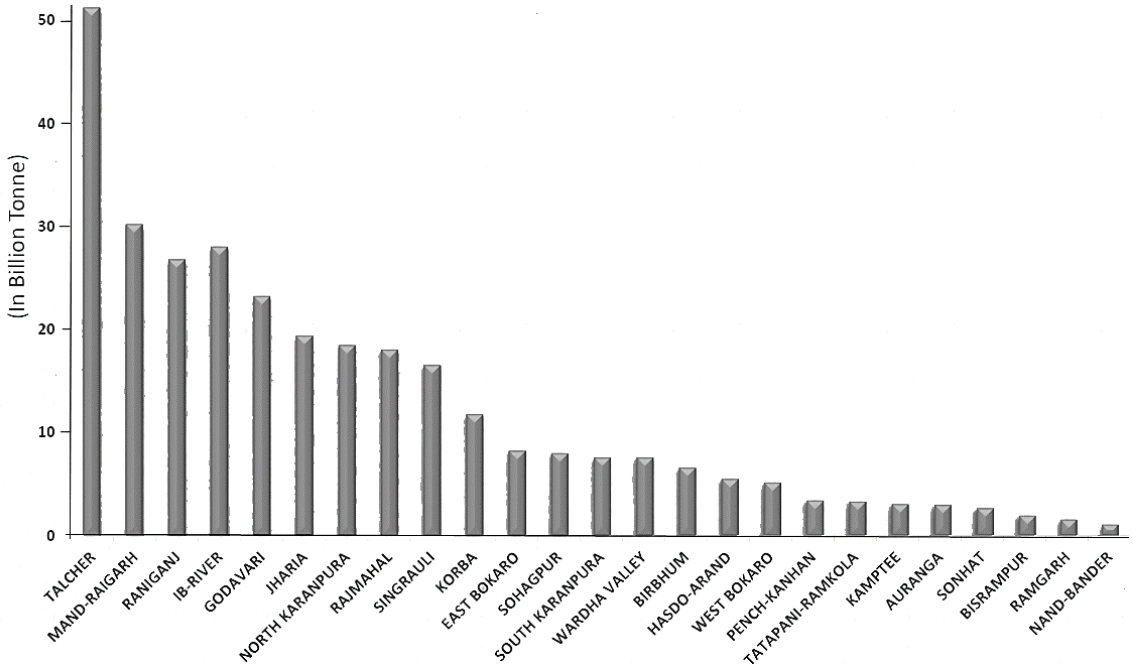


Figure 1.2 Coalfield-wise inventory of geological reserve of Indian coal as of April 1, 2018 (Geological Survey of India 2018).

Out of the total, 319.02 Gt of the net geological resources assessed for coal, leaving the mined out quantity, 1.588 Gt of coal are present in the Cenozoic coalfields, whereas Gondwana coalfields account for 317.433 Gt (99.50%) of the total coal. These coals vary in type as prime coking, medium coking, semi coking, and non-coking (Table 1.1) (Geological Survey of India 2018).

Table 1.1 Type-wise inventory of geological reserves (proved, indicated, and inferred combined) of Indian coals up to a depth of 1200 m, as on April 1, 2018 (Geological Survey of India 2018).

Type of coal	Reserve (in Gt)
Prime coking	5.313
Medium coking	27.502
Semi coking	1.707
Non-coking	282.910
Total	319.020

In the Indian context, the demand-supply gap for coal is increasing, which needs imports of coking and non-coking coal. China is the largest global producer of coal and produces

nearly four times as much as the next largest producer, the United States of America (USA) (Breeze 2015). China has given much attention to the cleaner production of coal (Fangneng 2003; Osborne 2013; Duan *et al.* 2018), extraction of valuable trace elements from coal (Dai *et al.* 2012; Gong *et al.* 2016; Dianshi *et al.* 2018) and on other advanced technical concepts utilized in this field. Technological advancements and research on Indian coal will facilitate the sustainable development of Indian coal-based industries.

1.2.1 The geological occurrence of the Gondwana coal

About 270 million years ago, during the Permian period, South Africa, South America, Antarctica, Australia, India, and Madagascar formed a large landmass called Gondwanaland (Mukhopadhyay *et al.* 2010). Gondwana coals formed in Gondwanaland. In the case of India, Gondwana sediments occur in eastern and central parts with minor occurrences in the northeastern part, especially in Assam and Sikkim. The maximum concentration of coalfields is in the north-eastern region of the peninsular plateau of India comprising parts of Jharkhand, Chhattisgarh, Orissa, eastern Madhya Pradesh, and the western part of West Bengal adjoining Jharkhand. The southern parts of Madhya Pradesh, the eastern part of Andhra Pradesh, and the eastern part of Maharashtra also have large coal deposits. The Gondwana coal mines are located in the river valleys of the Damodar (Jharkhand-West Bengal), the Mahanadi (Chhattisgarh-Odisha), the Godavari and the Wardha (Maharashtra-Andhra Pradesh), the Son (Madhya Pradesh Jharkhand), the Indravati, the Panch, the Narmada, the Koel, and some more.

The Damodar valley is home to the largest coalfields in the Jharkhand-West Bengal coal belt. Gondwana coalfields are located in several places such as Jharia, Raniganj, Bokaro, Karanpura, Giridih, Tatapani, Chandrapur, Talcher, Korba, Singrauli, etc. The Jharia coalfield, located in the south of the Dhanbad district of Jharkhand state, is one of India's richest coalfields, containing reserves of the highest quality bituminous coal. Raniganj

Coalfield is the oldest coalfield in India, where mining started in 1774. Presently, Eastern Coalfield Limited produces bituminous coal from several underground and opencast mines operating over an area of 1,530 km^2 (Das and Chakrapani 2011). The Raniganj, Barakar, and Karharbari formations are the three geological units containing most of the Gondwana coals. Chronologically, Karharbari Formation is the oldest coal formation in India, followed by Barakar and Raniganj. The geology of different Gondwana basins of India is mentioned in Chapter 2 of the thesis. The South Karanpura coalfield contains sediments of the Lower Gondwana. The Barakar Formation is the main coal-bearing horizon of the South Karanpura coalfield. The state-wise distribution of Gondwana coalfields of India is presented in Table 1.2. The important coalfields of India are presented in Figure 1.3.

Table 1.2 State-wise distribution of Gondwana coalfields in India (Indian Bureau of Mines 2018).

State	Important coalfields
West Bengal	Raniganj, Barjora, Birbhum, Darjeeling
Jharkhand	Raniganj, Jharia, East Bokaro, West Bokaro, Ramgarh, North Karanpura, South Karanpura, Aurangabad, Hutar, Daltongunj, Deogarh, Rajmahal
Bihar	Rajmahal
Madhya Pradesh	Johilla, Umaria, Pench-Kanhan, Pathakhera, Gurgunda, Mohpani, Sohagpur, Singrauli
Chattisgarh	Sohagpur, Sonhat, Jhilimili, Chirimiri, Bisrampur, East Bisrampur, Lakhanpur, Panchbahini, Hasdeo-arand, Sendurgarh, Korba, Mand-Raigarh, Tatapani-Ramkola
Uttar Pradesh	Singrauli
Maharashtra	Wardha-valley, Kamptee, Umrer Makardhokra, Nand Bander, Bokhara
Odisha	Ib-River, Talcher
Andhra Pradesh	Godavari Valley
Telangana	Godavari Valley
Sikkim	Rangit Valley
Assam	Singrimari

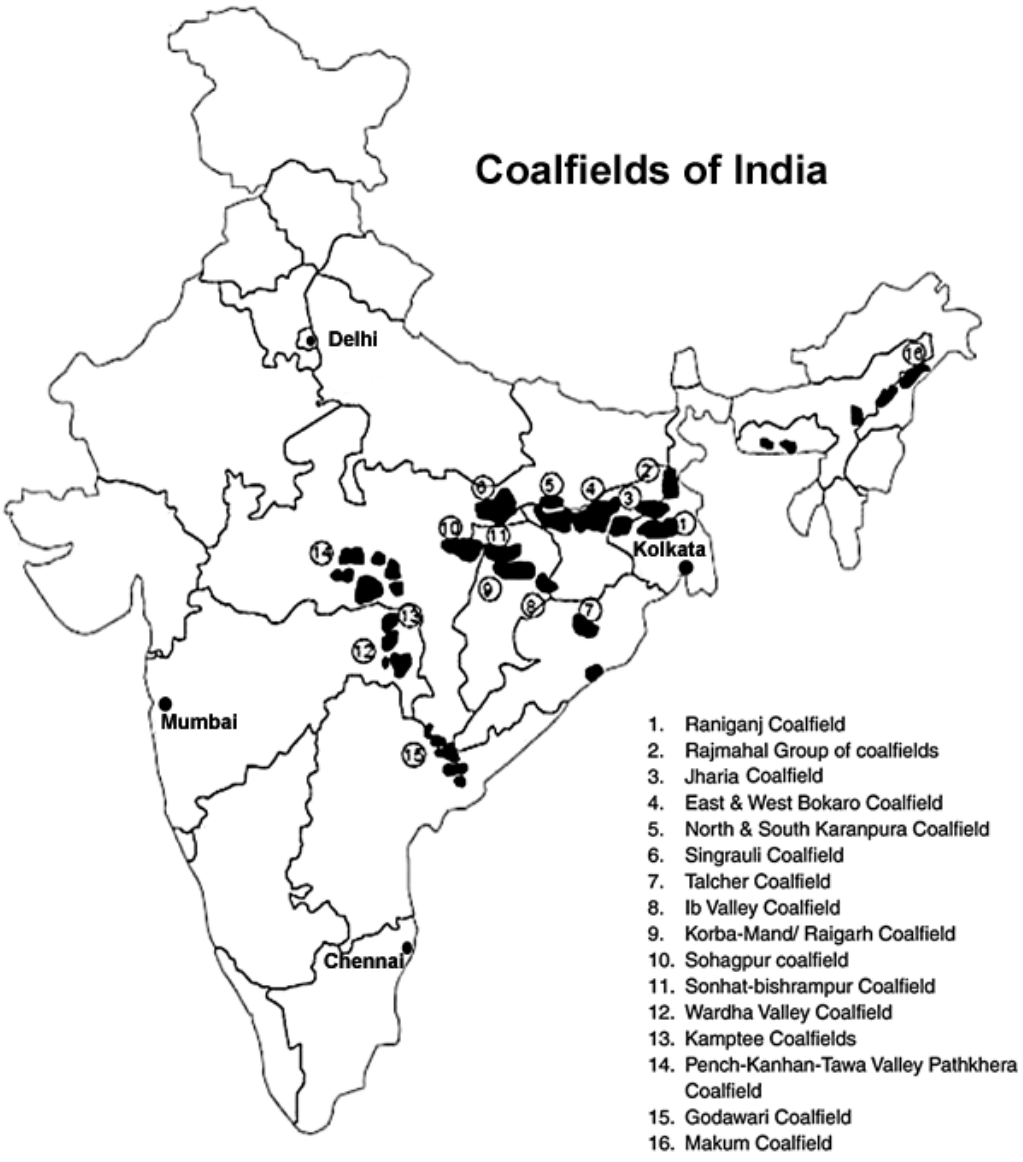


Figure 1.3 Important Gondwana coalfields of India (Dutta et al. 2011a).

1.2.2 The geological occurrence of the Cenozoic coal and lignite

Cenozoic coal-bearing sediments are mainly confined to the states of Assam, Arunachal Pradesh, Nagaland, and Meghalaya (Pareek 1988; Chabukdhara and Singh 2016), whereas the major parts of the lignite resources are located in Tamilnadu (36.135 Gt) followed by Rajasthan (6.35 Gt), Gujarat (2.72 Gt), Pondicherry (416.61 Mt), Jammu and Kashmir (27.55 Mt), Kerala (9.65 Mt) and West Bengal (3.93 Mt) (Geological Survey of India 2018).

Table 1.3 State-wise distribution of Cenozoic coal/lignite fields (Raja Rao 1981; Geological Survey of India 2018).

Types of Coalfields	State	Main coalfields
Cenozoic Coalfields	Arunachal Pradesh	Namchik-Namphuk, Miao Bum
	Assam	Dayang valley, Disai valley, Dikhau valley (Nazira), Saffrai valley, Makum, Mikir hills, Dilli-Jeypore etc.
	Meghalaya	Balphakram-Pendeguru, Siju, Mawlong-Shella, Bapung, Jayanti Hills (minor coalfields), West Daranggiri, East Daranggiri, Langrin, Khasi Hills (minor coalfields)
	Jammu and Kashmir	Chakkar, Kura, Kalakot etc.
	Nagaland	Borjan, Jhanzi-Disai, Tuen Sang, Tiru valley
Cenozoic Lignite Fields	Tamilnadu	Cuddalore-Pondicherry, Tanjavour and Trichirapalli regions
	Rajasthan	Barmer, Bikaner, Nagaur
	Gujarat	Kutch, Bhavnagar, Surat and Bharuch region
	Kerala	Quilon, Trivendrum and Kannanore region
	Jammu and Kashmir	Kupwarea region
	Other states	Karnataka, Maharashtra, West Bengal and Assam

In the case of Cenozoic coals, coalfields of Meghalaya, Mikir hills of Upper Assam, and coals of Jammu coalfields formed in Lower Eocene; lignites of Palana, Rajasthan, and Kutch formed in the Paleocene, coals of the Arunachal Pradesh, Nagaland, and Makum coalfields of Assam originated during the Late Eocene to Oligocene (Raja Rao 1981; Singh & Singh 2001; Singh *et al.* 2012; Mathews *et al.* 2020). The lignite fields of Tamilnadu and Kerala formed during the Miocene. Lignites in the Kashmir valley are of a more recent age and formed during Late Pliocene to the Early Pleistocene (Chandra and Chakrabarti 1989). Generally, Cenozoic coals have a high amount of sulphur and high moisture (Chandra *et al.* 1983; Singh and Singh 2000). The Makum coalfield of the Tinsukia district, Assam, is the most developed Cenozoic coalfield. The Neyveli Lignite field of Tamilnadu is the largest lignite field in India. Susceptibility to spontaneous combustion of lignite makes its mining difficult (Misra and Singh 1994). The state-wise distribution of Cenozoic coal or lignite fields of India is presented in Table 1.3.

1.3 Review work on Gondwana coals in general

Gondwana sediments, as the storehouse of premium quality coals, attracted the attention of early authors. Fox (1931) and Gee (1940) discussed the Gondwana system and the

origin of its different formations and emphasized its drift origin. Several authors discussed the petrographical and physical characteristics of Gondwana coals (Navale 1971; Navale and Saxena 1989; Misra *et al.* 1990). Sedimentary-tectonic environmental analysis of Gondwana sediments present in Saharjuri coalfield, Burhai basin, and Jayanti coalfield of Jharkhand (earlier Bihar) was done by Niyogi and his coauthors (Niyogi 1961, 1966; Niyogi and Sanyal 1962). Paleontological studies of different Gondwana sediments have been carried out by several authors (Chatterjee and Hotton 1986; Veevers 2006). Sedimentological studies of different sequences of Gondwana basins have been carried out by authors in much detail (Casshyap 1970; Chakraborty *et al.* 2003a; Chakraborty and Ghosh 2008). Recently, with the advancement of geochemical and petrographic techniques, advanced methods of characterization have been used by several authors to determine the source rock characteristics, depositional environment, coal bed methane potential of these coals, etc. (Mukhopadhyay *et al.* 1979; Mishra *et al.* 1990; Prachiti *et al.* 2011; Singh *et al.* 2013d; Naik *et al.* 2016; Singh and Jha 2018c).

1.4 Review work on South Karanpura coals

The mining history of South Karanpura coalfield dates to the East India Company. Mapping of Karanpura coalfield was first done by Williams (1852), a geological surveyor in the service of the East India Company. Hughes (1871) confirmed the further presence of thick Gondwana sediments in South Karanpura coalfield during his mapping of the entire coalfield during 1867 and 1868. Several unpublished articles by the workers of the Geological Survey of India also added significant contributions in understanding the geology of the area (Raja Rao 1987).

Sedimentary geological studies of South Karanpura coalfield were carried out by several workers (Banerjee 1963, 1964; Gupta *et al.* 2000; Holz *et al.* 2002). Banerjee (1960)

discussed the sedimentology of the area and interpreted the depositional environment, post-depositional changes in sedimentation, and mutual grain to grain relationships of the hard rocks belonging to the different Lower Gondwana Formations in the area (Banerjee 1960).

Paleobotanical studies have been carried out by several workers (Kulkarni 1879; Venkatachala and Kar 1964; Bharadwaj 1970; Bharadwaj *et al.* 1978; De *et al.* 2003; Srivastava and Agnihotri 2013; Murthy *et al.* 2014).

Klootwijk (1974) has conducted a paleo-magnetic study of Panchet clay beds from the Karanpura region.

Singh (2006) done a case study in the Argada area of South Karanpura Coalfield. He tried to evaluate the existing mining policy in India, the influence of mining on the environment, measures taken, occupational health hazards, and quality of life in the vicinity of such coal mines.

Using the remote sensing technique, Kumar & Pandey (2013) studied the impact of coal mining in the area.

A preliminary study of methane and carbon dioxide sorption characteristics of a few samples of this coalfield has been carried out by Dutta *et al.* (2011).

Mahesh *et al.* (2015) presented a relation between fusinite and semifusinite macerals as charcoal remains and their importance as paleofire indicators. The other workers have also made efforts to evaluate the shale gas potential and petrophysical characterization of Gondwana shales of South Karanpura coalfield (Mendhe *et al.* 2016; Sarkar and Singh 2016). The environmentalist also made hydrochemistry of coal mine water and risk to human health in the nearby coal mine region (Neogi et al. 2018).

To facilitate the coal bed methane exploration, cleat orientation and in-situ stress analysis in different coal seams of South Karanpura Coalfield has been done by Ali *et al.* (2017). The CBM potential of some of the coal seams of this coalfield was identified by Kumar *et al.* (2018b).

The hydrocarbon potential of few seams of South Karanpura coalfield has been discussed by Singh & Jha (2018a, c). An attempt was also made to classify coals of the Barka Sayal area of South Karanpura Coalfield with emphasis on the proper utilization of these coals (Singh and Jha 2018c). The interrelation between the mechanical and petrographic properties of these coals have also been discussed by (Singh and Jha 2020). Kumar et al. (2018a) have also used bacterial tools for the demineralization of these coals.

1.5 The objective and scope of the present work

The previous studies of South Karanpura coals were made for mine development with prime emphasis on the maximum production of coal from mines. During these studies, aspects of the depositional environment of coal seams were not covered, which is a prime controlling factor in many aspects of coal utilization. Though, some workers have generated some sporadic data on the petrographic and geochemical components of the South Karanpura coals in general. However, there has been no attempt made so far to characterize these coals on a regional scale to comment upon the depositional environment and hydrocarbon source rock characteristics.

The objectives of this thesis are:

- To undertake a detailed petrographic and geochemical study of coals from South Karanpura coalfield, Jharkhand, India for the determination of lateral as well as vertical variations in megascopic (lithotype) and microscopic (maceral and

microlithotype composition) constituents and geochemical characteristics (proximate constituents, ultimate constituents, major oxides, and trace elements).

- To interpret the depositional environment, ancient ecosystem, and peat-forming communities of these coals based on a review of published coal petrography based models and present-day environmental significance of geochemical constituents.
- To study the coal seams, to evaluate the source rock characteristics as well as efficient utilization of these coals in the industry.

This study discusses the depositional environment and elemental distribution of the South Karanpura coals. It will facilitate future researchers, mining operators in the area of the South Karanpura coalfield to draw important insight into these coals. This study also focuses on the potential environmental contamination studies and the effective utilization of these coals, followed by the proper classification method. To tackle the future energy crisis, an attempt has been made to find out the hydrocarbon potential of these coals. South Karanpura coalfield is a major Gondwana coalfield; hence, the studies done for this coalfield may also be valid for the other Gondwana coalfields of India.

1.6 Fieldwork

The fieldwork was conducted in three different field seasons of the year 2014-2015. Coal samples were collected from all the exposed seams present in different underground and open cast coal mines of South Karanpura coalfield following the pillar sampling method. The immediate roof and floor rocks of the coal seams were also studied and recorded. Discontinuities present in the coal seams were observed. The coal samples collected mainly belong to two areas, Barka Sayal and Argada. Coal samples of the Sayal, Sayal Balkudra, Upper Semana, Lower Semana, Hathidari, and Bansgarha seams were collected from different underground and opencast mines present in the Barka Sayal area. Coal

samples of the Argada, Argada-A, Argada-B, Argada-C, Argada-D, Argada-I, and Argada-J were collected from different underground and open cast mines present in the Argada area.

1.7 Laboratory work

The laboratory work includes different analyses done for the samples collected during the field visit. The work done at the laboratory is mainly categorized into four parts, 1) Sample preparation for the analysis; 2) Petrographic analyses; 3) Geochemical analyses; and 4) Data collection, storage, and presentation. Most of the laboratory work was done in the Geology and Geochemistry laboratory of the Rajiv Gandhi Institute of Petroleum Technology, Jais, Amethi. Macropetrographic seam characteristics were identified using the classification scheme proposed by Diessel, for banded coal (Diessel 1965), whereas microscopic analysis was made following the recommendations of the International Committee of Coal and Organic Petrology (ICCP) (International Committee for Coal and Organic Petrology 1971, 1975, 1998, 2001). The geochemical analysis, which is a major part of this analysis includes a proximate analysis, ultimate analysis, Rock-Eval pyrolysis, Fourier Transform Infrared (FTIR) Spectroscopy, X-ray diffraction (XRD), X-ray fluorescence (XRF) and Gas chromatography-mass spectroscopy (GC-MS). Proximate analysis was done using Indian standards to determine the moisture, ash, volatile matter, and fixed carbon content present in these coals. The ultimate analysis was carried out at the Central Drug Research Institute, Lucknow, to identify the Carbon, Hydrogen, Nitrogen, Sulphur, and Oxygen quantity present. FTIR study was done to determine the presence of different organic and inorganic compounds in coal as well as low-temperature ash derived from these coals. To understand the source rock characteristics of these coals, the Rock-Eval pyrolysis was done at Keshava Deva Malaviya Institute of Petroleum Exploration (KDMIPE), Dehradun. Inorganic identification such as the presence of trace

elements, major oxides, and minerals was done using the facility of XRF and XRD provided by Jawaharlal Nehru University, New Delhi, and Oil and Natural Gas Corporation (ONGC), Ahmedabad respectively on low-temperature ash samples derived from representative coal samples following the recommendations by Swanson and Huffman (1976). Geochemical analysis, such as the identification of biomarkers, was made in the Birbal Sahni Institute of Paleosciences, Lucknow, using gas chromatography-mass spectroscopy (GC-MS) apparatus. The details of the methods applied for the present work for different analyses are mentioned in Chapter 4 of this thesis.

2 CHAPTER 2. GEOLOGY

2.1 Introduction

The lithological and paleontological studies of the units indicate their origin and depositional environment. Genetic factors, such as paleo slope, water energy, paleoclimate, geological age, and different controls over sedimentation, affect the deposition of different facies of sedimentary rocks. A coal petrographic facies based on coal types can also deduce vital information about the environment of deposition (Navale and Saxena 1989). The South Karanpura Coalfield is a part of the Damodar valley belonging to the Gondwana basins of India. Therefore, the geology of the South Karanpura Coalfield is closely linked with the geology of the Gondwana basin and Damodar valley. The geology of the Gondwana basins is described below in detail.

2.2 Geology of the Gondwana basins of India

The geology of the Gondwana basin of India has been described by several authors (Fox 1931; Casshyap 1970; Rogers and Callahan 1987; Navale and Saxena 1989; Dutta 2002; Tewari and Maejima 2010). The main part of the Gondwana is well developed in the Eastern and Central regions of India. All these basins have graben or half-graben geometry. The Gondwana Basins of Peninsular India occur in four major linear belts (Mukhopadhyay *et al.* 2010) (Figure 2.1), namely:-

(1) The Trans-Indian basin belt, including the Satpura and Son Valley basins, having an ENE-WSW trend, and the Damodar-Koel Valley basins, trending E-W to WNW-ESE;

(2) The Wardha-Pranhita Godavari Valley basin belt, having a trend of NNW-SSE;

(3) The NW-SE-trending Mahanadi Valley basin belt that deviates to the WNW-ESE direction in the southernmost Talcher coalfield; and

(4) The Purnea-Rajmahal-Galsi basin belt with an NNW-SSE trend.

It is believed that the deposition of Gondwana basins initiated in the glacially-modified basement depressions with a much larger dimension and might be a single master basin whose remnants are now preserved caused by faulting at later stages (Mukhopadhyay *et al.* 2010). Repeated thick sediment accumulations caused the syn-sedimentary subsidence along with the faults of intra-basin nature suggests subsidence due to severe faulting to provide the required accommodation (Chakraborty and Ghosh 2008). The tectonic-sedimentary evolutionary study brings out crucial information about the origin of these basins. Old reactivated shear zones formed these basins in Proterozoic orogenic belts. The Lower Gondwana sediments such as the Talchir and Barakar formations are supposed to have been deposited in initial sag basins, whereas Upper Gondwana formations were deposited as syn-rift sedimentation in the evolving rift basins (Krook *et al.* 1986). A reactivation of palaeo-sutures and graben formation generated the intra-cratonic Gondwana basins (Casshyap and Tewari 2009). The Narmada–Son–Damodar, Pranhita–Godavari, and Mahanadi basins, the main riftogenic Gondwana continental basins formed during the Permian to Jurassic, converge to meet at the Satpura area in central India.

The Talchir Formation, a glaciogenic facies, formed during the late Carboniferous covering the Precambrian basement (Dutta 2002). The Talchir Formation is characterized by the presence of tillite, boulder bed, conglomerate, sandstone, shale, and varve deposits. The Karharbari Formation had formed as a small basin at the marginal part with fluvial conditions prevailed (Mukhopadhyay *et al.* 2010) has been identified only in few Gondwana basins. This formation contains conglomerate, pebbly coarse and medium-grained sandstone, fine clastics, and some coal beds.



Figure 2.1 Gondwana basins of India (Mukhopadhyay *et al.* 2010).

The Barakar Formation was deposited in a tectonically active environment and contains pebbly sandstone, sandstone, siltstone, black to grey shale, fireclay, and thick coal seams. The Barren Measures are made up of sandstone, grey micaceous shale, and black carbonaceous shale. Ferruginous bands and siderite bands are also common. This formation does not contain thick coal seams; however, some occurrence of thin coal seams and coal stringers may be present. This formation is known as the Motur Formation

in the Satpura basin. The Raniganj Formation overlies Barren Measures with a gradational contact and is characterized by the presence of carbonaceous shale, siltstone, thinner coal seams as compared to the Barakar Formation and fine to coarse-grained sandstone of greenish colour. This formation is known as the Bijori Formation in the Satpura basin. The bulk of the Panchet Formation is formed by alternate yellowish sandstone and red shale with some coal-bearing sediments. The Panchet Formation is known as the Maleri Formation in the Pranhita-Godavari valley, the Pali-Tiki in the Son Basin, and the Pachmarhi-Denwa in the Satpura Basin. The Mahadeva Formation has a lithological association of conglomerate, coarse to medium-grained sandstone, pebbly sandstone, and pink or buff coloured kaolinite clay lenses. In the Pranhita-Godavari valley, this formation is known as the Kota Formation, the Parsora in the Son basin, and the Bagra in the Satpura basin (Mukhopadhyay *et al.* 2010).

2.3 Geology of the Damodar Valley

The Damodar river basin is a sub-basin of the Ganges river basin. This funnel-shaped basin covers an area of 23,370.98 km^2 in the states of Jharkhand and West Bengal in India (Gupta 1999). Geographically, the basin lies between latitude 22°15' to 24°30' N and longitude 84°30' to 88°15' E. The larger area covering the upper catchment is situated in Jharkhand, whereas the state of West Bengal is covered by the low-lying floodplains of this basin. The important coalfield belonging to the Damodar basin are the Raniganj, Jharia, South Karanpura, North Karanpura, East Bokaro, West Bokaro, and Ramgarh (Figure 2.2). This basin is a repository of 46% of Indian coal reserves, mainly bituminous to sub-bituminous rank (Tiwary and Dhar 1994).

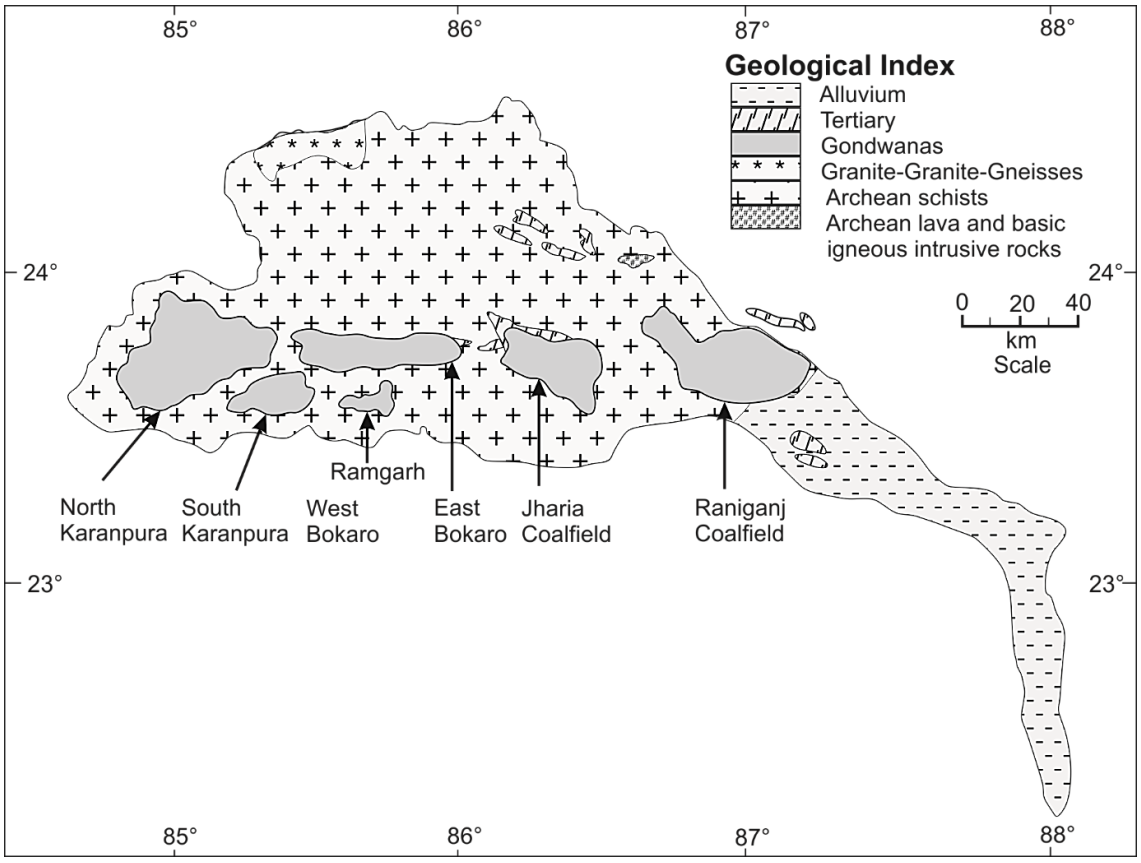


Figure 2.2 Geological map of Damodar River Basin.

The Damodar river basin contains a variety of rocks ranging from Archean to the recent age (Figure 2.2). The lower basin is characterized by alluvium soil lying over the solid rocks of the Cenozoic age. In the Damodar valley basins, the Archean basement is composed of quartzites, quartz-mica-schists, biotite-gneiss, and schist, garnetiferous gneiss and schist, acid granulites with hornblende, and amphibolites (Srivastava and Agnihotri 2013). Igneous intrusions, faults, and lineaments disturb the host rock at several places. Gondwana rocks consisting of sandstones, shales, and fire clays with coal seams compose the catchments of Tenughat, Panchet, and Durgapur Barrage. The Geological Formation of the Damodar basin is also associated with fire clay, bauxite, mica, and limestone. In the Damodar valley, the Gondwana sediments overlie the Chhotanagpur granite gneiss complex, exhibiting broad concordance with the regional structure of the surrounding basement. Its sedimentary sequences preserve about 200 Ma of the geological record. Phanerozoic sedimentation on the Neoproterozoic basement started

with the deposition of Late Carboniferous Gondwana sediments in Damodar valley basins. Table 2.1 presents the stratigraphic sequence of the Gondwana sediments of the Damodar valley (Raja Rao 1987).

Table 2.1 The stratigraphic succession of the Damodar Valley Basin (Raja Rao 1987).

Age		Damodar Valley Basins
Lower Cretaceous		Lamprophyre and dolerite intrusive
Jurassic	Upper	
	Middle	Non-Deposition
	Lower	
Upper Triassic	Rhaetic	Supra-Panchet Unit
	Noric	Infra-Norian erosional surface
	Carnic	
Lower Triassic		Panchet Formation
	Upper	Raniganj Formation
		Barren Measures
	Lower	Barakar Formation
Upper Carboniferous		Talchir Formation

The Talchir Formation formed during the early Permian and mainly has the glaciogenic nature of sedimentary deposits. The Barakar Formation, Barren Measure Formation, and the Raniganj Formation overlie the Talchir Formation consecutively, from bottom to top (Table 2.1). The Talchir Formation occurs as isolated patches in all the coalfields and has a conformable contact with the overlying sandstones of the Barakar Formation and unconformably overlies the Archaean granitic basement. The Talchir Formation is overlain by the Karharbari Formation, which is underlain by the Barakar Formation (Mukhopadhyay *et al.* 2010). Barakar Formation makes a conformable contact with the overlying ironstone-shale of the Barren Measures Formation. The Barakar Formation is well developed in all the coalfields of Damodar Valley and exhibits a variation in thickness from 300 m to 1200 m, while it has limited distribution in the subsidiary belt. The Jharia, East Bokaro, and South Karanpura coalfields have the thickest pile of Barakar rocks (Raja Rao 1987). The Barakar Formation is intruded by igneous intrusive (dykes and sills), which increased the rank of coals at numerous places in Jharia, Bokaro,

Chirimari, and in other coalfields (Chakraborty and Ghosh 2008; Sarana and Kar 2011). The topmost unit of the Lower Gondwana Group is the Raniganj Formation formed during Upper Permian. The Panchet Formation is the bottommost unit of the Upper Gondwana Group conformably overlies the Raniganj Formation, which is overlain by the Supra Panchet formation comprising coarse-grained sandstones and conglomerates. Soft-sediment deformation structures are present in both Upper and Lower Gondwana sediments (Chatterjee *et al.* 1990). An E-W trending major fault outlines the southern boundary of all the coalfields. There are several major and minor intra-basinal faults present in the area (Chakraborty *et al.* 2003b).

2.4 Geology of Karanpura basin

The Karanpura Coalfields form roughly an ellipsoid-shaped basin surrounded by the Precambrian metamorphic basement rocks. The Gondwana sediments have been deposited on a very uneven Archaean floor. It makes the largest patch of Gondwana situated at the western extremity of the Damodar basin. Geographically the area covers Latitudes 23°38' to 23°58' and Longitudes 84°46' to 85°28'. Karanpura basin is a combination of two basins, North Karanpura and South Karanpura. North Karanpura covers an area of about 1230. 24 km^2, falling in the Hazaribagh, Ranchi and Palamau districts of Jharkhand, while the South Karanpura coalfield is an elongated strip of about 194 km^2 in the south-east and falling in the Ramgarh district of Jharkhand state. The Karanpura basin forms the swollen core of the master sigmoidal basin formed by the Karanpura and Bokaro along with the minor outliers of Auranga and Hutar, whereas Bokaro and Hutar–Auranga basins represent the narrow extensions of the sigmoidal basin (Chakraborty *et al.* 2003b).

Table 2.2 Stratigraphic sequences of Formations in Karanpura Basin (Raja Rao 1987).

	Alluvium
	Dolerite and Mica Peridotite
Upper Gondwana	Mahadeva series-Fine grained sandstones of brick-red colour with subangular iron-stained pebbles.
----------Unconformity----------	
Lower Gondwana	Panchet series-Panchet sandstone, shale and clay of pink and green
	Damuda series:
	Raniganj stage-Sandstones and shales in association with calcareous sands. Few coal seams.
	Barren Measures-Light grey to blackish Ironstone shales and Micaceous shaly sandstones.
	Barakar stage-Sandstones, shales, and fireclay with inter-bedded coal seams.
	Karharbari stage-Gritty sandstones, shales, conglomerates, fireclay, and coal seams.
	Talchir series: Talchir stage-Olive green to greenish-yellow laminated shales, khaki-green fine sandstones, and boulder bed of green matrix. Two bands of varved clay in the Bachra, Ray, and Ghaghra areas.
----------Unconformity----------	
Archean	Metamorphics-Include a variety of schists and gneisses. Crystalline limestones occur as bands in quartz-schist and sericite-quartz-schist

Jowett (1925) provided the nomenclature for the northern part of Karanpura coalfield as the North Karanpura and the southern part as the South Karanpura coalfields, respectively, and this is in practice today. There are many interconnected basins of sediments in the coalfields, and the sediments rest unconformably on the Archaeans. The stratigraphic sequence of rocks that follows is based on the workers of the Geological Survey of India and their unpublished reports. It is only in the North Karanpura coalfield that a complete succession of rocks is traceable. The Formation such as Panchet and Mahadeva has not been recorded in the South Karanpura coalfield.

An East-West trending prominent fault zone marks the southern margin of the Karanpura basin with evidence of strike-slip movement. The northern margin also shows faults at places. The basin-fill strata have low dips and their outcrops grossly conform to the basin margins defining a synclinal structure with centripetal dips. The intra-basinal normal faults generally trend along NW–SE, while some of them have trended towards E–W.

2.5 About the South Karanpura

South Karanpura is situated in the Ramgarh district of Jharkhand state. The area is well connected with nearby places such as Ranchi, Patratu, Ramgarh, and Hazaribagh. National Highway No.33 running from Hazaribagh to Ranchi, is one of the easiest methods of accessibility to South Karanpura. The South Karanpura Coalfield lie between Latitudinal extent of 23° 30' N to 23° 45' N and Longitudinal extent of 85° 15' E to 85° 30' E.

2.6 Regional geology of South Karanpura

South Karanpura Coalfield is a semi-elliptical basin occupying sediments of Lower Gondwana deposited in a narrow, elongated trough during Permian. It is a part of the east-west aligned Damodar group of basins. This coalfield was first mapped by Williams (1852), a geological surveyor in the service of East India Company. Further several workers from the Geological Survey of India, Indian Bureau of Mines, Coal India Limited, etc., have added a significant contribution to the geological information of the area (Raja Rao 1957; Gokul *et al.* 1960; Banerjee 1963). The general strike of the beds is east-west, dipping southward on the northern side and northward on the southern side of the coalfield. Present mining activities are carried out in the Barka Sayal and Argada area of the South Karanpura coalfield. Coal seams belonging to the Barka Sayal area are thinner than the coal Seams present in the Argada area. The geological map of the area is given in Figure 2.3, and the lithological succession is described in Table 2.3 (after Raja Rao, 1987).

The lithological units present in different Formations occurring in South Karanpura coalfield are mentioned below:

2.6.1 Precambrian basement

The Precambrian basement rocks are composed of gneisses, granite, mica schist, quartzite, and few limestones. These are exposed all along the periphery of the area. The foliation is mainly WNW-ESE to East-West.

Table 2.3 Generalized stratigraphy of South Karanpura Coalfield (after Raja Rao, 1987).

Age	Formation	Lithology	Approximate thickness (m)
Early Cretaceous	Intrusive	Lamprophyre and dolerite dykes and sills.	
Late Permian	Raniganj	Fine-grained sandstones; grey, medium to coarse-grained, calcareous sandstones; mudstones; carbonaceous shale; a few thin coal seams	610
Middle Permian	Barren Measures	Medium-grained sandstone; siltstone; micaceous and carbonaceous shales; ironstone shales.	304-457
Early Permian	Barakar	Coarse-grained sandstone, shales; various economic coal seams	1053
Early Permian	Karharbari	Pebbly to coarse-grained sandstones, shales, and coal seams	74
Early Permian to Late Carboniferous	Talchir	Olive green shales/ green mudstones; fine to medium-grained sandstones; conglomerate; rhythmites and diamictites.	3-16
Precambrian	Basement	Granite, gneisses, mica schist, quartzite and limestone	

2.6.2 Talchir Formation

Talchir rocks comprising greenish shales and tillites conformably lie in the basement. The Talchir tillites are composed of angular to sub-angular pebbles of quartz, quartzite, or granite with the size of the pebbles varying up to 5 cm. Sporadic and lenticular occurrences of Talchir shales and sandstones are noticed along the fringes of the coalfield at the northern and eastern margins. A broad patch of Talchir Formation connects with the North Karanpura coalfield at the East of Hendegir. The thickness of this formation varies from 3 m to 16 m.

2.6.3 Karharbari Formation

The Karharbari Formation, with a pebbly to coarse-grained, dirty grey coloured sandstone rock type, conformably overlies the Talchir Formation. The formation attains a maximum thickness of about 74 m. This has been recognized in the Argada block and Gidi 'C' block present in the eastern and north-eastern parts of this coalfield, respectively. Intercalations with coal horizons of 0.61 m to 13.61 m have also been observed.

2.6.4 Barakar Formation

The Barakar is the main coal-bearing formation and covers a massive part of the coalfield. According to the stratigraphic order, it is above the Karharbari, but over the major part of the coalfield, it lies unconformably over the metamorphic basement. It conformably overlies the Karharbari Formation in the eastern and north-eastern parts of this coalfield, attaining a maximum thickness of 1053 m. Coarse-grained sandstone is dominant, whereas the lower part of the sequence is characterized by the presence of a pebble-bearing horizon. The middle portion of the Barakar Formation in South Karanpura coalfield is exceedingly rich in coal. The upper part of the Formation consists of fine-grained sandstone, siltstone, and shale.

2.6.5 Barren Measure Formation

The Barren Measure Formation having characteristic ironstone, shale, medium-grained sandstones, siltstones, micaceous shale, and carbonaceous shale is exposed in the central part of the coalfield. The Barren Measure forms a gradational contact with Barakar Formation. Outcrops of Barren Measures are found in streams and brook sections, where they consist of dark grey shales with bands of ironstone along with flaggy sandstone. The thickness of the Barren Measure Formation varies from 304 m to 457 m.

2.6.6 Raniganj Formation

The Raniganj Formation, existing in the south-central part of the coalfield and forming a conformable contact with the Barren Measure, attains a maximum thickness of 610 m. Fine-grained micaceous sandstones, micaceous flaggy sandstone, calcareous nodules, a thin bed of grey shales, and carbonaceous shales are the main lithological units present in this formation. The formation is truncated by a fault in the top part.

2.6.7 Igneous intrusive

Igneous intrusive such as mica-peridotite sills and dolerite dykes are present in this coalfield. Dolerite dykes are more common than mica-peridotite sills. Mica-peridotite exhibits porphyritic texture and consists of olivine, biotite, and alkali feldspar. Mica-peridotite sills are found affecting the several coal seams in the Argada and Sayal 'D' block of the area, whereas widely distributed dolerite dykes have minimal effect upon the strata in which they occur. Dolerite dykes exhibit ophitic texture and consist of labradorite, augite, and magnetite.

2.6.8 Structures

An ENW-WSW trending narrow ridge of metamorphic rocks separates South Karanpura coalfield from North Karanpura coalfield; however, a narrow path of Talchir rocks joins both coalfields at the western part. The northern, eastern, and western boundary of South Karanpura coalfield is normal, whereas the southern boundary is faulted. A metamorphic inlier is present in the eastern margin. Eleven out of seventeen faults deciphered in the area run parallel to one another with a general trend of NW-SE. Several faults present in the area, disturb coal seams in a few instances.

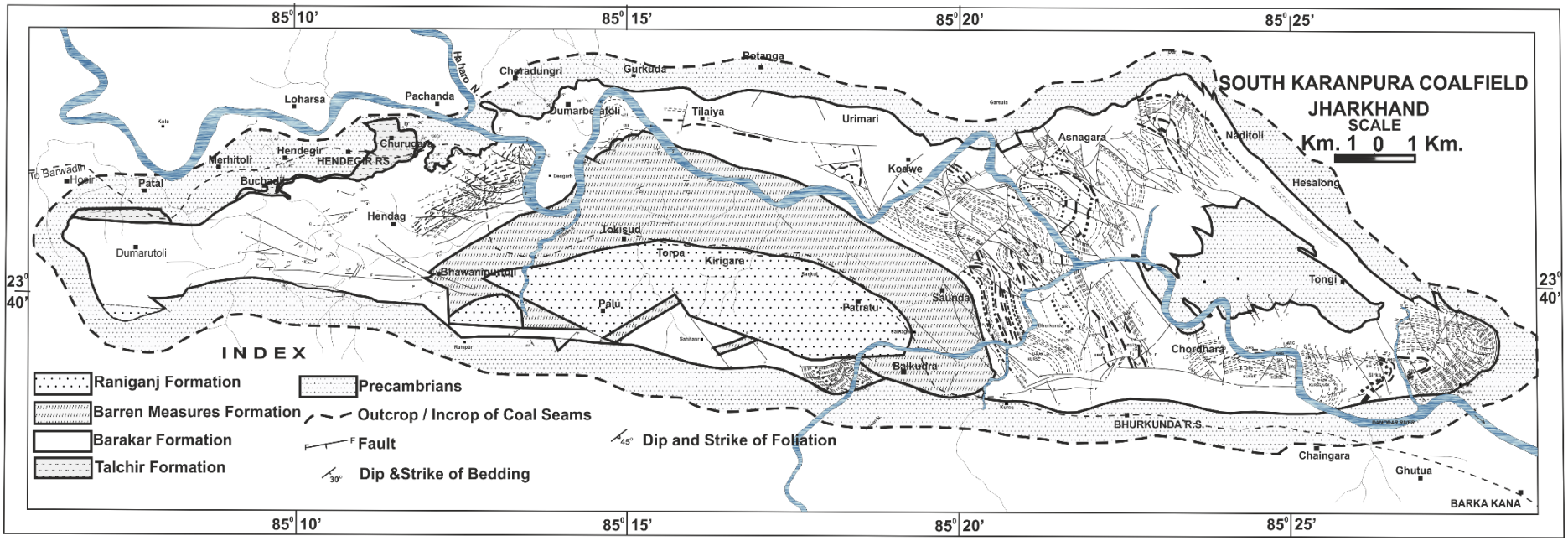


Figure 2.3 The geological map of South Karanpura Coalfield (after Raja Rao, 1987).

2.7 Location and communication of the study area

The area (South Karanpura coalfield), one of the most important coalfields of India, is situated in the western part of the Damodar valley and located in Ramgarh district of Jharkhand (Fig. 1.1). This coalfield covers an area of 194 km^2 bounded by latitudes 23°38'–23°45'N and longitudes 85°05'–85°28'E (Raja Rao, 1987). The area is well connected with the means of transport. The Barkakana railway junction is situated at the southeast edge of the field at a distance of 3.2 km. Two railway lines, Chandil-Barkakana and Gomoh-Barkakana, pass through the area. Besides this, road transport connects well the nearby cities such as Bokaro, Ramgarh, Hazaribagh, and Ranchi. Barkakana is connected with Bhurkunda, Argada, and Gidi by a well-maintained gravel road. Patratu, Bhurkunda, Saunda, Gidi, and Simratanr are important urban settlements.

2.8 Topography and drainage

South Karanpura coalfield is a plateau area having undulating topography and an average elevation of 335.28 meters. The highest point is 419 m, whereas the lowest point is 341 m above mean sea level. A few ridges are present near the metamorphic boundaries. Evergreen type forests cover the hilly terrain formed by isolated erosional remnants of Archean gneisses, whereas agricultural lands are located mainly in the plain areas.

Damodar River is the mainstream, which flows from north-west to south-east and passes through the vicinity of the coal mining areas with Nalkari River as its main tributary. Batuka and Haharo brooks join the Damodar River at the western boundary of this coalfield. Many small streams drain the area and discharge their loads into the Damodar River.

2.9 Climate

The climate of the area is tropical, and during summer, the temperature varies from 18°C to 45°C while during winter varies from 4°C to 24°C. The area receives annual rainfall precipitation of 1472 mm with significant seasonal variation (Kumar and Pandey 2013).

2.10 Vegetation

The eastern part of this coalfield has a few patches of forest, mostly having Sal trees, but the western part is covered with a thin growth of the forest. Sal and Mahua are the main trees, including some others in less amount such as Palas, Bair, Amla, Khair, Shimul, Karam, Sisir, etc.

2.11 Mode of Occurrence of Coal Seams in South Karanpura coalfield

2.11.1 Introduction

South Karanpura Coalfield exhibits a massive thickness of Lower Gondwana sediments. There are 42 coal seams reported from the area that can be correlated with each other. Some important seams are being exploited (Table 2.4).

Table 2.4 Location and name of the individual seam present in South Karanpura Coalfield.

Coalfield	Area	Name of the Seam	Location of the Seam
South Karanpura	Barka Sayal	Sayal	Sayal D underground (UG) mine
		Sayal Balkudra	Urimari opencast (OC) mine
		Upper Semana	Sirka opencast (OC) mine
		Lower Semana	Sirka opencast (OC) mine
		Hathidari	Bhurkunda underground (UG) mine
		Bansgarha	Bhurkunda underground (UG) mine
	Argada	Argada	Gidi A opencast (OC) mine
		Argada-A	Religara opencast (OC) mine
		Argada-B	Religara opencast (OC) mine
		Argada-C	Gidi C opencast (OC) mine
		Argada-D	Gidi C opencast (OC) mine
		Argada-I	Argada underground (UG) mine
		Argada-J	Argada underground (UG) mine

The thickness and the presence of these seams vary from place to place. Some seams are locally developed covering a very less regional extent hence can not be correlated. Field

photographs from the area are shown in Figure 2.4 and Figure 2.5. Figure 2.6 presents the geological map of South Karanpura coalfield, showing the locations of mapping.

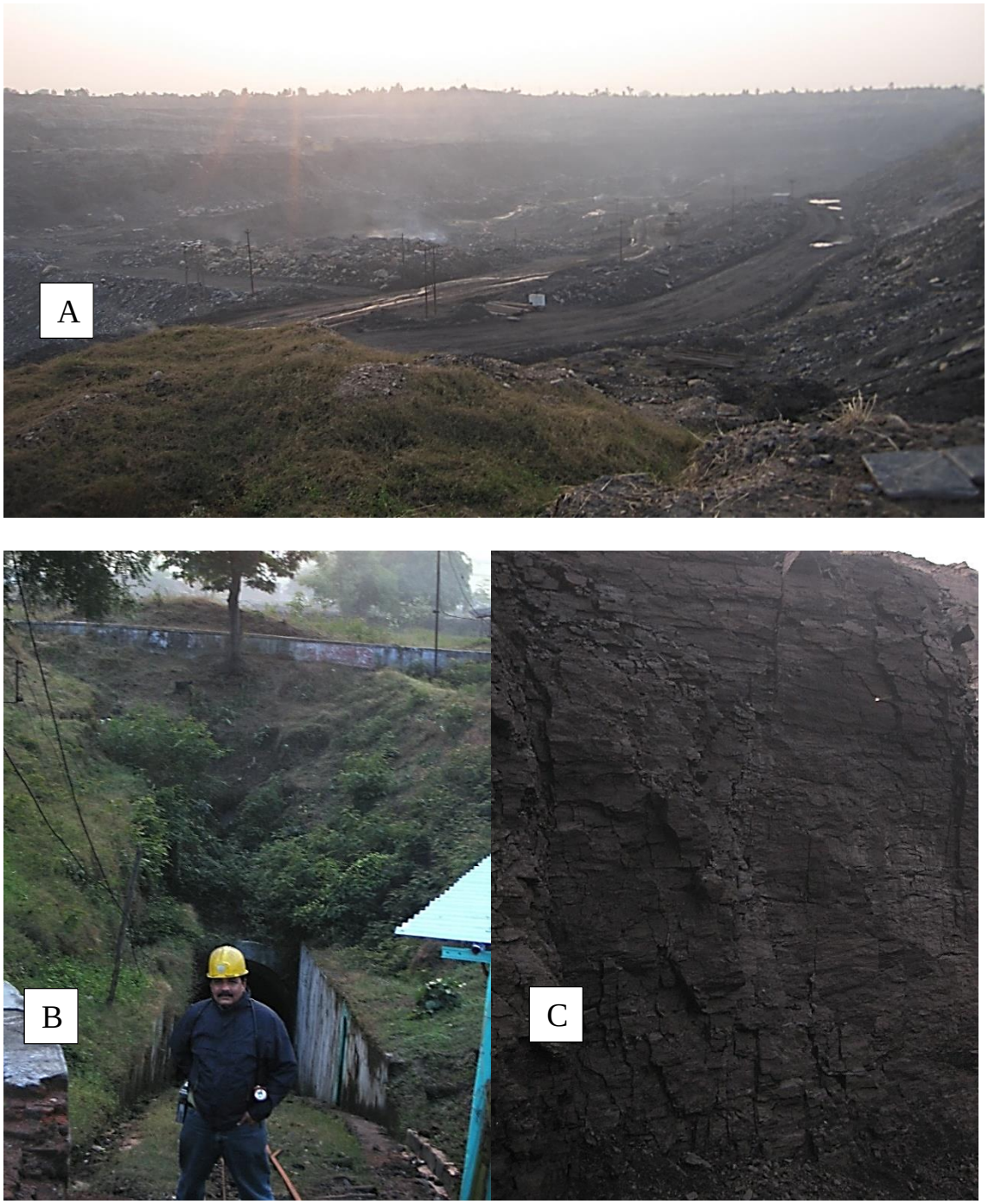


Figure 2.4 Field photographs showing A) Panoramic view of Bhurkunda colliery, Barka Sayal area, South Karanpura coalfield, B) Adit (entry point) of Argada underground mine. C) Coal seams showing banded nature, cleats, and fractures.

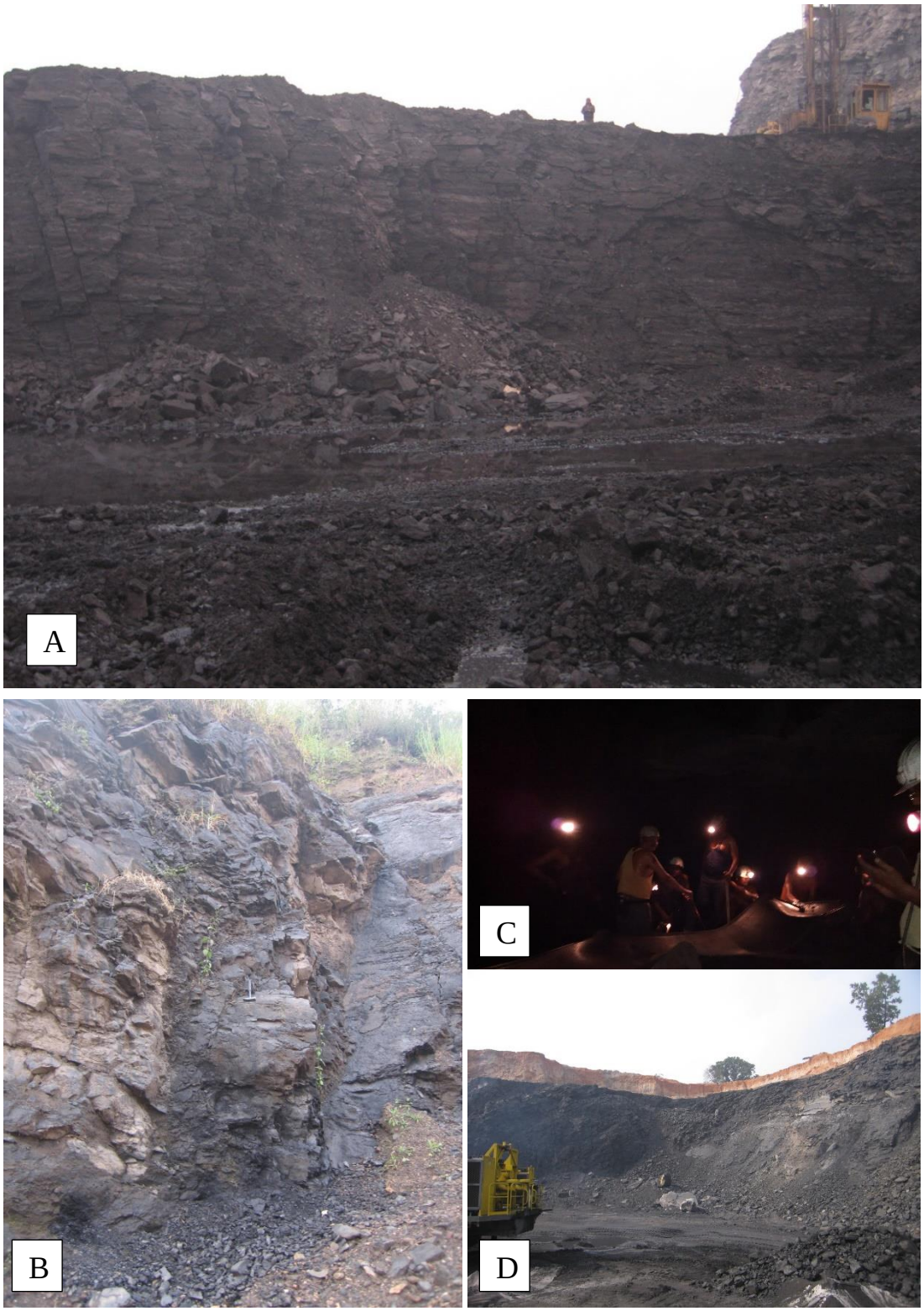
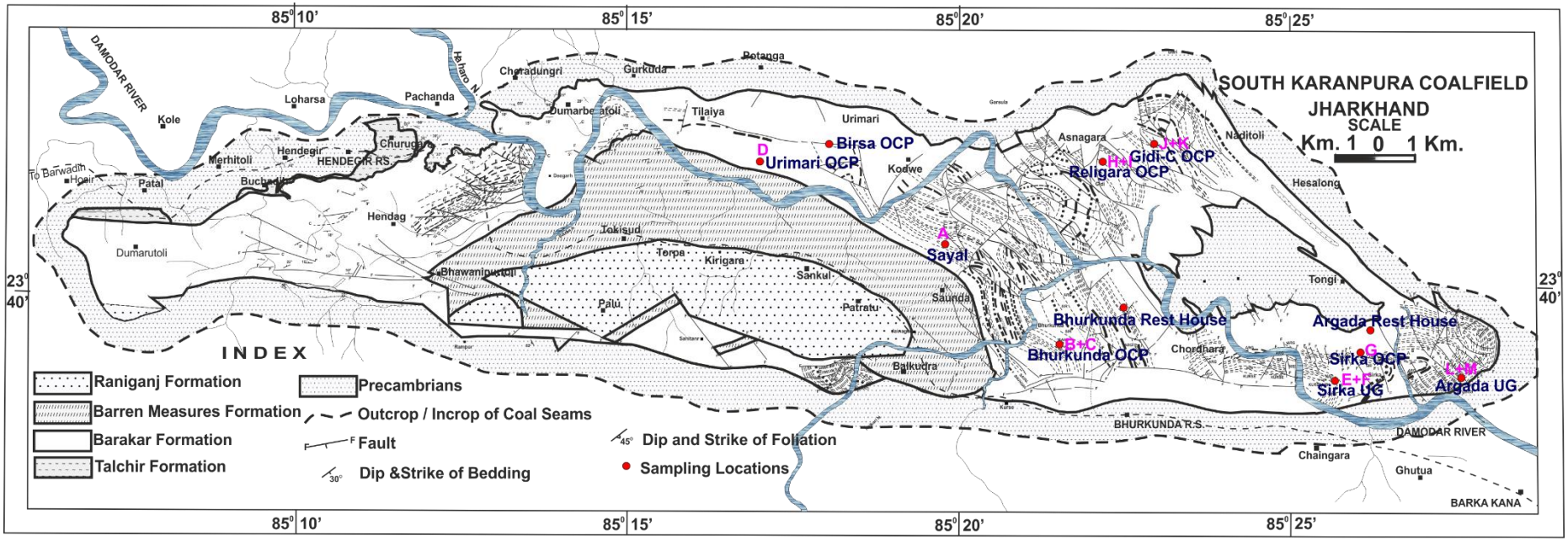


Figure 2.5 Field photographs showing A) open cast mine, parting bands, coal heaps and joints in seam present in the Gidi-C colliery, South Karanpura coalfield, B) An exposed coal seam, C) working conditions in the underground mine, and D) Bench of an open cast mine.



A- Sayal, B- Bansgarha, C- Hathidari, D- Sayal Balkudra, E- Upper Semana, F- Lower Semana, G- Argada, H- AG A, I- AG B, J- AG C, K- AG D, L- AG I, M- AG J

Figure 2.6 Geological map of South Karanpura coalfield showing sampling locations.

2.11.2 The regional occurrence of coal seams

The present mining activity in South Karanpura Coalfields is being carried out by Central Coalfields Limited (CCL), a subsidiary of Coal India Limited (CIL). For efficient administrative controls, Central Coalfield Limited has divided this coalfield into two areas: Barka Sayal and Argada.

The prominent coal seams belonging to the Barka Sayal area included for the present study are- the Sayal, Sayal Balkudra, Upper Semana, Lower Semana, Hathidari, and Bansgarha coals, whereas the important coal seams belonging to the Argada area are- the Argada, Argada-A, Argada-B, Argada-C, Argada-D, Argada-I, and Argada-J coals.

There are nine important underground (UG) and open cast (OC) collieries present in the Barka Sayal area. Coal seams have been collected from all the working coal seams of the Barka Sayal area. The important coal seams and their nature of exposure in these collieries are presented in Table 2.5.

Table 2.5 Collieries of Barka Sayal area with important coal seams present and their nature of exposure.

Colliery Name	Type of project	Coal seams exposed/present
Bhurkunda	OC+ UG	Argada (Sangram), Upper /Lower Sirka, Argada-A (OC) Upper Semana, Lower Semana, Upper Nakari, Lower Nakari, Hathidari, Bansgarha, (UG)
Saunda	UG	Hathidari, Bansgarha-C, Bansgarha, Argada-A
C. Saunda	UG	Bansgarha, Bansgarha C
Saunda D	OC+ UG	Saunda/ Lower Saunda/ Upper & Lower Sayal/ Upper and Lower Balkudra (OC) Argada (Sangram), Upper /Lower Sirka, Argada-A (UG)
Sayal D	UG	Upper Balkudra, Saunda, Sayal, Hathidari, Bansgarha, Semana-A
Urimari U/G (Sayal D)	UG	Hathidari, Bansgarha (UG)
Urimari	OC	Saunda, Balkudra/Sayal
N. Urimari (Birsa)	OC	Argada, Argada-A/Argada-B, Argada Top
Hindegir	UG	IV

The Barka Sayal area contains nine important collieries: Bhurkunda, Saunda, Central Saunda, Saunda D, Sayal D, Urimari Underground project, Urimari open cast project,

North Urimari/ Birsa, and Hindegir. This area comprises coal seams of a younger age than the Argada area. The Bhurkunda colliery has good exposure of the Upper Semana, Lower Semana, Upper Nakari, Lower Nakari, Hathidari, and Bansgarha coals. The latter coals are being exploited using underground mining methods while Upper Sirka and Lower Sirka coal seams are being exploited using the open cast mining method. The Saunda colliery has the Hathidari, Bansgarha C, and Bansgarha seams being exploited using underground methods. The Central Saunda underground mine has well-developed Bansgarha and Bansgarha C seam exposures. In the Saunda D colliery, the Saunda, Lower Saunda, Upper Sayal, and Lower Sayal seams are exposed at a shallow level and are exploited using the opencast technique while the Bansgarha, Semana A, Sirka, Upper Semana, and Lower Semana seams are being exploited using the underground mining method. Sayal D is an underground colliery and shows good development of most of the seams in the area, the major ones being the Upper Balkudra, Saunda, Sayal, Hathidari, Bansgarha, and Semana A seams. The Urimari underground project has exposed the Hathidari and Bansgarha seams, while the Urimari open cast project exploits the Saunda and Balkudra/Sayal seams. The Hindegir underground colliery covers an area of 5 km^2. and is present in the western part of the South Karanpura basin. The regional strike in the Barakar rocks present in the area is generally ENE-WSW and beds dipping at an angle of 12° to 14°.

The Argada area, with five important collieries in this area, is on the eastern side of the South Karanpura coalfield. Coal samples were collected from all the working coal seams of the Argada area following the pillar sampling method. The important coal seams and their nature of exposure in these collieries are presented in Table 2.6.

Table 2.6 Collieries of Argada area with important coal seams present and their nature of exposure.

Colliery Name	Type of Project	Coal seams exposed/present
Gidi A	OC	Argada, Argada-A, Argada-B
Religara	OC+UG	Argada, Argada-A, Argada-B, Argada-C&D, (OC), Argada-D (UG)
Gidi C	OC	Argada-A, Argada-B, Argada-C and D, Argada-L, M, N, O (Combined)
Argada	UG	Argada-K, Argada-J, Argada-I
Sirka	UG+OC	Up. Semana, Lr. Semana, Nakari, (UG) Argada, Argada-A, Sirka (OC)

The Argada area contains five collieries Gidi A opencast project, Religara combined project, Gidi C, Argada, and Sirka. Lower coal seams from Argada to Argada-T are present in this area. The present mining activities do not expose all of these seams. The Sirka colliery of this area, which is one of the oldest collieries, contains the Upper Semana, Lower Semana, Nakari, Argada, and Argada-A seams, whereas lower seams are expected at greater depth. The Argada, Argada-A, and Argada-B seams are well developed and exposed in the Gidi A colliery. The Religara colliery contains the Argada, Argada-A, Argada-B, and Argada-C&D coal seams exposed in open cast mines, whereas the Argada-D coal is exploited using the underground technique. The Gidi C colliery contains seams from the Argada to Argada-O, whereas the Argada underground mine contains only lower seams exposed at a greater depth such as Argada-I, Argada-J, and Argada-K.

2.11.2.1 Characteristics of coal seams of the Barka Sayal area

Sayal- The Sayal seam is well developed in the SW sector of the Bhurkunda Colliery and Jainagar Block. It got split into two sections in Central Saunda and Saunda ‘D’ Colliery, which coalesce again in Sayal ‘D’ block. The thickness of this seam varies from 5 to 10 m and attains its maximum thickness at Khas Karanpura Colliery and Urimari Block.

Sayal Balkudra- The Sayal Balkudra seam formed as the combination of the Upper Balkudra and Lower Balkudra seams at the Khas Karanpura Colliery. It is in the merged form in the Jainagar, Bhurkunda SW block, Central Saunda, Saunda 'A', Sayal 'D', and Urimari blocks. The thickness of the seam varies from 2 to 10 m.

Upper Semana- This seam attains its maximum thickness at the Sirka colliery and the Chordhara block (up to 9 m.). This seam is consistent in other blocks except for the Argada and Bhurkunda blocks, but the thickness varies from 2 to 5 m.

Lower Semana- Like the Upper Semana, this seam is also present in most of the blocks except the Argada block. The thickness of the seam is maximum in the Bhurkunda SW block (up to 6.5 m). The general thickness of the seam varies from 0.4 to 6 m.

Hathidari- The general thickness of the seam varies from 2 to 4 m. In the Jainagar block, the seam attains its maximum thickness up to 7.55 m, whereas in the Sayal-D block, it goes down to 0.33 m to 1.46 m thickness.

Bansgarha- The Bansgarha seam, also one of the consistent seams present in the area, is well developed in the Bhurkunda SW, Associated Karanpura, Khas Karanpura, Sayal-D, Gidi-A, and Urimari blocks. The thickness of the seam exceeds 4 m.

2.11.2.2 Characteristics of coal seams of the Argada area

Argada – The Argada seam is the thickest and most consistent seam of the entire coalfield. The average thickness of the seam varies from 15 to 25 m. It attains its maximum thickness in the Jainagar block (54.24 m.) whereas, in the Khas Karanpura, Saunda A, Gidi-A, Religara, and Urimari blocks its thickness reaches about 20 m.

Argada-A - This seam is well developed in the Sirka Colliery, Bhurkunda SW block, Central Saunda, Saunda-A, Associated Karanpura, Khas Karanpura, Sayal-A, Saunda-D, Gidi-A, Religara, Gidi-C, Urimari, and Jainagar blocks. In the Sirka colliery, the seam

attains its maximum thickness (16.4 to 31.27 m), whereas, in other parts, the thickness of the seam varies from 6.64 m to 16.64 m, with an average thickness of around 10 m.

Argada-B - This seam is well developed in the Argada, Central Saunda, Saunda-A, Associated Karanpura, Khas Karanpura, Sayal-A, Sayal-D, Gidi-A, Religara, Gidi-C, Urimari, and Jainagar blocks. The average thickness of the seam varies from 5 to 6 m and attains its maximum thickness of 10.06 m in the Jainagar block.

Argada-C - The seam has a localized development mainly in the Argada, Central Saunda, Saunda-A, Sayal-A, Gidi-A, Religara, Gidi-C, and Jainagar blocks. The thickness of the seam varies from 1 m to 4 m and attains its maximum thickness from 2.74 m to 4.26 m in the Central Saunda and Saunda blocks.

Argada-D - The thickness of the seam varies from 2.84 m to 8.61 m in the Central Saunda, Saunda-A, Sayal-A, Religara, Gidi-C, and Jainagar blocks, whereas in the Argada and Gidi-A blocks the seam thickness varies between 0.76 m and 6.27 m.

Argada-I - This seam has a localized development in the Argada, Gidi-A, and Gidi-C blocks. The thickness of the seam varies from 0.98 to 3.09 m in the Gidi-A block, whereas in the Argada and Gidi-C block, the thickness of the seam varies from 1.77 to 6.71 m.

Argada-J - This is a thin seam having a localized development in the Argada, Gidi-A, Religara, and Gidi-C blocks.

Besides these important coal seams, there are a few other coal seams also present in the area:- they were inaccessible, thus not included in this study.

3 CHAPTER 3. SAMPLING AND METHODS OF STUDY

3.1 Introduction

In the present study, all the major coal seams of the Barka Sayal and Argada area of the South Karanpura Coalfield have been included. The pillar coal samples were collected from all the working coal seams, from the open cast and underground mines. In aggregate, the coal samples were derived from seam sections located at distant places representing the entire coal occurrence of the South Karanpura coalfield of the Damodar Valley.

The collected coal samples were studied megascopically, and the macropetrographic coal seam profile of different sections was made. The individual megascopic bands were considered as one sample for different analyses. The coal petrography was carried out on the polished particulate mount, which includes the study of vitrinite reflectance and qualitative and quantitative evaluation of macerals, microlithotype, and mineral matter using white light as well as the fluorescence mode. The geochemical studies include proximate analysis, ultimate analysis, X-ray fluorescence (XRF), X-ray diffraction (XRD), Fourier transform infrared (FTIR) spectroscopy, Rock-Eval pyrolysis including total organic carbon (TOC) determination, and organic geochemical studies using Gas chromatography-mass spectroscopy (GC-MS).

The details of various analytical techniques used in the present study are described in the following sections.

3.2 Method of coal sampling

Sampling is the process of obtaining representative fractions of a bulk material that is required to be analyzed to identify the nature, composition, and other properties of coal. The implementation of an adequate sampling technique is essential for the interpretation

and reliability of the analyses (Stach *et al.* 1982). Coal is a heterogeneous material, making its sampling a complicated task. Coal sampling is mainly divided into two types. 1) *In situ* sampling and 2) *Ex situ* sampling (Thomas 2012). *In situ* coal samples are taken from exposed coal seam faces of underground or opencast mines, whereas *ex situ* coal samples are taken from coal transport containers or coal stockpiles. There are methods described for coal sampling in the various literature (Schopf 1960; Speight 2005a). The standards and guidelines for coal sampling also vary from country to country.

For the present study in situ sampling technique, the pillar sampling method was used. Samples were collected from all the working seams present in the South Karanpura coalfield belonging to the Barka Sayal and Argada areas. Samples were taken from bottom to top from coal seams exposed in the underground or opencast mines in such a way that if spread the samples in the laboratory, the entire thickness of the seam can be presented, and numbered accordingly. These samples were kept in airtight plastic bags.

The coal samples collected from different seams occurring in the Barka Sayal area/ Argada area were studied megascopically following Diessel's classification scheme (Diessel 1965). The coal samples were grouped according to their megascopic similarity in the form of a composite band. This led to the construction of the seam profiles.

3.3 Preparation of Coal Samples

3.3.1 Sample preparation for petrographic studies

For the petrographic study of all the coal samples collected from the working mines of South Karanpura coalfield, sample preparation was done systematically. Sample preparation for the petrographic study was done following the Indian standards IS 9127 (Part 2): 2002, which is similar to the standard ISO 7404-2: 1985.

3.3.1.1 Sample crushing

The coal samples collected from the field using the pillar sampling method were air-dried to remove the free moisture. A required amount (200 gm) is taken from each sample. The samples were crushed (upper size of 1 mm with a minimum production of fines) manually using mortar and pestle followed by sieving with 18 mesh (1000 microns) sieve, in small intervals to maintain the homogeneity of fine and coarse particles in the sample. Through coning and quartering, one-quarter of the sample was kept for petrography while the rest of the samples were processed for different geochemical analyses. The individual representative fractions of the <18-mesh sample (following the separation of the petrology sample) were crushed to 60 mesh (250 microns) and 72 mesh (212 microns) for Rock-Eval Pyrolysis and other geochemical analyses, respectively. Powdered samples were collected and stored in airtight glass bottles.

3.3.1.2 Embedding

The coal pellets were prepared from the -18 mesh fraction of all the samples for the microscopic study of these coals. To prepare a coal pellet, five gm of -18 mesh coal particle was mixed with 5 grams of cold settling hardener of GeoSyn make further poured with 10 ml of synthetic resin also of GeoSyn and mixed thoroughly until it made a semi-solid liquid to prevent settling and segregation of the grains. This mixture was passed into a silicon rubber mould of 2.5cm diameter and kept for a few hours at room temperature. No external pressure was applied in this process. After hardening, the specimens were taken out of the mould and properly marked to avoid confusion. Particles of coal were evenly dispersed with at least 60% of the cross-sectional area of the polished surface as coal.

3.3.1.3 Grinding

After the particulate mount (pellet) was prepared, the pellet was ground on a polishing machine to produce a smooth surface for measurement of vitrinite reflectance as well as quantitative and qualitative analysis of maceral, microlithotype, and mineral matter. The specimens were ground off on a rotating disk with 200 rotations per minute (rpm) fitted with different grit sizes (first coarser then finer) of abrasive silicon carbide paper using grinding and polishing machine. The same abrasive was used to grind off any irregularities on the surface of the specimen. A forceful jet of tap water was used thoroughly to wash the sample, silicon carbide paper, lap cloth, and the rotating disk after each stage of grinding and polishing to avoid scratches on samples.

3.3.1.4 Polishing

To prepare a smooth surface, two stages of polishing were done after the grinding on the high-speed rotating polishing machine. The first stage of polishing was done using magnesium carbonate (50 Microns) slurry on a blazer cloth. The second stage of polishing was carried out on velvet cloth using Alumina grade 3 (0.5-1 micron). After polishing, it was ensured that the polished surface was flat, relief-less, and free from pits and scratches.

3.3.2 Sample preparation for geochemical analyses

For the geochemical analysis, the coal samples were crushed using steel mortar and pastel. Nearly, 150 grams of sample was crushed to <60- and <72-mesh size. The coal powder was used for different geochemical analyses.

For Rock-Eval Pyrolysis, the samples were crushed to less than 60-mesh fragments and made free from moisture. These samples were directly subjected to pyrolysis.

For Fourier Transform Infrared Spectroscopy (FTIR) and Gas Chromatography-Mass Spectrometry (GC-MS), less than 72-mesh fragments of all the samples were further crushed into a very fine powder using an agate mortar and pestle.

For X-ray diffraction (XRD) and X-ray fluorescence (XRF) analyses, the crushed samples (<72 mesh) were converted into ash using low-temperature, as described in U.S. Geological Survey Circular 735 (Swanson & Huffman 1976). Each crushed sample was placed in a silica crucible in a muffle furnace. The temperature was gradually raised to 450 °C. After the evaporation of moisture and the burning of volatile matter, the temperature was gradually raised to 525 °C to complete the ashing process followed by occasional mixing of the coal present in the crucible to assure there is no unburnt organic matter remaining. Since XRD and XRF are mostly intended to identify the inorganic characteristics of the rock, hence only the prepared ash from the coal samples was subjected to these analyses, not the raw coal.

3.4 Methods of study

The characterization of coal under study was carried out with advanced and updated techniques and types of equipment. The methods used are as follows:

3.4.1 Petrographic study

The petrographic studies were employed to determine the macroscopic and microscopic properties of these coals. There are several standards available for the petrographic analysis of coal, which varies from country to country. Most of these standards follow the recommendations of the International Committee for Coal and Organic Petrology (ICCP).

3.4.1.1 Macroscopic petrographic study

The macroscopic petrographic analysis was the first analysis in which several lithotypes of coal were determined based on the bright and dull constituents. Lithotypes are

macroscopically identifiable units of coal. Based on the colour, lustre, texture, and type of stratification, humic coals have four lithotypes, vitrain, clarain, durain, and fusain. Vitrain and clarain are commonly called bright bands while durain and fusain are referred to as dull bands. The classification scheme for banded coal (Diessel 1965) was used for the macroscopic studies of these coals. The pillar samples collected from the coal seams present in the South Karanpura coalfield were spread on the laboratory floor and based on the proportions of its bright and dull constituents, it was categorized into several lithotypes. The samples having similar megascopic properties were kept in a single band, and their macro petrographic seam profile was constructed, showing the thickness, orientation, and type of lithotype present for all the coal seams.

3.4.1.2 Microscopic petrographic study

At the microscopic level, coal is composed of several organic and inorganic constituents. The organic microscopic entity of coal is called ‘maceral’. The association of macerals with macerals or mineral matter (<5%) is known as microlithotype. The maceral and mineral (5% to 60%) association at the microlithotype scale is called ‘carbominerite’. There are the prescribed methods of identification of macerals and microlithotype, which generally follows the recommendations of the ICCP. Microscopic analysis was done using a reflected light microscope, and the macerals were identified under immersion oil media with a refractive index of 1.518. The macerals were identified based on their relative reflectance, colour, size, and morphology. Their proportions are determined by a point count procedure. The microscopic organic constituents of coal (macerals) are categorized into three groups: vitrinite, liptinite, and inertinite.

3.4.1.2.1 Determination of maceral, maceral group, and visible mineral matter

Maceral analysis was performed using white incident light as well as under fluorescence mode using an advanced petrological microscope equipped with fluorescence microscopy

attachment, photometry for reflectance measurement and photographic unit in the Geology and Geochemistry Laboratory, Rajiv Gandhi Institute of Petroleum Technology, Jais, Amethi. An oil-immersion objective of 50x magnification and ocular of 10x magnification was used in this analysis with the help of an immersion oil of a refractive index of 1.518. The nomenclature and identification of the microscopic constituents (macerals) were made as per the recommendations of ICCP (International Committee for Coal and Organic Petrology 1963, 1975, 1998, 2001; Pickel *et al.* 2017), Stach et al. (1982) and Taylor et al. (1998). The quantitative assessment of the macerals was done using the stepping stage and software-controlled automatic point counter. With each step, from line to line and point to point, set to 400 microns, the complete particulate block was scanned, resulting in more than 1000 counts for an individual sample. The cross wires of the eyepiece were used as an observation point, and the maceral lying on the intersection of the crosswire was counted based on its group, specification, relative reflectance, colour, size, and morphology.

3.4.1.2.2 Determination of microlithotype and carbominerite

The microlithotype analysis was performed as per the recommendations of the ICCP (International Committee for Coal and Organic Petrology 1963, 1975, 1998, 2001; Pickel *et al.* 2017), Stach et al. (1982), and Taylor et al. (1998). The identification of a microlithotype was determined by the maceral or maceral groups occurring within an area of at least 50 µm x 50 µm and present in an amount equal to or exceeding 5 % by surface area. Hence, they can comprise a single maceral or maceral group if it exceeds these dimensions. Microlithotypes may include up to 20 % by volume of minerals such as argillaceous, carbonates, or siliceous minerals and up to 5% by volume of sulphide minerals. If the content of mineral matter exceeds these amounts, it is designated as minerite or carbominerite depending on the proportions of coal and mineral matter. A 20-

point graticule (Kotter's graticule) was fixed in the ocular of the petrological microscope used for the microlithotype analysis, where each square represents 5% area. The qualitative analysis of the microlithotype was performed simultaneously with the maceral analysis using the same instrument and keeping the line to line and point to point distance of 400 microns. For quantitative assessment of the microlithotype, a manual point counter was used. For each coal pellet, more than 600 points were counted.

3.4.1.2.3 Fluorescence Microscopy

Fluorescence microscopy was carried out using the same microscope, which was used for white light microscopy. Fluorescence characteristics of the macerals were observed using a fluorescence light attachment. The fluorescence occurs due to the phytopolymer inherited aromatic and phenolic compounds present in macerals, especially in the macerals of the liptinite group (Pradier *et al.* 1991). The fluorescence system consists of a blue excitation filter, dichroic mirror, and suppression filter. Routine maceral counting was made for reassuring the presence of fluorescent maceral.

3.4.1.2.4 Reflectance measurement

The vitrinite reflectance (VRo%) measurement was performed using the same microscope added with the photometry system. The random vitrinite reflectance (VRo%) measurement was carried out as per the ISO standard (ISO 7404-5 2009) on scratch-free collotelinite grains under monochromatic light of 546 nm. The standard used for the measurement was spinel having a reflectance value of 0.420, Yttrium-Aluminium-Garnet having a reflectance value of 0.902, and Gadolinium-Gallium-Garnet having a reflectance value of 1.715. A total of 100 measurements was taken for each particulate block covering the entire surface area.

3.4.2 Chemical analyses of coal

3.4.2.1 Proximate analysis

The proximate analysis of coal includes the determination of moisture, volatile matter, ash, and fixed carbon. The proximate analysis was carried out by following the Indian Standard (BIS 2003b). Proximate constituents are widely used for coal characterization and provide vital information for the selection of coal for industrial utilization.

3.4.2.1.1 Determination of moisture

Coal absorbs or loses moisture according to the humidity and temperature because of its hygroscopic nature. Moisture in coal may be present as adsorbed water on the external surface of coal or in the capillary of pores called free or accidental moisture. It is also present as combined water, as the water of hydration of inorganic constituents, as dissolved water resulting from the decomposition of an organic compound, distinguished as inherent moisture. Air-drying can remove the free moisture, but the removal of inherent moisture requires drying the crushed coal samples in an oven at 110°C for about an hour. The added amount of free and inherent moisture is called total moisture.

For the present study, the moisture content was analyzed using a glass dish, desiccator, and an air oven. At first, the weight of the glass dish was taken and noted as ‘A’. One gram of <72 mesh size air-dried coal sample was kept in the dish and spread uniformly. The combined weight of the dish and the sample was noted as ‘B’. The dish was kept in an air oven operating at a temperature of 110°C for one hour. The dish was brought out from the air oven and kept in a desiccator having some coarse dry silica gel filled in it. The final combined weight of the glass dish and sample after heating was noted as ‘C’. The weight loss was calculated as weight (wt.) percent (%) using the formula.

$$\text{Moisture (wt.\%)} = (\text{B} - \text{C})/(\text{B} - \text{A}) \times 100$$

3.4.2.1.2 Determination of ash yield

The residue, generally inorganic substances, left after the burning of coal is known as ash. The ash yield was determined using a silica crucible without the lid, desiccator, and a muffle furnace. The weight of the silica crucible without a lid was taken and noted as 'A'. One gram of <72 mesh size air-dried coal sample was kept in the crucible and spread uniformly. The combined weight of the crucible and the sample was noted as 'B'. The crucible was kept in a well-ventilated muffle furnace and heated for 30 minutes at a temperature of 500°C further; the temperature was ramped to 815±10°C, and the sample was heated for one more hour. The crucible was brought out from the muffle furnace and kept in a desiccator for cooling. The final combined weight of the crucible and sample residue after heating was noted as 'C'. The weight of the residue was determined and noted as wt. % using formula.

$$\text{Ash yield (wt.\%)} = (\text{C} - \text{A})/(\text{B} - \text{A}) \times 100$$

3.4.2.1.3 Determination of volatile matter

The volatile matter consists mainly of gases, water, and tarry vapours that evolved from coal when it is heated at high temperatures. The volatile matter was determined using a silica crucible with a lid, desiccator, and a muffle furnace. The weight of the silica crucible with lid was measured and noted as 'A'. One gram of <72-mesh size air-dried coal sample was kept in the crucible and spread uniformly. The combined weight of the crucible with lid and the sample was noted as 'B'. The closed lid crucible having a sample was kept in a muffle furnace and heated for 7 minutes in the absence of air at a temperature of 900±10°C. The crucible was brought out from the muffle furnace and allowed to cool in a desiccator. The final combined weight of the crucible with lid and sample after heating was noted as 'C'. The loss in weight of the heated sample was determined and noted as wt. % using below mentioned formula, which is the combined weight of moisture

and volatile matter. The content of volatile matter was determined by subtracting the previously calculated moisture content of the same sample.

$$\text{Volatile matter} + \text{Moisture (wt.\%)} = (\text{B} - \text{C})/(\text{B} - \text{A}) \times 100$$

Hence,

$$\text{Volatile matter (wt.\%)} = \left[\frac{\text{B} - \text{C}}{\text{B} - \text{A}} \times 100\right] - \text{Moisture (wt.\%)}$$

3.4.2.1.4 Calculation of fixed carbon

The fixed carbon is a calculated amount of nonvolatile material in a coal sample after subtracting the ash yield. The fixed carbon content shows a positive correlation with the rank of the coal. The amount of fixed carbon is calculated using following formula.

$$\text{Fixed carbon (wt.\%)} = 100 - [\text{Moisture (wt.\%)} + \text{Ash yield (wt.\%)} + \text{Volatile Matter (wt.\%)}]$$

3.4.2.2 Ultimate analysis

The ultimate analysis of these samples was carried out at the Sophisticated Analytical Instrument Facility (SAIF) laboratory, Central Drug Research Institute (CDRI), Lucknow. The Carbon, Hydrogen, Nitrogen, and Sulphur content of these coals were determined using Euro EA3000 Element Analyzer. The instrument mainly works as per ASTM D5373-08 (2008) in which combustion takes place in a catalytic tube in an oxygenated CO_2 atmosphere and high temperature. A non-reactive gas such as helium act as flushing and carrier gas while the combustion gases are made free from the mixing of foreign gases. The carbon, hydrogen, nitrogen, and sulphur components were separated from each other using a specific adsorption column and determined with the thermal conductive detector. The oxygen content was determined by subtracting the total content of carbon, hydrogen, nitrogen, and sulphur from 100.

3.4.2.3 Fourier transform infrared (FTIR) spectroscopy

The FTIR is a vital tool useful in understanding the structure/composition of organic and inorganic coal constituents. For FTIR analysis, samples were crushed into a very fine powder using an agate mortar. Representative coal samples were prepared by thoroughly mixing the samples having the same physicochemical properties, for each seam. The representative sample was divided into two fractions. One fraction was used as it is. The second fraction was converted to ash following low-temperature ashing techniques (Swanson & Huffman 1976) to identify the inorganic compounds present. The samples were analyzed with an FTIR spectrum and recorded in FTIR Spectrophotometer Perkin Elmer Spectrum under the ‘‘Attenuated Total Reflectance’’ (ATR) mode. PIKE MIRacle^{TM} ATR accessory equipped with ZnSe ATR crystal has been used for IR determination. A total of 20 scans were taken with a spectral resolution of 4 cm^{-1} at a range of 400 to 4000 cm^{-1}.

3.4.2.4 Gas chromatography-mass spectrometry (GC-MS)

To identify biomarkers, the extraction of coal was performed, starting with the powdering of the samples using a mortar into a very fine powder. The soluble organic matter was extracted with dichloromethane: methanol (9:1) mixture from oven-dried powdered samples by ultrasonication for 30 minutes. Subsequently, asphaltenes were removed by precipitation using an excess of n-hexane (40 ml). The fractionation was accomplished by passing the extract through a chromatography column containing activated silica gel using n-hexane (for saturates) and dichloromethane: hexane in the ratio 1:4 (for aromatic). The representative coal samples from all the coal seams were subjected to extraction of organic matter from coals. Fractionated samples were analysed with a combination of GC-MS. The GC was fitted with an HP–5MS fused silica capillary column (30 m×0.25 mm internal diameter, 0.25 µm film thickness), and helium (He) was used as the carrier gas at a flow rate of 1 ml/min. During each analysis, the GC oven temperature was held at an initial 40

°C for 5 minutes, and then ramped to 310 °C at 4 °C/min, which was held for a final 5.5 minutes. Full scan (m/z 50-550) 70 eV mass spectra were acquired with a source temperature of 300 °C. Data processing is done using Chemstation software. Peak assignments were based on GC retention time and mass spectral data, including a comparison to MS library and published mass spectra.

3.4.2.5 Rock-Eval pyrolysis

Rock-Eval pyrolysis has been widely used to identify the type and maturity of organic matter and to identify petroleum potential in sediments. For this process, the coal samples were crushed into fine powder less than 250 microns (60 mesh sieve). Crushed coal samples were analysed at Keshava Deva Malaviya Institute of Petroleum Exploration (KDMIPE), Dehradun, India, using the Rock-Eval 6 apparatus. Several authors have discussed the functionality and working principles of the Rock-Eval analyser (Espitalié *et al.* 1977; Horsfield *et al.* 1988; Lafargue *et al.* 1998).

For Rock-Eval pyrolysis, coal samples were kept in a vessel and progressively heated up to 650°C under an inert atmosphere (Helium). The hydrocarbons already present in the sample were escaped out at a moderate temperature of 350°C and recorded as S1 peak. The quantity of hydrocarbons generated from the thermal cracking of kerogen during heating at 350°C to 650°C was recorded as S2 peak. The CO_2 produced is noted as the S3 peak. Tmax denotes the temperature at the peak of S2 indicating maximum hydrocarbon generation during 350°C to 650°C.

3.4.2.6 Total organic carbon (TOC) determination

For the samples of South Karanpura coalfield, the Total Organic Carbon (TOC) usually having the unit as wt. % organic carbon per weight of dry rock (milligrams hydrocarbon per gram of rock) was determined through Rock-Eval pyrolysis.

3.4.2.7 X-ray fluorescence (XRF) analysis

XRF analysis was performed at Jawaharlal Nehru University, New Delhi. For this analysis, the representative coal samples were crushed and converted to low-temperature

ash following the recommendations by Swanson and Huffman (1976). The instrument works on a principle that an incoming X-Ray hits out an electron from one of the orbitals adjacent to the nucleus of an atom of the sample producing a hole in the orbit, resulting in an unstable configuration for the atom. To maintain equilibrium, an electron from higher energy states of outer orbital drops into the hole emitted excess energy in the form of a fluorescent X-Ray. The emitted fluorescent X-ray is the characteristic of any particular element making specific elements analysed.

3.4.2.8 X-ray diffraction (XRD) analysis

The XRD analysis was carried out at the Oil and Natural Gas Corporation (ONGC), Ahmedabad. XRD is a rapid and powerful method for phase determination of the crystalline material and mineralogical characterization of the coal. It is widely used for the identification of unknown crystalline materials. For XRD, the inorganic residue of the sample was prepared by following the low-temperature ashing technique (Swanson and Huffman 1976). XRD works on the principle of constructive interference between monochromatic X-rays and a crystalline sample. A cathode-ray tube generates X-rays, which get filtered to produce monochromatic radiation. The concentrated monochromatic radiation is directed toward the sample. The interaction of the incident X-rays with the sample produces diffracted rays characteristics to a particular lattice pattern. The law called Bragg's Law ($n\lambda=2d \sin \theta$) relates the wavelength of electromagnetic energy to the diffraction angle and the lattice space in a crystalline sample. These diffracted X-rays are then sensed and counted. By changing the 2θ angles, all possible diffraction directions of the lattice were determined. Conversion of the diffraction peaks to d-spacing permits the identification of the mineral containing a unique set of d-spacing. Standard reference patterns help in comparison to the d-spacing.

4 CHAPTER 4. COAL PETROGRAPHY

4.1 Introduction

The energy demand of the world is increasing day by day; fossil fuels are lacking to fulfill the requirements. Coal is generally utilized in thermal power generation, combustion, steel production, and chemical industries. Technological research leads to excessive use of coal as a raw material; hence their utility is unforeseen. In that case, the organic petrographic study reveals a better insight into the characteristics of the coal and provides useful information about its properties and suitability for various utilization. The biological and physicochemical processes working in swamps convert the plant debris into coal and determine its technological behaviour. The petrographical study of coal can trace these controlling processes. The branch of organic petrology, which has evolved from coal petrology, can also be used for basin analysis, fossil fuel resources exploration, and other multidisciplinary studies (Suárez-Ruiz *et al.* 2012). Coal is different from other rocks of the earth's crust due to its organic origin and complex nature, which makes its petrographic study complicated and challenging. Coal petrography is one of the important aspects of coal petrology, mainly dealing with the identification of macroscopic and microscopic constituents of coal to identify its inherent properties. Macroscopically coal may be characterized as banded or humic coal or non-banded or sapropelic coal. The macroscopic petrography mainly deals with the lithotype (macroscopically recognizable bands) present in coal, such as vitrain, clarain durain, and fusain. In contrast, microscopic petrography deals with the microscopic constituents of coals called macerals of organic origin and fine size minerals of inorganic origin. Microscopically, coals are made of numerous optically distinguishable entities that are derived from organic and inorganic natural materials. The organic fractions are the coalified remains of plant material, while

the mineral present in coal represents the inorganic fraction. Organic entities of coals are known as macerals, while inorganic entities are mineral matter.

4.2 History of Coal Microscopy

The microscopic study of coal was first started in the nineteenth century with the study of coal in a thin section (Witham 1831). Hutton (1833) published the first text material describing the cell structure of the coal. In 1870 with the identification of spore in coal, it was clear that terrestrial plants had acted as the precursor of coal. The origin of coal by White and Theissen in the form of a treatise was one of the important milestones having a thin section study of coal (White & Thiessen, 1913). The study of coal under transmitted light becomes popular in the USA and Europe after Theissen's microscopic study. Further contribution in this field was made by Seyler, Stach, Mackowsky, and Teichmüller. In 1925, Prof. E. Stach initiated the use of oil immersion objectives to identify the macerals of prepared coal blocks during microscopic studies of coal. Hoffmann and Jenkner (1932) had used the Berek photometer for the quantitative measurement of reflected light by vitrinite surfaces. This method was revolutionary in the field of coal microscopy and evolved the concept of coal rank with different reflectance values. The technique developed in the form of fluorescence microscopy helped to identify the hydrogen-rich microscopic constituents and provided criteria for maturity determination of low-rank coal (Schochardt 1936; Teichmüller & Wolf 1977). Significant contributions have been made by various authors (Ammosov & Ermakova 1950; Jacob 1964, 1974, 1952; Wolf 1966; Stach 1969; Gijzel 1971; Alpern *et al.* 1972; Ottenjann *et al.* 1974; Teichmüller 1974b; Preuss 1977; Alpern & Cheymol 1978; Robert 1979, 1980; Alpern 1980; von Jacob 1980; Hutton *et al.* 1980; Khorasani 1987; Murchison 1987b; Akande *et al.* 1992; Karayigit *et al.* 1998; Suggate 1998; Kruszewska 2003; Naeth *et al.* 2004; Ercegovac & Kostić 2006; López *et al.* 2008; Ojha *et al.* 2011; Valentim *et al.* 2013; Liu *et al.* 2019a;

Mirkowski & Jelonek 2019; Ndip *et al.* 2019; Chen *et al.* 2020). Several coal petrologists have used the new techniques of coal rank, fluorescence microscopy, and the study of coal blocks (Murchison 1987b; Misra 1992; Abdullah 1999; Hower *et al.* 2000; Cressler *et al.* 2010; Hackley *et al.* 2012; Friederich and van Leeuwen 2017).

Nowadays, fluorescence microscopy has become an essential tool for the hydrocarbon exploration program in the oil and gas industries. In India, these techniques have been used by various authors to understand the source rock characteristics and hydrocarbon potential of Permian and Cenozoic coals as well as lignite deposits (Singh and Singh 1996b, 2000, 2004; Singh 2002; Singh and Jha 2018a; Varma *et al.* 2018; Singh and Kumar 2020).

The International Committee for Coal and Organic Petrology was founded in 1951with objectives to secure the continuing international exchange of scientific information relating directly or indirectly to organic petrology and to develop and publish globally recognized and acceptable definitive descriptions and methods in the field of coal/organic petrology and petrography. The committee has formalized coal petrographic nomenclatures and published the International Handbook of Coal Petrography, its revisions, and supplements (International Committee for Coal and Organic Petrology 1963, 1975, 1998, 2001). The terms discussed in the book had formed the basis for different standards used in the field of coal science by different international organizations such as ISO, ASTM, BIS, etc. The committee had implemented the new worldwide definitions and nomenclature of microscopic constituents of coal under ICCP System 1994 (International Committee for Coal and Organic Petrology 1998, 2001; Sýkorová *et al.* 2005; Pickel *et al.* 2017).

Professor Erich Stach of Krefeld, Germany, is known as the founding father of modern Coal Petrology. In his Original book Lehrbuch der Kohlenpefro-graphie published in 1935, he emphasized the heterogeneity of coal using the study of polished sections and oil immersion objectives. The new edition was published in the English language in 1975, authored by E. Stach, M.Th. Mackowsky, and M. Teichmüller and R. Teichmüller, like the original textbook, it was profusely illustrated with excellent photomicrographs and diagrams. The book was a comprehensive survey of nearly all aspects of coal petrology and certainly filled an important gap in the fundamental scientific literature. Further, the third revised and enlarged edition was authored by E. Stach, M.Th. Mackowsky, M. Teichmüller, G. H. Taylor, D. Chandra, and R. Teichmüller, translated by D. G. Murchison, G. H. Taylor and F. Zierke in 1982 (Stach *et al.* 1982), was acted as a milestone in this field. In the year 1998, a new handbook named "Organic Petrology" incorporating some revised parts of Stach's Textbook of Coal Petrology was published by G.H. Taylor; M. Teichmüller; A. Davis; C.F.K. Diessel; R. Littke and P. Robert (Taylor *et al.* 1998). This book has filled the scientific gap of two decades in the field of organic petrology with additional information about petroleum. With time, several authors have published books and publications in the forms of journal articles adding significant contributions in the field (Teichmüller 1986; Speight 1995; Singh *et al.* 2008; Suárez-Ruiz and Crelling 2008; Ward and Suárez-Ruiz 2008; Flores *et al.* 2010; Hakimi *et al.* 2010; O'Keefe *et al.* 2011; Gürdal and Bozcu 2011; Richardson *et al.* 2012; Suárez-Ruiz *et al.* 2012; Valentine *et al.* 2013; Wang *et al.* 2013, 2016; Lakshmi *et al.* 2014; Blumenberg *et al.* 2015; Mani *et al.* 2015; Ribeiro *et al.* 2016; Sen 2016; Sen *et al.* 2016a; Dai *et al.* 2017; Teng *et al.* 2017; Dai and Finkelman 2018; Mastalerz *et al.* 2018; Ghassal *et al.* 2018; Małachowska *et al.* 2019; Misch *et al.* 2019; Ndip *et al.* 2019; Guo *et al.* 2019; Liu *et al.* 2019a; Qi *et al.* 2020).

4.3 History of Coal Petrography in India

Lomax (1911) had first reported the microscopic constituents of Indian coal. The systematic petrography of Indian coals belonging to Raniganj coalfield was reported by Fox (1926). Banerjee (1932) reported woody tissue present in Gondwana coals through a petrographic examination. The microstructural details of fusain from Gondwana coals were given by Chatterjee (1940). Ganju (1955) presented a systematic petrographic study of Indian coals using internationally recommended nomenclature. After the year 1950, the petrographic studies of Indian coals caught its pace and important contributions were made by early workers (Lahiri 1951; Lahiri and Basu 1952; Iyengar and Lahiri 1957; Chandra 1958, 1966; Mazumdar *et al.* 1959, 1962; Pareek 1964, 1966a, 1981; Ghosh 1964, 1969, 1971; Lahiri *et al.* 1968; Navale 1971, 1979; Lele and Chandra 1975; Ghosh *et al.* 1975; Navale and Misra 1980; Pareek and Bardhan 1985; Chandra and Chandra 1988; Chandra and Chakrabarti 1989; Misra *et al.* 1990; Rajarathnam *et al.* 1996). Due to the presence of abundant indigenous coal, the Indian coal had not drawn much attention for its systematic studies, and most of the prior studies were concentrated on mine development as well as for coal winning processes. With the raised requirement, systematic studies were implemented for several important coalfields of India. The workers have studied palynology, petrography, etc. of the coal and associated rock using petrographic techniques for different coalfields of India. Coalfields of Damodar river basins such as Jharia coalfield (Pareek 1964, 1966b; Verma *et al.* 1979; Mishra *et al.* 1990; Mishra and Cook 1992; Singh *et al.* 2013d, 2007, 2008; Mishra and Pandey 2011; Paul and Chatterjee 2011; Chatterjee and Paul 2013; Sen and Banerjee 2015), East and West Bokaro coalfield (Navale and Saxena 1989; Singh and Banerjee 2006; Mahesh *et al.* 2015b; Singh *et al.* 2015c; Tewari and Khan 2015; Bhowmick *et al.* 2017; Mendhe *et al.* 2017), North and South Karanpura coalfield (Venkatachala and Kar 1968; Mukherjee

and Arabinda 1969; Pareek 1986; Chakrabarti 1991; Singh 2000; Ali *et al.* 2017; Mendhe *et al.* 2017) and Raniganj coalfield (Ganju and Pant 1963; Navale and Saxena 1989; Hazra *et al.* 2016; Sen *et al.* 2016b; Acharyya 2019) also acquired the attention of the workers. Several authors have added significant contributions in the petrographic study of different other coalfields of India, Rajmahal coalfield (Singh and Singh 1995, 1998, 2011; Singh 2004; Singh *et al.* 2017b), Pench-Kanhan (Pareek *et al.* 1964; Pareek 1969a; Singh and Shukla 2004; Srivastava and Agnihotri 2013), Pathakhera (Nandgaonkar 1977), Mohpani (Chakraborty *et al.* 2003a), Sohagpur (Pareek 1987; Chakrabarti 1991), Singrauli (Pareek 1969b, 1970; Singh *et al.* 1987, 2014b; Singh and Navale 1989; Misra and Singh 1993), Chirimiri (Pattanaik *et al.* 2011), Lakhanpur (Kumar and Patel 2008), Korba (Singh and Singh 1991; Singh and Dwivedi 1994; Varma *et al.* 2013; Singh *et al.* 2016a), Wardha-valley (Pareek and Pande 1970), Talcher (Pareek 1963, 1986; Navale and Tiwari 1966; Navale and Srivastava 1969; Cheepurupalli *et al.* 2015; Singh 2016a, b), Ib-river valley (Pareek 1986; Singh *et al.* 2013e; Chakravarty *et al.* 2015). The coalfields of North-East India were evaluated by several workers using petrographic techniques (Ahmad 1971; Ahmed and Bharali 1984; Singh *et al.* 1992, 2013b, 2015a; Mishra 1992; Misra 1992; Ahmed 1996; Mishra and Ghosh 1996; Singh and Singh 2000, 2001, 2003, 2005, 2013; Phukan 2002; Nath 2005; Saikia 2009; Nayak *et al.* 2009; Dutta *et al.* 2011c; Sharma *et al.* 2014; Singh 2015, 2018). Some of the authors focused their study on low-rank coal (Misra and Singh 1994; Singh 2002, 2012; Singh *et al.* 2016b, 2017c, d, 2013a, 2016d; Paul *et al.* 2015; Singh and Kumar 2017, 2018, 2020; Kumar *et al.* 2019).

There are very few works available for petrographic studies of coal deposits of South Karanpura coalfield (Banerjee 1960; Pareek 1986; Chakrabarti 1991; Mahesh *et al.* 2015a; Singh and Jha 2018a, 2020). A glimpse of the petrographic information about South Karanpura coal comes from unpublished articles of the Geological Survey of India.

4.4 Present Work

The previous petrographic study of South Karanpura coals lacks systematic sampling techniques and the implementation of advanced petrographic equipment. The present investigation has been framed in such a way as to fill up the gaps of information, and an attempt has been made to carry out the petrographic study of coal deposits of South Karanpura coalfield on a regional scale employing modern techniques. In this connection, a large no of coal samples has been collected from all the working faces of open cast and underground coal mines and exposed faces of South Karanpura coalfield.

4.5 Megascopically recognizable constituents

Coal is a stratified mass of degraded plant material. The degradation is brought to the plant litter through the physical, biochemical, and dynamochemical processes of nature. These processes eventually convert plant material into megascopically distinct bands having variations in chemical composition. These megascopically recognizable ingredients can be further resolved into smaller microscopic units called 'Maceral'.

Coal is genetically classified into two broad groups as Sapropelic and Humic. Megascopically the Sapropelic coals are homogeneous and non-banded. They show dull or slightly greasy lustre and break with a conchoidal fracture. Depending upon the type of organic facies, the sapropelic coals can be resolved into two lithotypes, i.e., Cannel and Boghead. The cannel coals are rich in spore and pollen, while boghead coals contain abundant algal matter. The cannel coals are generally black with a black streak, whereas the boghead coals are slightly brown and produce a brown streak.

The humic coal is generally banded in nature. These bands represent variations in facies during the evolution of coal and differ in their physical properties, chemical composition, and maceral constitution. Several workers discussed and elaborated the

concept of the megascopic coal lithotype identification with the lithotype nomenclature (Stopes 1919; Thiessen and Sprunk 1935; Schopf 1960; Diessel 1965; Hower *et al.* 1990; Standards of Australia 1993; Larkin and Green 2012; Rusnak 2017). Stopes (1919) was the first to recognize and describe four fundamental banded ingredients of coal as vitrain, durain, clarain, and fusain. Later, Seyler (1954) designated these bands collectively as "lithotype". The minimum thickness for a band to be considered as a lithotype varies between 3 and 10 mm in different countries. In India, three millimeters (3 mm) are considered to be minimum thickness. As mentioned above, these bands differ significantly in their physical appearances such as colour, lustre, nature of stratification, and hardness. Table 4.1 presents a comparison of coal lithotype nomenclature.

Table 4.1 Comparison of coal lithotype nomenclature (modified after Rusnak 2017).

Stopes (1919)	Thiessen & Sprunk (1935)	Schopf (1960)	Diessel (1965)	Hower *et al.* (1990)	Standards of Australia (1993)	Larkin & Green (2012)	Rusnak (2017)	Associated Structure
Vitrain	Bright Coal	Bright	Bright (B)	Vitrain <10% Dull	C1 bright (B) <10% Dull	Bright (BR) <10% Dull	Bright Coal <10% Dull	Friable
Clarain	Semi-splint Coal	Moderately Bright	Banded Bright (Bb)	Bright Clarain 65-90% Bright	C2 Bright Banded (Bb) 60-90% Bright	Banded Bright coal (BB) 60-90% Bright	Banded Bright Coal 45-90% Bright	Semi-Blocky
		Midlustrous	Banded Coal	Clarain	C3 Interbanded	Interbanded (BD)	Banded Dull Coal 10-45% Bright	
Durain	Splint Coal	Moderately Dull	Banded Dull (Db)	Dull Clarain 10-35% Bright	C4 Dull w/minor bright (Db) 10-40% Bright	Banded Dull coal (DB) 10-40% Bright		Blocky
		Dull	Dull Coal (D)	Durain < 10% Bright	C5 Dull banded (Dmb) 1-10% Bright	Dull coal w/Minor Bright (DM) 1-10% Bright	Dull Coal <10% Bright	
					C6 Dull (D) <1% Bright	Dull (DD) <1% Bright		

Seams of humic coals have its banded nature because of the alternations of different layers present such as vitrain (bright bands), clarain (semi-bright bands), durain (dull bands), and fusain (mineral charcoal) as the macroscopically distinguishable coal bands (Figure

4.1). Vitrain and clarain are classified together as bright bands, whereas clarain and fusain are classified together as dull bands. These terms are described below in detail.



Figure 4.1 Different macroscopic bands present in banded humic coal. As per Diessel's classification scheme, the band will be 'Banded coal' having 40 to 60 % bright bands.

4.5.1 Vitrain

Vitrain is the brightest among the banded ingredients having vitreous lustre. Vitrain bands have black colour and very bright lustre. During mining, it produces fines breaking into cubes because of its brittle nature and the presence of fine cracks. The minimum thickness of this layer is 3 mm. The thicker bands exhibit conchoidal fracture. Humic coals contain widely distributed vitrain bands consisting of microlithotype mainly, vitrite and clarite-v. Vitrain is the dominant lithotype of all the coal seams of South Karanpura coalfield.

4.5.2 Clarain

Clarain bands are bright to semi-bright in appearance (lustre) and composed of alternate layers of bright (vitrain) and dull (durain and fusain) lustre. The thickness of individual

laminae remains less than 3 mm, but the clarain band's cumulative thickness should be more than 3 mm. Clarain has a silky lustre but does not have a conchoidal fracture. Clarain is frequently present in humic coals. At the microscopic level, clarain is composed of vitrite, clarite, durite, duroclarite, clarodurite, and fusite microlithotypes and the macerals forming these microlithotypes. In South Karanpura coals, this lithotype is also present in a good amount.

4.5.3 Durain

Durain bands have black or grey colour with the dullest appearance, and they exhibit irregular fracture and faintly greasy lustre for black durain. Its thickness is more than 3 mm. The bands having less than 3 mm thickness are recorded as clarain. Microscopically, durain is composed of the microlithotype durite and trimacerite with the occasional presence of liptinite-rich clarite. It is the hardest band and tends to break into large blocky fragments and is less frequently present than vitrain and clarain. Due to being dull in appearance, it looks, sometimes, like carbonaceous shale. In South Karanpura coals, a significant amount of durain bands are present. They are comparatively rich in the coals of the Argada area than the Barka Sayal area.

4.5.4 Fusain

Fusain resembles wood charcoal. It has silky lustre, black colour, and generally soft fibrous nature. It occurs as lenses of parallel orientation with coal seams and plays only a minor part of the entire seam. Fusain can be hard with fusite impregnated with mineral matter. It soils the hand. The presence of this band is indicative of fire horizons. Few bands of fusain have been observed in the coals of South Karanpura coalfield.

4.6 Macroscopic Description of Coal Seams of South Karanpura Coalfield

For the coals of South Karanpura Coalfield, lithotype names proposed by Diessel (1965) have been utilized because of their applicability for banded coals and the determination of lithotype based on bright and dull bands. The bright bands contain vitrain and clarain, while dull bands are composed of durain and fusain. According to Diessel's classification scheme, banded coal is divided into Bright coal, banded bright coal, banded coal, banded dull coal, and dull coal (Diessel, 1965) (Table 4.2). It is difficult to identify and differentiate these bands when the concentration of bright or dull components is nearer to the boundary line of two consecutive bands.

Table 4.2 The classification of Black coal lithotypes (after Diessel 1965).

Lithotype	Symbol	Description
Bright coal (vitrain)	B	Vitreous to subvitreous lustre; even to conchoidal fracture; brittle; may contain up to 10% dull coal in bands less than 5mm thick
Banded bright coal (clarain)	Bb	Mainly bright coal containing thin (less than 5 mm) dull coal bands ranging in proportion between 10 and 40%; even fracture
Banded coal (duroclarain)	BD	Contains bright and dull coal bands (all less than 5 mm) the ranging proportion between 40 and 60% each
Banded dull coal (clarodurain)	Db	Mainly dull coal containing thin (less than 5 mm) bright bands ranging in proportion between 10 and 40%; uneven fracture
Dull coal (durain)	D	Matt lustre and uneven fracture; may contain 10% of bright coal bands less than 5mm thick

All the bands have been recognized in the coals of South Karanpura coalfield (Figure 4.2 and Figure 4.3) (Table 4.3 and Table 4.4). The description of each band and their concentration in the coals of South Karanpura coalfield are undermentioned.

4.6.1 Bright coal

The bright coal band exhibits vitreous to sub-vitreous lustre and contains less than 10% dull component. These bands are brittle. The occurrence of bright coal is very less in the coals of South Karanpura, and its presence is only detected in the Lower Semana seam in the Barka Sayal area and Argada-A seam of the Argada area.

4.6.2 Banded bright coal

The bands have more than 60%, but less than 90% bright components are identified as Banded bright coal. These bands exhibit even fracture. South Karanpura coals have a moderate occurrence of banded bright coal. Coals of the Barka Sayal area have a comparatively higher occurrence of Banded bright coals than coals of the Argada area. This band constitutes 50% thickness of the Sayal Balkudra seam. In the coals of the Argada area, these bands are in low concentration and mark presence only in Argada and Argada-A seam.

4.6.3 Banded coal

Banded coal contains bright and dull coal bands (all less than 5 mm) ranging in proportion between 40% and 60% each. Banded coal is the dominant lithotype in the coals of South Karanpura coalfield. Its occurrence has been observed in both the area and in all the seams. The highest occurrence of this band is in the Bansgarha seam, where it constitutes 72% of the entire thickness of the seam. Its lowest concentration occurs in the Argada-I seam, where it covers only 11% of the entire thickness.

4.6.4 Banded dull coal

Banded dull coal is comparatively dull in appearance due to being rich in dull components varying between 60% and 90%. It is also a prime lithotype of South Karanprua coals. Its occurrence is higher in Argada coals compared to the coals of the Barka Sayal area. Its highest occurrence was observed in the coals of the Argada-I seam, where it covers 65% of the seam’s thickness. This band is absent in the Lower Semana and Bansgarha seam.

4.6.5 Dull coal

Dull coal is recognized by its dull appearance. It may only contain less than 10% bright component. Coals of the Argada area comparatively contain high concentration than coals

of the Barka Sayal area. In the case of coals of the Barka Sayal area, only the seam Upper Semana exhibit the presence of dull coal where it covers 20% of the seam's thickness. In the Argada area, all the seams contain dull coal bands. Its maximum concentration is observed in the coals of the Argada-A seam, where it covers 30% of the entire thickness of the seam.

4.7 Macroscopic Seam Profiles of South Karanpura Coalfield

Coal belonging to South Karanapura Coalfield is banded in nature. Banded coal is the most dominant lithotype and remains present throughout the seams. All the thirteen coal seams understudy of Barka Sayal as well as the Argada area exhibit a high thickness of banded coals. Thin layers of 'Bright coal' has also been observed in a few seams. As compared to the Barka Sayal area, the Argada area has thicker seams in which most of the thickness are being covered by banded coal and banded dull coal. Bright constituents are higher in all the coal seams of the Barka Sayal area compared to the coal seams of the Argada area, probably due to relatively dry, but with stagnant shallow water conditions, which helped the preservation of the woody plant material, and relatively high occurrence of bright constituents.

4.7.1 Coal seams of Barka Sayal area

Coal seams of the Barka Sayal area occur at relatively shallow depths. Sayal seam is the first exposed seam from the top, and Bansgarha is the bottom-most coal seam of the area. Sayal seam contains lithotypes such as - banded dull coal (12%), banded coal (53%), and banded bright coal (35%). It has a total exposed thickness of about 2.55 m. In this coals seam, Banded coal is the dominant lithotype and is present in the upper and lower part of the seam. Banded bright coal is present in the middle part of the seam. Banded dull coal is present at the bottom portion of the coal seam (Figure 4.2).

Table 4.3 Macropetrogrphic seam characteristics of Coals seams of the Barka Sayal area.

	Sayal		Sayal Balkudra		Upper Semana		Lower Semana		Hathidari		Bansgarha	
	Width (cm)	%	Width (cm)	%	Width (cm)	%	Width (cm)	%	Width (cm)	%	Width (cm)	%
Bright Coal		0		0		0	20	9		0		0
Banded Bright Coal	90	35	450	50	30	12	120	52	90	33	70	28
Banded Coal	135	53	200	22	125	50	90	39	135	49	180	72
Banded Dull Coal	30	12	250	28	45	18		0	50	18		0
Dull Coal		0		0	50	20		0		0		0
Shale/Claystone		0		0		0		0		0		0
Total	255	100	900	100	250	100	230	100	275	100	250	100

The exposed thickness of the Sayal Balkudra seam is 9 m. This seam also contains the same lithotype as the Sayal seam, but the thickness of the lithotype varies. In the Sayal Balkudra seam, banded bright coal is the dominant lithotype and covers about 50% of the total thickness while banded dull coal and banded coal covers about 28% and 22% of the total thickness, respectively. In this seam, banded bright coal occupies the top and bottom portion of the seam, while banded dull coal and banded coal are present in the center of the seam (Figure 4.2).

The exposed thickness of the Upper Semana is 2.5 m in which banded coal is the dominant lithotype (50%) followed by dull coal (20%) banded dull coal (18%), and banded bright coal (12%). Banded coal is present throughout the seam, while banded bright coal covers the bottom portion. Dull coal is present in the central portion of the seam (Figure 4.2).

The Lower Semana coal seam has an exposed thickness of 2.30 m. Banded bright coal covers 52% thickness of the entire seam. Banded coal (39%) is the second most dominant lithotype of this seam, followed by bright coal (9%). Banded coal is present at the top and bottom of the seam, whereas banded bright coal is present in the middle of the seam with some intercalation of bright coal and banded coal (Figure 4.2).

Hathidari coal seam has an exposed thickness of 2.75 m. The Banded coal covers about 49% of the total thickness of the seam, followed by banded bright coal (33%) and banded

dull coal (18%). Banded bright coal is present at the bottom and middle portion of the seam. Banded coal lithotype is present at the top portion of the seam, whereas banded dull coal is present near the bottom of the seam (Figure 4.2).

Banded coal is the most dominant lithotype of the Bansgarha seam and is present throughout the seam covering 72% of the total exposed thickness of 2.50 m. The remaining 28% of the seam is banded bright coal present in the central part (Figure 4.2).

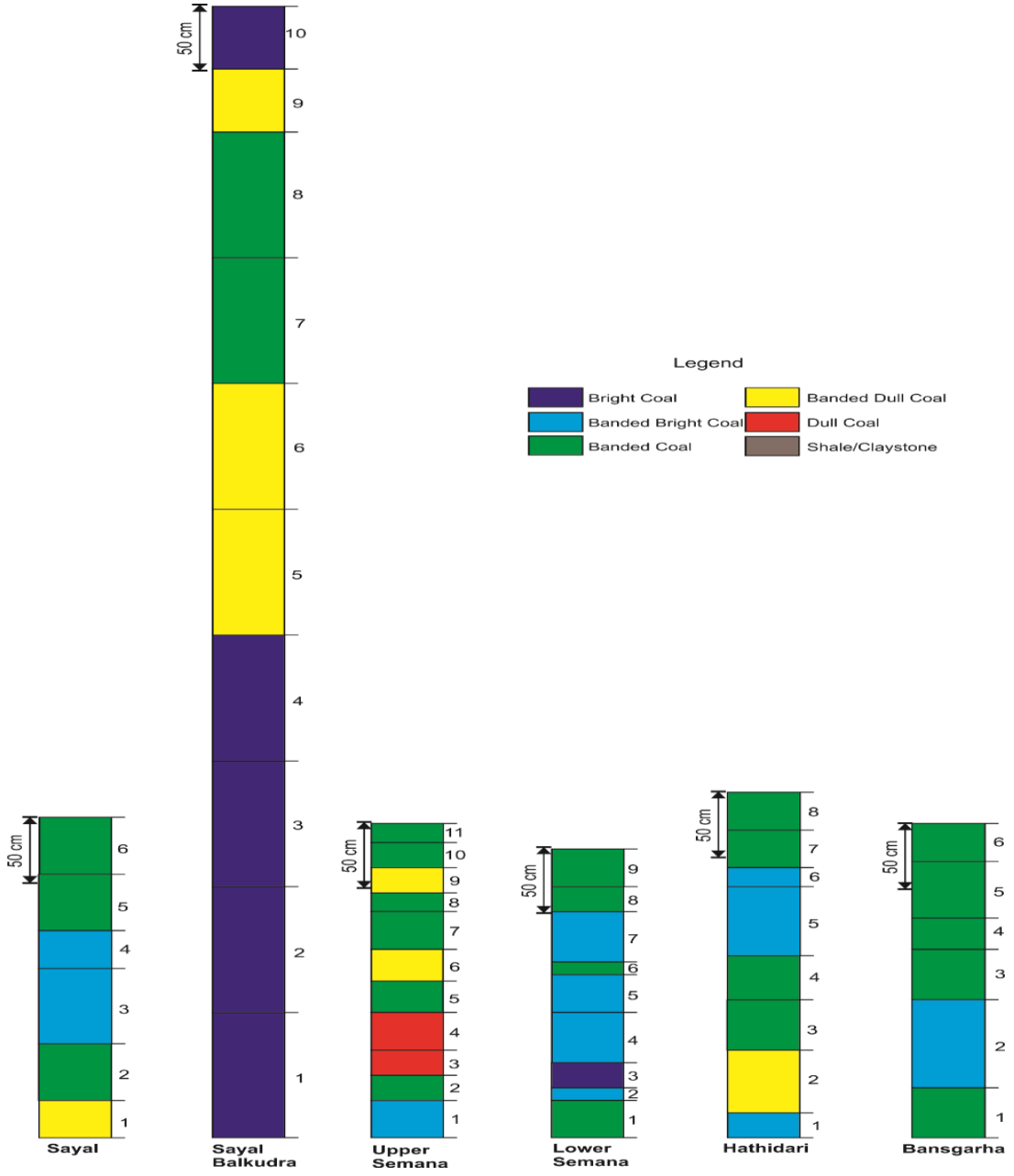


Figure 4.2 Macropetrographic seam profiles of coal seams of the Barka Sayal area.

4.7.2 Coal seams of Argada area

The coal seams present in the Argada area are thicker than the coal seams present in the Barka Sayal area. The seams of the Argada area occur at relatively deeper horizons than coal seams of the Barka Sayal area. Argada main seam has a total exposed thickness of about 10.50 m. Banded coal is the most dominant lithotype (33%) of this seam, followed by dull coal (26%), banded dull coal (21%), and banded bright coal (19%). Banded bright coal is concentrated at the bottom of the seam, whereas banded coal is present at the top of the seam. Dull coal is present near the top portion of the seam. Banded coal occupies thin layers throughout the complete seam and is available at the bottom, middle and top portions too (Figure 4.3).

The total exposed thickness of the Argada A seam is 7.60 m. Banded coal is the dominant lithotype of this seam and occupies 42% of the entire thickness. Dull coal covered 30% of the total thickness and was observed at the top and bottom parts of the seam. Banded dull coal is present in the central portion of the seam along with thin bands of shale, banded dull coal, and dull coal. Bright coal (3%) is present near the bottom of this seam with banded bright coal (13%) (Figure 4.3).

Argada B is having a total exposed thickness of 7.50 m in which most of the part is covered by banded dull coal (53%). Dull coal and banded coal covers 24% and 23% thickness respectively and remains present as a thin band in the bottom portion of the seam (Figure 4.3).

Banded coal is the most dominant lithotype of Argada C and covers 56% of the total thickness of 4.50 m. Banded dull coal is also present in a high amount (40%), whereas dull coal (4%) covers a very small portion of the seam. There is a rhythmic appearance of banded coal, and banded dull coal is present (Figure 4.3).

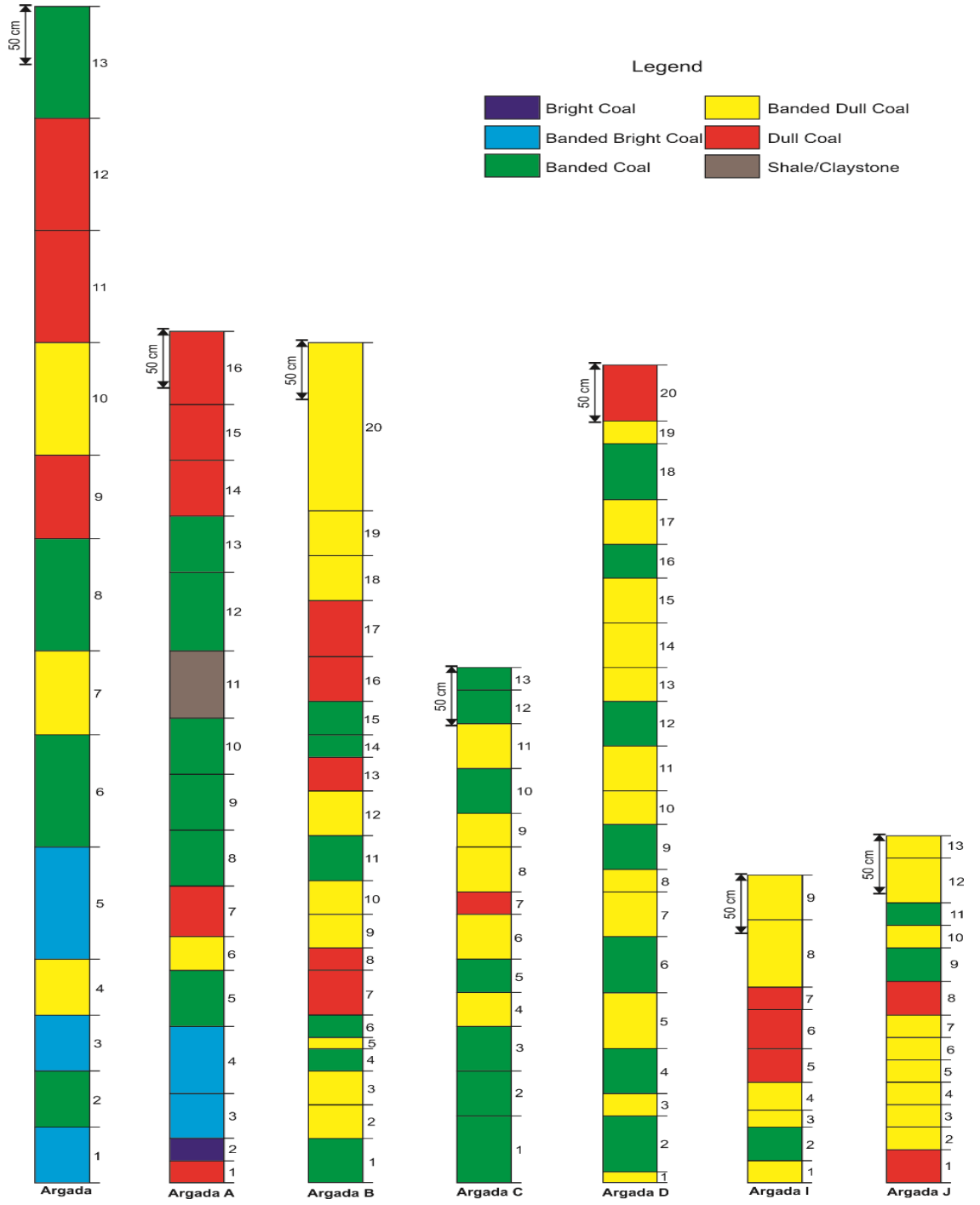


Figure 4.3 Macropetrographic seam profiles of coal seams of the Argada area.

Argada D shows an exposed thickness of 7.30 m in which banded dull coal is the dominant lithotype (52%) followed by banded coal (41%) and dull coal (7%). The seam shows an interband of banded coal and banded dull coal (Figure 4.3).

Argada I has a comparatively low thickness of 2.75 m. Banded dull coal (58%) is the most dominant lithotype of this seam, followed by dull coal (31%) and banded coal

(11%). Banded dull coal is present at the top and bottom portion of the seam, whereas dull coal occupies the central part. Banded coal is present near the bottom of this seam (Figure 4.3).

Argada J has a total thickness of 3.10 m, whose 65% is covered by banded dull coal. Dull coal and banded coal covers 19% and 16% of the thickness, respectively. Dull coal is present at the bottom of the seam, whereas banded dull coal is present at the top part of the seam. Thin layers of banded coal and dull coal occupy the central portion of the seam (Figure 4.3).

Table 4.4 Macropetrogrphic seam characteristics of Coals seams of the Argada area.

	Argada		**Argada-A**		**Argada-B**		**Argada-C**		**Argada-D**		**Argada-I**		**Argada-J**	
	Width (cm)	%	Width (cm)	%	Width (cm)	%	Width (cm)	%	Width (cm)	%	Width (cm)	%	Width (cm)	%
Bright Coal	0		20	3		0		0		0		0		0
Banded Bright Coal	200	19	100	13		0		0		0		0		0
Banded Coal	350	33	320	42	170	23	250	56	300	41	30	11	50	16
Banded Dull Coal	225	21	30	4	400	53	180	40	380	52	160	58	200	65
Dull Coal	275	26	230	30	180	24	20	4	50	7	85	31	60	19
Shale/Claystone	0		60	8		0		0		0		0		0
Total	1050	100	760	100	750	100	450	100	730	100	275	100	310	100

4.8 Microscopically recognizable constituents in coal seams of South Karanpura

The coal is heterogeneous because of its formation from a variety of plants and their organs and further varying degree of syngenetic and epigenetic modifications. The heterogeneity of coal can be perceptible by the naked eye, but a microscopic study of coal can reveal the coal constituents in detail. Analogous to minerals in rocks, coal contains macerals, the microscopic organic entity, as constituents of the coal. Apart from macerals, coals also contain a variable quantity of inorganic matter called mineral matter. To avoid the ambiguity in the microscopic study of coal throughout the world, the International Committee for Coal and Organic Petrology (ICCP) has established standards, rules and described the microscopic constituents present in coal. The present nomenclature scheme

prevailed is known as the "ICCP system 1994". International Committee for Coal and Organic Petrology (ICCP) in its 46th meeting in Oviedo (Spain) accepted the new set of drafts of definitions of the vitrinite group of macerals, which differ substantially from the Stopes Heerlen System (Stopes 1935) included in the 1963 edition of the International Handbook of Coal Petrology (International Committee for Coal and Organic Petrology 1963). In the new ICCP System 1994, the maceral group is defined based on reflectance, maceral subgroup based on the degree of destruction, while macerals are primarily categorized based on their morphology and/or degree of gelification (International Committee for Coal and Organic Petrology 1998) (Table 4.5).

Table 4.5 Subdivision of the maceral group vitrinite (International Committee for Coal and Organic Petrology 1998)

Subgroup	Maceral
Telovitrinite	Telinite Collotelinite (old term- telocollinite)
Detrovitinite	Vitrodetrinite Collodetrinite (old term- desmocollinite)
Gelovitrinite	Corpogelinite Gelinite (old term- gelocollinite)

Further members of ICCP published a classification system for huminite (Sýkorová *et al.* 2005), inertinite (International Committee for Coal and Organic Petrology & International Committee for Coal and Organic Petrology (ICCP) 2001) and liptinite (Pickel *et al.* 2017) and kept these under the ICCP system 1994. Besides the identifications of maceral and mineral matter, the constituents are also characterized as an association of two or more macerals called microlithotype and also as maceral-mineral associations called carbominerite. All microlithotypes bear the suffix "ite" to distinguish them from macerals, which bear the suffix "inite". An area of 50 × 50 μ is considered on the polished surface of coal perpendicular to the bedding plane for microlithotype analysis. It should also contain at least 5% of any maceral group. In addition to the

maceral content, 20–60 vol.% of silicate, carbonate, or argillaceous minerals or 5–20 vol.% sulfide minerals redefine the microlithotype as a carbominerite.

4.8.1 Maceral Analysis

Macerals are microscopically recognizable organic entities. The term ‘maceral’ was first used by Stopes (1935) for a constituent of coal isolated by the maceration process, i.e., selective oxidation treatment. The coals of South Karanpura coalfield constitute macerals of all the three groups’ vitrinite, liptinite, and inertinite. The qualitative and quantitative studies of the macerals and the associated minerals have been useful to know their quantitative variation along with the profiles of working coal seams of South Karanpura coalfield. The identification of macerals of the liptinite group has been performed both under white incident light as well as fluorescence mode, which made identification of the unstructured liptinite macerals such as bituminite, exsudatinite, and fluorinite possible. Besides the macerals, the qualitative and quantitative occurrence of mineral matter has also been recorded. The organic entities ‘macerals’ are characterized based on their morphology, hardness, colour, relief, internal structure, and reflectance. The macerals of one group show similarity in their chemical properties and technological behaviour but differ significantly from the maceral of other groups. Vitrinites formed by coalification products of humic substances originated from the lignin and cellulose of plant cell walls. Liptinites are derived from relatively hydrogen-rich plat remains such as sporopollenin, waxes, resins, and fats, whereas inertinites are derived from the transformation of the original plant substances. In the coal of a particular rank, vitrinites are comparatively rich in oxygen, liptinites in hydrogen, and inertinites in carbon (Ward and Suárez-Ruiz 2008). A comparison of the key characteristics of the three group macerals are presented in Table 4.6 (Osborne 2013).

Table 4.6 Comparison of key characteristics of group macerals (Osborne, 2013).

Characteristics	Vitrinite	Liptinite	Inertinite
Abundance	Major	Minor	Major, especially in the Southern hemisphere coals
Appearance in hand specimen	Bright, vitreous, or glassy	Resinous	Dull and dusty
Appearance under reflect light	Low to moderate and consistent reflectance	Relatively low in reflectance	Moderate to high and variable reflectance
Chemistry	Intermediate hydrogen content and volatile matter	Higher hydrogen content and volatile matter, more aliphatic	Lower hydrogen content and volatile matter, high carbon content
Reactivity during carbonisation	Reactive, principal reactive component of coking coals	Highly reactive	Inert

4.8.1.1 Vitrinite Group

The term Vitrinite has originated from the Latin word vitrum, meaning glass, and was first introduced by Stopes (1935). According to the new ICCP System, 1994 vitrinite group of macerals is defined as a group of macerals having grey colour and reflectance between inertinite and liptinite.

Due to geochemical gelification, open-textured different huminite macerals mix and form more or less homogeneous vitrinite. Table 4.7 presents a correlation of the huminite macerals of brown coals and lignites (ICCP 1971, 1975) with macerals of bituminous coals (ICCP 1971, 1975) and vitrinite classification by ICCP system 1994 (ICCP 1998). During peatification and coalification, the hydrolysable substances of plants such as disaccharides, starch, cellulose, hemicellulose, pentosans, pectins, and proteins get decomposed and form gaseous and liquid products such as carbon dioxide, ammonia, methane, and water, whereas remainder humic substances participate in the coal formation. Lignin-rich wood exhibits better preservation potential than cellulose-rich tissues of herbaceous plants.

Coals of the South Karanpura coalfield are generally vitrinite rich. All the macerals of the vitrinite group (telinite, collotelinite, vitrodetrinite, collodetrinite, gelinite, and corpogelinite) have been observed in these coals.

4.8.1.1.1 Telovitrinite

Telovitrinite term is derived from two Latin terms tela (means tissue) and vitrum (means glass). The ICCP introduced the term in 1994. This is a subgroup of the vitrinite group of macerals and represents vitrinites with preserved botanical cell structure, which may or may not be apparent in reflected white light. Telovitrinite comprises macerals telinite and collotelinite. Both of these macerals are distinct from their different degree of gelification (vitrinitization). Parenchymatous and woody tissues of roots, stems, barks, and leaves composed of cellulose and lignin originating from arborescent and herbaceous plants are responsible for the formation of these macerals. The dominance of these macerals indicates the excellent preservation of cell tissue under wet forested peatlands or forested wet raised bogs, which may have low-pH conditions.

Telinite

Telinite consists of clearly visible cell walls having intact plant tissue. The term telinite was first proposed by Jongmans & Koopmans (1933) for the vitrinite having visible cell structure. Telinite has originated from woody parts, leaves, and roots of the plants. It is commonly found in low-rank coal. It has variable size, shape, and openness of cell lumens mainly controlled by the original plant material, section orientation, and history of deformation. Colloidal masses, resins, or minerals can partly or totally fill the cell lumens of telinite.

Table 4.7 Correlation of the huminite macerals of brown coals and lignite (ICCP 1971, 1975) and (Sýkorová *et al.* 2005).

<table>
<tr><td colspan="4">Brown coal - lignite (ICCP 1971, 75)</td><td colspan="5">Brown coal - lignite</td></tr>
<tr><td>Maceral Group</td><td>Maceral Subgroup</td><td>Maceral</td><td>Maceral type</td><td>Maceral group</td><td>Maceral subgroup</td><td>Maceral</td><td>Maceral type</td><td>Maceral Variety</td></tr>
<tr><td rowspan="8">Huminite</td><td rowspan="3">Humotelinite</td><td rowspan="2">Textinite</td><td rowspan="2"></td><td rowspan="8">Huminite</td><td rowspan="3">Telohuminite</td><td rowspan="2">Textinite</td><td rowspan="2"></td><td>A (dark)</td></tr>
<tr><td>B (Light)</td></tr>
<tr><td>Ulminite</td><td>Textoulminite
Euulminite</td><td rowspan="2">Ulminite</td><td rowspan="2"></td><td>A (dark)</td></tr>
<tr><td></td><td></td><td>B (light)</td></tr>
<tr><td rowspan="3">Humocollinite</td><td>Gelinite</td><td>Levigelinite
Porigelinite</td><td rowspan="3">Gelohuminite</td><td>Gelinite</td><td>Levigelinite</td><td rowspan="3"></td></tr>
<tr><td></td><td></td><td></td><td></td><td>Porigelinite</td></tr>
<tr><td>Corpohuminite</td><td>Phlobaphinite
Pseudophlobaphinite</td><td>Corpohuminite</td><td>Phlobaphinite</td></tr>
<tr><td></td><td></td><td></td><td></td><td></td><td></td><td>Pseudophlobaphinite</td></tr>
<tr><td rowspan="2">Humodetrinite</td><td rowspan="2">Attrinite
Densinite</td><td rowspan="2"></td><td rowspan="2">Detrohuminite</td><td>Attrinite</td><td rowspan="2"></td><td rowspan="2"></td></tr>
<tr><td></td><td>Densinite</td></tr>
<tr><td colspan="9">transformation through maturation</td></tr>
</table>

Table 4.8 Correlation of the macerals of bituminous coals (ICCP 1971, 1975) and Vitrinite-94 (ICCP 1998).

<table>
<tr><td colspan="3">Bituminous coal (ICCP 1971, 75)</td><td colspan="3">Bituminous coal (ICCP 1994)</td></tr>
<tr><td>Maceral type</td><td>Maceral</td><td>Maceral group</td><td>Maceral</td><td>Maceral Subgroup</td><td>Maceral</td></tr>
<tr><td rowspan="2">Telinite1

Telinite2</td><td></td><td rowspan="5">Vitrinite</td><td>Telinite</td><td rowspan="2">Telovitrinite</td><td rowspan="5">Vitrinite</td></tr>
<tr><td>Telinite</td><td>Collotelinite</td></tr>
<tr><td>Telocollinite
Gelocollinite
Desmocollinite
Corpocollinite</td><td rowspan="2">Collinite</td><td>Corpogelinite</td><td rowspan="2">Gelovitrinite</td></tr>
<tr><td>Gelinite</td></tr>
<tr><td></td><td rowspan="2">Vitrodetrinite</td><td>Vitrodetrinite</td><td rowspan="2">Detrovitrinite</td></tr>
<tr><td colspan="2">Collodetrinite</td></tr>
<tr><td colspan="6">transformation through gelification</td></tr>
</table>

In South Karanpura coals, cell lumens of telinite are occasionally empty but usually closed by gelified swollen cell walls. Cell lumens are found to be filled with gelinite (Figure 4.4 A and B), resinite, micrinite, clay minerals (Figure 4.4 C), and carbonates. Its presence is scarce than collotelinite in coals of the study area. There are no characteristics differences in telinite present in the Barka Sayal area as well as in the Argada area.

Collotelinite

Collotelinite is a nearly structureless and homogeneous maceral of vitrinite group formed by the geochemical gelification (vitrinitization). Its reflectance value is used for the determination of the rank of coal or organic sediment. The term ‘collotelinite’ was introduced by ICCP introduced in the year 1994 for the vitrinite maceral devoid of any botanical structure. It is also derived from the woody parts, leaves, and roots of the plants. The collotelinite bands appear homogeneous due to the infilling of colloidal humic gel in the cell lumens to telinite. This maceral is most abundant in vitrain bands. It can also be

found in coaly shales. The reflectance of collotelinite acts as the rank parameter for coal as well as organic matter in sediments. It actively takes part in technological processes such as coal carbonization, liquefaction, etc.

In the coals of South Karanpura coalfield, collotelinite is found with disappeared primary structure (Figure 4.4 D, E, and F), containing few desiccation cracks. It is the most dominant maceral of the vitrinite group. Collotelinite occurs as thick and thin bands having grey colour in coals of the Barka Sayal area as well as in the Argada area.

4.8.1.1.2 Detrovitrinite

The term detrovitrinite has originated from two Latin terms detritus (means abrasion) and vitrum (means glass). The term was first introduced by ICCP in 1994 to denote particulate vitrinite materials. It indicates that macerals of this subgroup consist of finely fragmented vitrinitised vegetal relics occurring isolated or cemented by amorphous vitrinitic matter. The macerals vitrodetrinite and collodetrinite belong to this subgroup. The macerals of this subgroup also originate from cellulose or lignin-containing parenchymatous and woody tissues of roots, leaves, or stem originating from herbaceous and arborescent plants, but they suffer substantial decay which may be chemical decay or mechanical attrition. The high occurrence of these macerals indicates neutral or weakly alkaline and oxidizing conditions prevailed during peat formation (Diessel 1992). These are slightly darker in colour and lower in reflectance compared to the macerals of telovitrinite. During the combustion of medium rank coal, detrovitrinites form cenospheres, whereas, in carbonization, it is fusible.

Collodetrinite

This maceral seems as mottled vitrinitic groundmass formed by a mixture of vitrinite particles less than 10 μm. Collodetrinite lacks textural continuity and appears as irregular

patches with the less markedly layered perpendicular to the bedding. Its reflectance remains lower than collotelinite in coals having 0.5% to 1.4% VRo. With bituminization, these macerals may have variable fluorescence colour and intensity. They may originate due to substantial decomposition of cellulose-rich parenchymatous and woody tissues of roots, stems, and leaves at the beginning of the peat formation followed by cementing of small particles by humic colloids subsequently homogenized by geochemical gelification. It is the main constituent of the clarite band. Collodetrinite contains a high amount of volatile matter which degasses and contribute during technological processes such as carbonization or liquefaction.

In South Karanpura coals, it appears as amorphous vitrinitic groundmass binding other coal components and submicroscopic inorganic substances (Figure 4.4 G and H).

Vitrodetrinite

ICCP adopted the term vitrodetrinite in the year1970 for the maceral occurring as discrete vitrinite fragments of small size. It exhibits a size of less than 10 µm for rounded grains and 10 µm in the minimum direction for the fragments in thread form. The maceral becomes distinct when bounded by non-vitrinitic matter. The gelification of vitrodetrinite occurs either before the transportation and deposition or after sedimentation. Vitrodetrinite is derived by extensive comminution of parenchymatous and woody tissues of stems, roots, and leaves made up of cellulose and lignin. It commonly occurs in microlithotype vitrinertite and trimacerite such as clarodurite, duroclarite and vitrinertoliptite. Vitrodetrinite acts as a significant source for the generation of natural gas in the case of sedimentary rocks.

Coals of the Argada area have a significant concentration of vitrodetrinite (mean 4.07%) compared to the coals of the Barka Sayal area (mean 2.87%), which suggests that coals of the Argada area had suffered higher chemical decay or mechanical attrition.

4.8.1.1.3 Gelovitrinite

The term gelovitrinite is derived from two Latin terms gelu and vitrum, which means frost or stiffening and glass, respectively. ICCP introduced this term in 1994. These macerals originate by the gelification of humic solution derived from the decaying of plant cells as colloidal gels within voids or cavities and do not correspond to any particular plant tissue. Gelinite and corpogelinite are the macerals belonging to the subgroup of gelovitrinite.

Gelinite

ICCP adopted the term gelinite in 1994. Collinite or gelocollinite are the related terms to gelinite, which was previously used in the literature. Gelinite is a maceral of secondary origin consisting of structureless, homogenous infillings in cracks and voids occurring either as matrix embedding mylonitised coal particles or in cell cavities of funginite, fusinite, and semifusinite. It exhibits the lowest relief and often slightly higher reflectance than other vitrinites. It was formed by humic colloids during early diagenesis and precipitated as a colloidal gel (Figure 4.5 A and B). The occurrence of this maceral is rare and generally seen in the coals disturbed by tectonic activities during the early stages of coalification. Because of its rare occurrence, there is not any particular practical importance of this maceral, but acting like a maceral of vitrinite group, it actively takes part in technological processes.

Coals of both the area of the South Karanpura coalfield contain very less amount of gelinite.

Corpogelinite

Corpogelinite term is derived from two Latin terms corpus (means body) and gelu (means stiffening). The term ‘corpogelinite’ was adopted by ICCP in 1994. It is a maceral of subgroup gelovitrinite and group vitrinite. It exhibits a homogenous, structureless, and discrete body formed by humic cell infillings. It may occur isolated surrounded by fragmented bodies due to degradation of the inclosing plant tissue or may be found at its original place incorporated within telovitrinite. The size of the corpogelinite may go up to 300 microns (Soos 1963). It has a higher reflectance than other vitrinite macerals, possibly due to the oxidation of tannins (Stach *et al.* 1982). It generally exhibits a smooth outline with the variable shape of a sphere, oval or elongated depending on the orientation. Corpogelinite primarily originates from the secretion of the cell walls or the tannin in part. Secondarily, as gel precipitated from humic solutions during the early coalification stage. The related or previously used term for corpogelinite was phlobaphinite (Soos 1963) and corpocollinite in the case of brown coals.

Coals of the South Karanpura coalfield generally contain oval-shaped corpogelinite (Figure 4.5 C and D), but their occurrence is not high. There is no characteristic difference in the corpogelinite maceral present in the Barka Sayal as well as in the Argada area.

Dark Vitrinite

Dark vitrinite term was adopted by ICCP in 1994 for vitrinite exhibiting low reflectance and strong fluorescence compared to the normal vitrinite in the steam coal. The associated lipoid components are the reason for their lower reflectance. It generally appears in sapropelic coal (cannel and boghead) and few hydrogen-rich humic coals. It exhibits a dark grey colour under white incident light and possesses orange to dark brown colour fluorescence in UV irradiation. The fluorescence of dark vitrinite may be of primary or

secondary origin. First, it develops its fluorescence due to the inception of biopolymers in vitrinite, which decreases from the peat formation stage to the subbituminous stage and is taken over at 0.55 mean vitrinite reflectance. The secondary vitrinite fluorescence reaches a maximum at the high volatile bituminous stage at 0.8% mean vitrinite reflectance. This stage also indicates the second coalification jump where a lipoid substance in coal is adsorbed over the vitrinite macerals (Teichmüller & Teichmüller 1982). Because of having rich in lipoid substances and hydrogen content, dark vitrinite actively participates in the coal liquefaction process.

Some occurrences of dark vitrinite have been observed in the coals of the South Karanpura coalfield (Figure 4.5 E and F).

Pseudovitrinite

Pseudovitrinite is also derived from parenchymatous or woody tissues of barks, roots, stem, and leaves composed of cellulose and lignin and originating from herbaceous and arborescent plants. It is recognized by its higher reflectance than other macerals of the vitrinite group (approx. 0.05% higher) (Mastalerz *et al.* 2005) in the same coal. However, a change in reflectance varies with rank. In India, it is termed semivitrinite that indicates a transition stage between vitrinite and inertinite, thus having chemical and optical properties lying between the properties of vitrinite and inertinite. In the coking coal of India, The concentration of pseudovitrinite reaches up to 25% in Indian coking coals, which reduces the coking property of these coals. It may exhibit cell structure and generally have small slits known as comma slits. In the coals of South Karanpura coalfield, pseudovitrinite is found to have serrated margins of the fragment (Figure 4.5 G) and comma slits (Figure 4.5 H). Coals of the Barka Sayal area contain more Pseudovitrinite than coals of the Argada area.

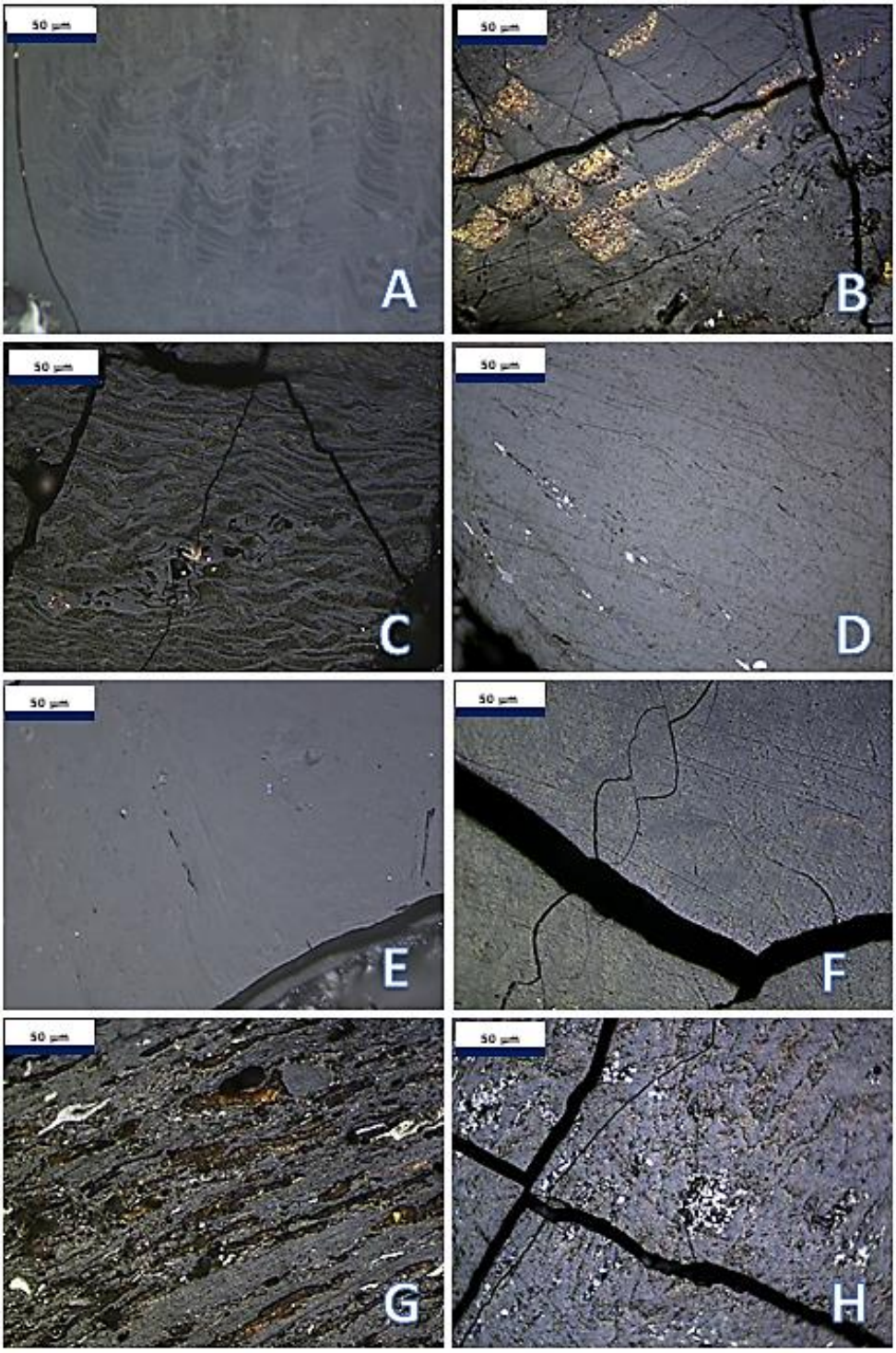


Figure 4.4 Representative photomicrographs of macerals, microlithotype, and mineral matter of South Karanpura coals (Polished surface, oil immersion, scale bar= 50 µm). The corresponding microlithotype name is provided in brackets. A) Gelinite filled in cell lumens of Telinite (Vitrite), B) Micrinite and corpogelinite filled in cell lumens of telinite (Vitrinertite V), C) Clay minerals filled in cell lumens (Clarite V), D) Collotelinite with inertodetrinite (Vitrite), E) Collotelinite Band (Vitrite), F) Collotelinite grain having crack filled with clay minerals, G) Collodetrinite with sporinite (Clarite V), H) Collodetrinite with micrinite (Vitrinertite V).

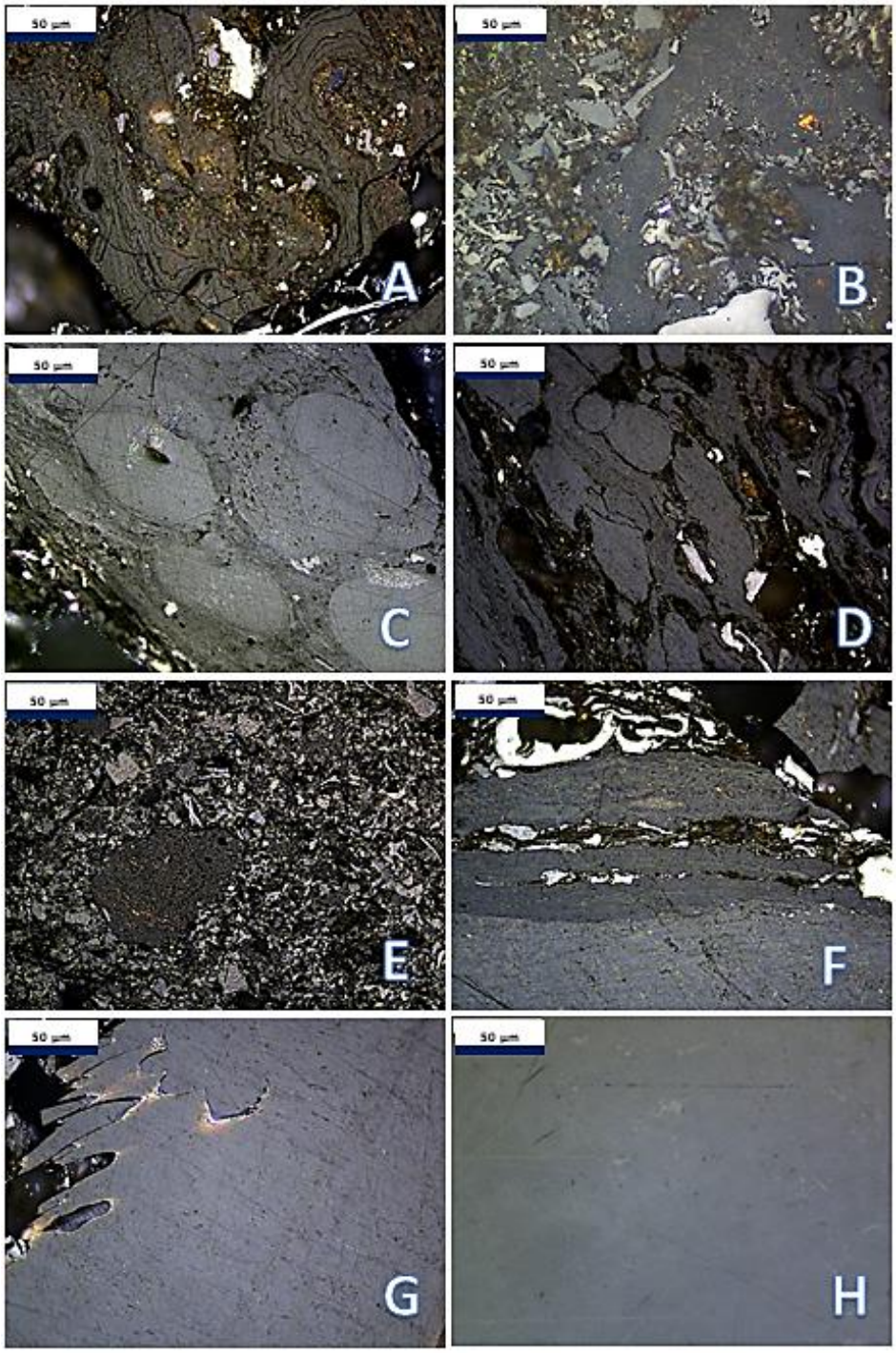


Figure 4.5 Representative photomicrographs of macerals, microlithotype, and mineral matter of South Karanpura coals (Polished surface, oil immersion, scale bar= 50 µm). The corresponding microlithotype name is provided in brackets. A) Gelinite with inertodetrinite and spores (Vitrinertite V), B) Gelinite grain with inertodetrinite (Vitrinertite V), C) Oval shaped corpogelinite (Vitrite), D) Oval shaped corpogelinite with sporinite (Clarite V), E) A dark vitrinite grain surrounded by other liptinite and inertinite macerals (Duroclarite), F) A band of dark vitrinite with collotelinite and sporinite (Duroclarite), G) Pseudovitrinite with serrated margin (Vitrite), H) Pseudovitrinite microband having comma slits (Vitrite).

4.8.1.2 Liptinite Group

The liptinite term was first introduced by Ammosov (1956) based on the Greek word 'Leiptos' meaning to remain or to leave behind because of the high perseveration and resistive nature of these macerals. The macerals belonging to the Liptinite group in the ICCP System 1994 are sporinite, cutinite, resinite, suberinite, exsudatinite, alginite, chlorophyllinite, liptodetrinite, and bituminite (Pickel *et al.* 2017). Liptinite is derived from non-humifiable plant matter remains relatively rich in hydrogens such as sporopollen, waxes, resins, and fats. The related term in the old literature was Exinite (Stopes 1935), which was used for the only outermost wall (skin as exine) occurring in coals. Later, Jongmanns *et al.* (1935) included coalified cuticles of leaf and the macerals derived from algae and resin in this group. However, Seyler (1932) had already used the terms resinite, alginite, sporinite, and cutinite for the macerals derived from resin, algae, spores, and cuticles, respectively. The macerals of liptinite are generally dark grey to black in reflected white light. However, the reflectance increases with increasing rank up to VRo% of about 1.3%, but fluorescence decreases. The fluorescence colour of liptinite macerals ranges from yellow (under blue light excitation) at low rank to orange at a higher rank. They are hydrogen-rich and contains more aliphatic constituents. Alginite has the highest ratio of aliphatic to aromatic components, followed by bituminite, resinite, cutinite, and sporinite. With the advancement of coalification, the identification of liptinite macerals becomes hard due to the converge of reflectance with that of vitrinite and loss in fluorescence property (Pradier *et al.* 1991). The liptinite macerals based on their morphology can be divided into two types, primary liptinite macerals having definite shape and morphology containing cutinite, resinite, suberinite, sporinite, alginite, and chlorophyllinite and secondary liptinite macerals exhibiting no particular structure containing bituminite, exsudatinite and fluorinite macerals (Table 4.9). These

unstructured macerals are understood to have generated during the first coalification jump at mean vitrinite reflectance of 0.5% (Teichmüller 1974b, a; Hutton 1987). It is hard to identify unstructured liptinite macerals under white incident light because of their similarity with argillaceous minerals, so blue light irradiation was used for the identification of these macerals in South Karanpura coals using their fluorescence properties (Teichmüller 1974b, a; Hutton 1987).

Table 4.9 Classification of Liptinite Group of Macerals (Pickel *et al.* 2017).

Maceral Group	Type	Maceral
Liptinite	Primary Liptinite Macerals	Cutinite
		Resinite
		Suberinite
		Sporinite
		Alginite
		Chlorophyllinite
	Secondary Liptinite Macerals	Liptodetrinite
		Fluorinite
		Bituminite
		Exsudatinite

4.8.1.2.1 Sporinite

Sporinite maceral arises from the exines and perines of plant spores and pollens (Seyler 1943). In low-rank coal, it attains its original shape and displays hollow, approximately rounded, triangular, or spindle shape. Guennel (1952) used the term 'miospore' for both microsporinite and pollen grains due to their close resemblance. The size of sporinite varies from 10 to 2000 µm. Based on the size, they are divided into two types, miospores or microsporinite of smaller size ranging from 20 to 180 microns (Figure 4.6 A and B) and megaspores of bigger size (Figure 4.6 C, D, E, and F) having a size greater than 200 microns. Megaspores typically show weaker fluorescence compared to miospores. Sporinite possesses rusty brown, dark grey or occasionally nearly black colour in coals of low rank. Sporinite may be thin-walled called tenuisporinite or may possess a thick wall called crassisporinite. Thin-walled tenuispores are characteristic of wet, arborescent

lycopod swamps, whereas thick-walled crassisporinite is characteristic of the relatively dry environment (Smith 1962). In high-rank coal, sporinite becomes light grey and gradually matches the colour of the vitrinite. Under blue-light radiation, sporinite gives fluorescence bright yellow to orange to brown which disappears at a rank of about 1.3% vitrinite reflectance. It occurs generally associated with bright layers of coal.

In the coals of the South Karanpura coalfield, the occurrence of sporinite is mainly characterized by their brown to black colour in reflected light and bright yellow fluorescence under blue light radiation (Figure 4.6 A, B, C, D, E, and F). It is the most dominant maceral of the liptinite group in these coals. There is no difference in the characteristics of sporinite belonging to both areas. Few occurrences of sporangium are also recorded in the coals of the study area (Figure 4.6 G and H). Crassispores are rarely present in these coals. A thick wall of the spore is designated as a protective cover against dehydration, hence the dominance of tenui type sporinite in these coals represent a relatively wet environment (Diessel 1992).

4.8.1.2.2 Cutinite

The term cutinite was first introduced by Stopes (1935) for the waxy cuticular coating on the epidermal tissues of leaves, stalks, shoots, needles, or thin stems. The maceral cutinite is formed by cuticles (skin) of leaves and stems. Its exhibit colour varying from dark grey to black under white light and fluorescence of yellow to orange under blue-light excitation. It seems as narrow bands with one-sided serrated margins when seen perpendicular to the stratification while except perpendicular plane, it can be confused with macrospores due to a similar look. Occasionally the underlying epidermal cells can also be observed. It occurs in clarite bands, and a large part of it mainly originates from leaves compared to stems. Based on size cutinite can be divided into two types

microcutinite having a size range of 20 to 180 microns and megacutinite having a size more than 200 microns.

In the coals of the study area, the presence of cutinite is not much high (mean approx. 0.4%). They are identifiable due to their serrated margin (Figure 4.7 A, B, C, D, E, and F) and brownish fluorescence under blue light irradiation (Figure 4.7 F).

4.8.1.2.3 Resinite

The term resinite was proposed by Stopes (1935) for oval, spherical, spindle-shaped resinous bodies produced by the metabolic activity of plants. It may occur as discrete bodies, diffused impregnations, or as infillings in cell cavities of telinite. It possesses black to dark grey colour in ordinary white light with shape varying from circular, oval to rod-shaped having frequently light grey coloured zoned structure sometimes containing gas bubbles. It may often show yellow or orange colour with red internal reflections. The fluorescence colour of resinite varies from yellow, orange to light brown under blue-light excitation with weaker fluorescence in the outer oxidation rim. Depending on the precursor of liptinite, resinites are divided into two types, terpene resinites formed from resins and lipid resinites formed from waxes. Lipid resinites do not show the form of plant cell lumina. The high concentration of resinite in the coal makes it a potential source of liquid hydrocarbons (Snowdon 1980; Snowdon and Powell 1982). It may also act as a source of various chemicals on a commercial scale (Teot 1982). Based on its observation in bituminous coal, Jones & Murchison (1963) categorised resinite into two types, primary resinite occurring as globular bodies and filling of cell cavities of telinite and secondary resinite occurring in interconnected globules and fractures exhibiting mobile phase due to increased temperature and pressure condition. Further, Teichmüller (1974b) characterized the mobile phase as a secondary liptinite maceral called exsudatinite.

Coals of the South Karanpura coalfield contain less resinite generally having rod shape (Figure 4.7G and H) and oval-shaped (Figure 4.8 A and B). Round to oval-shaped resinite of variable size is found in the coals of Barka Sayal as well as the Argada area, as isolated bodies or as in situ cell fillings. They are dark grey to black under white light but show greenish-yellow colour under fluorescence light.

4.8.1.2.4 Suberinite

Suberinite is a maceral of the liptinite group mainly derived from coalified cell walls. In reflected light, it appears medium to dark grey or almost black. In blue-light excitation, the fluorescence colour may be lemon-yellow to yellow-orange and brown. It displays more or less rectangular, brick-like, or patterns of an irregular polygon. Suberinite often appears together with corpogelinite (Figure 4.8 C and D). It originates due to the suberinization process in which suberin lamellae are formed after injury in the bark, roots, and fruits of plants as wound tissue. Suberinite commonly occurs in Cenozoic brown coal but is rarely present in Mesozoic coals and is unknown from Carboniferous coals (Teichmüller 1989). Similarly, suberinite is rarely present in the coals of the study area.

4.8.1.2.5 Alginite

Alginite is the maceral of algal origin. The term alginite was first introduced by Hevia Rodríguez (1953). Based on morphology Hutton *et al.* (1980) categorized alginite as alginite A and alginite B, which was further termed as telalginite and lamalginite, respectively, by Cook (1982). Telalginite commonly shows its botanical structure, appears dark in reflected white light and occurs as discrete lenses, flattened disks, or fan-shaped masses (Figure 4.8 E and F). It has a high fluorescence intensity (Figure 4.8 F). It can originate from lipid-rich algae such as *Tasmanites* and *Gloeocapsomorpha* in a marine environment or from *Botryococcus* and related forms in a non-marine environment. Lamalginite occurs as thin lamellae (<5 μm) and having a less lateral extent

(<80 µm). It is derived from smaller algae and generally does not exhibit botanical structures. It can originate from *Acritarchs* and *Dinoflagellates* in the marine environment and *Pediastrum* in a lacustrine environment. Both types of alginite have a high content of hydrogen mainly dominated by aliphatic compounds. Because of high H/C ratios, alginite gives a high yield of hydrocarbon during pyrolysis. Coals rich in alginite are also suitable for coal liquefaction. Some of the algae are also indicative of paleoenvironments. Such as the presence of Tasmanites indicates a marine paleoenvironment, whereas *Botryococcus* generally indicate a lacustrine environment while Pediastrum is an indicator of freshwater paleoenvironment.

Coals of the South Karanpura coalfield rarely contain alginite. Its presence was only recognized near the top portion of the Sayal Balkudra coal seam, which may be an indicator of marine influence in that part (Figure 4.8 E and F).

4.8.1.2.6 Bituminite

The term bituminite was first defined by (Teichmüller 1974b) for an unfigured autochthonous maceral of the liptinite group, occurring in petroleum source rocks. The ICCP introduced this term in 1975. Bituminite is a structure-less maceral of the liptinite group. It may have a close association with minerals giving rise to internal reflection in white reflected light. It is derived from the degradation of algae, faunal plankton, bacterial bodies, and bodies of higher animals in anoxic to suboxic conditions. It is a characteristic maceral of many oil source rocks. The name bituminite indicates the bituminous character of this maceral, which gives high yields of bitumen, hydrocarbons, tar, and volatile matter (Powell *et al.* 1982). Cook (1981) indicates the origin of bituminite from the degradation of higher plants or algae and occurs in amorphous and lamellar forms.

In the South Karanpura coals, it is present in very less amount. It appears dark grey, brown to black in white reflected light (Figure 4.8 G), and shows a varying degree of

fluorescence intensities (pale yellow, pale orange, light to dark brown) (Figure 4.8 H) to non-fluorescence under blue-light excitation.

4.8.1.2.7 Fluorinite

In the new ICCP System 1994, fluorinite is considered as a variety of resinite (Pickel *et al.* 2017). The term fluorinite was first described by (Teichmüller 1974b) because of its characteristic fluorescence property under the incident fluorescence light. Teichmüller (1974b) It is originated from plant oils or other liptinitic plant material (Teichmüller 1974b; Hutton 1987). The size of fluorinite varies from 0.1 µm to 0.5 µm with the lamellar or nodular shape. Fluorinite is considered a secondary maceral formed in the process of oil generation (Mukhopadhyay *et al.* 1979).

In the coals of the South Karanpura coalfield, fluorinite is present in low amounts. Wherever they are present, they exhibit a close association with humic matter and cutinite maceral (Figure 4.9 A, B, C, and D).

4.8.1.2.8 Exsudatinite

The term exsudatinite was first introduced by Teichmüller (1974b) to describe a maceral closely related to the generation of liquid hydrocarbons. Exsudatinite is the solid residue of the petroleum-like substance of secondary origin generated by liptinite or possibly by perhydrous vitrinites during the coalification process. It is a secondary maceral that has been generated during coalification and occupies the voids such as cracks, fissures, or cell cavities(Teichmüller 1974b; Pépin *et al.* 2014). It generally possesses the same colour, reflectance, and fluorescence property that of the maceral from which it is derived. Due to its rare occurrence, it has insignificant practical importance. In the South Karanpura coals, the presence of exsudatinite is low (Figure 4.9 E, F, G, and H).

4.8.1.2.9 Liptodetrinite

Liptodetrinite is a maceral of liptinite group, formed by fragmentation of other liptinite due to mechanical or biochemical degradation. The ICCP first introduced the term in 1971. Its colour is dark brown, dark grey, or black. The fluorescence colour varies from greenish-yellow, yellow, orange, to light brown, depending on precursor material and stage of coalification. It is widely distributed in coals as well as sedimentary rocks other than coal. Association of liptodetrinite can be seen with attrital layers, together with detrovitrinite, resinite, and sporinite.

This maceral is present in a good amount in both of the areas, the Barka Sayal (mean 1.4%) and Argada (mean 1.8%), and forms the second dominant maceral of the liptinite group (Figure 4.9 C and D).

4.8.1.2.10 Chlorophyllinite

ICCP first introduced the term chlorophyllinite in 1971. Chlorophyllinite is a maceral of liptinite group having a small rounded shape of 1 to 5 μm diameter and possessing red-coloured fluorescence, which fades into weak orange colour after excitation for a few minutes. It appears black and can be confused with liptodetrinite when observing in reflected white light. Chlorophyllinite originates from chloroplasts in plants formed in leaves, younger stems, and fruits. A strong anaerobic condition favours the fossilization of chlorophyll. This maceral is rarely present in the coals of the South Karanpura coalfield.

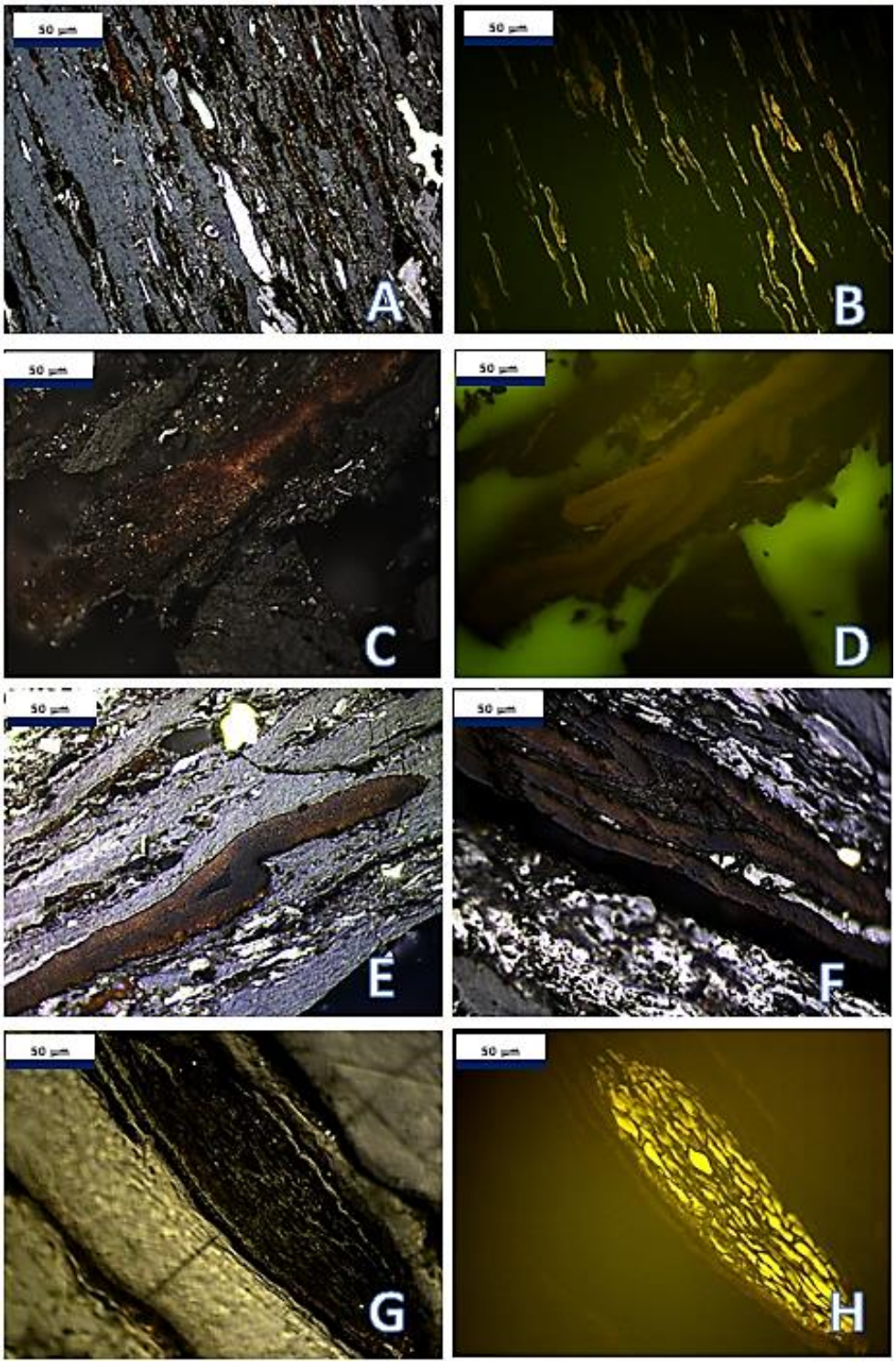


Figure 4.6 Representative photomicrographs of macerals, microlithotype, and mineral matter of South Karanpura coals (Polished surface, oil immersion, scale bar= 50 µm). The corresponding microlithotype name is provided in brackets. A) Miospores in the groundmass of collodetrinite (Duroclarite), B) Image A under fluorescence light, C) Megaspore (Clarite L), D) Image C under fluorescence light, E) Megaspore (Vitrienertolitptite), F) Megaspore associated with inertodetrinite (Liptite, specifically Sporite), G) Sporangium (Liptite, specifically Sporite), H) Image G under fluoresce light.

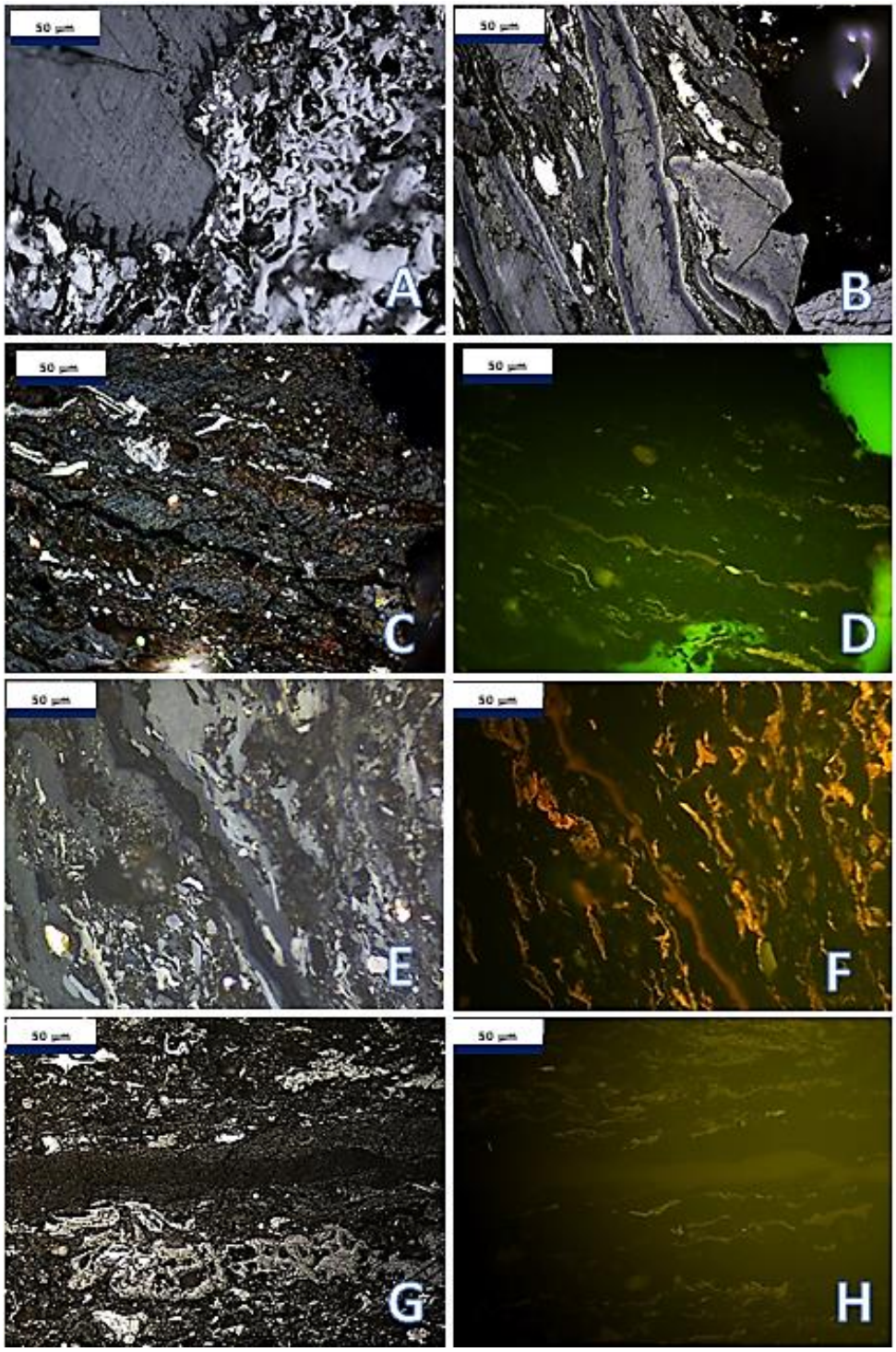


Figure 4.7 Representative photomicrographs of macerals, microlithotype, and mineral matter of South Karanpura coals (Polished surface, oil immersion, scale bar= 50 µm). The corresponding microlithotype name is provided in brackets. A) A mega cuticle surrounding the collotelinite microband (Duroclarite), B) Cutinite associated with collotelinite and collodetrinite (Clarite V), C) Cutinite occurring with collodetrinite and inertodetrinite (Duroclarite), D) Image C under fluorescence light, E) A mega cuticle showing serrated margin (Clarite L), F) Image E under fluorescence light, G) Large resinite associated with dark vitrinite (Clarite V), H) Image G under fluorescence light.

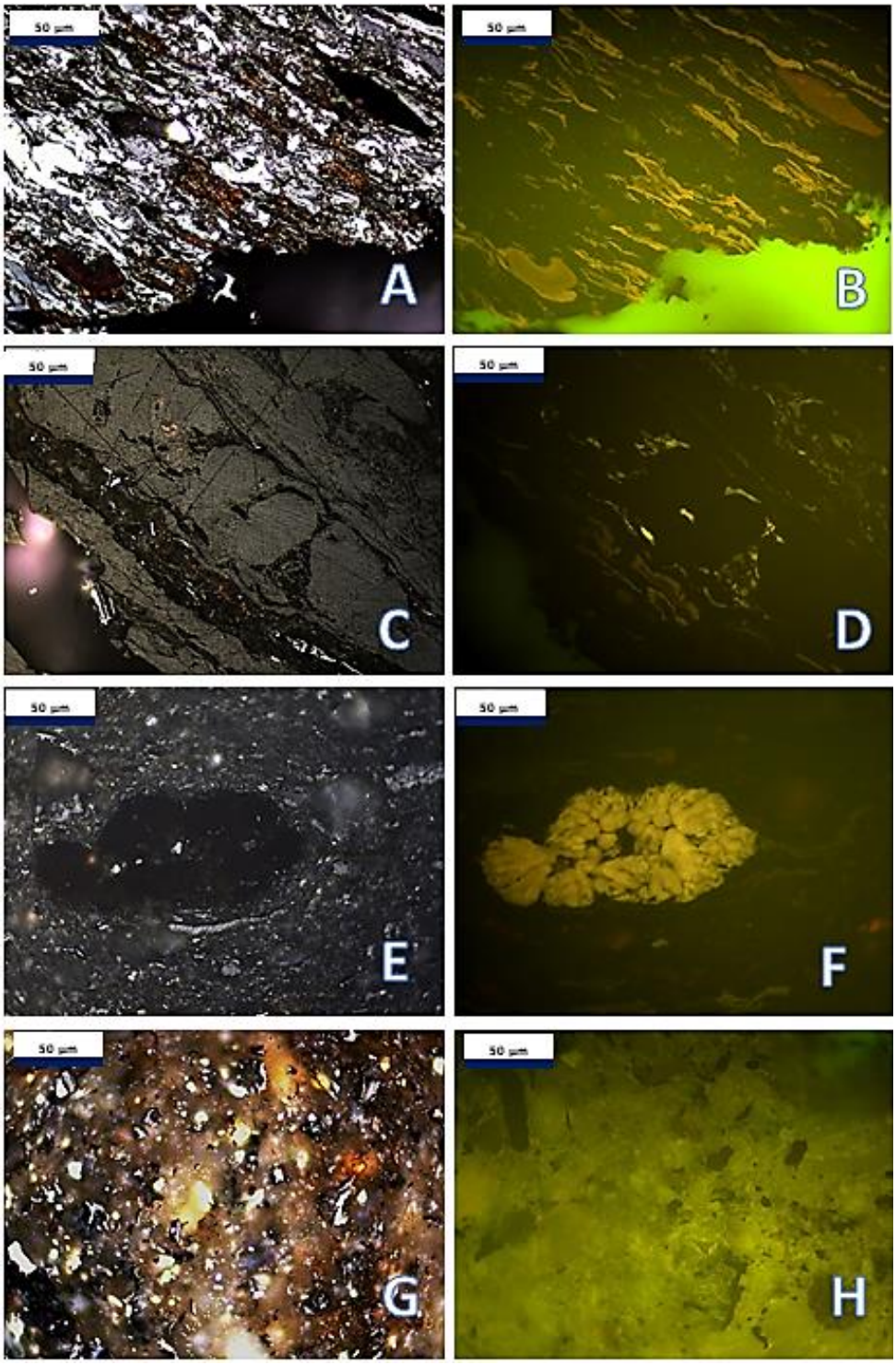


Figure 4.8 Representative photomicrographs of macerals, microlithotype, and mineral matter of South Karanpura coals (Polished surface, oil immersion, scale bar= 50 µm). The corresponding microlithotype name is provided in brackets. A) Oval-shaped resinite occurring with inertodetrinite, sporinite and minerals (Clarodurite), B) Image A under fluorescence light C) Suberinite associated with corpogelinite (Duroclarite), D) Field of view of Image C under fluoresce light, E) Alginite (Carbargilite), F) Image A in fluorescence light, G) Dispersed bituminite associated with carbonate minerals and detrital macerals (Carbankerite), H) Image G in fluorescence light.

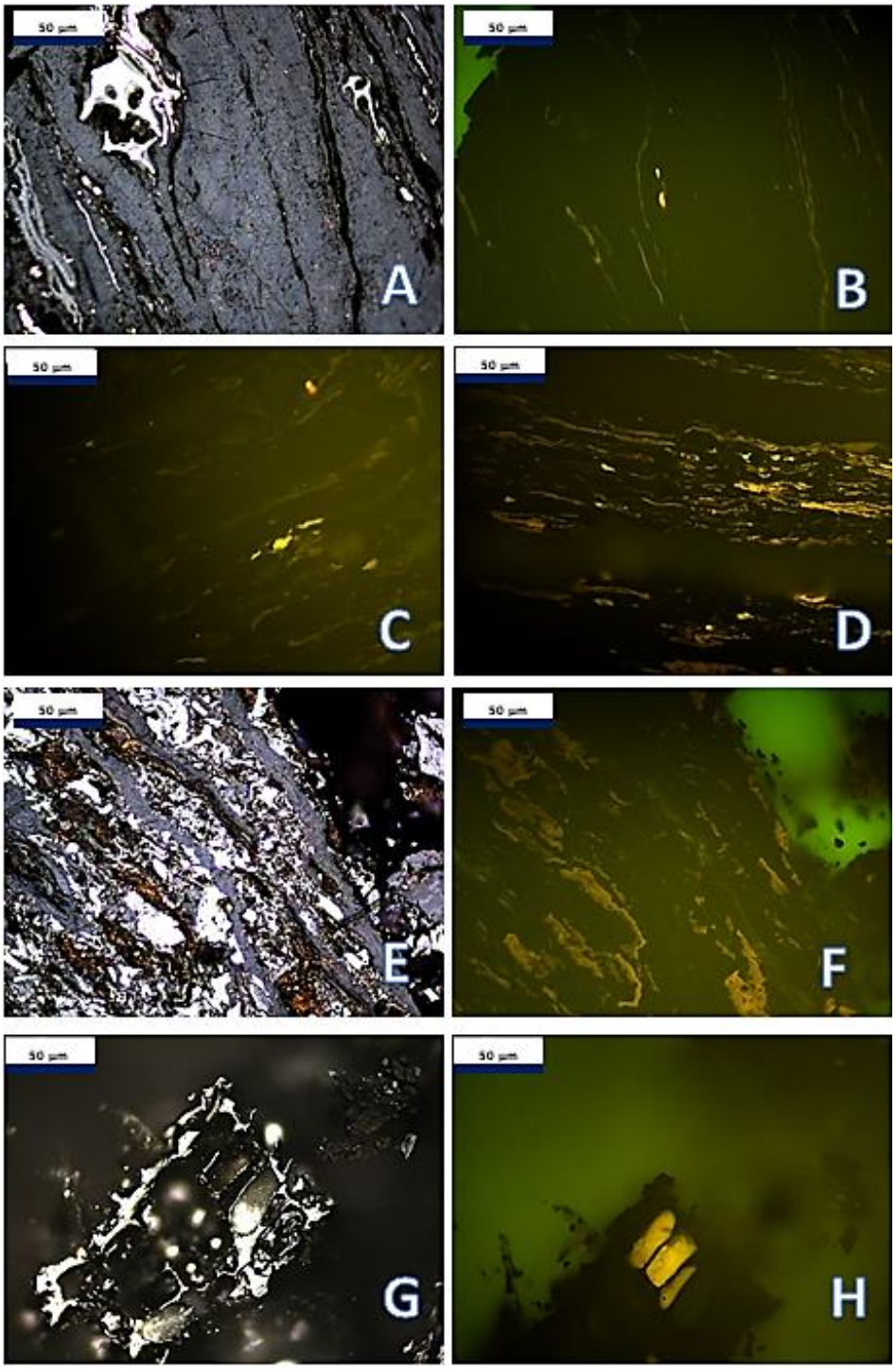


Figure 4.9 Representative photomicrographs of macerals, microlithotype, and mineral matter of South Karanpura coals (Polished surface, oil immersion, scale bar= 50 µm). The corresponding microlithotype name is provided in brackets. A) Fluorinite and Exsudatinite associated with collotelinite and cutinite (Clarite V), B) Image A under fluorescence light, C) Fluorinite occurring with sporinite and liptodetrinite under fluorescence light, D) Fluorinite with cutinite and miospores under fluorescence light, E) Exsudatinite filled in cracks of collotelinite (Clarodurite), F) Image E under fluorescence light, exsudatinite showing greenish fluorescence colour, G) Exsudatinite filled in cell lumens of fusinite, H) Image G under fluorescence light.

4.8.1.3 Inertinite Group

Inertinite is a group of macerals exhibiting higher reflectance compared to macerals of vitrinite and liptinite groups in low and medium rank coal. According to the new inertinite classification (ICCP System 1994), the macerals belonging to this group are fusinite, semifusinite, micrinite, macrinite, inertodetrinite, funginite, and secretinite (Table 4.10). In this new classification, the old sclerotinite macerals are replaced by funginite and secretinite macerals. The term inertinite is derived from the Latin term inertia meaning inactivity. The macerals of the inertinite group are more inert than other macerals during the carbonization process (Suárez-Ruiz and Crelling 2008). Inertinite macerals either exhibit no or very little fluorescence. The macerals fusinite, semifusinite, and funginite exhibit cell structure, whereas macerals such as secretinite, macrinite, and micrinite do not exhibit plant cell structure (Table 4.10). Inertodetrinite is supposed to be formed by the fragmentation of other inertinite macerals. Inertinite macerals originate from tissues of fungi or higher plants at various stages of compaction but primarily expressing the depositional environment. It may also be derived from fine detrital fragments, gelified amorphous material or cell secretions altered by biochemical redox processes during coalification. Inertinite macerals are characterized by high carbon content but less hydrogen and oxygen content in comparison to other macerals.

Table 4.10 Macerals of the inertinite group (International Committee for Coal and Organic Petrology 2001).

Macerals with cell structures:	Fusinite
	Semifusinite
	Funginite
Macerals lacking plant cell structures:	Secretinite
	Macrinite
	Micrinite
Fragmented inertinite:	Inertodetrinite

Coals of the South Karanpura coalfield contain an appreciable amount of inertinite macerals. Semifusinite is the most dominant macerals of this group followed by inertodetrinite, and fusinite.

4.8.1.3.1 Fusinite

The term fusinite was first introduced by Stopes (1935). Fusinite maceral exhibits high reflectance, the well-preserved cell structure of parenchyma, collenchyma or sclerenchyma formed by lignin and cellulose. The cell lumina of fusinite are generally empty, but sometimes it may be filled with gelinite, exsudatinite, or minerals. It occurs either as regular and well-preserved tissues with empty cell lumina (sieve structure) or as arc-shaped fragments of collapsed former cell tissues (Bogen structure). Fusinite exhibits colour varying from greyish white to yellowish-white but does not have fluorescence property. The variety of fusinite formed by wildfire is called pyrofusinite, whereas the variety generated by decarboxylation of plant tissues with bacterial action or by dehydration and weathering is called degradofusinite (Scott 2002). Degradofusinite exhibit a well-developed cellular structure and greyish white colour with high reflectance. Sometimes, the transitional stage between collotelinite and degradofusinite can be noticed. Pyrofusinite exhibit higher reflectance than degradofusinite with a well-preserved cell structure of yellowish-white to white colour. Due to its friable nature, fusinite generally concentrates on fine particles.

Fusinite present in the South Karanpura coals contains both sieve structure (Figure 4.10 A and C) and bogen structure (Figure 4.10 B and D). Both pyro (Figure 4.10 A and B) and degrado (Figure 4.10 C and D) varieties were recognized in these coals. The fusinite of the Argada area has more cell lumens filled with mineral matter compared to the fusinite occurring in the Barka Sayal area, possibly due to the high influx of terrigenous mineral matter during the formation of coals of the Argada area.

4.8.1.3.2 Semifusinite

Semifusinite exhibits intermediate reflectance and structure in between fusinite and collotelinite. The term ‘semifusinite’ was first given by Jongmans *et al.* (1938). It contains vague or partially visible cell cavities generally empty or sometimes filled with other macerals such as exsudatinite or minerals like clay. Fluorescence in these macerals can be visible on longer wavelength irradiation, which decreases with rank and degree of dehydration and oxidation. The presence of low reflectance and distinct fluorescence in semifusinite may indicate adsorbed bituminous matter by it.

In the coals of the South Karanpura coalfield, semifusinite is the most dominant maceral of the inertinite group. Its colour varies from grey to white, and reflectance lies in between fusinite and vitrinite in the same coal. Both degradosemifusinite (Figure 4.10 E, F, and H) and pyrosemifusinite (Figure 4.10 G) were recognized in these coals.

4.8.1.3.3 Macrinite

The term ‘macrinite’ was first introduced by Stach & Alpern (1966) for a massive (non-granular) inertinite maceral characterized by high reflectance. Macrinite originates from flocculated humic matrix materials, which go through dehydration and redox processes during early peatification due to the lowered water table (International Committee for Coal and Organic Petrology 2001). Further researchers discussed the origin of macrinite as the result of severe alteration by non-plant entities (fungi, bacteria, and animals) and possibly has originated from the multi-generational coprolites of wood-eating and coprophageous insects (Hower *et al.* 2009, 2011, 2013a, b; O’Keefe *et al.* 2013). It occurs as discrete structureless bodies of variable shapes or as an amorphous matrix of 10 µm to 40 µm size. It is light grey to white with variable reflectance but always higher than accompanying vitrinites. It generally occurs in durite, sometimes associated with collodetrinite.

In the South Karanpura coals, very few occurrences of macrinite were detected (Figure 4.11 A and B).

4.8.1.3.4 Micrinite

The term ‘micrinite’ was first introduced by Stopes (1935) for an inertinite maceral having a very small size and rounded grains. Thiessen (1920) was one of the early workers who recognized and shown this maceral in the photomicrographs. Ammosov (1956) described this maceral as mixtinite to characterize the association of vitrinite and micrinite. Diessel (1992) described the size of the micrinite as <2 µm. It is thought to be formed by the coalification product of former sclerenchyma or lipoid substances, especially bituminite and hydrogen-rich vitrinite (Stach 1968; Teichmüller 1971). Micrinite occurs in aggregates distinguished by its granularity.

In coals of the South Karanpura coalfield, micrinite shows pale grey to white colour with high reflectance than vitrinite macerals but often lower than other inertinite macerals of the same coal (Figure 4.11 C and D). It does not fluoresce. Relief of micrinite is hard to distinguish due to its tiny size, generally, it is supposed to be very low to negligible (International Committee for Coal and Organic Petrology 2001).

4.8.1.3.5 Secretinite

The term ‘secretinite’ was first introduced by Lyons *et al.* (1986) for a maceral of inertinite group having high reflectance and round to oblong, non-cellular form. Later, the term was accepted by ICCP in 1997. It may possess an oxidized rim of lower or higher reflectance and internal notches. It shows pale grey to a yellowish-white colour. Under blue-light excitation, it does not fluoresce. Secretinite having higher reflectance shows considerable relief. The size of the secretinite generally varies from 60 µm to 400 µm, whereas smaller and larger secretinite have also been reported.

Coals of the study area show the presence of secretinite macerals in a minimal concentration, and it is generally recognized by its internal notches and high reflectance (Figure 4.11 E and F).

4.8.1.3.6 Funginite

Funginite maceral is derived by the oxidation or humic gelification of single or multi-celled fungal spores, sclerotia, hyphae and mycelia, and other fungal remains. The colour of funginite varies from pale grey to white, rarely yellowish white. It does not fluoresce. It occurs in the form of roundish unicellular to multicellular oval form in Cenozoic and younger deposits. It may also exhibit spindle-shaped form, multicellular roundish, or tubular forms. In coals of older ages presence of funginite is rare. In the coals of the South Karanpura coalfield, it is present in very less amount, mainly in the Argada D and Sayal Balkudra seams (Figure 4.11 G and H).

4.8.1.3.7 Inertodetrinite

The term ‘inertodetrinite’ was introduced by Stach & Alpern (1966) and was adopted by ICCP in 1971 for the discrete small (<10 μm) inertinite fragments of varying shape. It is non-fluorescent, but the colour may vary significantly in the same coal from light grey to white. Its shape and degree are mainly controlled by the degree of desiccation, mechanical crushing, and attrition of fusinized plant cell walls, phlobaphene, spores, or constituents with fungal affinities. Wildfires probably created them in or around the peatland. It forms a significant portion of microlithotype duroclarite, clarodurite, vitrinertoliptite, durite, and vitrinertite. It may also be associated with minerals such as clay or pyrite caused by allochthonous origin.

In coals of the South Karanprua coalfield, inertodetrinite is present in good concentration (Figure 4.11 H). It is a dominating maceral of the inertinite group in these coals.

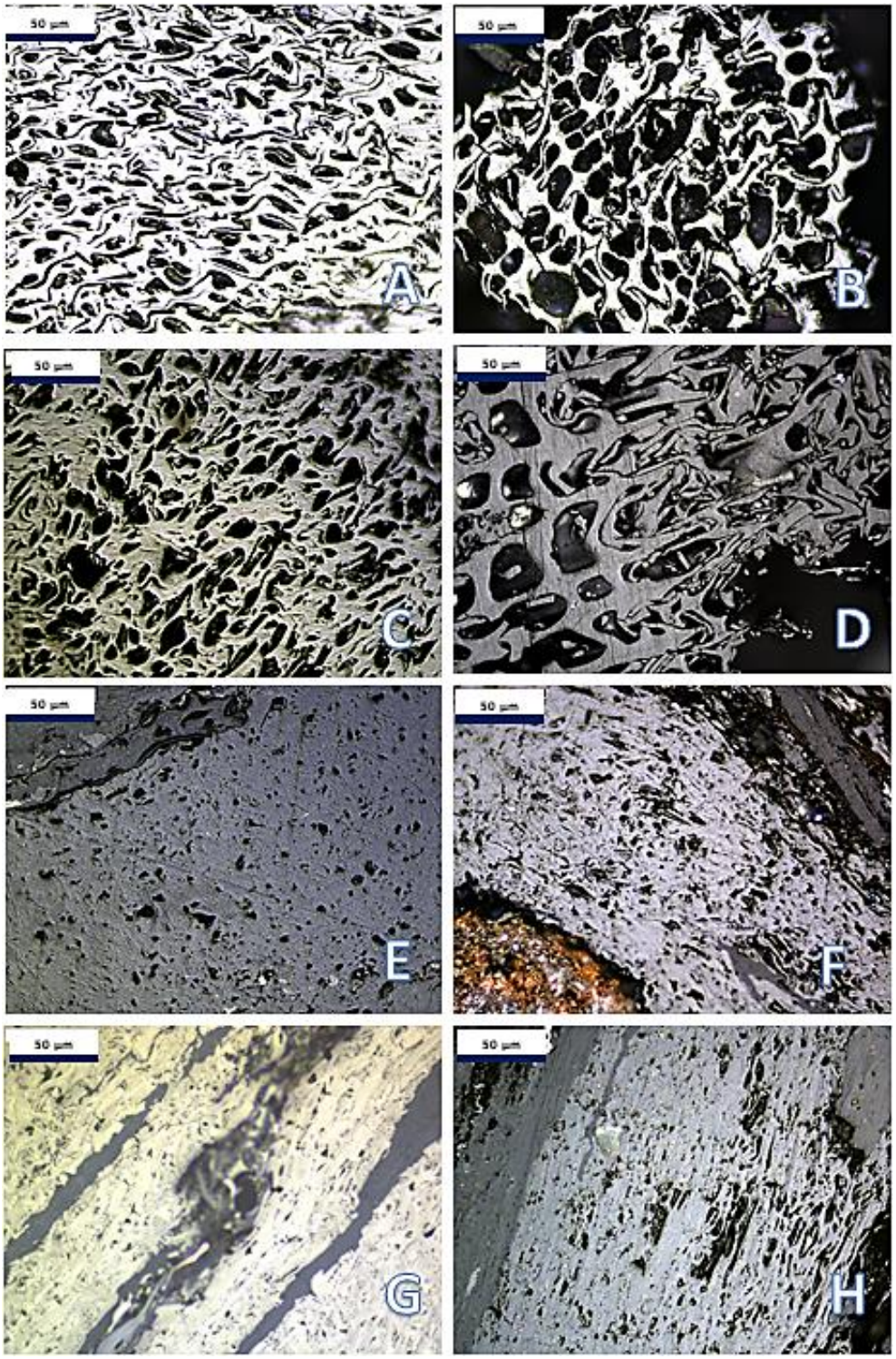


Figure 4.10 Representative photomicrographs of macerals, microlithotype, and mineral matter of South Karanpura coals (Polished surface, oil immersion, scale bar= 50 µm). Microlithotype name is Inertite for all photomicrographs. A) Pyrofusinite with sieve structure, B) Pyrofusinite with bogen structure, C) Degradofusinite with sieve structure, D) Degradofusinite with bogen structure, E) Degradosemifusinite, F) Semifusinite with carbonate minerals, G) Pyrosemifusinite, H) Degradosemifusinite.

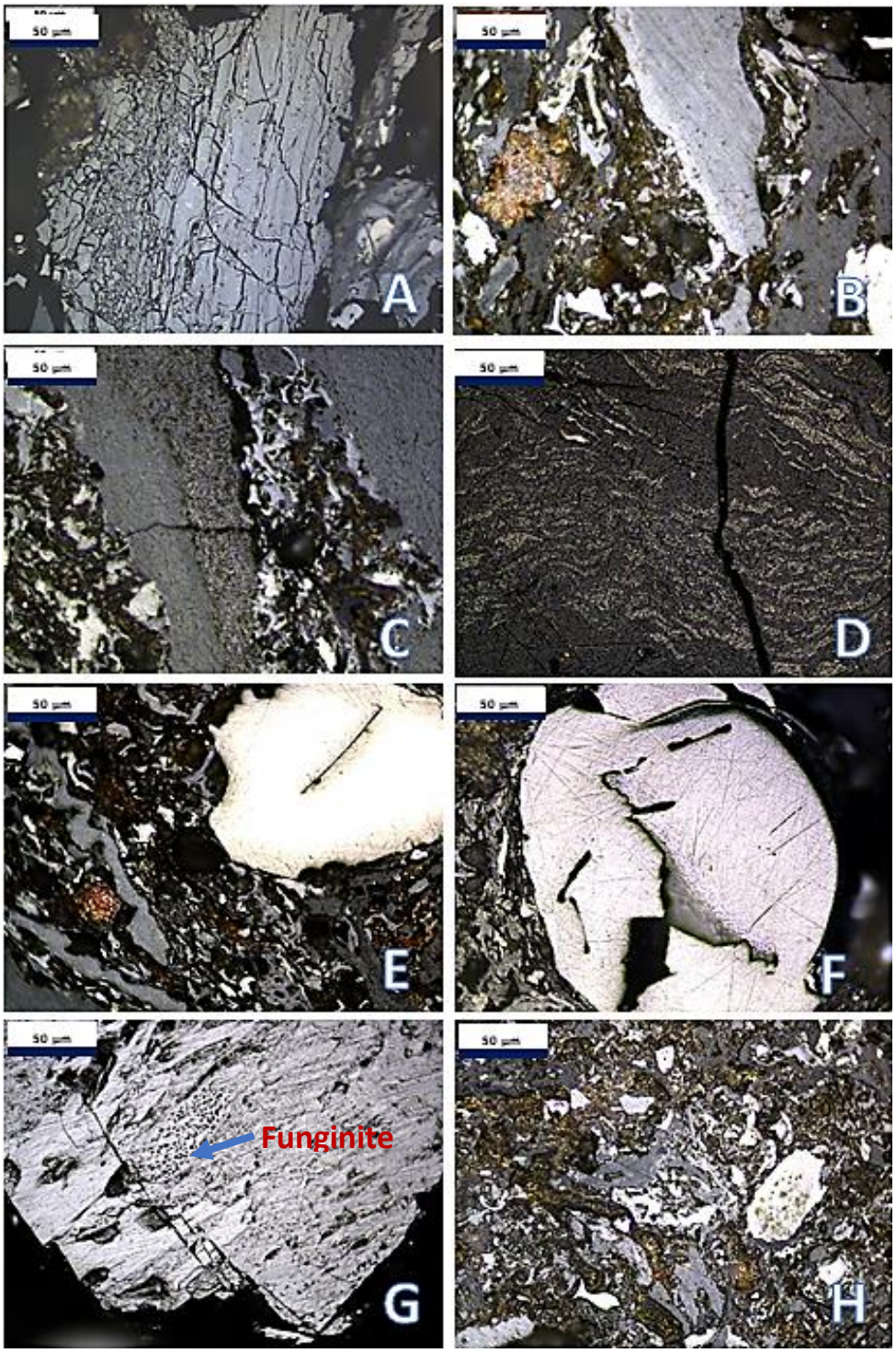


Figure 4.11 Representative photomicrographs of macerals, microlithotype, and mineral matter of South Karanpura coals (Polished surface, oil immersion, scale bar= 50 µm). The corresponding microlithotype name is provided in brackets. A) A macrinite grain in the middle (Inertite), B) Macrinite grain with collotelinite, inertodetrinite and carbonate minerals (Vitrinertite I), C) Micrinite occurring with collodetrinite (Vitrinertite V), D) Micrinite filled in cell lumens of telinite (Vitrinertite V), E) Secretinite with clay minerals (Carbargilite), F) Secretinite (Inertite), G) Funginite occurring with semifusinite (Inertite), H) Funginite grain occurring with inertodetrinite, vitrodetrinite, and carbonate minerals.

4.8.1.4 Mineral Matter

The sum of the minerals and inorganic matter associated with coal is called mineral matter. It may contain dissolved salts or inorganic substances present in coal's pore water, inorganic elements incorporated within the organic components or macerals, and discrete crystalline or non-crystalline inorganic particles (Ward 2016). The mineral matter incorporated into coal can be present in coal forming plant communities, or it may be syngenetic (deposited with coal bands) or epigenetic (incorporated after the formation of coal). Generally, the syngenetic mineral occurs in intimate association with organic constituents, whereas epigenetic minerals occupy places like cleats, fissures, cracks, and cell cavities. Microscopically visible mineral matter includes fine layers and other concentrations intimately intergrown with the maceral components, as well as discrete mineral fragments or crystals and a range of nodules, lenticels, veins, pore infillings, and cell-replacement structures. Mineral matter present in coal causes most of the problems associated with the utilization of coal.

The textural relationships revealed by microscopy indicate the formation of the mineral matter, or how it might respond to coal preparation and utilisation processes. It may also provide information on the depositional conditions and geologic history of the coal and associated seams. Due to difficulty in distinguishing small mineral particles as separate entities during point counting, the total proportion of microscopically visible minerals evaluated is found to be smaller than the mineral matter evaluated in the same coal using chemical analysis. It should also be noted that mineral matter determined by the point counting technique reflects the vol.% of the mineral matter present in the coal seam, whereas mineral matter identified through low-temperature ashing technique reflects the mass % of the mineral matter.

The South Karanpura coalfield contains a significant portion of visible mineral matter. Argillaceous, carbonate, and pyrite minerals are easily recognizable mineral constituents of these seams. In general, the argillaceous minerals are the more dominant mineral matter in these coal seams and are characterized by their black colour. They occur as lenticular bodies, microbands, and as infillings of the fissure, crack, cleat, and cell cavities of fusinite. The carbonate minerals occur as a dispersed form, as groundmass, as cell cavity fillings as well as in the form of carbonate nodules. Pyrites are found as disseminated particles as well as discrete grains; sometimes, they also occur as fissure fillings. Quantitative analysis of visible mineral matter present in the coals of the South Karanpura coalfield is shown in Table 4.12 and Table 4.16.

4.8.1.4.1 Argillaceous minerals

Argillaceous minerals include clay minerals. They occur as fine granular groundmass acting as infilling in fissures cracks, cavities, or cleats (Figure 4.12 A and B). They may also occupy cell lumens of telinite, fusinite, and secretinite. These minerals exhibit a dark colour. Coals of the Barka Sayal area exhibit a high amount of argillaceous mineral matter compared to coal seams of the Argada area.

4.8.1.4.2 Carbonate minerals

Carbonate minerals are originated from secondary precipitation. They may occur as infillings in cell cavities (Figure 4.12 C), fissures (Figure 4.12 E), and cleats. They may also form nodules (Figure 4.12 D and H) or groundmass as the replacement of collotelinite. In the case of carbonate minerals, the coals of the Argada area contain high concentrations compared to the coals of the Barka Sayal area.

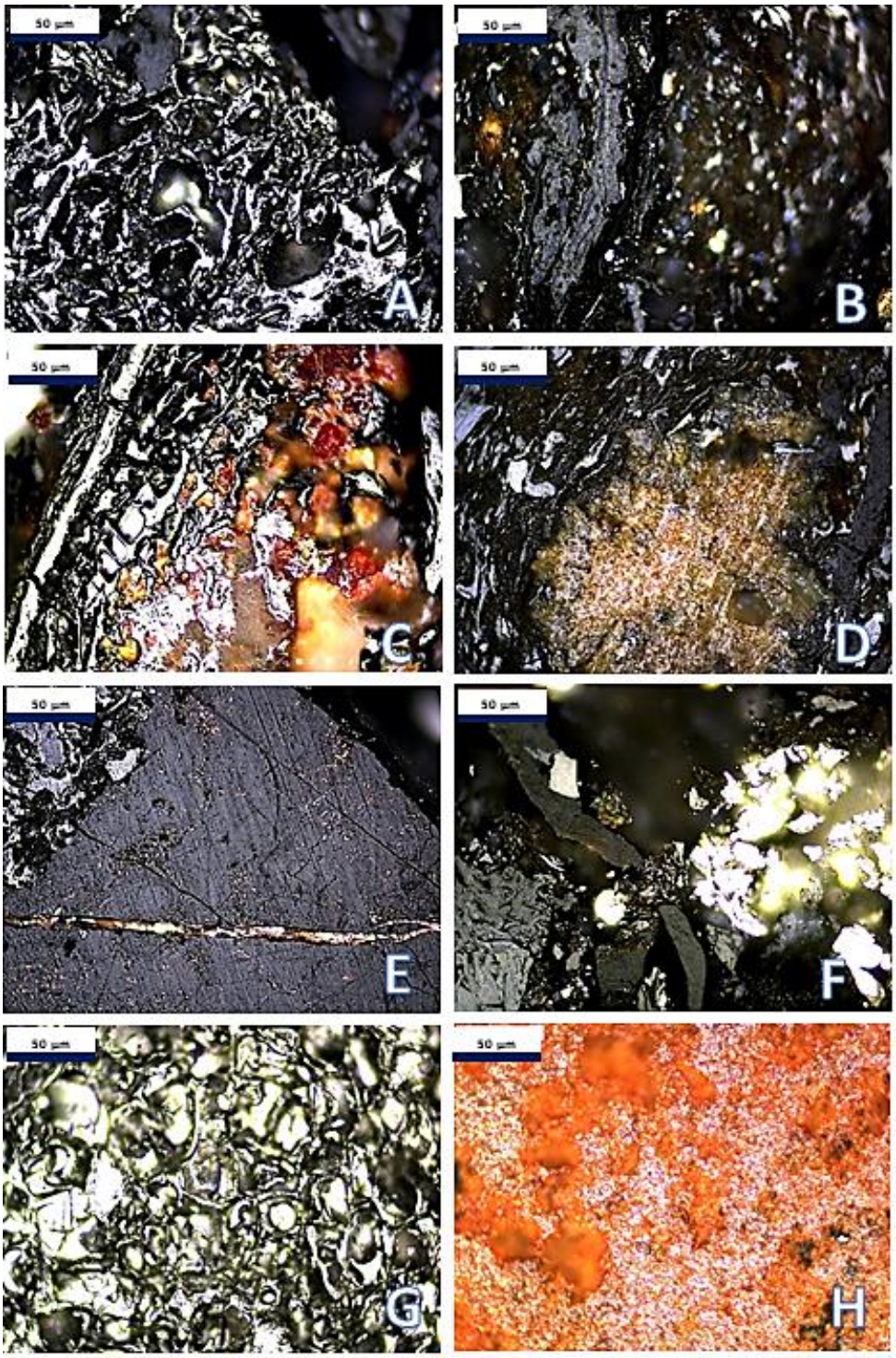


Figure 4.12 Representative photomicrographs of macerals, microlithotype, and mineral matter of South Karanpura coals (Polished surface, oil immersion, scale bar= 50 µm). The corresponding microlithotype name is provided in brackets. A) Clay minerals filled in cell lumens of fusinite (Carbargilite), B) Argillaceous minerals associated with vitrodetrinite and inertodetrinite (Carbargilite), C) Carbonate minerals filled in cell lumens of fusinite (Carbankerite), D) A carbonate nodule (Carbankerite), E) Carbonate minerals filling in the crack of collotelinite (Vitrite), F) Pyrite (Carbopyrite), G) A discrete weathered pyrite grain (Minerite), H) A grain of carbonate mineral (Minerite).

4.8.1.4.3 Sulphide minerals

These minerals are represented by pyrite and marcasite. Mainly pyrite is the dominant sulphide in these coals, only a few occurrences of other sulphide minerals were observed. They occur as dissemination, as a massive replacement, as a fissure or cracks infillings, as cavity infilling, as framboidal mass (Figure 4.12 F), and as discrete grains (Figure 4.12 G),). Coals of the Barka Sayal area contain high pyrite in comparison to the coals of the Argada area.

4.8.1.4.4 Siliceous minerals

Quartz, with a clastic origin, is the important constituent of this mineral group. It occurs associated with argillaceous minerals as discrete grains generally subrounded to subangular in shape. During the microscopic study, quartz was rarely found in the coals of the South Karanpura coalfield.

4.8.1.5 Microlithotype analysis

The term ‘microlithotype’ was introduced by Seyler (1952). The maceral and mineral composition of a coal seam may change over short distances both vertically and laterally based on the conditions that prevailed during the formation of the original peat swamps (Stach et al., 1982). These changes can be quantified by petrographic assessment of assemblage of maceral-maceral and maceral-mineral termed as microlithotype and carbominerite, respectively. It may also help in the evaluation of the characteristics of coal for technological and industrial purposes.

Microlithotypes are the natural assemblages of macerals at the microscopic level. For the demarcation of different microlithotypes, ICCP (1971) formulated two rules. According to these rules, the minimum dimension of an area to be called a microlithotype should be 50 µm x 50 µm, and the 5% rule. The 5% rule states that a microlithotype can have 5%

accessory macerals. The microlithotype is classified as monomaceral (macerals of one group covering more than 95% of the surface area of 50 µm x 50 µm), bimaceral (composed of macerals belonging to two groups), and trimaceral (macerals of all the three groups combined). An assemblage of maceral and mineral matter at microlithotype scale is termed as carbominerite if it contains 20–60 vol.% of silicate, carbonate, argillaceous minerals or a combination of two or more minerals or 5–20 vol.% sulfide minerals and called carbosilicite, carbankerite, carbargilite, carbopolyminerite and carbopyrite respectively.

A classification of microlithotypes and carbominerite is shown in Table 4.11 and Table 4.12, respectively.

Table 4.11 Summary of the microlithotype of hard coal.

Microlithotype Group	Maceral composition and quantity (Vol.%)	Microlithotype
Monomaceral	V > 95%	Vitrite
	L > 95%	Liptite
	I > 95%	Inertite
Bimaceral	V + L > 95% and V > L (Each >5%)	Clarite V
	V + L > 95% and L > V (Each >5%)	Clarite L
	V + I > 95% and V > I (Each >5%)	Vitrinertite V
	V + I > 95% and I > V (Each >5%)	Vitrinertite I
	I + L > 95% and I > L (Each >5%)	Durite I
	I + L > 95% and L > I (Each >5%)	Durite L
Trimaceral	V + I + L > 95% and V > I & L (Each >5%)	Duroclarite
	V + I + L > 95% and L > I & V (Each >5%)	Vitrinertoliptite
	V + I + L > 95% and I > V & L (Each >5%)	Clarodurite

V- Vitrinite, L- Liptinite and I- Inertinite.

Table 4.12 Summary of the carbominerite.

Microlithotype Group	Mineral composition and quantity (Vol. %)	Microlithotype
Carbominerite	Coal macerals + 20-60% clay minerals	Carbargilite
	Coal macerals + 20-60% carbonate minerals	Carbankerite
	Coal macerals + 20-60% silicate minerals	Carbosilicite
	Coal macerals + 20-60% various minerals	Carbopolyminerite
	Coal macerals + 5-20% sulphide minerals	Carbopyrite
Minerite	Mineral > 60%	Minerite

The microlithotype analysis of coal under study was carried out under white incident light. In these coals, all the microlithotype groups occur where monomaceral is

represented by vitrite, liptite and inertite, bimaceral by clarite vitrinertite and durite, and the trimaceral by duroclarite and clarodurite. The most dominating microlithotype groups are vitrite and clarite, followed by inertite, durite, liptite, and duroclarite in descending order. Vitrite is composed of collotelinite and telinite, liptite of sporinite, and resinite and inertite of semifusinite and fusinite. In most cases, the clarite and vitrinertite is vitrinite rich. Durite is low in concentration. The trimacerite is represented by duroclarite, clarodurite is in a lower concentration. The carbominerite is chiefly represented by carbargilite and carbankerite with a lower concentration of carbopolyminerite and carbopyrite.

At the microlithotype level, coals of the Barka Sayal area are Vitrite-rich, followed by inertite, vitrinertite-V, and clarite-V. In the case of carbominerite, coals of the Barka Sayal area are carbargilite rich, followed by carbankerite. Both carbopolyminerite and carbopyrite occur in less concentration.

Coals of the Argada area are inertite rich, followed by vitrite, vitrinertite-V, and vitrinertite-I. All other microlithotypes are in low concentration. Among the carbominerites, carbankerite is dominant, followed by carbargilite. Carbpolyminerite and carbopyrite occur in low concentrations in this area too.

In the South Karanpura coals, collotelinite is the major constituting maceral for the microlithotype- vitrite. The coals of the Barka Sayal area are Vitrite-rich (Figure 4.4 A, D, E and F; Figure 4.5 B, C, G, and H) compared to the coals of the Argada area.

The occurrence of liptite microlithotype is scarce in coals of the South Karanpura coalfield. A few occurrences of liptite microlithotype were observed formed by megasporinite, and it is termed as sporite. (Figure 4.6 F, G, and H)

Inertite in these coals is mainly characterised by the presence of macerals fusinite and semifusinite (Figure 4.10 A to H; Figure 4.11 A, F, and G). Coals of the Argada area are more inertite rich compared to the coals of the Barka Sayal area.

The South Karanpura coals have a little amount of clarite. Clarite V (Figure 4.4 C and G; Figure 4.5 D; Figure 4.7 B and G; Figure 4.9 A) is abundant compared to clarite L (Figure 4.6 C; Figure 4.7E). Coals of the Barka Sayal area are more clarite rich compared to the coals of the Argada area. South Karanpura coal has a low amount of durite. Durite-I is more common than durite-L in these coals. In the case of durite concentration, the coals of the Argada area are slightly higher than the coals of the Barka Sayal area.

Coals of South Karanpura are more enriched in vitrinertite-V (Figure 4.4 B and H, Figure 4.5 A; Figure 4.11 C and D) compared to vitrinertite-I. The coals of the Argada area exhibit a higher concentration of vitrinertite. Coals of the Argada area also show comparitiverly higher concentration of trimacerite, especially duroclarite.

Duroclarite is the most abundant trimaceral microlithotype in these coals, generally represented by a combination of macerals such as collodetrinite, vitrodetrinite, inertodetrinite, and sporinite (Figure 4.5 E and F; Figure 4.6 A; Figure 4.7 A and C; Figure 4.8 C). The occurrence of clarodurite was also observed in these coals (Figure 4.8 A; Figure 4.9 E). The presence of vitrinertoliptite is very low in these coals.

In the case of carbominerite, carbargilite are present in these coals in a high amount (Figure 4.8 E; Figure 4.11 E; Figure 4.12 A and B). It is also the most dominant carbominerite in the coals of the Barka Sayal area. Carbankerite is the most dominant carbominerite of the coals of the Argada area (Figure 4.8 G; Figure 4.12 C and D). The presence of carbopyrite (Figure 4.12 F) is very less in these coals. The carbopolyminerite microlithotype is also found in very few amounts in these coals.

4.9 Quantitative Occurrence of Microscopic constituents

The ternary diagram shows a relative percentage of all the three groups of macerals present in the different seams of the South Karanpura coalfield (Figure 4.13). This figure clearly shows the dominance of vitrinite and inertinite in these seams. Collotelinite is the most dominant maceral of vitrinite group present in the coals of South Karanpura coalfield. In the coals of the Barka Sayal area, the range of collotelinite varies from 16.8% to 82.9%, mean 47.8%, whereas, in coals of Argada area, its concentration varies in between nil and 64.8%, mean 26.2%.

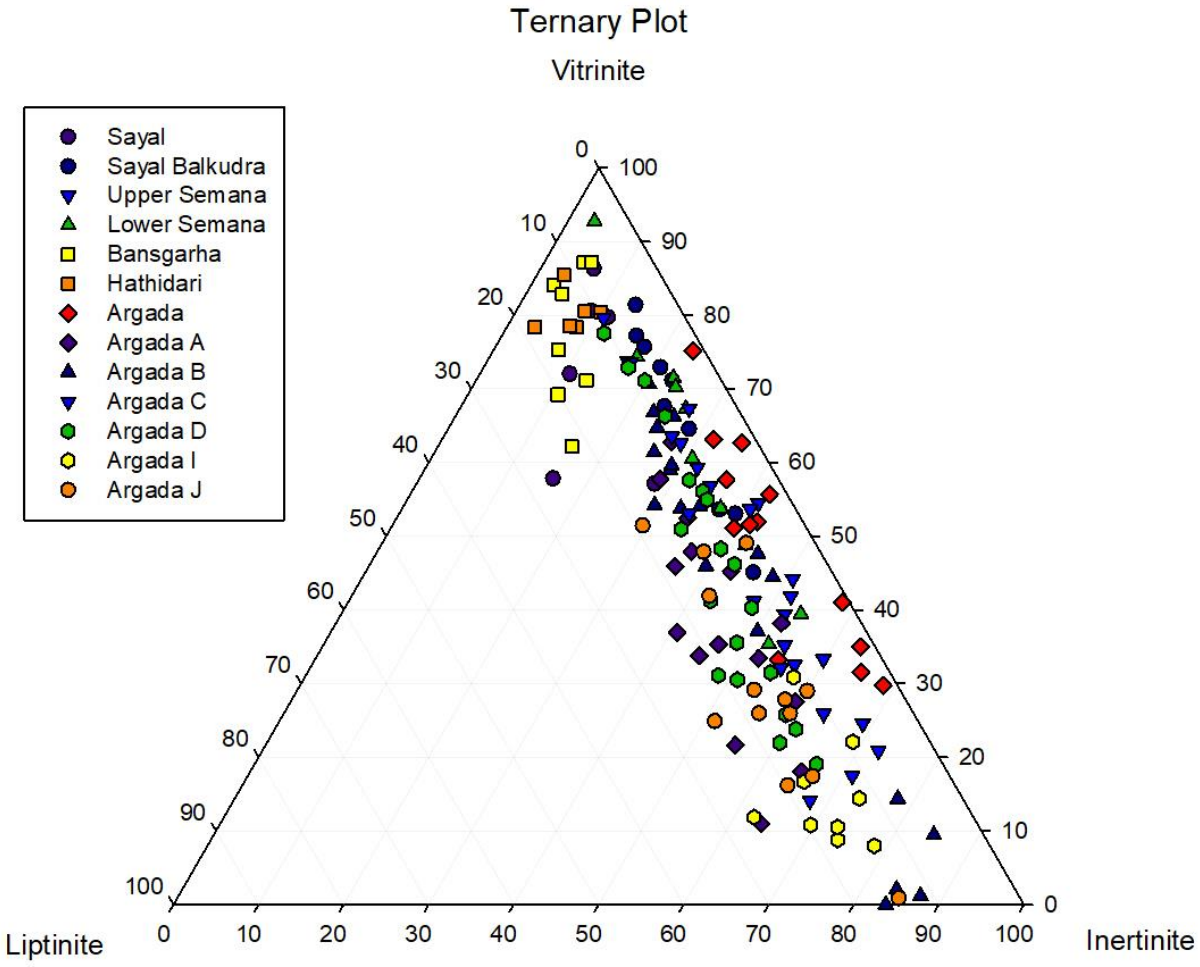


Figure 4.13 Distribution of group of macerals in South Karanpura coals.

4.9.1 Quantitative distribution of microscopic constituents in coal seams of the Barka Sayal Area

4.9.1.1 Maceral composition

The quantitative analysis of maceral content with visible mineral matter of the Barka Sayal area is presented in Table 4.12, while Table 4.13 presents the maceral content of Barka Sayal coals on a mineral matter free basis. All the seams of Barka Sayal area are vitrinite rich. The vitrinite content of the coals of the Barka Sayal area varies from 19.5% to 91.2%, mean 52.9% (20.8% - 92.7%, mean 66%, mmf basis). The inertinite content ranges from 2.2% to 67.9%, mean 19.6% (2.7% - 72.5%, mean 23.4%, mmf basis). The liptinite content in the coals of the Barka Sayal area varies between 3.6% and 14%, a mean of 8.1% (4%- 26.5%, mean 10.6%, mmf basis). Collotelinite is the dominant maceral of the vitrinite group, sporinite is dominant among liptinite, whereas in the inertinite group semifusinite is dominant. Figure 4.14 to Figure 4.19 presents the macro-petrographic section, microscopic (maceral and microlithotype) seam profiles, and range of mean vitrinite reflectance of different coal seams of the Barka Sayal.

4.9.1.2 Mineral matter

Coal seams of the Barka Sayal area have visible mineral matter in the range of 1.6% to 54.7%, mean 19.4%. Among the mineral matter, argillaceous minerals, carbonate minerals, and pyrite are the easily visible and distinguishable minerals present in these coals at the microscopic level. The argillaceous minerals in these coals are ranging from 0.5% to 37.3%, mean 14.5%. Carbonate minerals in these coals range in between nil to 38.6%, mean 4%, while pyrite in these coals lies in the range of nil to 13.3%, mean 0.9%. Table 4.12 presents the different visible macerals present in the coals of the Barka Sayal area of South Karanpura coalfield.

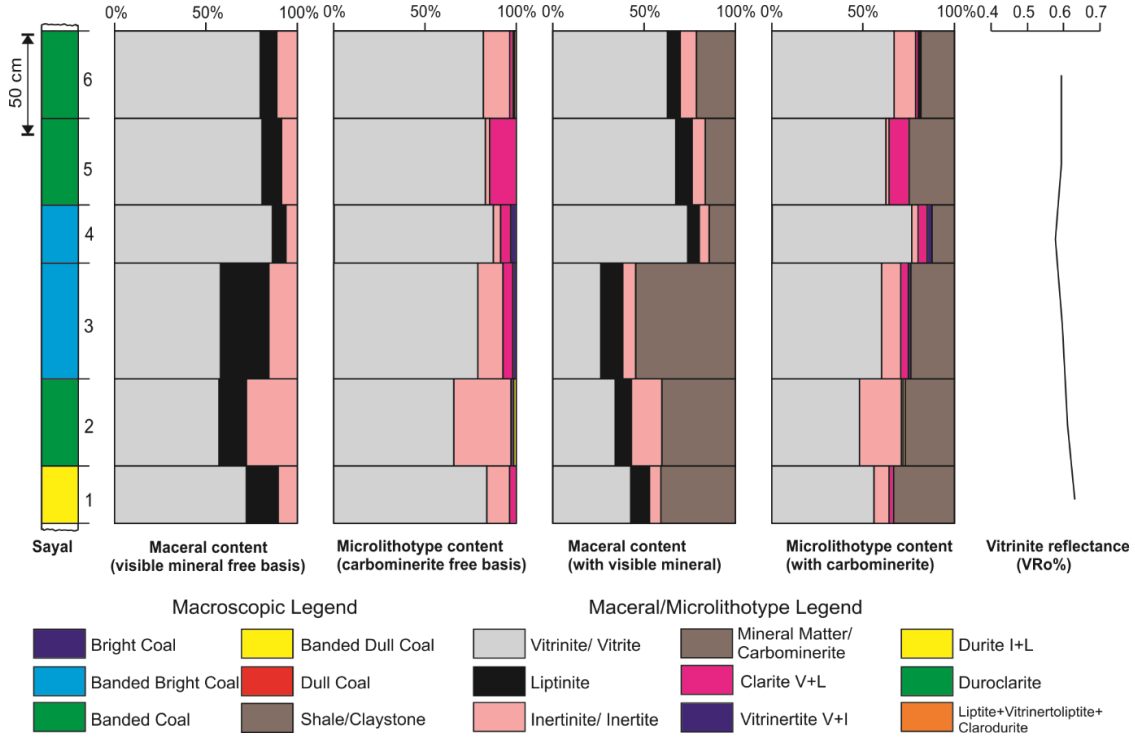


Figure 4.14 Macro-petrographic section, microscopic (maceral and microlithotype) seam profiles and range of mean vitrinite reflectance of Sayal Seam, South Karanpura Coalfield, Jharkhand.

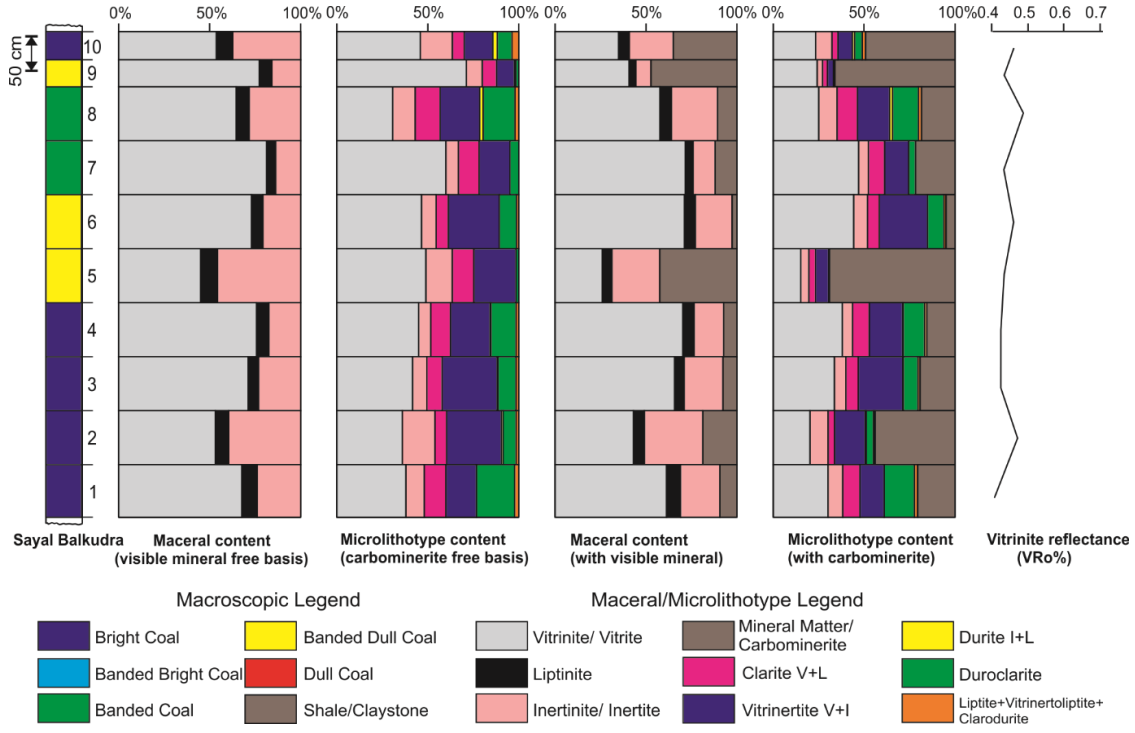


Figure 4.15 Macro-petrographic section, microscopic (maceral and microlithotype) seam profiles, and range of mean vitrinite reflectance of Sayal Balkudra Seam, South Karanpura Coalfield, Jharkhand.

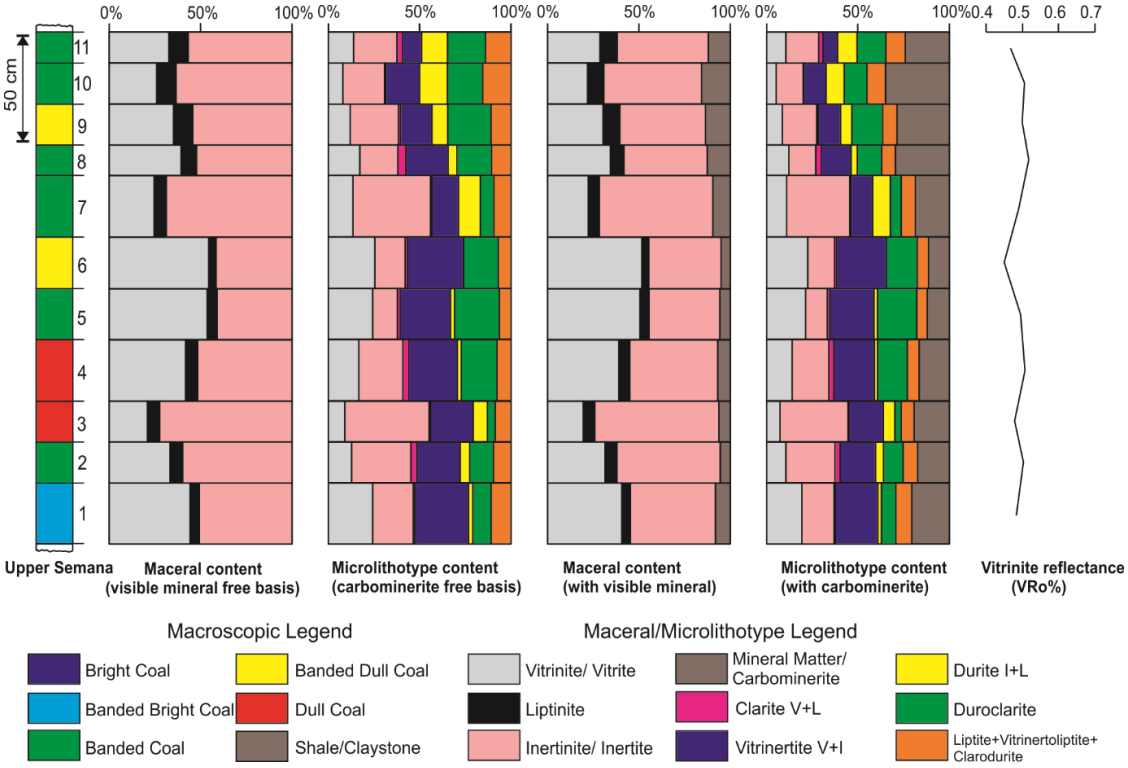


Figure 4.16 Macro-petrographic section, microscopic (maceral and microlithotype) seam profiles, and range of mean vitrinite reflectance of Upper Semana Seam, South Karanpura Coalfield, Jharkhand.

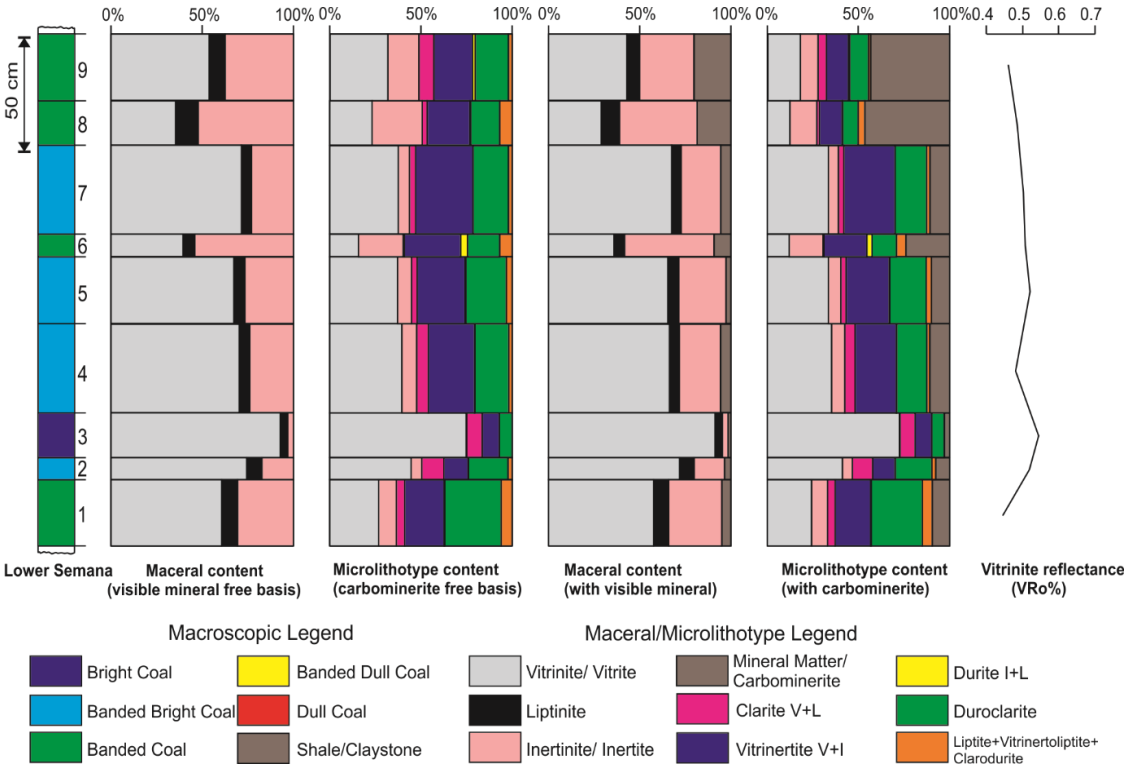


Figure 4.17 Macro-petrographic section, microscopic (maceral and microlithotype) seam profiles and range of mean vitrinite reflectance of Lower Semana Seam, South Karanpura Coalfield, Jharkhand.

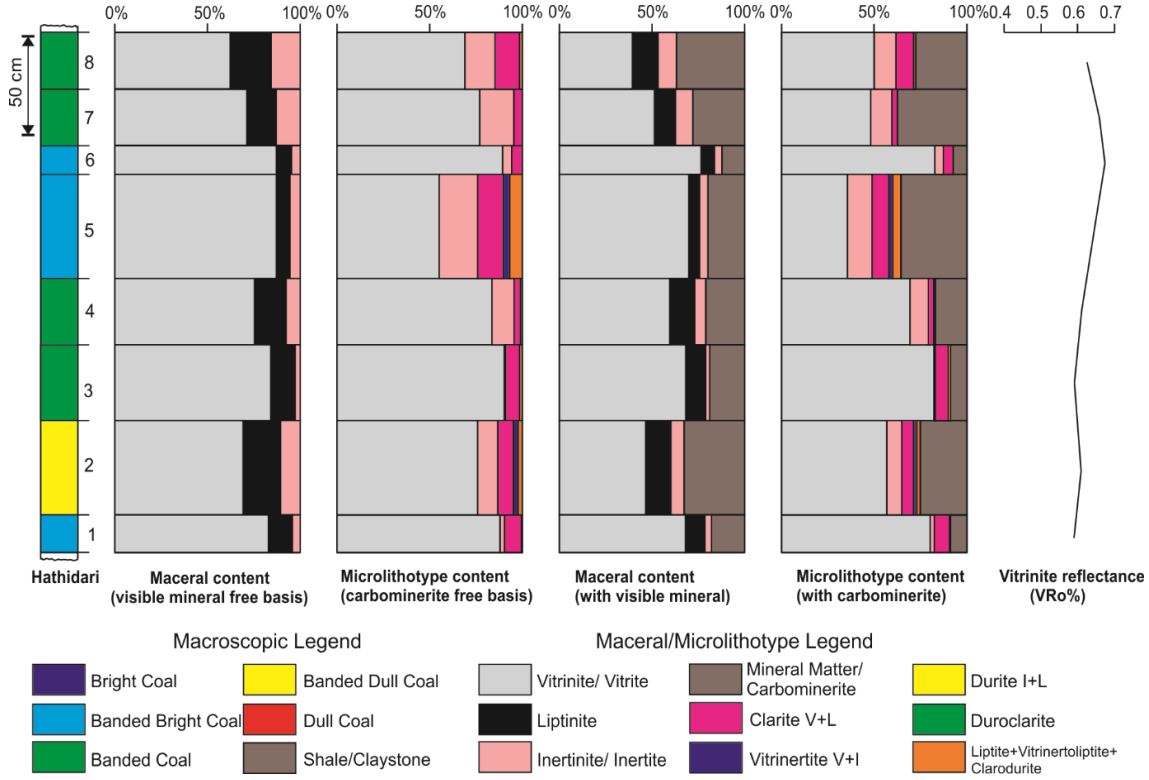


Figure 4.18 Macro-petrographic section, microscopic (maceral and microlithotype) seam profiles, and range of mean vitrinite reflectance of Hathidari Seam, South Karanpura Coalfield, Jharkhand.

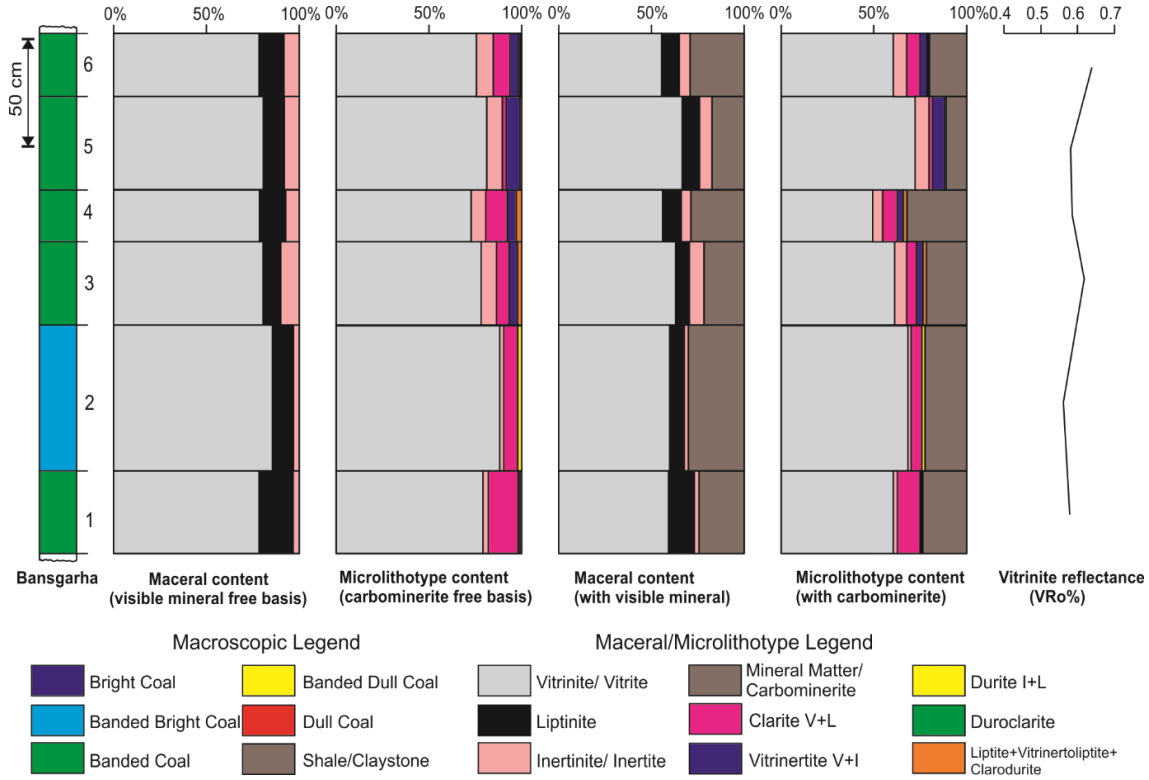


Figure 4.19 Macro-petrographic section, microscopic (maceral and microlithotype) seam profiles, and range of mean vitrinite reflectance of Bansgarha Seam, South Karanpura Coalfield, Jharkhand.

4.9.1.3 Microlithotypes

In case of microlithotype, the coals of Barka Sayal area are vitrite rich, concentration ranging from 5.2% to 82.8%, mean 43.5% (7.9%-90.3%, mean 56.2%, carbominerite free basis) followed by inertite from 0.2% to 37.2%, mean 9.8% (0.2%-46.1%, mean 13.3%, carbominerite free basis); vitrinertite-V from nil to 23%, mean 6.9% (nil-25.8%, mean 8.9%, carbominerite free basis), duroclarite from nil to 28%, mean 5.9% (nil-30.9%, mean 7.5%, carbominerite free basis), clarite-V from nil to 12.2%, mean 4.9% (nil-16.0%, mean 6.4%, carbominerite free basis). All other microlithotypes such as liptite, clarite-L, vitrinertite-I, durite-I, durite-L, vitrinertoliptite, and clarodurite are in less concentration (mean values <3% for each). Table 4.14 presents the quantitative distribution of different microlithotype present in the coal seams of the Barka Sayal area, while Table 4.15 presents microlithotype content present in these seams carbominerite free basis.

4.9.1.4 Carbominerites

Among the carbominerites of the Barka Sayal area, the carbargilite is the most dominant (0.6%- 36.5%, mean 15%), followed by carbankerite (nil - 59.2%, mean 7.2%) while carbopyrite (nil-3.6%, mean 0.5%) and carbopolyminerite (nil-2.9%, mean 0.4%) are in very less concentration. Table 4.14 presents the quantitative distribution of different carbominerite present in the coal seams of the Barka Sayal area.

Table 4.13 Maceral and mineral matter content (vol.%) of different coals seams of Barka Sayal area, South Karanpura Coalfield, Jharkhand, India

	Tl	Ctl	Vdr	Cdr	Cgl	Gl	DV	SV	Spo	Cut	Res	Alg	Sub	Ldr	Flo	Exu	Bit	Micr	Macr	Sfu	Fu	Scr	Idr	Arg	Carb	Py	Vit	Lipt	Inert	MM
Sayal																														
6 (top)	0.3	60.7	nil	nil	0.3	nil	1.0	0.3	3.7	0.3	0.3	nil	nil	1.7	0.3	0.3	0.3	nil	nil	6.4	1.4	nil	1.0	20.0	0.7	0.7	62.7	7.1	8.8	21.4
5	0.3	64.4	nil	nil	2.5	nil	nil	nil	2.2	1.0	1.3	0.3	0.6	1.0	0.6	1.0	1.0	nil	nil	2.5	1.6	nil	3.2	11.1	0.6	4.8	67.3	8.9	7.3	16.5
4	0.3	72.9	0.3	nil	nil	nil	nil	0.3	3.0	0.3	0.3	0.3	nil	1.0	0.3	nil	1.0	nil	nil	1.7	0.7	1.3	1.7	13.0	nil	1.3	73.9	6.4	5.4	14.4
3	0.4	24.9	0.9	nil	nil	nil	nil	nil	5.8	1.3	0.9	nil	nil	0.9	0.4	1.3	1.3	nil	nil	3.1	1.8	nil	2.2	37.3	4.0	13.3	26.2	12.0	7.1	54.7
2	0.3	29.4	3.1	nil	nil	nil	0.3	1.0	3.8	0.7	nil	nil	nil	2.1	0.3	0.3	1.7	nil	nil	9.2	2.7	1.0	3.8	37.2	1.7	1.4	34.1	8.9	16.7	40.3
1 (bottom)	0.4	37.1	3.7	nil	0.4	0.4	nil	0.7	4.8	1.1	nil	nil	nil	0.7	0.7	0.7	1.5	nil	nil	0.7	1.8	nil	3.7	34.9	2.2	3.7	42.7	10.3	6.3	40.8
Min	0.3	24.9	nil	nil	nil	nil	nil	nil	2.2	0.3	nil	nil	nil	0.7	0.3	nil	0.3	nil	nil	0.7	0.7	nil	1.0	11.1	nil	0.7	26.2	6.4	5.4	14.4
Max	0.4	72.9	3.7	nil	2.5	0.4	1.0	1.0	5.8	1.3	1.3	0.3	0.6	2.1	0.7	1.3	1.7	nil	nil	9.2	2.7	1.3	3.8	37.3	4.0	13.3	73.9	12.0	16.7	54.7
Mean	0.4	48.2	1.3	nil	0.5	0.1	0.2	0.4	3.9	0.8	0.5	0.1	0.1	1.2	0.5	0.6	1.1	nil	nil	4.0	1.7	0.4	2.6	25.6	1.5	4.2	51.2	8.9	8.6	31.3
SD	0.0	18.5	1.5	nil	0.9	0.1	0.4	0.4	1.2	0.4	0.5	0.2	0.2	0.5	0.2	0.4	0.4	nil	nil	3.0	0.6	0.6	1.0	11.2	1.3	4.3	17.8	1.9	3.8	14.8
Sayal Balkudra																														
10 (top)	0.6	27.5	2.4	2.6	0.4	0.2	nil	1.0	2.6	nil	0.2	0.2	nil	1.2	nil	1.6	nil	0.8	nil	10.5	2.4	nil	10.5	14.4	19.8	0.8	34.8	5.9	24.3	35.0
9	0.5	32.2	4.4	3.0	0.7	nil	nil	nil	1.6	nil	0.4	nil	nil	0.5	nil	1.2	nil	0.4	nil	1.9	3.1	nil	3.0	8.7	38.6	nil	40.7	3.7	8.4	47.3
8	1.3	48.5	3.3	3.6	0.8	0.2	nil	nil	3.1	nil	0.6	nil	nil	0.8	nil	1.9	nil	0.6	nil	8.4	5.0	nil	11.3	3.8	6.9	nil	57.7	6.3	25.3	10.7
7	0.5	58.0	4.7	6.6	1.6	0.2	nil	nil	2.8	0.2	0.2	nil	nil	0.5	0.4	0.4	nil	0.5	nil	3.5	3.1	nil	4.9	4.7	7.3	nil	71.6	4.4	12.0	12.0
6	0.7	60.0	3.3	6.9	nil	0.2	nil	nil	4.1	nil	0.3	nil	nil	0.7	nil	1.0	nil	1.5	0.3	6.3	5.1	nil	7.1	0.5	2.1	nil	71.0	6.1	20.3	2.6
5	1.0	19.7	2.5	2.7	nil	nil	nil	nil	2.8	0.2	0.7	nil	nil	1.0	nil	0.7	nil	0.2	nil	5.5	1.8	0.2	18.6	6.0	36.5	nil	25.9	5.4	26.3	42.5
4	0.5	59.0	6.6	3.0	0.9	0.2	nil	nil	1.9	0.2	0.4	nil	nil	1.1	nil	2.8	nil	0.4	0.2	2.3	6.3	nil	7.2	4.7	2.6	nil	70.2	6.3	16.2	7.3
3	4.6	54.9	4.5	1.1	0.6	nil	nil	nil	2.7	0.1	0.4	nil	nil	0.6	nil	1.5	nil	0.6	0.3	4.3	5.2	nil	10.9	4.8	2.5	0.4	65.7	5.3	21.3	7.7
2	1.4	35.8	3.7	1.8	0.4	nil	nil	nil	3.5	nil	0.2	nil	nil	0.5	nil	1.8	nil	nil	nil	7.2	6.5	0.2	18.2	11.1	7.6	0.2	43.0	6.0	32.1	18.9
1 (bottom)	1.0	52.9	3.8	3.2	0.3	nil	nil	nil	2.6	nil	0.9	nil	nil	1.0	nil	3.2	nil	0.2	nil	4.4	6.7	0.2	10.2	6.1	3.2	nil	61.3	7.7	21.7	9.4
Min	0.5	19.7	2.4	1.1	nil	nil	nil	nil	1.6	nil	0.2	nil	nil	0.5	nil	0.4	nil	nil	nil	1.9	1.8	nil	3.0	0.5	2.1	nil	25.9	3.7	8.4	2.6
Max	4.6	60.0	6.6	6.9	1.6	0.2	nil	1.0	4.1	0.2	0.9	0.2	nil	1.2	0.4	3.2	nil	1.5	0.3	10.5	6.7	0.2	18.6	14.4	38.6	0.8	71.6	7.7	32.1	47.3
Mean	1.2	44.9	3.9	3.5	0.6	0.1	nil	0.1	2.8	0.1	0.4	0.0	nil	0.8	0.0	1.6	nil	0.5	0.1	5.4	4.5	0.1	10.2	6.5	12.7	0.1	54.2	5.7	20.8	19.4
SD	1.2	14.0	1.2	1.8	0.4	0.1	nil	0.3	0.7	0.1	0.2	0.1	nil	0.3	0.1	0.9	nil	0.4	0.1	2.6	1.7	0.1	4.9	3.8	13.4	0.3	15.9	1.1	6.7	15.3
Up. Semana																														
11 (top)	nil	24.2	2.1	1.3	0.8	0.2	nil	nil	6.1	0.2	1.5	nil	nil	0.4	0.2	1.0	nil	1.5	0.4	23.2	5.0	0.2	19.6	6.5	5.6	nil	28.6	9.4	49.9	12.1
10	0.1	16.8	3.3	1.4	0.2	nil	nil	nil	6.1	0.4	1.1	nil	nil	1.0	nil	0.4	nil	0.5	0.2	20.6	4.5	0.1	27.5	9.8	5.8	0.2	21.8	8.9	53.5	15.8
9	1.2	19.8	5.8	2.3	1.0	nil	nil	0.2	6.4	nil	0.6	nil	nil	1.4	nil	0.6	0.2	0.2	0.2	19.7	8.2	0.2	18.5	8.0	5.6	nil	30.4	9.1	46.9	13.6
8	nil	28.8	4.1	0.7	0.3	0.2	0.3	nil	3.5	nil	0.5	nil	nil	1.0	nil	2.5	nil	0.2	0.2	17.4	5.4	nil	22.4	6.3	6.4	nil	34.4	7.4	45.6	12.7
7	nil	19.9	2.3	nil	nil	nil	nil	nil	4.6	nil	0.7	nil	nil	0.7	nil	0.2	nil	nil	0.2	35.6	6.5	nil	19.9	5.6	4.1	nil	22.2	6.0	62.2	9.6
6	0.3	46.7	3.0	1.2	0.3	nil	0.1	0.1	2.4	0.1	0.1	nil	nil	0.9	nil	0.3	nil	0.7	nil	13.8	6.9	nil	18.0	2.9	2.2	nil	51.7	3.8	39.4	5.1

Table 4.13 Maceral and mineral matter content (vol.%) of different coals seams of Barka Sayal area, South Karanpura Coalfield, Jharkhand, India

	Tl	Ctl	Vdr	Cdr	Cgl	Gl	DV	SV	Spo	Cut	Res	Alg	Sub	Ldr	Flo	Exu	Bit	Micr	Macr	Sfu	Fu	Scr	Idr	Arg	Carb	Py	Vit	Lipt	Inert	MM
5	nil	45.7	3.2	0.7	0.4	nil	0.1	0.4	3.2	nil	0.7	nil	nil	0.7	nil	0.5	nil	1.6	0.1	14.1	4.7	nil	18.1	2.9	2.8	nil	50.5	5.1	38.7	5.7
4	0.2	35.9	1.4	1.2	0.4	nil	nil	nil	3.5	nil	0.4	nil	nil	1.0	nil	1.2	nil	0.6	nil	17.5	9.2	nil	20.9	3.7	3.1	nil	39.0	6.0	48.2	6.8
3	0.4	16.9	1.8	0.4	nil	nil	0.2	nil	3.2	0.2	0.5	nil	nil	1.1	nil	1.3	nil	0.2	0.2	29.4	12.0	nil	26.2	3.2	3.1	nil	19.5	6.3	67.9	6.3
2	nil	29.1	2.4	nil	nil	nil	nil	nil	4.0	0.2	0.9	nil	nil	0.9	nil	0.6	nil	1.1	0.2	26.7	7.3	nil	21.2	2.4	3.1	nil	31.4	6.6	56.5	5.5
1 (bottom)	0.2	36.6	3.6	0.2	nil	nil	nil	nil	2.9	nil	0.4	nil	nil	0.9	nil	0.4	nil	0.9	nil	18.6	8.2	nil	18.9	4.4	3.8	nil	40.6	4.7	46.6	8.2
Min	nil	16.8	1.4	nil	nil	nil	nil	nil	2.4	nil	0.1	nil	nil	0.4	nil	0.2	nil	nil	nil	13.8	4.5	nil	18.0	2.4	2.2	nil	19.5	3.8	38.7	5.1
Max	1.2	46.7	5.8	2.3	1.0	0.2	0.3	0.4	6.4	0.4	1.5	nil	nil	1.4	0.2	2.5	0.2	1.6	0.4	35.6	12.0	0.2	27.5	9.8	6.4	0.2	51.7	9.4	67.9	15.8
Mean	0.2	29.1	3.0	0.8	0.3	0.0	0.1	0.1	4.2	0.1	0.7	nil	nil	0.9	0.0	0.8	0.0	0.7	0.2	21.5	7.1	0.1	21.0	5.1	4.1	0.0	33.6	6.7	50.5	9.2
SD	0.3	10.4	1.2	0.7	0.3	0.1	0.1	0.1	1.4	0.1	0.4	nil	nil	0.2	0.1	0.6	0.1	0.5	0.1	6.4	2.2	0.1	3.1	2.3	1.4	0.1	10.5	1.8	8.6	3.6
Lr. Semana																														
9 (top)	0.3	38.1	2.7	1.2	nil	nil	nil	0.6	4.3	nil	0.3	nil	nil	1.3	nil	1.0	nil	0.5	0.2	9.6	5.0	nil	14.5	9.2	11.0	0.2	42.9	7.0	29.8	20.3
8	0.2	25.2	2.8	0.3	nil	nil	0.2	0.2	7.1	0.2	0.3	nil	nil	1.2	nil	1.2	0.2	0.5	nil	14.0	7.9	0.2	20.1	7.1	11.5	nil	28.8	10.0	42.6	18.6
7	nil	61.3	2.8	2.6	nil	nil	nil	0.8	3.6	nil	0.5	nil	nil	0.8	nil	0.3	nil	0.2	0.2	5.1	5.6	nil	10.7	3.4	2.2	nil	67.5	5.1	21.8	5.6
6	0.2	30.7	3.2	1.5	0.2	nil	nil	nil	4.0	nil	0.4	nil	nil	1.1	nil	0.4	nil	0.8	0.2	16.2	10.5	0.2	21.1	4.0	5.1	0.2	35.8	5.9	49.1	9.3
5	0.2	59.0	2.8	0.8	0.3	0.2	nil	2.1	4.3	0.2	0.7	nil	nil	0.7	nil	0.2	nil	2.3	nil	8.1	4.9	nil	10.5	0.8	2.0	nil	65.4	5.9	25.9	2.8
4	0.4	59.4	2.9	1.4	1.0	nil	0.2	1.0	3.5	0.2	0.6	nil	nil	0.6	nil	0.6	nil	0.6	0.4	8.4	4.7	nil	8.4	3.3	2.2	0.2	66.3	5.5	22.6	5.7
3	0.2	82.9	4.3	1.8	0.4	0.4	nil	1.2	1.4	0.2	0.6	nil	nil	0.8	0.2	0.8	nil	0.4	nil	nil	0.4	nil	2.2	0.6	1.0	nil	91.2	4.1	3.1	1.6
2	nil	65.8	3.3	2.3	0.2	nil	nil	0.2	5.2	0.2	1.2	nil	nil	0.6	nil	0.8	nil	1.0	nil	5.2	3.7	nil	6.8	1.9	1.7	nil	71.8	8.0	16.7	3.5
1 (bottom)	nil	52.7	1.8	2.0	0.8	0.2	nil	nil	5.8	nil	0.8	nil	nil	1.0	0.2	0.4	nil	1.2	0.2	12.3	3.6	nil	11.9	1.6	3.4	nil	57.6	8.3	29.2	5.0
Min	nil	25.2	1.8	0.3	nil	nil	nil	nil	1.4	nil	0.3	nil	nil	0.6	nil	0.2	nil	0.2	nil	nil	0.4	nil	2.2	0.6	1.0	nil	28.8	4.1	3.1	1.6
Max	0.4	82.9	4.3	2.6	1.0	0.4	0.2	2.1	7.1	0.2	1.2	nil	nil	1.3	0.2	1.2	0.2	2.3	0.4	16.2	10.5	0.2	21.1	9.2	11.5	0.2	91.2	10.0	49.1	20.3
Mean	0.2	52.8	3.0	1.6	0.3	0.1	0.0	0.7	4.4	0.1	0.6	nil	nil	0.9	0.0	0.6	0.0	0.8	0.1	8.8	5.2	0.0	11.8	3.6	4.4	0.1	58.6	6.7	26.7	8.1
SD	0.1	17.3	0.6	0.7	0.3	0.1	0.1	0.7	1.5	0.1	0.3	nil	nil	0.3	0.1	0.3	0.1	0.6	0.1	4.7	2.7	0.1	5.7	2.7	3.8	0.1	18.5	1.8	12.8	6.4
Hathidari																														
8 (top)	0.4	32.7	5.9	nil	0.4	nil	nil	nil	4.8	1.5	1.1	nil	0.4	2.9	0.7	1.1	1.5	nil	nil	4.8	2.6	nil	2.6	34.6	1.1	1.1	39.3	14.0	9.9	36.8
7	0.4	46.6	3.4	nil	nil	0.4	0.4	nil	5.9	1.3	nil	nil	nil	1.7	0.4	0.4	1.7	nil	nil	3.4	3.0	nil	3.0	27.1	nil	0.9	51.3	11.4	9.3	28.0
6	0.3	75.5	0.7	nil	nil	nil	nil	nil	2.0	0.3	0.7	nil	nil	0.7	0.7	0.3	2.4	nil	nil	1.7	0.7	nil	1.7	11.9	nil	0.3	76.5	7.1	4.1	12.2
5	0.7	66.4	1.7	0.3	0.3	nil	nil	0.3	2.1	0.3	0.3	nil	nil	2.1	0.3	0.3	0.3	nil	nil	2.1	1.4	0.7	0.3	19.2	nil	0.7	69.9	5.8	4.5	19.9
4	nil	57.3	1.9	nil	nil	nil	nil	0.4	5.6	1.5	nil	nil	0.4	3.4	0.8	0.4	1.5	nil	nil	3.0	2.3	nil	0.8	18.4	1.9	0.8	59.6	13.5	6.0	21.0
3	nil	67.9	nil	nil	0.3	nil	nil	nil	2.8	0.6	nil	nil	nil	4.1	0.6	0.9	1.6	nil	nil	0.6	0.3	0.3	0.9	18.9	nil	nil	68.2	10.7	2.2	18.9
2	0.3	44.3	1.0	nil	0.3	nil	nil	0.7	7.4	0.3	0.7	0.3	0.7	2.6	0.3	nil	1.3	nil	nil	4.5	1.0	nil	1.6	31.7	nil	1.0	46.6	13.6	7.1	32.7
1 (bottom)	0.3	66.8	nil	0.3	nil	0.3	nil	0.3	3.8	1.0	0.6	nil	nil	2.6	0.3	0.6	1.6	nil	nil	1.6	1.0	nil	1.0	17.9	nil	nil	68.1	10.6	3.5	17.9
Min	nil	32.7	nil	nil	nil	nil	nil	nil	2.0	0.3	nil	nil	nil	0.7	0.3	nil	0.3	nil	nil	0.6	0.3	nil	0.3	11.9	nil	nil	39.3	5.8	2.2	12.2
Max	0.7	75.5	5.9	0.3	0.4	0.4	0.4	0.7	7.4	1.5	1.1	0.3	0.7	4.1	0.8	1.1	2.4	nil	nil	4.8	3.0	0.7	3.0	34.6	1.9	1.1	76.5	14.0	9.9	36.8

Table 4.13 Maceral and mineral matter content (vol.%) of different coals seams of Barka Sayal area, South Karanpura Coalfield, Jharkhand, India

	Tl	Ctl	Vdr	Cdr	Cgl	Gl	DV	SV	Spo	Cut	Res	Alg	Sub	Ldr	Flo	Exu	Bit	Micr	Macr	Sfu	Fu	Scr	Idr	Arg	Carb	Py	Vit	Lipt	Inert	MM
Mean	0.3	57.2	1.8	0.1	0.2	0.1	0.1	0.2	4.3	0.9	0.4	0.0	0.2	2.5	0.5	0.5	1.5	nil	nil	2.7	1.5	0.1	1.5	22.5	0.4	0.6	59.9	10.8	5.8	23.4
SD	0.2	13.7	1.9	0.1	0.2	0.2	0.1	0.2	1.8	0.5	0.4	0.1	0.2	1.0	0.2	0.3	0.5	nil	nil	1.4	0.9	0.2	0.9	7.3	0.7	0.4	12.2	2.8	2.6	7.7
Bansgarha																														
6 (top)	0.3	49.7	4.4	nil	nil	nil	0.7	0.3	4.4	1.0	nil	nil	nil	2.0	0.7	0.7	0.7	nil	nil	4.1	0.3	nil	1.4	27.9	nil	1.4	55.4	9.5	5.8	29.3
5	0.5	57.6	7.1	nil	nil	nil	nil	1.3	4.9	0.9	0.5	0.5	0.5	0.9	0.5	0.5	0.5	nil	nil	4.9	0.5	nil	1.3	16.5	nil	0.9	66.5	9.4	6.7	17.4
4	0.4	50.0	4.5	nil	nil	nil	nil	1.1	3.0	0.8	0.8	nil	0.4	3.4	0.8	0.4	0.8	nil	nil	2.6	1.1	nil	1.5	26.1	1.5	1.1	56.0	10.1	5.2	28.7
3	0.4	60.2	2.4	nil	nil	nil	nil	nil	4.7	0.8	0.8	nil	nil	1.2	nil	nil	nil	nil	nil	3.5	2.0	0.8	1.6	21.7	nil	nil	63.0	7.5	7.9	21.7
2	0.4	54.9	4.4	nil	nil	nil	nil	nil	3.1	0.4	0.9	0.4	nil	1.3	0.4	0.4	0.9	nil	nil	0.9	0.9	nil	0.4	30.1	nil	nil	59.7	8.0	2.2	30.1
1 (bottom)	0.4	54.6	2.5	nil	nil	nil	nil	1.7	6.7	0.4	0.8	nil	nil	3.4	0.4	0.8	1.3	nil	nil	0.8	0.4	nil	1.3	22.7	1.7	nil	59.2	13.9	2.5	24.4
Min	0.3	49.7	2.4	nil	nil	nil	nil	nil	3.0	0.4	nil	nil	nil	0.9	nil	nil	nil	nil	nil	0.8	0.3	nil	0.4	16.5	nil	nil	55.4	7.5	2.2	17.4
Max	0.5	60.2	7.1	nil	nil	nil	0.7	1.7	6.7	1.0	0.9	0.5	0.5	3.4	0.8	0.8	1.3	nil	nil	4.9	2.0	0.8	1.6	30.1	1.7	1.4	66.5	13.9	7.9	30.1
Mean	0.4	54.5	4.2	nil	nil	nil	0.1	0.8	4.5	0.7	0.6	0.2	0.1	2.0	0.5	0.5	0.7	nil	nil	2.8	0.9	0.1	1.2	24.2	0.5	0.6	60.0	9.7	5.1	25.3
SD	0.0	3.8	1.6	nil	nil	nil	0.3	0.7	1.3	0.2	0.3	0.2	0.2	1.0	0.2	0.3	0.4	nil	nil	1.5	0.6	0.3	0.4	4.5	0.8	0.6	3.9	2.1	2.1	4.6

Tl- Telinite, Ctl- Collotelinite, Vdr- Vitrodetrinite, Cdr- Collodetrinite, Cgl- Corpogelinite, Gl- Gelinite, DV- Dark Vitrinite, SV- Pseudovitrinite, Spo- Sporinite, Cut- Cutinite, Res- Resinite, Alg- Alginite, Sub- Suberinite, Ldr- Liptodetrinite, Flo- Fluorinite, Exu- Exsudatinite, Bit- Bituminite, Micr- Micrinite, Macr - Macrinite, Sfu- Semifusinite, Fu- Fusinite, Scr- Secretinite, Idr- Inertodetrinite, Arg- Argillaceous minerals, Carb- Carbonate minerals, Py- Pyrite, Vit- Total Vitrinite, Lipt- Total Liptinite, Inert- Total Inertinite, MM- Total Mineral matter

Table 4.14 Maceral content (mineral matter free) basis (vol.%) of different coals seams of Barka Sayal area, South Karanpura Coalfield, Jharkhand, India

	Tl	Ctl	Vdr	Cdr	Cgl	Gl	DV	SV	Spo	Cut	Res	Alg	Sub	Ldr	Flo	Exu	Bit	Micr	Macr	Sfu	Fu	Scr	Idr	Vit	Lipt	Inert
Sayal																										
6 (top)	0.4	77.2	1.3	nil	0.4	nil	nil	0.4	4.7	0.4	0.4	nil	nil	2.2	0.4	0.4	0.4	nil	nil	8.2	1.7	nil	1.3	79.7	9.1	11.2
5	0.4	77.2	nil	nil	3.0	nil	nil	nil	2.7	1.1	1.5	0.4	0.8	1.1	0.8	1.1	1.1	nil	nil	3.0	1.9	nil	3.8	80.6	10.6	8.7
4	0.4	85.2	0.4	nil	nil	nil	nil	0.4	3.5	0.4	0.4	0.4	nil	1.2	0.4	nil	1.2	nil	nil	2.0	0.8	1.6	2.0	86.3	7.4	6.3
3	1.0	54.9	2.0	nil	nil	nil	nil	nil	12.8	2.9	2.0	nil	nil	2.0	1.0	2.9	2.9	nil	nil	6.9	3.9	nil	4.9	57.8	26.5	15.7
2	0.6	49.1	5.1	nil	nil	nil	0.6	1.7	6.3	1.1	nil	nil	nil	3.4	0.6	0.6	2.9	nil	nil	15.4	4.6	1.7	6.3	57.1	14.9	28.0
1 (bottom)	0.6	62.7	6.2	nil	0.6	0.6	nil	1.2	8.1	1.9	nil	nil	nil	1.2	1.2	1.2	2.5	nil	nil	1.2	3.1	nil	6.2	72.1	17.4	10.6
Min	0.4	49.1	nil	nil	nil	nil	nil	nil	2.7	0.4	nil	nil	nil	1.1	0.4	0.4	0.4	nil	nil	1.2	0.8	nil	1.3	57.1	7.4	6.3
Max	1.0	85.2	6.2	nil	3.0	0.6	0.6	1.7	12.8	2.9	2.0	0.4	0.8	3.4	1.2	2.9	2.9	nil	nil	15.4	4.6	1.7	6.3	86.3	26.5	28.0
Mean	0.6	67.7	2.5	nil	0.7	0.1	0.1	0.6	6.3	1.3	0.7	0.1	0.1	1.9	0.7	1.3	1.8	nil	nil	6.1	2.7	0.6	4.1	72.3	14.3	13.4
SD	0.2	13.0	2.4	nil	1.1	0.2	0.2	0.6	3.4	0.9	0.8	0.2	0.3	0.8	0.3	0.9	1.0	nil	nil	4.9	1.3	0.8	1.9	11.3	6.4	7.1
Sayal Balkudra																										
10 (top)	0.9	42.4	3.7	4.1	0.6	0.3	nil	1.6	4.1	nil	0.3	0.3	nil	1.9	nil	2.5	nil	1.3	nil	16.2	3.7	nil	16.2	53.6	9.0	37.4
9	1.0	61.1	8.3	5.6	1.3	nil	nil	nil	3.0	nil	0.7	nil	nil	1.0	nil	2.3	nil	0.7	nil	3.6	5.9	nil	5.6	77.2	6.9	15.8
8	1.5	54.3	3.7	4.1	0.9	0.2	nil	nil	3.4	nil	0.6	nil	nil	0.9	nil	2.2	nil	0.6	nil	9.4	5.6	nil	12.7	64.6	7.1	28.3
7	0.6	65.9	5.4	7.5	1.8	0.2	nil	nil	3.2	0.2	0.2	nil	nil	0.6	0.4	0.4	nil	0.6	nil	4.0	3.6	nil	5.5	81.4	5.0	13.7
6	0.7	61.6	3.4	7.1	nil	0.2	nil	nil	4.2	nil	0.3	nil	nil	0.7	nil	1.0	nil	1.5	0.3	6.4	5.3	nil	7.3	72.9	6.3	20.8
5	1.7	34.3	4.4	4.7	nil	nil	nil	nil	4.9	0.3	1.2	nil	nil	1.7	nil	1.2	nil	0.3	nil	9.6	3.2	0.3	32.3	45.1	9.3	45.6
4	0.6	63.7	7.2	3.2	0.9	0.2	nil	nil	2.1	0.2	0.4	nil	nil	1.1	nil	3.0	nil	0.4	0.2	2.5	6.8	nil	7.7	75.7	6.8	17.5
3	5.0	59.5	4.9	1.2	0.6	nil	nil	nil	2.9	0.2	0.5	nil	nil	0.6	nil	1.7	nil	0.6	0.3	4.7	5.6	nil	11.8	71.2	5.8	23.1
2	1.7	44.1	4.6	2.2	0.4	nil	nil	nil	4.4	nil	0.2	nil	nil	0.7	nil	2.2	nil	nil	nil	8.9	8.0	0.2	22.4	53.0	7.4	39.6
1 (bottom)	1.1	58.4	4.1	3.6	0.4	nil	nil	nil	2.8	nil	0.9	nil	nil	1.1	nil	3.6	nil	0.2	nil	4.9	7.3	0.2	11.3	67.6	8.5	23.9
Min	0.6	34.3	3.4	1.2	nil	nil	nil	nil	2.1	nil	0.2	nil	nil	0.6	nil	0.4	nil	nil	nil	2.5	3.2	nil	5.5	45.1	5.0	13.7
Max	5.0	65.9	8.3	7.5	1.8	0.3	nil	1.6	4.9	0.3	1.2	0.3	nil	1.9	0.4	3.6	nil	1.5	0.3	16.2	8.0	0.3	32.3	81.4	9.3	45.6
Mean	1.5	54.5	4.9	4.3	0.7	0.1	nil	0.2	3.5	0.1	0.5	0.0	nil	1.0	0.0	2.0	nil	0.6	0.1	7.0	5.5	0.1	13.3	66.2	7.2	26.6
SD	1.3	10.1	1.5	1.9	0.5	0.1	nil	0.5	0.8	0.1	0.3	0.1	nil	0.4	0.1	0.9	nil	0.4	0.1	3.9	1.6	0.1	8.0	11.4	1.3	10.3
Up. Semana																										
11 (top)	nil	27.5	2.4	1.5	0.9	0.2	nil	nil	7.0	0.2	1.8	nil	nil	0.4	0.2	1.1	nil	1.8	0.4	26.4	5.7	0.2	22.3	32.5	10.7	56.8
10	0.2	19.9	3.9	1.6	0.3	nil	nil	nil	7.3	0.4	1.3	nil	nil	1.2	nil	0.4	nil	0.6	0.3	24.4	5.4	0.2	32.7	25.9	10.6	63.5
9	1.4	23.0	6.8	2.7	1.1	nil	nil	0.2	7.4	nil	0.7	nil	nil	1.6	nil	0.7	0.2	0.2	0.2	22.8	9.5	0.2	21.4	35.1	10.6	54.3
8	nil	33.0	4.7	0.8	0.4	0.2	0.4	nil	4.0	nil	0.6	nil	nil	1.1	nil	2.8	nil	0.2	0.2	20.0	6.2	nil	25.6	39.4	8.5	52.2
7	nil	22.0	2.5	nil	nil	nil	nil	nil	5.1	nil	0.7	nil	nil	0.7	nil	0.2	nil	nil	0.2	39.4	7.2	nil	22.0	24.6	6.7	68.8
6	0.3	49.2	3.2	1.2	0.3	nil	0.1	0.1	2.5	0.1	0.1	nil	nil	1.0	nil	0.3	nil	0.7	nil	14.6	7.3	nil	19.0	54.5	4.0	41.5
5	nil	48.5	3.4	0.7	0.4	nil	0.1	0.4	3.4	nil	0.7	nil	nil	0.7	nil	0.6	nil	1.7	0.1	15.0	5.0	nil	19.2	53.6	5.4	41.0

Table 4.14 Maceral content (mineral matter free) basis (vol.%) of different coals seams of Barka Sayal area, South Karanpura Coalfield, Jharkhand, India

	Tl	Ctl	Vdr	Cdr	Cgl	Gl	DV	SV	Spo	Cut	Res	Alg	Sub	Ldr	Flo	Exu	Bit	Micr	Macr	Sfu	Fu	Scr	Idr	Vit	Lipt	Inert
4	0.2	38.5	1.5	1.3	0.4	nil	nil	nil	3.8	nil	0.4	nil	nil	1.1	nil	1.3	nil	0.6	nil	18.8	9.8	nil	22.4	41.8	6.5	51.7
3	0.4	18.0	1.9	0.4	nil	nil	0.2	nil	3.4	0.2	0.6	nil	nil	1.2	nil	1.3	nil	0.2	0.2	31.4	12.8	nil	27.9	20.8	6.7	72.5
2	nil	30.8	2.5	nil	nil	nil	nil	nil	4.3	0.2	1.0	nil	nil	1.0	nil	0.6	nil	1.2	0.2	28.2	7.7	nil	22.4	33.3	7.0	59.8
1 (bottom)	0.2	39.9	3.9	0.2	nil	nil	nil	nil	3.1	nil	0.5	nil	nil	1.0	nil	0.5	nil	1.0	nil	20.3	8.9	nil	20.5	44.2	5.1	50.7
Min	nil	18.0	1.5	nil	nil	nil	nil	nil	2.5	nil	0.1	nil	nil	0.4	nil	0.2	nil	nil	nil	14.6	5.0	nil	19.0	20.8	4.0	41.0
Max	1.4	49.2	6.8	2.7	1.1	0.2	0.4	0.4	7.4	0.4	1.8	nil	nil	1.6	0.2	2.8	0.2	1.8	0.4	39.4	12.8	0.2	32.7	54.5	10.7	72.5
Mean	0.2	31.8	3.3	1.0	0.3	0.0	0.1	0.1	4.7	0.1	0.8	nil	nil	1.0	0.0	0.9	0.0	0.7	0.2	23.7	7.8	0.1	23.2	36.9	7.4	55.7
SD	0.4	10.5	1.4	0.8	0.4	0.1	0.1	0.1	1.7	0.1	0.4	nil	nil	0.3	0.1	0.7	0.1	0.6	0.1	7.0	2.2	0.1	3.9	10.6	2.3	9.6
Lr. Semana																										
9 (top)	0.4	47.9	3.4	1.5	nil	nil	nil	0.7	5.4	nil	0.4	nil	nil	1.7	nil	1.3	nil	0.6	0.2	12.1	6.3	nil	18.3	53.8	8.8	37.4
8	0.2	30.9	3.4	0.4	nil	nil	0.2	0.2	8.7	0.2	0.4	nil	nil	1.4	nil	1.4	0.2	0.6	nil	17.2	9.7	0.2	24.7	35.4	12.3	52.3
7	nil	64.9	3.0	2.8	nil	nil	nil	0.8	3.8	nil	0.5	nil	nil	0.8	nil	0.3	nil	0.2	0.2	5.4	5.9	nil	11.4	71.5	5.4	23.1
6	0.2	33.9	3.5	1.6	0.2	nil	nil	nil	4.4	nil	0.5	nil	nil	1.2	nil	0.5	nil	0.9	0.2	17.9	11.6	0.2	23.2	39.4	6.5	54.1
5	0.2	60.7	2.9	0.9	0.3	0.2	nil	2.2	4.4	0.2	0.7	nil	nil	0.7	nil	0.2	nil	2.4	nil	8.3	5.1	nil	10.9	67.3	6.1	26.6
4	0.4	63.0	3.1	1.5	1.0	nil	0.2	1.0	3.7	0.2	0.6	nil	nil	0.6	nil	0.6	nil	0.6	0.4	8.9	5.0	nil	8.9	70.3	5.8	23.9
3	0.2	84.3	4.4	1.9	0.4	0.4	nil	1.2	1.5	0.2	0.6	nil	nil	0.8	0.2	0.8	nil	0.4	nil	nil	0.4	nil	2.3	92.8	4.1	3.1
2	nil	68.2	3.4	2.4	0.2	nil	nil	0.2	5.3	0.2	1.3	nil	nil	0.6	nil	0.9	nil	1.1	nil	5.3	3.9	nil	7.1	74.4	8.3	17.3
1 (bottom)	nil	55.5	1.9	2.1	0.9	0.2	nil	nil	6.1	nil	0.9	nil	nil	1.1	0.2	0.4	nil	1.3	0.2	12.9	3.8	nil	12.5	60.6	8.7	30.7
Min	nil	30.9	1.9	0.4	nil	nil	nil	nil	1.5	nil	0.4	nil	nil	0.6	nil	0.2	nil	0.2	nil	nil	0.4	nil	2.3	35.4	4.1	3.1
Max	0.4	84.3	4.4	2.8	1.0	0.4	0.2	2.2	8.7	0.2	1.3	nil	nil	1.7	0.2	1.4	0.2	2.4	0.4	17.9	11.6	0.2	24.7	92.8	12.3	54.1
Mean	0.2	56.6	3.2	1.7	0.3	0.1	0.1	0.7	4.8	0.1	0.6	nil	nil	1.0	0.1	0.7	0.0	0.9	0.1	9.8	5.8	0.1	13.2	62.8	7.3	29.8
SD	0.2	15.9	0.6	0.7	0.4	0.1	0.1	0.7	1.9	0.1	0.3	nil	nil	0.4	0.1	0.4	0.1	0.6	0.1	5.5	3.1	0.1	7.0	16.9	2.3	15.3
Hathidari																										
8 (top)	0.6	51.7	9.3	nil	0.6	nil	nil	nil	7.6	2.3	1.7	nil	0.6	4.7	1.2	1.7	2.3	nil	nil	7.6	4.1	nil	4.1	62.2	22.1	15.7
7	0.6	64.7	4.7	nil	nil	0.6	0.6	nil	8.2	1.8	nil	nil	nil	2.4	0.6	0.6	2.4	nil	nil	4.7	4.1	nil	4.1	71.2	15.9	12.9
6	0.4	86.1	0.8	nil	nil	nil	nil	nil	2.3	0.4	0.8	nil	nil	0.8	0.8	0.4	2.7	nil	nil	1.9	0.8	nil	1.9	87.2	8.1	4.7
5	0.9	82.9	2.1	0.4	nil	0.4	nil	0.4	2.6	0.4	0.4	nil	nil	2.6	0.4	0.4	0.4	nil	nil	2.6	1.7	0.9	0.4	87.2	7.3	5.6
4	nil	72.5	2.4	nil	nil	nil	nil	0.5	7.1	1.9	nil	nil	0.5	4.3	1.0	0.5	1.9	nil	nil	3.8	2.8	nil	1.0	75.4	17.1	7.6
3	nil	83.7	nil	nil	0.4	nil	nil	nil	3.5	0.8	nil	nil	nil	5.0	0.8	1.2	1.9	nil	nil	0.8	0.4	0.4	1.2	84.1	13.2	2.7
2	0.5	65.9	1.4	nil	0.5	nil	nil	1.0	11.1	0.5	1.0	0.5	1.0	3.9	0.5	nil	1.9	nil	nil	6.7	1.4	nil	2.4	69.2	20.2	10.6
1 (bottom)	0.4	81.3	nil	0.4	nil	0.4	nil	0.4	4.7	1.2	0.8	nil	nil	3.1	0.4	0.8	2.0	nil	nil	2.0	1.2	nil	1.2	82.9	12.9	4.3
Min	nil	51.7	nil	nil	nil	nil	nil	nil	2.3	0.4	nil	nil	nil	0.8	0.4	nil	0.4	nil	nil	0.8	0.4	nil	0.4	62.2	7.3	2.7
Max	0.9	86.1	9.3	0.4	0.6	0.6	0.6	1.0	11.1	2.3	1.7	0.5	1.0	5.0	1.2	1.7	2.7	nil	nil	7.6	4.1	0.9	4.1	87.2	22.1	15.7
Mean	0.4	73.6	2.6	0.1	0.2	0.2	0.1	0.3	5.9	1.2	0.6	0.1	0.3	3.3	0.7	0.7	1.9	nil	nil	3.8	2.1	0.2	2.0	77.4	14.6	8.0

Table 4.14 Maceral content (mineral matter free) basis (vol.%) of different coals seams of Barka Sayal area, South Karanpura Coalfield, Jharkhand, India

	Tl	Ctl	Vdr	Cdr	Cgl	Gl	DV	SV	Spo	Cut	Res	Alg	Sub	Ldr	Flo	Exu	Bit	Micr	Macr	Sfu	Fu	Scr	Idr	Vit	Lipt	Inert
SD	0.3	11.3	2.9	0.2	0.2	0.2	0.2	0.3	2.9	0.7	0.6	0.2	0.4	1.3	0.3	0.5	0.6	nil	nil	2.3	1.4	0.3	1.3	8.7	5.0	4.3
Bansgarha																										
6 (top)	0.5	70.2	6.3	nil	nil	nil	1.0	0.5	6.3	1.4	nil	nil	nil	2.9	1.0	1.0	1.0	nil	nil	5.8	0.5	nil	1.9	78.4	13.5	8.2
5	0.5	69.7	8.7	nil	nil	nil	nil	1.6	6.0	1.1	0.5	0.5	0.5	1.1	0.5	0.5	0.5	nil	nil	6.0	0.5	nil	1.6	80.5	11.4	8.1
4	0.5	70.2	6.3	nil	nil	nil	nil	1.6	4.2	1.1	1.1	nil	0.5	4.7	1.1	0.5	1.1	nil	nil	3.7	1.6	nil	2.1	78.5	14.1	7.3
3	0.5	76.9	3.0	nil	nil	nil	nil	nil	6.0	1.0	1.0	nil	nil	1.5	nil	nil	nil	nil	nil	4.5	2.5	1.0	2.0	80.4	9.6	10.1
2	0.6	78.5	6.3	nil	nil	nil	nil	nil	4.4	0.6	1.3	0.6	nil	1.9	0.6	0.6	1.3	nil	nil	1.3	1.3	nil	0.6	85.4	11.4	3.2
1 (bottom)	0.6	72.2	3.3	nil	nil	nil	nil	2.2	8.9	0.6	1.1	nil	nil	4.4	0.6	1.1	1.7	nil	nil	1.1	0.6	nil	1.7	78.3	18.3	3.3
Min	0.5	69.7	3.0	nil	nil	nil	nil	nil	4.2	0.6	nil	nil	nil	1.1	nil	nil	nil	nil	nil	1.1	0.5	nil	0.6	78.3	9.6	3.2
Max	0.6	78.5	8.7	nil	nil	nil	1.0	2.2	8.9	1.4	1.3	0.6	0.5	4.7	1.1	1.1	1.7	nil	nil	6.0	2.5	1.0	2.1	85.4	18.3	10.1
Mean	0.5	72.9	5.6	nil	nil	nil	0.2	1.0	6.0	1.0	0.8	0.2	0.2	2.8	0.6	0.6	0.9	nil	nil	3.7	1.2	0.2	1.7	80.3	13.0	6.7
SD	0.1	3.5	1.9	nil	nil	nil	0.4	0.9	1.5	0.3	0.4	0.3	0.3	1.4	0.3	0.4	0.5	nil	nil	1.9	0.7	0.4	0.5	2.5	2.8	2.6

Tl- Telinite, Ctl- Collotelinite, Vdr- Vitrodetrinite, Cdr- Collodetrinite, Cgl- Corpogelinite, Gl- Gelinite, DV- Dark Vitrinite, SV- Pseudovitrinite, Spo- Sporinite, Cut- Cutinite, Res- Resinite, Alg- Alginite, Sub- Suberinite, Ldr- Liptodetrinite, Flo- Fluorinite, Exu- Exsudatinite, Bit- Bituminite, Micr- Micrinite, Macr - Macrinite, Sfu- Semifusinite, Fu- Fusinite, Scr- Secretinite, Idr- Inertodetrinite, Vit- Total Vitrinite, Lipt- Total Liptinite, Inert- Total Inertinite.

Table 4.15 Microlithotype and carbominerite content (vol.%) of different coals seams of Barka Sayal area, South Karanpura Coalfield, Jharkhand, India

	Vte	Lte	Ite	ClV	ClL	ViV	ViI	DuI	DuL	VIL	CLD	DUC	CAnk	CPy	CPoly	CArg	Mo	Bi	Tri	Cmin
Sayal																				
6 (top)	66.9	nil	11.8	1.5	nil	0.7	nil	0.7	nil	nil	nil	nil	0.7	1.5	1.5	14.7	78.7	2.9	nil	18.4
5	62.4	nil	1.8	10.9	nil	nil	nil	nil	nil	nil	nil	nil	5.5	3.6	0.6	15.2	64.2	10.9	nil	24.9
4	76.6	nil	3.5	4.8	nil	2.8	nil	nil	nil	nil	nil	nil	nil	2.8	nil	9.7	80.0	7.6	nil	12.4
3	60.1	nil	10.5	4.2	nil	1.3	nil	nil	nil	nil	nil	nil	1.4	nil	nil	22.5	70.6	5.5	nil	23.9
2	47.9	nil	22.9	nil	nil	1.0	nil	1.0	nil	nil	nil	nil	4.2	1.0	nil	21.9	70.8	2.1	nil	27.1
1 (bottom)	56.0	nil	8.3	2.4	nil	nil	nil	nil	nil	nil	nil	nil	1.2	2.4	nil	29.8	64.3	2.4	nil	33.3
Min	47.9	nil	1.8	nil	nil	nil	nil	nil	nil	nil	nil	nil	nil	nil	nil	9.7	64.2	2.1	nil	12.4
Max	76.6	nil	22.9	10.9	nil	2.8	nil	1.0	nil	nil	nil	nil	5.5	3.6	1.5	29.8	80.0	10.9	nil	33.3
Mean	61.7	nil	9.8	4.0	nil	1.0	nil	0.3	nil	nil	nil	nil	2.2	1.9	0.4	19.0	71.4	5.2	nil	23.3
SD	8.9	nil	6.9	3.5	nil	0.9	nil	0.4	nil	nil	nil	nil	2.0	1.2	0.6	6.6	6.2	3.2	nil	6.6
Sayal Balkudra																				
10 (top)	23.3	nil	8.9	2.9	0.4	6.0	1.9	0.8	0.4	0.2	1.7	4.2	27.7	0.6	2.9	18.1	32.2	12.5	6.0	49.3
9	24.1	nil	2.9	2.6	0.2	2.8	0.6	0.2	nil	nil	nil	0.6	48.8	nil	2.8	14.5	27.1	6.3	0.6	66.1
8	25.0	nil	10.0	10.8	0.4	15.6	2.2	1.6	nil	nil	1.8	14.2	12.0	nil	nil	6.5	35.0	30.5	15.9	18.5
7	47.0	nil	5.4	8.9	nil	11.6	1.4	0.2	nil	nil	nil	3.8	13.2	nil	0.5	8.0	52.3	22.1	3.8	21.8
6	44.2	nil	7.6	6.2	0.2	21.4	5.2	nil	nil	nil	1.2	9.0	4.4	nil	nil	0.6	51.8	33.0	10.2	5.0
5	15.1	nil	4.5	3.7	nil	5.5	1.6	nil	nil	nil	nil	0.4	59.2	nil	1.6	8.4	19.6	10.8	0.4	69.2
4	37.9	0.2	5.7	8.4	0.8	15.6	2.7	0.2	0.2	0.4	0.6	11.7	6.3	nil	0.6	8.8	43.8	27.9	12.7	15.6
3	33.7	nil	6.4	6.7	nil	20.0	4.4	0.4	nil	nil	1.2	8.1	10.8	0.6	0.2	7.7	40.0	31.5	9.2	19.2
2	20.2	nil	10.0	3.0	0.6	12.4	4.4	0.6	nil	0.2	0.6	4.0	16.8	0.2	1.4	25.8	30.1	21.0	4.8	44.1
1 (bottom)	30.1	nil	8.1	8.5	1.0	10.7	2.6	nil	nil	0.2	1.6	16.6	4.4	nil	0.2	16.0	38.2	22.8	18.4	20.6
Min	15.1	nil	2.9	2.6	nil	2.8	0.6	nil	nil	nil	nil	0.4	4.4	nil	nil	0.6	19.6	6.3	0.4	5.0
Max	47.0	0.2	10.0	10.8	1.0	21.4	5.2	1.6	0.4	0.4	1.8	16.6	59.2	0.6	2.9	25.8	52.3	33.0	18.4	69.2
Mean	30.1	0.0	6.9	6.2	0.4	12.2	2.7	0.4	0.1	0.1	0.9	7.2	20.4	0.1	1.0	11.4	37.0	21.9	8.2	32.9
SD	9.9	0.1	2.3	2.8	0.3	5.9	1.4	0.5	0.1	0.1	0.7	5.3	18.2	0.2	1.1	6.8	9.9	8.9	5.9	21.4
Up. Semana																				
11 (top)	10.5	nil	17.9	2.2	nil	5.2	2.8	10.7	nil	1.0	9.7	15.7	11.1	nil	nil	13.1	28.4	21.0	26.4	24.2
10	5.2	nil	14.9	0.4	nil	7.1	5.0	9.9	nil	0.6	9.5	12.5	13.5	0.2	1.0	20.2	20.0	22.4	22.6	34.9
9	8.4	nil	18.9	0.8	nil	8.6	3.6	6.0	0.2	nil	7.8	16.9	10.4	nil	1.2	17.1	27.3	19.3	24.7	28.7
8	12.1	nil	14.7	3.0	0.2	8.9	7.3	3.4	nil	0.6	6.9	13.3	11.7	nil	2.4	15.5	26.8	22.8	20.8	29.6
7	10.9	nil	34.5	0.6	nil	7.3	4.6	9.5	0.2	0.2	7.5	6.0	6.9	nil	0.2	11.5	45.4	22.2	13.7	18.7
6	22.5	nil	14.6	1.2	nil	19.0	8.1	0.2	nil	nil	6.1	16.8	4.7	nil	0.8	5.9	37.2	28.5	22.9	11.5
5	21.2	nil	11.9	1.4	nil	16.9	7.3	2.0	nil	0.4	5.4	21.4	5.0	0.2	0.2	6.8	33.1	27.6	27.2	12.1

Table 4.15 Microlithotype and carbominerite content (vol.%) of different coals seams of Barka Sayal area, South Karanpura Coalfield, Jharkhand, India

	Vte	Lte	Ite	ClV	ClL	ViV	ViI	DuI	DuL	VIL	CLD	DUC	CAnk	CPy	CPoly	CArg	Mo	Bi	Tri	Cmin
4	13.9	nil	20.1	2.6	0.2	13.9	8.3	1.8	nil	0.2	6.2	16.3	6.8	nil	0.8	8.9	34.0	26.8	22.7	16.5
3	7.2	nil	37.2	0.6	nil	9.2	9.6	6.2	0.2	0.2	6.8	3.4	8.6	0.2	0.4	10.2	44.4	25.8	10.4	19.4
2	10.5	nil	26.8	2.6	0.2	10.9	8.6	4.4	nil	0.2	7.8	10.7	9.2	nil	0.2	8.0	37.4	26.6	18.7	17.3
1 (bottom)	19.2	nil	17.6	0.7	nil	12.6	10.8	1.8	nil	0.2	8.5	8.0	9.2	nil	nil	11.4	36.8	25.9	16.7	20.6
Min	5.2	nil	11.9	0.4	nil	5.2	2.8	0.2	nil	nil	5.4	3.4	4.7	nil	nil	5.9	20.0	19.3	10.4	11.5
Max	22.5	nil	37.2	3.0	0.2	19.0	10.8	10.7	0.2	1.0	9.7	21.4	13.5	0.2	2.4	20.2	45.4	28.5	27.2	34.9
Mean	12.9	nil	20.8	1.5	0.1	10.9	6.9	5.1	0.1	0.3	7.5	12.8	8.8	0.1	0.7	11.7	33.7	24.4	20.6	21.2
SD	5.5	nil	8.0	0.9	0.1	4.1	2.4	3.5	0.1	0.3	1.3	5.1	2.7	0.1	0.7	4.3	7.3	2.9	5.0	7.1
Lr. Semana																				
9 (top)	18.1	nil	9.6	4.4	0.2	8.4	3.6	0.8	nil	0.2	1.0	10.2	24.3	0.2	1.4	17.5	27.7	17.5	11.5	43.4
8	12.4	nil	14.7	1.2	0.2	9.0	3.6	0.2	nil	nil	3.6	8.6	20.3	nil	1.0	25.3	27.1	14.1	12.2	46.6
7	33.5	nil	5.4	2.8	0.2	23.0	5.0	nil	nil	nil	1.8	17.3	3.6	nil	nil	7.3	38.9	31.1	19.2	10.9
6	12.0	nil	18.6	0.4	nil	16.2	7.4	2.6	0.2	nil	5.2	13.3	12.7	0.2	0.2	10.9	30.6	26.9	18.6	24.0
5	33.5	nil	6.9	2.8	nil	17.9	5.7	0.4	nil	nil	2.8	20.0	5.2	nil	nil	4.8	40.3	26.8	22.8	10.1
4	35.2	nil	7.3	5.7	nil	18.0	4.5	0.2	nil	nil	1.6	16.6	4.5	0.2	nil	6.3	42.5	28.3	18.2	10.9
3	72.5	nil	0.2	8.3	nil	8.5	0.6	nil	nil	nil	0.2	6.8	2.1	nil	nil	0.8	72.7	17.4	7.0	2.9
2	41.2	nil	5.4	10.7	0.4	9.7	2.6	0.2	nil	0.2	1.9	20.0	3.9	nil	0.2	3.7	46.6	23.6	22.1	7.7
1 (bottom)	24.2	nil	8.8	4.2	nil	15.9	3.6	0.2	0.2	0.8	4.6	28.0	5.4	nil	0.2	4.0	33.0	24.0	33.4	9.6
Min	12.0	nil	0.2	0.4	nil	8.4	0.6	nil	nil	nil	0.2	6.8	2.1	nil	nil	0.8	27.1	14.1	7.0	2.9
Max	72.5	nil	18.6	10.7	0.4	23.0	7.4	2.6	0.2	0.8	5.2	28.0	24.3	0.2	1.4	25.3	72.7	31.1	33.4	46.6
Mean	31.4	nil	8.5	4.5	0.1	14.1	4.1	0.5	0.1	0.1	2.5	15.6	9.1	0.1	0.3	8.9	39.9	23.3	18.3	18.5
SD	17.6	nil	5.1	3.1	0.1	5.0	1.8	0.8	0.1	0.3	1.6	6.3	7.7	0.1	0.5	7.4	13.2	5.4	7.3	15.2
Hathidari																				
8 (top)	50.0	nil	11.7	9.6	nil	nil	nil	1.1	nil	nil	nil	nil	2.1	2.1	nil	23.4	61.7	10.6	nil	27.7
7	48.1	nil	11.5	2.9	nil	nil	nil	nil	nil	nil	nil	nil	1.0	nil	nil	36.5	59.6	2.9	nil	37.5
6	82.8	nil	4.6	5.2	nil	nil	nil	nil	nil	nil	nil	nil	0.6	nil	nil	6.9	87.4	5.2	nil	7.5
5	35.6	2.2	13.3	8.9	nil	nil	nil	2.2	nil	2.2	nil	nil	nil	nil	nil	35.6	51.1	11.1	2.2	35.6
4	69.4	nil	9.9	2.7	nil	nil	nil	nil	nil	0.9	nil	nil	0.9	nil	nil	16.2	79.3	2.7	0.9	17.1
3	82.3	1.4	0.7	6.8	nil	nil	nil	nil	nil	nil	nil	nil	0.7	nil	nil	8.2	84.4	6.8	nil	8.8
2	56.8	1.8	8.1	6.3	nil	1.8	nil	nil	nil	nil	nil	nil	1.8	1.8	nil	21.6	66.7	8.1	nil	25.2
1 (bottom)	80.2	0.6	2.2	8.2	nil	nil	nil	nil	nil	nil	nil	nil	nil	nil	nil	8.8	83.0	8.2	nil	8.8
Min	35.6	nil	0.7	2.7	nil	nil	nil	nil	nil	nil	nil	nil	nil	nil	nil	6.9	51.1	2.7	nil	7.5
Max	82.8	2.2	13.3	9.6	nil	1.8	nil	2.2	nil	2.2	nil	nil	2.1	2.1	nil	36.5	87.4	11.1	2.2	37.5
Mean	63.1	0.7	7.8	6.3	nil	0.2	nil	0.4	nil	0.4	nil	nil	0.9	0.5	nil	19.7	71.6	7.0	0.4	21.0

Table 4.15 Microlithotype and carbominerite content (vol.%) of different coals seams of Barka Sayal area, South Karanpura Coalfield, Jharkhand, India

	Vte	Lte	Ite	ClV	ClL	ViV	ViI	DuI	DuL	VIL	CLD	DUC	CAnk	CPy	CPoly	CArg	Mo	Bi	Tri	Cmin
SD	16.9	0.9	4.4	2.4	nil	0.6	nil	0.8	nil	0.8	nil	nil	0.7	0.9	nil	11.1	12.7	3.0	0.8	11.4
Bansgarha																				
6 (top)	60.4	0.7	7.2	7.2	nil	3.6	nil	0.7	nil	nil	nil	nil	0.7	nil	nil	19.4	68.4	11.5	nil	20.1
5	72.2	nil	7.4	1.9	nil	6.5	nil	nil	nil	0.9	nil	nil	nil	nil	nil	11.1	79.6	8.3	0.9	11.1
4	49.4	2.0	5.3	7.9	nil	3.3	nil	nil	nil	nil	nil	nil	4.0	nil	nil	28.3	56.6	11.2	nil	32.2
3	61.2	1.8	6.5	5.3	nil	3.5	nil	nil	nil	nil	nil	nil	2.4	nil	nil	19.4	69.4	8.8	nil	21.8
2	68.3	nil	1.7	5.8	nil	nil	nil	1.7	nil	nil	nil	nil	0.8	nil	nil	21.7	70.0	7.5	nil	22.5
1 (bottom)	60.4	0.7	2.2	12.2	nil	0.7	nil	nil	nil	nil	nil	nil	3.6	2.2	2.2	15.8	63.3	13.0	nil	23.7
Min	49.4	nil	1.7	1.9	nil	nil	nil	nil	nil	nil	nil	nil	nil	nil	nil	11.1	56.6	7.5	nil	11.1
Max	72.2	2.0	7.4	12.2	nil	6.5	nil	1.7	nil	0.9	nil	nil	4.0	2.2	2.2	28.3	79.6	13.0	0.9	32.2
Mean	62.0	0.9	5.0	6.7	nil	2.9	nil	0.4	nil	0.2	nil	nil	1.9	0.4	0.4	19.3	67.9	10.1	0.2	21.9
SD	7.2	0.8	2.3	3.1	nil	2.1	nil	0.6	nil	0.4	nil	nil	1.5	0.8	0.8	5.3	7.0	2.0	0.4	6.2

Vte- Vitrite, Lte- Liptite, Ite- Inertite, ClV- Clarite V, ClL- Clarite L, ViV- Vitrinertite V, ViI- Vitrinertite I, DuI- Durite I, DuL- Durite L, VIL- Vitrinertoliptite, CLD- Clarodurite, DUC- Duroclarite, CAnk- Carbankerite, CPy- Carbopyrite, CPoly- Carbopolyminerite, CArg- Carbargilite, Mo- Monomacerals, Bi- Bimacerals, Tri- Trimacerals, Cmin- Total Carbominerite

Table 4.16 Microlithotype content (carbominerite free) basis (vol.%) of different coals seams of Barka Sayal area, South Karanpura Coalfield, Jharkhand, India

	Vte	Lte	Ite	ClV	ClL	ViV	ViI	DuI	DuL	VIL	CLD	DUC	Mo	Bi	Tri
Sayal															
6 (top)	82.0	nil	14.4	1.8	nil	0.9	nil	0.9	nil	nil	nil	nil	96.4	3.6	nil
5	83.1	nil	2.4	14.5	nil	nil	nil	nil	nil	nil	nil	nil	85.5	14.5	nil
4	87.4	nil	3.9	5.5	nil	3.2	nil	nil	nil	nil	nil	nil	91.3	8.7	nil
3	79.0	nil	13.7	5.5	nil	1.8	nil	nil	nil	nil	nil	nil	92.7	7.3	nil
2	65.7	nil	31.4	nil	nil	1.4	nil	1.4	nil	nil	nil	nil	97.2	2.9	nil
1 (bottom)	83.9	nil	12.5	3.6	nil	nil	nil	nil	nil	nil	nil	nil	96.4	3.6	nil
Min	65.7	nil	2.4	nil	nil	nil	nil	nil	nil	nil	nil	nil	85.5	2.9	nil
Max	87.4	nil	31.4	14.5	nil	3.2	nil	1.4	nil	nil	nil	nil	97.2	14.5	nil
Mean	80.2	nil	13.1	5.2	nil	1.2	nil	0.4	nil	nil	nil	nil	93.3	6.8	nil
SD	6.9	nil	9.5	4.6	nil	1.1	nil	0.6	nil	nil	nil	nil	4.1	4.1	nil
Sayal Balkudra															
10 (top)	45.9	nil	17.6	5.7	0.8	11.9	3.7	1.6	0.8	0.4	3.3	8.2	63.5	24.6	11.9
9	71.1	nil	8.7	7.5	0.6	8.1	1.7	0.6	nil	nil	nil	1.7	79.8	18.5	1.7
8	30.7	nil	12.3	13.3	0.5	19.1	2.7	1.9	nil	nil	2.2	17.4	43.0	37.4	19.6
7	60.1	nil	6.9	11.4	nil	14.8	1.8	0.2	nil	nil	nil	4.8	66.9	28.3	4.8
6	46.5	nil	8.0	6.5	0.2	22.5	5.5	nil	nil	nil	1.3	9.5	54.5	34.7	10.7
5	49.0	nil	14.6	11.9	nil	17.9	5.3	nil	nil	nil	nil	1.3	63.6	35.1	1.3
4	44.9	0.2	6.7	10.0	0.9	18.5	3.2	0.2	0.2	0.5	0.7	13.9	51.9	33.1	15.1
3	41.7	nil	7.9	8.3	nil	24.8	5.5	0.5	nil	nil	1.4	10.0	49.5	39.1	11.4
2	36.1	nil	17.9	5.4	1.1	22.1	7.9	1.1	nil	0.4	1.1	7.1	53.9	37.5	8.6
1 (bottom)	37.9	nil	10.2	10.7	1.3	13.5	3.3	nil	nil	0.3	2.0	20.9	48.1	28.8	23.2
Min	30.7	nil	6.7	5.4	nil	8.1	1.7	nil	nil	nil	nil	1.3	43.0	18.5	1.3
Max	71.1	0.2	17.9	13.3	1.3	24.8	7.9	1.9	0.8	0.5	3.3	20.9	79.8	39.1	23.2
Mean	46.4	0.0	11.1	9.1	0.5	17.3	4.1	0.6	0.1	0.2	1.2	9.5	57.5	31.7	10.8
SD	11.2	0.1	4.1	2.6	0.5	5.0	1.8	0.7	0.3	0.2	1.0	6.1	10.4	6.2	6.8
Up. Semana															
11 (top)	13.8	nil	23.7	2.9	nil	6.9	3.7	14.1	nil	1.3	12.8	20.7	37.5	27.7	34.8
10	7.9	nil	22.9	0.6	nil	11.0	7.6	15.2	nil	0.9	14.6	19.2	30.8	34.5	34.8
9	11.8	nil	26.5	1.1	nil	12.1	5.1	8.5	0.3	nil	11.0	23.7	38.3	27.0	34.7
8	17.2	nil	20.9	4.2	0.3	12.7	10.4	4.8	nil	0.9	9.9	18.9	38.0	32.4	29.6
7	13.4	nil	42.4	0.7	nil	9.0	5.6	11.7	0.2	0.2	9.3	7.3	55.9	27.3	16.8
6	25.5	nil	16.5	1.3	nil	21.4	9.2	0.2	nil	nil	6.9	19.0	42.0	32.1	25.9
5	24.2	nil	13.5	1.6	nil	19.2	8.4	2.3	nil	0.5	6.1	24.4	37.7	31.4	30.9
4	16.6	nil	24.1	3.1	0.2	16.6	9.9	2.2	nil	0.2	7.5	19.5	40.7	32.1	27.2
3	8.9	nil	46.2	0.7	nil	11.4	11.9	7.7	0.3	0.3	8.4	4.2	55.1	32.0	12.9
2	12.7	nil	32.5	3.1	0.2	13.2	10.3	5.3	nil	0.2	9.4	13.0	45.2	32.2	22.6
1 (bottom)	24.2	nil	22.2	0.9	nil	15.9	13.5	2.3	nil	0.3	10.7	10.1	46.4	32.6	21.0
Min	7.9	nil	13.5	0.6	nil	6.9	3.7	0.2	nil	nil	6.1	4.2	30.8	27.0	12.9
Max	25.5	nil	46.2	4.2	0.3	21.4	13.5	15.2	0.3	1.3	14.6	24.4	55.9	34.5	34.8
Mean	16.0	nil	26.5	1.9	0.1	13.6	8.7	6.8	0.1	0.4	9.7	16.4	42.5	31.0	26.5
SD	5.9	nil	9.6	1.2	0.1	4.1	2.9	4.9	0.1	0.4	2.4	6.4	7.3	2.4	7.1
Lr. Semana															
9 (top)	31.9	nil	17.0	7.8	0.4	14.9	6.4	1.4	nil	0.4	1.8	18.1	48.9	30.9	20.2
8	23.1	nil	27.6	2.2	0.4	16.8	6.7	0.4	nil	nil	6.7	16.0	50.8	26.5	22.8
7	37.6	nil	6.1	3.2	0.2	25.8	5.7	nil	nil	nil	2.0	19.5	43.7	34.8	21.5
6	15.8	nil	24.4	0.6	nil	21.3	9.8	3.5	0.3	nil	6.9	17.5	40.2	35.3	24.4
5	37.2	nil	7.6	3.1	nil	20.0	6.3	0.5	nil	nil	3.1	22.2	44.8	29.8	25.3
4	39.6	nil	8.2	6.4	nil	20.2	5.0	0.2	nil	nil	1.8	18.6	47.7	31.8	20.5
3	74.7	nil	0.2	8.5	nil	8.7	0.6	nil	nil	nil	0.2	7.0	74.9	17.9	7.2
2	44.7	nil	5.8	11.6	0.5	10.5	2.8	0.2	nil	0.2	2.1	21.6	50.5	25.6	24.0
1 (bottom)	26.8	nil	9.7	4.6	nil	17.6	3.9	0.2	0.2	0.9	5.1	31.0	36.5	26.6	37.0

Table 4.16 Microlithotype content (carbominerite free) basis (vol.%) of different coals seams of Barka Sayal area, South Karanpura Coalfield, Jharkhand, India

	Vte	Lte	Ite	ClV	ClL	ViV	ViI	DuI	DuL	VIL	CLD	DUC	Mo	Bi	Tri
Min	15.8	nil	0.2	0.6	nil	8.7	0.6	nil	nil	nil	0.2	7.0	36.5	17.9	7.2
Max	74.7	nil	27.6	11.6	0.5	25.8	9.8	3.5	0.3	0.9	6.9	31.0	74.9	35.3	37.0
Mean	36.8	nil	11.9	5.3	0.2	17.3	5.2	0.7	0.1	0.2	3.3	19.1	48.7	28.8	22.5
SD	15.8	nil	8.7	3.3	0.2	5.1	2.5	1.1	0.1	0.3	2.2	5.9	10.3	5.1	7.2
Hathidari															
8 (top)	69.1	nil	16.2	13.2	nil	nil	nil	1.5	nil	nil	nil	nil	85.3	14.7	nil
7	76.9	nil	18.5	4.6	nil	nil	nil	nil	nil	nil	nil	nil	95.4	4.6	nil
6	89.4	nil	5.0	5.6	nil	nil	nil	nil	nil	nil	nil	nil	94.4	5.6	nil
5	55.2	3.5	20.7	13.8	nil	nil	nil	3.5	nil	3.5	nil	nil	79.3	17.2	3.5
4	83.7	nil	12.0	3.3	nil	nil	nil	nil	nil	1.1	nil	nil	95.7	3.3	1.1
3	90.3	1.5	0.8	7.5	nil	nil	nil	nil	nil	nil	nil	nil	92.5	7.5	nil
2	75.9	2.4	10.9	8.4	nil	2.4	nil	nil	nil	nil	nil	nil	89.2	10.8	nil
1 (bottom)	88.0	0.6	2.4	9.0	nil	nil	nil	nil	nil	nil	nil	nil	91.0	9.0	nil
Min	55.2	nil	0.8	3.3	nil	nil	nil	nil	nil	nil	nil	nil	79.3	3.3	nil
Max	90.3	3.5	20.7	13.8	nil	2.4	nil	3.5	nil	3.5	nil	nil	95.7	17.2	3.5
Mean	78.6	1.0	10.8	8.2	nil	0.3	nil	0.6	nil	0.6	nil	nil	90.3	9.1	0.6
SD	11.3	1.2	7.0	3.6	nil	0.8	nil	1.2	nil	1.2	nil	nil	5.3	4.6	1.2
Bansgarha															
6 (top)	75.7	0.9	9.0	9.0	nil	4.5	nil	0.9	nil	nil	nil	nil	85.6	14.4	nil
5	81.2	nil	8.3	2.1	nil	7.3	nil	nil	nil	1.0	nil	nil	89.6	9.4	1.0
4	72.8	2.9	7.8	11.6	nil	4.9	nil	nil	nil	nil	nil	nil	83.5	16.5	nil
3	78.2	2.3	8.3	6.8	nil	4.5	nil	nil	nil	nil	nil	nil	88.7	11.3	nil
2	88.2	nil	2.2	7.5	nil	nil	nil	2.2	nil	nil	nil	nil	90.3	9.7	nil
1 (bottom)	79.3	0.9	2.8	16.0	nil	0.9	nil	nil	nil	nil	nil	nil	83.0	17.0	nil
Min	72.8	nil	2.2	2.1	nil	nil	nil	nil	nil	nil	nil	nil	83.0	9.4	nil
Max	88.2	2.9	9.0	16.0	nil	7.3	nil	2.2	nil	1.0	nil	nil	90.3	17.0	1.0
Mean	79.2	1.2	6.4	8.9	nil	3.7	nil	0.5	nil	0.2	nil	nil	86.8	13.0	0.2
SD	4.8	1.1	2.8	4.3	nil	2.5	nil	0.8	nil	0.4	nil	nil	2.9	3.1	0.4

Vte- Vitrite, Lte- Liptite, Ite- Inertite, ClV- Clarite V, ClL- Clarite L, ViV- Vitrinertite V, ViI- Vitrinertite I, DuI- Durite I, DuL- Durite L, VIL- Vitrinertoliptite, CLD- Clarodurite, DUC- Duroclarite, Mo- Monomacerals, Bi- Bimacerals, Tri- Trimacerals.

4.9.2 Quantitative distribution of microscopic constituents in Coal seams of the Argada Area

4.9.2.1 Macerals

The quantitative analysis of maceral content, with the visible mineral matter of the Argada area, is presented in Table 4.16, while Table 4.17 presents the maceral content of the coals of the Argada area on a mineral matter free basis. All the seams belonging to the Argada area are inertinite rich. The important coals seams belonging to the Argada area are Argada, Argada-A, Argada-B, Argada-C, Argada-D, Argada-I, and Argada-J. In the coals of Argada area, the inertinite content ranges from 9.4% to 68.8%, mean 39.7% (10.8% - 87.2%, mean 48.5%, mmf basis). The vitrinite content of the coals of the Argada area varies from nil to 70.1%, mean 33.2% (nil - 79.6%, mean 39.0%, mineral matter free basis). The liptinite content in the coals of Argada area varies in between 0.4% and 23.8%, mean 10.5% (0.8%- 25.8%, mean 12.5%, mmf basis). Collotelinite is the dominant maceral of the vitrinite group, sporinite is dominant among liptinite, whereas inertinite inertodetrinite and semifusinite are present in high amounts. Figure 4.20 to Figure 4.26 presents the macro-petrographic section, microscopic (maceral and microlithotype) seam profiles, and range of mean vitrinite reflectance of different coal seams of Argada area of South Karanpura Coalfield.

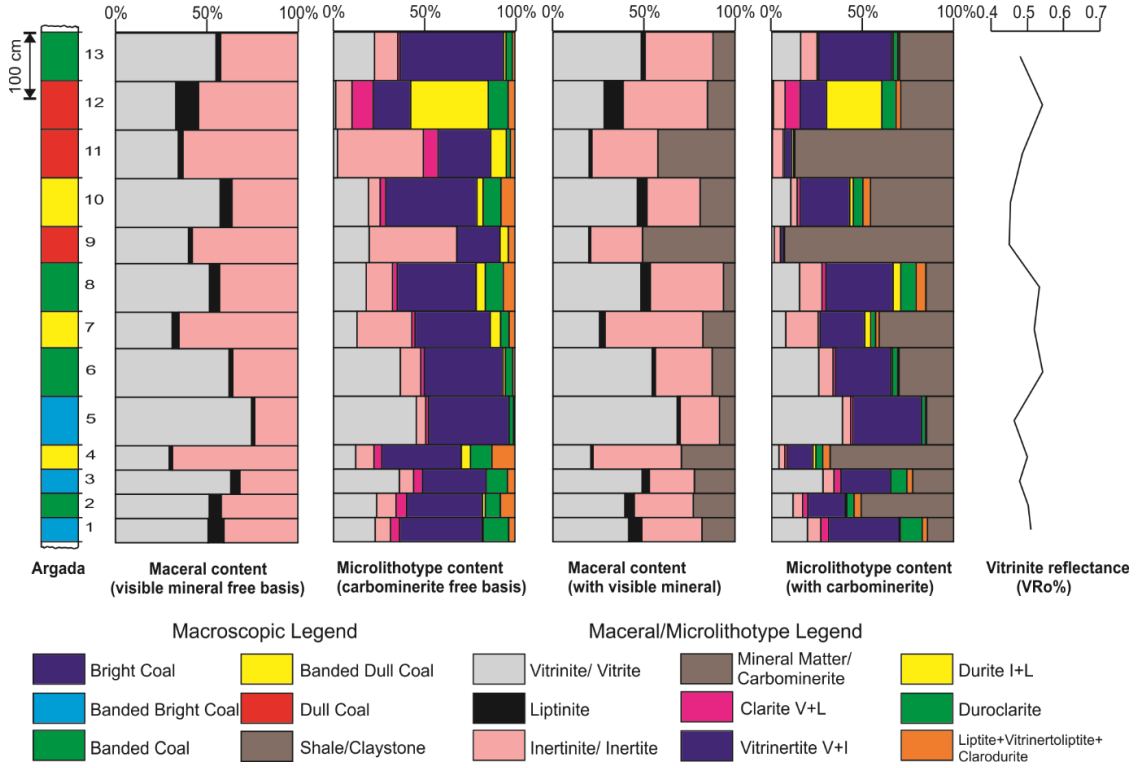


Figure 4.20 Macro-petrographic section, microscopic (maceral and microlithotype) seam profiles and range of mean vitrinite reflectance of Argada Seam, South Karanpura Coalfield, Jharkhand.

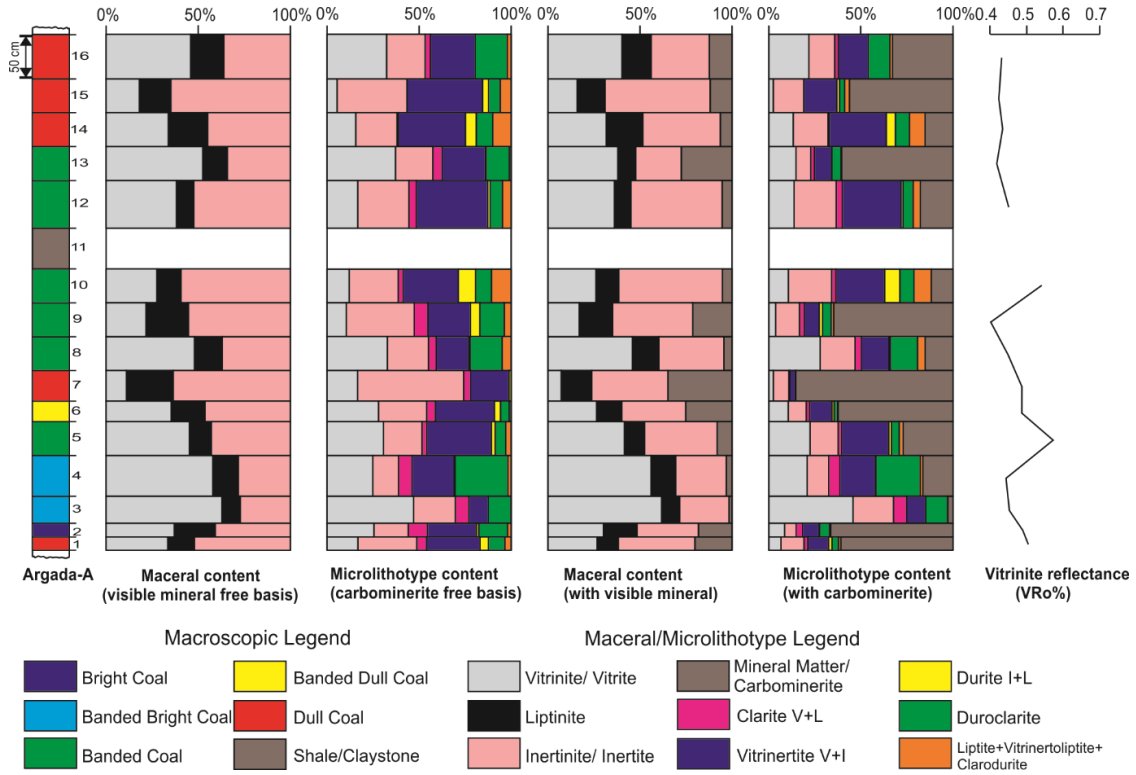


Figure 4.21 Macro-petrographic section, microscopic (maceral and microlithotype) seam profiles and range of mean vitrinite reflectance of Argada A Seam, South Karanpura Coalfield, Jharkhand.

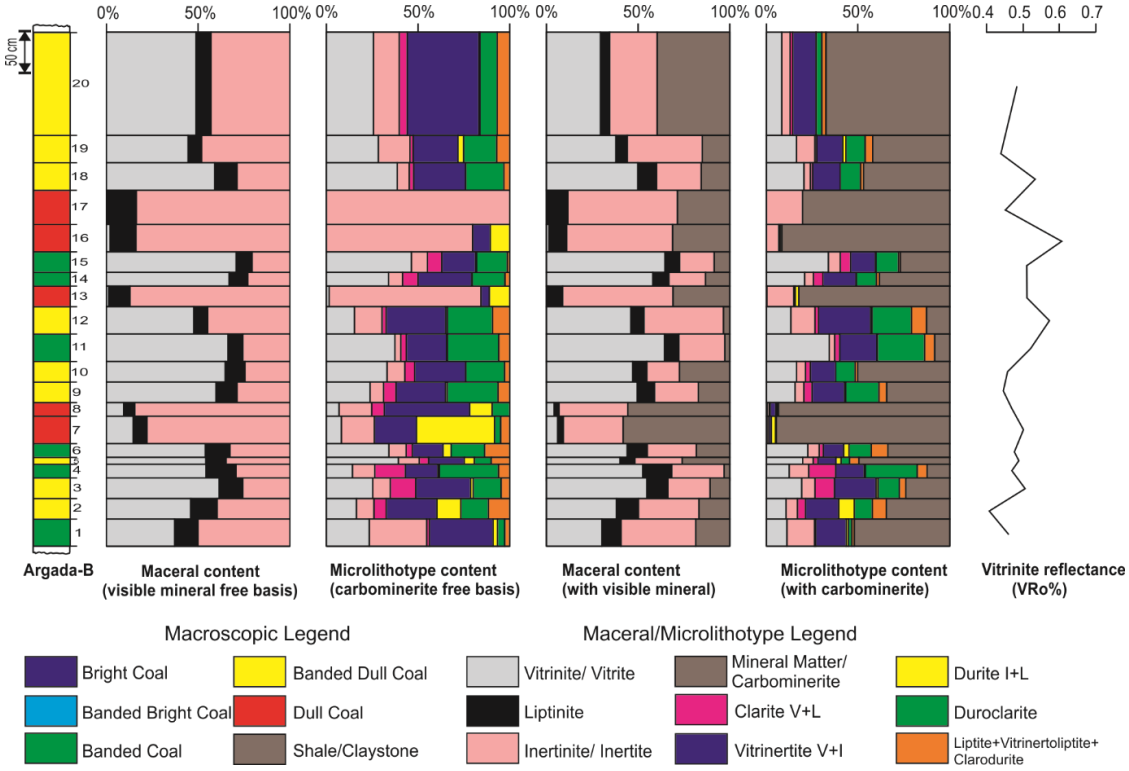


Figure 4.22 Macro-petrographic section, microscopic (maceral and microlithotype) seam profiles and range of mean vitrinite reflectance of Argada-B Seam, South Karanpura Coalfield, Jharkhand.

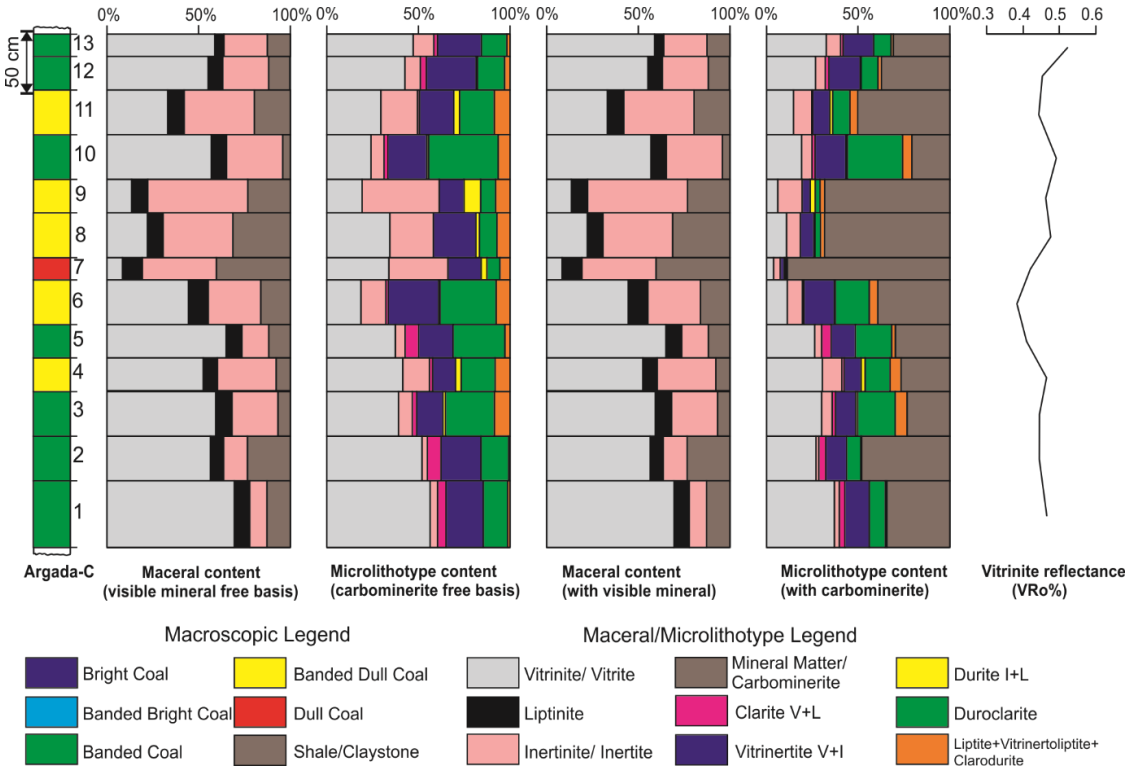


Figure 4.23 Macro-petrographic section, microscopic (maceral and microlithotype) seam profiles and range of mean vitrinite reflectance of Argada-C Seam, South Karanpura Coalfield, Jharkhand.

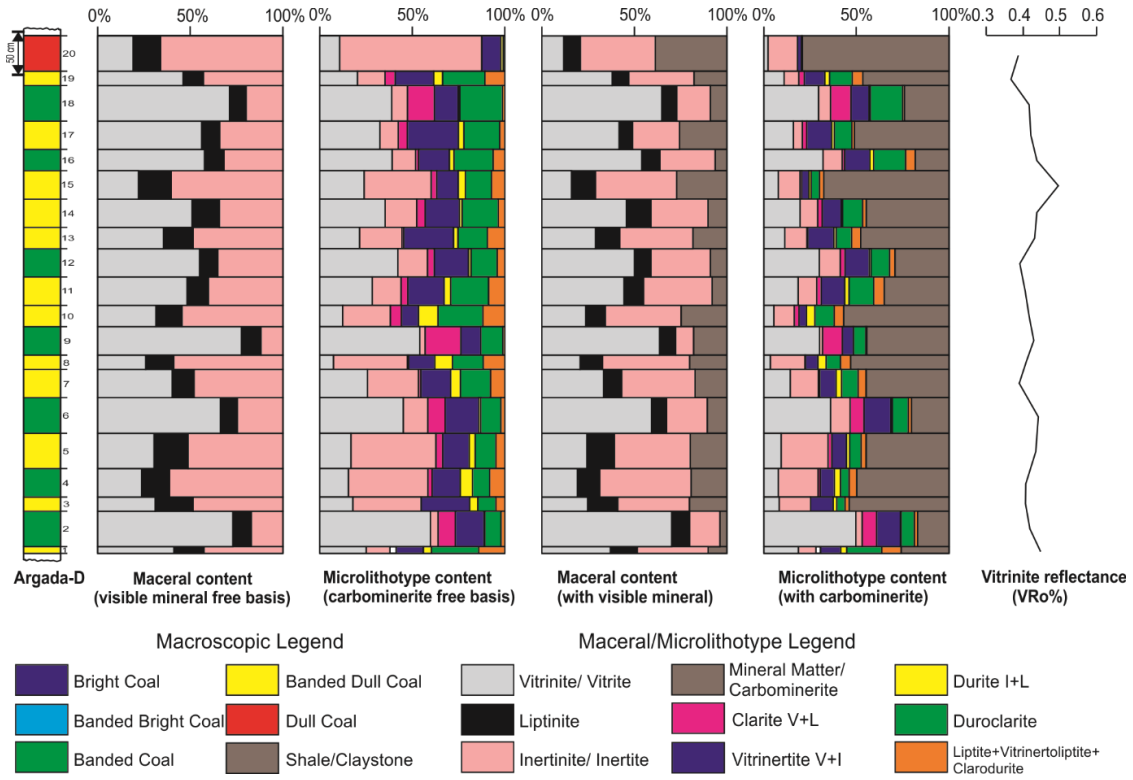


Figure 4.24 Macro-petrographic section, microscopic (maceral and microlithotype) seam profiles and range of mean vitrinite reflectance of Argada-D Seam, South Karanpura Coalfield, Jharkhand.

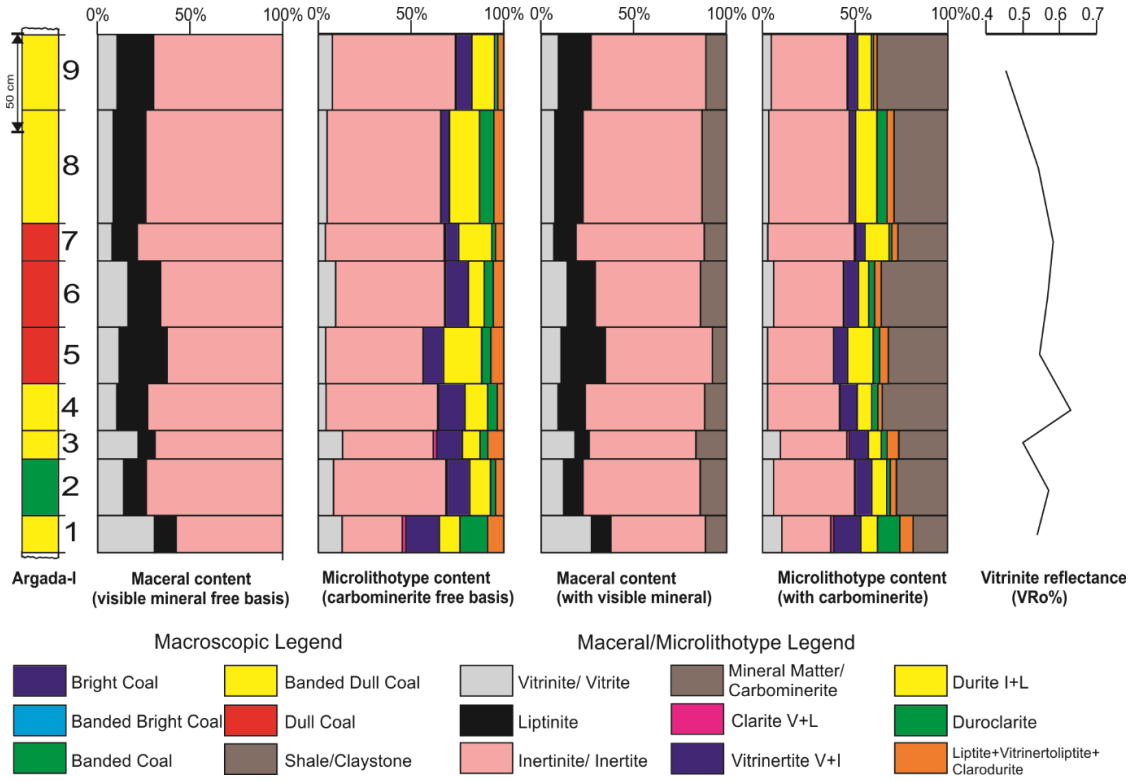


Figure 4.25 Macro-petrographic section, microscopic (maceral and microlithotype) seam profiles and range of mean vitrinite reflectance of Argada-I Seam, South Karanpura Coalfield, Jharkhand.

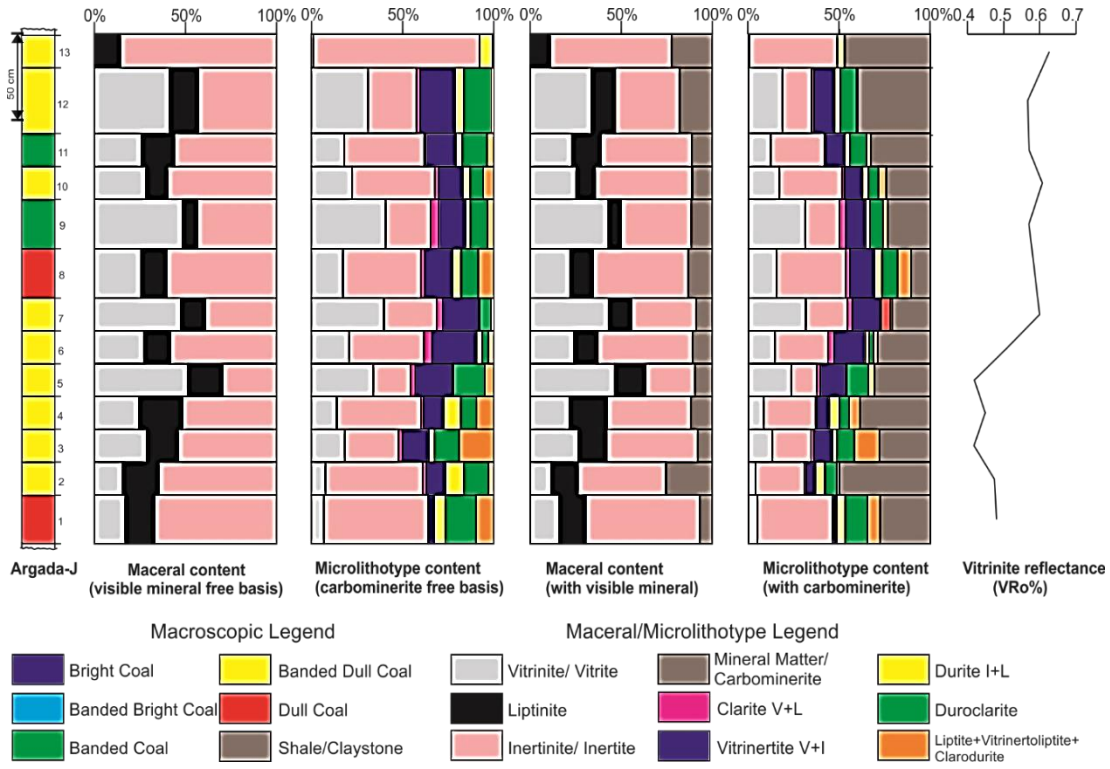


Figure 4.26 Macro-petrographic section, microscopic (maceral and microlithotype) seam profiles and range of mean vitrinite reflectance of Argada-J Seam, South Karanpura Coalfield, Jharkhand.

4.9.2.2 Mineral matter

Coal seams of the Argada area have visible mineral matter in the range of 1.8% to 58.2%, a mean of 16.6%. In these coals, argillaceous minerals, carbonate minerals, and pyrite are easily visible and distinguishable minerals at the microscopic level. The argillaceous minerals in these coals are ranging from nil to 28.6%, mean 6.2%. In the coals of the Argada area, carbonate minerals range from 0.2% to 52.2%, mean 10.3%, while pyrite in these coals lies in the range of nil to 1.4%, mean 0.1%. Table 4.16 presents the quantitative distribution of different types of minerals in the coals of the Argada area of South Karanpura coalfield.

The coals of the Argada seam of this area possess a high concentration of Argillaceous minerals ranging from 1% to 28.6%, mean 10.9%, followed by carbonate minerals having a range between 0.2% and 47.8%, mean 9.9% and pyrite lying in between nil and 1.4%, mean 0.6%.

4.9.2.3 Microlithotype concentration

In case of microlithotype, the coals of Argada area are inertite-rich, concentration ranging from 1% to 48.1%, mean 16.4% (2.8%-100%, mean 29.3%, carbominerite free basis) followed by vitrite, ranging from nil to 49.7%, mean 14.7% (nil-59.9%, mean 23.1%, carbominerite free basis); vitrinertite-V from nil to 33.1%, mean 9.7% (nil-43.8%, mean 16.1%, carbominerite free basis), duroclarite from nil to 30.1%, mean 7.7% (nil-37.9%, mean 10.7%, carbominerite free basis), vitrinertite-I from nil to 12.6%, mean 3.5% (nil-19.6%, mean 5.9%, carbominerite free basis). All other microlithotypes such as liptite, clarite-V, clarite-L, durite-I, durite-L, vitrinertoliptite, and clarodurite are in less concentration (mean values <3% for each). Table 4.18 presents the quantitative distribution of different microlithotype present in the coal seams of the Argada area, while Table 4.19 presents microlithotype content present in these seams carbominerite free basis.

4.9.2.4 Carbominerite concentration

In case of carbominerite concentration of the Argada area, the carbankerite is the most dominant (0.2%- 87.6%, mean 24.9%) followed by carbargilite (nil - 54.2%, mean 13%), carbopolyminerite (nil-12.5%, mean 1.6%) and carbopyrite (nil-1.3%, mean 0.1%). Table 4.18 presents the quantitative distribution of different carbominerite present in the coal seams of the Argada area.

Table 4.17 Maceral and mineral matter content (vol.%) of different coal seams of Argada area, South Karanpura coalfield, India

	Tl	Ctl	Vdr	Cdr	Cgl	Gl	DV	SV	Spo	Cut	Res	Alg	Sub	Ldr	Flo	Exu	Bit	Micr	Macr	Sfu	Fu	Scr	Idr	Arg	Carb	Py	Vit	Lipt	Inert	MM
Argada																														
13 (top)	7.6	24.2	10.0	6.0	0.8	0.2	nil	nil	0.8	0.8	0.2	nil	nil	nil	nil	nil	nil	2.4	nil	7.8	7.0	nil	19.8	6.6	5.2	0.6	48.8	1.8	37.0	12.4
12	0.8	4.0	21.4	1.4	0.6	nil	nil	nil	7.8	1.2	1.4	nil	nil	nil	nil	nil	nil	1.2	0.2	20.2	6.0	nil	18.6	4.0	11.2	nil	28.2	10.4	46.2	15.2
11	1.6	2.6	10.4	5.6	nil	nil	nil	nil	0.4	0.2	0.4	nil	nil	nil	nil	nil	nil	0.2	nil	11.4	3.6	nil	21.4	6.6	34.8	0.8	20.2	1.0	36.6	42.2
10	10.6	14.6	16.0	4.4	0.6	0.2	nil	0.2	3.6	0.2	0.8	nil	nil	0.4	nil	nil	nil	0.6	0.2	7.4	5.4	nil	15.6	7.2	11.8	0.2	46.6	5.0	29.2	19.2
9	2.6	4.4	8.8	3.6	0.2	0.6	nil	nil	nil	0.2	0.2	nil	nil	nil	nil	nil	nil	nil	nil	3.0	5.0	nil	20.6	2.0	47.8	1.0	20.2	0.4	28.6	50.8
8	7.2	22.8	16.6	2.0	nil	nil	nil	nil	2.8	0.4	1.8	nil	nil	nil	nil	nil	nil	0.4	0.2	14.2	10.4	nil	14.8	3.6	2.8	nil	48.6	5.0	40.0	6.4
7	3.0	12.6	6.0	3.8	0.2	0.2	0.2	nil	0.6	1.4	0.8	nil	nil	nil	nil	nil	nil	0.2	1.8	10.6	19.8	nil	21.2	11.2	5.0	1.4	26.0	2.8	53.6	17.6
6	1.0	41.6	7.2	4.6	0.2	0.2	nil	nil	0.6	0.4	0.6	nil	nil	nil	nil	nil	nil	0.8	1.2	6.8	8.4	nil	13.8	11.4	0.4	0.8	54.8	1.6	31.0	12.6
5	12.2	41.4	8.4	4.0	1.8	0.8	nil	nil	0.4	0.4	0.4	nil	nil	nil	nil	nil	nil	2.8	0.4	3.6	6.2	nil	8.4	1.0	6.8	1.0	68.6	1.2	21.4	8.8
4	2.4	9.2	7.8	1.0	0.4	nil	0.2	nil	nil	0.6	0.6	nil	nil	nil	nil	nil	nil	nil	1.2	10.0	2.6	nil	34.6	28.6	0.4	0.4	21.0	1.2	48.4	29.4
3	5.2	25.4	13.4	2.8	1.0	nil	1.2	nil	1.8	1.2	0.6	nil	nil	0.2	nil	nil	nil	0.8	1.0	5.2	4.2	nil	13.6	21.6	0.2	0.6	49.0	3.8	24.8	22.4
2	7.2	15.6	10.8	4.2	1.0	nil	1.0	nil	2.4	nil	1.2	1.2	nil	0.2	nil	nil	nil	0.4	2.6	9.6	6.6	nil	13.2	22.0	0.2	0.6	39.8	5.0	32.4	22.8
1 (bottom)	5.6	24.0	8.4	2.8	0.8	0.2	nil	nil	3.8	1.0	1.0	nil	nil	1.2	nil	nil	nil	2.0	2.6	4.2	8.8	nil	15.4	15.6	2.0	0.6	41.8	7.0	33.0	18.2
Min	0.8	2.6	6.0	1.0	nil	nil	nil	nil	nil	nil	0.2	nil	nil	nil	nil	nil	nil	nil	nil	3.0	2.6	nil	8.4	1.0	0.2	nil	20.2	0.4	21.4	6.4
Max	12.2	41.6	21.4	6.0	1.8	0.8	1.2	0.2	7.8	1.4	1.8	1.2	nil	1.2	nil	nil	nil	2.8	2.6	20.2	19.8	nil	34.6	28.6	47.8	1.4	68.6	10.4	53.6	50.8
Mean	5.2	18.7	11.2	3.6	0.6	0.2	0.2	0.0	1.9	0.6	0.8	0.1	nil	0.2	nil	nil	nil	0.9	0.9	8.8	7.2	nil	17.8	10.9	9.9	0.6	39.5	3.6	35.6	21.4
SD	3.5	12.4	4.3	1.5	0.5	0.2	0.4	0.1	2.1	0.4	0.5	0.3	nil	0.3	nil	nil	nil	0.9	0.9	4.6	4.2	nil	6.1	8.3	14.1	0.4	14.7	2.8	9.1	12.3
Argada-A																														
16 (top)	nil	36.8	2.5	0.3	0.6	nil	nil	nil	8.3	nil	1.1	nil	nil	5.0	nil	1.1	0.3	0.8	nil	8.9	8.3	nil	13.6	7.8	4.7	nil	40.2	15.8	31.6	12.5
15	nil	12.3	3.4	0.1	nil	nil	0.1	nil	11.2	0.1	0.5	nil	nil	2.7	0.1	0.3	0.3	0.5	0.3	15.9	3.4	nil	37.2	4.3	7.6	nil	15.9	15.1	57.1	11.9
14	nil	28.2	2.2	0.6	0.3	0.3	nil	nil	10.1	0.9	0.6	nil	0.3	6.1	nil	1.5	0.3	0.3	nil	18.1	6.4	nil	17.2	4.3	2.2	nil	31.6	19.9	42.0	6.4
13	0.2	34.0	2.8	0.7	nil	nil	0.1	nil	5.9	0.1	0.4	nil	nil	2.7	0.2	0.1	0.2	0.7	nil	7.3	4.0	0.1	12.6	5.1	22.6	nil	37.9	9.6	24.8	27.7
12	nil	31.9	3.8	0.3	0.1	nil	nil	nil	5.7	0.3	0.4	nil	nil	1.9	nil	0.5	0.3	1.3	nil	21.2	8.2	nil	18.8	1.6	3.9	nil	36.1	8.9	49.5	5.5
11																														
10	nil	25.4	nil	nil	0.6	nil	nil	nil	7.1	0.6	1.2	nil	0.6	2.4	nil	0.6	nil	0.6	nil	29.6	6.5	nil	19.5	2.4	3.0	nil	26.0	12.4	56.2	5.3
9	nil	14.7	2.0	0.3	nil	nil	nil	nil	13.2	0.3	0.4	nil	nil	2.3	nil	1.3	0.6	0.6	0.2	17.7	1.5	nil	23.6	7.1	14.2	nil	17.0	18.2	43.5	21.4
8	0.2	42.1	2.3	0.7	0.3	nil	0.2	nil	8.6	0.2	0.5	nil	nil	2.7	nil	2.5	nil	0.5	nil	10.5	13.3	nil	11.1	3.5	1.0	nil	45.8	14.4	35.3	4.5
7	nil	5.4	1.5	0.2	nil	nil	0.2	nil	10.6	0.2	0.2	nil	nil	4.4	0.2	1.0	0.2	0.8	0.2	10.6	1.0	nil	28.9	16.7	18.2	nil	7.1	16.6	41.4	34.9
6	nil	22.0	3.2	1.0	nil	0.2	nil	nil	9.3	nil	0.2	nil	nil	2.1	0.4	1.7	nil	1.0	nil	8.4	5.1	nil	20.3	8.0	17.3	nil	26.4	13.7	34.7	25.2
5	nil	37.5	2.9	1.0	nil	0.2	nil	nil	6.9	0.6	0.4	nil	nil	2.1	0.2	0.8	nil	0.8	0.2	10.1	7.1	nil	21.3	5.5	2.7	nil	41.5	10.9	39.4	8.2
4	0.1	50.4	3.8	1.3	0.3	0.1	nil	nil	6.7	nil	1.5	nil	nil	3.4	0.3	1.5	nil	1.8	nil	5.3	10.6	nil	9.7	1.4	1.8	nil	55.9	13.4	27.4	3.2
3	0.9	57.2	2.3	1.2	nil	nil	nil	nil	5.3	0.4	0.7	nil	nil	2.1	0.2	0.9	0.4	nil	nil	3.9	17.3	nil	5.5	0.9	0.9	nil	61.7	9.9	26.7	1.8
2	0.5	22.2	6.5	0.3	0.3	0.3	nil	nil	10.5	0.3	0.6	nil	nil	4.3	nil	1.4	1.1	1.1	0.5	6.8	3.0	0.3	21.6	7.5	10.9	nil	30.1	18.2	33.3	18.4
1 (bottom)	0.3	20.1	5.7	0.2	nil	nil	0.2	0.2	4.6	0.8	1.3	nil	nil	2.9	nil	1.3	0.8	1.1	0.3	14.0	3.7	0.2	22.4	5.7	14.6	nil	26.6	11.6	41.5	20.3
Min	nil	5.4	nil	nil	nil	nil	nil	nil	4.6	nil	0.2	nil	nil	1.9	nil	0.1	nil	nil	nil	3.9	1.0	nil	5.5	0.9	0.9	nil	7.1	8.9	24.8	1.8

Table 4.17 Maceral and mineral matter content (vol.%) of different coal seams of Argada area, South Karanpura coalfield, India

	Tl	Ctl	Vdr	Cdr	Cgl	Gl	DV	SV	Spo	Cut	Res	Alg	Sub	Ldr	Flo	Exu	Bit	Micr	Macr	Sfu	Fu	Scr	Idr	Arg	Carb	Py	Vit	Lipt	Inert	MM
Max	0.9	57.2	6.5	1.3	0.6	0.3	0.2	0.2	13.2	0.9	1.5	nil	0.6	6.1	0.4	2.5	1.1	1.8	0.5	29.6	17.3	0.3	37.2	16.7	22.6	nil	61.7	19.9	57.1	34.9
Mean	0.2	29.4	3.0	0.5	0.2	0.1	0.1	0.0	8.3	0.3	0.7	nil	0.1	3.1	0.1	1.1	0.3	0.8	0.1	12.5	6.6	0.0	18.9	5.5	8.4	nil	33.3	13.9	39.0	13.8
SD	0.2	13.7	1.5	0.4	0.2	0.1	0.1	0.0	2.4	0.3	0.4	nil	0.2	1.2	0.1	0.6	0.3	0.4	0.1	6.7	4.3	0.1	7.7	3.8	7.0	nil	14.2	3.3	9.6	9.9
Argada- B																														
20 (top)	0.4	20.0	5.4	1.6	1.8	nil	nil	0.2	2.8	nil	0.2	nil	nil	1.0	nil	0.8	0.2	0.2	nil	6.6	3.4	nil	15.6	nil	39.8	nil	29.4	5.0	25.8	39.8
19	0.6	28.6	7.2	1.0	0.4	nil	nil	nil	3.8	nil	0.2	nil	nil	1.0	0.2	1.0	nil	0.6	0.4	13.6	6.4	0.2	19.8	0.6	14.4	nil	37.8	6.2	41.0	15.0
18	0.2	38.4	8.6	1.8	0.8	nil	nil	nil	5.4	0.6	0.2	nil	nil	1.6	0.2	2.0	0.2	1.0	nil	5.2	2.2	0.4	15.6	0.2	15.4	nil	49.8	10.2	24.4	15.6
17	nil	nil	nil	nil	nil	nil	nil	nil	5.2	nil	0.2	nil	nil	3.2	nil	2.4	0.6	nil	0.4	16.8	9.8	nil	32.8	8.2	20.4	nil	nil	11.6	59.8	28.6
16	nil	1.0	0.4	nil	nil	nil	nil	nil	3.4	0.2	0.2	nil	nil	3.6	nil	2.2	nil	nil	0.4	18.2	1.0	nil	38.2	15.2	16.0	nil	1.4	9.6	57.8	31.2
15	1.6	47.8	6.6	2.4	5.0	0.8	nil	0.4	2.4	1.0	1.0	nil	nil	1.6	0.2	1.8	nil	2.0	0.4	6.0	4.2	nil	6.2	0.2	8.4	nil	64.6	8.0	18.8	8.6
14	0.4	43.2	7.8	2.6	2.8	0.2	nil	1.0	3.8	0.2	0.6	nil	nil	2.0	0.2	2.0	nil	0.8	0.4	6.4	3.2	nil	9.2	1.0	12.2	nil	58.0	8.8	20.0	13.2
13	nil	0.8	nil	nil	nil	nil	nil	nil	3.4	nil	0.4	nil	nil	2.2	nil	1.8	0.2	nil	0.4	18.4	6.4	nil	35.0	24.8	6.2	nil	0.8	8.0	60.2	31.0
12	0.6	39.2	4.6	1.0	0.2	nil	nil	0.4	3.6	0.6	0.2	nil	nil	0.4	0.2	2.2	nil	1.2	0.6	12.8	7.2	nil	21.6	nil	3.4	nil	46.0	7.2	43.4	3.4
11	2.0	52.6	2.8	3.6	2.4	nil	0.2	0.8	4.4	0.6	0.2	nil	nil	1.4	0.2	1.0	nil	2.4	0.6	6.0	3.8	nil	12.2	0.4	2.4	nil	64.4	7.8	25.0	2.8
10	0.6	36.8	4.4	2.0	2.8	nil	nil	0.4	3.4	nil	0.4	nil	nil	1.8	0.2	2.0	nil	0.4	0.6	3.6	3.8	nil	9.4	1.6	25.8	nil	47.0	7.8	17.8	27.4
9	2.4	36.0	8.0	2.8	0.2	nil	nil	nil	4.4	0.4	0.8	nil	nil	1.2	nil	2.6	0.2	0.6	0.6	8.0	3.2	nil	11.4	1.6	15.6	nil	49.4	9.6	23.8	17.2
8	0.2	2.6	1.4	nil	nil	nil	nil	nil	0.8	nil	0.2	nil	nil	1.2	nil	0.4	nil	0.4	0.4	7.8	0.2	nil	28.8	3.2	52.2	0.2	4.2	2.6	37.6	55.6
7	nil	2.2	3.2	0.6	nil	nil	nil	nil	0.8	0.2	0.2	nil	nil	0.8	nil	1.2	nil	0.2	0.8	6.6	1.2	nil	23.8	7.4	50.8	nil	6.0	3.2	32.6	58.2
6	0.6	36.6	5.0	1.6	0.2	nil	nil	nil	5.6	0.4	0.4	nil	nil	2.2	nil	2.2	0.2	nil	0.2	12.2	4.8	nil	9.6	3.4	14.8	nil	44.0	11.0	26.8	18.2
5	0.4	31.2	7.8	0.4	0.2	nil	nil	nil	3.6	0.6	1.0	nil	nil	1.2	nil	1.6	0.2	nil	0.4	12.2	2.8	nil	10.4	6.6	19.0	0.4	40.0	8.2	25.8	26.0
4	2.0	42.0	7.2	0.6	0.6	nil	nil	0.2	10.6	0.6	0.6	nil	nil	2.2	0.2	1.6	nil	1.4	0.6	7.8	10.4	nil	8.4	0.2	2.2	0.6	52.6	15.8	28.6	3.0
3	4.0	39.8	7.6	1.4	1.8	nil	nil	0.2	5.8	1.2	1.0	nil	0.2	1.2	0.2	1.6	0.2	0.2	0.4	8.8	5.4	nil	8.2	1.6	9.2	nil	54.8	11.4	23.0	10.8
2	0.8	27.8	8.4	1.2	nil	nil	nil	nil	6.2	1.4	0.8	nil	nil	1.6	0.2	1.6	0.2	0.8	0.6	12.8	5.2	nil	13.6	6.0	10.8	nil	38.2	12.0	33.0	16.8
1 (bottom)	6.8	10.6	6.8	4.6	0.8	0.4	nil	0.2	5.8	1.2	nil	nil	0.2	1.4	0.2	1.4	0.2	1.0	nil	12.4	10.4	nil	17.0	10.6	8.0	nil	30.2	10.4	40.8	18.6
Min	nil	nil	nil	nil	nil	nil	nil	nil	0.8	nil	nil	nil	nil	0.4	nil	0.4	nil	nil	nil	3.6	0.2	nil	6.2	nil	2.2	nil	nil	2.6	17.8	2.8
Max	6.8	52.6	8.6	4.6	5.0	0.8	0.2	1.0	10.6	1.4	1.0	nil	0.2	3.6	0.2	2.6	0.6	2.4	0.8	18.4	10.4	0.4	38.2	24.8	52.2	0.6	64.6	15.8	60.2	58.2
Mean	1.2	26.9	5.2	1.5	1.0	0.1	0.0	0.2	4.3	0.5	0.4	nil	0.0	1.6	0.1	1.7	0.1	0.7	0.4	10.1	4.8	0.0	17.3	4.6	17.4	0.1	35.9	8.7	33.3	22.1
SD	1.6	17.2	2.9	1.2	1.3	0.2	0.0	0.3	2.1	0.4	0.3	nil	0.1	0.8	0.1	0.6	0.2	0.7	0.2	4.3	2.9	0.1	9.5	6.2	14.2	0.2	21.4	3.0	13.1	15.2
Argada- C																														
13 (top)	0.8	53.8	2.8	nil	1.0	nil	nil	0.4	2.6	0.2	nil	nil	nil	1.2	nil	1.0	nil	nil	nil	10.0	1.8	nil	11.8	1.6	11.0	nil	58.8	5.0	23.6	12.6
12	nil	48.6	4.8	1.0	0.6	nil	nil	0.2	4.4	nil	0.2	nil	nil	1.6	0.2	1.4	0.2	0.4	0.2	6.8	3.2	nil	14.4	0.2	11.6	nil	55.2	8.0	25.0	11.8
11	0.5	27.7	3.7	0.6	0.3	nil	0.1	0.3	5.9	0.2	0.3	nil	nil	1.5	0.1	1.0	0.1	0.8	0.1	14.0	4.8	nil	18.7	0.5	19.2	nil	33.1	9.0	38.3	19.7
10	0.6	49.4	3.8	2.2	0.2	0.2	0.4	nil	5.2	0.2	0.2	nil	nil	1.2	0.2	1.4	nil	1.6	0.2	12.0	2.4	nil	14.4	0.4	3.8	nil	56.8	8.4	30.6	4.2
9	nil	11.6	1.6	nil	0.2	nil	nil	nil	6.8	0.2	0.2	nil	nil	1.0	0.2	0.4	nil	1.2	nil	19.0	4.2	nil	30.2	1.2	22.0	nil	13.4	8.8	54.6	23.2
8	0.2	18.6	2.0	0.2	0.2	nil	nil	0.8	5.6	0.2	0.2	nil	nil	1.8	0.2	0.6	nil	0.8	0.2	13.2	3.4	nil	20.4	0.6	30.8	nil	22.0	8.6	38.0	31.4
7	0.2	7.0	0.8	0.4	nil	nil	nil	nil	8.4	0.2	0.4	nil	nil	1.2	nil	0.4	0.2	0.2	nil	12.0	1.2	nil	27.0	0.6	39.8	nil	8.4	10.8	40.4	40.4

Table 4.17 Maceral and mineral matter content (vol.%) of different coal seams of Argada area, South Karanpura coalfield, India

	Tl	Ctl	Vdr	Cdr	Cgl	Gl	DV	SV	Spo	Cut	Res	Alg	Sub	Ldr	Flo	Exu	Bit	Micr	Macr	Sfu	Fu	Scr	Idr	Arg	Carb	Py	Vit	Lipt	Inert	MM
6	0.6	36.2	5.6	1.6	0.4	nil	nil	nil	7.2	0.2	0.6	nil	nil	1.0	nil	1.8	nil	0.8	nil	8.0	6.2	nil	13.6	nil	16.2	nil	44.4	10.8	28.6	16.2
5	0.8	52.6	5.0	1.2	5.4	nil	nil	nil	4.2	0.4	0.6	nil	nil	2.0	0.2	1.2	nil	1.0	nil	3.6	4.8	nil	5.2	nil	11.6	0.2	65.0	8.6	14.6	11.8
4	1.2	44.4	5.6	0.4	0.4	nil	0.2	0.2	4.0	0.2	0.2	nil	nil	2.0	nil	1.2	0.2	0.4	nil	15.8	5.2	nil	10.6	nil	7.8	nil	52.4	7.8	32.0	7.8
3	1.2	48.4	7.0	0.6	0.8	nil	0.6	0.6	4.8	0.2	0.2	nil	nil	1.6	nil	2.0	0.2	0.8	0.2	7.4	5.0	nil	11.6	nil	6.8	nil	59.2	9.0	25.0	6.8
2	0.2	42.8	8.6	1.4	3.4	nil	nil	nil	2.6	nil	0.6	nil	nil	1.6	nil	2.4	nil	0.4	0.6	2.8	1.4	nil	7.8	0.2	23.2	nil	56.4	7.2	13.0	23.4
1 (bottom)	0.4	59.4	6.6	1.4	1.6	nil	nil	nil	3.2	nil	0.2	nil	nil	2.0	0.2	2.8	nil	0.4	0.4	2.0	2.4	nil	4.2	0.2	12.6	nil	69.4	8.4	9.4	12.8
Min	nil	7.0	0.8	nil	nil	nil	nil	nil	2.6	nil	nil	nil	nil	1.0	nil	0.4	nil	nil	nil	2.0	1.2	nil	4.2	nil	3.8	nil	8.4	5.0	9.4	4.2
Max	1.2	59.4	8.6	2.2	5.4	0.2	0.6	0.8	8.4	0.4	0.6	nil	nil	2.0	0.2	2.8	0.2	1.6	0.6	19.0	6.2	nil	30.2	1.6	39.8	0.2	69.4	10.8	54.6	40.4
Mean	0.5	38.5	4.5	0.8	1.1	0.0	0.1	0.2	5.0	0.2	0.3	nil	nil	1.5	0.1	1.4	0.1	0.7	0.1	9.7	3.5	nil	14.6	0.4	16.7	0.0	45.7	8.5	28.7	17.1
SD	0.4	16.4	2.2	0.7	1.5	0.1	0.2	0.3	1.7	0.1	0.2	nil	nil	0.4	0.1	0.7	0.1	0.4	0.2	5.0	1.6	nil	7.5	0.5	9.8	0.1	19.3	1.4	12.0	9.9
Argada- D																														
20 (top)	0.1	6.4	4.0	0.8	0.3	nil	nil	nil	5.7	0.2	0.4	nil	nil	2.4	nil	0.3	0.1	0.7	0.3	14.0	3.7	nil	21.8	14.3	24.5	nil	11.7	9.1	40.5	38.7
19	nil	33.9	3.1	0.8	0.1	0.1	nil	nil	7.3	0.3	0.5	nil	nil	0.9	nil	0.1	nil	0.6	nil	14.0	2.2	nil	18.4	7.7	10.0	0.1	38.0	9.0	35.2	17.8
18	0.1	59.5	3.2	1.7	nil	nil	0.1	0.1	5.7	0.1	0.8	nil	nil	0.6	0.1	0.8	nil	0.8	nil	8.0	1.4	nil	7.9	3.1	5.9	nil	64.7	8.2	18.1	9.0
17	0.4	32.2	5.7	0.7	2.6	0.1	nil	nil	4.5	0.1	0.6	nil	nil	1.6	nil	0.4	nil	0.7	0.4	8.8	1.3	nil	14.2	10.4	15.3	nil	41.7	7.2	25.4	25.7
16	0.1	51.3	1.3	1.1	nil	0.2	nil	nil	7.3	0.1	0.7	nil	nil	1.5	nil	0.3	nil	0.4	0.1	13.7	1.5	0.1	14.0	2.8	3.7	nil	53.9	9.8	29.8	6.5
15	0.2	13.3	1.1	1.2	0.1	nil	nil	0.1	10.2	0.2	0.2	nil	nil	0.7	nil	1.4	0.1	0.2	0.1	16.7	1.9	nil	25.0	10.4	16.8	nil	16.0	12.9	43.9	27.2
14	0.7	36.6	4.6	2.7	0.4	0.4	0.1	0.1	10.9	0.2	0.5	nil	nil	1.3	nil	0.4	nil	0.3	nil	12.5	1.6	0.2	16.1	4.4	5.6	0.3	45.7	13.3	30.7	10.4
13	0.1	24.5	3.3	1.0	nil	nil	nil	nil	9.3	0.8	0.7	nil	nil	2.1	nil	0.2	nil	0.4	0.2	19.7	1.5	0.1	17.6	7.1	11.4	nil	29.0	13.0	39.5	18.5
12	nil	46.7	2.0	1.2	nil	nil	0.1	nil	6.5	0.3	0.5	nil	nil	1.2	nil	0.3	nil	0.8	nil	15.3	3.3	nil	12.7	3.4	5.3	0.3	50.0	8.9	32.1	9.1
11	0.2	41.6	1.5	0.8	nil	0.2	0.1	nil	6.8	0.2	0.5	nil	nil	2.3	nil	0.9	nil	1.0	0.1	16.6	4.9	nil	14.4	3.2	4.8	0.2	44.4	10.6	37.0	8.1
10	0.1	17.6	3.0	1.9	0.2	0.2	0.6	0.1	7.5	0.3	0.7	nil	nil	1.4	nil	0.6	nil	0.8	0.2	18.2	2.2	nil	19.5	9.3	15.5	0.1	23.6	10.6	40.9	24.8
9	0.5	54.3	6.4	1.6	0.6	0.2	nil	nil	4.6	0.2	0.7	nil	nil	2.3	0.1	0.9	nil	0.4	nil	3.0	0.8	nil	5.5	4.8	13.3	nil	63.5	8.7	9.7	18.1
8	0.2	14.1	5.3	0.7	0.1	nil	0.3	nil	9.3	0.3	0.8	nil	nil	1.4	0.1	0.1	0.2	0.4	0.5	22.2	4.6	nil	19.6	6.2	13.7	0.1	20.6	12.1	47.3	20.0
7	0.3	27.9	4.2	0.3	0.3	0.1	0.3	nil	6.7	0.3	0.7	nil	nil	1.8	nil	0.3	nil	0.5	0.3	18.2	4.9	nil	15.7	4.4	12.9	nil	33.3	9.8	39.6	17.3
6	0.3	55.8	1.9	1.0	0.2	nil	nil	nil	3.2	nil	0.5	nil	nil	1.5	nil	2.9	nil	0.5	0.2	8.1	6.8	nil	6.4	4.4	6.3	nil	59.2	8.1	22.0	10.7
5	nil	19.3	4.4	0.8	nil	nil	nil	nil	9.1	0.6	0.4	nil	nil	2.7	nil	2.1	nil	nil	0.4	21.6	6.3	nil	12.7	6.4	13.5	nil	24.4	14.8	40.9	19.9
4	0.1	14.9	3.7	0.1	nil	nil	0.1	0.1	9.2	0.4	0.7	nil	nil	1.4	nil	0.3	0.1	0.4	0.5	22.6	6.6	nil	19.3	3.4	16.1	nil	19.2	12.0	49.4	19.5
3	0.9	18.8	4.5	0.6	nil	nil	nil	nil	12.2	0.2	0.3	nil	nil	3.6	nil	nil	nil	0.2	0.2	18.4	6.4	0.2	13.4	7.6	12.7	nil	24.8	16.3	38.7	20.3
2	1.1	64.9	2.2	1.1	0.4	nil	nil	0.4	4.8	0.2	0.2	nil	nil	0.9	0.2	3.4	nil	0.7	0.2	4.5	1.9	0.2	8.9	0.9	2.8	0.2	70.1	9.7	16.4	3.9
1 (bottom)	2.0	31.4	2.2	0.8	0.4	nil	0.2	nil	10.4	0.4	0.6	nil	nil	1.6	0.2	1.4	nil	2.4	1.4	15.6	2.6	0.2	16.0	nil	10.2	nil	37.0	14.6	38.2	10.2
Min	nil	6.4	1.1	0.1	nil	nil	nil	nil	3.2	nil	0.2	nil	nil	0.6	nil	nil	nil	nil	nil	3.0	0.8	nil	5.5	nil	2.8	nil	11.7	7.2	9.7	3.9
Max	2.0	64.9	6.4	2.7	2.6	0.4	0.6	0.4	12.2	0.8	0.8	nil	nil	3.6	0.2	3.4	0.2	2.4	1.4	22.6	6.8	0.2	25.0	14.3	24.5	0.3	70.1	16.3	49.4	38.7
Mean	0.4	33.3	3.4	1.1	0.3	0.1	0.1	0.1	7.6	0.3	0.6	nil	nil	1.7	0.0	0.9	0.0	0.6	0.3	14.6	3.3	0.1	15.0	5.7	11.0	0.1	38.5	10.9	33.8	16.8
SD	0.5	17.1	1.5	0.6	0.6	0.1	0.2	0.1	2.4	0.2	0.2	nil	nil	0.7	0.1	0.9	0.1	0.5	0.3	5.5	2.0	0.1	5.0	3.4	5.4	0.1	17.1	2.5	10.4	8.3
Argada- I																														

Table 4.17 Maceral and mineral matter content (vol.%) of different coal seams of Argada area, South Karanpura coalfield, India

	Tl	Ctl	Vdr	Cdr	Cgl	Gl	DV	SV	Spo	Cut	Res	Alg	Sub	Ldr	Flo	Exu	Bit	Micr	Macr	Sfu	Fu	Scr	Idr	Arg	Carb	Py	Vit	Lipt	Inert	MM
9 (top)	nil	8.5	0.8	0.3	nil	nil	nil	nil	12.5	nil	0.3	nil	nil	3.0	nil	1.6	nil	nil	nil	31.9	14.7	nil	15.0	8.7	2.7	nil	9.5	17.4	61.6	11.4
8	0.3	6.9	nil	0.3	nil	nil	nil	nil	10.0	nil	1.0	nil	nil	2.4	nil	1.7	nil	nil	nil	34.5	12.8	nil	16.6	8.6	4.8	nil	7.6	15.2	63.8	13.5
7	nil	6.6	0.3	nil	nil	nil	nil	nil	6.3	nil	1.3	nil	nil	2.0	nil	2.0	0.3	nil	nil	41.9	12.0	nil	15.0	7.6	4.7	nil	7.0	12.0	68.8	12.3
6	nil	13.5	0.8	nil	nil	nil	nil	nil	8.7	nil	0.4	nil	nil	3.0	0.4	2.3	0.4	nil	nil	21.1	18.1	nil	17.3	7.9	6.4	nil	14.3	15.0	56.4	14.3
5	nil	10.9	nil	nil	nil	nil	nil	nil	15.8	1.0	1.5	nil	nil	2.0	nil	3.5	nil	0.5	1.0	32.7	nil	nil	23.3	5.9	2.0	nil	10.9	23.8	57.4	7.9
4	nil	8.3	1.0	nil	nil	nil	nil	nil	11.5	0.3	0.3	nil	nil	2.2	nil	0.3	nil	0.3	0.3	37.3	6.4	nil	19.8	10.2	1.9	nil	9.2	14.7	64.0	12.1
3	nil	17.6	0.8	nil	nil	nil	nil	nil	4.1	0.5	0.8	nil	nil	0.8	nil	1.4	nil	nil	0.3	32.2	8.1	nil	16.8	10.5	6.2	nil	18.4	7.6	57.3	16.8
2	nil	11.5	0.3	0.3	nil	nil	0.3	nil	7.8	nil	nil	nil	nil	1.3	nil	1.3	nil	nil	0.5	37.2	9.9	nil	15.2	8.6	5.9	nil	12.3	10.4	62.8	14.4
1 (bottom)	nil	25.4	1.9	nil	nil	nil	nil	nil	6.1	0.3	0.5	nil	nil	1.6	nil	1.9	nil	nil	nil	21.2	14.0	nil	15.6	6.6	5.0	nil	27.3	10.3	50.8	11.6
Min	nil	6.6	nil	nil	nil	nil	nil	nil	4.1	nil	nil	nil	nil	0.8	nil	0.3	nil	nil	nil	21.1	nil	nil	15.0	5.9	1.9	nil	7.0	7.6	50.8	7.9
Max	0.3	25.4	1.9	0.3	nil	nil	0.3	nil	15.8	1.0	1.5	nil	nil	3.0	0.4	3.5	0.4	0.5	1.0	41.9	18.1	nil	23.3	10.5	6.4	nil	27.3	23.8	68.8	16.8
Mean	0.0	12.1	0.6	0.1	nil	nil	0.0	nil	9.2	0.2	0.7	nil	nil	2.0	0.0	1.8	0.1	0.1	0.2	32.2	10.7	nil	17.2	8.3	4.4	nil	12.9	14.0	60.3	12.7
SD	0.1	5.7	0.6	0.1	nil	nil	0.1	nil	3.5	0.3	0.5	nil	nil	0.7	0.1	0.8	0.2	0.2	0.3	6.6	5.0	nil	2.6	1.4	1.7	nil	6.1	4.5	5.0	2.3
Argada- J																														
13 (top)	nil	0.7	nil	nil	nil	nil	nil	nil	8.1	0.4	0.7	nil	nil	1.5	nil	0.4	nil	nil	nil	38.3	13.9	nil	13.7	16.8	5.5	nil	0.7	11.1	66.0	22.2
12	nil	33.3	0.7	0.4	nil	nil	nil	nil	7.1	0.2	0.7	nil	nil	3.3	nil	2.0	nil	nil	nil	12.3	7.1	nil	15.2	11.7	6.1	nil	34.4	13.2	34.6	17.8
11	nil	22.6	0.2	nil	0.5	nil	nil	nil	12.0	0.7	0.5	nil	nil	2.9	nil	0.2	nil	nil	0.2	24.6	8.8	nil	16.5	5.2	5.2	nil	23.3	16.3	50.1	10.4
10	0.2	24.5	nil	0.2	1.1	nil	nil	nil	5.7	0.6	0.6	nil	nil	2.3	nil	0.6	nil	0.2	0.2	28.0	10.5	nil	14.9	6.3	4.2	nil	25.9	9.8	53.8	10.5
9	nil	41.6	0.3	nil	1.4	nil	nil	0.3	3.6	0.3	0.3	nil	nil	1.7	0.3	1.1	nil	nil	nil	12.7	10.8	nil	14.4	6.1	5.3	nil	43.5	7.2	38.0	11.4
8	nil	22.0	0.3	0.3	nil	nil	nil	nil	9.2	nil	1.0	nil	nil	1.5	nil	1.0	nil	0.5	0.3	24.3	7.2	nil	19.6	8.4	4.5	0.3	22.5	12.6	51.7	13.1
7	nil	42.7	nil	0.9	0.2	nil	nil	nil	7.0	0.2	0.7	nil	nil	2.2	nil	2.5	nil	0.2	0.2	15.6	9.7	nil	9.5	5.2	3.4	nil	43.7	12.5	35.1	8.6
6	nil	22.9	nil	0.8	1.1	nil	nil	nil	7.0	0.5	0.5	nil	nil	2.4	nil	2.2	nil	nil	nil	25.3	7.8	0.3	18.3	10.5	0.3	nil	24.8	12.7	51.8	10.8
5	nil	44.4	1.7	0.3	0.3	nil	nil	nil	9.7	0.3	0.6	nil	nil	3.4	0.3	3.1	nil	0.3	nil	13.1	4.6	0.3	8.6	5.1	4.0	nil	46.7	17.4	26.8	9.1
4	nil	20.7	1.3	nil	nil	nil	nil	nil	9.7	1.3	0.9	1.3	nil	5.3	nil	2.6	nil	nil	nil	26.0	8.4	nil	11.0	7.9	3.5	nil	22.0	21.2	45.4	11.5
3	nil	24.8	1.4	0.7	nil	nil	nil	nil	8.3	0.7	1.4	nil	nil	3.5	nil	2.1	nil	nil	nil	16.6	10.3	nil	22.8	5.5	2.1	nil	26.9	15.9	49.7	7.6
2	nil	11.0	1.1	nil	nil	nil	nil	nil	9.1	0.4	1.1	nil	nil	2.7	nil	1.5	nil	nil	nil	18.6	12.5	nil	17.1	15.2	9.9	nil	12.1	14.8	48.1	25.0
1 (bottom)	nil	14.0	2.3	nil	nil	nil	nil	nil	7.0	0.6	1.7	nil	nil	4.7	nil	1.2	nil	0.6	0.6	40.1	8.7	nil	12.2	4.1	2.3	nil	16.3	15.1	62.6	4.4
Min	nil	0.7	nil	nil	nil	nil	nil	nil	3.6	nil	0.3	nil	nil	1.5	nil	0.2	nil	nil	nil	12.3	4.6	nil	8.6	4.1	0.3	nil	0.7	7.2	26.8	4.4
Max	0.2	44.4	2.3	0.9	1.4	nil	nil	0.3	12.0	1.3	1.7	1.3	nil	5.3	0.3	3.1	nil	0.6	0.6	40.1	13.9	0.3	22.8	16.8	9.9	0.3	46.7	21.2	66.0	25.0
Mean	0.0	25.0	0.7	0.3	0.3	nil	nil	0.0	8.0	0.5	0.8	0.1	nil	2.9	0.0	1.6	nil	0.1	0.1	22.7	9.3	0.0	14.9	8.3	4.3	0.0	26.4	13.8	47.2	12.6
SD	0.1	12.4	0.8	0.3	0.5	nil	nil	0.1	2.0	0.3	0.4	0.4	nil	1.1	0.1	0.9	nil	0.2	0.2	8.8	2.4	0.1	3.9	3.9	2.2	0.1	12.7	3.4	10.7	5.4

Tl- Telinite, Ctl- Collotelinite, Vdr- Vitrodetrinite, Cdr- Collodetrinite, Cgl- Corpogelinite, Gl- Gelinite, DV- Dark Vitrinite, SV- Pseudovitrinite, Spo- Sporinite, Cut- Cutinite, Res- Resinite, Alg- Alginite, Sub- Suberinite, Ldr- Liptodetrinite, Flo- Fluorinite, Exu- Exsudatinite, Bit- Bituminite, Micr- Micrinite, Macr - Macrinite, Sfu- Semifusinite, Fu- Fusinite, Scr- Secretinite, Idr- Inertodetrinite, Arg- Argillaceous minerals, Carb- Carbonate minerals, Py- Pyrite, Vit- Total Vitrinite, Lipt- Total Liptinite, Inert- Total Inertinite, MM- Total Mineral matter

Table 4.18 Maceral content (vol.%) of different coal seams of Argada area, South Karanpura coalfield, Jharkhand, India

	Tl	Ctl	Vdr	Cdr	Cgl	Gl	DV	SV	Spo	Cut	Res	Alg	Sub	Ldr	Flo	Exu	Bit	Micr	Macr	Sfu	Fu	Scr	Idr	Vit	Lipt	Inert
Argada																										
13 (top)	8.7	27.6	11.4	6.9	0.9	0.2	nil	nil	0.9	0.9	0.2	nil	nil	nil	nil	nil	nil	2.7	nil	8.9	8.0	nil	22.6	55.7	2.1	42.2
12	0.9	4.7	25.2	1.7	0.7	nil	nil	nil	9.2	1.4	1.7	nil	nil	nil	nil	nil	nil	1.4	0.2	23.8	7.1	nil	21.9	33.3	12.3	54.5
11	2.8	4.5	18.0	9.7	nil	nil	nil	nil	0.7	0.4	0.7	nil	nil	nil	nil	nil	nil	0.4	nil	19.7	6.2	nil	37.0	35.0	1.7	63.3
10	13.1	18.1	19.8	5.5	0.7	0.3	nil	0.3	4.5	0.3	1.0	nil	nil	0.5	nil	nil	nil	0.7	0.3	9.2	6.7	nil	19.3	57.7	6.2	36.1
9	5.3	8.9	17.9	7.3	0.4	1.2	nil	nil	nil	0.4	0.4	nil	nil	nil	nil	nil	nil	nil	nil	6.1	10.2	nil	41.9	41.1	0.8	58.1
8	7.7	24.4	17.7	2.1	nil	nil	nil	nil	3.0	0.4	1.9	nil	nil	nil	nil	nil	nil	0.4	0.2	15.2	11.1	nil	15.8	51.9	5.3	42.7
7	3.6	15.3	7.3	4.6	0.2	0.2	0.2	nil	0.7	1.7	1.0	nil	nil	nil	nil	nil	nil	0.2	2.2	12.9	24.0	nil	25.7	31.6	3.4	65.1
6	1.1	47.6	8.2	5.3	0.2	0.2	nil	nil	0.7	0.5	0.7	nil	nil	nil	nil	nil	nil	0.9	1.4	7.8	9.6	nil	15.8	62.7	1.8	35.5
5	13.4	45.4	9.2	4.4	2.0	0.9	nil	nil	0.4	0.4	0.4	nil	nil	nil	nil	nil	nil	3.1	0.4	4.0	6.8	nil	9.2	75.2	1.3	23.5
4	3.4	13.0	11.1	1.4	0.6	nil	0.3	nil	nil	0.9	0.9	nil	nil	nil	nil	nil	nil	nil	1.7	14.2	3.7	nil	49.0	29.8	1.7	68.6
3	6.7	32.7	17.3	3.6	1.3	nil	1.6	nil	2.3	1.6	0.8	nil	nil	0.3	nil	nil	nil	1.0	1.3	6.7	5.4	nil	17.5	63.1	4.9	32.0
2	9.3	20.2	14.0	5.4	1.3	nil	1.3	nil	3.1	nil	1.6	1.6	nil	0.3	nil	nil	nil	0.5	3.4	12.4	8.6	nil	17.1	51.6	6.5	42.0
1 (bottom)	6.9	29.3	10.3	3.4	1.0	0.2	nil	nil	4.7	1.2	1.2	nil	nil	1.5	nil	nil	nil	2.4	3.2	5.1	10.8	nil	18.8	51.1	8.6	40.3
Min	0.9	4.5	7.3	1.4	nil	nil	nil	nil	nil	nil	0.2	nil	nil	nil	nil	nil	nil	nil	nil	4.0	3.7	nil	9.2	29.8	0.8	23.5
Max	13.4	47.6	25.2	9.7	2.0	1.2	1.6	0.3	9.2	1.7	1.9	1.6	nil	1.5	nil	nil	nil	3.1	3.4	23.8	24.0	nil	49.0	75.2	12.3	68.6
Mean	6.4	22.5	14.4	4.7	0.7	0.3	0.3	0.0	2.3	0.8	1.0	0.1	nil	0.2	nil	nil	nil	1.1	1.1	11.2	9.1	nil	24.0	49.2	4.4	46.5
SD	3.9	13.4	5.1	2.3	0.6	0.4	0.5	0.1	2.5	0.5	0.5	0.4	nil	0.4	nil	nil	nil	1.0	1.2	5.7	4.8	nil	11.2	13.6	3.3	13.5
Argada-A																										
16 (top)	nil	42.1	2.9	0.3	0.6	nil	nil	nil	9.5	nil	1.3	nil	nil	5.7	nil	1.3	0.3	1.0	nil	10.1	9.5	nil	15.5	45.9	18.0	36.1
15	nil	13.9	3.8	0.1	nil	nil	0.1	nil	12.7	0.1	0.6	nil	nil	3.1	0.1	0.3	0.3	0.6	0.3	18.0	3.8	nil	42.2	18.0	17.2	64.8
14	nil	30.2	2.3	0.7	0.3	0.3	nil	nil	10.8	1.0	0.7	nil	0.3	6.6	nil	1.6	0.3	0.3	nil	19.3	6.9	nil	18.4	33.8	21.3	44.9
13	0.3	47.1	3.9	1.0	nil	nil	0.2	nil	8.1	0.2	0.5	nil	nil	3.7	0.3	0.2	0.3	1.0	nil	10.1	5.6	0.2	17.4	52.5	13.3	34.2
12	nil	33.8	4.0	0.3	0.1	nil	nil	nil	6.0	0.3	0.4	nil	nil	2.0	nil	0.5	0.3	1.3	nil	22.5	8.6	nil	20.0	38.2	9.4	52.4
11																										
10	nil	26.9	nil	nil	0.6	nil	nil	nil	7.5	0.6	1.3	nil	0.6	2.5	nil	0.6	nil	0.6	nil	31.3	6.9	nil	20.6	27.5	13.1	59.4
9	nil	18.7	2.6	0.4	nil	nil	nil	nil	16.8	0.4	0.6	nil	nil	3.0	nil	1.7	0.7	0.7	0.2	22.6	1.9	nil	29.9	21.6	23.1	55.3
8	0.2	44.1	2.4	0.7	0.4	nil	0.2	nil	9.0	0.2	0.5	nil	nil	2.8	nil	2.6	nil	0.5	nil	10.9	13.9	nil	11.6	47.9	15.1	37.0
7	nil	8.2	2.2	0.3	nil	nil	0.3	nil	16.2	0.3	0.3	nil	nil	6.7	0.3	1.5	0.3	1.3	0.3	16.2	1.5	nil	44.4	11.0	25.4	63.6
6	nil	29.4	4.3	1.3	nil	0.3	nil	nil	12.4	nil	0.3	nil	nil	2.8	0.5	2.3	nil	1.3	nil	11.2	6.9	nil	27.2	35.3	18.3	46.5
5	nil	40.9	3.1	1.0	nil	0.2	nil	nil	7.5	0.6	0.4	nil	nil	2.3	0.2	0.8	nil	0.8	0.2	11.0	7.7	nil	23.2	45.2	11.8	43.0
4	0.1	52.0	3.9	1.3	0.3	0.1	nil	nil	6.9	nil	1.6	nil	nil	3.5	0.3	1.6	nil	1.9	nil	5.5	11.0	nil	10.0	57.8	13.9	28.3
3	0.9	58.3	2.3	1.3	nil	nil	nil	nil	5.4	0.4	0.7	nil	nil	2.2	0.2	0.9	0.4	nil	nil	4.0	17.6	nil	5.6	62.8	10.1	27.2
2	0.6	27.2	8.0	0.4	0.4	0.4	nil	nil	12.8	0.4	0.8	nil	nil	5.2	nil	1.8	1.4	1.4	0.6	8.4	3.7	0.4	26.4	36.9	22.3	40.8
1 (bottom)	0.4	25.3	7.2	0.2	nil	nil	0.2	0.2	5.8	1.0	1.6	nil	nil	3.6	nil	1.6	1.0	1.4	0.4	17.5	4.6	0.2	28.0	33.4	14.5	52.1
Min	nil	8.2	nil	nil	nil	nil	nil	nil	5.4	nil	0.3	nil	nil	2.0	nil	0.2	nil	nil	nil	4.0	1.5	nil	5.6	11.0	9.4	27.2

Table 4.18 Maceral content (vol.%) of different coal seams of Argada area, South Karanpura coalfield, Jharkhand, India

	Tl	Ctl	Vdr	Cdr	Cgl	Gl	DV	SV	Spo	Cut	Res	Alg	Sub	Ldr	Flo	Exu	Bit	Micr	Macr	Sfu	Fu	Scr	Idr	Vit	Lipt	Inert
Max	0.9	58.3	8.0	1.3	0.6	0.4	0.3	0.2	16.8	1.0	1.6	nil	0.6	6.7	0.5	2.6	1.4	1.9	0.6	31.3	17.6	0.4	44.4	62.8	25.4	64.8
Mean	0.2	33.2	3.5	0.6	0.2	0.1	0.1	0.0	9.8	0.4	0.8	nil	0.1	3.7	0.1	1.3	0.4	0.9	0.1	14.6	7.3	0.1	22.7	37.8	16.5	45.7
SD	0.3	13.7	1.9	0.4	0.2	0.1	0.1	0.1	3.5	0.3	0.4	nil	0.2	1.5	0.2	0.7	0.4	0.5	0.2	7.1	4.2	0.1	10.5	14.1	4.7	11.6
Argada- B																										
20 (top)	0.7	33.2	9.0	2.7	3.0	nil	nil	0.3	4.7	nil	0.3	nil	nil	1.7	nil	1.3	0.3	0.3	nil	11.0	5.7	nil	25.9	48.8	8.3	42.9
19	0.7	33.7	8.5	1.2	0.5	nil	nil	nil	4.5	nil	0.2	nil	nil	1.2	0.2	1.2	nil	0.7	0.5	16.0	7.5	0.2	23.3	44.5	7.3	48.2
18	0.2	45.5	10.2	2.1	1.0	nil	nil	nil	6.4	0.7	0.2	nil	nil	1.9	0.2	2.4	0.2	1.2	nil	6.2	2.6	0.5	18.5	59.0	12.1	28.9
17	nil	nil	nil	nil	nil	nil	nil	nil	7.3	nil	0.3	nil	nil	4.5	nil	3.4	0.8	nil	0.6	23.5	13.7	nil	45.9	nil	16.3	83.8
16	nil	1.5	0.6	nil	nil	nil	nil	nil	4.9	0.3	0.3	nil	nil	5.2	nil	3.2	nil	nil	0.6	26.5	1.5	nil	55.5	2.0	14.0	84.0
15	1.8	52.3	7.2	2.6	5.5	0.9	nil	0.4	2.6	1.1	1.1	nil	nil	1.8	0.2	2.0	nil	2.2	0.4	6.6	4.6	nil	6.8	70.7	8.8	20.6
14	0.5	49.8	9.0	3.0	3.2	0.2	nil	1.2	4.4	0.2	0.7	nil	nil	2.3	0.2	2.3	nil	0.9	0.5	7.4	3.7	nil	10.6	66.8	10.1	23.0
13	nil	1.2	nil	nil	nil	nil	nil	nil	4.9	nil	0.6	nil	nil	3.2	nil	2.6	0.3	nil	0.6	26.7	9.3	nil	50.7	1.2	11.6	87.3
12	0.6	40.6	4.8	1.0	0.2	nil	nil	0.4	3.7	0.6	0.2	nil	nil	0.4	0.2	2.3	nil	1.2	0.6	13.3	7.5	nil	22.4	47.6	7.5	44.9
11	2.1	54.1	2.9	3.7	2.5	nil	0.2	0.8	4.5	0.6	0.2	nil	nil	1.4	0.2	1.0	nil	2.5	0.6	6.2	3.9	nil	12.6	66.3	8.0	25.7
10	0.8	50.7	6.1	2.8	3.9	nil	nil	0.6	4.7	nil	0.6	nil	nil	2.5	0.3	2.8	nil	0.6	0.8	5.0	5.2	nil	13.0	64.7	10.7	24.5
9	2.9	43.5	9.7	3.4	0.2	nil	nil	nil	5.3	0.5	1.0	nil	nil	1.5	nil	3.1	0.2	0.7	0.7	9.7	3.9	nil	13.8	59.7	11.6	28.7
8	0.5	5.9	3.2	nil	nil	nil	nil	nil	1.8	nil	0.5	nil	nil	2.7	nil	0.9	nil	0.9	0.9	17.6	0.5	nil	64.9	9.5	5.9	84.7
7	nil	5.3	7.7	1.4	nil	nil	nil	nil	1.9	0.5	0.5	nil	nil	1.9	nil	2.9	nil	0.5	1.9	15.8	2.9	nil	56.9	14.4	7.7	78.0
6	0.7	44.7	6.1	2.0	0.2	nil	nil	nil	6.9	0.5	0.5	nil	nil	2.7	nil	2.7	0.2	nil	0.2	14.9	5.9	nil	11.7	53.8	13.5	32.8
5	0.5	42.2	10.5	0.5	0.3	nil	nil	nil	4.9	0.8	1.4	nil	nil	1.6	nil	2.2	0.3	nil	0.5	16.5	3.8	nil	14.1	54.1	11.1	34.9
4	2.1	43.3	7.4	0.6	0.6	nil	nil	0.2	10.9	0.6	0.6	nil	nil	2.3	0.2	1.7	nil	1.4	0.6	8.0	10.7	nil	8.7	54.2	16.3	29.5
3	4.5	44.6	8.5	1.6	2.0	nil	nil	0.2	6.5	1.4	1.1	nil	0.2	1.4	0.2	1.8	0.2	0.2	0.5	9.9	6.1	nil	9.2	61.4	12.8	25.8
2	1.0	33.4	10.1	1.4	nil	nil	nil	nil	7.5	1.7	1.0	nil	nil	1.9	0.2	1.9	0.2	1.0	0.7	15.4	6.3	nil	16.4	45.9	14.4	39.7
1 (bottom)	8.4	13.0	8.4	5.7	1.0	0.5	nil	0.3	7.1	1.5	nil	nil	0.3	1.7	0.3	1.7	0.3	1.2	nil	15.2	12.8	nil	20.9	37.1	12.8	50.1
Min	nil	nil	nil	nil	nil	nil	nil	nil	1.8	nil	nil	nil	nil	0.4	nil	0.9	nil	nil	nil	5.0	0.5	nil	6.8	nil	5.9	20.6
Max	8.4	54.1	10.5	5.7	5.5	0.9	0.2	1.2	10.9	1.7	1.4	nil	0.3	5.2	0.3	3.4	0.8	2.5	1.9	26.7	13.7	0.5	64.9	70.7	16.3	87.3
Mean	1.4	31.9	6.5	1.8	1.2	0.1	0.0	0.2	5.3	0.6	0.6	nil	0.0	2.2	0.1	2.2	0.2	0.8	0.6	13.6	5.9	0.0	25.1	43.1	11.0	45.9
SD	1.9	19.0	3.4	1.5	1.6	0.2	0.0	0.3	2.1	0.5	0.4	nil	0.1	1.1	0.1	0.7	0.2	0.7	0.4	6.4	3.5	0.1	18.1	23.4	3.0	23.2
Argada- C																										
13 (top)	0.9	61.6	3.2	nil	1.1	nil	nil	0.5	3.0	0.2	nil	nil	nil	1.4	nil	1.1	nil	nil	nil	11.4	2.1	nil	13.5	67.3	5.7	27.0
12	nil	55.1	5.4	1.1	0.7	nil	nil	0.2	5.0	nil	0.2	nil	nil	1.8	0.2	1.6	0.2	0.5	0.2	7.7	3.6	nil	16.3	62.6	9.1	28.3
11	0.6	34.5	4.6	0.7	0.4	nil	0.1	0.3	7.3	0.3	0.4	nil	nil	1.8	0.1	1.2	0.1	1.0	0.1	17.4	5.9	nil	23.3	41.1	11.2	47.7
10	0.6	51.6	4.0	2.3	0.2	0.2	0.4	nil	5.4	0.2	0.2	nil	nil	1.3	0.2	1.5	nil	1.7	0.2	12.5	2.5	nil	15.0	59.3	8.8	31.9
9	nil	15.1	2.1	nil	0.3	nil	nil	nil	8.9	0.3	0.3	nil	nil	1.3	0.3	0.5	nil	1.6	nil	24.7	5.5	nil	39.3	17.5	11.5	71.1
8	0.3	27.1	2.9	0.3	0.3	nil	nil	1.2	8.2	0.3	0.3	nil	nil	2.6	0.3	0.9	nil	1.2	0.3	19.2	5.0	nil	29.7	32.1	12.5	55.4
7	0.3	11.7	1.3	0.7	nil	nil	nil	nil	14.1	0.3	0.7	nil	nil	2.0	nil	0.7	0.3	0.3	nil	20.1	2.0	nil	45.3	14.1	18.1	67.8

Table 4.18 Maceral content (vol.%) of different coal seams of Argada area, South Karanpura coalfield, Jharkhand, India

	Tl	Ctl	Vdr	Cdr	Cgl	Gl	DV	SV	Spo	Cut	Res	Alg	Sub	Ldr	Flo	Exu	Bit	Micr	Macr	Sfu	Fu	Scr	Idr	Vit	Lipt	Inert
6	0.7	43.2	6.7	1.9	0.5	nil	nil	nil	8.6	0.2	0.7	nil	nil	1.2	nil	2.2	nil	1.0	nil	9.6	7.4	nil	16.2	53.0	12.9	34.1
5	0.9	59.6	5.7	1.4	6.1	nil	nil	nil	4.8	0.5	0.7	nil	nil	2.3	0.2	1.4	nil	1.1	nil	4.1	5.4	nil	5.9	73.7	9.8	16.6
4	1.3	48.2	6.1	0.4	0.4	nil	0.2	0.2	4.3	0.2	0.2	nil	nil	2.2	nil	1.3	0.2	0.4	nil	17.1	5.6	nil	11.5	56.8	8.5	34.7
3	1.3	51.9	7.5	0.6	0.9	nil	0.6	0.6	5.2	0.2	0.2	nil	nil	1.7	nil	2.2	0.2	0.9	0.2	7.9	5.4	nil	12.5	63.5	9.7	26.8
2	0.3	55.9	11.2	1.8	4.4	nil	nil	nil	3.4	nil	0.8	nil	nil	2.1	nil	3.1	nil	0.5	0.8	3.7	1.8	nil	10.2	73.6	9.4	17.0
1 (bottom)	0.5	68.1	7.6	1.6	1.8	nil	nil	nil	3.7	nil	0.2	nil	nil	2.3	0.2	3.2	nil	0.5	0.5	2.3	2.8	nil	4.8	79.6	9.6	10.8
Min	nil	11.7	1.3	nil	nil	nil	nil	nil	3.0	nil	nil	nil	nil	1.2	nil	0.5	nil	nil	nil	2.3	1.8	nil	4.8	14.1	5.7	10.8
Max	1.3	68.1	11.2	2.3	6.1	0.2	0.6	1.2	14.1	0.5	0.8	nil	nil	2.6	0.3	3.2	0.3	1.7	0.8	24.7	7.4	nil	45.3	79.6	18.1	71.1
Mean	0.6	44.9	5.3	1.0	1.3	0.0	0.1	0.2	6.3	0.2	0.4	nil	nil	1.8	0.1	1.6	0.1	0.8	0.2	12.1	4.2	nil	18.7	53.4	10.5	36.1
SD	0.4	17.1	2.6	0.7	1.8	0.1	0.2	0.3	3.0	0.1	0.2	nil	nil	0.4	0.1	0.8	0.1	0.5	0.2	6.8	1.8	nil	11.9	20.3	2.8	18.4
Argada- D																										
20 (top)	0.2	10.5	6.6	1.4	0.5	nil	nil	nil	9.3	0.3	0.7	nil	nil	3.9	nil	0.5	0.2	1.2	0.5	22.8	6.1	nil	35.6	19.1	14.8	66.1
19	nil	41.2	3.8	0.9	0.1	0.1	nil	nil	8.8	0.4	0.6	nil	nil	1.1	nil	0.1	nil	0.7	nil	17.1	2.7	nil	22.4	46.2	11.0	42.9
18	0.1	65.4	3.5	1.8	nil	nil	0.1	0.1	6.3	0.1	0.9	nil	nil	0.7	0.1	0.9	nil	0.9	nil	8.8	1.5	nil	8.7	71.1	9.0	19.9
17	0.6	43.3	7.6	1.0	3.4	0.2	nil	nil	6.1	0.2	0.8	nil	nil	2.1	nil	0.6	nil	1.0	0.6	11.8	1.7	nil	19.1	56.1	9.7	34.2
16	0.1	54.9	1.3	1.1	nil	0.2	nil	nil	7.8	0.1	0.7	nil	nil	1.6	nil	0.3	nil	0.4	0.1	14.6	1.7	0.1	15.0	57.6	10.5	31.9
15	0.3	18.2	1.5	1.6	0.2	nil	nil	0.2	14.0	0.3	0.3	nil	nil	1.0	nil	2.0	0.2	0.3	0.2	22.9	2.6	nil	34.3	22.0	17.7	60.3
14	0.8	40.9	5.2	3.0	0.5	0.5	0.1	0.1	12.1	0.2	0.6	nil	nil	1.5	nil	0.5	nil	0.3	nil	13.9	1.8	0.2	18.0	51.0	14.8	34.2
13	0.1	30.1	4.1	1.3	nil	nil	nil	nil	11.5	0.9	0.8	nil	nil	2.6	nil	0.2	nil	0.5	0.2	24.2	1.9	0.1	21.6	35.5	16.0	48.5
12	nil	51.4	2.2	1.3	nil	nil	0.1	nil	7.1	0.4	0.6	nil	nil	1.3	nil	0.4	nil	0.9	nil	16.9	3.6	nil	13.9	55.0	9.8	35.3
11	0.2	45.3	1.6	0.9	nil	0.2	0.1	nil	7.4	0.2	0.5	nil	nil	2.5	nil	1.0	nil	1.1	0.1	18.1	5.3	nil	15.6	48.3	11.5	40.2
10	0.1	23.4	4.0	2.6	0.2	0.2	0.7	0.1	10.0	0.4	1.0	nil	nil	1.8	nil	0.9	nil	1.1	0.2	24.2	2.9	nil	26.0	31.5	14.1	54.5
9	0.6	66.2	7.8	2.0	0.7	0.2	nil	nil	5.6	0.2	0.8	nil	nil	2.8	0.1	1.0	nil	0.5	nil	3.6	0.9	nil	6.8	77.6	10.6	11.9
8	0.2	17.6	6.6	0.8	0.1	nil	0.4	nil	11.6	0.3	1.0	nil	nil	1.8	0.1	0.1	0.2	0.5	0.6	27.7	5.7	nil	24.5	25.8	15.1	59.1
7	0.3	33.7	5.1	0.4	0.3	0.1	0.4	nil	8.1	0.3	0.9	nil	nil	2.2	nil	0.4	nil	0.6	0.3	22.0	6.0	nil	19.0	40.3	11.8	47.9
6	0.4	62.5	2.1	1.1	0.2	nil	nil	nil	3.6	nil	0.6	nil	nil	1.7	nil	3.2	nil	0.6	0.2	9.1	7.6	nil	7.2	66.3	9.1	24.6
5	nil	24.1	5.4	1.0	nil	nil	nil	nil	11.4	0.7	0.5	nil	nil	3.3	nil	2.6	nil	nil	0.5	27.0	7.8	nil	15.8	30.5	18.4	51.1
4	0.2	18.5	4.6	0.2	nil	nil	0.2	0.2	11.5	0.5	0.8	nil	nil	1.7	nil	0.4	0.2	0.5	0.6	28.0	8.1	nil	24.0	23.8	14.9	61.3
3	1.1	23.6	5.6	0.8	nil	nil	nil	nil	15.4	0.2	0.4	nil	nil	4.5	nil	nil	nil	0.2	0.2	23.0	8.1	0.2	16.9	31.1	20.4	48.5
2	1.2	67.5	2.3	1.2	0.4	nil	nil	0.4	5.0	0.2	0.2	nil	nil	1.0	0.2	3.5	nil	0.8	0.2	4.6	1.9	0.2	9.3	72.9	10.1	17.0
1 (bottom)	2.2	35.0	2.5	0.9	0.5	nil	0.2	nil	11.6	0.5	0.7	nil	nil	1.8	0.2	1.6	nil	2.7	1.6	17.4	2.9	0.2	17.8	41.2	16.3	42.5
Min	nil	10.5	1.3	0.2	nil	nil	nil	nil	3.6	nil	0.2	nil	nil	0.7	nil	nil	nil	nil	nil	3.6	0.9	nil	6.8	19.1	9.0	11.9
Max	2.2	67.5	7.8	3.0	3.4	0.5	0.7	0.4	15.4	0.9	1.0	nil	nil	4.5	0.2	3.5	0.2	2.7	1.6	28.0	8.1	0.2	35.6	77.6	20.4	66.1
Mean	0.4	38.7	4.2	1.3	0.4	0.1	0.1	0.1	9.2	0.3	0.7	nil	nil	2.0	0.0	1.0	0.0	0.7	0.3	17.9	4.0	0.1	18.6	45.1	13.3	41.6
SD	0.5	17.6	2.0	0.7	0.7	0.1	0.2	0.1	3.1	0.2	0.2	nil	nil	1.0	0.1	1.0	0.1	0.5	0.4	7.3	2.5	0.1	7.7	17.5	3.3	15.1
Argada- I																										

Table 4.18 Maceral content (vol.%) of different coal seams of Argada area, South Karanpura coalfield, Jharkhand, India

	Tl	Ctl	Vdr	Cdr	Cgl	Gl	DV	SV	Spo	Cut	Res	Alg	Sub	Ldr	Flo	Exu	Bit	Micr	Macr	Sfu	Fu	Scr	Idr	Vit	Lipt	Inert
9 (top)	nil	9.5	0.9	0.3	nil	nil	nil	nil	14.2	nil	0.3	nil	nil	3.4	nil	1.9	nil	nil	nil	36.0	16.6	nil	16.9	10.8	19.7	69.5
8	0.4	8.0	nil	0.4	nil	nil	nil	nil	11.6	nil	1.2	nil	nil	2.8	nil	2.0	nil	nil	nil	39.8	14.7	nil	19.1	8.8	17.5	73.7
7	nil	7.6	0.4	nil	nil	nil	nil	nil	7.2	nil	1.5	nil	nil	2.3	nil	2.3	0.4	nil	nil	47.7	13.6	nil	17.1	8.0	13.6	78.4
6	nil	15.8	0.9	nil	nil	nil	nil	nil	10.1	nil	0.4	nil	nil	3.5	0.4	2.6	0.4	nil	nil	24.6	21.1	nil	20.2	16.7	17.5	65.8
5	nil	11.8	nil	nil	nil	nil	nil	nil	17.2	1.1	1.6	nil	nil	2.2	nil	3.8	nil	0.5	1.1	35.5	nil	nil	25.3	11.8	25.8	62.4
4	nil	9.4	1.1	nil	nil	nil	nil	nil	13.0	0.4	0.4	nil	nil	2.5	nil	0.4	nil	0.4	0.4	42.4	7.3	nil	22.5	10.5	16.7	72.8
3	nil	21.1	1.0	nil	nil	nil	nil	nil	4.9	0.7	1.0	nil	nil	1.0	nil	1.6	nil	nil	0.3	38.6	9.7	nil	20.1	22.1	9.1	68.8
2	nil	13.4	0.3	0.3	nil	nil	0.3	nil	9.1	nil	nil	nil	nil	1.6	nil	1.6	nil	nil	0.6	43.4	11.6	nil	17.8	14.4	12.2	73.4
1 (bottom)	nil	28.7	2.1	nil	nil	nil	nil	nil	6.9	0.3	0.6	nil	nil	1.8	nil	2.1	nil	nil	nil	24.0	15.9	nil	17.7	30.8	11.7	57.5
Min	nil	7.6	nil	nil	nil	nil	nil	nil	4.9	nil	nil	nil	nil	1.0	nil	0.4	nil	nil	nil	24.0	nil	nil	16.9	8.0	9.1	57.5
Max	0.4	28.7	2.1	0.4	nil	nil	0.3	nil	17.2	1.1	1.6	nil	nil	3.5	0.4	3.8	0.4	0.5	1.1	47.7	21.1	nil	25.3	30.8	25.8	78.4
Mean	0.0	13.9	0.7	0.1	nil	nil	0.0	nil	10.5	0.3	0.8	nil	nil	2.3	0.1	2.0	0.1	0.1	0.3	36.9	12.3	nil	19.6	14.9	16.0	69.2
SD	0.1	6.6	0.6	0.2	nil	nil	0.1	nil	3.7	0.4	0.5	nil	nil	0.8	0.1	0.9	0.2	0.2	0.4	7.6	5.8	nil	2.6	7.0	4.7	6.1
Argada- J																										
13 (top)	nil	0.8	nil	nil	nil	nil	nil	nil	10.4	0.6	0.8	nil	nil	2.0	nil	0.6	nil	nil	nil	49.3	17.9	nil	17.7	0.8	14.3	84.9
12	nil	40.5	0.8	0.5	nil	nil	nil	nil	8.7	0.3	0.8	nil	nil	4.0	nil	2.4	nil	nil	nil	15.0	8.7	nil	18.4	41.8	16.1	42.1
11	nil	25.2	0.3	nil	0.5	nil	nil	nil	13.4	0.8	0.5	nil	nil	3.3	nil	0.3	nil	nil	0.3	27.5	9.8	nil	18.4	25.9	18.1	55.9
10	0.2	27.3	nil	0.2	1.2	nil	nil	nil	6.3	0.7	0.7	nil	nil	2.6	nil	0.7	nil	0.2	0.2	31.3	11.7	nil	16.6	29.0	11.0	60.1
9	nil	46.9	0.3	nil	1.6	nil	nil	0.3	4.1	0.3	0.3	nil	nil	1.9	0.3	1.3	nil	nil	nil	14.4	12.2	nil	16.3	49.1	8.1	42.8
8	nil	25.4	0.3	0.3	nil	nil	nil	nil	10.5	nil	1.1	nil	nil	1.7	nil	1.1	nil	0.6	0.3	27.9	8.3	nil	22.5	25.9	14.5	59.5
7	nil	46.7	nil	1.0	0.2	nil	nil	nil	7.7	0.2	0.8	nil	nil	2.4	nil	2.8	nil	0.2	0.2	17.1	10.6	nil	10.4	47.8	13.7	38.4
6	nil	25.7	nil	0.9	1.2	nil	nil	nil	7.9	0.6	0.6	nil	nil	2.7	nil	2.4	nil	nil	nil	28.4	8.8	0.3	20.5	27.8	14.2	58.0
5	nil	48.9	1.9	0.3	0.3	nil	nil	nil	10.7	0.3	0.6	nil	nil	3.8	0.3	3.5	nil	0.3	nil	14.4	5.0	0.3	9.4	51.4	19.1	29.5
4	nil	23.4	1.5	nil	nil	nil	nil	nil	11.0	1.5	1.0	1.5	nil	6.0	nil	3.0	nil	nil	nil	29.4	9.5	nil	12.4	24.9	23.9	51.2
3	nil	26.9	1.5	0.8	nil	nil	nil	nil	9.0	0.8	1.5	nil	nil	3.7	nil	2.2	nil	nil	nil	17.9	11.2	nil	24.6	29.1	17.2	53.7
2	nil	14.7	1.5	nil	nil	nil	nil	nil	12.1	0.5	1.5	nil	nil	3.5	nil	2.0	nil	nil	nil	24.8	16.7	nil	22.7	16.2	19.7	64.1
1 (bottom)	nil	14.9	2.5	nil	nil	nil	nil	nil	7.5	0.6	1.9	nil	nil	5.0	nil	1.2	nil	0.6	0.6	42.9	9.3	nil	13.0	17.4	16.2	66.5
Min	nil	0.8	nil	nil	nil	nil	nil	nil	4.1	nil	0.3	nil	nil	1.7	nil	0.3	nil	nil	nil	14.4	5.0	nil	9.4	0.8	8.1	29.5
Max	0.2	48.9	2.5	1.0	1.6	nil	nil	0.3	13.4	1.5	1.9	1.5	nil	6.0	0.3	3.5	nil	0.6	0.6	49.3	17.9	0.3	24.6	51.4	23.9	84.9
Mean	0.0	28.2	0.8	0.3	0.4	nil	nil	0.0	9.2	0.5	0.9	0.1	nil	3.3	0.1	1.8	nil	0.2	0.1	26.2	10.7	0.1	17.2	29.8	15.9	54.4
SD	0.1	13.7	0.8	0.4	0.5	nil	nil	0.1	2.4	0.4	0.4	0.4	nil	1.2	0.1	1.0	nil	0.2	0.2	10.4	3.3	0.1	4.6	14.0	3.8	13.6

Tl- Telinite, Ctl- Collotelinite, Vdr- Vitrodetrinite, Cdr- Collodetrinite, Cgl- Corpogelinite, Gl- Gelinite, DV- Dark Vitrinite, SV- Pseudovitrinite, Spo- Sporinite, Cut- Cutinite, Res- Resinite, Alg- Alginite, Sub- Suberinite, Ldr- Liptodetrinite, Flo- Fluorinite, Exu- Exsudatinite, Bit- Bituminite, Micr- Micrinite, Macr - Macrinite, Sfu- Semifusinite, Fu- Fusinite, Scr- Secretinite, Idr- Inertodetrinite, Vit- Total Vitrinite, Lipt- Total Liptinite, Inert- Total Inertinite

Table 4.19 Microlithotype and carbominerite content (vol.%) of coals seams of Argada area, South Karanpura Coalfield, India.

	Vte	Lte	Ite	ClV	ClL	ViV	ViI	DuI	DuL	VIL	CLD	DUC	CAnk	CPy	CPoly	CArg	Mo	Bi	Tri	Cmin
Argada																				
13 (top)	16.3	nil	9.0	0.8	nil	30.8	9.5	0.5	0.3	0.3	0.5	2.4	9.2	nil	1.8	18.7	25.3	41.8	3.2	29.7
12	1.1	0.2	6.4	7.3	0.9	7.1	7.5	29.1	1.3	nil	2.2	7.8	17.3	0.2	3.1	8.4	7.8	53.2	10.0	29.1
11	0.5	nil	6.0	1.0	nil	2.5	1.0	1.3	nil	nil	0.3	0.3	65.6	nil	4.8	16.8	6.5	5.8	0.5	87.2
10	10.7	nil	4.0	0.9	0.2	21.7	5.6	1.2	0.5	1.6	2.3	5.8	26.3	0.5	5.1	13.5	14.7	30.1	9.8	45.5
9	1.7	nil	3.4	nil	nil	1.4	0.2	0.2	nil	0.2	nil	nil	86.1	0.5	2.4	3.8	5.0	1.9	0.2	92.8
8	15.8	nil	12.0	1.2	0.9	24.9	12.0	2.8	1.7	0.9	4.5	8.2	7.5	0.2	0.5	6.8	27.8	43.5	13.7	15.1
7	7.9	nil	18.0	1.0	nil	12.8	11.6	2.5	1.0	1.0	1.0	2.5	10.4	0.5	3.0	26.9	25.9	28.9	4.4	40.7
6	26.1	nil	7.9	0.9	0.2	24.0	6.5	0.7	0.2	0.5	0.2	2.8	0.2	0.5	1.4	27.9	34.0	32.6	3.5	30.0
5	39.1	nil	4.5	1.3	nil	32.8	4.9	nil	nil	nil	0.5	2.2	9.4	1.3	0.9	3.1	43.5	39.1	2.7	14.7
4	4.3	nil	3.2	1.1	nil	11.7	2.4	1.7	nil	1.1	2.6	3.9	26.4	nil	5.8	35.9	7.6	16.9	7.6	68.0
3	28.5	nil	5.9	4.1	nil	22.6	4.5	nil	nil	0.9	2.3	8.8	10.6	0.9	0.9	10.0	34.4	31.2	12.0	22.4
2	12.1	nil	5.1	3.0	nil	14.4	6.3	0.4	nil	0.4	3.4	4.2	29.6	0.9	4.2	16.1	17.1	24.1	8.0	50.7
1 (bottom)	20.1	nil	7.2	3.8	0.5	33.1	5.8	0.5	nil	1.4	1.4	12.0	7.7	nil	0.7	5.8	27.3	43.7	14.9	14.2
Min	0.5	nil	3.2	nil	nil	1.4	0.2	nil	nil	nil	nil	nil	0.2	nil	0.5	3.1	5.0	1.9	0.2	14.2
Max	39.1	0.2	18.0	7.3	0.9	33.1	12.0	29.1	1.7	1.6	4.5	12.0	86.1	1.3	5.8	35.9	43.5	53.2	14.9	92.8
Mean	14.2	0.0	7.1	2.0	0.2	18.5	6.0	3.1	0.4	0.6	1.6	4.7	23.6	0.4	2.7	14.9	21.3	30.2	7.0	41.6
SD	11.4	0.1	3.9	1.9	0.3	10.5	3.5	7.5	0.6	0.5	1.3	3.5	24.1	0.4	1.8	9.8	12.0	14.5	4.7	25.5
Argada-A																				
16 (top)	21.7	nil	14.0	2.0	nil	12.0	4.3	nil	nil	nil	1.4	11.7	8.9	nil	2.3	21.7	35.7	18.3	13.1	32.9
15	2.4	nil	16.6	nil	nil	10.0	8.0	1.2	0.2	nil	2.6	2.8	35.2	nil	0.8	20.2	19.0	19.4	5.4	56.2
14	13.2	nil	19.0	0.6	nil	20.2	10.8	5.0	nil	nil	8.5	7.6	5.6	nil	1.2	8.5	32.2	36.6	16.1	15.2
13	14.7	nil	8.1	1.5	0.4	7.1	2.1	0.2	nil	nil	0.4	5.0	46.9	nil	1.4	12.2	22.8	11.4	5.4	60.4
12	13.6	nil	22.9	3.2	0.2	19.3	12.6	1.0	nil	0.6	3.4	5.5	11.1	nil	0.4	6.3	36.5	36.3	9.5	17.8
11																				
10	10.6	nil	23.5	2.4	nil	15.9	10.6	8.2	nil	nil	9.4	7.7	5.9	nil	1.8	4.1	34.1	37.1	17.1	11.8
9	3.6	nil	13.0	2.2	0.4	4.6	3.6	1.4	0.4	nil	1.4	4.6	48.5	nil	1.8	14.6	16.6	12.6	6.0	64.9
8	27.9	nil	18.9	3.5	nil	11.3	3.8	0.7	nil	nil	4.2	14.8	5.1	nil	0.7	9.3	46.8	19.2	18.9	15.1
7	2.4	nil	8.4	0.4	0.2	1.6	1.4	nil	nil	nil	nil	0.2	41.6	nil	7.0	36.9	10.8	3.6	0.2	85.5
6	10.5	nil	9.9	1.8	nil	10.1	2.0	1.2	nil	nil	0.4	1.8	43.7	nil	3.4	15.3	20.3	15.1	2.2	62.4
5	22.3	nil	15.3	1.9	nil	18.1	7.4	1.5	nil	nil	2.1	4.2	6.9	nil	1.9	18.3	37.6	29.0	6.3	27.1
4	20.8	nil	11.7	5.9	0.2	15.8	3.4	0.4	nil	nil	1.4	24.0	11.5	nil	0.2	4.7	32.5	25.7	25.5	16.4
3	45.7	nil	22.0	7.1	nil	9.2	1.1	nil	nil	nil	0.2	11.9	1.1	nil	nil	1.8	67.7	17.4	12.1	2.8
2	8.5	nil	6.3	3.5	nil	7.3	1.6	0.4	nil	nil	0.6	5.3	45.3	nil	1.8	19.3	14.8	12.8	5.9	66.5
1 bottom)	6.5	nil	12.6	1.8	0.2	8.5	2.8	1.8	nil	0.6	0.8	3.4	34.2	nil	3.6	23.1	19.0	15.2	4.9	60.9
Min	2.4	nil	6.3	nil	nil	1.6	1.1	nil	nil	nil	nil	0.2	1.1	nil	nil	1.8	10.8	3.6	0.2	2.8

Table 4.19 Microlithotype and carbominerite content (vol.%) of coals seams of Argada area, South Karanpura Coalfield, India.

	Vte	Lte	Ite	ClV	ClL	ViV	ViI	DuI	DuL	VIL	CLD	DUC	CAnk	CPy	CPoly	CArg	Mo	Bi	Tri	Cmin
Max	45.7	nil	23.5	7.1	0.4	20.2	12.6	8.2	0.4	0.6	9.4	24.0	48.5	nil	7.0	36.9	67.7	37.1	25.5	85.5
Mean	15.0	nil	14.8	2.5	0.1	11.4	5.0	1.5	0.0	0.1	2.5	7.4	23.4	nil	1.9	14.4	29.8	20.6	9.9	39.7
SD	11.1	nil	5.4	1.9	0.1	5.3	3.7	2.2	0.1	0.2	2.8	5.9	18.1	nil	1.7	8.9	14.2	9.8	6.8	25.4
Argada- B																				
20 (top)	8.3	nil	4.6	1.4	nil	9.5	3.2	0.2	nil	0.2	2.0	3.0	67.6	nil	nil	nil	12.9	14.3	5.2	67.6
19	16.4	nil	10.0	1.0	nil	7.8	6.4	1.4	0.4	0.2	3.9	10.5	41.2	nil	0.4	0.4	26.4	17.0	14.6	42.0
18	20.4	nil	3.5	1.0	0.2	12.2	2.9	nil	0.2	0.2	1.4	10.9	46.6	nil	0.4	nil	23.9	16.5	12.6	47.0
17	nil	nil	19.8	nil	nil	nil	nil	nil	nil	nil	nil	nil	48.7	nil	4.8	26.8	19.8	nil	nil	80.3
16	nil	nil	6.7	nil	nil	0.6	0.2	0.8	nil	nil	nil	nil	36.2	nil	12.6	42.9	6.7	1.7	nil	91.6
15	33.9	nil	6.3	5.5	0.2	10.6	2.9	0.4	nil	0.2	0.8	12.2	26.1	nil	0.4	0.4	40.2	19.6	13.3	26.9
14	20.9	nil	4.8	5.2	nil	14.5	3.5	0.2	nil	0.4	1.2	11.0	36.0	nil	0.4	1.9	25.7	23.4	12.6	38.3
13	0.2	nil	14.7	nil	nil	0.4	0.4	1.9	nil	nil	nil	nil	19.5	nil	8.6	54.2	14.9	2.7	nil	82.4
12	13.3	nil	13.1	1.9	nil	21.5	6.9	0.9	nil	2.2	6.0	21.5	12.7	nil	nil	nil	26.5	31.2	29.7	12.7
11	34.3	nil	3.0	2.3	0.4	15.8	4.4	0.4	nil	2.1	3.4	25.7	7.6	nil	nil	0.6	37.3	23.4	31.2	8.2
10	16.4	nil	4.8	2.5	0.2	12.6	1.3	nil	nil	0.2	1.3	10.5	47.9	nil	0.4	1.9	21.2	16.6	12.0	50.2
9	15.6	nil	4.9	4.4	nil	14.4	3.4	0.4	0.2	1.1	3.2	18.1	32.7	nil	nil	1.7	20.5	22.8	22.4	34.4
8	0.4	nil	1.2	0.2	0.2	2.2	0.8	0.4	0.4	nil	nil	0.6	87.4	nil	2.9	3.3	1.6	4.3	0.6	93.5
7	0.4	0.2	1.0	nil	nil	1.0	0.2	2.3	nil	nil	nil	0.2	80.7	0.2	2.3	11.4	1.7	3.5	0.2	94.6
6	22.5	0.2	6.3	1.9	0.4	7.1	4.0	2.3	0.6	5.2	3.8	12.1	30.2	nil	0.4	3.1	29.0	16.3	21.0	33.8
5	19.8	nil	5.8	2.6	nil	6.8	3.0	1.9	0.9	3.2	1.9	4.7	35.8	0.4	7.7	5.5	25.6	15.1	9.8	49.5
4	12.5	nil	10.6	14.0	0.7	10.2	5.4	0.7	nil	1.9	3.5	28.3	11.2	0.7	0.2	0.2	23.1	30.9	33.7	12.3
3	19.2	nil	7.3	9.2	1.5	16.5	6.3	0.8	0.2	2.1	1.5	11.7	20.0	0.2	0.8	2.9	26.5	34.4	15.2	24.0
2	10.7	nil	6.3	3.8	0.6	13.4	4.6	5.9	2.7	3.1	4.4	9.9	23.3	nil	0.8	10.5	17.0	31.0	17.4	34.6
1 (bottom)	11.1	nil	15.1	0.5	0.2	13.0	3.7	1.2	nil	0.5	0.9	1.9	29.4	nil	1.9	20.8	26.2	18.5	3.2	52.1
Min	nil	nil	1.0	nil	nil	nil	nil	nil	nil	nil	nil	nil	7.6	nil	nil	nil	1.6	nil	nil	8.2
Max	34.3	0.2	19.8	14.0	1.5	21.5	6.9	5.9	2.7	5.2	6.0	28.3	87.4	0.7	12.6	54.2	40.2	34.4	33.7	94.6
Mean	13.8	0.0	7.5	2.9	0.2	9.5	3.2	1.1	0.3	1.1	2.0	9.6	37.0	0.1	2.3	9.4	21.3	17.2	12.7	48.8
SD	10.1	0.1	4.8	3.4	0.4	6.0	2.1	1.3	0.6	1.4	1.7	8.4	21.1	0.2	3.4	14.9	9.9	10.2	10.5	27.0
Argada- C																				
13 (top)	32.5	nil	7.8	1.2	0.2	14.3	2.0	0.2	nil	nil	1.2	9.6	28.8	nil	0.6	1.4	40.3	18.0	10.8	30.9
12	26.7	nil	5.3	2.0	nil	14.3	2.7	0.4	0.2	nil	1.8	9.2	36.3	0.2	0.2	0.6	32.0	19.6	11.0	37.4
11	14.7	nil	9.9	0.5	nil	6.8	2.6	1.5	0.1	0.5	3.4	9.4	48.9	0.1	0.8	1.0	24.6	11.5	13.3	50.7
10	19.1	nil	5.7	1.6	nil	13.2	3.7	0.8	nil	nil	5.1	30.1	20.3	nil	nil	0.4	24.8	19.3	35.2	20.7
9	6.1	nil	13.3	nil	nil	2.5	1.8	2.9	nil	nil	2.5	2.7	62.5	0.2	2.5	3.3	19.4	7.1	5.1	68.4
8	11.0	nil	7.5	nil	nil	4.9	2.4	0.6	nil	0.2	2.0	3.0	67.1	nil	0.6	0.6	18.5	7.9	5.3	68.4
7	3.9	nil	3.7	nil	nil	1.4	0.6	0.4	nil	nil	0.6	0.8	87.6	nil	1.0	nil	7.5	2.4	1.4	88.6

Table 4.19 Microlithotype and carbominerite content (vol.%) of coals seams of Argada area, South Karanpura Coalfield, India.

	Vte	Lte	Ite	ClV	ClL	ViV	ViI	DuI	DuL	VIL	CLD	DUC	CAnk	CPy	CPoly	CArg	Mo	Bi	Tri	Cmin
6	11.3	nil	8.2	0.8	nil	13.1	3.5	0.6	nil	1.0	3.7	18.4	39.1	nil	nil	0.2	19.5	18.0	23.2	39.3
5	26.3	nil	3.7	5.2	nil	10.8	2.5	nil	nil	0.4	1.5	19.9	29.6	0.2	nil	nil	30.0	18.4	21.7	29.8
4	30.4	nil	10.6	1.3	nil	6.7	2.5	1.9	0.4	0.6	5.4	13.5	26.7	nil	nil	nil	41.0	12.7	19.6	26.7
3	30.1	nil	5.7	1.6	0.2	8.6	2.5	1.0	nil	1.0	5.5	20.5	23.3	nil	nil	nil	35.8	13.9	27.0	23.3
2	27.0	nil	1.4	3.7	0.2	9.9	1.4	nil	nil	0.2	0.2	7.8	47.5	nil	0.4	0.2	28.4	15.2	8.2	48.2
1 (bottom)	37.0	nil	2.6	2.8	0.2	12.2	1.2	nil	nil	0.4	0.4	8.7	33.8	nil	0.6	nil	39.7	16.4	9.5	34.4
Min	3.9	nil	1.4	nil	nil	1.4	0.6	nil	nil	nil	0.2	0.8	20.3	nil	nil	nil	7.5	2.4	1.4	20.7
Max	37.0	nil	13.3	5.2	0.2	14.3	3.7	2.9	0.4	1.0	5.5	30.1	87.6	0.2	2.5	3.3	41.0	19.6	35.2	88.6
Mean	21.2	nil	6.6	1.6	0.1	9.1	2.3	0.8	0.1	0.3	2.6	11.8	42.4	0.1	0.5	0.6	27.8	13.9	14.7	43.6
SD	10.4	nil	3.3	1.5	0.1	4.2	0.8	0.8	0.1	0.4	1.8	8.1	19.0	0.1	0.7	0.9	9.7	5.2	9.5	19.7
Argada- D																				
20 (top)	2.2	nil	15.9	nil	nil	1.8	0.4	0.2	nil	nil	nil	0.2	46.7	nil	2.6	30.0	18.1	2.4	0.2	79.3
19	10.9	nil	7.9	3.0	nil	8.3	2.8	2.2	0.4	0.6	5.2	12.3	24.8	0.2	2.0	19.6	18.8	16.6	18.0	46.5
18	29.5	nil	6.4	10.2	1.0	8.2	1.6	0.6	nil	nil	1.0	17.5	18.9	nil	0.2	5.0	35.9	21.5	18.5	24.1
17	15.9	nil	4.8	2.4	nil	11.9	1.6	1.4	nil	0.2	1.2	9.5	33.8	nil	1.0	16.3	20.7	17.3	10.9	51.1
16	31.9	nil	10.4	1.2	0.2	11.2	2.3	2.1	nil	0.4	4.8	17.2	14.1	0.2	0.2	3.9	42.3	17.0	22.4	18.3
15	7.7	nil	11.7	0.8	0.2	2.8	1.0	1.0	0.2	0.2	2.2	4.6	50.4	nil	0.8	16.5	19.4	6.0	6.9	67.7
14	19.5	nil	9.4	2.6	nil	9.0	1.2	0.6	0.2	0.2	1.8	10.8	32.8	0.6	0.2	11.2	28.9	13.6	12.8	44.8
13	11.2	nil	12.0	0.6	nil	8.1	5.9	0.8	0.4	0.4	4.5	8.3	36.4	0.2	0.4	10.8	23.2	15.9	13.2	47.8
12	29.8	nil	11.4	2.6	nil	11.4	1.8	0.8	0.2	0.2	2.8	10.0	20.8	1.0	0.4	7.1	41.2	16.7	12.9	29.2
11	18.4	nil	10.1	2.0	0.4	8.1	4.6	2.2	0.2	0.2	5.5	13.3	27.5	0.4	0.2	6.9	28.5	17.4	19.0	35.1
10	5.3	nil	11.1	2.4	0.2	2.8	1.2	4.4	0.2	0.4	4.7	10.5	33.4	0.2	1.8	21.5	16.4	11.1	15.6	56.9
9	30.0	nil	1.7	10.1	0.6	4.3	1.5	0.2	nil	nil	0.6	6.6	32.0	nil	0.6	11.8	31.6	16.7	7.2	44.4
8	3.4	nil	18.7	0.4	nil	4.0	2.6	4.4	nil	1.2	4.2	7.8	41.0	0.4	1.6	10.2	22.1	11.5	13.3	53.2
7	14.2	nil	15.2	0.8	nil	7.7	1.2	3.0	nil	nil	4.3	8.9	30.5	nil	1.0	13.4	29.3	12.6	13.2	44.9
6	36.0	0.2	10.6	4.9	2.6	11.8	2.6	0.8	nil	0.4	1.0	8.7	11.6	nil	0.4	8.3	46.8	22.8	10.2	20.3
5	9.3	0.2	25.3	1.2	0.8	5.8	2.1	1.2	0.6	0.4	2.1	6.2	34.2	0.2	1.0	9.5	34.8	11.7	8.6	44.9
4	7.8	nil	21.5	1.2	nil	5.1	2.5	2.9	0.4	0.4	3.7	4.7	39.3	nil	1.6	9.0	29.2	12.1	8.8	49.9
3	8.2	nil	17.0	nil	nil	6.5	5.5	2.0	nil	0.2	2.0	4.5	40.5	nil	0.8	12.7	25.2	14.1	6.8	54.0
2	49.7	0.4	3.3	6.4	1.4	10.7	2.1	0.4	nil	0.4	1.0	7.2	13.5	0.2	0.8	2.5	53.4	21.1	8.6	17.0
1 (bottom)	18.5	nil	9.5	2.3	0.2	7.2	3.8	2.3	0.8	3.2	7.4	19.0	25.9	nil	nil	nil	28.0	16.6	29.5	25.9
Min	2.2	nil	1.7	nil	nil	1.8	0.4	0.2	nil	nil	nil	0.2	11.6	nil	nil	nil	16.4	2.4	0.2	17.0
Max	49.7	0.4	25.3	10.2	2.6	11.9	5.9	4.4	0.8	3.2	7.4	19.0	50.4	1.0	2.6	30.0	53.4	22.8	29.5	79.3
Mean	18.0	0.0	11.7	2.8	0.4	7.3	2.4	1.7	0.2	0.5	3.0	9.4	30.4	0.2	0.9	11.3	29.7	14.7	12.8	42.8
SD	12.4	0.1	5.8	2.9	0.6	3.1	1.5	1.2	0.2	0.7	2.0	4.6	10.6	0.3	0.7	6.9	9.9	4.8	6.3	16.1
Argada- I																				

Table 4.19 Microlithotype and carbominerite content (vol.%) of coals seams of Argada area, South Karanpura Coalfield, India.

	Vte	Lte	Ite	ClV	ClL	ViV	ViI	DuI	DuL	VIL	CLD	DUC	CAnk	CPy	CPoly	CArg	Mo	Bi	Tri	Cmin
9 (top)	5.0	nil	40.9	0.3	nil	2.5	2.8	7.5	nil	nil	1.9	1.1	8.6	nil	3.0	26.5	45.9	13.0	3.0	38.1
8	3.6	nil	43.3	nil	nil	1.1	2.2	11.6	nil	nil	3.6	5.4	7.2	nil	1.1	20.9	46.9	14.8	9.0	29.2
7	3.0	nil	46.7	0.3	nil	2.3	3.0	13.0	nil	nil	3.3	1.3	8.0	nil	0.3	18.7	49.7	18.7	4.7	27.0
6	6.3	nil	37.5	0.4	nil	5.5	2.3	5.5	nil	nil	3.5	3.1	14.8	nil	3.1	18.0	43.8	13.7	6.6	35.9
5	2.9	nil	35.6	nil	nil	3.4	4.2	13.8	nil	nil	4.6	3.4	5.9	nil	0.4	25.9	38.5	21.3	8.0	32.2
4	3.0	nil	38.7	0.3	nil	3.9	5.3	7.9	nil	nil	2.3	3.3	3.3	nil	1.3	30.8	41.6	17.4	5.6	35.4
3	9.8	nil	35.8	1.4	nil	5.7	4.4	7.1	nil	nil	6.3	3.0	9.8	nil	0.8	15.9	45.6	18.6	9.3	26.5
2	6.2	nil	43.7	0.3	nil	5.1	3.8	8.1	nil	nil	3.2	1.9	8.4	nil	1.9	17.5	49.9	17.3	5.1	27.8
1 (bottom)	10.6	nil	26.1	1.7	nil	9.0	5.6	9.2	nil	nil	7.3	11.8	7.6	nil	1.1	10.1	36.7	25.5	19.1	18.8
Min	2.9	nil	26.1	nil	nil	1.1	2.2	5.5	nil	nil	1.9	1.1	3.3	nil	0.3	10.1	36.7	13.0	3.0	18.8
Max	10.6	nil	46.7	1.7	nil	9.0	5.6	13.8	nil	nil	7.3	11.8	14.8	nil	3.1	30.8	49.9	25.5	19.1	38.1
Mean	5.6	nil	38.7	0.5	nil	4.3	3.7	9.3	nil	nil	4.0	3.8	8.2	nil	1.5	20.5	44.3	17.8	7.8	30.1
SD	2.8	nil	5.7	0.6	nil	2.2	1.2	2.7	nil	nil	1.7	3.1	3.0	nil	1.0	6.0	4.3	3.7	4.4	5.7
Argada- J																				
13 (top)	0.7	nil	48.1	nil	nil	nil	nil	3.8	nil	nil	nil	0.4	6.0	nil	1.1	39.9	48.8	3.8	0.4	47.0
12	18.7	nil	15.9	1.3	nil	10.4	1.1	2.8	nil	nil	0.9	9.1	7.6	nil	1.3	30.9	34.6	15.7	1nil	39.8
11	12.2	nil	29.4	0.5	nil	8.6	2.5	2.3	nil	nil	2.3	9.5	11.3	nil	0.5	21.0	41.6	13.8	11.8	32.8
10	17.0	nil	34.3	1.3	nil	7.0	3.2	3.0	nil	nil	4.5	5.3	7.5	nil	nil	17.0	51.3	14.5	9.8	24.5
9	31.3	nil	18.8	3.3	nil	8.0	3.1	1.9	nil	nil	2.8	7.2	9.1	nil	0.8	13.6	50.1	16.3	10.0	23.6
8	15.4	nil	38.0	2.0	nil	8.9	4.9	3.9	nil	nil	7.5	8.5	7.9	nil	3.0	nil	53.4	19.7	16.1	10.8
7	31.4	nil	22.9	2.6	nil	12.4	3.1	0.6	nil	nil	1.3	4.8	4.3	nil	1.1	15.5	54.3	18.7	6.1	20.9
6	14.8	nil	28.8	3.3	nil	13.7	3.6	2.0	nil	nil	2.3	2.3	9.4	nil	1.3	18.6	43.5	22.7	4.6	29.3
5	23.7	nil	13.7	2.3	nil	12.3	1.4	0.6	nil	nil	3.4	11.7	13.7	nil	2.9	14.3	37.4	16.6	15.1	30.9
4	8.5	nil	28.1	0.9	nil	6.3	0.9	5.4	nil	nil	5.8	5.4	11.2	nil	3.1	24.6	36.6	13.4	11.2	38.8
3	13.1	nil	21.4	1.4	nil	9.7	0.7	2.8	nil	nil	13.8	9.0	9.7	nil	0.7	17.9	34.5	14.5	22.8	28.3
2	3.8	nil	26.9	0.8	nil	3.4	1.5	5.7	nil	nil	1.9	6.4	15.9	nil	1.5	32.2	30.7	11.4	8.3	49.6
1 (bottom)	5.0	nil	41.1	nil	nil	1.1	1.7	4.4	nil	nil	7.2	11.7	8.3	nil	1.7	17.8	46.1	7.2	18.9	27.8
Min	0.7	nil	13.7	nil	nil	nil	nil	0.6	nil	nil	nil	0.4	4.3	nil	nil	nil	30.7	3.8	0.4	10.8
Max	31.4	nil	48.1	3.3	nil	13.7	4.9	5.7	nil	nil	13.8	11.7	15.9	nil	3.1	39.9	54.3	22.7	22.8	49.6
Mean	15.0	nil	28.3	1.5	nil	7.8	2.1	3.0	nil	nil	4.1	7.0	9.4	nil	1.5	20.3	43.3	14.5	11.2	31.1
SD	9.3	nil	9.7	1.1	nil	4.1	1.3	1.5	nil	nil	3.6	3.2	3.0	nil	0.9	9.6	7.7	4.8	5.8	10.3

Vte- Vitrite, Lte- Liptite, Ite- Inertite, ClV- Clarite V, ClL- Clarite L, ViV- Vitrinertite V, ViI- Vitrinertite I, DuI- Durite I, DuL- Durite L, VIL- Vitrinertoliptite, CLD- Clarodurite, DUC- Duroclarite, CAnk- Carbankerite, CPy- Carbopyrite, CPoly- Carbopolyminerite, CArg- Carbargilite, Mo- Monomacerals, Bi- Bimacerals, Tri- Trimacerals, Cmin- Total Carbominerite

Table 4.20 Microlithotype content (carbominerite free) basis (vol.%) of different coals seams of Barka Sayal area, South Karanpura Coalfield, Jharkhand, India

	Vte	Lte	Ite	ClV	ClL	ViV	ViI	DuI	DuL	VIL	CLD	DUC	Mo	Bi	Tri
Argada															
13 (top)	23.2	nil	12.7	1.1	nil	43.8	13.5	0.8	0.4	0.4	0.8	3.4	36.0	59.6	4.5
12	1.6	0.3	9.1	10.3	1.3	1nil	10.6	40.9	1.9	nil	3.1	10.9	10.9	75.0	14.1
11	3.9	nil	47.1	7.8	nil	19.6	7.8	9.8	nil	nil	2.0	2.0	51.0	45.1	3.9
10	19.7	nil	7.3	1.7	0.4	39.7	10.3	2.1	0.9	3.0	4.3	10.7	26.9	55.1	18.0
9	23.3	nil	46.7	nil	nil	20.0	3.3	3.3	nil	3.3	nil	nil	70.0	26.7	3.3
8	18.6	nil	14.1	1.4	1.1	29.4	14.1	3.3	1.9	1.1	5.3	9.7	32.7	51.3	16.1
7	13.3	nil	30.4	1.7	nil	21.7	19.6	4.2	1.7	1.7	1.7	4.2	43.8	48.8	7.5
6	37.3	nil	11.2	1.3	0.3	34.3	9.2	1.0	0.3	0.7	0.3	4.0	48.5	46.5	5.0
5	45.8	nil	5.2	1.6	nil	38.5	5.8	nil	nil	nil	0.5	2.6	51.1	45.8	3.1
4	13.5	nil	10.1	3.4	nil	36.5	7.4	5.4	nil	3.4	8.1	12.2	23.7	52.7	23.7
3	36.7	nil	7.6	5.3	nil	29.2	5.8	nil	nil	1.2	2.9	11.4	44.3	40.2	15.5
2	24.5	nil	10.3	6.0	nil	29.2	12.9	0.9	nil	0.9	6.9	8.6	34.8	48.9	16.3
1 (bottom)	23.5	nil	8.4	4.5	0.6	38.6	6.7	0.6	nil	1.7	1.7	14.0	31.8	50.8	17.3
Min	1.6	nil	5.2	nil	nil	10.0	3.3	nil	nil	nil	nil	nil	6.8	26.7	3.1
Max	45.8	0.3	47.1	10.3	1.3	43.8	19.6	40.9	1.9	3.4	8.1	14.0	93.2	75.0	23.7
Mean	21.9	0.0	16.9	3.5	0.3	30.0	9.8	5.6	0.5	1.3	2.9	7.2	38.9	49.7	11.4
SD	12.2	0.1	14.1	3.0	0.4	9.5	4.2	10.6	0.8	1.2	2.5	4.4	14.4	10.6	6.7
Argada-A															
16 (top)	32.3	nil	20.9	3.0	nil	17.9	6.4	nil	nil	nil	2.1	17.5	53.2	27.2	19.6
15	5.5	nil	37.9	nil	nil	22.8	18.3	2.7	0.5	nil	5.9	6.4	43.4	44.3	12.3
14	15.5	nil	22.4	0.7	nil	23.8	12.8	5.9	nil	nil	10.0	9.0	37.9	43.1	19.0
13	37.1	nil	20.5	3.9	1.0	18.1	5.4	0.5	nil	nil	1.0	12.7	57.6	28.8	13.7
12	16.6	nil	27.8	3.8	0.2	23.5	15.4	1.2	nil	0.7	4.1	6.7	44.4	44.1	11.5
11															
10	12.0	nil	26.7	2.7	nil	18.0	12.0	9.3	nil	nil	10.7	8.7	38.7	42.0	19.3
9	10.2	nil	36.9	6.3	1.1	13.1	10.2	4.0	1.1	nil	4.0	13.1	47.2	35.8	17.1
8	32.8	nil	22.3	4.1	nil	13.3	4.5	0.8	nil	nil	4.9	17.4	55.1	22.7	22.3
7	16.4	nil	57.5	2.7	1.4	11.0	9.6	nil	nil	nil	nil	1.4	74.0	24.7	1.4
6	27.8	nil	26.2	4.8	nil	26.7	5.4	3.2	nil	nil	1.1	4.8	54.0	40.1	5.9
5	30.6	nil	20.9	2.6	nil	24.9	10.2	2.1	nil	nil	2.9	5.8	51.6	39.8	8.6
4	24.9	nil	14.0	7.0	0.2	18.8	4.1	0.5	nil	nil	1.7	28.7	38.9	30.7	30.4
3	47.0	nil	22.7	7.3	nil	9.5	1.1	nil	nil	nil	0.2	12.3	69.7	17.9	12.4
2	25.5	nil	18.8	10.3	nil	21.8	4.9	1.2	nil	nil	1.8	15.8	44.2	38.2	17.6
1 (bottom)	16.6	nil	32.1	4.7	0.5	21.8	7.3	4.7	nil	1.6	2.1	8.8	48.7	38.9	12.4
Min	5.5	nil	14.0	nil	nil	9.5	1.1	nil	nil	1.4	nil	nil	37.9	17.9	1.4
Max	47.0	nil	57.5	10.3	1.4	26.7	18.3	9.3	1.1	30.4	1.6	10.7	74.0	44.3	28.7
Mean	23.4	nil	27.2	4.3	0.3	19.0	8.5	2.4	0.1	14.9	0.2	3.5	50.6	34.6	11.3
SD	11.0	nil	10.3	2.6	0.5	5.1	4.5	2.6	0.3	6.8	0.4	3.1	10.3	8.3	6.5
Argada- B															
20 (top)	25.5	nil	14.3	4.4	nil	29.2	9.9	0.6	nil	0.6	6.2	9.3	39.8	44.1	16.2
19	28.3	nil	17.3	1.8	nil	13.4	11.0	2.5	0.7	0.4	6.7	18.0	45.6	29.3	25.1
18	38.5	nil	6.6	2.0	0.4	23.0	5.5	nil	0.4	0.4	2.7	20.6	45.1	31.1	23.7
17	nil	nil	100.0	nil	nil	nil	nil	nil	nil	nil	nil	nil	100.0	nil	nil
16	nil	nil	80.0	nil	nil	7.5	2.5	10.0	nil	nil	nil	nil	80.0	20.0	nil
15	46.4	nil	8.7	7.5	0.3	14.5	3.9	0.6	nil	0.3	1.1	16.8	55.0	26.8	18.2
14	33.9	nil	7.7	8.4	nil	23.5	5.7	0.3	nil	0.7	2.0	17.8	41.6	37.9	20.5
13	1.2	nil	83.3	nil	nil	2.4	2.4	10.7	nil	nil	nil	nil	84.5	15.5	nil
12	15.3	nil	15.0	2.2	nil	24.6	7.9	1.0	nil	2.5	6.9	24.6	30.3	35.7	34.0
11	37.4	nil	3.2	2.5	0.5	17.2	4.8	0.5	nil	2.3	3.7	28.0	40.6	25.5	33.9
10	32.9	nil	9.7	5.1	0.4	25.3	2.5	nil	nil	0.4	2.5	21.1	42.6	33.3	24.1
9	23.8	nil	7.4	6.8	nil	21.9	5.1	0.6	0.3	1.6	4.8	27.7	31.2	34.7	34.1
8	6.3	nil	18.8	3.1	3.1	34.4	12.5	6.3	6.3	nil	nil	9.4	25.0	65.6	9.4
7	7.7	3.9	19.2	nil	nil	19.2	3.9	42.3	nil	nil	nil	3.9	30.8	65.4	3.9
6	34.0	0.3	9.4	2.8	0.6	10.7	6.0	3.5	0.9	7.9	5.7	18.2	43.7	24.5	31.8

Table 4.20 Microlithotype content (carbominerite free) basis (vol.%) of different coals seams of Barka Sayal area, South Karanpura Coalfield, Jharkhand, India

	Vte	Lte	Ite	ClV	ClL	ViV	ViI	DuI	DuL	VIL	CLD	DUC	Mo	Bi	Tri
5	39.2	nil	11.4	5.1	nil	13.5	5.9	3.8	1.7	6.3	3.8	9.3	50.6	30.0	19.4
4	14.3	nil	12.1	16.0	0.7	11.6	6.2	0.7	nil	2.2	3.9	32.3	26.4	35.2	38.4
3	25.2	nil	9.6	12.1	1.9	21.6	8.2	1.1	0.3	2.7	1.9	15.3	34.8	45.2	20.0
2	16.4	nil	9.6	5.8	1.0	20.5	7.1	9.0	4.2	4.8	6.7	15.1	26.0	47.4	26.6
1 (bottom)	23.2	nil	31.4	1.0	0.5	27.1	7.7	2.4	nil	1.0	1.9	3.9	54.6	38.7	6.8
Min	nil	nil	3.2	nil	nil	nil	nil	nil	nil	nil	nil	nil	25.0	nil	nil
Max	46.4	3.9	100.0	16.0	3.1	34.4	12.5	42.3	6.3	7.9	6.9	32.3	100.0	65.6	38.4
Mean	22.5	0.2	23.7	4.3	0.5	18.1	5.9	4.8	0.7	1.7	3.0	14.6	46.4	34.3	19.3
SD	13.9	0.8	27.8	4.1	0.8	8.6	3.0	9.2	1.6	2.2	2.4	9.6	19.9	14.8	12.1
Argada- C															
13 (top)	47.0	nil	11.2	1.8	0.3	20.7	3.0	0.3	nil	nil	1.8	13.9	58.3	26.0	15.7
12	42.7	nil	8.5	3.3	nil	22.8	4.2	0.7	0.3	nil	2.9	14.7	51.1	31.3	17.6
11	29.8	nil	20.1	1.1	nil	13.7	5.2	3.0	0.2	0.9	6.9	19.1	49.9	23.2	26.9
10	24.1	nil	7.2	2.1	nil	16.7	4.6	1.0	nil	nil	6.4	38.0	31.3	24.4	44.4
9	19.4	nil	41.9	nil	nil	7.7	5.8	9.0	nil	nil	7.7	8.4	61.3	22.6	16.1
8	34.6	nil	23.7	nil	nil	15.4	7.7	1.9	nil	0.6	6.4	9.6	58.3	25.0	16.7
7	33.9	nil	32.1	nil	nil	12.5	5.4	3.6	nil	nil	5.4	7.1	66.1	21.4	12.5
6	18.6	nil	13.5	1.4	nil	21.6	5.7	1.0	nil	1.7	6.1	30.4	32.1	29.7	38.2
5	37.5	nil	5.3	7.4	nil	15.3	3.5	nil	nil	0.6	2.1	28.3	42.8	26.3	31.0
4	41.5	nil	14.5	1.7	nil	9.1	3.4	2.6	0.6	0.9	7.4	18.5	56.0	17.3	26.7
3	39.2	nil	7.5	2.1	0.3	11.2	3.2	1.3	nil	1.3	7.2	26.7	46.7	18.1	35.2
2	52.0	nil	2.8	7.1	0.4	19.1	2.8	nil	nil	0.4	0.4	15.1	54.8	29.4	15.9
1 (bottom)	56.5	nil	4.0	4.3	0.3	18.5	1.9	nil	nil	0.6	0.6	13.3	60.5	25.0	14.5
Min	18.6	nil	2.8	nil	nil	7.7	1.9	nil	nil	nil	0.4	7.1	31.3	17.3	12.5
Max	56.5	nil	41.9	7.4	0.4	22.8	7.7	9.0	0.6	1.7	7.7	38.0	66.1	31.3	44.4
Mean	36.7	nil	14.8	2.5	0.1	15.7	4.3	1.9	0.1	0.5	4.7	18.7	51.5	24.6	23.9
SD	11.3	nil	11.3	2.4	0.2	4.6	1.5	2.4	0.2	0.5	2.6	9.1	10.4	4.0	10.1
Argada- D															
20 (top)	10.6	nil	76.9	nil	nil	8.7	1.9	1.0	nil	nil	nil	1.0	87.5	11.5	1.0
19	20.4	nil	14.8	5.6	nil	15.6	5.2	4.1	0.7	1.1	9.6	23.0	35.2	31.1	33.7
18	38.9	nil	8.4	13.4	1.3	10.8	2.1	0.8	nil	nil	1.3	23.1	47.2	28.4	24.4
17	32.5	nil	9.9	4.9	nil	24.3	3.3	2.9	nil	0.4	2.5	19.3	42.4	35.4	22.2
16	39.0	nil	12.8	1.4	0.2	13.7	2.8	2.6	nil	0.5	5.9	21.0	51.8	20.8	27.4
15	23.9	nil	36.2	2.5	0.6	8.6	3.1	3.1	0.6	0.6	6.8	14.1	60.1	18.4	21.5
14	35.2	nil	17.1	4.6	nil	16.4	2.1	1.1	0.4	0.4	3.2	19.6	52.3	24.6	23.1
13	21.4	nil	23.0	1.2	nil	15.6	11.3	1.6	0.8	0.8	8.6	16.0	44.4	30.4	25.3
12	42.1	nil	16.1	3.6	nil	16.1	2.5	1.1	0.3	0.3	3.9	14.1	58.2	23.6	18.3
11	28.4	nil	15.6	3.1	0.6	12.5	7.0	3.4	0.3	0.3	8.5	20.4	43.9	26.8	29.3
10	12.4	nil	25.7	5.5	0.5	6.4	2.8	10.1	0.5	0.9	11.0	24.3	38.1	25.7	36.2
9	53.9	nil	3.0	18.2	1.1	7.8	2.6	0.4	nil	nil	1.1	11.9	56.9	30.1	13.0
8	7.3	nil	39.9	0.9	nil	8.6	5.6	9.4	nil	2.6	9.0	16.7	47.2	24.5	28.3
7	25.7	nil	27.5	1.4	nil	13.9	2.1	5.4	nil	nil	7.9	16.1	53.2	22.9	23.9
6	45.2	0.3	13.3	6.1	3.3	14.8	3.3	1.0	nil	0.5	1.3	11.0	58.7	28.6	12.8
5	16.8	0.4	45.9	2.2	1.5	10.5	3.7	2.2	1.1	0.8	3.7	11.2	63.1	21.3	15.7
4	15.5	nil	42.9	2.5	nil	10.2	4.9	5.7	0.8	0.8	7.4	9.4	58.4	24.1	17.6
3	17.8	nil	36.9	nil	nil	14.2	12.0	4.4	nil	0.4	4.4	9.8	54.7	30.7	14.7
2	59.9	0.5	4.0	7.8	1.6	12.9	2.6	0.5	nil	0.5	1.2	8.7	64.3	25.4	10.3
1 (bottom)	25.0	nil	12.8	3.1	0.3	9.7	5.1	3.1	1.1	4.3	9.9	25.6	37.8	22.4	39.8
Min	7.3	nil	3.0	nil	nil	6.4	1.9	0.4	nil	nil	nil	1.0	35.2	11.5	1.0
Max	59.9	0.5	76.9	18.2	3.3	24.3	12.0	10.1	1.1	4.3	11.0	25.6	87.5	35.4	39.8
Mean	28.6	0.1	24.1	4.4	0.6	12.6	4.3	3.2	0.3	0.8	5.4	15.8	52.8	25.3	21.9
SD	14.1	0.1	17.5	4.4	0.8	4.0	2.8	2.7	0.4	1.0	3.4	6.2	11.6	5.1	9.1
Argada- I															
9 (top)	8.0	nil	66.1	0.5	nil	4.0	4.5	12.1	nil	nil	3.1	1.8	74.1	21.0	4.9
8	5.1	nil	61.2	nil	nil	1.5	3.1	16.3	nil	nil	5.1	7.7	66.3	20.9	12.8

Table 4.20 Microlithotype content (carbominerite free) basis (vol.%) of different coals seams of Barka Sayal area, South Karanpura Coalfield, Jharkhand, India

	Vte	Lte	Ite	ClV	ClL	ViV	ViI	DuI	DuL	VIL	CLD	DUC	Mo	Bi	Tri
7	4.1	nil	63.9	0.5	nil	3.2	4.1	17.8	nil	nil	4.6	1.8	68.0	25.6	6.4
6	9.8	nil	58.5	0.6	nil	8.5	3.7	8.5	nil	nil	5.5	4.9	68.3	21.3	10.4
5	4.3	nil	52.5	nil	nil	4.9	6.2	20.4	nil	nil	6.8	4.9	56.8	31.5	11.7
4	4.6	nil	59.9	0.5	nil	6.1	8.1	12.2	nil	nil	3.6	5.1	64.5	26.9	8.6
3	13.4	nil	48.7	1.9	nil	7.8	6.0	9.7	nil	nil	8.6	4.1	62.1	25.3	12.6
2	8.6	nil	60.5	0.4	nil	7.1	5.2	11.2	nil	nil	4.5	2.6	69.0	23.9	7.1
1 (bottom)	13.1	nil	32.1	2.1	nil	11.0	6.9	11.4	nil	nil	9.0	14.5	45.2	31.4	23.5
Min	4.1	nil	32.1	nil	nil	1.5	3.1	8.5	nil	nil	3.1	1.8	45.2	20.9	4.9
Max	13.4	nil	66.1	2.1	nil	11.0	8.1	20.4	nil	nil	9.0	14.5	74.1	31.5	23.5
Mean	7.9	nil	55.9	0.7	nil	6.0	5.3	13.3	nil	nil	5.6	5.3	63.8	25.3	10.9
SD	3.5	nil	9.8	0.7	nil	2.8	1.6	3.8	nil	nil	2.0	3.7	8.0	3.9	5.2
Argada- J															
13 (top)	1.3	nil	90.8	nil	nil	nil	nil	7.1	nil	nil	nil	0.8	92.1	7.1	0.8
12	31.1	nil	26.4	2.2	nil	17.3	1.8	4.7	nil	nil	1.4	15.2	57.4	26.0	16.6
11	18.2	nil	43.8	0.7	nil	12.8	3.7	3.4	nil	nil	3.4	14.1	62.0	20.5	17.5
10	22.5	nil	45.4	1.7	nil	9.3	4.2	3.9	nil	nil	5.9	7.0	67.9	19.2	13.0
9	40.9	nil	24.6	4.4	nil	10.5	4.0	2.5	nil	nil	3.6	9.4	65.6	21.4	13.0
8	17.3	nil	42.7	2.2	nil	9.9	5.5	4.4	nil	nil	8.5	9.6	59.9	22.1	18.0
7	39.7	nil	29.0	3.3	nil	15.7	4.0	0.7	nil	nil	1.6	6.1	68.7	23.6	7.7
6	20.9	nil	40.7	4.7	nil	19.4	5.0	2.9	nil	nil	3.2	3.2	61.5	32.0	6.5
5	34.3	nil	19.8	3.3	nil	17.8	2.1	0.8	nil	nil	5.0	16.9	54.1	24.0	21.9
4	13.9	nil	46.0	1.5	nil	10.2	1.5	8.8	nil	nil	9.5	8.8	59.9	21.9	18.3
3	18.3	nil	29.8	1.9	nil	13.5	1.0	3.9	nil	nil	19.2	12.5	48.1	20.2	31.7
2	7.5	nil	53.4	1.5	nil	6.8	3.0	11.3	nil	nil	3.8	12.8	60.9	22.6	16.5
1 (bottom)	6.9	nil	56.9	nil	nil	1.5	2.3	6.2	nil	nil	10.0	16.2	63.9	10.0	26.2
Min	1.3	nil	19.8	nil	nil	nil	nil	0.7	nil	nil	nil	0.8	48.1	7.1	0.8
Max	40.9	nil	90.8	4.7	nil	19.4	5.5	11.3	nil	nil	19.2	16.9	92.1	32.0	31.7
Mean	21.0	nil	42.2	2.1	nil	11.1	2.9	4.7	nil	nil	5.8	10.2	63.2	20.8	16.0
SD	12.0	nil	17.8	1.4	nil	5.7	1.6	2.9	nil	nil	4.9	4.8	9.9	6.1	7.9

Vte- Vitrite, Lte- Liptite, Ite- Inertite, ClV- Clarite V, ClL- Clarite L, ViV- Vitrinertite V, ViI- Vitrinertite I, DuI- Durite I, DuL- Durite L, VIL- Vitrinertoliptite, CLD- Clarodurite, DUC- Duroclarite, Mo- Monomacerals, Bi- Bimacerals, Tri- Trimacerals.

5 CHAPTER 5. GEOCHEMICAL CHARACTERISTICS

5.1 Introduction

The geochemical characterization of coal is essential in illuminating the reactivity of organic matter and inorganic constituents in coal. The organic petrography, chemical, and mineralogical characteristics of the coal control its technological behaviour, by-product characteristics, environmental impact, and effects on human health as well as ecology. Information about the geochemical characteristics of this complex, abundant fossil fuel facilitates the identification of water salinity, depositional environment, redox conditions during sedimentation, source-rock characteristics, tectonic setting, utilization potential, classification, etc. (Ayinla *et al.* 2017).

The geochemical characterization of coal is a difficult task due to the diversity originated by different peat-forming communities, coalification trends etc. Despite the challenges, a thorough understanding of the geochemical properties of coal provides vital information about this vital source of energy. During the coalification process, due to physical, chemical, and microbiological changes, the quantities of elemental constituents change in the different types of coal. Chemical analysis of coal provides vital information about the quality (i.e., rank and grade) and genetic characteristics of coal. The proximate analysis is a robust tool for qualitative and quantitative assessment of organic (fixed carbon and volatile matter) and inorganic (ash and moisture) matter present in coal.

In the present study, the various geochemical constituents which show their presence in the coals of South Karanpura coalfield have been identified by different analytical techniques such as proximate analysis, ultimate analysis, XRD, XRF, FTIR, and GC-MS. For these analyses, samples were taken from the coal seams present in Barka Sayal as well as in the Argada area of the South Karanpura coalfield, Jharkhand, India. The

detailed analytical procedures for different geochemical analyses are described in Chapter III. The Rock-Eval Pyrolysis has also been conducted, which has been discussed in Chapter VI.

5.2 Proximate analysis

The proximate analysis is mostly used in the grading and quality assessment of the coal for its industrial utilization. It includes the determination of moisture (M), volatile matter (VM), ash yield (A), and fixed carbon (FC). The Indian standard (BIS 2003b) was used for the analysis of these coals. All the coal samples were analysed for proximate constituents (M, A, VM, FC), which are also subjected to microscopic study. The result of the proximate analysis is given on a “dry basis” and “daf basis” in the text as well as in Table 5.1 and Table 5.2 and Figure 5.1 to Figure 5.13.

5.2.1 Moisture

The water contents in coal may present in various forms, such as films on the surface of the coal particles, inside the capillaries, incorporated with organic compounds, and forming the part of the crystal structure of the minerals. The water content present in coal is known as the moisture content of the coal. During proximate analysis, adventitious moisture present on the surface evaporates in the laboratory atmosphere. However, the inherent moisture, which is mainly affected by stages of maturation, is calculated as the moisture content of the coal following the process, as mentioned in Chapter 3.

In the coals of South Karanpura coalfield, the moisture content of the coal seams of Barka Sayal area is slightly higher in comparison to the Argada area and varies from 1.45% to 6.47%, mean 3.67%, whereas for coals of Argada area the moisture content lies in the range of 0.19%- 3.74%, mean 1.81% (Table 5.1 and Table 5.2)

.

5.2.2 Ash Yield

The ash yield represents the non-combustible inorganic residue left after the burning of the coal. The coals of the Barka Sayal area have ash yield lying in the range of 4% to 52.11%, mean 22.49%, while coals of the Argada area exhibit comparatively higher ash yield, ranging from 8.85% to 68.53%, mean 26.28% (Table 5.1 and Table 5.2). Some bands of the Sayal seam of the Barka Sayal area exhibit a relatively very high content of ash because of the presence of a high concentration of minerals.

5.2.3 Volatile Matter

The organic components of the coal liberated at high temperature in a vacuum condition, excluding the moisture content, are known as volatile matter. The volatile matter content of coal seams of the Barka Sayal area lies in the range of 21.29% to 36.68%, mean 30.36%, while coals of the Argada area have volatile matter content in between 14.12% and 37.13%, mean 27.94% (Table 5.1 and Table 5.2). The VM (daf basis) is also used to predict the rank of South Karanpura coals. Coals seams of the Argada area exhibit lower VM content compared to the coal seams of the Barka Sayal area due to the variation in the microscopic constituents and lithological stress.

5.2.4 Fixed Carbon

The solid combustible material of coal after the expulsion of volatile components is called fixed carbon. Fixed carbon is determined by the difference discussed in Chapter 3. The fixed carbon content of the coals of the Barka Sayal area lies between 19.30% and 56.51%, mean 43.48% (42.87%-70.59%, mean 58.41%, daf basis). Coals of Argada area have fixed carbon content in the range of 16.30% to 54.32%, mean 43.97% (52.43%-68.93%, mean 60.96%, daf basis) (Table 5.1 and Table 5.2).

5.2.5 Distribution of Proximate constituents

In the present study, the pillar coal samples were drawn from all working sections of the Barka Sayal and Argada areas. The coal samples have been subjected to proximate analysis to see the variation in the distribution of proximate constituents along with the coal seam profiles from top to bottom of the seams.

5.2.5.1 Coal Seams of Barka Sayal area

Coal seams of the Barka Sayal area exhibit relatively less moisture (mean 3.67%) while ash (mean 22.49%), volatile matter (mean 30.36%), and fixed carbon contents (mean 43.48%) are comparatively high. These changes in proximate constituents are being mainly guided by the presence of mineral matter and microscopic constituents of the coal, which is controlling the type of band present in the seam. Bright bands are exhibiting high volatile matter and fixed carbon, whereas duller bands exhibit higher ash yield.

The coals of the Sayal seam contain moisture content 2.71% to 4.33%, mean 3.49% on the air-dried basis. The ash yield from 16.56% to 52.11%, mean 30.57%. Some of the bands of this seam exhibit high ash yield due to the presence of a high amount of hematite. The volatile matter lies between 23.54% and 35.79%, mean 28.67% (29.41%- 57.13%, mean 44.66% daf basis) (Table 5.1). From top to bottom, the moisture content first increases until the midpoint, then decreases towards bottom. Ash yield becomes high in the middle part of the seam, while volatile content decreases towards the bottom. Fixed carbon content first decreases then increases in the bottom of the seam (Figure 5.1).

The coals of the Sayal Balkudra seam contain moisture range content from 2.71% to 4.33%, mean 3.49%, on the air-dried basis. The ash yield of these coals lies in the range of 16.56% to 52.11%, mean 30.57%. The volatile matter lies between 21.29% and 34.56%, mean 28.69% (38.83%- 50.97%, mean 42.83% on daf basis). The fixed carbon

content lie between 23.44% and 50.33%, mean 39.13% (49.03%- 61.17%, mean 57.17%, on daf basis) (Table 5.1). Ash yield varies with the types of banding present in the coal seam and is highest in the 'banded dull coal' present in the middle part of the seam. Fixed carbon content increases towards the bottom of the seam. Moisture and volatile matter show the difference influenced by the presence of different types of bands (Figure 5.2).

Moisture content in the coals of the Upper Semana seam lies in the range of 1.57% to 4.58%, mean 3.01%. These coals have ash yield from 12.30% to 22.12%, mean 15.40%. The volatile matter content lies in the range of 27.76% to 33.59%, mean 30.76% (33.37%-40.31%, mean 37.72%, on daf basis). The fixed carbon content varies from 46.24% to 55.43%, mean 50.83% (59.69-66.63, mean 62.28%, on daf basis) (Table 5.1). Moisture and fixed carbon content increase towards the bottom of the seam while ash yield and volatile matter decrease in the bottom portion of the seam due to the presence of brighter bands in the bottom of the seam (Figure 5.3).

The coals of Lower Semana seam, the exhibit moisture content in the range of 1.45% to 4.75%, mean 2.84%. These coals have a relatively less ash yield, which varies from 4% to 25.38%, mean 14.93%. The volatile matter in these coals lies in the range of 28% to 36.01%, mean 32.76% (37.68%- 41.28%, mean 39.84%, daf basis). Fixed carbon content in these coals lie in between 43.31% and 55.25%, mean 49.46% (58.72%-62.32%, mean 60.16%, daf basis) (Table 5.1). The variation of proximate constituents along the coal seam profile is presented in (Figure 5.4). Moisture, volatile matter, and fixed carbon increase towards the bottom portion of the coal seam (Figure 5.4).

The coals of the Hathidari seam have a moisture content lying in the range of 3.09% to 4.68%, mean 3.90%. The ash yield varies from 13.10% to 29.99%, mean 21.80%. Volatile matter is in between 25.47% and 36.68%, mean 31.30% (35.96%-46.13%, mean 42.17%.

Fixed carbon content varies in the range of 35.62%-46.14%, mean 43% (53.87%-64.04%, mean 57.83% daf basis) (Table 5.1). Moisture, volatile matter, and fixed carbon content increase towards the bottom part of the seam (Figure 5.5).

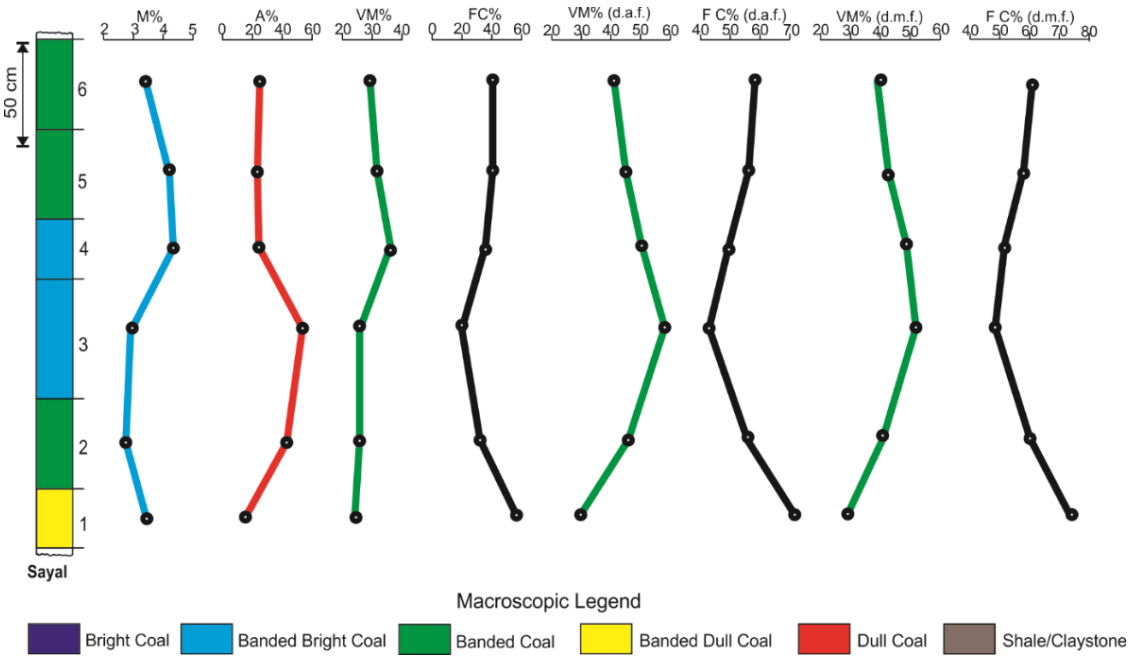


Figure 5.1 Variation of proximate constituents along the macropetrographic seam section of Sayal seam.

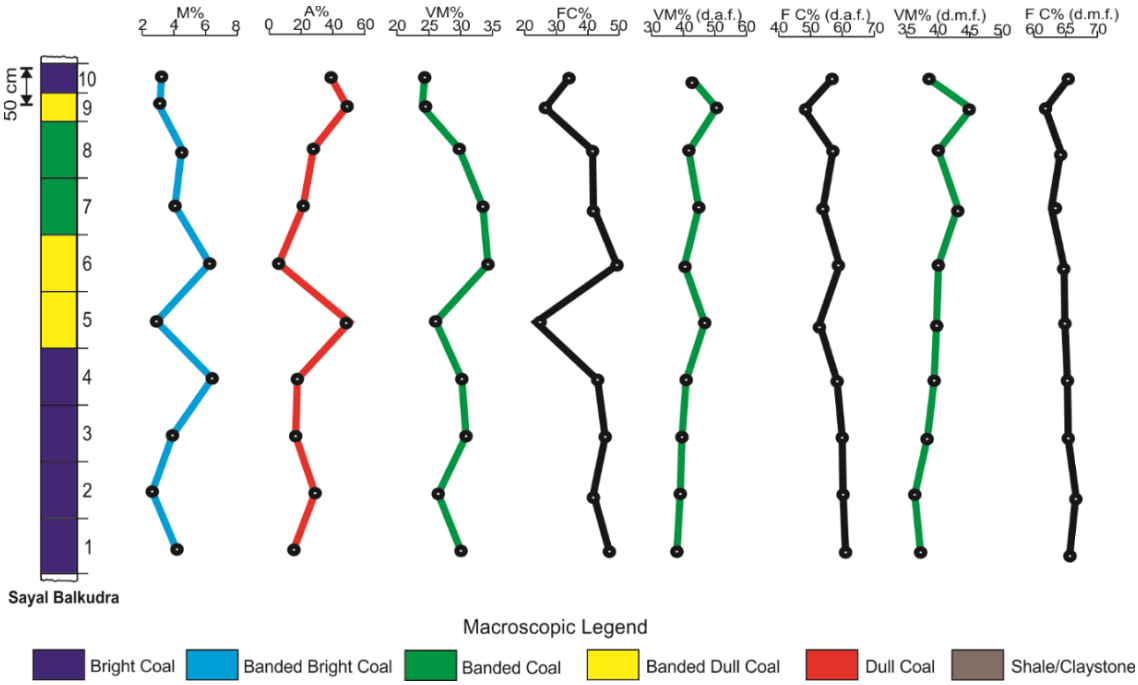


Figure 5.2 Variation of proximate constituents along the macropetrographic seam section of Sayal Balkudra seam.

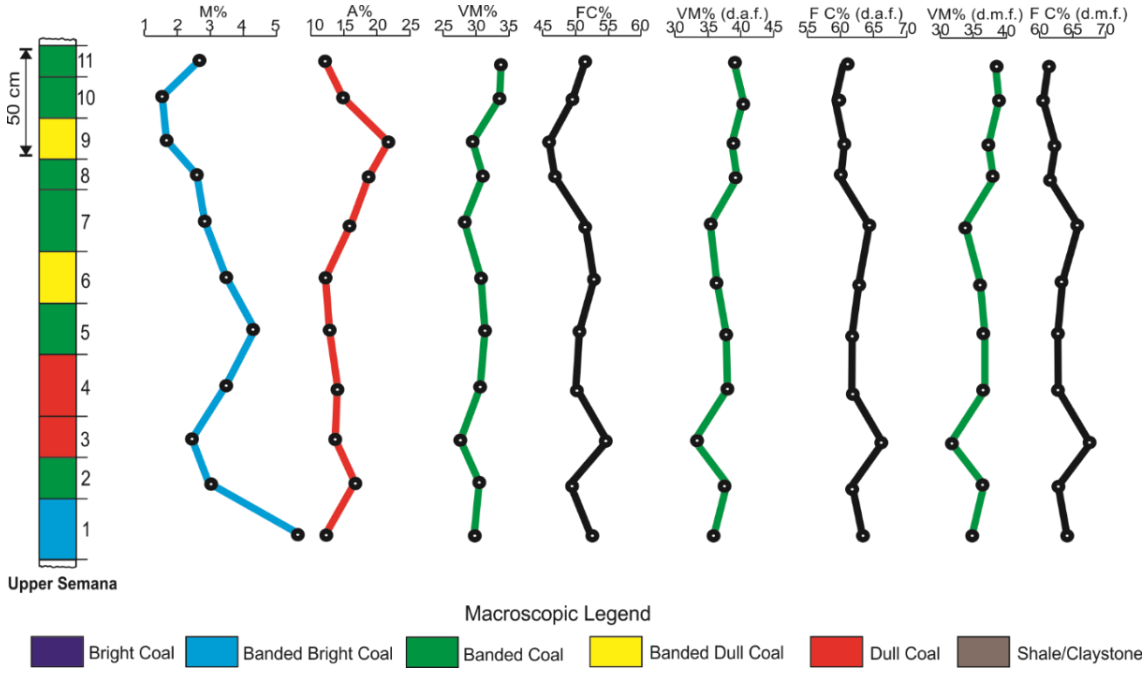


Figure 5.3 Variation of proximate constituents along the macropetrographic seam section of Upper Semana seam.

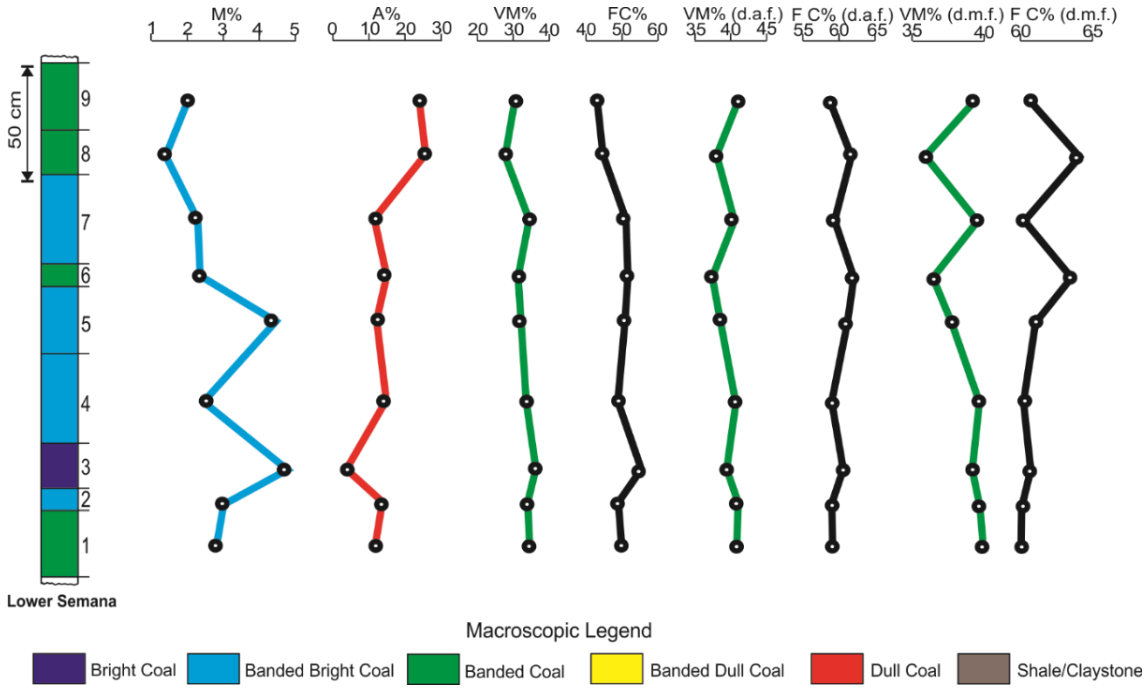


Figure 5.4 Variation of proximate constituents along the macropetrographic seam section of Lower Semana seam.

The Bansgarha coals show moisture content in the range of 3.10% to 5.42%, mean 4.52%. Ash yield varies from 18.93% to 32.38%, mean 24.31%. Volatile matter lies in between 28.63% and 33.98%, mean 29.97% (38.87%-49.59%, mean 42.33%, daf basis). Fixed

carbon ranges from 33.34% to 47.01%, mean 41.20% (50.41%-61.13%, mean 57.67%, daf basis) (Table 5.1). Moisture, volatile matter, and ash yield exhibit an increasing trend towards the bottom of the seam (Figure 5.6).

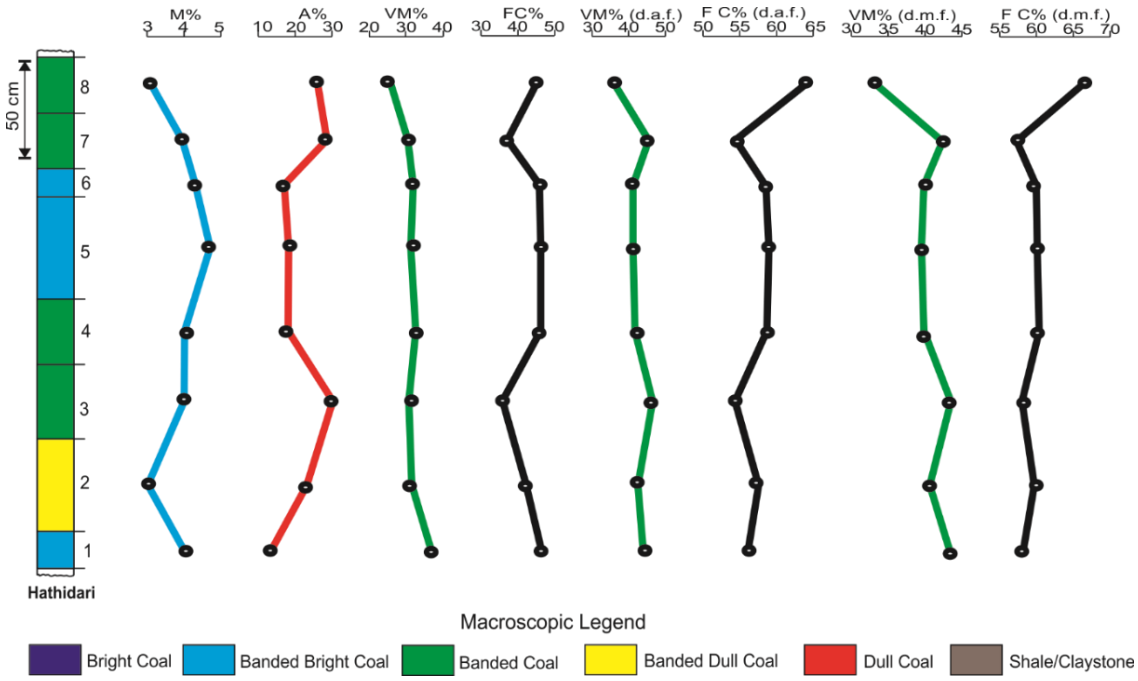


Figure 5.5 Variation of proximate constituents along the macropetrographic seam section of Hathidari seam.

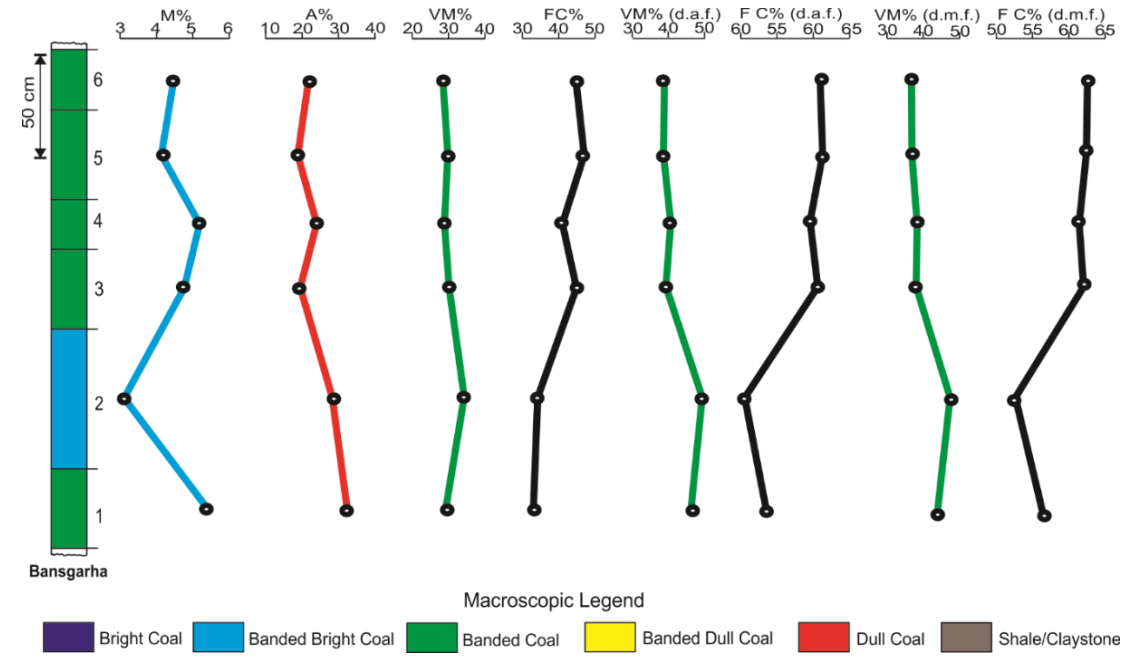


Figure 5.6 Variation of proximate constituents along the macropetrographic seam section of Bansgarha seam.

Table 5.1 Proximate constituents (wt%) of coal seams of Barka Sayal area, South Karanpura coalfield.

Seam name and Sample No.	As received basis				Dry Basis			Daf basis		Dmf basis		
	Moisture	Ash	Volatile Matter	Fixed Carbon	Ash	Volatile Matter	Fixed Carbon	Volatile Matter	Fixed Carbon	Volatile Matter	Fixed Carbon	Fuel Ratio
Sayal												
6 (top)	3.44	25.52	29.63	41.40	26.43	30.69	42.88	41.71	58.29	39.54	60.46	1.40
5	4.21	23.31	32.11	40.37	24.34	33.52	42.15	44.30	55.70	42.45	57.55	1.26
4	4.33	24.87	35.79	35.01	26.00	37.41	36.60	50.55	49.45	48.75	51.25	0.98
3	2.88	52.11	25.71	19.30	53.65	26.47	19.87	57.13	42.87	51.51	48.49	0.75
2	2.71	41.05	25.24	31.00	42.19	25.94	31.87	44.88	55.12	40.54	59.46	1.23
1 (bottom)	3.38	16.56	23.54	56.51	17.14	24.37	58.49	29.41	70.59	27.92	72.08	2.40
Min	2.71	16.56	23.54	19.30	17.14	24.37	19.87	29.41	42.87	27.92	48.49	0.75
Max	4.33	52.11	35.79	56.51	53.65	37.41	58.49	57.13	70.59	51.51	72.08	2.40
Mean	3.49	30.57	28.67	37.27	31.63	29.73	38.64	44.66	55.34	41.78	58.22	1.34
SD	0.61	12.11	4.29	11.29	12.37	4.62	11.74	8.48	8.48	7.55	7.55	0.52
Sayal Balkudra												
10 (top)	3.39	39.85	24.52	32.24	41.25	25.38	33.38	43.19	56.81	38.90	61.10	1.32
9	3.51	48.68	24.37	23.44	50.45	25.26	24.29	50.97	49.03	45.41	54.59	0.96
8	4.54	24.16	30.09	41.22	25.31	31.52	43.18	42.19	57.81	40.17	59.83	1.37
7	4.23	21.02	33.79	40.96	21.95	35.29	42.77	45.21	54.79	43.62	56.38	1.21
6	6.31	8.79	34.56	50.33	9.38	36.89	53.72	40.71	59.29	40.09	59.91	1.46
5	3.01	51.54	21.29	24.16	53.14	21.95	24.91	46.84	53.16	40.04	59.96	1.14
4	6.47	19.43	30.43	43.67	20.77	32.53	46.69	41.06	58.94	39.48	60.52	1.44
3	4.12	18.10	30.97	46.82	18.87	32.30	48.83	39.81	60.19	38.37	61.63	1.51
2	2.70	29.73	26.69	40.88	30.55	27.43	42.02	39.49	60.51	36.71	63.29	1.53
1 (bottom)	4.27	17.92	30.21	47.59	18.73	31.56	49.72	38.83	61.17	37.38	62.62	1.58
Min	2.70	8.79	21.29	23.44	9.38	21.95	24.29	38.83	49.03	36.71	54.59	0.96
Max	6.47	51.54	34.56	50.33	53.14	36.89	53.72	50.97	61.17	45.41	63.29	1.58
Mean	4.25	27.92	28.69	39.13	29.04	30.01	40.95	42.83	57.17	40.02	59.98	1.35
SD	1.20	13.53	4.10	8.97	13.85	4.55	9.68	3.64	3.64	2.53	2.53	0.19
Up. Semana												
11 (top)	2.69	12.30	33.46	51.55	12.64	34.39	52.97	39.36	60.64	38.47	61.53	1.54
10	1.57	15.10	33.59	49.74	15.34	34.13	50.54	40.31	59.69	39.21	60.79	1.48
9	1.73	22.12	29.92	46.24	22.50	30.44	47.05	39.29	60.71	37.47	62.53	1.55

Seam name and Sample No.	As received basis				Dry Basis			Daf basis		Dmf basis		
	Moisture	Ash	Volatile Matter	Fixed Carbon	Ash	Volatile Matter	Fixed Carbon	Volatile Matter	Fixed Carbon	Volatile Matter	Fixed Carbon	Fuel Ratio
8	2.65	18.91	31.18	47.26	19.42	32.03	48.54	39.75	60.25	38.27	61.73	1.52
7	2.88	16.76	28.54	51.83	17.25	29.38	53.36	35.51	64.49	34.14	65.86	1.82
6	3.55	12.64	30.81	53.00	13.11	31.95	54.95	36.77	63.23	35.80	64.20	1.72
5	4.39	12.86	31.51	51.23	13.46	32.96	53.58	38.09	61.91	37.11	62.89	1.63
4	3.51	14.52	31.17	50.80	15.05	32.31	52.65	38.03	61.97	36.91	63.09	1.63
3	2.51	14.31	27.76	55.43	14.68	28.47	56.85	33.37	66.63	32.20	67.80	2.00
2	3.09	16.91	30.46	49.54	17.45	31.43	51.12	38.07	61.93	36.74	63.26	1.63
1 (bottom)	4.58	13.02	29.93	52.47	13.64	31.37	54.99	36.32	63.68	35.30	64.70	1.75
Min	1.57	12.30	27.76	46.24	12.64	28.47	47.05	33.37	59.69	32.20	60.79	1.48
Max	4.58	22.12	33.59	55.43	22.50	34.39	56.85	40.31	66.63	39.21	67.80	2.00
Mean	3.01	15.40	30.76	50.83	15.87	31.71	52.42	37.72	62.28	36.51	63.49	1.66
SD	0.91	2.91	1.70	2.47	2.90	1.73	2.77	1.98	1.98	1.95	1.95	0.15
Lr. Semana												
9 (top)	2.00	24.23	30.45	43.31	24.73	31.07	44.20	41.28	58.72	39.29	60.71	1.42
8	1.45	25.38	28.00	45.17	25.76	28.41	45.83	38.27	61.73	36.05	63.95	1.61
7	2.27	12.20	34.68	50.85	12.49	35.49	52.03	40.55	59.45	39.69	60.31	1.47
6	2.37	14.91	31.17	51.55	15.27	31.93	52.80	37.68	62.32	36.54	63.46	1.65
5	4.42	12.47	32.21	50.90	13.05	33.70	53.25	38.76	61.24	37.82	62.18	1.58
4	2.49	14.98	33.73	48.81	15.36	34.59	50.05	40.86	59.14	39.77	60.23	1.45
3	4.75	4.00	36.01	55.25	4.20	37.80	58.00	39.46	60.54	39.19	60.81	1.53
2	2.99	13.86	33.97	49.18	14.29	35.02	50.69	40.86	59.14	39.85	60.15	1.45
1 (bottom)	2.86	12.39	34.61	50.14	12.75	35.63	51.61	40.84	59.16	39.97	60.03	1.45
Min	1.45	4.00	28.00	43.31	4.20	28.41	44.20	37.68	58.72	36.05	60.03	1.42
Max	4.75	25.38	36.01	55.25	25.76	37.80	58.00	41.28	62.32	39.97	63.95	1.65
Mean	2.84	14.93	32.76	49.46	15.32	33.74	50.94	39.84	60.16	38.69	61.31	1.51
SD	1.03	6.11	2.38	3.32	6.16	2.67	3.84	1.25	1.25	1.42	1.42	0.08
Hathidari												
8 (top)	3.12	26.05	25.47	45.36	26.89	26.29	46.82	35.96	64.04	33.51	66.49	1.78
7	3.94	28.63	30.50	36.93	29.80	31.75	38.45	45.23	54.77	42.80	57.20	1.21
6	4.34	17.27	32.25	46.14	18.05	33.71	48.24	41.14	58.86	39.81	60.19	1.43
5	4.68	17.91	31.70	45.71	18.78	33.26	47.96	40.95	59.05	39.55	60.45	1.44
4	4.01	18.27	31.99	45.73	19.03	33.33	47.64	41.16	58.84	39.75	60.25	1.43
3	3.89	29.99	30.50	35.62	31.21	31.73	37.06	46.13	53.87	43.57	56.43	1.17

Seam name and Sample No.	As received basis				Dry Basis			Daf basis		Dmf basis		
	Moisture	Ash	Volatile Matter	Fixed Carbon	Ash	Volatile Matter	Fixed Carbon	Volatile Matter	Fixed Carbon	Volatile Matter	Fixed Carbon	Fuel Ratio
2	3.09	23.17	31.34	42.39	23.91	32.34	43.74	42.51	57.49	40.64	59.36	1.35
1 (bottom)	4.09	13.10	36.68	46.13	13.66	38.24	48.10	44.29	55.71	43.40	56.60	1.26
Min	3.09	13.10	25.47	35.62	13.66	26.29	37.06	35.96	53.87	33.51	56.43	1.17
Max	4.68	29.99	36.68	46.14	31.21	38.24	48.24	46.13	64.04	43.57	66.49	1.78
Mean	3.90	21.80	31.30	43.00	22.67	32.58	44.75	42.17	57.83	40.38	59.62	1.38
SD	0.51	5.67	2.87	4.06	5.85	3.07	4.27	3.00	3.00	3.04	3.04	0.18
Bansgarha												
6 (top)	4.46	22.29	28.63	44.63	23.33	29.96	46.71	39.08	60.92	37.16	62.84	1.56
5	4.18	18.93	29.89	47.01	19.75	31.19	49.06	38.87	61.13	37.33	62.67	1.57
4	5.21	24.17	28.65	41.98	25.49	30.22	44.28	40.56	59.44	38.46	61.54	1.47
3	4.75	19.73	29.81	45.71	20.71	31.30	47.99	39.47	60.53	37.85	62.15	1.53
2	3.10	28.38	33.98	34.54	29.29	35.07	35.64	49.59	50.41	47.42	52.58	1.02
1 (bottom)	5.42	32.38	28.86	33.34	34.24	30.51	35.25	46.40	53.60	43.46	56.54	1.16
Min	3.10	18.93	28.63	33.34	19.75	29.96	35.25	38.87	50.41	37.16	52.58	1.02
Max	5.42	32.38	33.98	47.01	34.24	35.07	49.06	49.59	61.13	47.42	62.84	1.57
Mean	4.52	24.31	29.97	41.20	25.47	31.38	43.16	42.33	57.67	40.28	59.72	1.38
SD	0.76	4.76	1.87	5.36	5.02	1.72	5.64	4.15	4.15	3.84	3.84	0.22

5.2.5.2 Coal Seams of the Argada area

The coals of the Argada area exhibit lesser moisture (mean 1.81%), volatile matter (27.94%), and approximately same fixed carbon (mean 43.97%) content compared to the coals of the Barka Sayal area. These coals also possess higher ash yield (mean 26.28%) because of the presence of high mineral matter in these coals.

The coals belonging to Argada seam exhibit moisture content lying in the range of 0.19% to 1.51%, mean 0.76%. The ash yield varies from 12.77% to 64.99%, mean 29.62%. The volatile matter lies in the range of 15.99% to 36.63%, mean 28.16% (32.62%-48.57%, mean 41.01%, daf basis). The fixed carbon content varies -between 17.74% and 53.20%, mean 41.47% (51.43%- 67.38%, mean 58.99%, daf basis) (Table 5.2). Volatile matter and fixed carbon are high in the top and bottom portion of this seam and low in the middle part. Moisture content increases towards the bottom. The middle part of the seam exhibit a higher ash yield compared to the top and bottom portion (Figure 5.7).

Moisture content in the coals of Argada-A varies from 0.86% to 3.43%, mean 1.69%. The ash yield lies between 11.13% and 45.29%, mean 24.95%. Volatile content lies in the range of 22.17% and 32.97%, mean 28.07% (34.70%-42.77%, mean 38.44%, daf basis). The fixed carbon content varies from 31.68% to 54.32%, mean 45.29% (57.23%-65.30%, mean 61.56%, daf basis) (Table 5.2). In this coal seam, the moisture, volatile matter, and fixed carbon are increasing towards the bottom of the seam, whereas the ash yield decrease towards the bottom portion indicating coal of high quality is present in the bottom portion of the seam (Figure 5.8).

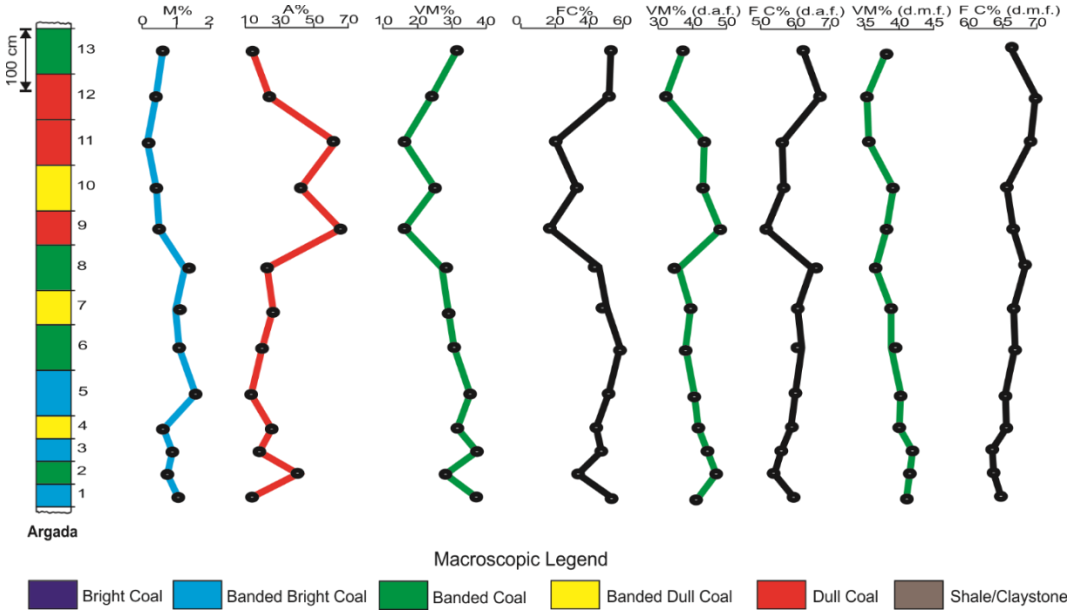


Figure 5.7 Variation of proximate constituents along the macropetrographic seam section of Argada seam.

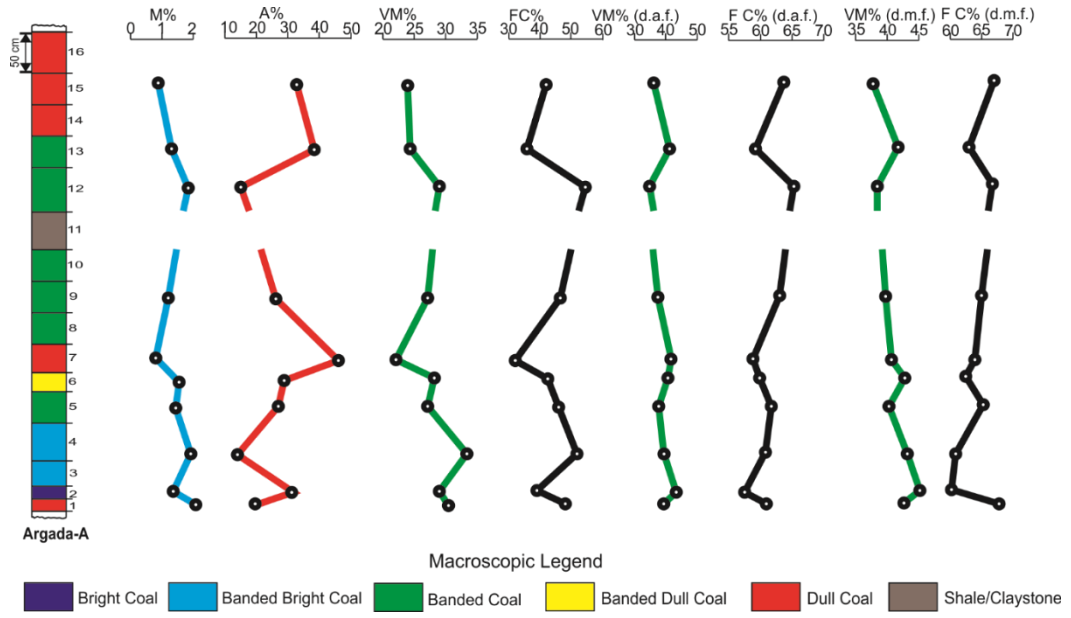


Figure 5.8 Variation of proximate constituents along the macropetrographic seam section of Argada-A seam.

The coals of Argada-B seam exhibit moisture content in the range of 0.89% to 3.74%, mean 2.14%. The ash yield varies from 8.85% to 68.53%, mean 31.74%. The volatile matter lies in the range of 14.12% to 37.13%, mean 27.11% (32.31%-47.62%, mean 41.13%, daf basis). The fixed carbon content varies from 16.30% to 51.09%, mean

39.01% (52.38%-67.69%, mean 58.87%, daf basis) (Table 5.2). Argada B coal seam also exhibits approximately the same trend as Argada-A coal seam and exhibits moisture, volatile matter, and fixed carbon content increasing towards the bottom portion of the seam. In contrast, ash yield decreases towards the bottom of the seam, along with the fluctuations guided by the presence of different bands (Figure 5.9).

The coals of Argada-C seam have a moisture content lying in the range of 1.24% to 3.47%, mean 2.35%. The ash yield lies between 12.49% and 43.04%, mean 24.04%. The volatile matter varies from 23.96% to 33.54%, mean 29.51% (36.70%-43%, mean 40.25%, daf basis). The fixed carbon content in these coals varies from 31.76% to 52.37%, mean 44.10% (57%-63.30%, mean 59.75%, daf basis) (Table 5.2). Moisture content first decreases then increases from bottom to top. Ash yield exhibit a decreasing trend towards the top, whereas fixed carbon content and volatile matter increase towards the top part of the seam. (Figure 5.10).

The coals of Argada-D seam exhibit moisture content 0.62% to 3.20%, mean 1.72%. The ash yield of coals of this seam ranges from 13.90% to 47.42%, mean 22.36%. The volatile matter is in between 22.94% and 35.81%, mean 30.77% (35.81%-44.94%, mean 40.67%, daf basis). The fixed carbon content varies from 28.41% to 52.55%, mean 45.15% (55.06%-64.19%, mean 59.33%, daf basis) (Table 5.2). Moisture, volatile matter, and fixed carbon decrease towards the top, whereas ash yield increasing towards the top (Figure 5.11).

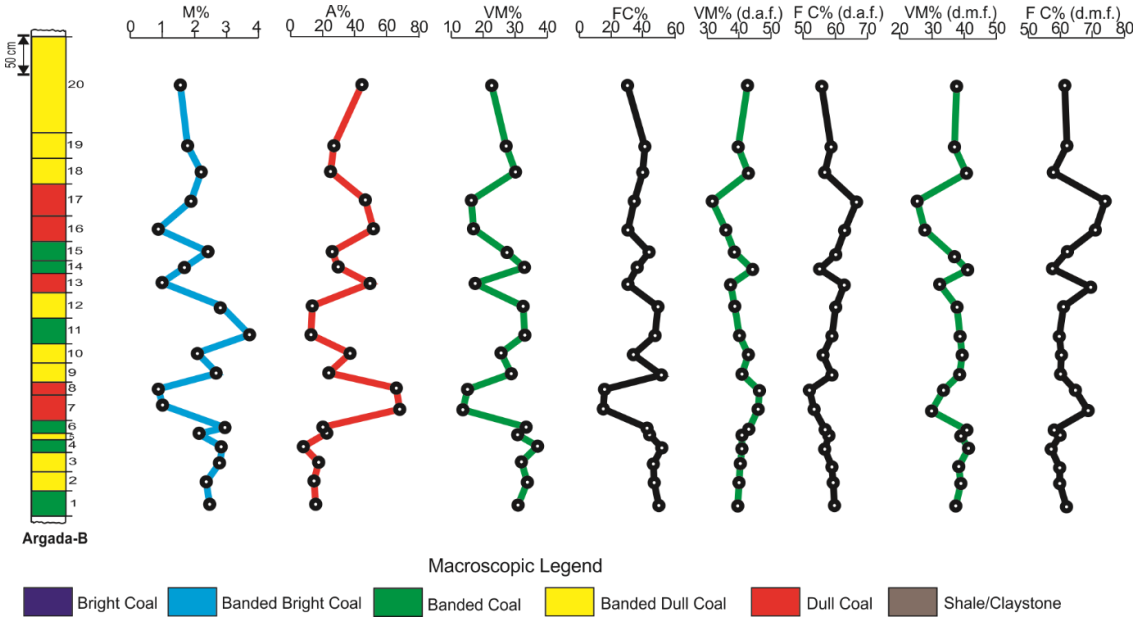


Figure 5.9 Variation of proximate constituents along the macropetrographic seam section of Argada-B seam.

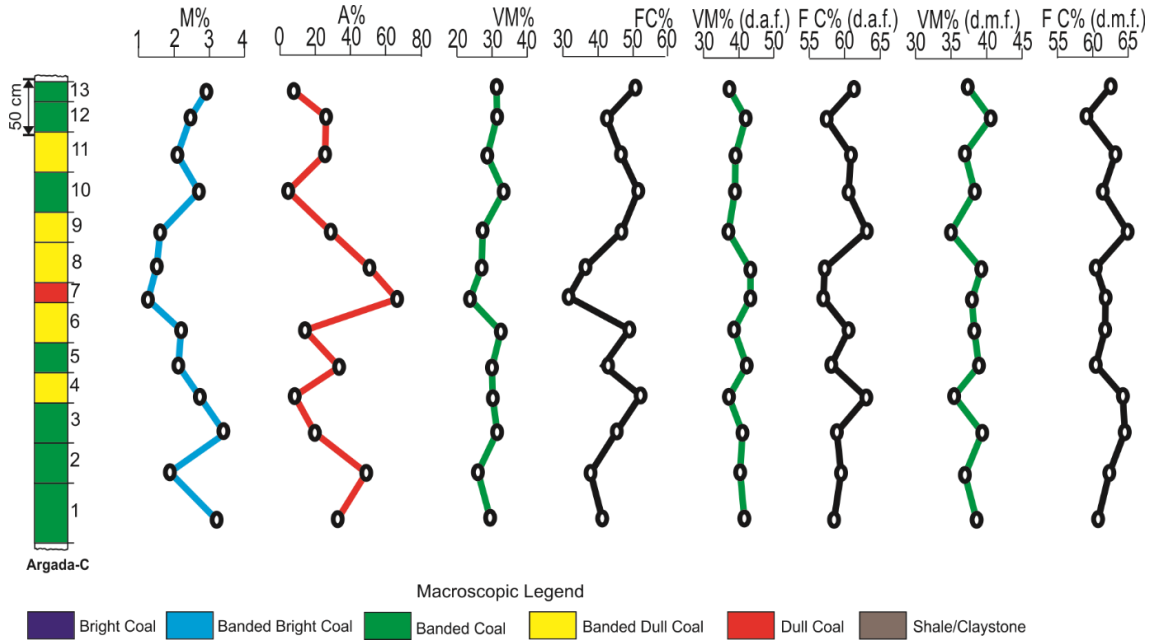


Figure 5.10 Variation of proximate constituents along the macropetrographic seam section of Argada-C seam.

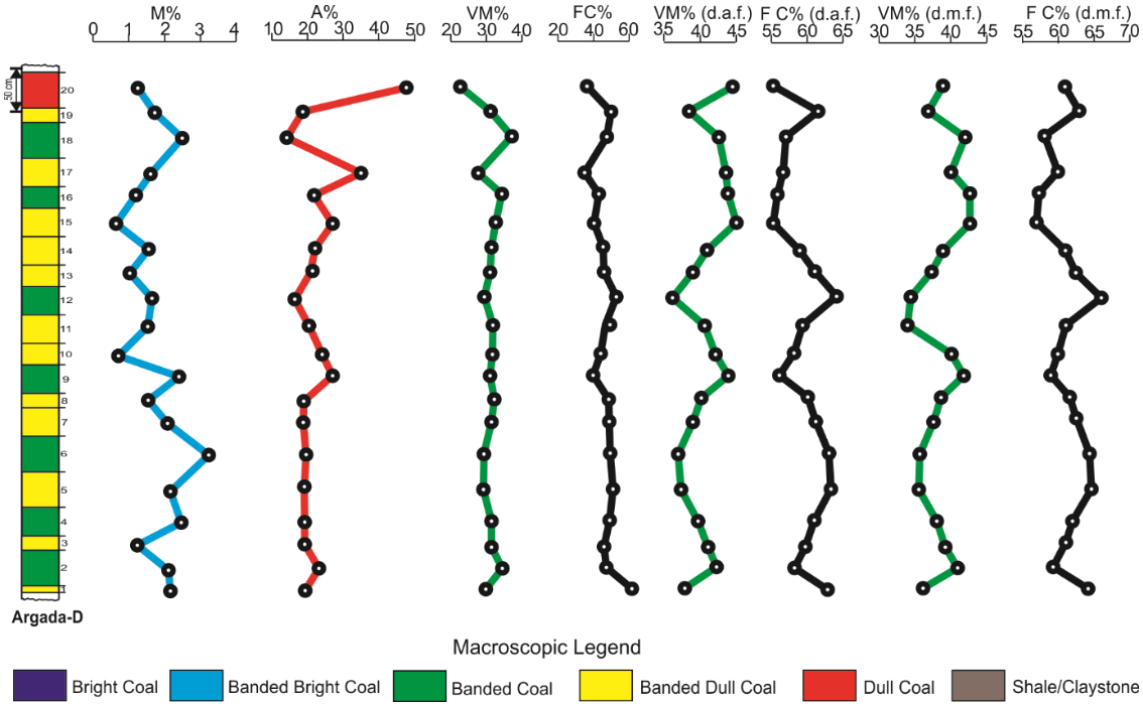


Figure 5.11 Variation of proximate constituents along the macropetrographic seam section of Argada-D seam.

The coals belonging to the Argada-I seam have a moisture content lying in the range of 1.35% to 2.63%, mean 1.84%. The ash yield varies between 20.04% and 33.67%, mean 25.95%. The volatile matter ranges from 21.55% to 25.94%, mean 23.70% (31.07%-35.08%, mean 32.85%, daf basis). The fixed carbon content in these coals are in between 43.44% and 52.78%, mean 48.50% (64.92%-68.93%, mean 67.15%, daf basis) (Table 5.2). Moisture volatile matter and fixed carbon increase towards the bottom of the seam, whereas visible minerals and ash yield decrease towards the bottom (Figure 5.12).

The moisture content of the coals of the Argada-J seam varies from 1.41% to 3.30%, mean 2.19%. The ash yield varies between 17.14% and 36.60%, mean 25.30%. The volatile matter lies in the range of 19.90% to 32.05% mean 28.26% (32.10%-45.59%, mean 38.92%, daf basis). The fixed carbon content varies from 36.59% to 48.66%, mean 44.25% (54.41%-67.90%, mean 61.08%, daf basis) (Table 5.2). Moisture content exhibits a decreasing trend towards the top part of the seam. Volatile matter and fixed carbon show

a fluctuating trend in this seam. Ash yield first decreases then increases towards the bottom to the top portion of the seam (Figure 5.13).

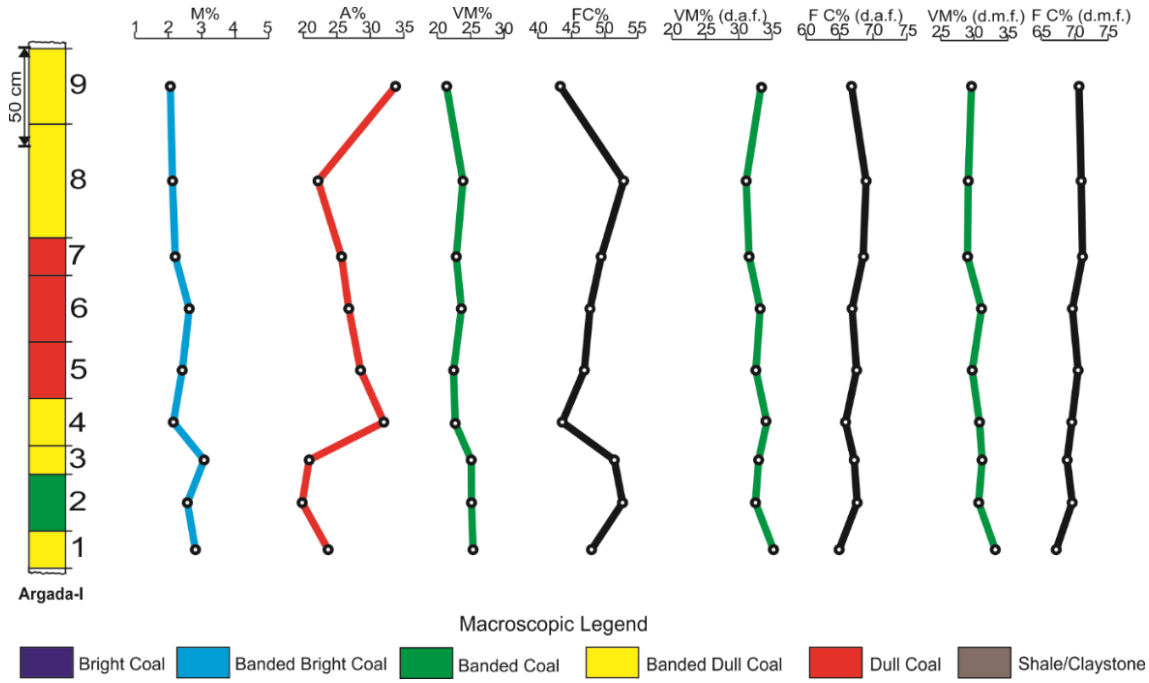


Figure 5.12 Variation of proximate constituents along the macropetrographic seam section of Argada-I seam.

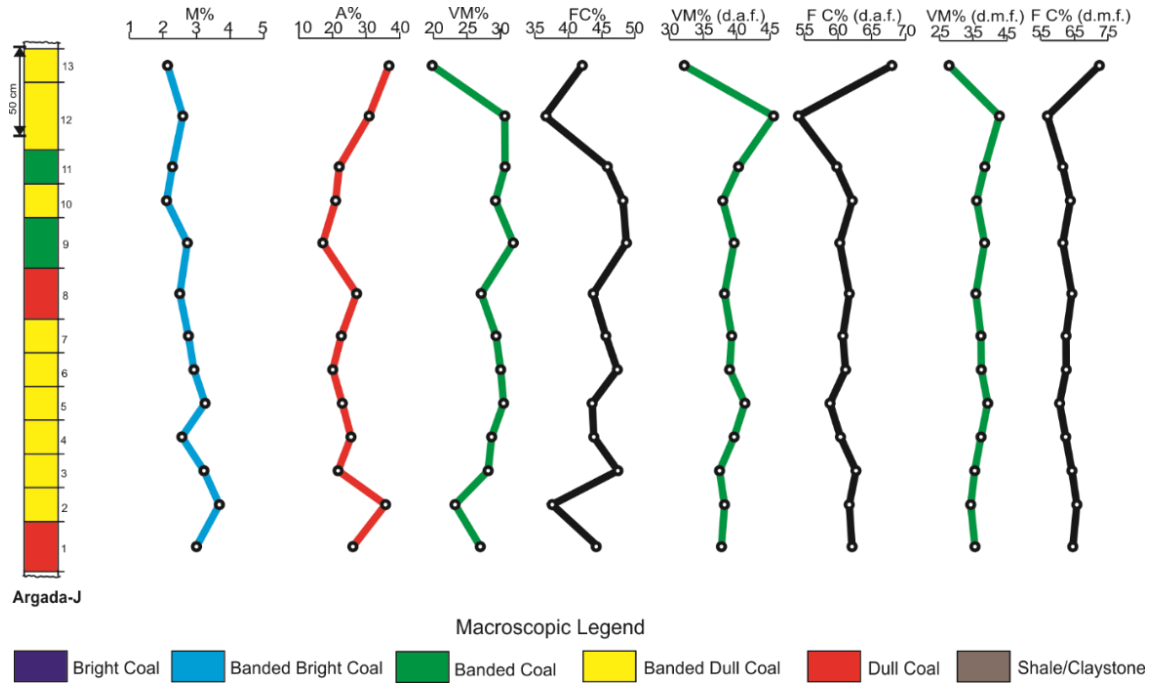


Figure 5.13 Variation of proximate constituents along the macropetrographic seam section of Argada-J seam.

Table 5.2 Proximate constituent (wt.%) of coal seams of Argada area, South Karanpura coalfield.

Seam name and Sample No.	As received basis				Dry basis			Daf basis		Dmf basis		
	Moisture	Ash	Volatile Matter	Fixed Carbon	Ash	Volatile Matter	Fixed Carbon	Volatile Matter	Fixed Carbon	Volatile Matter	Fixed Carbon	Fuel ratio
Argada												
13 (top)	0.60	14.43	31.78	53.20	14.51	31.97	53.52	37.40	62.60	36.32	63.68	1.67
12	0.41	24.80	24.40	50.40	24.90	24.50	50.60	32.62	67.38	30.31	69.69	2.07
11	0.19	62.63	15.99	21.19	62.75	16.02	21.23	43.01	56.99	31.46	68.54	1.33
10	0.43	42.17	24.83	32.57	42.35	24.94	32.71	43.26	56.74	38.76	61.24	1.31
9	0.52	64.99	16.75	17.74	65.32	16.84	17.83	48.57	51.43	36.63	63.37	1.06
8	1.18	22.74	27.11	48.96	23.01	27.44	49.55	35.64	64.36	33.66	66.34	1.81
7	0.93	25.84	28.78	44.45	26.08	29.05	44.86	39.31	60.69	37.09	62.91	1.54
6	1.04	19.69	30.58	48.69	19.90	30.90	49.20	38.58	61.42	37.01	62.99	1.59
5	1.51	13.26	34.76	50.47	13.46	35.29	51.25	40.78	59.22	39.85	60.15	1.45
4	0.61	24.87	30.86	43.66	25.03	31.05	43.92	41.42	58.58	39.39	60.61	1.41
3	0.78	16.99	36.63	45.60	17.13	36.91	45.96	44.54	55.46	43.37	56.63	1.25
2	0.67	39.86	27.46	32.02	40.12	27.65	32.23	46.17	53.83	42.31	57.69	1.17
1 (bottom)	0.96	12.77	36.11	50.16	12.89	36.46	50.65	41.86	58.14	40.99	59.01	1.39
Min	0.19	12.77	15.99	17.74	12.89	16.02	17.83	32.62	51.43	30.31	56.63	1.06
Max	1.51	64.99	36.63	53.20	65.32	36.91	53.52	48.57	67.38	43.37	69.69	2.07
Mean	0.76	29.62	28.16	41.47	29.80	28.39	41.81	41.01	58.99	37.47	62.53	1.46
SD	0.35	16.99	6.26	11.28	17.01	6.37	11.44	4.18	4.18	3.78	3.78	0.26
Argada-A												
16 (top)	1.73	33.63	26.08	38.57	34.22	26.54	39.24	40.34	59.66	37.07	62.93	1.48
15	0.94	33.28	24.00	41.78	33.59	24.23	42.18	36.48	63.52	33.10	66.90	1.74
14	1.47	21.97	28.11	48.46	22.29	28.53	49.18	36.71	63.29	34.84	65.16	1.72
13	1.35	38.56	24.64	35.45	39.09	24.98	35.94	41.00	59.00	36.96	63.04	1.44
12	1.84	14.98	28.86	54.32	15.26	29.41	55.34	34.70	65.30	33.50	66.50	1.88
11												
10	1.48	15.49	29.01	54.02	15.73	29.45	54.83	34.94	65.06	33.71	66.29	1.86
9	1.15	25.76	27.17	45.92	26.06	27.48	46.45	37.17	62.83	34.88	65.12	1.69
8	2.22	15.37	31.77	50.64	15.72	32.49	51.79	38.55	61.45	37.39	62.61	1.59
7	0.86	45.29	22.17	31.68	45.68	22.36	31.96	41.16	58.84	35.76	64.24	1.43
6	1.57	28.83	27.91	41.69	29.29	28.35	42.36	40.09	59.91	37.51	62.49	1.49
5	2.16	23.87	27.57	46.40	24.40	28.18	47.42	37.27	62.73	35.18	64.82	1.68

Seam name and Sample No.	As received basis				Dry basis			Daf basis		Dmf basis		
	Moisture	Ash	Volatile Matter	Fixed Carbon	Ash	Volatile Matter	Fixed Carbon	Volatile Matter	Fixed Carbon	Volatile Matter	Fixed Carbon	Fuel ratio
4	1.90	14.03	32.97	51.11	14.30	33.60	52.10	39.21	60.79	38.18	61.82	1.55
3	3.43	11.13	31.65	53.80	11.52	32.77	55.71	37.04	62.96	36.21	63.79	1.70
2	1.34	31.33	28.79	38.54	31.76	29.19	39.06	42.77	57.23	39.97	60.03	1.34
1 (bottom)	1.98	20.73	30.32	46.97	21.15	30.93	47.92	39.22	60.78	37.55	62.45	1.55
Min	0.86	11.13	22.17	31.68	11.52	22.36	31.96	34.70	57.23	33.10	60.03	1.34
Max	3.43	45.29	32.97	54.32	45.68	33.60	55.71	42.77	65.30	39.97	66.90	1.88
Mean	1.69	24.95	28.07	45.29	25.34	28.56	46.10	38.44	61.56	36.12	63.88	1.61
SD	0.61	9.73	2.90	6.86	9.78	3.07	7.15	2.28	2.28	1.87	1.87	0.16
Argada- B												
20 (top)	1.57	44.83	23.37	30.23	45.54	23.75	30.71	43.60	56.40	38.46	61.54	1.29
19	1.82	28.28	28.23	41.68	28.80	28.76	42.45	40.39	59.61	37.87	62.13	1.48
18	2.19	26.81	30.55	40.44	27.41	31.24	41.35	43.03	56.97	40.80	59.20	1.32
17	1.93	47.44	16.36	34.27	48.37	16.68	34.95	32.31	67.69	25.31	74.69	2.09
16	0.91	51.33	17.24	30.52	51.80	17.40	30.80	36.09	63.91	28.40	71.60	1.77
15	2.45	26.78	28.07	42.70	27.45	28.78	43.77	39.67	60.33	37.30	62.70	1.52
14	1.67	30.12	30.27	37.95	30.63	30.78	38.59	44.37	55.63	41.80	58.20	1.25
13	1.02	48.91	18.56	31.52	49.41	18.75	31.84	37.06	62.94	30.25	69.75	1.70
12	2.87	14.82	32.70	49.61	15.26	33.66	51.08	39.73	60.27	38.62	61.38	1.52
11	3.74	14.47	33.19	48.59	15.04	34.48	50.48	40.59	59.41	39.52	60.48	1.46
10	2.13	38.13	25.89	33.84	38.96	26.46	34.58	43.34	56.66	39.48	60.52	1.31
9	2.73	24.91	29.81	42.55	25.61	30.65	43.74	41.20	58.80	39.11	60.89	1.43
8	0.89	66.47	15.54	17.10	67.07	15.68	17.25	47.62	52.38	34.22	65.78	1.10
7	1.05	68.53	14.12	16.30	69.26	14.27	16.47	46.42	53.58	30.84	69.16	1.15
6	2.95	20.46	32.96	43.63	21.08	33.97	44.95	43.04	56.96	41.47	58.53	1.32
5	2.16	22.46	31.30	44.09	22.95	31.99	45.06	41.51	58.49	39.72	60.28	1.41
4	2.92	8.85	37.13	51.09	9.12	38.25	52.63	42.09	57.91	41.50	58.50	1.38
3	2.86	18.97	31.85	46.32	19.53	32.79	47.68	40.75	59.25	39.27	60.73	1.45
2	2.44	15.48	33.31	48.77	15.87	34.14	49.99	40.58	59.42	39.44	60.56	1.46
1 (bottom)	2.54	16.74	31.63	49.09	17.17	32.46	50.37	39.19	60.81	37.90	62.10	1.55
Min	0.89	8.85	14.12	16.30	9.12	14.27	16.47	32.31	52.38	25.31	58.20	1.10
Max	3.74	68.53	37.13	51.09	69.26	38.25	52.63	47.62	67.69	41.80	74.69	2.09
Mean	2.14	31.74	27.11	39.01	32.32	27.75	39.94	41.13	58.87	37.06	62.94	1.45
SD	0.77	17.00	6.85	9.83	17.08	7.15	10.27	3.38	3.38	4.59	4.59	0.22

Seam name and Sample No.	As received basis				Dry basis			Daf basis		Dmf basis		
	Moisture	Ash	Volatile Matter	Fixed Carbon	Ash	Volatile Matter	Fixed Carbon	Volatile Matter	Fixed Carbon	Volatile Matter	Fixed Carbon	Fuel ratio
Argada- C												
13 (top)	2.94	14.82	31.51	50.72	15.27	32.47	52.26	38.32	61.68	37.19	62.81	1.61
12	2.47	23.16	31.48	42.89	23.74	32.28	43.97	42.33	57.67	40.48	59.52	1.36
11	2.11	22.55	29.28	46.06	23.04	29.91	47.05	38.86	61.14	36.98	63.02	1.57
10	2.64	12.49	33.54	51.33	12.83	34.45	52.72	39.52	60.48	38.61	61.39	1.53
9	1.60	23.89	27.62	46.89	24.28	28.07	47.65	37.07	62.93	34.99	65.01	1.70
8	1.51	35.08	27.20	36.22	35.62	27.61	36.77	42.89	57.11	39.54	60.46	1.33
7	1.24	43.04	23.96	31.76	43.58	24.26	32.16	43.00	57.00	38.23	61.77	1.33
6	2.15	17.17	31.94	48.75	17.54	32.64	49.82	39.58	60.42	38.27	61.73	1.53
5	2.13	26.10	30.11	41.65	26.67	30.77	42.56	41.96	58.04	39.77	60.23	1.38
4	3.20	14.08	30.36	52.37	14.54	31.36	54.10	36.70	63.30	35.60	64.40	1.73
3	3.47	20.01	31.43	45.08	20.73	32.56	46.71	41.08	58.92	39.50	60.50	1.43
2	1.91	33.92	26.05	38.11	34.58	26.56	38.86	40.60	59.40	37.28	62.72	1.46
1 (bottom)	3.19	26.16	29.17	41.48	27.02	30.13	42.85	41.29	58.71	39.03	60.97	1.42
Min	1.24	12.49	23.96	31.76	12.83	24.26	32.16	36.70	57.00	34.99	59.52	1.33
Max	3.47	43.04	33.54	52.37	43.58	34.45	54.10	43.00	63.30	40.48	65.01	1.73
Mean	2.35	24.04	29.51	44.10	24.57	30.24	45.19	40.25	59.75	38.11	61.89	1.49
SD	0.68	8.65	2.58	5.97	8.71	2.78	6.29	2.02	2.02	1.58	1.58	0.13
Argada- D												
20 (top)	1.23	47.42	22.94	28.41	48.00	23.23	28.77	44.67	55.33	39.04	60.96	1.24
19	1.78	18.68	30.60	48.94	19.02	31.15	49.83	38.47	61.53	36.99	63.01	1.60
18	2.47	13.90	35.81	47.81	14.26	36.72	49.03	42.82	57.18	41.85	58.15	1.34
17	1.61	34.84	27.63	35.93	35.41	28.08	36.51	43.47	56.53	40.19	59.81	1.30
16	1.19	22.28	33.87	42.66	22.55	34.28	43.17	44.26	55.74	42.59	57.41	1.26
15	0.62	27.38	32.36	39.65	27.55	32.56	39.89	44.94	55.06	42.76	57.24	1.23
14	1.53	22.02	31.31	45.14	22.36	31.80	45.84	40.96	59.04	39.20	60.80	1.44
13	1.00	20.54	30.64	47.82	20.75	30.95	48.30	39.05	60.95	37.41	62.59	1.56
12	1.60	16.54	29.31	52.55	16.81	29.79	53.40	35.81	64.19	34.48	65.52	1.79
11	1.50	19.92	31.84	46.74	20.22	32.33	47.45	40.52	59.48	38.98	61.02	1.47
10	0.71	23.97	31.62	43.70	24.14	31.84	44.02	41.98	58.02	40.07	59.93	1.38
9	2.34	26.85	31.11	39.70	27.49	31.86	40.65	43.93	56.07	41.72	58.28	1.28
8	1.55	19.08	31.68	47.70	19.38	32.17	48.45	39.91	60.09	38.43	61.57	1.51
7	2.08	18.45	30.92	48.55	18.84	31.58	49.58	38.91	61.09	37.45	62.55	1.57

Seam name and Sample No.	As received basis				Dry basis			Daf basis		Dmf basis		
	Moisture	Ash	Volatile Matter	Fixed Carbon	Ash	Volatile Matter	Fixed Carbon	Volatile Matter	Fixed Carbon	Volatile Matter	Fixed Carbon	Fuel ratio
6	3.20	19.00	28.92	48.88	19.63	29.88	50.50	37.17	62.83	35.60	64.40	1.69
5	2.13	19.15	29.11	49.60	19.57	29.75	50.68	36.99	63.01	35.41	64.59	1.70
4	2.39	19.03	30.92	47.66	19.50	31.68	48.83	39.35	60.65	37.84	62.16	1.54
3	1.19	22.62	31.07	45.12	22.89	31.45	45.67	40.78	59.22	38.97	61.03	1.45
2	2.08	17.01	34.00	46.92	17.37	34.72	47.91	42.02	57.98	40.77	59.23	1.38
1 (bottom)	2.14	18.55	29.71	49.60	18.96	30.36	50.69	37.46	62.54	35.96	64.04	1.67
Min	0.62	13.90	22.94	28.41	14.26	23.23	28.77	35.81	55.06	34.48	57.24	1.23
Max	3.20	47.42	35.81	52.55	48.00	36.72	53.40	44.94	64.19	42.76	65.52	1.79
Mean	1.72	22.36	30.77	45.15	22.73	31.31	45.96	40.67	59.33	38.79	61.21	1.47
SD	0.63	7.29	2.57	5.48	7.34	2.62	5.68	2.71	2.71	2.37	2.37	0.17
Argada- I												
9 (top)	1.35	33.67	21.55	43.44	34.13	21.84	44.03	33.15	66.85	29.50	70.50	2.02
8	1.40	22.03	23.79	52.78	22.34	24.13	53.53	31.07	68.93	29.03	70.97	2.22
7	1.58	25.77	22.87	49.78	26.19	23.24	50.58	31.48	68.52	28.96	71.04	2.18
6	1.94	26.63	23.60	47.83	27.16	24.07	48.77	33.04	66.96	30.45	69.55	2.03
5	1.83	28.54	22.66	46.97	29.07	23.08	47.85	32.54	67.46	29.66	70.34	2.07
4	1.48	32.35	22.56	43.62	32.83	22.89	44.27	34.08	65.92	30.70	69.30	1.93
3	2.63	20.80	25.14	51.43	21.36	25.82	52.82	32.83	67.17	30.96	69.04	2.05
2	2.04	20.04	25.24	52.68	20.45	25.76	53.78	32.39	67.61	30.61	69.39	2.09
1 (bottom)	2.31	23.75	25.94	48.00	24.31	26.55	49.13	35.08	64.92	32.93	67.07	1.85
Min	1.35	20.04	21.55	43.44	20.45	21.84	44.03	31.07	64.92	28.96	67.07	1.85
Max	2.63	33.67	25.94	52.78	34.13	26.55	53.78	35.08	68.93	32.93	71.04	2.22
Mean	1.84	25.95	23.70	48.50	26.43	24.15	49.42	32.85	67.15	30.31	69.69	2.05
SD	0.41	4.59	1.38	3.31	4.60	1.49	3.45	1.15	1.15	1.16	1.16	0.11
Argada- J												
13 (top)	1.41	36.60	19.90	42.09	37.13	20.18	42.69	32.10	67.90	27.83	72.17	2.12
12	1.98	30.77	30.66	36.59	31.39	31.28	37.33	45.59	54.41	42.98	57.02	1.19
11	1.63	21.94	30.76	45.67	22.30	31.27	46.43	40.24	59.76	38.48	61.52	1.48
10	1.47	21.00	29.37	48.16	21.31	29.81	48.88	37.88	62.12	36.15	63.85	1.64
9	2.15	17.14	32.05	48.66	17.52	32.75	49.73	39.71	60.29	38.40	61.60	1.52
8	1.90	26.99	27.23	43.89	27.51	27.76	44.74	38.29	61.71	35.85	64.15	1.61
7	2.26	22.63	29.46	45.66	23.15	30.14	46.71	39.22	60.78	37.33	62.67	1.55
6	2.43	20.14	30.11	47.32	20.65	30.86	48.50	38.89	61.11	37.25	62.75	1.57

Seam name and Sample No.	As received basis				Dry basis			Daf basis		Dmf basis		
	Moisture	Ash	Volatile Matter	Fixed Carbon	Ash	Volatile Matter	Fixed Carbon	Volatile Matter	Fixed Carbon	Volatile Matter	Fixed Carbon	Fuel ratio
5	2.80	22.93	30.55	43.72	23.59	31.43	44.98	41.13	58.87	39.26	60.74	1.43
4	1.93	25.49	28.75	43.83	25.99	29.32	44.69	39.61	60.39	37.42	62.58	1.52
3	2.74	21.63	28.21	47.43	22.23	29.00	48.76	37.30	62.70	35.45	64.55	1.68
2	3.30	35.59	23.31	37.80	36.81	24.10	39.09	38.14	61.86	34.31	65.69	1.62
1 (bottom)	2.52	26.09	27.03	44.37	26.76	27.72	45.52	37.85	62.15	35.50	64.50	1.64
Min	1.41	17.14	19.90	36.59	17.52	20.18	37.33	32.10	54.41	27.83	57.02	1.19
Max	3.30	36.60	32.05	48.66	37.13	32.75	49.73	45.59	67.90	42.98	72.17	2.12
Mean	2.19	25.30	28.26	44.25	25.87	28.89	45.23	38.92	61.08	36.63	63.37	1.58
SD	0.54	5.66	3.22	3.55	5.80	3.29	3.59	2.84	2.84	3.30	3.30	0.20

5.3 Ultimate analysis

5.3.1 Introduction

The ultimate analysis has been carried out to determine the essential elements present in coals of the South Karanpura coalfield. It identifies the elemental composition of the coal. Carbon, hydrogen, nitrogen, and sulfur are analysed experimentally, and oxygen was determined by subtracting the combined weight % from 100. The determination of these elements is essential because carbon and hydrogen help in the evaluation of rank and stage of coalification. They are also helpful in determining the suitability of coal for hydrogenation and gasification purposes. Sulphur and nitrogen are potential pollutants to the environment. The representative samples from different coal seams of South Karanpura coalfield have been subjected to ultimate analysis. The quantitative occurrence of the ultimate constituents of Barka Sayal is given in Table 5.3, whereas Table 5.4 presents the ultimate constituents of the coals of the Argada area.

5.3.2 Carbon

The carbon content of coal seams of Barka Sayal area varies from 29.08% to 88.30%, mean 74.34% (daf basis), whereas coal seams of Argada area exhibit a range of 72.69% to 85.99%, mean 79.36% (daf basis). The nature of the banding present mainly influences the carbon content of coals in these seams. These coals have high concentration of inorganic constituents which is reflected from their ash yield (mean 22.49%). It makes carbon concentration lower in these coals. Bright bands exhibit higher carbon content compared to dull bands because of the presence of carbon-rich vitrinite macerals while dull bands contain less vitrain (Hower *et al.* 1990), at microscopic level dull bands are having a higher concentration of inertinite macerals and lower concentration of vitrinite

macerals. Dull bands also exhibit higher concentrations of inorganic constituents. This phenomenon has been observed in the coal seams of both areas.

5.3.3 Hydrogen

Coal seams of Barka Sayal area exhibit Hydrogen content (daf basis) from 3.12% to 6.87%, mean 5.13%, whereas coal seams of Argada area show a range of 3.96% to 5.77%, mean 4.92%. Dull bands exhibit more hydrogen content compared to bright bands, possibly affected by high moisture content and liptinite macerals present in these bands.

5.3.4 Nitrogen

The Nitrogen content (daf basis) of the coal seams of the Barka Sayal area varies from 0.34% to 2.41%, mean 1.52%, whereas coal seams of the Argada area exhibit a range of nil to 2.46%, mean 2.03%. Nitrogen content does not show any clear correlation with the banding nature of these coals.

5.3.5 Sulphur

The Sulphur content in the coal seams of Barka Sayal area varies from nil to 1.18%, mean 0.78% (daf basis), whereas, for coal seams of Argada area, the range lies between nil to 0.69%, mean 0.38% (daf basis). Sulphur content in coal can be influenced by several physicochemical and biological activities such as sulphur derived from plant materials or in the form of sulphate from seawater.

5.3.6 Oxygen

The oxygen content of coal seams of Barka Sayal area varies from 3.26% to 63.30%, mean 17.64% (daf basis), whereas coal seams of Argada area exhibit oxygen content from 5.99% to 20.06%, mean 13.31% (daf basis). Dull bands show more oxygen content than bright bands in these coals, possibly due to the presence of high inertinite macerals present in these coals and the breaking down of high mineral content present in these bands.

5.3.7 Distribution of Ultimate constituents

The coal samples from the South Karanpura coalfield have been subjected to an ultimate analysis, and the result is presented in Table 5.3 and Table 5.4 on a dry basis and dry ash-free basis. Coal is a heterogeneous mixture of organic and inorganic constituents. The variation of ultimate constituents in coal is guided by several factors such as composition, rank, as well as syn and post-depositional activities. The moisture content present in coal affects the hydrogen and oxygen content of the coal. The result presented on a dry basis, or dry ash-free basis represents the accurate elemental constituents of the coal. The variation of the ultimate constituents along the seam profile has also been discussed (Figure 5.14 to Figure 5.26).

5.3.7.1 Coal seams of Barka Sayal area

In general, all the coal seams of the Barka Sayal area contain high carbon (mean 57.18%, dry basis) and oxygen content (mean 13.51%, dry basis) but they exhibit less hydrogen (mean 3.90%, dry basis), nitrogen (mean 1.17%, dry basis) and sulphur (mean 0.58%, dry basis). In comparison to other elements, the concentration of nitrogen is very low.

In the coals of Sayal seam, the carbon content is high, which ranges from 39.34% to 57.40%, mean 49.38% on a dry basis (47.48%-88.30%, mean 72.25% on daf basis). The oxygen content of these coals are between 2.12% and 39.77%, mean 16.03% on a dry basis (3.26%-48%, mean 20.94% daf basis). The hydrogen content ranges from 2.59% to 3.91%, mean 3.32% on a dry basis (3.12%-6.01%, mean 4.86%, daf basis). The nitrogen content varies from 0.28% to 0.93%, mean 0.62%, dry basis (0.34%-1.44%, mean 0.92% daf basis). The sulphur content in these coals lies in the range of 0.64%-0.88%, mean 0.71% on a dry basis (0.89%-1.16%, mean 1.02%, daf basis) (Table 5.3) Carbon, hydrogen and nitrogen content first increases then slightly decreases from bottom to top of the seam. The sulphur content decreases towards the top (Figure 5.14).

The coals of Sayal Balkudra seam, carbon content lies in the range of 22.21% to 60.57%, mean 41.80% on a dry basis (29.08%-77.92%, mean 64.41%, daf basis). The oxygen content varies from 9.19% to 48.34%, mean 19.05% on dry basis (14.12% to 63.30%, mean 27.49%, daf basis). Hydrogen lies in between 2.76% and 5.25%, mean 3.71% on a dry basis (4.65%-6.87%, mean 5.58% on daf basis). The nitrogen content lying in the range of 0.57% to 1.68%, mean 1.22% on dry basis (0.75%-2.29%, mean 1.89%, daf basis). The sulphur content ranges from nil to 0.58%, mean 0.38% on a dry basis (nil to 1.18%, mean 0.63% on daf basis) (Table 5.3) Carbon, hydrogen and nitrogen content decreases towards the bottom to the top part of the seam, whereas sulphur and oxygen content increases towards the top (Figure 5.15).

The coals of Upper Semana have carbon content ranging in between 58.79% and 70.90%, mean 65.98% on a dry basis (74.80%-81.92%, mean 77.82%, daf basis). The oxygen content of these coals are in between 9.09% and 15.96%, mean 12.55% on a dry basis (10.51%-18.48%, mean 14.84%, daf basis). The hydrogen content in this seam varies from 3.69% to 4.33%, mean 4.12% on a dry basis (4.27%- 5.28%, mean 4.87%, daf basis). The nitrogen content varies from 1.59% to 1.92%, mean 1.74%, dry basis (1.87%-2.22%, mean 2.05% daf basis). The sulphur content in these coals lie in the range of 0.30%-0.46%, mean 0.35% on a dry basis (0.35%-0.53%, mean 0.42%, daf basis) (Table 5.3) Carbon and hydrogen decrease towards the bottom while sulphur, nitrogen, and oxygen first decrease then increase towards the bottom (Figure 5.16).

The coals of the Lower Semana seam have carbon content lying in the range of 59.09% to 76.05%, mean 68.09% on a dry basis (77.58%-79.98%, mean 79.20%, daf basis). The oxygen content varies from 9.22% to 12.49%, mean 10.79% on dry basis (11.47% to 14.28%, mean 12.54%, daf basis). Hydrogen is in between 4.31% and 5.08%, mean 4.61% on a dry basis (5.10%-5.77%, mean 5.37% on daf basis). The nitrogen content

lying in the range of 1.66% to 2.11%, mean 1.92% on a dry basis (1.99%- 2.41%, mean 2.24%, daf basis). The sulphur content ranges from 0.38% to 0.70%, mean 0.56% on dry basis (0.45% to 0.80%, mean 0.65% on daf basis) (Table 5.3). In this seam, carbon and hydrogen content reaches a maximum near to the bottom, whereas nitrogen, sulphur, and oxygen do not show much variation (Figure 5.17).

In the coals of Hathidari seam, the carbon content ranges from 51.06% to 66.03%, mean 60.62% on a dry basis (71.26%- 81.92%, mean 77.62% on daf basis). The oxygen content of these coals are moderate, in between 8.04% and 16.78%, mean 11.98% on a dry basis (10.74%- 22.62%, mean 15.34% daf basis). The hydrogen content is low, which ranges from 3.22% to 4.58%, mean 3.95% on a dry basis (4.49%- 5.30%, mean 5.05%, daf basis). The nitrogen content varies from 0.43% to 1.06%, mean 0.81%, dry basis (0.59%-1.30%, mean 1.02% daf basis). The sulphur content in these coals lie in the range of 0.68%-0.86%, mean 0.75% on dry basis (0.83%-1.13%, mean 0.97%, daf basis) (Table 5.3). Carbon, hydrogen, and nitrogen contents show a decreasing trend towards the top, while sulphur first increases, then decrease and further increases towards the top. Oxygen content first decreases then increases towards the top part of the seam (Figure 5.18).

The coals of Bansgarha seam have carbon content ranging in between 47.90% and 63.66%, mean 57.21% on a dry basis (72.83%- 83.26%, mean 78.33%, daf basis). The oxygen content of these coals are in between 6.26% and 15.02%, mean 10.64% on a dry basis (8.85%-20.62%, mean 14.67%, daf basis). The hydrogen content in this seam varies from 3.11% to 4.05%, mean 3.66% on a dry basis (4.62%- 5.73%, mean 5.03%, daf basis). The nitrogen content varies from 0.44% to 0.91%, mean 0.73% on dry basis (0.68%-1.21%, mean 0.99% on daf basis). The sulphur content in these coals lie in the range of 0.67%- 0.75%, mean 0.71% on dry basis (0.91%- 1.14%, mean 0.99%, daf basis) (Table 5.3). Carbon, hydrogen, and nitrogen content first increases then decreases towards the

top, whereas oxygen content exhibit a reverse trend to this. Sulphur content decreases from bottom to top (Figure 5.19).

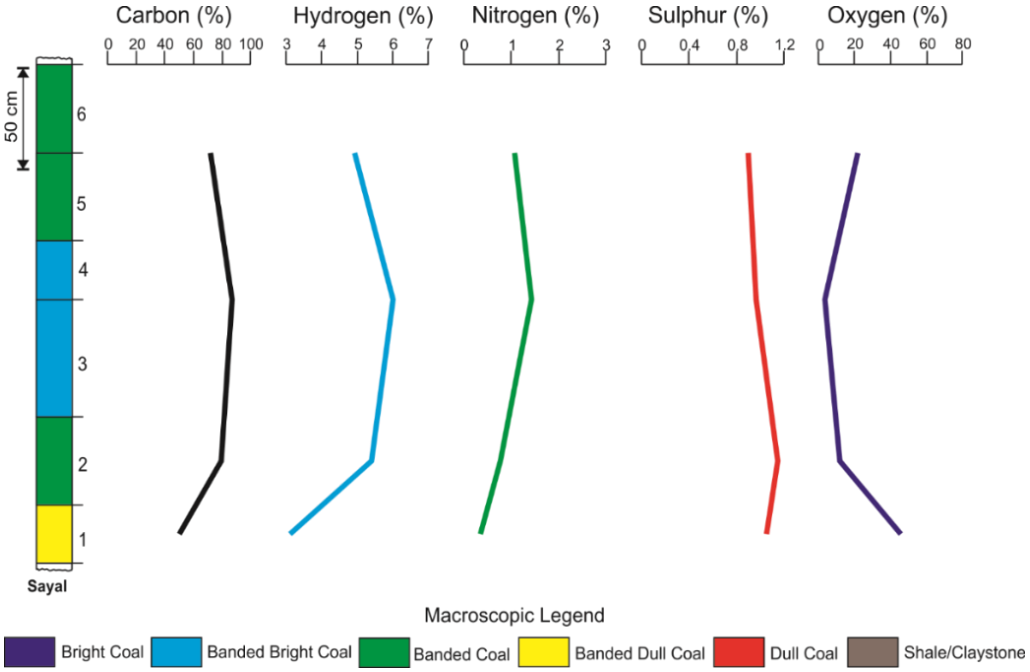


Figure 5.14 Variation of ultimate constituents along the macropetrographic seam section of Sayal seam.

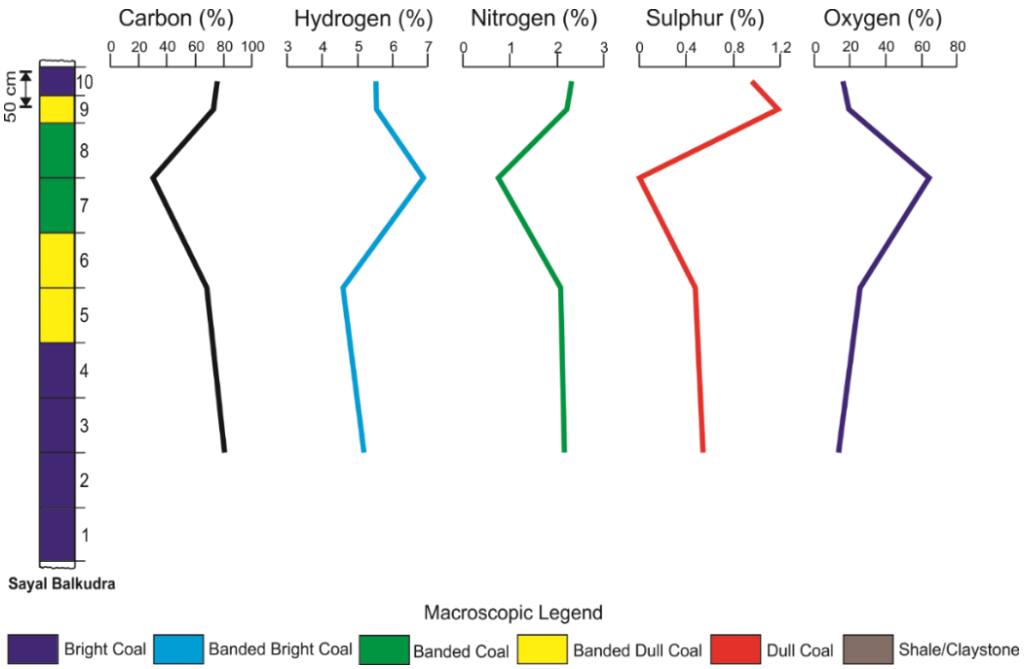


Figure 5.15 Variation of ultimate constituents along the macropetrographic seam section of Sayal Balkudra seam.

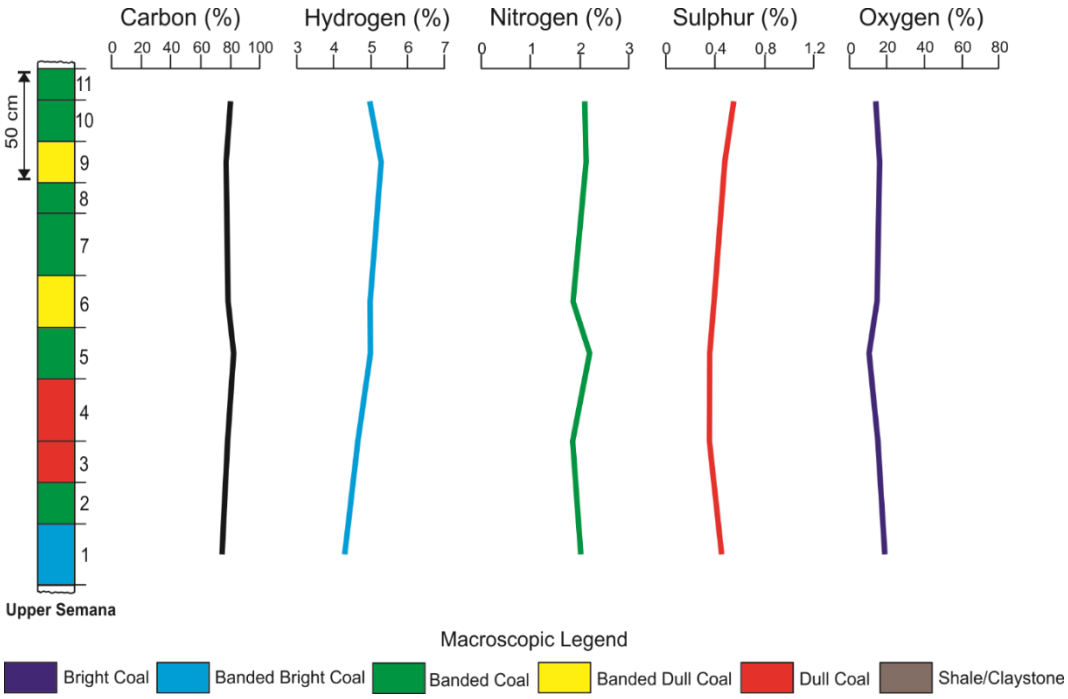


Figure 5.16 Variation of ultimate constituents along the macropetrographic seam section of Upper Semana seam.

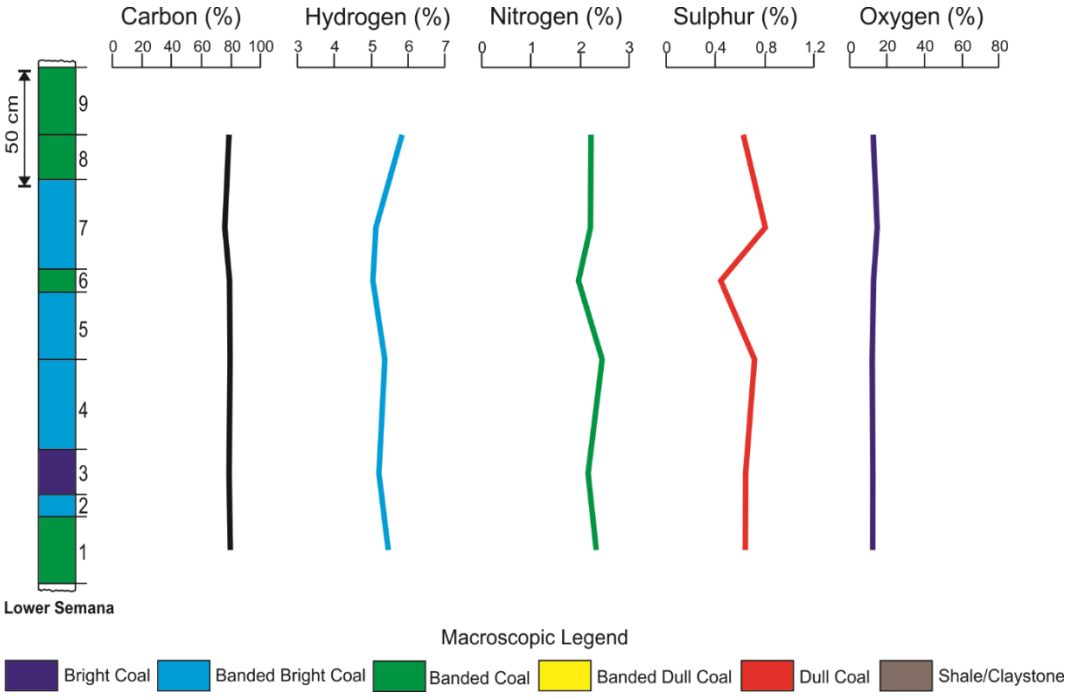


Figure 5.17 Variation of ultimate constituents along the macropetrographic seam section of Lower Semana seam.

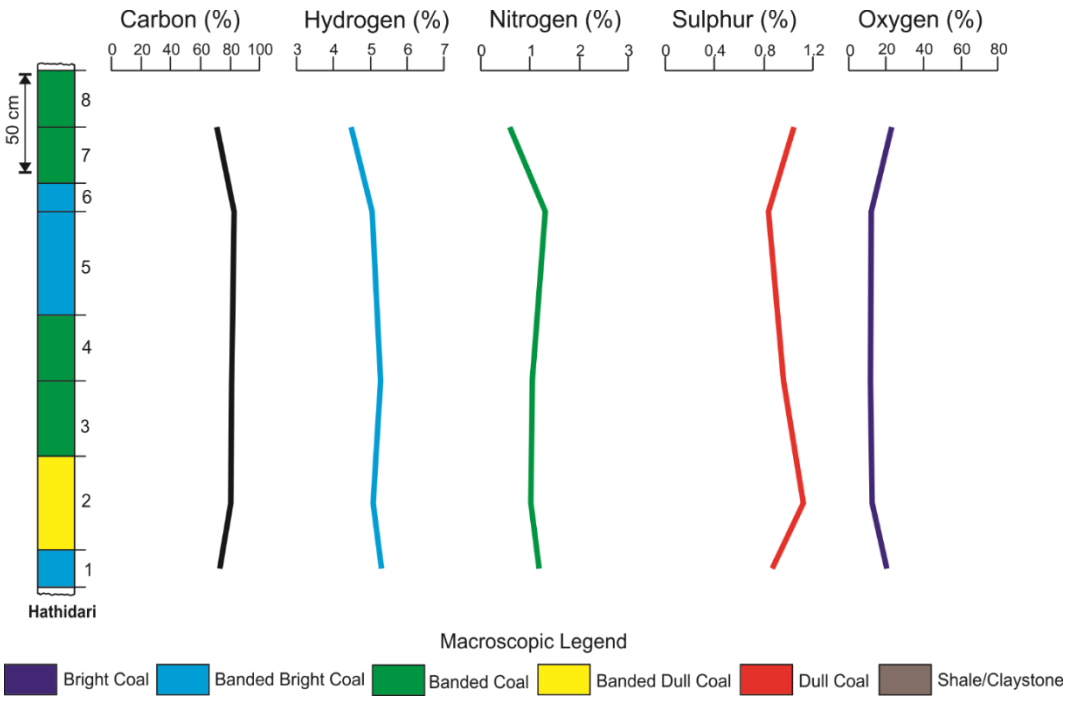


Figure 5.18 Variation of ultimate constituents along the macropetrographic seam section of Hathidari seam.

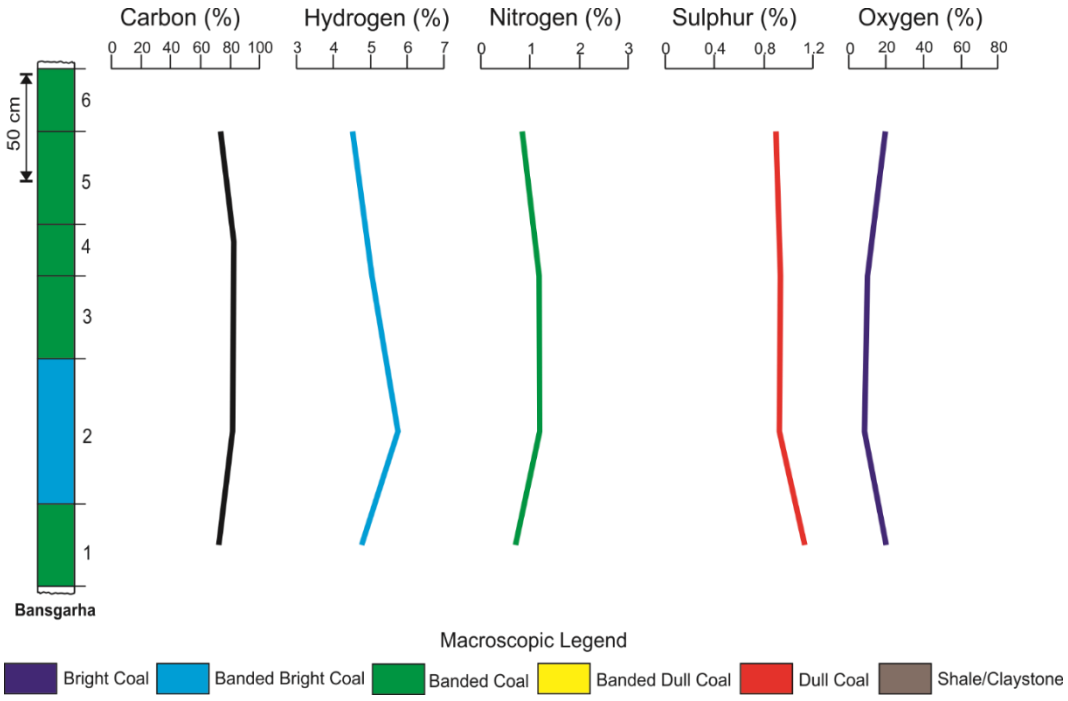


Figure 5.19 Variation of ultimate constituents along the macropetrographic seam section of Bansgarha seam.

Table 5.3 Ultimate analysis of coals seams present in the Barka Sayal area, South Karanpura coalfield.

	Ash	Moisture	Dry basis					Dry ash-free (daf) basis						
	(wt.%)	(wt.%)	C%	H%	N%	S%	O%	C%	H%	N%	S%	O%	H/C	O/C
Sayal														
SL/5+6	24.42	3.83	54.12	3.68	0.82	0.67	15.32	72.53	4.94	1.10	0.89	20.54	0.82	0.21
SL/3+4	33.74	3.61	57.40	3.91	0.93	0.64	2.12	88.30	6.01	1.44	0.99	3.26	0.82	0.03
SL/2	41.05	2.71	46.64	3.11	0.46	0.67	6.92	80.69	5.38	0.80	1.16	11.97	0.80	0.11
SL/1	16.56	3.38	39.34	2.59	0.28	0.88	39.77	47.48	3.12	0.34	1.06	48.00	0.79	0.76
Min	16.56	2.71	39.34	2.59	0.28	0.64	2.12	47.48	3.12	0.34	0.89	3.26	0.79	0.03
Max	41.05	3.83	57.40	3.91	0.93	0.88	39.77	88.30	6.01	1.44	1.16	48.00	0.82	0.76
Mean	28.94	3.38	49.38	3.32	0.62	0.71	16.03	72.25	4.86	0.92	1.02	20.94	0.81	0.28
SD	9.27	0.42	6.98	0.51	0.26	0.10	14.50	15.35	1.07	0.40	0.10	16.77	0.01	0.29
Sayal Balkudra														
SBK/10	39.85	3.39	43.71	3.26	1.35	0.56	9.86	74.40	5.55	2.29	0.96	16.79	0.90	0.17
SBK/9	48.68	3.51	35.93	2.76	1.09	0.58	9.19	72.51	5.57	2.20	1.18	18.55	0.92	0.19
SBK/7+8	22.59	4.39	22.21	5.25	0.57	nil	48.34	29.08	6.87	0.75	nil	63.30	2.84	1.63
SBK/5+6	30.17	4.66	46.56	3.18	1.41	0.33	16.87	68.12	4.65	2.06	0.49	24.68	0.82	0.27
SBK/1+2+3+4	21.30	4.39	60.57	4.08	1.68	0.42	10.97	77.92	5.25	2.17	0.54	14.12	0.81	0.14
Min	21.30	3.39	22.21	2.76	0.57	nil	9.19	29.08	4.65	0.75	nil	14.12	0.81	0.14
Max	48.68	4.66	60.57	5.25	1.68	0.58	48.34	77.92	6.87	2.29	1.18	63.30	2.84	1.63
Mean	32.52	4.07	41.80	3.71	1.22	0.38	19.05	64.41	5.58	1.89	0.63	27.49	1.26	0.48
SD	10.44	0.51	12.62	0.88	0.38	0.21	14.90	17.95	0.73	0.58	0.41	18.24	0.79	0.58
Up. Semana														
Up. Sm/10+11	13.70	2.13	67.21	4.32	1.85	0.46	12.16	78.15	5.03	2.15	0.53	14.14	0.77	0.14
Up. Sm/9	22.12	1.73	58.79	4.09	1.67	0.36	12.58	75.87	5.28	2.15	0.47	16.23	0.84	0.16
Up. Sm/6	12.64	3.55	68.25	4.26	1.65	0.33	12.40	78.54	4.91	1.90	0.38	14.28	0.75	0.14
Up. Sm/5	12.86	4.39	70.90	4.33	1.92	0.31	9.09	81.92	5.00	2.22	0.36	10.51	0.73	0.10
Up. Sm/3+4	14.42	3.01	66.12	4.01	1.59	0.30	13.12	77.66	4.71	1.87	0.35	15.41	0.73	0.15
Up. Sm/1	13.02	4.58	64.59	3.69	1.74	0.37	15.96	74.80	4.27	2.02	0.43	18.48	0.69	0.19
Min	12.64	1.73	58.79	3.69	1.59	0.30	9.09	74.80	4.27	1.87	0.35	10.51	0.69	0.10
Max	22.12	4.58	70.90	4.33	1.92	0.46	15.96	81.92	5.28	2.22	0.53	18.48	0.84	0.19
Mean	14.79	3.23	65.98	4.12	1.74	0.35	12.55	77.82	4.87	2.05	0.42	14.84	0.75	0.14
SD	3.33	1.06	3.75	0.23	0.11	0.05	2.00	2.25	0.32	0.13	0.07	2.42	0.05	0.03
Lr. Semana														
Lr. Sm/8+9	24.81	1.73	59.09	4.31	1.66	0.48	9.22	79.04	5.77	2.23	0.64	12.33	0.88	0.12
Lr. Sm/7	12.20	2.27	67.89	4.47	1.95	0.70	12.49	77.58	5.11	2.23	0.80	14.28	0.79	0.14
Lr. Sm/6	14.91	2.37	67.32	4.32	1.69	0.38	11.03	79.45	5.10	1.99	0.45	13.02	0.77	0.12
Lr. Sm/4+5	13.73	3.46	68.44	4.61	2.07	0.62	10.04	79.78	5.38	2.41	0.73	11.70	0.81	0.11
Lr. Sm/3	4.00	4.75	76.05	5.08	2.11	0.62	11.94	79.39	5.30	2.20	0.65	12.46	0.80	0.12
Lr. Sm/1	12.39	2.86	69.78	4.84	2.05	0.57	10.01	79.98	5.55	2.35	0.65	11.47	0.83	0.11
Min	4.00	1.73	59.09	4.31	1.66	0.38	9.22	77.58	5.10	1.99	0.45	11.47	0.77	0.11
Max	24.81	4.75	76.05	5.08	2.11	0.70	12.49	79.98	5.77	2.41	0.80	14.28	0.88	0.14
Mean	13.67	2.91	68.09	4.61	1.92	0.56	10.79	79.20	5.37	2.24	0.65	12.54	0.81	0.12
SD	6.09	0.98	4.97	0.28	0.18	0.11	1.15	0.79	0.24	0.13	0.11	0.93	0.03	0.01
Hathidari														
HD/7+8	27.34	3.53	51.06	3.22	0.43	0.75	16.21	71.26	4.49	0.59	1.04	22.62	0.76	0.24
HD/5+6	17.59	4.51	66.03	4.13	1.06	0.68	9.68	80.94	5.06	1.30	0.83	11.87	0.75	0.11
HD/3+4	24.13	3.95	61.34	3.95	0.81	0.73	8.04	81.92	5.28	1.08	0.97	10.74	0.77	0.10
HD/2	23.17	3.09	61.44	3.88	0.73	0.86	9.18	80.74	5.10	0.96	1.13	12.06	0.76	0.11
HD/1	13.10	4.09	63.23	4.58	1.01	0.74	16.78	73.23	5.30	1.17	0.86	19.44	0.87	0.20
Min	13.10	3.09	51.06	3.22	0.43	0.68	8.04	71.26	4.49	0.59	0.83	10.74	0.75	0.10
Max	27.34	4.51	66.03	4.58	1.06	0.86	16.78	81.92	5.30	1.30	1.13	22.62	0.87	0.24
Mean	21.07	3.83	60.62	3.95	0.81	0.75	11.98	77.62	5.05	1.02	0.97	15.34	0.78	0.15
SD	5.07	0.49	5.07	0.44	0.23	0.06	3.73	4.45	0.29	0.24	0.11	4.77	0.04	0.06
Bansgarha														
BG/5+6	20.61	4.32	58.40	3.62	0.70	0.71	15.02	74.44	4.62	0.89	0.91	19.15	0.74	0.19
BG/3+4	21.95	4.98	63.66	3.88	0.91	0.73	7.73	82.78	5.04	1.18	0.94	10.06	0.73	0.09

	Ash	Moisture	Dry basis					Dry ash-free (daf) basis						
	(wt.%)	(wt.%)	C%	H%	N%	S%	O%	C%	H%	N%	S%	O%	H/C	O/C
BG/2	28.38	3.10	58.88	4.05	0.86	0.67	6.26	83.26	5.73	1.21	0.95	8.85	0.83	0.08
BG/1	32.38	5.42	47.90	3.11	0.44	0.75	13.56	72.83	4.73	0.68	1.14	20.62	0.78	0.21
Min	20.61	3.10	47.90	3.11	0.44	0.67	6.26	72.83	4.62	0.68	0.91	8.85	0.73	0.08
Max	32.38	5.42	63.66	4.05	0.91	0.75	15.02	83.26	5.73	1.21	1.14	20.62	0.83	0.21
Mean	25.83	4.46	57.21	3.66	0.73	0.71	10.64	78.33	5.03	0.99	0.99	14.67	0.77	0.14
SD	4.79	0.87	5.76	0.35	0.18	0.03	3.72	4.73	0.43	0.22	0.09	5.26	0.04	0.06

5.3.7.2 Coal seams of Argada area

All the coal seams of Argada area contain high carbon (mean 58.93%, dry basis) and high oxygen content (mean 9.62%, dry basis) but they exhibit less nitrogen (mean 1.50%, dry basis), sulphur (mean 0.29%, dry basis) and hydrogen content (mean 3.61%, dry basis). Coals of the Argada area possesses high concentration of inertinite and mineral matter compared to the coals of the Barka Sayal area, the compositional variation is ultimately guiding the variation of ultimate constituents in these coals.

In the coals of Argada seam, the carbon content ranges from 25.20% to 71.05%, mean 56.02% on a dry basis (72.69%- 81.78%, mean 78.57% on daf basis). The oxygen content of these coals lie between 6.96% and 9.70%, mean 8.99% on a dry basis (10.65%-20.06%, mean 13.92%, daf basis). The hydrogen content ranges from 1.73% to 4.23%, mean 3.47% on a dry basis (4.68%- 5.52%, mean 4.99%, daf basis). The nitrogen content varies from 0.78% to 1.90%, mean 1.51%, dry basis (2.09%- 2.24%, mean 2.16% daf basis). The sulphur content in these coals lie in the range of nil to 0.47%, mean 0.29% on a dry basis (nil- 0.55%, mean 0.36%, daf basis) (Table 5.4). Carbon, hydrogen, nitrogen, and sulphur content is high in the bottom part of the seam, which decreases continuously till the middle section of the seam further increases towards the top, whereas oxygen content exhibit a reverse trend (Figure 5.20).

In the coals of Argada-A seam, carbon content lying in the range of 54.07% to 67.67%, mean 60.59% on a dry basis (78.97%-80.71%, mean 79.87%, daf basis). The oxygen content varies from 7.90% to 11.53%, mean 9.31% on dry basis (11.17% to 13.45%, mean 12.22%, daf basis). Hydrogen lies between 3.63% and 4.08%, mean 3.79% on a dry basis

(4.60%- 5.37%, mean 5.02% on daf basis). The nitrogen content lying in the range of 1.61% to 1.86%, mean 1.73% on a dry basis (2.12%-2.36%, mean 2.28%, daf basis). The sulphur content ranges from 0.41% to 0.59%, mean 0.46% on dry basis (0.52% to 0.69%, mean 0.61% on daf basis) (Table 5.4). Carbon, hydrogen, and nitrogen content increases towards the bottom while sulphur and oxygen content increase then decrease towards the bottom (Figure 5.21).

The coals of Argada-B have carbon content ranging in between 38.14% and 70.30%, mean 55.91% on a dry basis (72.96%- 82.73%, mean 77.94%, daf basis). The oxygen content of these coals are in between 7.77% and 12.99%, mean 10.01% on a dry basis (9.47%-19.67%, mean 14.51%, daf basis). The hydrogen content in this seam varies from 2.88% to 4.04%, mean 3.44% on a dry basis (4.43%- 5.77%, mean 4.92%, daf basis). The nitrogen content varies from 1.11% to 2%, mean 1.61%, dry basis (2.19%- 2.35%, mean 2.25% daf basis). The sulphur content in these coals lie in the range of nil to 0.59%, mean 0.30% on a dry basis (nil- 0.69%, mean 0.38%, daf basis) (Table 5.4). Carbon, hydrogen, sulphur, and nitrogen first increases then decreases and again increases towards the top, whereas oxygen content first decreases then increases in the top portion of the seam (Figure 5.22).

The coals of Argada-C seam have carbon content lying in the range of 45.53% to 67.40%, mean 58.96% on a dry basis (77.07%-79.20%, mean 77.72%, daf basis). The oxygen content varies from 8.63% to 13.96%, mean 11.35% on dry basis (13.44% to 16.01%, mean 14.98%, daf basis). Hydrogen is in between 2.82% and 3.79%, mean 3.46% on a dry basis (4.22%-5.01%, mean 4.60% on daf basis). The nitrogen content lying in the range of 1.27% to 2.14%, mean 1.81% on a dry basis (2.25%- 2.45%, mean 2.38%, daf basis). The sulphur content ranges from nil to 0.38%, mean 0.23% on dry basis (nil to 0.51%, mean 0.32% on daf basis) (Table 5.4). Carbon, hydrogen, nitrogen, and oxygen

do not show much variation in the top and bottom portion of the seam, but in the middle portion, its quantity decreases. Sulphur content exhibits more variation and decreases to its minimum near to the top of the seam but further increases in the topmost part of the seam (Figure 5.23).

In the coals of Argada-D seam, the carbon content ranges from 37.81% to 70.69%, mean 60.08% on a dry basis (72.72%- 82.43%, mean 79.47% on daf basis). The oxygen content of these coals are in between 8.25% and 11.01%, mean 9.68% on a dry basis (9.62%- 19.68%, mean 13.39% daf basis). The hydrogen content ranges from 2.65% to 4.40%, mean 3.46% on a dry basis (3.96%- 5.14%, mean 4.64%, daf basis). The nitrogen content varies from 1.15% to 2.11%, mean 1.71%, dry basis (2.12%- 2.46%, mean 2.28% daf basis). The sulphur content in these coals lie in the range of nil to 0.30%, mean 0.17% on a dry basis (nil to 0.35%, mean 0.23%, daf basis) (Table 5.4). Carbon, hydrogen, and nitrogen content first increases, but further does not show much variation towards the bottom of the seam. Sulphur content decreases towards the bottom, whereas oxygen content roughly increases in the bottom portion of the seam (Figure 5.24).

The coals of Argada-I seam have carbon content ranging in between 58.45% and 64.97%, mean 60.52% on a dry basis (74.33%- 81.68%, mean 80.08%, daf basis). The oxygen content of these coals are in between 8.48% and 14.90%, mean 10.33% on a dry basis (11.21%- 18.95%, mean 13.60%, daf basis). The hydrogen content in this seam varies from 3.40% to 4.02%, mean 3.71% on a dry basis (4.55%- 5.11%, mean 4.91%, daf basis). The nitrogen content varies from nil to 1.58%, mean 0.85% on a dry basis (nil to 2.09%, mean 1.12%, daf basis). The sulphur content in these coals lie in the range of 0.16%- 0.29%, mean 0.23% on dry basis (0.22%- 0.38%, mean 0.30%, daf basis) (Table 5.4). Nitrogen and sulphur content also increases towards the bottom, whereas oxygen content first increases then decreases towards the bottom (Figure 5.25).

The carbon content of the coals of Argada-J seam varies from 51.88% to 67.98%, mean 60.42% on a dry basis (78.93%- 85.99%, mean 81.89%, daf basis). The oxygen content ranges in between 4.39% and 10.16%, mean 7.68% on a dry basis (5.99%- 15.45%, mean 10.54%, daf basis). The hydrogen content lies in the range of 3.44% to 4.55%, mean 3.97% on a dry basis (5.24%- 5.52%, mean 5.38%, daf basis). Nitrogen varies from nil to 1.77%, mean 1.30% on a dry basis (nil to 2.20%, mean 1.72%, daf basis). Sulphur content is in between 0.25% and 0.41%, mean 0.35% on dry basis (0.37%- 0.56%, mean 0.47% on daf basis) (Table 5.4). Carbon hydrogen, nitrogen, and sulphur first increase then do not exhibit much variation towards the bottom of the seam, whereas oxygen content decreases towards the bottom (Figure 5.26).

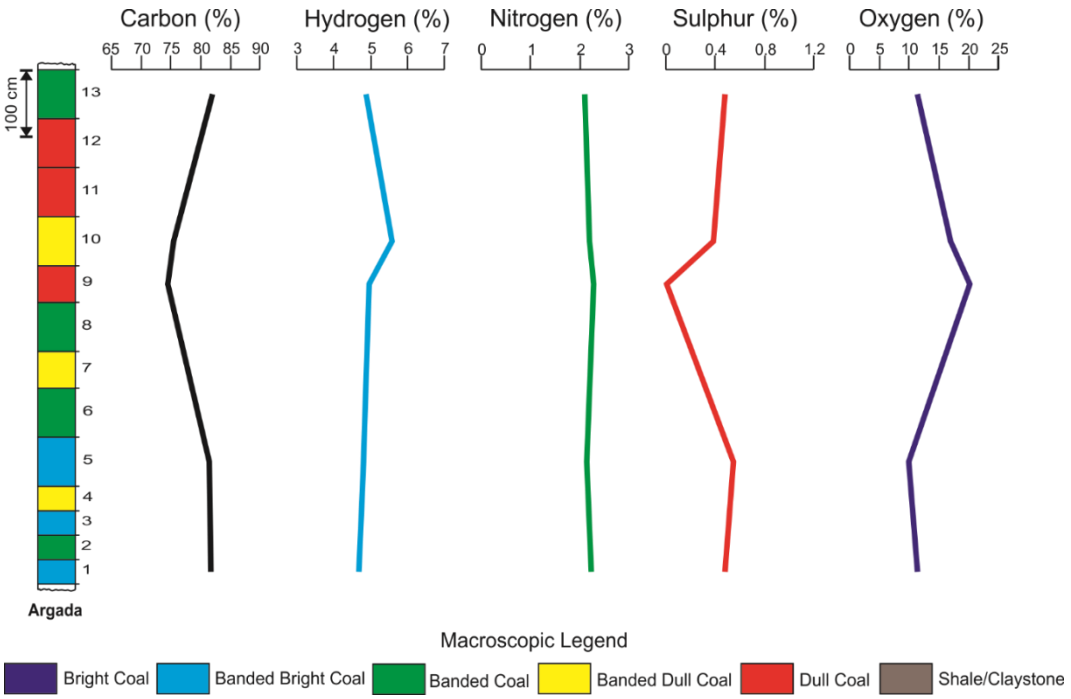


Figure 5.20 Variation of ultimate constituents along the macropetrographic seam section of Argada seam.

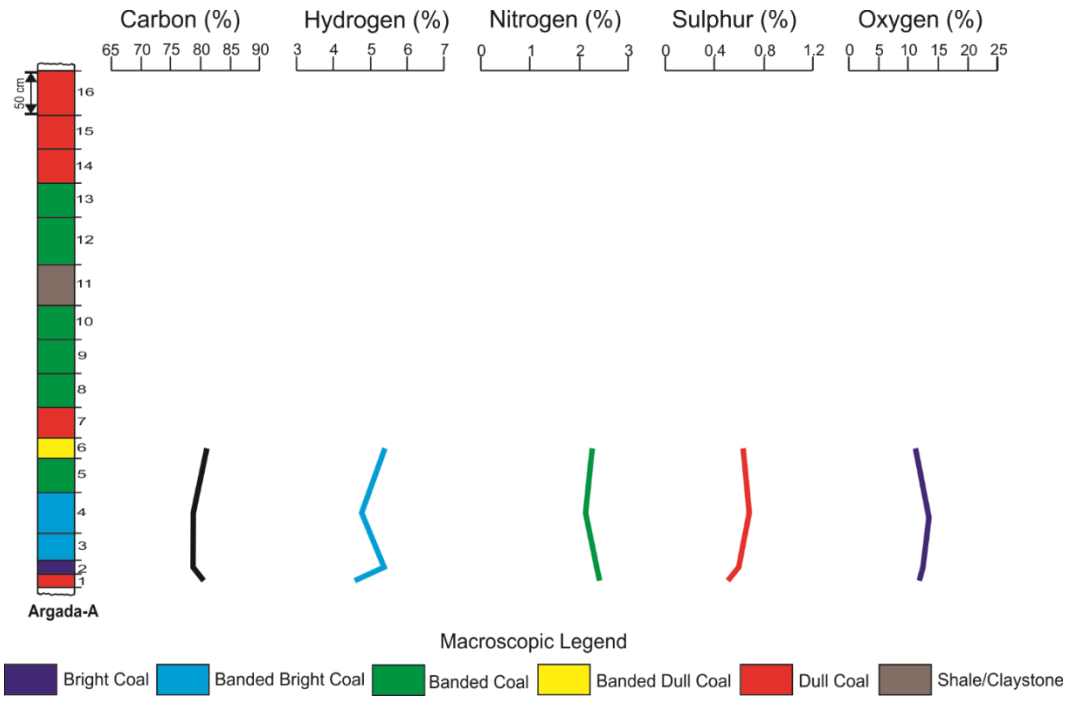


Figure 5.21 Variation of ultimate constituents along the macropetrographic seam section of Argada-A seam.

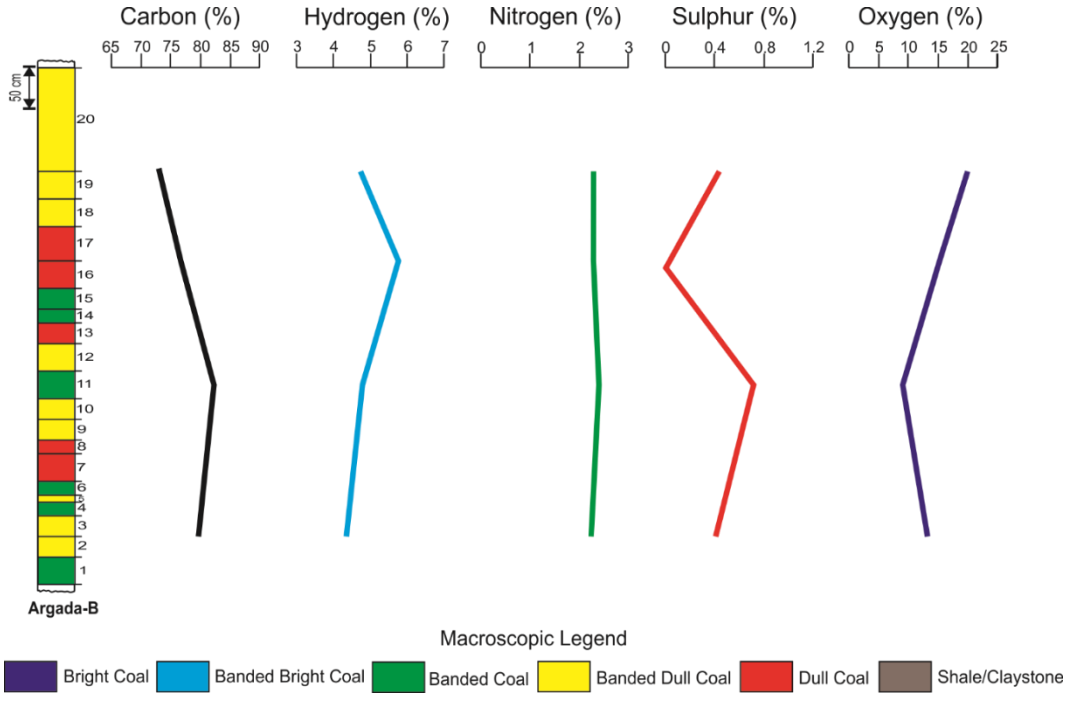


Figure 5.22 Variation of ultimate constituents along the macropetrographic seam section of Argada-B seam.

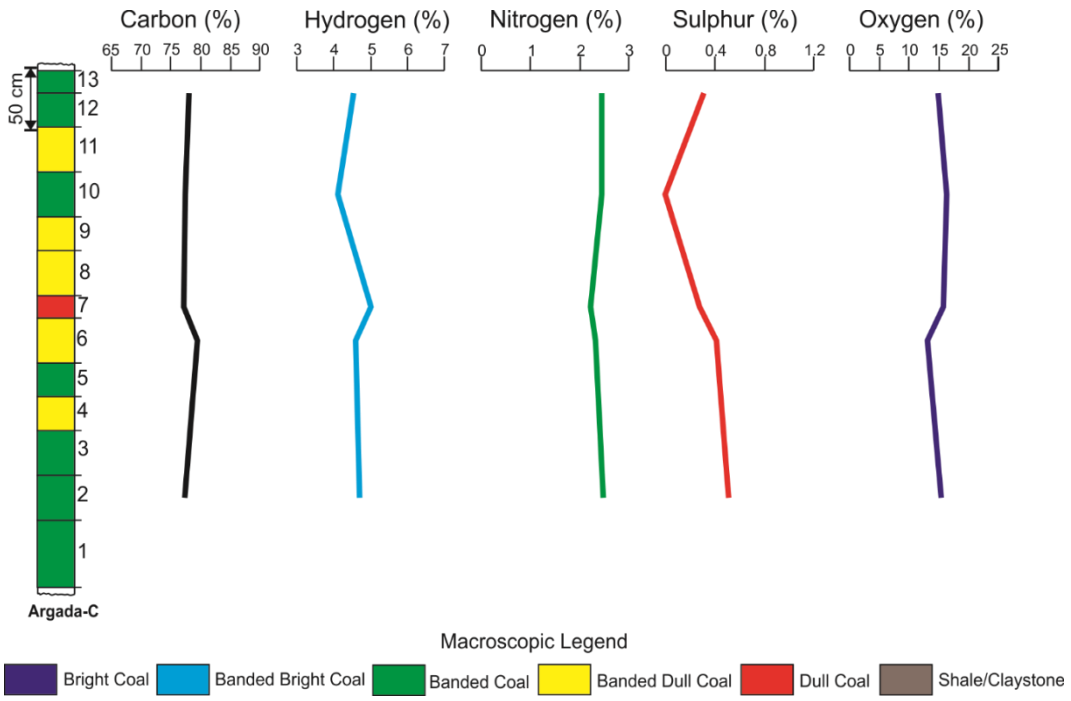


Figure 5.23 Variation of ultimate constituents along the macropetrographic seam section of Argada-C seam.

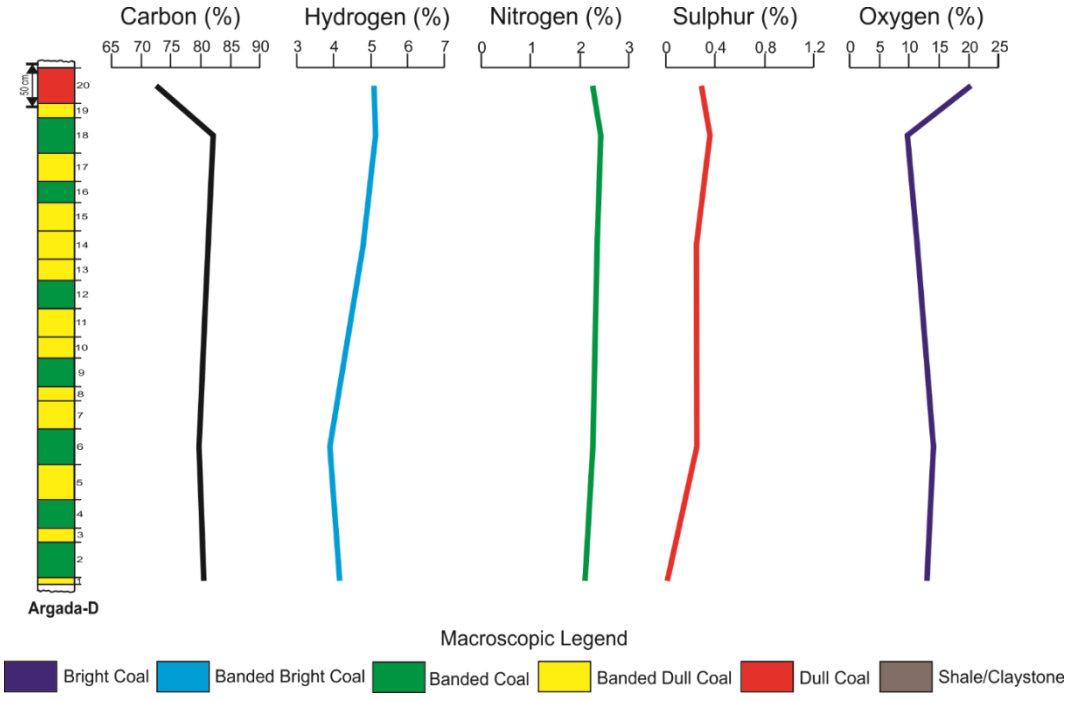


Figure 5.24 Variation of ultimate constituents along the macropetrographic seam section of Argada-D seam.

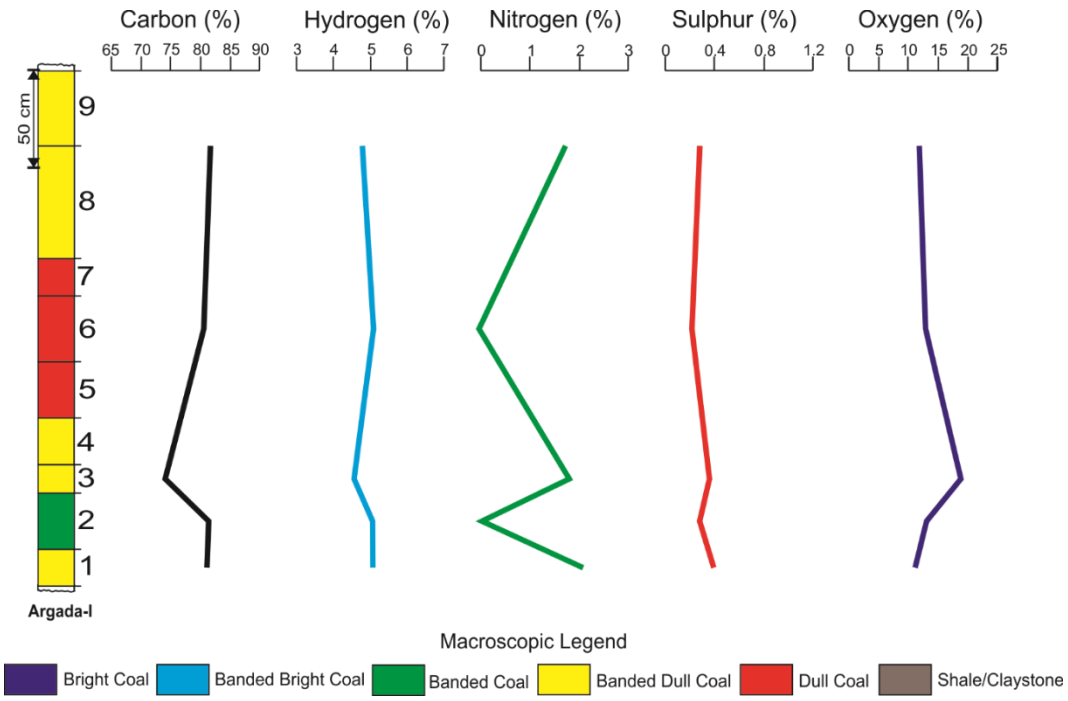


Figure 5.25 Variation of ultimate constituents along the macropetrographic seam section of Argada-I seam.

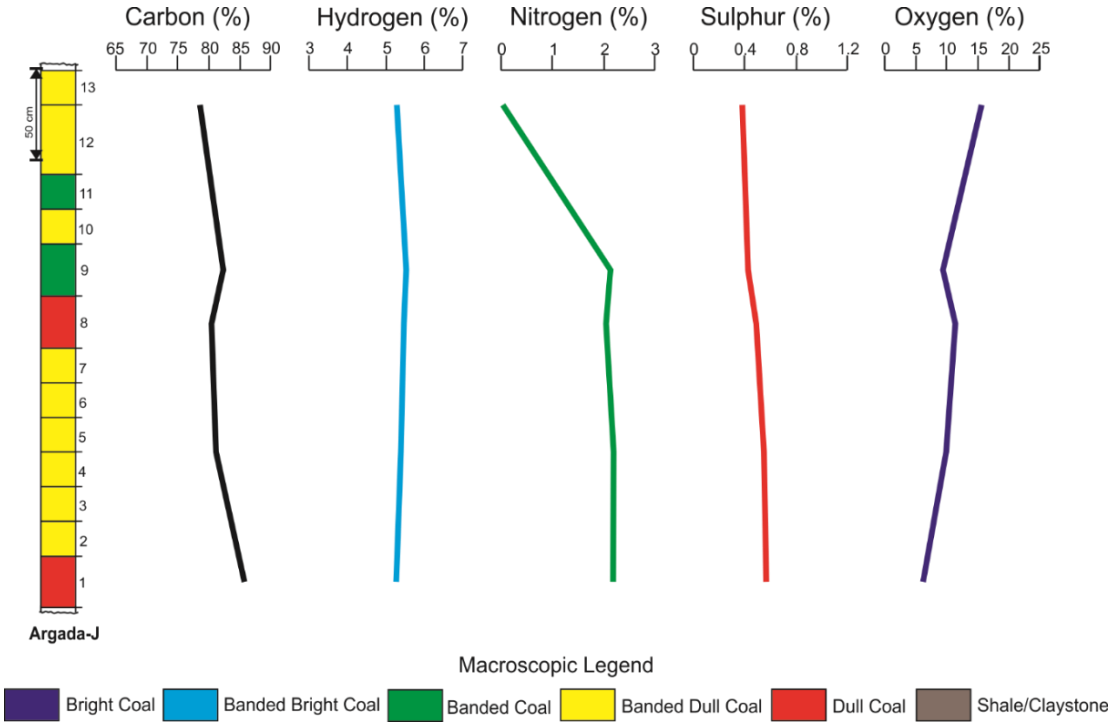


Figure 5.26 Variation of ultimate constituents along the macropetrographic seam section of Argada-J seam.

Table 5.4 Ultimate constituents (wt.%) of coal seams of the Argada area.

	Ash	Moisture	Dry Basis					Dry ash-free (daf) basis						
	(wt.%)	(wt.%)	C%	H%	N%	S%	O%	C%	H%	N%	S%	O%	H/C	O/C
Argada														
AG/13	14.43	0.60	69.67	4.14	1.78	0.39	9.50	81.51	4.85	2.09	0.45	11.11	0.71	0.10
AG/10	42.17	0.43	43.41	3.18	1.25	0.22	9.59	75.31	5.52	2.16	0.39	16.63	0.88	0.17
AG/9	64.99	0.52	25.20	1.73	0.78	nil	6.96	72.69	5.00	2.24	nil	20.06	0.83	0.21
AG/5	13.26	1.51	70.77	4.23	1.86	0.47	9.22	81.78	4.88	2.15	0.55	10.65	0.72	0.10
AG/1	12.77	0.96	71.05	4.08	1.90	0.38	9.70	81.57	4.68	2.18	0.44	11.13	0.69	0.10
Min	12.77	0.43	25.20	1.73	0.78	nil	6.96	72.69	4.68	2.09	nil	10.65	0.69	0.10
Max	64.99	1.51	71.05	4.23	1.90	0.47	9.70	81.78	5.52	2.24	0.55	20.06	0.88	0.21
Mean	29.52	0.80	56.02	3.47	1.51	0.29	8.99	78.57	4.99	2.16	0.36	13.92	0.76	0.13
SD	20.93	0.40	18.65	0.95	0.44	0.17	1.03	3.82	0.28	0.05	0.19	3.78	0.07	0.04
Argada-A														
AG/A/6	28.83	1.57	56.97	3.77	1.62	0.44	7.90	80.57	5.34	2.29	0.62	11.17	0.80	0.10
AG/A/4	14.03	1.90	67.67	4.08	1.82	0.59	11.53	78.97	4.76	2.12	0.69	13.45	0.72	0.13
AG/A/2	31.33	1.34	54.07	3.66	1.61	0.41	8.49	79.24	5.37	2.35	0.60	12.44	0.81	0.12
AG/A/1	20.73	1.98	63.64	3.63	1.86	0.41	9.31	80.71	4.60	2.36	0.52	11.81	0.68	0.11
Min	14.03	1.34	54.07	3.63	1.61	0.41	7.90	78.97	4.60	2.12	0.52	11.17	0.68	0.10
Max	31.33	1.98	67.67	4.08	1.86	0.59	11.53	80.71	5.37	2.36	0.69	13.45	0.81	0.13
Mean	23.73	1.70	60.59	3.79	1.73	0.46	9.31	79.87	5.02	2.28	0.61	12.22	0.75	0.11
SD	6.84	0.26	5.36	0.18	0.12	0.08	1.38	0.78	0.34	0.09	0.06	0.84	0.05	0.01
Argada- B														
AG/B/18+19+20	33.31	1.86	48.20	3.11	1.48	0.28	12.99	72.96	4.71	2.24	0.43	19.67	0.77	0.20
AG/B/16+17	49.39	1.42	38.14	2.88	1.11	nil	7.77	76.43	5.77	2.23	nil	15.57	0.91	0.15
AG/B/11	14.47	3.74	70.30	4.04	2.00	0.59	8.04	82.73	4.76	2.35	0.69	9.47	0.69	0.09
AG/B/2	15.48	2.44	66.99	3.73	1.84	0.34	11.23	79.62	4.43	2.19	0.41	13.35	0.67	0.13
Min	14.47	1.42	38.14	2.88	1.11	nil	7.77	72.96	4.43	2.19	nil	9.47	0.67	0.09
Max	49.39	3.74	70.30	4.04	2.00	0.59	12.99	82.73	5.77	2.35	0.69	19.67	0.91	0.20
Mean	28.16	2.37	55.91	3.44	1.61	0.30	10.01	77.94	4.92	2.25	0.38	14.51	0.76	0.14
SD	14.36	0.87	13.28	0.47	0.34	0.21	2.19	3.64	0.51	0.06	0.25	3.69	0.09	0.04
Argada- C														
AG/C/12+13	18.99	2.71	62.67	3.59	1.97	0.26	11.99	77.87	4.46	2.45	0.32	14.90	0.69	0.14
AG/C/10	12.49	2.64	67.40	3.68	2.14	nil	13.96	77.32	4.22	2.45	nil	16.01	0.66	0.16
AG/C/7	43.04	1.24	43.53	2.82	1.27	0.17	8.63	77.15	5.01	2.25	0.30	15.30	0.78	0.15
AG/C/6	17.17	2.15	65.30	3.79	1.90	0.38	11.08	79.20	4.60	2.30	0.46	13.44	0.70	0.13
AG/C/1+2+3	26.70	2.86	55.89	3.43	1.77	0.37	11.06	77.07	4.73	2.44	0.51	15.25	0.74	0.15
Min	12.49	1.24	43.53	2.82	1.27	nil	8.63	77.07	4.22	2.25	nil	13.44	0.66	0.13
Max	43.04	2.86	67.40	3.79	2.14	0.38	13.96	79.20	5.01	2.45	0.51	16.01	0.78	0.16
Mean	23.68	2.32	58.96	3.46	1.81	0.23	11.35	77.72	4.60	2.38	0.32	14.98	0.71	0.14
SD	10.71	0.59	8.63	0.34	0.30	0.14	1.72	0.79	0.26	0.09	0.18	0.85	0.04	0.01
Argada- D														
AG/D/20	47.42	1.23	37.81	2.65	1.15	0.15	10.23	72.72	5.09	2.22	0.29	19.68	0.84	0.20
AG/D/18	13.90	2.47	70.69	4.40	2.11	0.30	8.25	82.43	5.14	2.46	0.35	9.62	0.75	0.09
AG/D/13+14+15	23.31	1.38	62.13	3.68	1.80	0.19	8.57	81.37	4.81	2.35	0.24	11.22	0.71	0.10
AG/D/6	19.00	3.20	64.20	3.18	1.79	0.20	11.01	79.88	3.96	2.22	0.25	13.70	0.59	0.13
AG/D/1	18.55	2.14	65.59	3.40	1.72	nil	10.33	80.93	4.20	2.12	nil	12.75	0.62	0.12
Min	13.90	1.23	37.81	2.65	1.15	nil	8.25	72.72	3.96	2.12	nil	9.62	0.59	0.09
Max	47.42	3.20	70.69	4.40	2.11	0.30	11.01	82.43	5.14	2.46	0.35	19.68	0.84	0.20
Mean	24.44	2.08	60.08	3.46	1.71	0.17	9.68	79.47	4.64	2.28	0.23	13.39	0.70	0.13
SD	11.87	0.72	11.49	0.58	0.31	0.10	1.07	3.47	0.48	0.12	0.12	3.43	0.09	0.04
Argada- I														
AG/I/8+9	27.85	1.38	58.48	3.40	1.20	0.20	8.48	81.49	4.74	1.68	0.27	11.82	0.70	0.11
AG/I/5+6+7	26.98	1.78	59.24	3.68	nil	0.16	9.44	81.68	5.08	nil	0.22	13.02	0.75	0.12
AG/I/3	20.80	2.63	58.45	3.57	1.44	0.27	14.90	74.33	4.55	1.83	0.34	18.95	0.73	0.19
AG/I/2	20.04	2.04	64.97	4.02	nil	0.23	10.33	81.67	5.05	nil	0.29	12.99	0.74	0.12
AG/I/1	23.75	2.31	61.47	3.87	1.58	0.29	8.48	81.21	5.11	2.09	0.38	11.21	0.75	0.10
Min	20.04	1.38	58.45	3.40	nil	0.16	8.48	74.33	4.55	nil	0.22	11.21	0.70	0.10
Max	27.85	2.63	64.97	4.02	1.58	0.29	14.90	81.68	5.11	2.09	0.38	18.95	0.75	0.19

	Ash	Moisture	Dry Basis					Dry ash-free (daf) basis						
	(wt.%)	(wt.%)	C%	H%	N%	S%	O%	C%	H%	N%	S%	O%	H/C	O/C
Mean	23.88	2.03	60.52	3.71	0.85	0.23	10.33	80.08	4.91	1.12	0.30	13.60	0.74	0.13
SD	3.15	0.43	2.48	0.22	0.70	0.05	2.39	2.88	0.22	0.92	0.05	2.76	0.02	0.03
Argada- J														
AG/J/12+13	33.69	1.70	51.88	3.44	nil	0.25	10.16	78.93	5.24	nil	0.37	15.45	0.80	0.15
AG/J/9	17.14	2.15	67.98	4.55	1.77	0.34	7.85	82.41	5.52	2.14	0.41	9.52	0.80	0.09
AG/J/8	26.99	1.90	58.44	3.97	1.51	0.34	8.23	80.62	5.47	2.08	0.47	11.35	0.81	0.11
AG/J/2-7	24.74	2.58	60.81	4.01	1.64	0.41	7.74	81.50	5.37	2.20	0.55	10.38	0.79	0.10
AG/J/1	26.09	2.52	62.98	3.86	1.60	0.41	4.39	85.99	5.28	2.18	0.56	5.99	0.74	0.05
Min	17.14	1.70	51.88	3.44	nil	0.25	4.39	78.93	5.24	nil	0.37	5.99	0.74	0.05
Max	33.69	2.58	67.98	4.55	1.77	0.41	10.16	85.99	5.52	2.20	0.56	15.45	0.81	0.15
Mean	25.73	2.17	60.42	3.97	1.30	0.35	7.68	81.89	5.38	1.72	0.47	10.54	0.79	0.10
SD	5.29	0.34	5.30	0.35	0.66	0.06	1.86	2.35	0.11	0.86	0.07	3.05	0.03	0.03

5.4 Determination of Major oxides in coals of South Karanpura coalfield

The determination of the major oxide was carried out on selected whole coal samples of South Karanpura coalfield. The oxides which are quantitatively calculated include SiO_2, Al_2O_3, Fe_2O_3, MnO, CaO, MgO, K_2O, Na_2O, TiO_2, and P_2O_5. Due to the insignificant intra-seam variation of the geochemical constituents, one or two representative samples were selected from each seam, and their mean values were discussed. The inter-seam variation of major oxides has been presented for both the area Barka Sayal as well as Argada (Figure 5.27 and Figure 5.28). The intraseam or interseam variation of major oxides reflects the mineralogical variations present in these coals. The metamorphic progression and leaching behaviour of different minerals, phases, and elements during coalification result in essential changes in the mineral and chemical composition of coals (Vassilev *et al.* 1996). Enrichment of SiO_2 may indicate the presence of quartz and silicate minerals. A high concentration of Al_2O_3 may indicate a high influx of clay minerals in the coal. The high content of FeO may occur due to the presence of iron-bearing minerals such as hematite, magnetite, and ilmenite. Gypsum as well as other carbonate minerals such as siderite, ankerite, dolomite etc. may be responsible for the enrichment of CaO in the coal. Halite influence the Na content in the coal. A high concentration of iron content generally indicates river-borne sediments, whereas a high concentration of sulphur

indicates marine influence (Schweinfurth 2002). Although, in the case of pyrite, syngenetic pyrite may form due to the introduction of SO_4 in the peat by marine water which further reduced to S_2 and forms pyrite after combining with iron (Casagrande, 1987). This pyrite can be classified as marine sediment but epigenetic pyrite gets introduced in coal during coalification which may not be classified as marine sediments. Higher TiO_2 content might be related to the additional terrigenous input of anatase during coal formation (Chen *et al.* 2015a). The determination of major oxides was carried out on the ash of selected samples using the XRF instrument. The results are presented in Table 5.5 and shown in Figure 5.27 and Figure 5.28.

5.4.1 The occurrence of Major Oxides in the coals of the South Karanpura

5.4.1.1 Barka Sayal area

The most abundant oxide present in the coals of the Barka Sayal area is SiO_2. Its range varies from 37.41% to 64.02%, mean 55.31% in this area. In these coals, the Al_2O_3 concentration varies from 19.30% to 32.97%, mean 28.32%. FeO content in the coals of Barka Sayal area ranges from 1.22% to 25.39%, mean 7.21%. As compared to SiO_2 and Al_2O_3 content, the high occurrence of FeO is sporadic and observed in the samples of Sayal and Bansgarha seam, which indicate the presence of hematite in these seams. All other oxides are in a low concentration. TiO_2 content of Barka Sayal area varies from 0.87% to 2.23%, mean 1.66%. MnO content of the coals of Barka Sayal area varies from Nil to 0.24%, mean 0.06%. The MgO content in the coals of the Barka Sayal area varies from 0.26% to 1.97%, mean 0.98%. The concentration of CaO is in between Nil to 8.45%, mean 2.44%. Na_2O content of this area lies in between 0.17% and 0.42%, mean 0.22%. K_2O of the coals of the Barka Sayal area lies between 0.80% and 3.07%, mean 1.97%. The P_2O_5 content of the Barka Sayal area lies in between 0.07% and 5.87%, mean 1.82% (Table 5.5).

The coals of Sayal seam have a high amount of SiO_2, Al_2O_3, and FeO, while other major oxides are comparatively very less. The mean values of SiO_2, Al_2O_3, and FeO content of the coals of this seam are 40.38%, 20.48%, and 25.10%, respectively. The oxides of the other major elements such as CaO, TiO_2, MnO, MgO, Na_2O, K_2O, and P_2O_5 are in very less amount having mean values 5.73%, 0.97, 0.21, 1.66, 0.21, 1.42, and 3.83 respectively (Table 5.5).

The analysis of major oxide concentration of the coals of Sayal Balkudra seam shows the enrichment of SiO_2, Al_2O_3, and FeO in these coals having mean concentration values 60.88%, 28.32%, and 3.89% respectively. Other oxides contribute less than 8%. The mean values of TiO_2, MnO, MgO, CaO, Na_2O, K_2O and P_2O_5 are 1.79%, 0.03%, 1.25%, 0.50%, 0.22%, 2.72% and 0.40% respectively (Table 5.5).

Coals of the Upper Semana seam also show a high abundance of SiO_2 and Al_2O_3 having mean values 52.26% and 31.89%, respectively. The mean concentrations of other major oxides such as TiO_2, FeO, MnO, MgO, CaO, Na_2O, K_2O, and P_2O_5 are 1.97, 2.64, 0.01, 0.31, 5.42, 0.25, 1.22 and 4.03 respectively (Table 5.5).

The mean SiO_2 concentration of the coals of the Lower Semana seam is 58.65%. The Al_2O_3 concentration of these coals shows an average value of 30.21%. The mean concentration of other major oxides such as TiO_2, FeO, MnO, MgO, CaO, Na_2O, K_2O, and P_2O_5 are 1.94, 1.83, 0.01, 0.35, 2.69, 0.17, 1.71 and 2.45 respectively (Table 5.5).

Coals of Hathidari seam also show a high abundance of SiO_2 and Al_2O_3 having mean values of 63.23% and 29.58%, respectively. The mean concentration of other major oxides such as TiO_2, FeO, MnO, MgO, CaO, Na_2O, K_2O, and P_2O_5 is 1.72, 1.76, nil, 0.86, 0.02, 0.30, 2.43 and 0.10 respectively (Table 5.5).

The coals of the Bansgarha seam contain a high amount of SiO_2, Al_2O_3, and FeO having mean values 56.46%, 29.42%, and 8.06%. The average values for TiO_2, MnO, MgO, CaO, Na_2O, K_2O, and P_2O_5 are 1.59%, 0.09%, 1.43, 0.30, 0.18, 2.35 and 0.11% respectively (Table 5.5).

5.4.1.2 Argada area

In the Argada area also the SiO_2 is present in a very high concentration, indicating the presence of quartz and silicate minerals in it. The SiO_2 range lies in between 44.48% and 63.21%, mean 55.35%. Coals of Argada area exhibit Al_2O_3 range from 29.86% to 39.19%, mean 33.72%. The coals of Argada area are comparatively rich in Al_2O_3 indicate the higher presence of clay minerals in these coals compared to coals belonging to Barka Sayal area. In the coals of Argada area, the FeO content varies from 1.09% to 25.39%, mean 5.22%. The seams of this area contain a fewer amount of iron-bearing minerals. Argada A and Argada J seams exhibit the sporadic occurrence of FeO in this area. For Argada area, the TiO_2 content of the coal varies from 2.10% to 4.42%, mean 2.77%. The MnO content is in between nil to 0.12%, mean 0.02%. The coals of Argada area exhibit the MgO concentration lying between 0.22% and 1.01%, mean 0.50%. Coals of Argada area exhibit CaO range varying from nil to 5.25% mean 1.36%. In this area the Na_2O content varies from 0.16% to 0.62%, mean 0.23%. Coals of Argada area possess K_2O content in between 0.92% and 1.98%, mean 1.53%. Coals of Argada area have P_2O_5 content ranging from 0.07% to 5.87%, mean 1.46% (Table 5.5).

The coals of Argada seam have a high concentration of SiO_2 as well as Al_2O_3, and other major oxides are lower in concentration. The mean SiO_2 and Al_2O_3 content of the coals of this seam is 58.01% and 34.28% respectively. The oxides of other major elements such as TiO_2, FeO, MnO, MgO, CaO, Na_2O, K_2O, and P_2O_5 are in very less amount having mean values 2.20%, 2.46, 0.02, 0.47, 0.31, 0.17, 1.73, and 0.35% respectively (Table 5.5).

The analysis of major oxide concentration of the coals of Argada-A seam shows the enrichment of SiO_2, Al_2O_3, and FeO in these coals having mean concentration values 54.45%, 32.01%, and 4.61% respectively. Other oxides contribute less than 10%. The mean values of TiO_2, MnO, MgO, CaO, Na_2O, K_2O, and P_2O_5 are 2.24%, 0.03%, 0.29%, 2.83%, 0.21%, 0.96%, and 2.36% respectively (Table 5.5).

Coals of Argada-B seam also show a high abundance of SiO_2 and Al_2O_3 having mean values of 61.20% and 31.61%, respectively. The mean concentration of other major oxides such as TiO_2, FeO, MnO, MgO, CaO, Na_2O, K_2O, and P_2O_5 is 2.92, 1.38, nil, 0.46, 0.14, 0.19, 1.72 and 0.36 respectively (Table 5.5).

Table 5.5 The concentration of oxide of major elements present in coals of South Karanpura Coalfield.

Seam Name and Sample No.	Ash Wt.%	Concentrations of oxides of the major elements in weight %									
		SiO_2	TiO_2	Al_2O_3	FeO	MnO	MgO	CaO	Na_2O	K_2O	P_2O_5
SL 3	33.74	43.36	1.07	21.66	25.39	0.24	1.66	3.01	0.20	1.63	1.79
SL 5	24.42	37.41	0.87	19.30	24.81	0.19	1.65	8.45	0.23	1.22	5.87
SBK 5	30.17	62.58	2.04	30.28	1.62	nil	0.72	0.04	0.20	2.37	0.15
SBK 9	48.68	59.18	1.55	26.36	6.16	0.05	1.79	0.95	0.23	3.07	0.65
US 3+4	14.42	51.28	1.77	30.82	2.83	0.01	0.26	6.95	0.29	0.80	5.00
US 9	22.12	53.23	2.16	32.97	2.46	0.02	0.35	3.89	0.21	1.65	3.07
LS 4+5	13.73	53.54	1.65	30.60	2.31	0.01	0.32	5.28	0.17	1.41	4.70
LS 8+9	24.81	63.75	2.23	29.81	1.35	nil	0.37	0.09	0.17	2.00	0.20
HD 3	24.13	62.44	1.63	28.85	2.29	0.01	1.27	nil	0.42	3.02	0.07
HD7	27.34	64.02	1.80	30.31	1.22	nil	0.46	0.03	0.18	1.84	0.13
BG 1	32.38	61.60	1.80	30.69	1.97	0.01	0.90	0.10	0.19	2.64	0.10
BG 2+3	28.38	51.33	1.38	28.15	14.16	0.16	1.97	0.49	0.17	2.06	0.13
AG 9	64.99	59.93	2.15	31.28	3.53	0.03	0.56	0.15	0.17	1.98	0.22
AG 10	42.17	56.10	2.24	37.28	1.40	0.01	0.38	0.46	0.16	1.48	0.48
AG A 8+9+10	18.87	52.21	2.13	32.02	7.10	0.05	0.36	2.59	0.24	0.92	2.39
AG A 14+15	27.62	56.69	2.36	31.99	2.13	0.01	0.22	3.08	0.19	1.00	2.34
AG B 16+17	49.39	63.21	3.45	29.86	1.09	nil	0.35	0.03	0.20	1.48	0.33
AG B 18	33.31	59.20	2.39	33.36	1.66	nil	0.57	0.29	0.19	1.96	0.39
AG C 1+2+3	26.70	55.83	2.10	33.02	1.80	nil	0.52	2.36	0.62	1.79	1.95
AG C 7	43.04	57.12	2.84	35.94	1.50	nil	0.50	nil	0.27	1.73	0.09
AG D 20	47.42	52.54	2.63	39.19	2.87	0.01	0.45	0.35	0.16	1.66	0.14
AG I 1	23.75	57.17	3.55	33.48	2.62	0.02	0.61	0.15	0.16	1.80	0.45
AG I 5+6+7	26.98	57.23	4.42	34.44	1.56	0.01	0.34	0.14	0.16	1.40	0.32
AG J 9	17.14	47.77	2.86	33.87	4.45	0.04	0.57	5.25	0.19	1.39	3.61
AG J 12+13	33.69	44.48	2.91	32.67	12.34	0.12	1.01	2.89	0.25	1.28	2.06

The mean SiO_2 concentration of the coals of Argada-C seam is 56.47%. The Al_2O_3 concentration of these coals shows an average value of 34.48%. The mean concentration of other major oxides such as TiO_2, FeO, MnO, MgO, CaO, Na_2O, K_2O, and P_2O_5 is 2.47, 1.65, nil, 0.51, 1.18, 0.45, 1.76 and 1.02 respectively (Table 5.5).

Coals of Argada-D seam also show a high abundance of SiO_2 and Al_2O_3 having mean values of 52.54% and 39.19%, respectively. The mean concentration of other major oxides such as TiO_2, FeO, MnO, MgO, CaO, Na_2O, K_2O, and P_2O_5 are 2.63, 2.87, 0.01, 0.45, 0.35, 0.16, 1.66 and 0.14 respectively (Table 5.5).

The coals of Argada-I seam contain a high amount of SiO_2 and Al_2O_3 having mean values of 57.20% and 33.96%, respectively. The average values for TiO_2, FeO, MnO, MgO, CaO, Na_2O, K_2O and P_2O_5 are 3.98%, 2.09%, 0.01, 0.47, 0.15, 0.16, 1.60 and 0.38% respectively (Table 5.5).

The coals of Argada-J seam contain a high amount of SiO_2, Al_2O_3, and FeO having mean 46.13%, 33.27%, and 8.39%. The average values for TiO_2, MnO, MgO, CaO, Na_2O, K_2O, and P_2O_5 are 2.89%, 0.08%, 0.79, 4.07, 0.22, 1.33, and 2.84% respectively (Table 5.5).

5.4.2 Distribution of Major oxides in coals of South Karanpura coalfield

5.4.2.1 Barka Sayal area

The variation diagram of major oxides in different coal seams of the Barka Sayal area is presented in Figure 5.27. The variation of the major oxides are being mainly guided by the presence of mineral constituents in different bands and seams. In coals of Barka Sayal area, the maximum concentration of SiO_2 has been observed in Bansgarha coal seam, whereas Sayal seam exhibits the minimum. Coals of Upper Semana seam exhibit a maximum concentration of Al_2O_3, whereas its minimum concentration was observed in the coals of the Sayal seam. FeO concentration is found highest in coals of Sayal seam, whereas its least abundance was found in the coals of Lower Semana seam. Coals of Sayal

seam also exhibit a higher concentration of CaO compared to other seams of the area. The lowest concentration of CaO was observed in Hathidari seam. TiO_2 is found maximum in Upper Semana and minimum in Sayal seam. The concentration of MnO in these coals is very low. Its highest concentration occurs in the Sayal seam and it is undetectable in the Hathidari seam. MgO is found in maximum concentration in the Upper Semana and minimum in Bansgarha seam. The concentration of Na_2O is also very low in the coals of the Barka Sayal area. It is found maximum concentration in Hathidari and minimum concentration in Lower Semana seam. Sayal Balkudra exhibits the highest concentration of K_2O, while the coals of Upper Semana have the lowest distribution of K_2O. P_2O_5 is highest in the coals of Upper Semana and lowest in the coals of the Hathidari seam.

5.4.2.2 Argada area

The variation diagram of major oxides in different coal seams of the Barka Sayal area is presented in Figure 5.28. In the coals of the Argada area, the maximum concentration of SiO_2 has been observed in Argada-B and the minimum in Argada-J. Al_2O_3 is highest in Argada-D, whereas its minimum concentration was observed in the coals of Argada-B seam. FeO concentration is found highest in coals of Argada-J seam, whereas its least abundance was found in the coals of Argada-B seam. Coals of Argada-J seam also exhibit a higher concentration of CaO compared to other seams of the area. The lowest concentration of CaO was observed in the coals of Argada-I seam. The maximum TiO_2 is found in Argada-I seam and the minimum in Argada seam. The concentration of MnO in these coals is very less. Its highest concentration occurs in Argada-J seam and undetectable in Argada-B and Argada-C seam. MgO is found in maximum concentration in Argada-J seam, whereas Argada-A seam exhibits its minimum concentration. The concentration of Na_2O is also very less in the coals of the Argada area. It is found in maximum concentration in Argada-C seam and minimum concentration in Argada-D

seam. Argada seam exhibits the highest concentration of K_2O, while the coals of Argada-A seam have the lowest concentration of K_2O. P_2O_5 is highest in the coals of Argada-A seam and lowest in the coals of Argada-D seam.

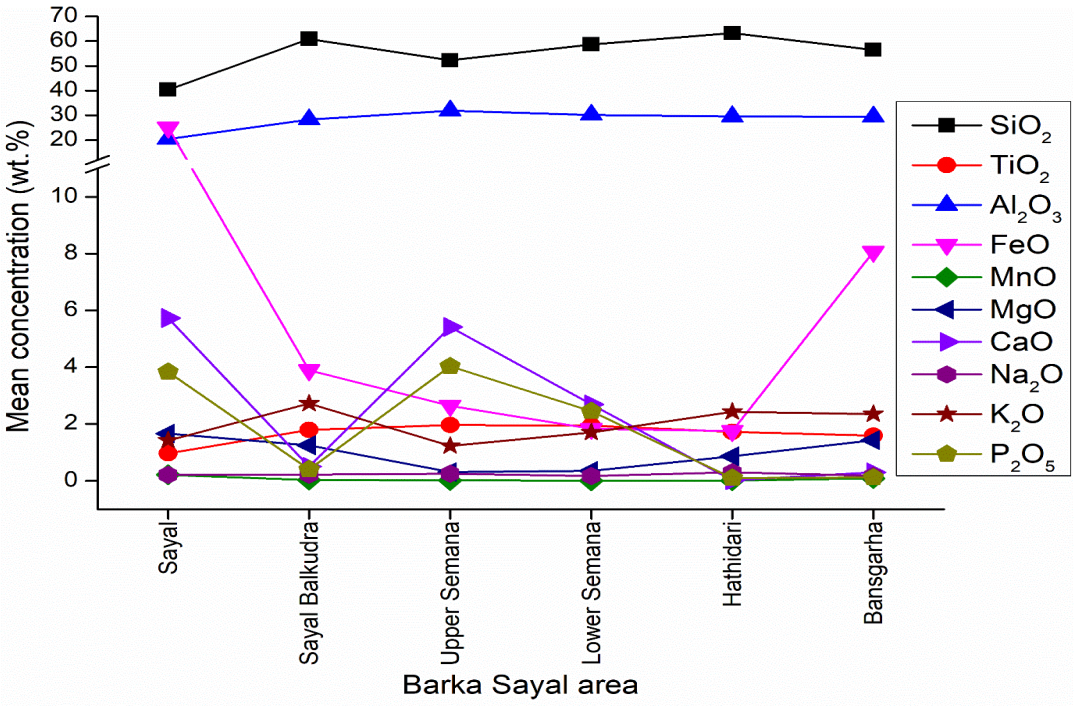


Figure 5.27 Variation of major oxides in coals of Barka Sayal area, South Karanpura coalfield.

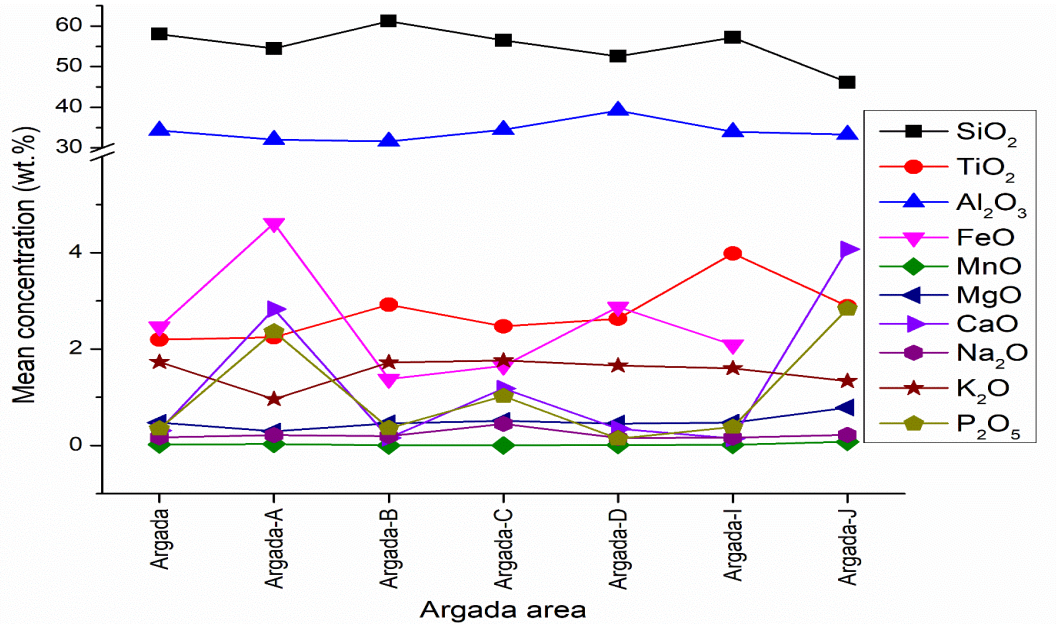


Figure 5.28 Variation of major oxides in coals of Argada area, South Karanpura coalfield.

5.5 Distribution of Major Elements in coals of South Karanpura coalfield

The chemical data as oxides have been recalculated to respective cationic proportions and then converted to a hundred per-cent. The quantitative details of major elements are given in Table 5.6, and the variation has been shown in Figure 5.29 Figure 5.30. They follow the same trend of distribution as their respective oxides.

Table 5.6 The concentration of major elements in coals of South Karanpura Coalfield.

Sample name	Ash (wt.%)	Si	Ti	Al	Fe	Mn	Mg	Ca	Na	K	P
SL 3	33.74	20.27	0.64	11.46	19.73	0.18	1.00	2.15	0.15	1.35	0.78
SL 5	24.42	17.49	0.52	10.22	19.29	0.15	1.00	6.04	0.17	1.01	2.56
SBK 5	30.17	29.25	1.22	16.03	1.26	nil	0.43	0.03	0.15	1.97	0.06
SBK 9	48.68	27.66	0.93	13.95	4.79	0.04	1.08	0.68	0.17	2.55	0.29
US 3+4	14.42	23.97	1.06	16.31	2.20	0.01	0.16	4.96	0.21	0.66	2.18
US 9	22.12	24.88	1.30	17.45	1.91	0.01	0.21	2.78	0.16	1.37	1.34
LS 4	13.73	25.03	0.99	16.20	1.79	0.01	0.19	3.77	0.13	1.17	2.05
LS 8+9	24.81	29.80	1.34	15.78	1.05	nil	0.23	0.07	0.13	1.66	0.09
HD 3	24.13	29.19	0.98	15.27	1.78	0.01	0.77	nil	0.31	2.51	0.03
HD7	27.34	29.92	1.08	16.04	0.95	nil	0.28	0.02	0.14	1.53	0.06
BG 1	32.38	28.79	1.08	16.24	1.53	nil	0.54	0.07	0.14	2.19	0.04
BG 2+3	28.38	23.99	0.83	14.90	11.01	0.13	1.19	0.35	0.13	1.71	0.06
AG 9	64.99	28.01	1.29	16.56	2.74	0.02	0.34	0.11	0.13	1.65	0.09
AG 10	42.17	26.23	1.35	19.73	1.09	nil	0.23	0.33	0.12	1.23	0.21
AG A 8+9+10	18.87	24.41	1.28	16.95	5.52	0.04	0.22	1.85	0.17	0.76	1.04
AG A 14+15+16	27.62	26.50	1.41	16.93	1.65	0.01	0.13	2.20	0.14	0.83	1.02
AG B 16+17	49.39	29.55	2.07	15.80	0.85	nil	0.21	0.02	0.15	1.23	0.14
AG B 18	33.31	27.67	1.43	17.65	1.29	nil	0.34	0.21	0.14	1.63	0.17
AG C 1+2+3	26.70	26.10	1.26	17.48	1.40	nil	0.32	1.69	0.46	1.49	0.85
AG C 7	43.04	26.70	1.70	19.02	1.17	nil	0.30	nil	0.20	1.43	0.04
AG D 20	47.42	24.56	1.58	20.74	2.23	0.01	0.27	0.25	0.12	1.38	0.06
AG I 1	23.75	26.72	2.13	17.72	2.03	0.01	0.37	0.11	0.12	1.49	0.20
AG I 5+6+7	26.98	26.75	2.65	18.23	1.21	nil	0.20	0.10	0.12	1.16	0.14
AG J 9	17.14	22.33	1.72	17.93	3.46	0.03	0.34	3.75	0.14	1.15	1.58
AG J 12+13	33.69	20.79	1.75	17.29	9.59	0.09	0.61	2.06	0.19	1.06	0.90

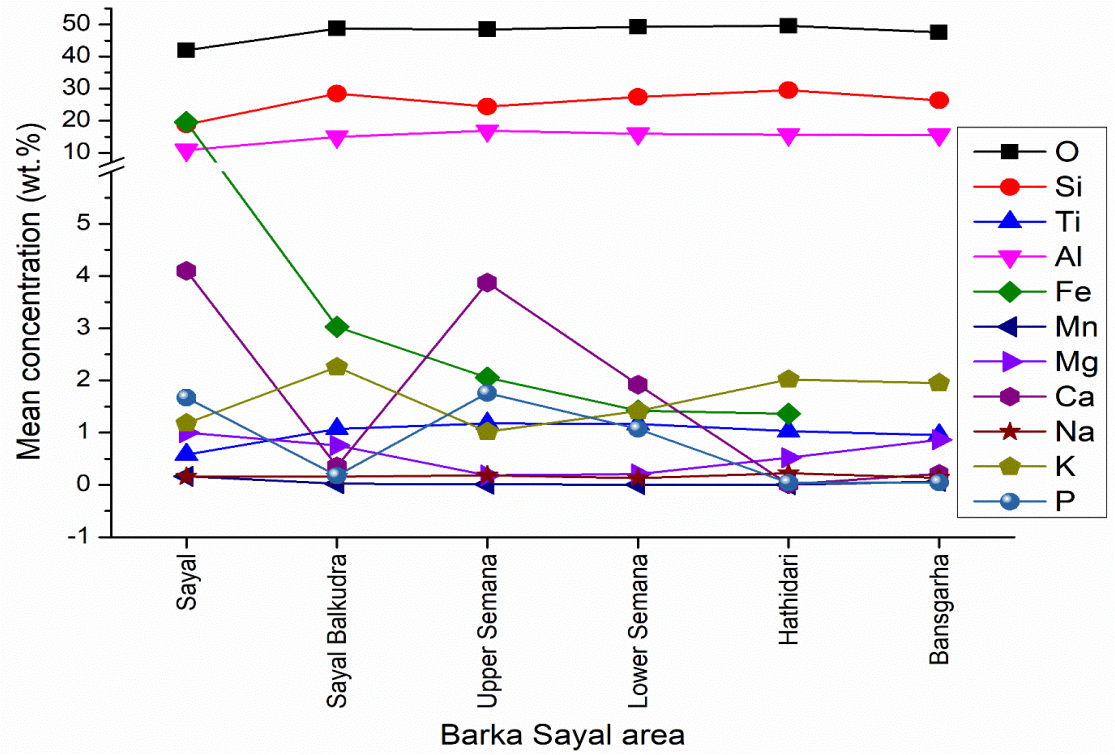


Figure 5.29 Variation of major elements in coals of Barka Sayal area, South Karanpura coalfield.

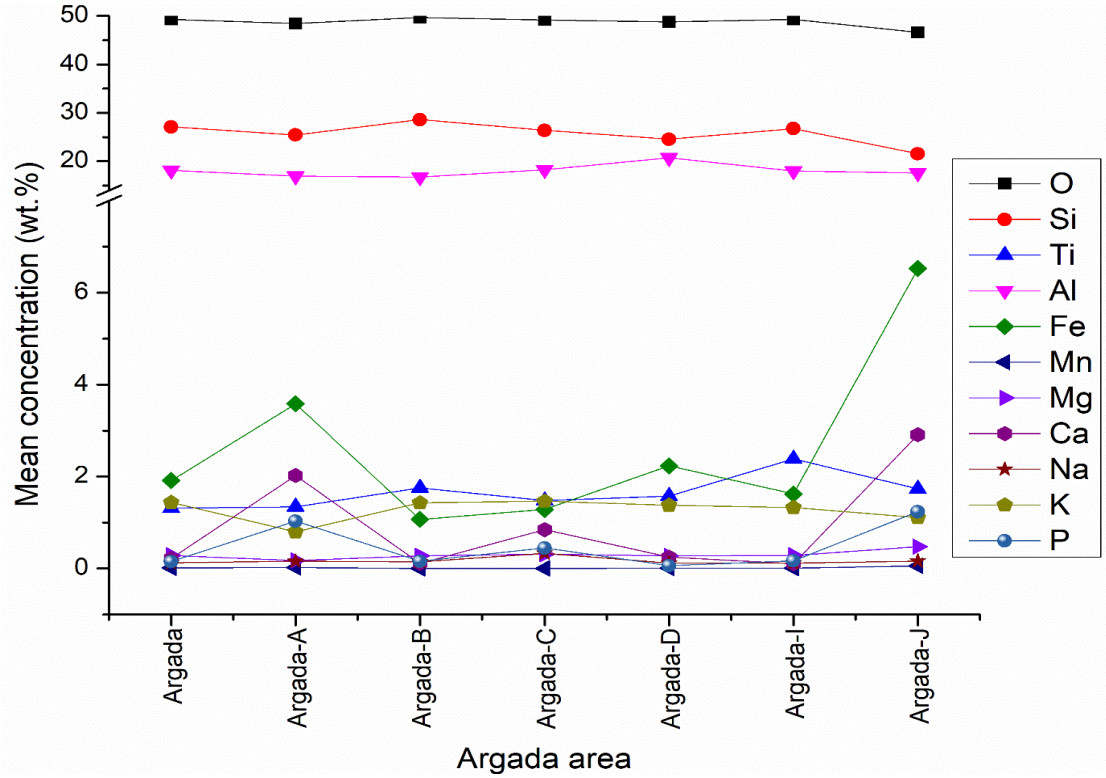


Figure 5.30 Variation of major elements in coals of Argada area, South Karanpura coalfield.

5.5.1 Relation of Major Elements with Ash Yield

Minerals are the prime contributors of the major elements in the coal and its ash yield. Besides a significant contribution of elements also come from organic part of the coal where peat-forming plant communities absorb the elements like C, H, O, N, S, P, K, Ca, Mg, Mn, Cu, Zn, B, Mo and Ga for their growth (Gluskoter 1975; Cameron *et al.* 1989; Dai *et al.* 2014a).

The scatter plot of major elements versus ash yield shows that the elements like Si, Fe, Mn, Mg, and K have a positive correlation with ash yield in the coals of Barka Sayal area, whereas elements Ti, Al, Ca, Na, P and O are in negative correlation (Figure 5.31 and Figure 5.32). For the coals of Argada area Si, Al, K, and O exhibit positive correlation with ash yield, whereas elements like Ti, Fe, Mn, Mg, Ca, Na, and P are found in negative correlation (Figure 5.33 and Figure 5.34). The elemental correlation with ash yield for both the area differs from each other, which suggests that the mineralogical compositions of both areas are slightly different.

The elements Si and K are found in positive correlation with ash yield in both the areas, whereas elements like Ti, Ca, Na, and P are found in negative correlation in both the areas which suggests the affinity of Silicon and Potassium with inorganic constituents and enrichment of their concentration with ash yield. In contrast, titanium, calcium, sodium, and phosphorous possibly have a more organic affinity, or during low-temperature ashing process, these elements do not concentrate in the residue. Although, these can be controlled by sources and the mechanism of bonding with organic matter, and the fate along with coal-rank advance (Dai *et al.* 2020a).

Some of the elements, like Na, Al, and Ti, have very low R^2 value (coefficient of determination). This decreases the confidence of these data for correlation purposes.

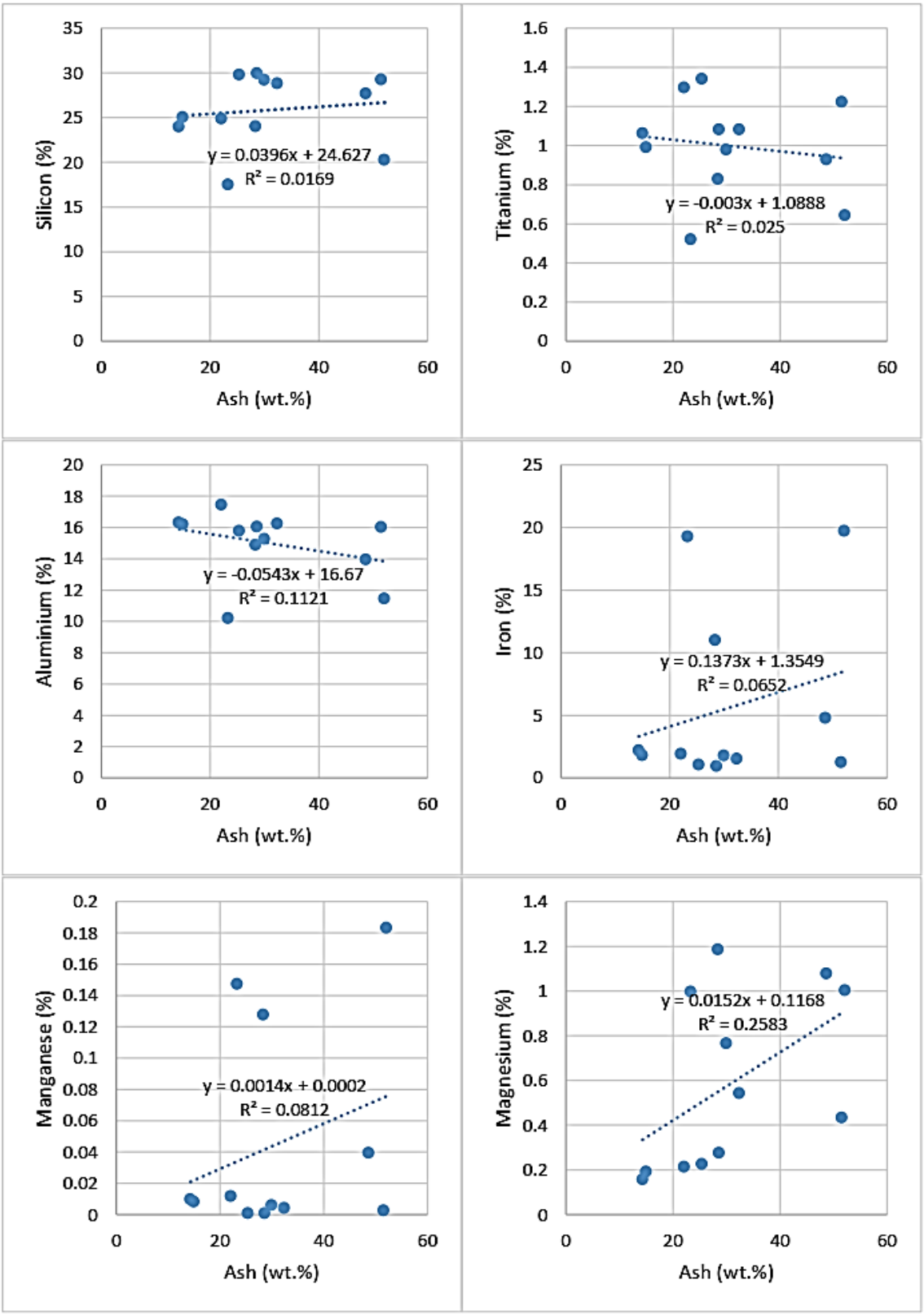


Figure 5.31 Scatter plot of major elements (Si, Ti, Fe, Al, Mn, and Mg) with ash yield for coals of Barka Sayal area, South Karanpura coalfield.

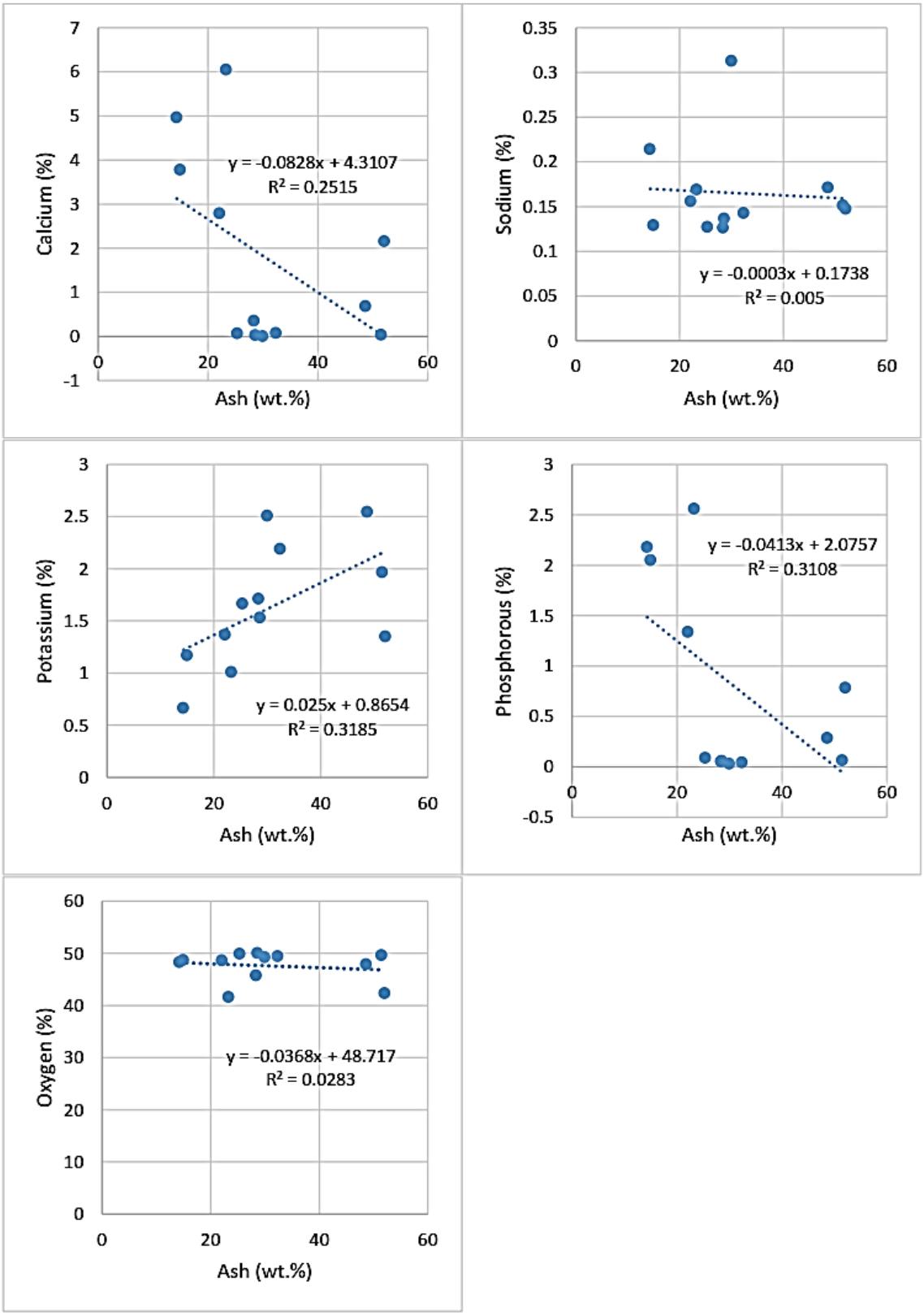


Figure 5.32 Scatter plot of major elements (Ca, Na, K, P, and O) with ash yield for coals of Barka Sayal area, South Karanpura coalfield.

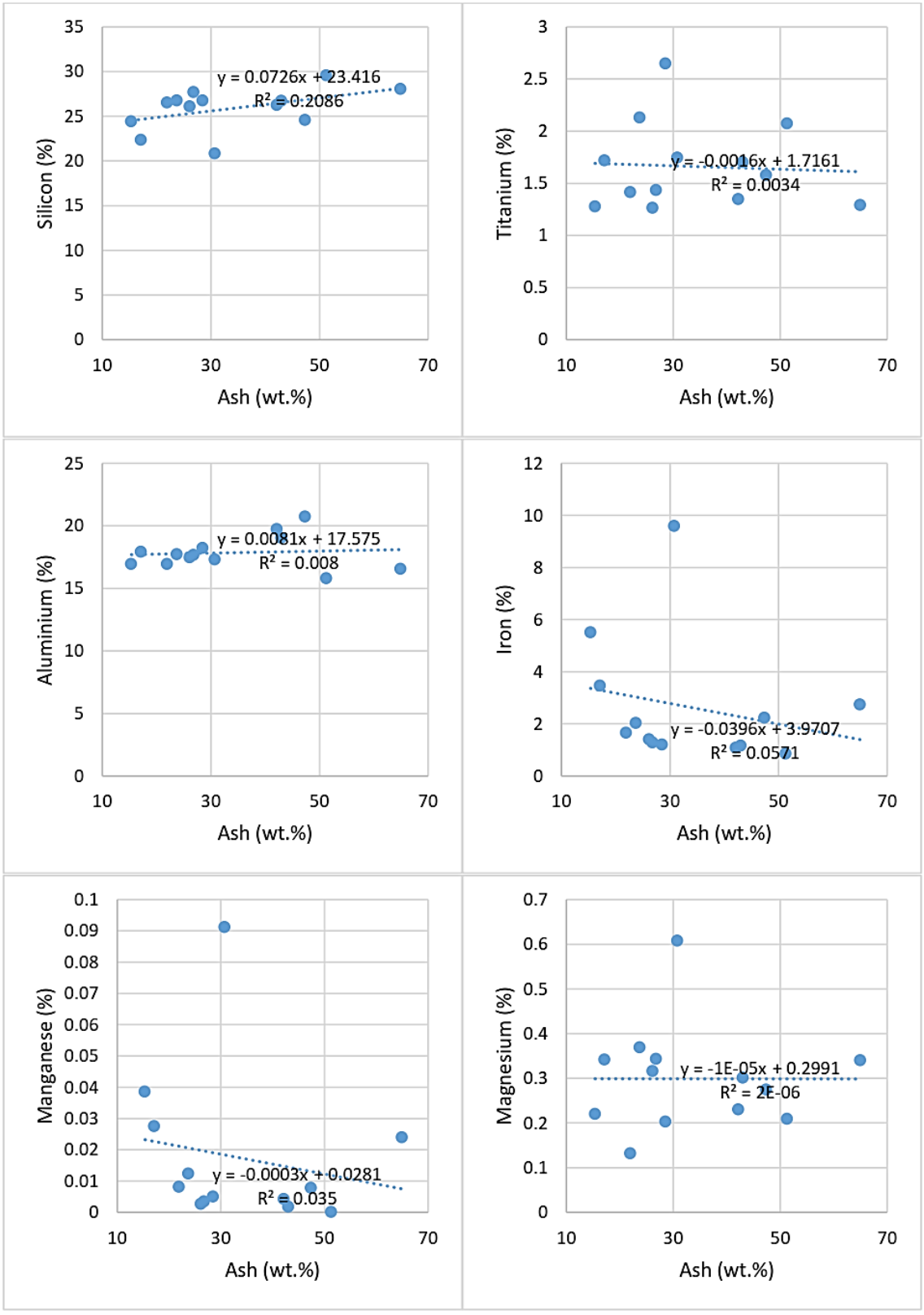


Figure 5.33 Scatter plot of major elements (Si, Ti, Fe, Al, Mn, and Mg) with ash yield for coals of Argada area, South Karanpura coalfield.

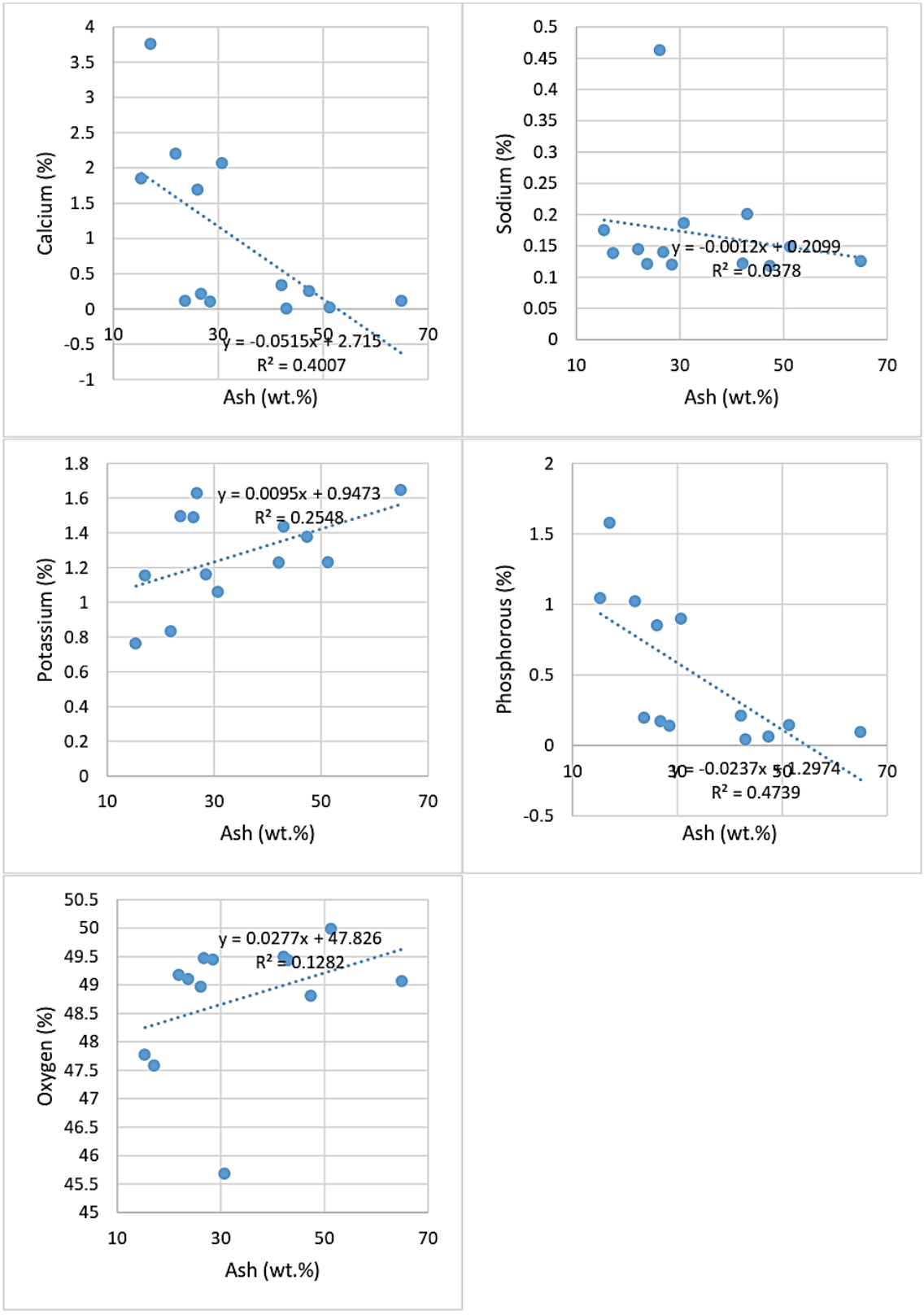


Figure 5.34 Scatter plot of major elements (Ca, Na, K, P, and O) with ash yield for coals of Argada area, South Karanpura coalfield.

The paleoclimate controls not only the deposition of organic content but also the deposition of inorganic constituents. The unstable minerals convert into more stable minerals due to weathering. This is the reason that feldspar ultimately breaks down to form clay minerals as a function of acidity, climate and depositional setting in the swamp. Coal as a sedimentary rock is a combination of both organic and inorganic constituents. A careful study of its inorganic constituents of coal, considering its mode of occurrence and the types of origin can reveal crucial information about the paleodepositional environmental conditions (Querol *et al.* 1997b; Singh *et al.* 2016c; Hakimi *et al.* 2017). Besides this, it can also be helpful in the determination of the nature of provenance (Hayashi *et al.* 1997; Yang *et al.* 2018), redox conditions (Biester *et al.* 2012; Liang *et al.* 2020), paleosalinity (Ingram and Sloan 1992; Wang *et al.* 2011; Wei *et al.* 2018b), effect on the thermal efficiency of boilers (Querol *et al.* 1997b; Mardon and Hower 2004; Papanicolaou *et al.* 2004; Koukouzas *et al.* 2009; Dai *et al.* 2010), and steps for coal conversion processes (Steller *et al.* 2006; Milici 2009; Vasireddy *et al.* 2011; Finkelman *et al.* 2019). The scientists identified these properties and several indices were proposed by the researchers to quantify the paleodepositional condition using major oxide concentration and elemental concentration of the rock and coal, such as the chemical index of alteration (CIA) (Nesbitt and Young 1982), chemical index of weathering (CIW) (Harnois 1988), and index of compositional variability (ICV) (Cox *et al.* 1995). High CIA and CIW indicate the formation of mud in high concentrations under tropical conditions, whereas its low concentration indicates a glacial environment. The warm-humid climate facilitates the chemical wreathing of the source area and causes an increase in the values of CIA and CIW. The components like Fe_2O_3, K_2O, Na_2O, CaO, MgO, MnO, and TiO2 can be easily leached out due to chemical weathering, whereas Al is hard to migrate. So the rocks and minerals having more weathering susceptible elements can alter easily. The

presence of a high concentration of quartz and clay minerals indicated by a high concentration of SiO_2 and Al_2O_3 and low concentration of unstable minerals indicate a recycling process. The formation of South Karanpura coals with the geochemical point of view is discussed in detail in Chapter 7.

5.6 Trace Element in the coals of South Karanpura coalfield

The distribution of trace elements in coal is controlled by their geological factors such as sedimentary environments, epigenetic hydrothermal activity, and deposition by groundwater. Zhang et al. (2002) found that clay minerals in the Late Permian coals have high concentrations of Ba, Be, Cs, F, Ga, Nb, Rb, Th, U, and Zr; quartz is very low in trace elements except for Zr. Calcite has high concentrations of As, Mn, and Sr and pyrite has high concentrations of As, Cd, Hg, Mo, Sb, Se, Tl, and Zn. Based on their strong geochemical affinity, trace elements can be classified into several groups, such as siderophile, chalcophile, lithophile, atmophile, or biophile (Pareek and Bardhan 1985). In the context of organic or inorganic affinity, Ge, Be, and B exhibit greatest organic affinities; whereas Hg, Zr, Zn, As, Cd, Pb, Mn, and Mo are generally inorganically combined; P, Ga, Sb, Ti, and V tend to be allied with the other elements having organic affinities; and Co, Ni, Cr, Se, and Cu more closely associated with the inorganically combined elements (Gluskoter 1975). Although, methods adopted for determining the modes of occurrence of non-mineral elements in coal includes statistics, density- and size-separation, selective leaching techniques, in-situ direct microanalyses, and various chemical investigations, with having their respective limitations (Dai *et al.* 2020a). In early works, gross assumptions about associations were made based on float/sink data.

Mukherjee & Dutta (1950) initiated the study of trace elements in Indian coals. Further, Iyer & Sundaram (1955) and Rao & Rao (1955) added some significant contributions in

this field by discussing the presence and mode of occurrence of Ge and Co in some of the Indian coals. In 1970, one of the important major attempts to analyse several trace elements in the Umaria coalfield, Madhya Pradesh, having coals of the Gondwana period, was made by Rishi (1970). Further, contributions were made by several authors to analyse the presence of trace elements in different Gondwana and Cenozoic coals and lignite in India (Pareek and Bardhan 1985; Roy *et al.* 2006; Kumar and Ahmad 2007; Nayak *et al.* 2009; Prakash *et al.* 2012; Saikia *et al.* 2014; Singh *et al.* 2014a, 2017b; Equeenuddin *et al.* 2016; Singh and Singh 2016; Srikanth and Raju 2019; Verma and Verma 2019)

The first attempt on the trace element study of South Karanpura coal was made by Pareek & Bardhan (1985). Mukherjee *et al.* (1988) discussed the affinity of the trace element for Gondwana coals, selecting a few samples from South Karanpura coalfield along with other major Gondwana coalfields. In the book, 'Trace metals in Indian Coal,' Banerjee *et al.* (2000) discussed the distribution of trace elements from South Karanpura coalfield, but the analysis was done on unsystematically collected samples.

In the present study, pillar coal samples from the coal seam sections of South Karanpura coalfield were subjected to trace element determination to know their quantitative occurrence and distribution in the coal seam sections. Also, an effort has been made to focus on their organic and inorganic associations.

5.6.1 The occurrence of Trace Elements in Coals of South Karanpura coalfield

The important trace elements analysed in these coals are V, Cr, Co, Ni, Cu, Zn, Rb, Sr, Zr, and Pb. The result of the quantitative analysis is given in Table 5.7. Due to minor intra-seam variations of the geochemical components, few representative samples were analyzed for trace elements from each seam, and their mean values have been discussed. The fluctuating pattern of distribution of the trace elements Pb, V, Ba, Sr and Cr appears

to be related directly to the proportion of the ash yield. The inter-seam variation of the trace elements has been presented for both the areas in Figure 5.35 and Figure 5.36.

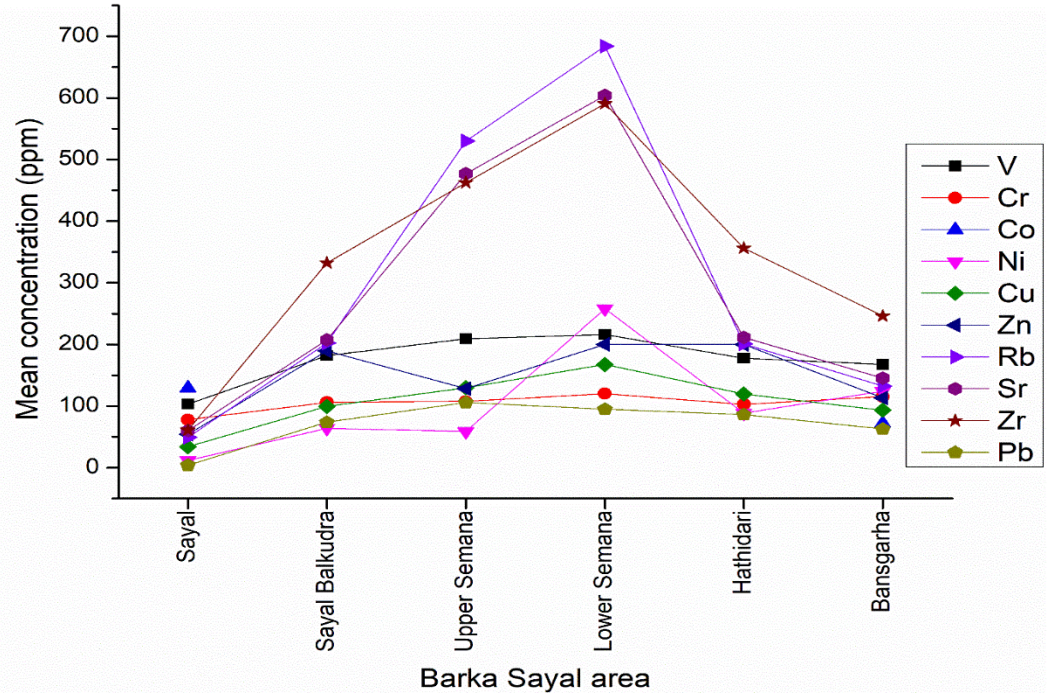


Figure 5.35 Variation of trace elements in coals of Barka Sayal area, South Karanpura coalfield.

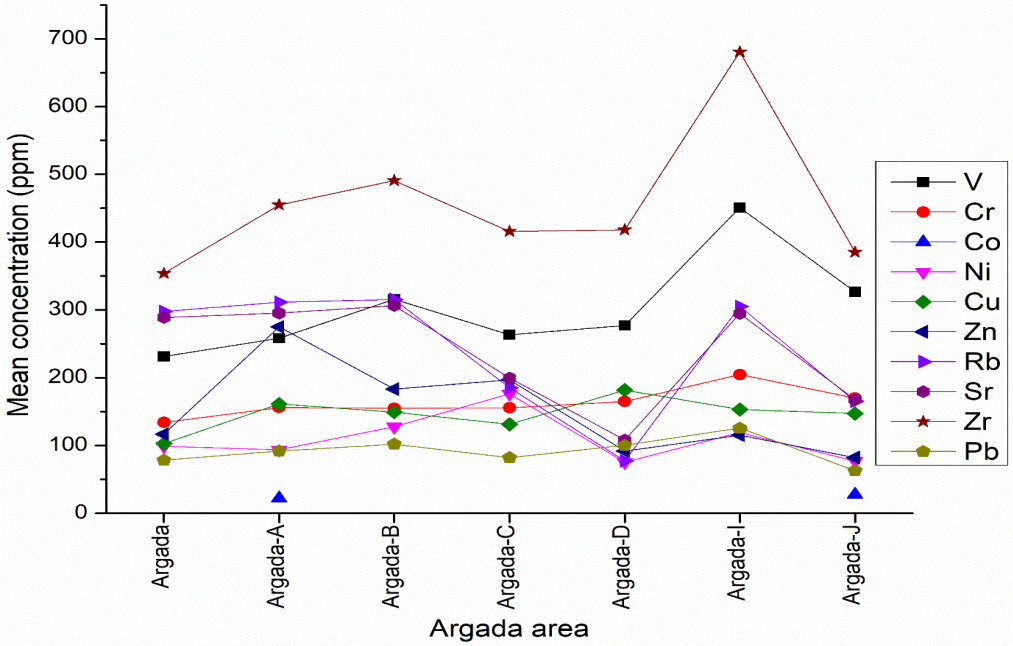


Figure 5.36 Variation of trace elements in coals of Argada area, South Karanpura coalfield.

Vanadium (V) : The concentration of vanadium in the coals of the Barka Sayal area varies from 89 ppm to 246 ppm, mean 176 ppm. Its concentration is found to increase with depth. The coal seams of the Argada area have comparatively more vanadium concentration, ranging from 222 ppm to 500 ppm, mean 305 ppm. The lithophile nature of vanadium may guide this distribution; hence their high concentration is with increasing mineral content in coal (Raask 1985; Li *et al.* 2018). Coals of Argada area contain more clay minerals comparatively so also contain high concentration of vanadium.

Chromium (Cr) : In the coals of the Barka Sayal area, the chromium concentration varies from 73 ppm to 140 ppm, mean 105 ppm, whereas coal seams of Argada area exhibit chromium concentration of 110 ppm to 208 ppm, mean 163 ppm.

Cobalt (Co) : Cobalt content varies from nil to 137 ppm in the coals of the Barka Sayal area, whereas in coals of Argada area, the content lies in between nil and 55 ppm. Most of the seams do not exhibit cobalt content in a detectable amount. It is only detected in the coals of Sayal, Bansgarha, Argada-A, and Argada-J seams.

Nickel (Ni): Nickel content in the coal of the Barka Sayal area varies from 5 to 259 ppm, mean 101 ppm. In coals of Argada area it varies from 72 to 272 ppm, mean 112 ppm.

Copper (Cu) : The copper content in the coals of the Barka Sayal area varies from 28 ppm to 168 ppm, mean 107 ppm. In the coals of the Argada area, the copper content lies in the range of 61 ppm to 201 ppm, mean 144 ppm.

Zinc (Zn) : The coals of the Barka Sayal area exhibit zinc content ranging from 49 ppm to 254 ppm, mean 148 ppm. Coals of Argada area have zinc content ranging in between 82 ppm to 399 ppm, mean 156 ppm.

Rubidium (Rb) : The rubidium content of the coals of the Barka Sayal area lies in between 44 ppm and 1192 ppm, mean 300 ppm, whereas the coals of the Argada area have rubidium content lying in between 70 ppm and 441 ppm, mean 249 ppm.

Strontium (Sr) : The strontium content of coal seams of the Barka Sayal area varies from 56 ppm to 1018 ppm, mean 284 ppm. Coals of Argada area have strontium content in between 104 ppm and 397 ppm, mean 247 ppm.

Zirconium (Zr) : The content of zirconium varies from 57 ppm to 689 ppm, mean 341 ppm in coals of Barka Sayal area, whereas coals of Argada area have zirconium content ranging from 313 ppm to 769 ppm, mean 460 ppm.

Lead (Pb) : The coals of the Barka Sayal area have lead content varying in between 4 ppm and 112 ppm, mean 71 ppm, while coals of Argada area have lead content ranging from 49 ppm to 152 ppm, mean 91 ppm.

Table 5.7 The concentration of selected trace elements (in ppm) in coals of South Karanpura Coalfield on ash basis.

Sample name	Ash (wt.%)	V	Cr	Co	Ni	Cu	Zn	Rb	Sr	Zr	Pb
SL 3	33.74	117	82	137	5	29	59	44	56	57	5
SL 5	24.42	89	74	122	19	40	49	54	64	65	4
SBK 5	30.17	209	108	nil	79	122	151	200	210	364	94
SBK 9	48.68	155	105	nil	49	77	229	205	205	301	54
US 3+4	14.42	186	92	nil	50	108	106	486	439	425	99
US 9	22.12	233	123	nil	68	152	151	574	514	500	113
LS 4+5	13.73	185	101	nil	259	167	216	1192	1019	492	81
LS 8+9	24.81	246	140	nil	257	168	184	175	189	689	109
HD 3	24.13	166	109	nil	97	115	254	112	136	332	84
HD7	27.34	190	97	nil	80	125	146	290	287	380	89
BG 1	32.38	188	111	nil	151	120	138	155	173	352	86
BG 3+4	28.38	147	120	72	98	67	88	110	118	140	40
AG 9	64.99	226	153	nil	83	101	101	280	272	313	78
AG 10	42.17	236	115	nil	114	105	133	315	305	394	79
AG A 8+9+10	18.87	258	202	22	97	177	399	441	397	465	94
AG A 14+15+16	27.62	258	110	nil	90	145	151	182	193	445	90
AG B 16+17	49.39	375	163	nil	80	164	100	411	386	559	117
AG B 18	33.31	256	147	nil	175	134	266	220	227	423	88
AG C 1+2+3	26.70	222	190	nil	272	201	295	300	294	383	96
AG C 7	43.04	304	121	nil	81	61	99	70	105	449	68
AG D 20	47.42	277	165	nil	75	182	92	77	108	418	100
AG I 1	23.75	402	208	nil	148	181	129	351	332	592	152
AG I 5+6+7	26.98	500	201	nil	91	125	102	259	258	769	99
AG J 9	17.14	315	168	1	82	149	83	173	179	435	77
AG J 12+13	33.69	338	172	55	72	145	82	158	156	335	49

Not only the major oxides and major/minor elements provide the clues for the paleodepositional environment, but also the trace element concentration is a good indicator of the conditions that prevailed during the deposition of organic and inorganic constituents of the coal. Elements like vanadium (V) and nickel (Ni) are the redox-sensitive. The high concentration of V represents the anoxic environment (Galarraga *et al.* 2008; Chen *et al.* 2011). The high vanadium concentration of Argada-B and Argada-I seam indicates more anoxic conditions prevailed during the formation of coal of these seams. Zirconium (Zr) is a resistant element for chemical weathering (Ward *et al.* 1999). The high concentration of Zr in these coals indicate the provenance of the inorganic content supplying to these coals of felsic nature. The paleodepositional environment is discussed in Chapter 7 in more detail, considering the geochemical characteristics of the coals of South Karanpura coalfield.

5.7 X-ray Diffraction Study of Coals of South Karanpura

The X-ray diffraction pattern is a characteristic of the substance under investigation. XRD technique is useful in determining the minerals of crystalline nature present in coal (Singh *et al.* 2015d, 2017b; Banerjee *et al.* 2016; Mishra and Singh 2017; Karayiğit *et al.* 2018; Mendhe *et al.* 2018). Quartz, orthoclase, microcline, albite, dolomite, pyrite, siderite, ilmenite, hematite, pyrrhotite, andalusite, illite, smectite, kaolinite, and nontronite are among the mineral identified by XRD analysis of ash of the coals derived by technique described in Swanson & Huffman (1976) (Figure 5.37 and Table 5.8). Mineral in the coal can be of two types, syn-genetic (those formed with the formation of coal) and epigenetic (those formed after the formation of coal) (Dai *et al.* 2014b). Mineralogically, all the coal seams of the study area exhibit differences. Quartz is the most dominant mineral in all the seams ranging from 35% to 88%, mean 71.46%. The mean values of Hematite and Illite are 7.15% and 7.12%, respectively. Other minerals such as microcline, orthoclase, albite,

dolomite, pyrite, siderite, ilmenite, pyrrhotite, andalusite, smectite, kaolinite, and nontronite together constitute only less than 15% of the entire part (Figure 5.37).

5.7.1 X-ray Diffraction Study of Coal seams of Barka Sayal area

Coal seams of the Barka Sayal area exhibit quartz content lying in the range of 20% to 88%, mean 64.08%. Next dominant maceral is a clay mineral illite, ranging from 1% to 59%, mean 11.33%. Hematite is also high, ranging from nil to 51%, mean 10.83%. Except for these dominant minerals, other minerals are in low quantity (Table 5.8).

Sayal seam of Barka Sayal area contains a high amount of minerals such as hematite, ilmenite, siderite, and pyrite. Hematite (mean 45.5%) is the most dominant mineral of this seam (Table 5.8 and Figure 5.37). Clay minerals (mean 3%) are present in lower concentrations than in the Sayal seam. This seam is devoid of smectite or kaolinite, but pyrrhotite and albite are only present in this seam.

Quartz is again the most dominant mineral (mean 81%) in LTA of Sayal Balkudra coal seam of Barka Sayal area. Clay minerals such as illite, smectite, kaolinite, and nontronite are also present in good concentration. Felsic minerals such as orthoclase and albite are also present but in very less concentration (mean 2% each).

The coals of Upper Semana seam exhibit quartz content 73% (mean value) followed by siderite (mean 6.5%), pyrite (mean 3.5%), and microcline (mean 3%). Three minerals, orthoclase, albite, and illite, have a mean concentration of 2.5% for each. Other minerals such as pyrrhotite, hematite, smectite, and ilmenite are in less quantity ($\leq$ 2% each).

The coals of Lower Semana seam also have a high amount of quartz (mean 78.5%) followed by illite (mean 4%), siderite (mean 3.5%), and microcline (mean 3%). Ilmenite, hematite, and smectite are 2%. Other minerals such as orthoclase, albite, pyrite, and nontronite are in less amount ($\leq$ 1% each).

Coals of Hathidari seam also have the highest amount of quartz (mean 86.5%). Microcline (mean 4.5%), illite (mean 2.5%), smectite (mean 2.5%), siderite (2%), and ilmenite (mean 2%) are the only other minerals detected in these coals using XRD.

The coals of Bansgarha seam is having a high amount of illite (mean 51%) followed by quartz (mean 24%). Hematite (mean 12.5%), microcline (mean 6.5%), siderite (mean 3%), and ilmenite (mean 1.5%) are also present in this seam.

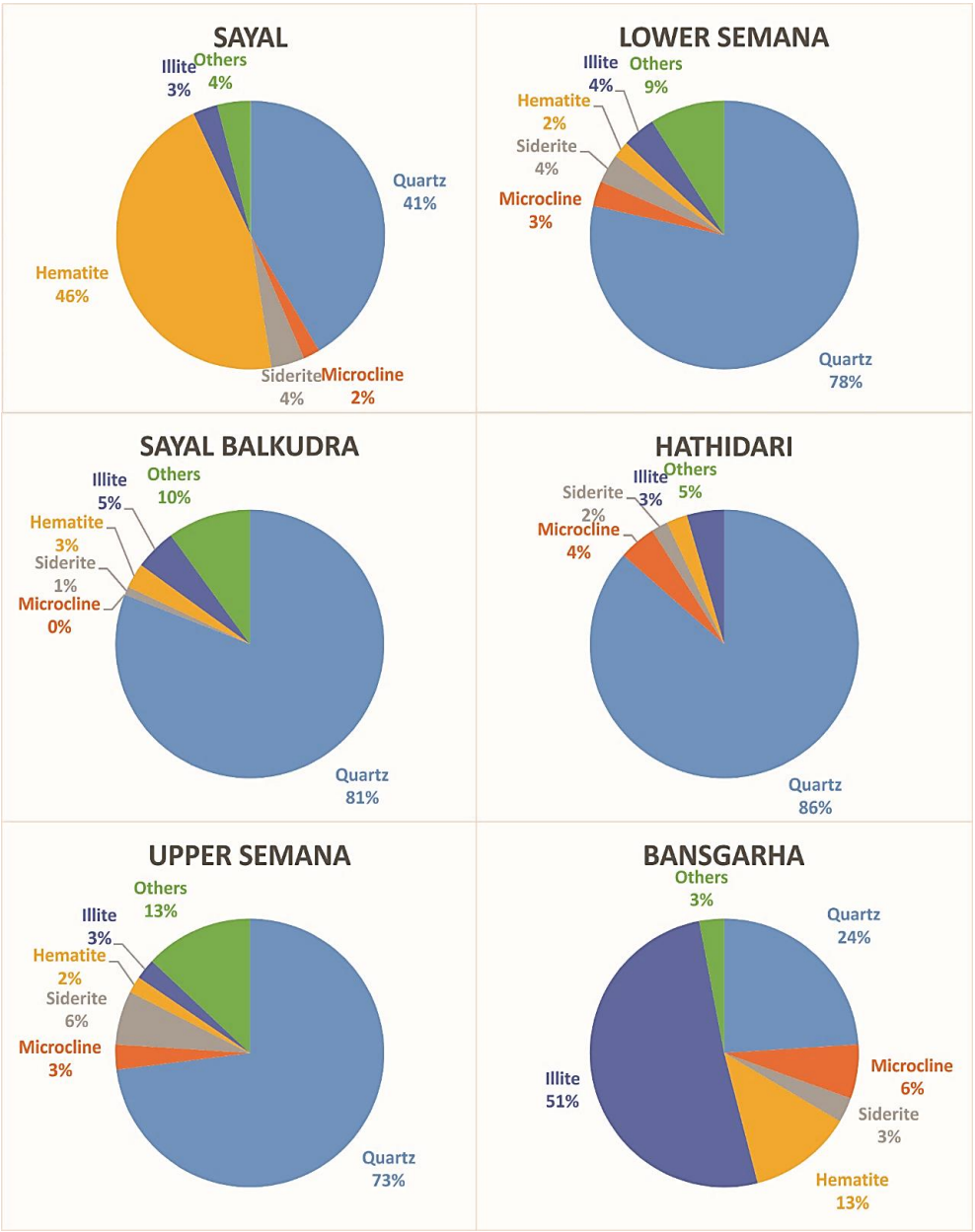


Figure 5.37 Pie chart showing main mineral components present in the low-temperature ash (LTA) of coals of the Barka Sayal area (Table 5.8).

Table 5.8 XRD analysis of coal ash samples of South Karanpura coalfield, Jharkhand, India.

	Felsic Minerals (%)				Carbonate Minerals (%)	Heavy Minerals (%)						Clay Minerals (%)			
Sample No.	**Quartz**	**Orthoclase**	**Microcline**	**Albite**	**Dolomite**	**Pyrite**	**Siderite**	**Ilmenite**	**Hematite**	**Pyrrhotite**	**Andalusite**	**Illite**	**Smectite-Kaolinite**	**Kaolinite**	**Nontronite**
SL 3	48	nil	nil	5	nil	nil	1	1	40	nil	nil	5	nil	nil	nil
SL 5	35	nil	4	nil	nil	1	7	nil	51	1	nil	1	nil	nil	nil
Sayal	41.5	nil	2	2.5	nil	0.5	4	0.5	45.5	0.5	nil	3	nil	nil	nil
SBK 5	84	3	nil	1	nil	nil	nil	4	nil	nil	nil	5	3	nil	nil
SBK 9	78	1	nil	3	nil	1	2	1	6	nil	nil	5	1	1	1
Sayal Balkudra	81	2	nil	2	nil	0.5	1	2.5	3	nil	nil	5	2	0.5	0.5
US 3+4+5	69	5	1	3	1	6	8	1	nil	4	nil	1	1	nil	nil
US 9	77	nil	5	2	nil	1	5	nil	4	nil	nil	4	2	nil	nil
Upper Semana	73	2.5	3	2.5	0.5	3.5	6.5	0.5	2	2	nil	2.5	1.5	nil	nil
LS 4+5	71	nil	5	1	1	1	5	2	4	3	nil	4	2	nil	1
LS 8	86	2	1	1	nil	nil	2	2	nil	nil	nil	4	2	nil	nil
Lower Semana	78.5	1	3	1	0.5	0.5	3.5	2	2	1.5	nil	4	2	nil	0.5
HD 3	85	nil	5	nil	nil	nil	2	2	nil	nil	nil	4	2	nil	nil
HD 7	88	nil	4	nil	nil	nil	2	2	nil	nil	nil	1	3	nil	nil
Hathidari	86.5	nil	4.5	nil	nil	nil	2	2	nil	nil	nil	2.5	2.5	nil	nil
BG 1	20	nil	7	nil	nil	nil	4	1	24	nil	nil	43	1	nil	nil
BG 2	28	nil	6	nil	nil	nil	2	2	1	nil	nil	59	2	nil	nil
Bansgarha	24	nil	6.5	nil	nil	nil	3	1.5	12.5	nil	nil	51	1.5	nil	nil
AG 5	84	nil	1	2	nil	nil	2	2	2	nil	nil	4	3	nil	nil
AG 9	84	nil	1	2	nil	nil	1	2	3	nil	nil	5	2	nil	nil

	Felsic Minerals (%)				Carbonate Minerals (%)	Heavy Minerals (%)						Clay Minerals (%)			
Sample No.	**Quartz**	**Orthoclase**	**Microcline**	**Albite**	**Dolomite**	**Pyrite**	**Siderite**	**Ilmenite**	**Hematite**	**Pyrrhotite**	**Andalusite**	**Illite**	**Smectite-Kaolinite**	**Kaolinite**	**Nontronite**
AG 10	84	nil	nil	3	nil	nil	2	1	2	nil	nil	5	3	nil	nil
Argada	84.0	nil	1.0	2.3	nil	nil	1.7	1.7	2.3	nil	nil	4.7	2.7	nil	nil
AG A 8+9+10	75	nil	2	1	nil	1	3	1	13	nil	nil	2	2	nil	nil
AG A 14+15+16	79	nil	2	1	nil	nil	4	1	8	1	nil	2	2	nil	nil
Argada-A	77	nil	2	1	nil	0.5	3.5	1	10.5	0.5	nil	2	2	nil	nil
AG B 16+17	87	nil	2	2	nil	nil	2	2	nil	nil	nil	2	3	nil	nil
AG B 18+19+20	82	nil	9	1	nil	nil	2	2	nil	nil	nil	2	2	nil	nil
Argada-B	84.5	nil	5.5	1.5	nil	nil	2	2	nil	nil	nil	2	2.5	nil	nil
AG C 1+2+3	78	nil	7	1	nil	nil	4	1	3	1	nil	3	2	nil	nil
AG C 7	84	nil	4	1	nil	nil	3	2	nil	nil	nil	3	3	nil	nil
Argada-C	81	nil	5.5	1	nil	nil	3.5	1.5	1.5	0.5	nil	3	2.5	nil	nil
AG D 20	77	nil	7	3	nil	nil	1	2	2	nil	nil	5	2	1	nil
Argada-D	77	nil	7	3	nil	nil	1	2	2	nil	nil	5	2	1	nil
AG I 1	83	nil	4	3	nil	nil	2	2	2	nil	1	3	nil	nil	nil
AG I 5+6+7	81	nil	1	3	nil	nil	3	3	2	nil	nil	3	3	1	nil
Argada-I	82	nil	2.5	3	nil	nil	2.5	2.5	2	nil	0.5	3	1.5	0.5	nil
AG J 9	56	2	2	8	2	2	7	4	8	nil	nil	6	3	nil	nil
AG J 12	55	3	5	5	2	1	6	3	11	3	nil	4	1	nil	1
Argada-J	55.5	2.5	3.5	6.5	2	1.5	6.5	3.5	9.5	1.5	nil	5	2	nil	0.5

5.7.2 X-ray Diffraction Study of Coal seams of Argada area

The coals of the Argada area also exhibit the enrichment of quartz (55%-87%, mean 77.79%). Other important minerals are hematite (nil-13%, mean 4%), microcline (1%-9%, mean 3.62%) and illite (2%-6%, mean 3.50%) and siderite (1%-7%, mean 3%) (Table 5.8 and Figure 5.38). Coals of Argada area show relatively more enrichment of felsic minerals and carbonate minerals and the deficiency of iron-rich minerals and clay minerals compared to coals of the Barka Sayal area.

The coals of Argada seam are quartz-rich (mean 84%) followed by illite (mean 4.7%). Other minerals present in these coals are smectite (2.7%), hematite (2.3%), albite (2.3%), siderite (1.7%), ilmenite (1.7%) and microcline (1%).

The coals of Argada-A seam exhibit the dominance of quartz (mean 77%). Heavy minerals such as hematite (mean 10.5%) and siderite (mean 3.5%) are also present in high amount. Other minerals contributing to low concentration (≤ 2%) are microcline, albite, pyrite, ilmenite, pyrrhotite, illite, and smectite.

The analyzed coals of Argada-B seam is characterized by the presence of the high amount of quartz (mean 84.5%) followed by microcline (mean 5.5%) and smectite (mean 2.5%). Other minerals having a lower concentration (≤ 2% for each) are albite, siderite, ilmenite, and illite.

Coals of Argada-C seam upon analysis confirms the high occurrence of quartz (mean 81%) in these coals followed by microcline (mean 5.5%) and siderite (mean 3.5%). Clay minerals such as illite (mean 3%) and smectite (mean 2.5%) are also present in these coals. Besides these minerals, there are other minerals (concentration ≤ 1.5% for each) identified in these coals are albite, ilmenite, hematite, and pyrrhotite.

Analysis of the coals of Argada-D seam shows the dominance of quartz (mean 77%) followed by microcline (7%), illite (5%), and albite (3%). Other minerals present in less concentration (≤ 2% for each) are siderite, ilmenite, hematite, smectite, and kaolinite.

The Argada-I coals are characterized by a high content of quartz (mean 82%). Albite and illite are in equal concentration (mean 3%). Microcline, siderite, ilmenite shows the mean concentration of 2.5%. Hematite, andalusite, smectite, and kaolinite are also present in these coals, but in very less concentration (≤ 2% for each).

The analyzed Argada-J coals are characterized by a relatively higher concentration of heavy minerals. Although quartz is still the dominant mineral present in these coals, their concentration got reduced to a mean value of 55.5% in these coals. Heavy minerals such as Hematite (mean 9.5%), siderite (mean 6.5%) are in high concentration. Other important minerals identified in these coals are albite (mean 6.5%), illite (mean 5%), microcline (mean 3.5%), ilmenite (mean 3.5%) and other minerals such as orthoclase, dolomite, pyrite, pyrrhotite, smectite, and nontronite exhibit concentration ≤ 2.5% for each.

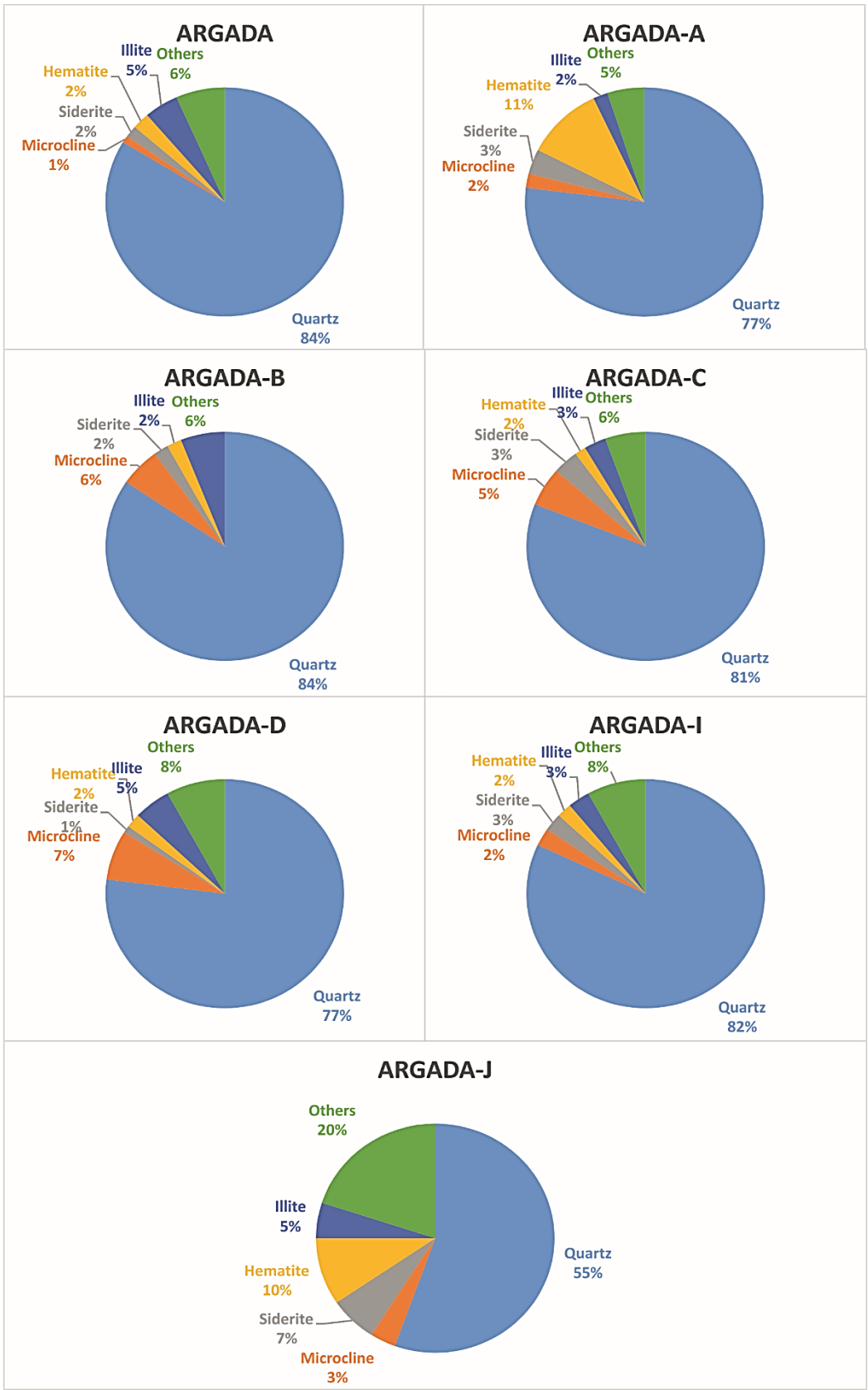


Figure 5.38 Pie chart showing main mineral components present in the coal seams of the Argada area (Table 5.8).

5.8 Fourier Transform Infrared (FTIR) Spectroscopy of Coals of South Karanpura

Fourier Transform Infrared (FTIR) Spectroscopy is one of the oldest and most efficient techniques applied in the field of organic geochemistry. Several scientists proposed and used the spectra obtained from FTIR spectroscopy to identify the organic compounds (Painter *et al.* 1985; Sobkowiak and Painter 1992; Walker and Mastalerz 2004; Mastalerz *et al.* 2010) as well as inorganic compounds (Painter *et al.* 1982; Sharma and Wadhwa 1997; Singh 2004; Gupta 2007; Bandopadhyay 2010; Kumar *et al.* 2018a). Nowadays, it is one of the most important tools for coal characterization especially in various utilization of coals like combustion and coke making processes (Guo and Bustin 1998; Dutcher and Crelling 2000; Yaman *et al.* 2001; Vandenbroucke 2003; Mastalerz *et al.* 2010; Yao *et al.* 2012; Zodrow *et al.* 2012; Balachandran 2014; D'Angelo and Zodrow 2015; Zhang *et al.* 2016; Presswood *et al.* 2016; Karayiğit *et al.* 2017a; Rajak *et al.* 2018; Jing *et al.* 2019; Małachowska *et al.* 2019)

FTIR spectrum peaks were identified based on the FTIR library and previous studies (Painter *et al.* 1978; Sobkowiak and Painter 1992; Saikia *et al.* 2007; Chen *et al.* 2015b).

FTIR spectra of the raw coal exhibit important peaks present at wavenumber (cm^{-1}) 3698, 3620, 2950, 2920, 2850, 1650, 1450, 1375, 1100, 1000, 1034, 790, 750, 689 and 541 (Figure 5.39) (Table 5.9). Peak present at wavenumber (cm^{-1}) 2950 is attributed to Aliphatic CH_3, whereas 2920 and 2850 cm^{-1} can be attributed to Aliphatic CH, CH_2, and CH_3 molecules. C=O and CO stretching in between 1640-1750 cm^{-1} is attributed to phenolic ester, carboxylic acid, and conjugated ketonic structures. 1450 cm^{-1} is for CH_2 and CH_3 with a possibility of some aromatic ring modes. 1375 cm^{-1} represents CH_3 groups. Several peaks forming in between 1300-1100 cm^{-1} is because of the C-O stretch and O-H bend in phenoxy structures. The peaks present in between 1000 to 1100 cm^{-1}

can be attributed to aliphatic ethers and alcohols, whereas peaks present in between 900 to 700 cm^{-1} shows aromatic C-H out-of-plane bending modes.

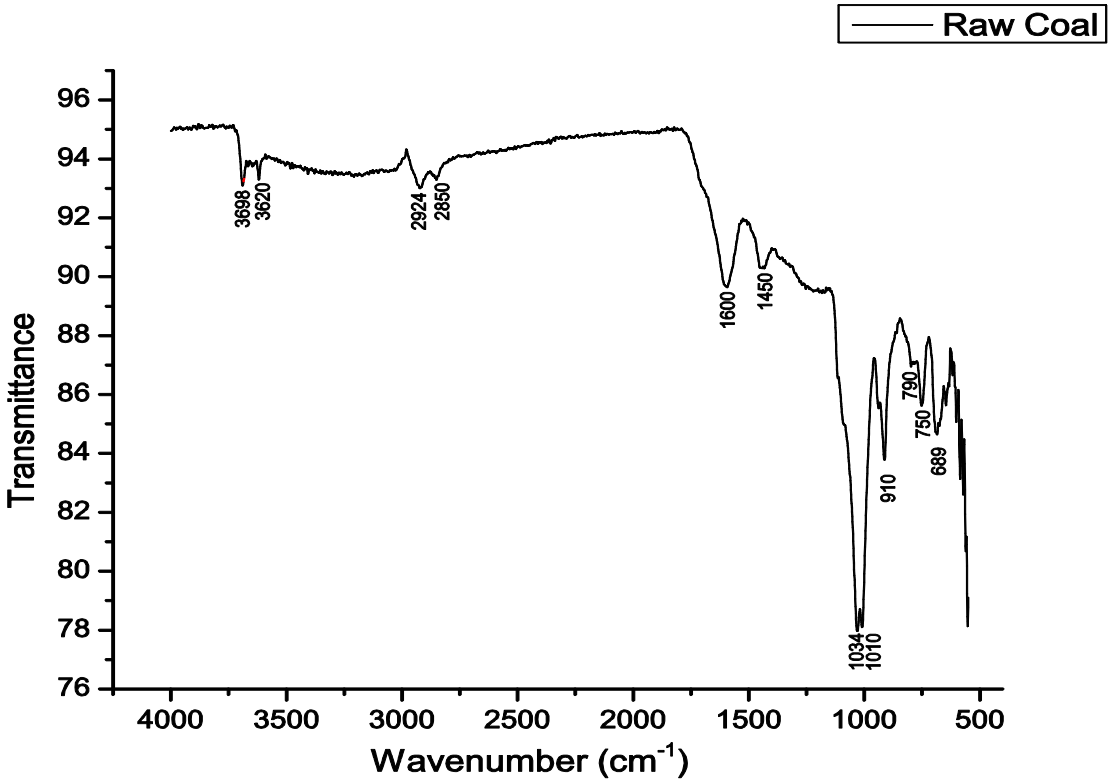


Figure 5.39 FTIR spectra of the raw coal, Bansgarha Seam, South Karanpura Coalfield, Jharkhand, India.

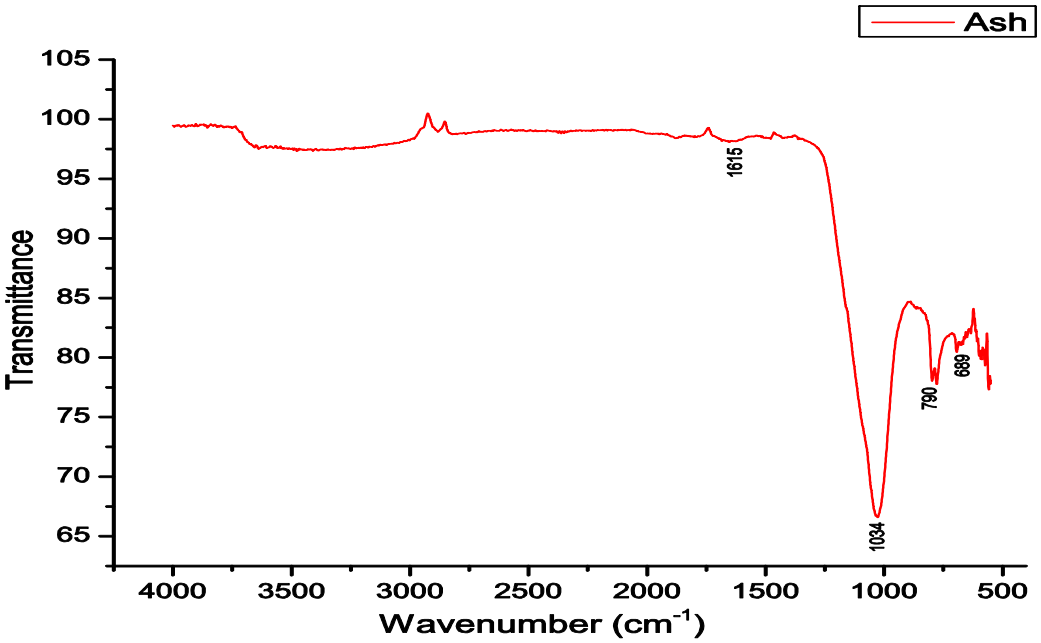


Figure 5.40 FTIR Spectra of the ash of the coal obtained using low-temperature.

The ash of these coals was generated by following low-temperature ashing techniques were further analyzed by FTIR, and the spectra are shown in Figure 5.40. The spectra clearly show the different inorganic functional groups present in these coals. The most prominent peak present at 1034 cm^{-1} and 689 cm^{-1} is attributed to the presence of a high amount of clay minerals, mainly in the form of kaolinite. 790 cm^{-1} shows the presence of quartz. A small peak present at 1615 cm^{-1} indicates the presence of a small amount of gypsum. The bands of OH group observed at 3600-3800 cm^{-1} are in close association with the band assigned for clay minerals. The IR bands between 1100 and 400 cm^{-1} are also associated with clay minerals such as kaolinite, illite, and montmorillonite. The IR bands from 3600-3800 cm^{-1} are associated with quartz and kaolinite.

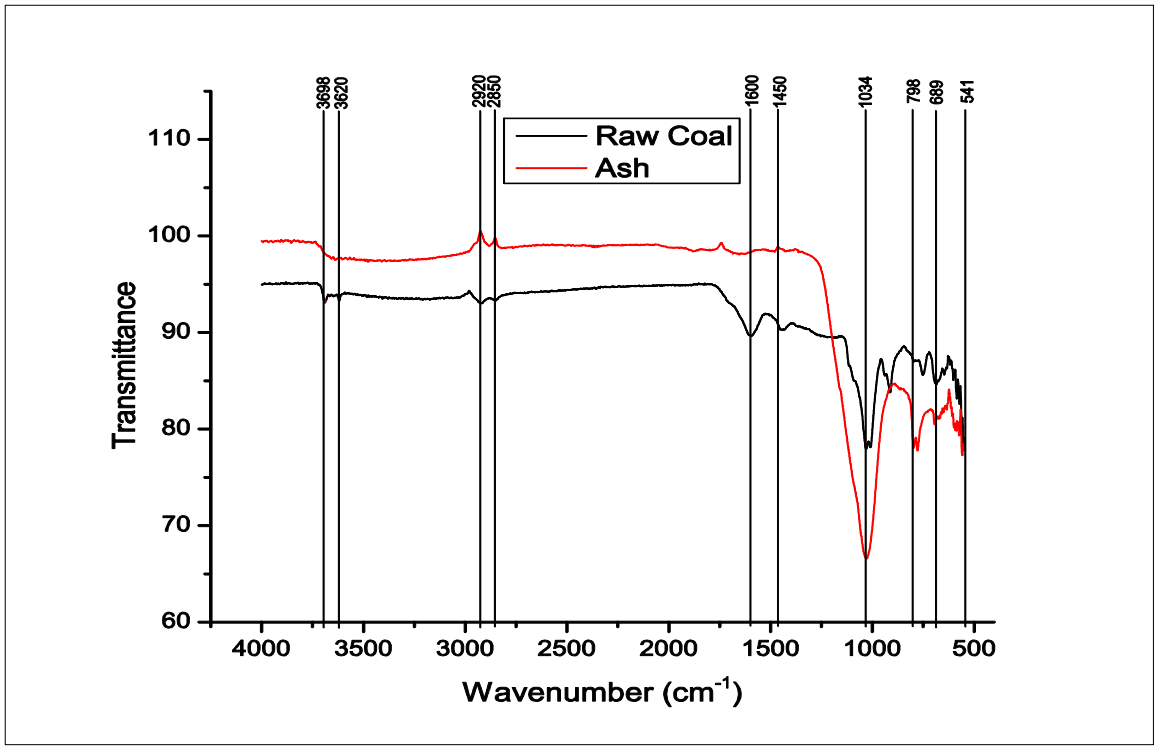


Figure 5.41 Combined FTIR Spectra of the raw coal and ash of the coals of Bansgarha seam, South Karanpura Coalfield, Jharkhand, India.

Figure 5.41 presents a comparative view of the FTIR spectra of all the two portions of the raw coal and ash from the same coal. Here it is seen that raw coal has same mineral peaks, but not all of the same peaks, which are also present in the spectra of ash, but the spectra

obtained for ash shows the inorganic constituents such as kaolinite, quartz, and gypsum present in these coals, whereas other spectra observed in raw coal except spectra observed in ash show the presence of several aliphatic, aromatic and other organic compounds.

5.8.1 FTIR Spectroscopy of Coals of Barka Sayal area

The FTIR spectra of the coals of the Barka Sayal area do not show much difference from one another. The result of composite samples of each seam of the Barka Sayal area is presented in Figure 5.42. The peak intensity assigned to minerals is higher in the spectra of coal seams of the Barka Sayal area. The spectra of coals of Upper Semana and Lower Semana show similar attributes. The most prominent peaks are present at wavenumber (cm^{-1}) 689, 750, 790, 910, 1010, 1034, 1450, 1600, 2850, 2920, 3620, and 3698 cm^{-1}. Peaks present at wavenumber 689, 1034, and 3698 cm^{-1} are due to the presence of kaolinite, while 790 and 1615 cm^{-1} can be attributed to minerals quartz and gypsum, respectively. The peak at 750, 910, and 1600 cm^{-1} represents aromatic hydrocarbon. Wavenumber 1010 cm^{-1} is for aliphatic ethers or alcohol. Wavenumber 2850 and 2920 cm^{-1} represents aliphatic hydrocarbons.

Table 5.9 Prominent peaks identified in the FTIR Spectra of the raw coal and ash of the coals of Bansgarha seam, South Karanpura Coalfield, Jharkhand, India using the library and published literature (Painter *et al.* 1978; Sobkowiak and Painter 1992; Chen *et al.* 2015b).

Raw Coal		Ash	
Wavenumber (cm-1)	**Assignment**	**Wavenumber (cm-1)**	**Assignment**
689	Kaolinite	689	Kaolinite
750	Aromatic C-H	790	Quartz
790	Quartz	1034	Kaolinite
910	Aromatic C-H	1615	Gypsum
1010	Aliphatic ethers, alcohols		
1034	Kaolinite		
1450	CH_2 and CH_3 bend		
1600	Aromatic ring		
2850	Aliphatic CH, CH_2, and CH_3		
2920	Aliphatic CH, CH_2, and CH_3		
3620	Kaolinite		
3698	Kaolinite		

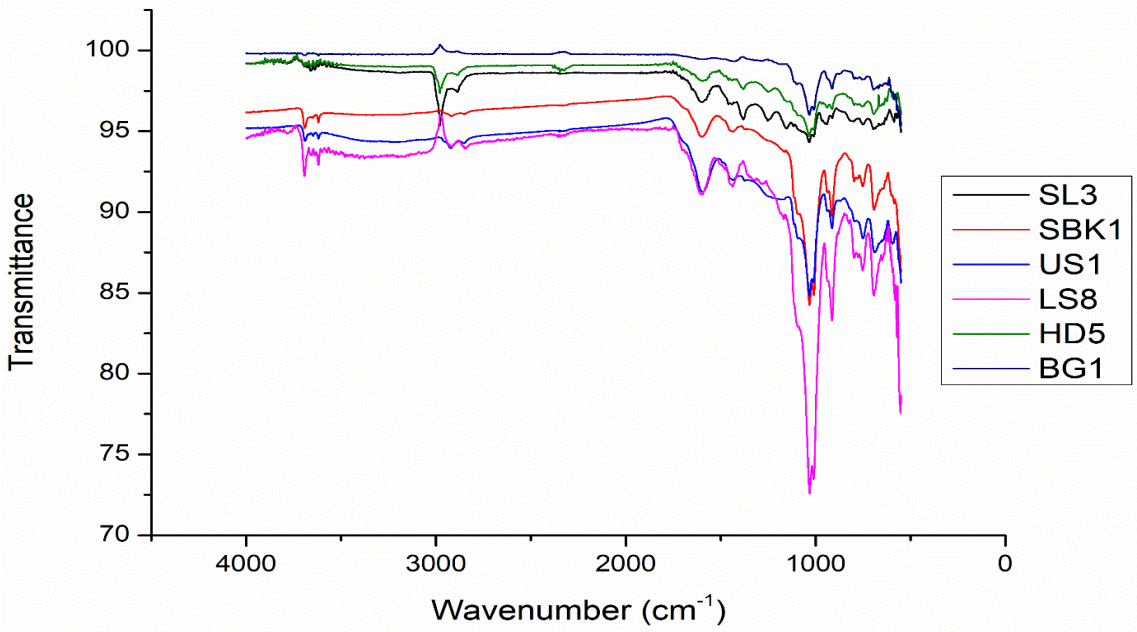


Figure 5.42 Combined FTIR Spectra of the raw coal of the coals of Barka Sayal area, South Karanpura Coalfield, Jharkhand, India.

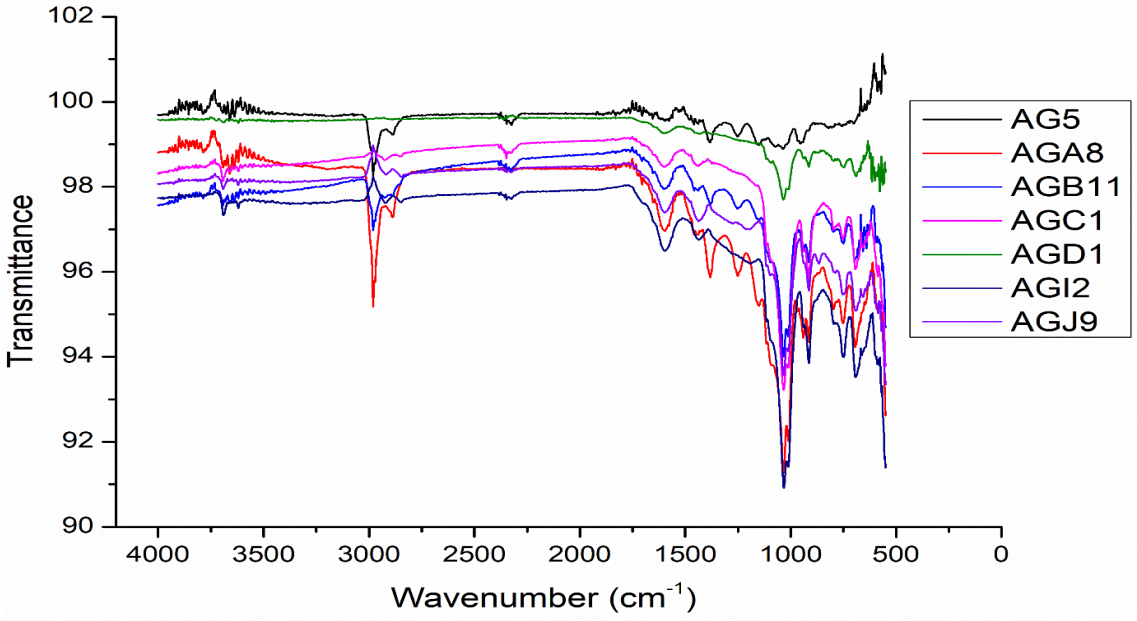


Figure 5.43 Combined FTIR Spectra of the raw coal of the coals of Argada area, South Karanpura Coalfield, Jharkhand, India.

5.8.2 FTIR Spectroscopy of Coals of Argada area

FTIR spectra obtained for coals of Argada area also have prominent peaks at wavenumber (cm^{-1}) 689, 750, 790, 910, 1010, 1034, 1450, 1600, 2850, 2920, 3620 and 3698 cm^{-1}

(Figure 5.43). Peaks assigned to kaolinite are 689, 1034, 3620, and 3698 cm^{-1}, whereas peaks present at 750 and 910 cm^{-1} can be assigned to the aromatic hydrocarbons. 2850 and 2920 cm^{-1} represent the aliphatic hydrocarbons.

5.9 Organic Geochemistry of Coals of South Karanpura

Biological markers, also called biomarkers, are altered remains of a biological state or condition that can be identified. Gas chromatography-Mass spectrometry (GC-MS) was used to identify the different biomarkers present in the coal of the study area. Biomarker's chemical structures provide a distinct link to natural products like lipids, terpenoids, or pigments, identified in extant descendants of coal–forming flora (Bechtel *et al.* 2007a). The concentration of biomarkers generally decreases with an increase in rank (Radke *et al.* 1984; White *et al.* 1998). Biomarker distribution can be effectively used to characterize source environment (Fowler *et al.* 1991; Huang *et al.* 2014; Song *et al.* 2015; Qian *et al.* 2018), vegetation type (Ikeda *et al.* 2008; Stefanova *et al.* 2013; Mitrović *et al.* 2016; Radhwani *et al.* 2018), or maturity (Peters and Cassa 1994; Hakimi *et al.* 2016; López-Días *et al.* 2016; Jaroszewicz *et al.* 2018) of the coal. Investigation of the macromolecular composition of the saturated fraction has been performed on the samples of South Karanpura coalfield.

5.9.1 Organic geochemical analysis of coal seams of Barka Sayal area

The coal samples collected from different seams of the Barka Sayal area were clubbed together based on their similar petrochemical properties and got analyzed using GC-MS. The major biomarker compounds identified in these samples are given in Table 5.10**.** Various biomarker parameters were also calculated are given in Table 5.11.

Table 5.10 Biomarker compounds identified in the studied samples of the Barka Sayal area.

Peak no.	Compound	Base Peak	Mol. ion
1	C_{15}-bicyclic sesquiterpane	193	208
2	4β(H)-eudesmane	109	208
3	8β(H)-drimane	123	208
4	8β(H)-homodrimane	123	222
5	C_{18}-diterpane	233	248
6	C_{19}-tricyclic terpane	123	262
7	C_{18}-norpimarane	233	262
8	C_{19}-tricyclic terpane	191	262
9	ent-beyerane	123	274
10	C_{20}-diterpane	123	274
11	α-phyllocladane	123	274
12	Sandaracopimaradiene	257	272
13	17,21-secohopane (C_{24})	191	330
14	17,21-secohopane (C_{25})	191	344
15	17α(H)-22,29,30-trisnorhopane (Tm)	191	370
16	17β(H)-22,29,30-trisnorhopane	149	370
17	17α(H),21β(H)-30-norhopane	191	398
18	17β(H),21α(H)-30-norhopane	177	398
19	βα-hopane	191	412
20	αβ-hopane	191	412
21	17α(H),21β(H)-Homohopane (22 S)	191	426
22	17α(H),21β(H)-Homohopane (22 R)	191	426
23	17β(H),21β(H)-Homohopane	205	426
24	17α(H),21β(H)-Bishomohopane	191	440
25	17β(H),21β(H)-Bishomohopane	191	440

n-alkanes and isoprenoids

The *n*-alkanes and isoprenoids were identified based on the selected mass chromatogram m/z 57. The *n*-alkane hydrocarbon fractions are dominated by the homologous series ranging from C_{14} to C_{33}. The unimodal *n*-alkane distribution pattern is evident in all the samples with the dominance of medium-chain (*n*-C_{23}, *n*-C_{25}) hydrocarbons. The acyclic isoprenoid hydrocarbons, pristine (Pr), and phytane (Ph) are identified in all samples with an abundance of pristine over phytane. The Pr/Ph ratio varies from 2.95 to 8.04. The carbon preference index (CPI) varies from 0.57 to 1.90, and the terrigenous/aquatic ratio

(TAR) varies from 0.43 to 1.82. Proxy aqueous ($P_{aq)}$ varies from 0.19 to 1.00, whereas Proxy wax ($P_{wax)}$ is between 0.89 and 0.97.

Terpenoids

Terpenoids identified include sesquiterpanes, diterpanes, and triterpanes. C_{15}-bicyclic sesquiterpane, 4β(H)-eudesmane, C_{15} 8β(H)-drimane, and C_{16} 8β(H)-homodrimane are the sesquiterpenoids identified. Diterpenoids found in the extracts include 18-norisopimarane, *ent*-beyerane, α-phyllocladane, norabieta-3,8,11,13-tetraene, sandaracopimaradiene, and unknown C_{18}, C_{20} diterpenoids. Tricyclic terpanes found are C_{15} and C_{19} hydrocarbons.

Table 5.11 Biomarker parameters calculated for the studied samples of the Barka Sayal area.

Sample no.	CPI	TAR	P_{aq}	P_{wax}	Pr/Ph	Pr/*n*-C_{17}	Ph/*n*-C_{18}
SL 1	1.90	0.89	0.95	0.16	3.33	0.93	0.14
SL 4	0.58	1.03	0.94	0.16	3.10	0.57	0.14
SL 5+6	0.57	1.57	0.96	0.15	2.95	2.26	0.29
BG 2	0.62	1.22	0.91	0.20	5.11	2.89	0.41
BG 3+4+5+6	1.89	0.43	0.97	0.12	6.83	2.13	0.25
HD 2	1.60	1.40	0.90	0.26	3.74	2.29	0.25
HD 5+6	1.82	1.63	0.95	0.18	3.86	3.21	0.31
HD 7+8	1.79	1.82	0.94	0.19	3.03	2.56	0.24
SBK	2.64	1.59	1.00	0.09	1.39	0.49	0.28

The triterpenoid biomarkers were detected using the characteristic ion extract *m/z*-191. The samples are characterized by the high relative abundance of hopane type of pentacyclic triterpenoids. In all samples, the highest abundances are shown by 17α(H)-22,29,30-trisnorhopane, and 17β(H), 21α(H)-hopane (βα-moretane). Both βα and αβ hopanes are identified but ββ counterpart is absent. The overall distribution of hopanes is similar in all samples indicating not many changes happened in the microbial activity during the deposition of the sequence. Tetracyclic 17, 21-secohopanes (C_{24} and C_{25} homologues) are also present in these samples.

5.9.2 Organic geochemical analysis of coal seams of Argada area

The combined coal samples collected from seams of the Argada area were analyzed using GC-MS. The major biomarker compounds identified in these samples are given in Table 5.12 and Table 5.13. Various biomarker parameters were also calculated (Table 5.14).

Table 5.12 *n*-alkanes and isoprenoids compounds identified in the studied samples of the Argada area.

Sl.no	Carbon no.	AG-A	AG-B	AG-C	AG-D	AG-I	AG-J
1	13	0	0	0	0	19193	17811
2	14	0	0	0	0	31141	26022
3	15	189865	0	0	0	28352	24909
4	16	894641	310	30224	84919	29965	29232
5	17	2946202	7275	119236	180385	41882	46058
6	PR	45332	0	8126	85844	11718	20050
7	18	2654516	9512	166147	139617	53102	50315
8	PH	364475	0	2950	31156	9466	9088
9	19	3227175	19763	292921	145611	55975	58215
10	20	5686374	42667	663337	169717	63274	55464
11	21	7704866	75453	1407638	206870	60839	60233
12	22	11174007	132576	2676920	247098	55712	48272
13	23	17462553	245637	5786978	315273	51529	50553
14	24	11938740	195423	4389739	290010	35614	32031
15	25	17062747	300921	7917347	264774	29749	27286
16	26	4014069	80908	1846836	122589	9585	8336
17	27	4334908	106712	2379614	114471	3327	0
18	28	1213803	31167	602601	0	0	0
19	29	847638	32625	531789	0	0	0
20	30	361139	0	196166	0	0	0
21	31	172991	0	148188	0	0	0
22	32	0	0	59423	0	0	0

n-alkanes and isoprenoids

The *n*-alkane hydrocarbon fractions are dominated by the homologous series ranging from C_{13} to C_{32}. The unimodal *n*-alkane distribution pattern is evident in all the samples with the dominance of medium-chain (*n*-C_{23}, *n*-C_{25}) hydrocarbons. The coal seams present in shallow depth are having lower chains, whereas deeper seams such as Argada I and Argada J shows the presence of higher carbon chains. The acyclic isoprenoid hydrocarbons, pristane (Pr), and phytane (Ph) are identified in all samples with an

abundance of pristane over phytane except the seam Argada-A, where it is opposite. The pristane/phytane ratio in coal reveal both the paleo-redox settings and intensity of methane formation. In the coals of Argada-A, low pristane/phytane ratios indicate prevailed reducing conditions during sediment deposition (Orphan *et al.* 2001) or may be generation of high content of methane during diagenesis by methanogenic archaebacterial biomass (Tomoaia-Cotisel *et al.* 1992).

Terpenoids

In the case of terpenoids, C_{15} tricyclic terpane are present in the coals of the Argada area. In all samples, the highest abundances are shown by 17α(H)-22,29,30-Trisnorhopane. Both βα and αβ hopanes are identified along with ββ homohopane. The overall similar distribution of hopanes indicates that very few changes happened in the microbial activity during the deposition of the coal seams of the Argada area.

Table 5.13 Biomarker compounds present in the samples of the Argada area of South Karanpura coalfield.

Peak	Compound	Base peak	Mol. ion
1	C15 tricyclic terpane	191	206
2	17α (H)-22, 29,30-Trisorhopane	191	370
3	αα/αβ-30-Norhopane	191	398
4	ββ-30-Norhopane	177	398
5	αβ-Hopane	191	412
6	βα-Hopane	191	412
7	αβ-Homohopane (22S)	191	426
8	αβ-Homohopane (22R)	191	426
9	ββ-Homohopane	205	426
10	αβ-Bishomohopane (22S)	191	440
11	αβ-Bishomohopane (22R)	191	440

Table 5.14 Biomarker parameters calculated for the studied samples of the Argada area.

Sample no.	CPI	TAR	P_{aq}	P_{wax}	Pr/Ph	Pr/*n*-C_{17}	Ph/*n*-C_{18}
AG	0.77	0.45	0.89	0.22	8.04	1.43	0.15
AG-A	1.95	0.84	0.97	0.13	0.12	0.02	0.14
AG-B	2.16	5.15	0.94	0.20	nil	nil	nil
AG-C	2.36	7.42	0.95	0.18	2.75	2.07	0.02
AG-D	1.46	0.35	1.00	0.16	5.76	0.48	0.22
AG-I	1.24	0.03	1.00	0.04	1.24	0.28	0.18
AG-J	1.29	nil	1.00	nil	2.21	0.44	0.18

6 CHAPTER 6. MATURATION (RANK) AND SOURCE ROCK POTENTIAL OF COALS OF SOUTH KARANPURA COALFIELD

6.1 Introduction

Maturation or rank of organic matter refers to the physicochemical stage of coalification, which is influenced by post-depositional subsidence. With subsidence, followed by sedimentation, the temperature and pressure increase in response to the geothermal gradient and thickening of overburden. It is an irreversible process. During physicochemical transformation, the lignite changes to subbituminous coal then bituminous, semi-anthracite, anthracite, and lastly, in meta-anthracite. During the process of diagenesis, catagenesis, and metagenesis various changes occur in the organic matter such as alteration in micro constituents (Smith and Cook 1980; Chandra and Chakrabarti 1989), loss of CO and CO_2 (Kopp and Bennett 2001), loss of volatiles (Hayatsu *et al.* 1988; Kopp *et al.* 2000; Murchison 2004), etc., which also affects the petrographic and physicochemical properties of the organic matter (Gorbanenko and Ligouis 2014; Varma *et al.* 2018; Acharyya 2019). Several proxies may act as maturity indicators of the organic matter, some of them are fluorescence intensity measurement (for low-rank coal), carbon content, volatile matter, moisture content, calorific value, spore colour (Thermal Alteration Index/TAI), vitrinite/ huminite reflectance, production index (PI), and Tmax (°C) obtained by Rock-Eval Pyrolysis (Wilkins *et al.* 1992). Among these parameters, vitrinite reflectance is the most widely used, because humic materials respond to temperature during coalification. Besides, assessing the rank of the coal vitrinite reflectance can also trace the paleogeothermometric settings of the basin (Bostick 1979; Barker and Elders 1981; Qiu *et al.* 2007).

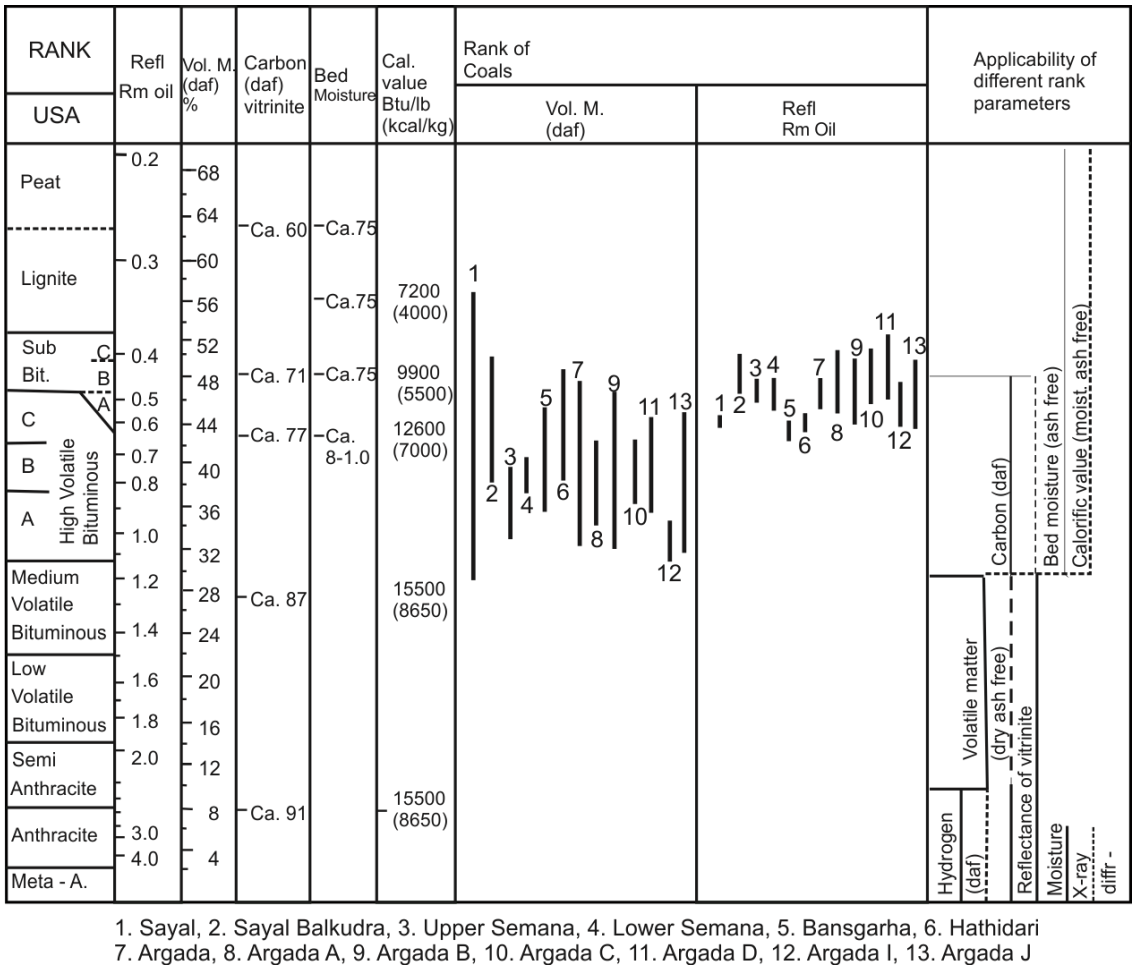
Coal is formed by organic substances and may have the capability to generate liquid or gaseous hydrocarbons. A rock that is capable of generating or that has generated movable quantities of hydrocarbons is called a source rock. In the context of petroleum/ hydrocarbon generation potential, organic matter can be classified as immature, mature, or over-mature. The assessment of any rock as a source rock is done based on the quantitative and qualitative assessment of the organic matter, type of kerogen (insoluble organic matter), bitumen, and maturity level. Rock-Eval pyrolysis is also a robust method to identify the degree of maturation of organic matter and quantify distillable materials generated from the source rock.

The maturity assessment of the coals of South Karanpura coalfield has been carried out with the help of chemical and optical parameters. The chemical parameters utilised are volatile matter (daf basis), carbon (daf basis), and Rock-Eval pyrolysis. The mean vitrinite reflectance (VRo %) was employed as an optical parameter. Further, the source rock potential of these coals has been analysed.

6.2 Rank based on Chemical and Petrological Parameters

In the scheme of rank determination given by North American ASTM classification (ASTM D388-15, 2015), the coals of Barka Sayal area of South Karanpura coalfield show their rank from Subbituminous C to high volatile B bituminous (mean VRo% between 0.40% and 0.66%), whereas the coals of Argada are also characterised as Subbituminous C to high volatile B bituminous in rank (mean VRo% from 0.37% and 0.63%) (Figure 6.1). Based on the volatile matter, which ranges between 29.41% and 57.13% (daf basis) the coals of the Barka Sayal area can be characterized as High volatile A bituminous to Subbituminous C in rank, whereas coals of Argada area exhibit volatile content ranging in between 31.07% and 48.57%, which suggests rank ranging from High volatile A

bituminous to Subbituminous C (Figure 6.1). Few samples show abnormally high volatile content, ranks up to lignite because of enrichment of chemically resistant, hydrogen-bearing liptinite macerals in these coals. The rank of these coals also suggests that part of these coals are in the bituminization stage (VRo% in between 0.5% and 0.6%) (Teichmüller 1989).



1. Sayal, 2. Sayal Balkudra, 3. Upper Semana, 4. Lower Semana, 5. Bansgarha, 6. Hathidari
7. Argada, 8. Argada A, 9. Argada B, 10. Argada C, 11. Argada D, 12. Argada I, 13. Argada J

Figure 6.1 Rank of coals of the South Karanpura Coalfield, Jharkhand, India, based on Random Vitrinite reflectance (VRo %) and V.M. (daf basis) in the scheme representing the different stages of coalification according to North American (ASTM) and West German (DIN) classification and their distinction based on different physical and chemical parameters. The last column shows the applicability of various rank parameters to different coalification stage (after Stach *et al.* 1982).

In the scheme of rank determination proposed by Kotter (1960) using maximum vitrinite reflectance values (Vrmax.%) and volatile matter (daf) (wt. %) as parameters, the rank of the coals of South Karanpura coalfield varies from Flammkohle to Gaskohle (Figure 6.2).

The discussion provided above concludes that the rank of coals of South Karanpura coalfield ranges from subbituminous to high volatile bituminous.

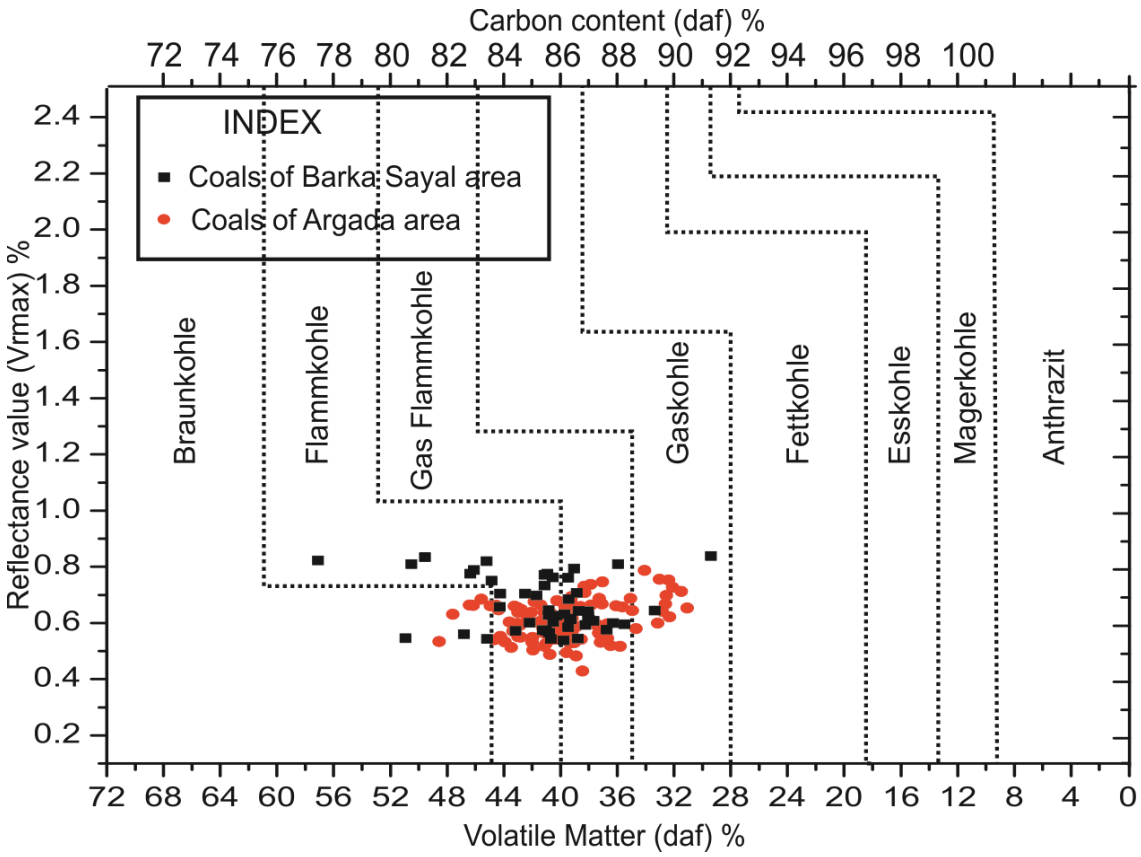


Figure 6.2 Rank of South Karanpura coals in the diagram proposed by Kotter (1960) using reflectance and Volatile Matter (daf) as parameters.

6.3 Maturity assessed by Rock-Eval Pyrolysis Method

A better understanding of the mechanisms of hydrocarbon generation, expulsion, storage, and retention, thermal cracking of sedimentary organic matter, and its maturity constitutes a key point to estimate the oil and gas in-place, free or adsorbed, for their exploration and exploitation. This is best accomplished by a rapid screening of organic-rich rocks using the Rock-Eval Pyrolyzer (Baudin *et al.* 2015; Singh and Kumar 2018). The IFP Energies Nouvelles (IFPEN) also known as French Institute of Petroleum (in French: Institut Français du Pétrole, IFP) in 1970, designed and developed a method to assess the oil potential of a sedimentary rock called the Rock-Eval technique using a standardized

pyrolysis apparatus (Lafargue *et al.* 1998). The data obtained through rock-eval provides crucial information about the quantity, type, and degree of thermal maturity of organic matter occurring as concentrated organic matter (coal) or as dispersed organic matter (DOM) in sedimentary rocks. The significant part of this technique is that organic matter is analysed without separating it from the rock, and a large number of samples may be analysed sequentially in a short period of time. The analysis is performed under controlled temperature, and an organic matter sample (approx. 100 mg) is heated in the absence of air. The organic compounds thus produced may be assessed quantitatively. During the heating, the oxygenated compounds released from mineral matter are excluded. It gives the quantitative measurement of various fractions of volatile/ nonvolatile organic compounds, source rock potential, and degree of maturation. The analytical procedure has been discussed in Chapter-3. Initially, the pyrolysis oven temperature was kept isothermally at 300°C for 3 minutes, and the free hydrocarbons were volatilized and measured as the S1 peak (detected by a flame ionization detector). The temperature was then raised from 300° to 550°C at a rate of 25°C/min, and the hydrocarbons released from this thermal cracking were measured as the S2 peak (detected by a flame ionization detector). The temperature at which S2 reaches its maximum is called Tmax, which depends on the kerogen's nature and maturity. The CO_2 issued from kerogen cracking was trapped in the 300°-390°C range. The trap was heated, and a thermal conductivity detector detected released CO_2 during the cooling of the pyrolysis oven as S3 peak. The instrument also calculated the total organic carbon (TOC). Other derived parameters include the genetic potential that is the addition of S1 and S2. The production index denotes the ratio of S1 and S1+S2. It is used to characterize the evolution level of the organic matter. Hydrogen Index (HI) corresponds to the quantity of the pyrolysable organic compounds (S2) relative to the total organic carbon and calculated by formula HI

= [100 x S2] /TOC. It acts as a parameter to characterize hydrocarbon origin because lipid and protein-rich marine organisms are rich in hydrogen compared to the carbohydrate-rich land plants. Oxygen Index (OI) corresponds to the ratio of oxygen to carbon and calculated by formula OI = [100 x S3] /TOC. The details of the parameter, as suggested by Larter (1984) and modified by Murchison (1987) for Rock-Eval pyrolysis, are given below:

Peak S1	Quantity of hydrocarbon and related material liberated from organic material during heating at 250°C for 5 min. in helium - approximately equivalent to material extracted through the solvent procedure.
Peak S2	The quantity of carbon dioxide produced during pyrolysis of the sediment over the temperature range of 250-550°C per minute in helium approximately equivalent to the thermal degradation of kerogen.
Peak S3	Quantity of carbon dioxide produced during the pyrolysis of the sediments over the temperature range of 250-390°C.
T max	The temperature of the maximum Kerogen decomposition rate (maximum peak S2 evolution) - relatable to the maturity of the sample. It is given by the amplitude of the peak above S2.
TOC	Total organic carbon
S1 + S2	Genetic potential
S1 /S1+S2	Production Index
S2 /TOC	Hydrogen Index (HI) - Hydrogen Index corresponds to the quantity of the pyrolysable organic compounds "hydrocarbon" (HC) from S2 relative to the total organic carbon (TOC or C org) in Sample (mg Hydrocarbon / g organic carbon = mg HC/g C org)
S3/TOC	Oxygen index (OI) - Oxygen Index corresponds to the quantity of CO_2 from S_3 relative to the TOC (mg CO_2 / g C org).

Several eminent workers applied the Rock-Eval pyrolysis technique for source rock characterization (Davis *et al.* 2007; Gretskaya and Dakhnova 2010; Hakimi *et al.* 2013; Karayiğit *et al.* 2018; Qian *et al.* 2018), quantification of organic matter (Kondla *et al.* 2016; Singh *et al.* 2016e; Van de Wetering *et al.* 2016; Qian *et al.* 2018), etc. The guideline for interpreting the source rock potential of organic matter with the help of Rock-Eval pyrolysis data is given below (Peters 1986; McCarthy *et al.* 2011) (Table 6.1 to Table 6.5).

Table 6.1 Geochemical parameters describing source rock generative potential (Peters 1986).

Quantity	TOC (Wt. %)	S1 (mg HC/g rock)	S2 (mg HC/g rock)
Poor	0-0.5	0.05	0-2.5
Fair	0.5-1.0	0.5-1.0	2.5-5.0
Good	1.0-2.0	1.0-2.0	5.0-10.0
Very Good	>2.0	>2.0	>10.0

Table 6.2 Total Organic Carbon and their Source Rock Implications (after, Peters 1986).

TOC (Wt. %)	Source Rock Implications
<0.5	Negligible Source Capacity
0.5-1.0	Slight Source Capacity
1.0-2.0	Moderate Source Capacity
>2.0	Good to Excellent Source Capacity

Table 6.3 Hydrogen index and their principal products (after, Peters 1986).

HI (mg HC/g C_{org})	Principal Product	Relative Quantity
<150	Gas	Small
150-300	Oil and Gas	Small
300-450	Oil	Moderate
450-600	Oil	Large
>600	Oil	Very Large

Table 6.4 Maturation based on Production Index (PI), Temperature (Tmax), and Vitrinite Reflectance (VRo %) (after, Peters 1986).

Maturation	PI [S1/(S1+S2)]	Tmax (°C)	VRo %
Top Oil Window (birth line)	~0.1	~435-445	~0.6
Bottom Oil Window (death line)	~0.4	~470	~1.4

Table 6.5 Geochemical parameters describing the type of hydrocarbon generated (after, Peters 1986)

Type	HI (mg HC/g TOC)	S2/S3*
Gas	0-150	0-3
Gas and Oil	150-300	3-5
Oil	>300	>5

** Assuming level of thermal maturation equivalent to VRo = 0.6%*

The analytical result of Rock-Eval pyrolysis of the coals of South Karanpura coalfield is given in Table 6.6 and

Table 6.7. The Total Organic Carbon (TOC) content in the coals of the South Karanpura coalfield is high, which varies from 16.97 (wt. %) to 81.93 (wt. %), mean 54.37 (wt. %). The value of the S1 peak (free hydrocarbon) is low, varying from 0.14 mg HC/g rock to 2.84 mg HC/g rock, mean 0.90 mg HC/g rock. The S2 peak represents the number of hydrocarbons generated through the thermal cracking of non-volatile organic matter. In the coals of South Karanpura coalfield, the values of the S2 peak varies from 29.97 mg HC/g rock to 153.50 mg HC/g rock, mean 93.87 mg HC/g rock. The S3 content of these coals varies from 1.07 mg CO_2/g rock to 23.74 mg CO_2/g rock, mean 7.79 mg CO_2/g rock. Tmax for these coals varies from 129 °C to 435 °C, mean 422 °C. The Hydrogen Index (HI) of the coals of South Karanpura coalfield varies from 65 mg HC/g TOC to 262 mg HC/g TOC, mean 175.02 mg HC/g TOC. The Oxygen Index (OI) for coals of South Karanpura coalfield lies in the range of 2 mg CO_2/g TOC to 67 mg CO_2/g TOC, mean 16.16 mg CO_2/g TOC. The production index of South Karanpura coals varies from nil to 0.03 and does not possess any characteristic difference in both the areas. As per the guidelines of source rock generative potential (Peters, 1986), the geochemical parameters obtained by rock-eval pyrolysis (S1, S2, and Tmax) indicate that the coals of South Karanpura coalfield may act as the excellent source rock for hydrocarbon generation.

6.3.1 Maturity of coals of Barka Sayal area

There are six prominent coal seams present in the Barka Sayal area: Sayal, Sayal Balkudra, Upper Semana, Lower Semana, Hathidari, and Bansgarha. Bansgarha is the bottom-most seam of the area, whereas Sayal is the top-most seam. The Total Organic Carbon (TOC) content in the coals of the Barka Sayal area varies from 17.33 (wt. %) to

81.93 (wt. %), mean 54.21 (wt. %). The value of the S1 peak (free hydrocarbon) in the Barka Sayal area of South Karanpura coalfield varies from 0.14 mg HC/g rock to 1.05 mg HC/g rock, mean 0.57 mg HC/g rock. The S2 peak, which represents the number of hydrocarbons generated through thermal cracking of non-volatile organic matter varies from 31.61 mg HC/g rock to 139.02 mg HC/g rock, mean 91.04 mg HC/g rock for coals of the Barka Sayal area. The S3 content of the coals of the Barka Sayal area varies from 7.61 mg CO_2/g rock to 23.74 mg CO_2/g rock, mean 10.36 mg CO_2/g rock. Tmax for the coals of the Barka Sayal area varies from 422 °C to 435 °C, mean 426.18 °C. The Hydrogen Index (HI) of the coals of the Barka Sayal area varies from 65 mg HC/g TOC to 234 mg HC/g TOC, mean 171.64 mg HC/g TOC. The Oxygen Index (OI) for coals of Barka Sayal area lies in the range of 11 mg CO_2/g TOC to 67 mg CO_2/g TOC, mean 22.22 mg CO_2/g TOC. The production index of the coals of South Karanpura coalfield varies from nil to 0.03 and does not possess any characteristic difference in both the areas. The coals of Sayal seam exhibit the minimum value to TOC, whereas the coals of Bansgarha seam have the highest TOC content. The coals of the Sayal seam also exhibit the lowest S2, PI, and Tmax values, which suggests that due to lower concentration of organic material and the highest concentration of mineral matter, the coals of this seam have not much hydrocarbon generation potential. The coals of the Hathidari seam exhibit the minimum values of S1 and HI but maximum values of S3 and Tmax; this suggests that due to thermal maturation, the coals of this seam have low hydrocarbon generation potential exhibited by the lower values of S2 and lowest values of HI. The coals of Bansgarha seam exhibit the highest TOC and HI values and minimum OI value, suggesting that these coals have a high source rock potential. The sample-wise detailed analytical result of source rock evaluation data of the coals of the Barka Sayal area is presented in Table 6.6. As per the guidelines of source rock generative potential (Peters,

1986), the geochemical parameters obtained by rock-eval pyrolysis (S1, S2, HI, and Tmax) indicate that the coals of Barka Sayal area may act as a very good source rock for hydrocarbon generation.

Table 6.6 Source Rock Evaluation Data of coals of Barka Sayal area, South Karanpura coalfield, Jharkhand, India.

Sample Name	TOC	S1	S2	S3	S2/S3	Tmax	HI	OI	PI	MINC
SL 5+6	48.01	0.32	59.21	13.31	4.45	431	123	28	0.01	1.80
SL 3+4	17.33	0.15	31.61	11.54	2.74	424	182	67	nil	2.89
SL 2	29.78	0.46	62.08	8.77	7.08	425	208	29	0.01	1.79
SL 1	36.66	0.44	70.88	8.22	8.62	422	193	22	0.01	1.79
SBK-7+8	60.07	1.05	132.15	8.93	14.80	422	220	15	0.01	1.31
SBK-5+6	50.29	0.67	96.43	8.45	11.41	424	192	17	0.01	1.27
SBK-1+2+3+4	60.57	0.75	109.23	9.60	11.38	426	180	16	0.01	1.43
Up. Sm-9	62.64	0.80	117.44	7.61	15.43	429	187	12	0.01	1.19
Up. Sm-5	71.37	0.61	114.05	9.19	12.41	429	160	13	0.01	1.49
Up. Sm-1	69.48	0.45	87.84	12.01	7.31	430	126	17	0.01	1.60
Lr. Sm-7	68.18	0.83	128.80	8.65	14.89	425	189	13	0.01	1.42
Lr. Sm-3	71.57	0.68	132.40	8.68	15.25	428	185	12	0.01	2.64
Lr. Sm-1	67.55	0.76	139.02	8.85	15.71	426	206	13	0.01	2.53
HD 7+8	57.12	0.92	120.90	12.40	9.75	425	212	22	0.01	1.69
HD 5+6	62.64	0.14	40.45	23.74	1.70	435	65	38	nil	2.75
HD 3+4	35.52	0.32	56.84	14.23	3.99	428	160	40	0.01	1.50
HD 2	56.45	0.41	61.64	12.51	4.93	425	109	22	0.01	2.03
HD 1	28.28	0.29	35.06	9.90	3.54	424	124	35	0.01	2.13
BG 5+6	50.39	0.61	76.07	8.99	8.46	422	151	18	0.01	1.80
BG 3+4	35.05	0.41	76.40	10.17	7.51	424	218	29	0.01	1.64
BG 2	34.36	0.47	80.34	11.21	7.17	428	234	33	0.01	1.71
BG 1	81.93	0.40	66.74	9.00	7.42	424	81	11	0.01	2.77
BS MIN	17.33	0.14	31.61	7.61	1.70	422	65	11	nil	1.19
BS MAX	81.93	1.05	139.02	23.74	15.71	435	234	67	0.01	2.89
BS MEAN	52.51	0.54	86.16	10.73	8.91	426	168	23.73	0.01	1.87
BS SD	16.86	0.24	32.86	3.36	4.35	3.19	45.21	12.93	nil	0.51

TOC= Total organic carbon (wt.%); S1= free hydrocarbons (mg HC/g rock); S2= amount of hydrocarbons (mg HC/g rock); S3= released carbon dioxide (mg CO2/g rock); S2/S3 =Hydrogen richness; Tmax= temperature maximum (°C); HI (Hydrogen Index) = (S2/TOC) × 100 (mg HC/g TOC); OI (Oxygen Index) = (S3/TOC) × 100 (mg CO_2/g TOC); PI (Production Index) = S1/(S1+S2); MINC=Mineral content (%); mg/g= Milligram/gram; wt.= Weight; BS= Barka Sayal area, SL= Sayal; SBK= Sayal Balkudra; US= Upper Semana; LS= Lower Semana; HD= Hathidari; BG= Bansgarha; MIN= Minimum, MAX=Maximum, MEAN= Arithmetic average, SD= Standard deviation.

6.3.2 Maturity of coals of Argada area

The Argada, Argada-A, Argada-B, Argada-C, Argada-D, Argada-I and Argada-J are the most prominent coal seams of the Argada area. Argada-J is the bottom-most seam while Argada is the top-most seam in this area.

The analytical result of the Rock-Eval pyrolysis of the coals of the Argada area of South Karanpura coalfield is given in

Table 6.7. The TOC content of the Argada area is from 16.97 wt.% to 74.64 wt.%, mean 56.22 wt.%. For the Argada area, the S1 peak values lie in the range of 0.32 mg HC/g rock to 2.84 mg HC/g rock, mean 1.20 mg HC/g rock. The S2 peak values lie in between 29.97 mg HC/g rock and 153.50 mg HC/g rock, mean 101.59 mg HC/g rock. The S3 content for coals of Argada area the range lies in between 1.07 mg CO_2/g rock and 8.30 mg CO_2/g rock, mean 4.93 mg CO_2/g rock. Coals of Argada area exhibit, Tmax lying in the range of 129 °C to 435 °C, mean 417.07 °C. Coals of Argada area the values of the hydrogen index (HI) lie in between 82 mg HC/g TOC and 262 mg HC/g TOC, mean 181.64 mg HC/g TOC. The Oxygen Index (OI) for coals of the Argada area lies in between 2 mg CO_2/g TOC and 19 mg CO_2/g TOC, mean 8.59 mg CO_2/g TOC.

The coals of Argada seam contain minimum as well as maximum TOC concentration in their different bands, possibly due to extreme variation in the depositional environment during the formation of different bands of this seam. It also exhibits the highest values of S1 and Tmax. The coals of Argada-A seam contain the highest mineral matter concentration and residual organic carbon, which suggests that the high mineral content of these coals possibly hindered the pyrolysis process. The coals of Argada-B seam exhibit the minimum concentration of S2 HI and OI; hence the coals belonging to this seam has not high source potential, which is also supported by low TOC content of these coals. The coals of Argada-C seam exhibit the highest values for S2 and HI but the lowest values for S3 and Tmax, which suggests that these coals have a good source rock potential but low maturity.

Table 6.7 Source Rock Evaluation Data of coals of Argada area, South Karanpura coalfield, Jharkhand, India.

Sample Name	TOC	S1	S2	S3	S2/S3	Tmax	HI	OI	PI	MINC
AG 10	44.36	2.62	99.41	2.31	43.03	433	224	5	0.03	n.d.
AG 9	16.97	0.92	39.85	1.63	24.45	433	235	10	0.02	n.d.
AG 8	74.64	2.84	133.14	4.35	30.61	433	178	6	0.02	n.d.
AG 13	72.32	2.76	133.18	4.04	32.97	435	184	6	0.02	n.d.
AG/A-14+15+16	66.20	1.26	101.70	8.23	12.36	430	154	12	0.01	7.99
AG/A-8+9+10	61.85	1.36	112.12	4.65	24.11	432	181	8	0.01	1.60
AG/A-2	71.05	1.65	125.82	7.01	17.95	431	177	10	0.01	1.92
AG/B-18+19+20	46.08	0.86	104.42	1.80	58.01	430	227	4	0.01	3.99
AG/B-13	36.45	0.77	29.97	1.38	21.72	431	82	4	0.03	2.37
AG/B-1	59.86	1.29	129.78	1.45	89.50	430	217	2	0.01	6.96
AG/C-7	40.39	0.66	105.70	1.07	98.79	432	262	3	0.01	4.22
AG/C-6	64.15	1.30	153.50	7.40	20.74	129	239	12	0.01	1.49
AG/C-1+2+3	55.09	1.06	114.39	2.41	47.46	432	208	4	0.01	4.83
AG/D-20	36.96	0.32	49.70	7.01	7.09	428	134	19	0.01	1.09
AG/D-12	65.05	0.80	115.64	8.30	13.93	432	178	13	0.01	2.21
AG/D-1	63.60	1.11	129.48	7.64	16.95	429	204	12	0.01	1.32
AG/I-7	59.98	1.70	73.81	6.29	11.73	432	123	10	0.02	2.37
AG/I-2	61.51	0.90	97.23	6.17	15.76	432	158	10	0.01	2.33
AG/I-1	58.84	0.95	92.11	6.18	14.90	434	157	11	0.01	1.90
AG/J-13	51.46	0.54	57.24	5.35	10.70	429	111	10	0.01	1.47
AG/J-9	69.39	0.64	131.32	7.01	18.73	432	189	10	0.01	1.99
AG/J-1	60.67	1.21	105.32	5.01	21.02	433	174	8	0.01	1.21
AG MIN	16.97	0.32	29.97	1.07	7.09	129	82	2	0.01	1.09
AG MAX	74.64	2.84	153.50	8.30	98.79	435	262	19	0.03	7.99
AG MEAN	56.22	1.25	101.58	4.85	29.66	418	181.64	8.59	0.01	2.85
AG SD	13.85	0.68	32.14	2.42	23.85	63	43.49	3.96	0.01	1.94

TOC= Total organic carbon (wt.%); S1= free hydrocarbons (mg HC/g rock); S2= amount of hydrocarbons (mg HC/g rock); S3= released carbon dioxide (mg CO2/g rock); S2/S3 =Hydrogen richness; Tmax= temperature maximum (°C); HI (Hydrogen Index) = (S2/TOC) × 100 (mg HC/g TOC); OI (Oxygen Index) = (S3/TOC) × 100 (mg CO_2/g TOC); PI (Production Index) = S1/(S1+S2); MINC=Mineral content (%); mg/g= Milligram/gram; wt.= Weight; AG= Argada, AG/A=Argada-A seam; AG/B=Argada-B seam; AG/C=Argada-C seam; AG/D=Argada-D seam; AG/I=Argada-I seam; AG/J=Argada-J seam; MIN= Minimum, MAX=Maximum, MEAN= Arithmetic average, SD= Standard deviation.

6.4 Coals of South Karanpura as a Hydrocarbon Source Rock

Liquid hydrocarbon generation from coals and coaly source rocks is now known from many parts of the world, especially in the Australian region (Macgregor 1994; Todd *et al.* 1997). Oil-prone sequences are also identified in Indonesia, Canada, and New Zealand. Although, these oil accumulations have been generated from Cenozoic coals and only minor quantities of oil appear to be related to coals of other ages caused by the variation in vegetation with age (Petersen 2005).

The petrological and geochemical characteristics of the South Karanpura coals were used to evaluate these coal's source rock characteristics and to explore the possibility of their participation in hydrocarbon generation. The potentiality of a source rock type to generate hydrocarbon depends on the three factors, the type of organic matter, its quantity, and the source rock maturity. Each of these three factors is discussed in the following paragraphs.

6.4.1 Type of Organic Matter

The organic matter acting as a precursor of hydrocarbon is called kerogen. It constitutes 80% to 99% of the total organic matter; the rest is composed of bitumen (Tissot and Welte 1984). Petrographically, kerogen is related to the original organic matter and products of their alteration. Accordingly, each type of kerogen can be characterized using the terminology of coal macerals (Pashin 2008). The alginite maceral of coal can be the signature maceral of the type I kerogen; in contrast, macerals belonging to the liptinite group such as sporinite, cutinite, resinite, bituminite, exsudatinite, and suberinite can be characterized as type II kerogen. Macerals belonging to the vitrinite group are part of type III kerogen except for per-hydrous (dark) vitrinite (hydrogen more than 5.5 wt.%), whereas all the macerals of inertinite group can be considered as type IV kerogen (Pashin 2008). The behaviour of coal macerals during the liquefaction processes justifies its source rock characteristics. Vitrinite macerals actively participate and help in liquefaction

because of their thermoplastic nature, and liptinite provides higher yield due to the presence of more aliphatic content whereas, inertinite remains less reactive or inert during the process (Suárez-Ruiz and Crelling 2008).

Cornford et al. (1979) discussed the relation between macerals and kerogen using a triangular diagram, which based on the concept that the liptinites are hydrogen-rich, thus acting as Type I or II kerogens, while inertinites, remaining inert in all situation, act as Type IV kerogen (although a few reactive inertinites such as semifusinite may generate some hydrocarbons). Microscopic petrographic analysis data plotted on this diagram shows that macerals of the Barka Sayal coals, as well as the Argada area of South Karanpura coalfield, mostly act as Type III kerogen, whereas few inertinite-rich bands act as type IV kerogen (Figure 6.3).

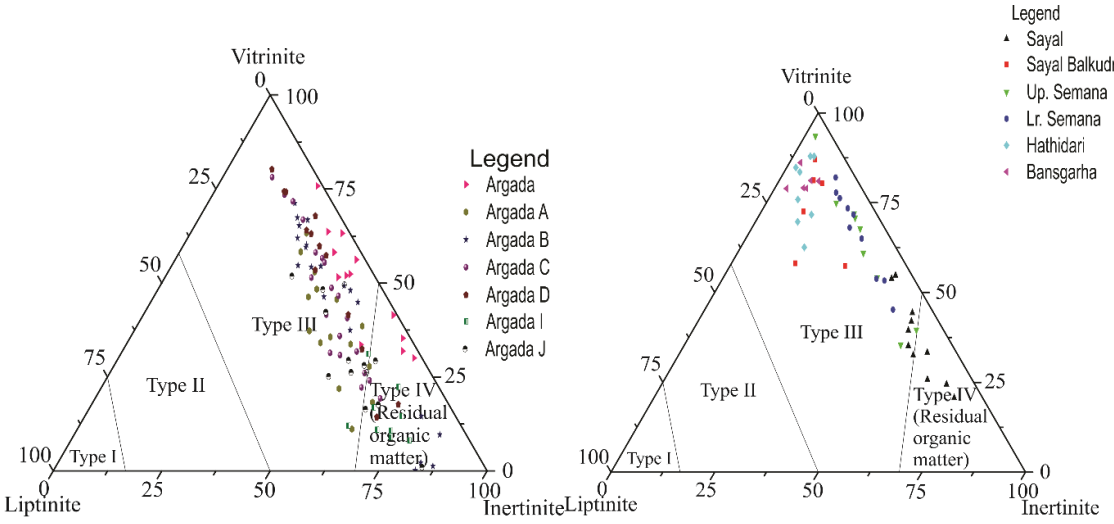


Figure 6.3 Type of kerogen present in coal seams of South Karanpura coalfield (after Cornford, 1979).

Further, the type of organic matter is also determined by the Hydrogen Index (HI) (S2/TOC*100) and Oxygen Index (OI) (S3/TOC*100), calculated from parameters of rock-eval pyrolysis. HI and OI of the coals of South Karanpura coalfield plotted based on a model proposed by Peters (1986), lies in between Type II and III kerogen (Figure 6.4). The input of terrigenous organic matter increases the TOC thus affecting the outcome.

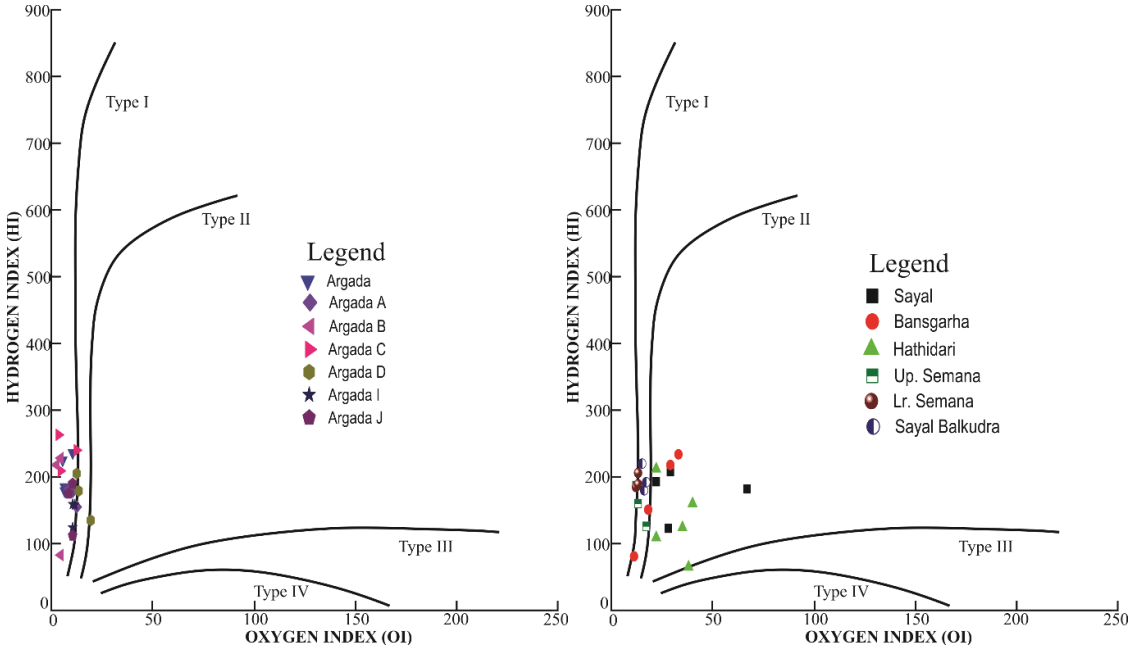


Figure 6.4 Plot of Hydrogen index (HI) versus oxygen index (OI) showing various hydrocarbon generative types (after Peters, 1986).

A cross plot between vitrinite reflectance and HI (Figure 6.5) of the coals of South Karanpura coalfield also support the previous outcome (Petersen 2005).

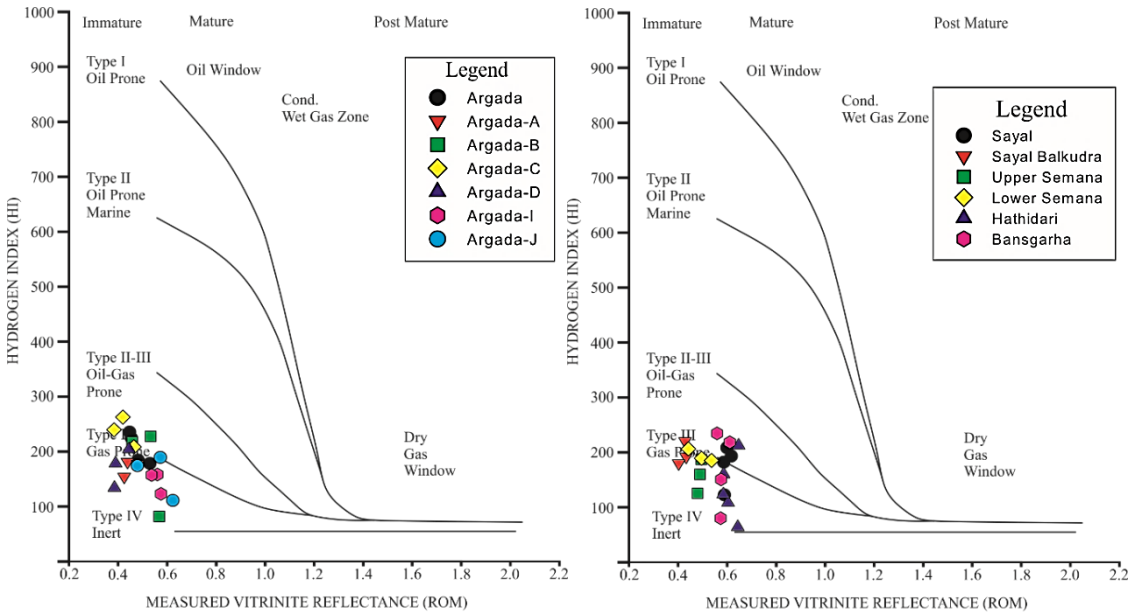


Figure 6.5 Cross plot between vitrinite reflectance (VRo %) and Hydrogen Index (HI) of coals of Barka Sayal and Argada area, South Karanpura coalfield (adopted after Petersen, 2005).

It suggests that most of these coals contain Type III kerogen, which can generate gas only, and that some of them also contain mixed Type II and III kerogen, which is oil as well as

gas prone. Almost all the coal belonging to the South Karanpura coalfield is of immature nature exhibited by the low vitrinite reflectance.

Langford and Blanc-Valleron, (1990) also discussed and established a relationship among types of kerogen, its origin, nature of expelled hydrocarbon with S2 peak of Rock-Eval pyrolysis and Total Organic Carbon (TOC). Plotted pyrolysis data of coals of South Karanpura coalfield again support the presence of gas prone type III kerogen in these coals, whereas few coal bands also contain mix type kerogen, which can generate a mixed liquid and gaseous hydrocarbon (Figure 6.6).

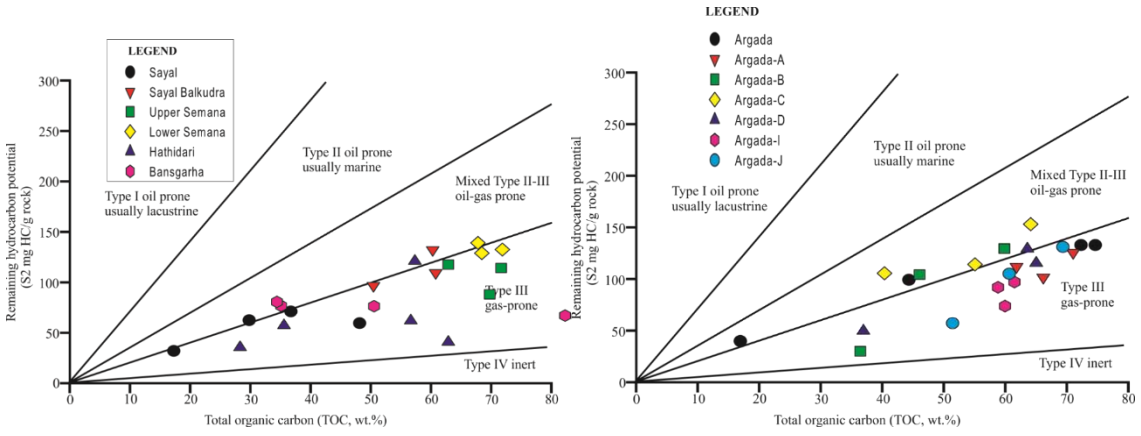


Figure 6.6 Plot of remaining hydrocarbon potential (S2) versus TOC for coals of Barka Sayal area and Argada area (after Langford and Blanc-Valleron, 1990).

Rock-Eval pyrolysis data shows a visual and authentic representation of hydrocarbons present or capable of being expelled from a source rock, but it is also not free from shortcomings (Katz 1983). Lafargue et al. (1998) discussed the incomplete combustion of mineral-rich coals during the oxidation process of Rock-Eval pyrolysis, thus leading to the determination of lower TOC than the actual TOC. Higher rank coals (VRo > 2%) show more variation of TOC during this process. Thus, they suggest that the atomic H/C ratio and O/C ratio are more authentic than the hydrogen index (HI) and oxygen index (OI). Hence, the ultimate analysis data have also been used to determine the type of kerogen (Jones and Edison 1978) (Figure 6.7).

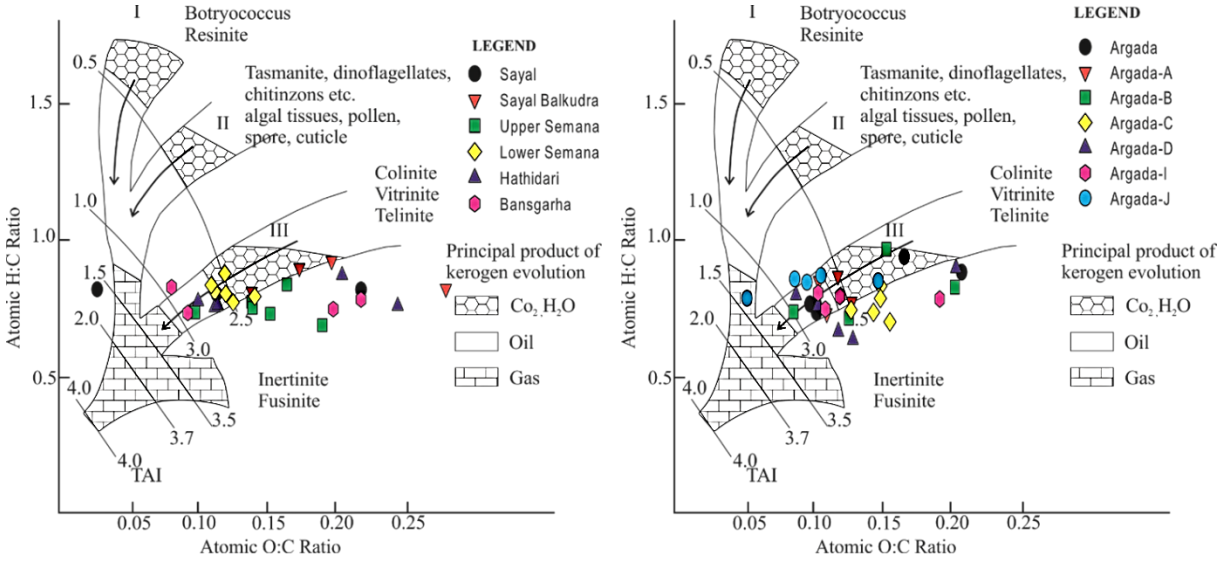


Figure 6.7 Kerogen types of the coals of Barka Sayal as well as the Argada area (after Jones and Edison, 1978).

For South Karanpura coals, the H/C value ranging from 0.59 to 0.91 and O/C values ranging from 0.03 to 0.25 put these coals as Type III kerogen indicating few samples are capable of generating oil as well as gas, but most of them can produce only gaseous hydrocarbons.

The FTIR analyses have also been used to depict the kerogen type, source rock characteristics, and maturity of the coals of South Karanpura coalfield. The relative ratios of aliphatic and aromatic bands are called as A-Factor, and the relative ratio of carbonyl to carboxyl and an aromatic band called as C-Factor is calculated using the following equations (Ganz and Kalkreuth 1987, 1991; Misra *et al.* 2019, 2020):

A-Factor= (2930 cm^{-1} + 2860 cm^{-1})/ (2930 cm^{-1} + 2860 cm^{-1} + 1630 cm^{-1})

C-Factor= 1710 cm^{-1} / (1710 cm^{-1} + 1630 cm^{-1})

Concerning the van Krevelen diagram, plots of A-factor and C-factor shows that in both the areas of South Karanpura coalfield, Barka Sayal as well as in Argada type III and admixed type II/III are the dominant kerogens which are in agreement with the values obtained by rock eval pyrolysis studies. Although the difference in the result of Rock-

Eval pyrolysis and FTIR analysis may occur due to a change in the behaviour of the macerals during pyrolysis (Misra *et al.* 2018).

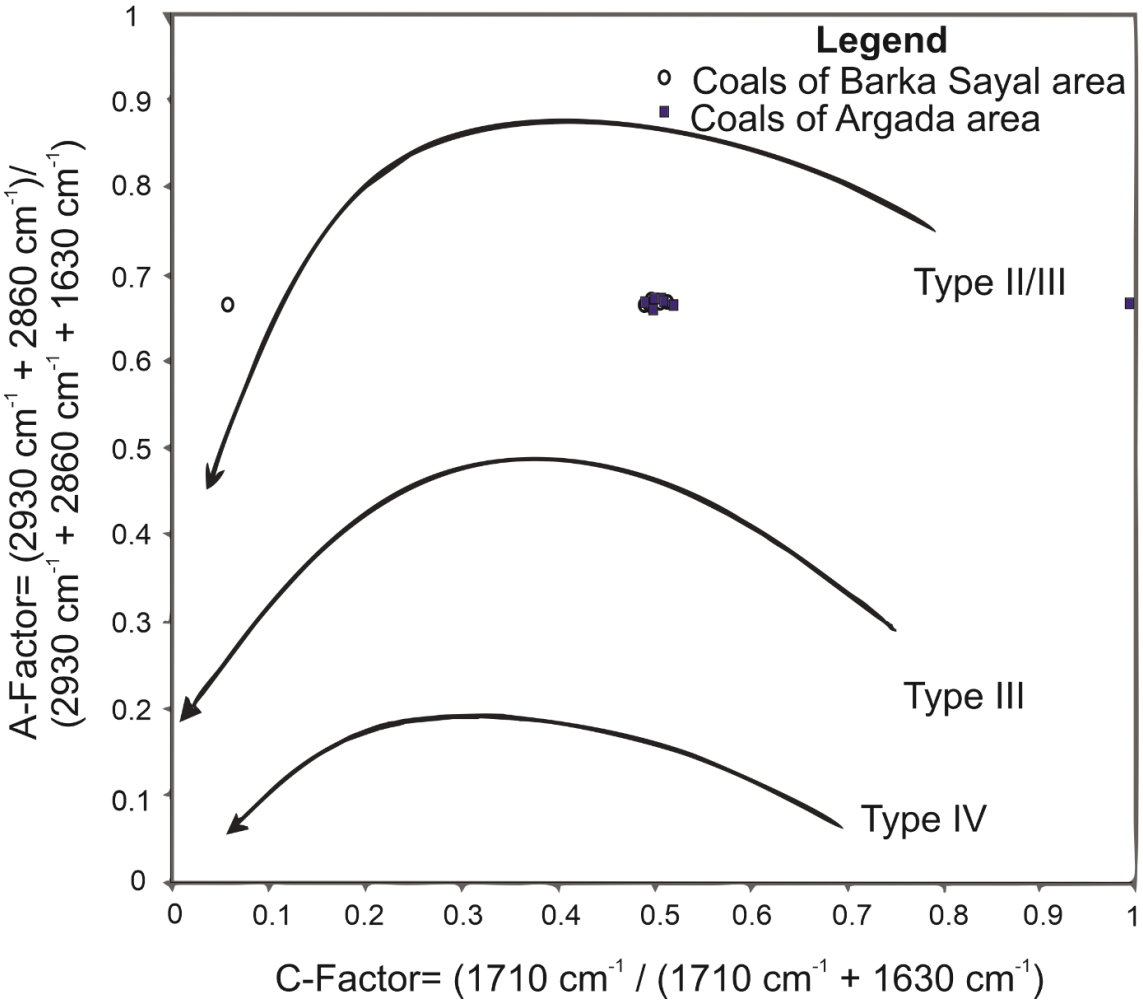


Figure 6.8 Kerogen types present in South Karanpura coalfield based on A-factor (aliphatic/aromatic peak intensity) and C-factor (carbonyl/aromatic peak intensity) (modified after Ganz and Kalkreuth, 1987).

6.4.2 The quantity of Organic Matter

The quantity of organic matter can be estimated by assessing the total organic carbon (TOC) content determined from the Rock-Eval pyrolysis. The total number of reactive macerals (vitrinite and liptinite) can also provide an idea about the organic matter present in the coal. Kerogen and bitumen both are parts of the TOC. In a reducing environment, TOC content increases; when it exceeds 2%, it indicates an excellent source capacity (Bustin 1997). Petersen and Nytoft (2006) discussed the hydrocarbon generative potential

of coals of different ages and found Permian coals have good potential because the S2 values in these coals are several folds higher than the S1 values, suggesting that expelled hydrocarbon during maturation is much more than the hydrocarbons present in free form. The S2 denotes the retained hydrocarbon present in source rock that can be expelled during maturation. TOC present in South Karanpura coals shows that these coals have an excellent hydrocarbon generating potential upon maturation (Peters and Cassa 1994; Dembicki 2009) (Figure 6.9).

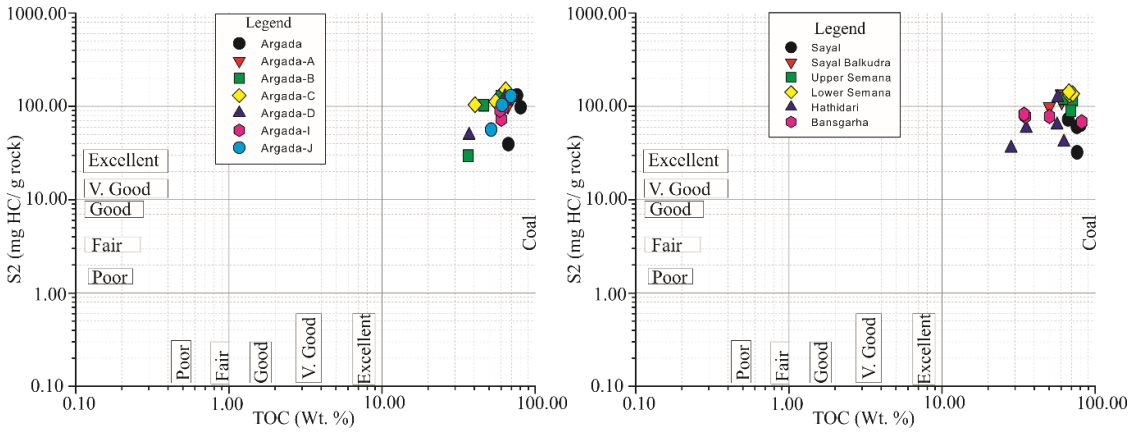


Figure 6.9 Cross plot between total organic carbon (TOC) and fixed hydrogen potential (S2) of analysed coal samples of Barka Sayal and Argada area of South Karanpura coalfield (after Peters & Cassa 1994; Dembicki 2009).

The outcome was further supported by the cross plot of genetic potential (S1+S2) versus TOC and shows that the coals of both Barka Sayal area as well as Argada area belonging to South Karanpura coalfield exhibit excellent source rock potential due to high concentration of TOC, free hydrocarbons (S1), and the hydrocarbons expelled during thermal cracking (S2) (Figure 6.10).

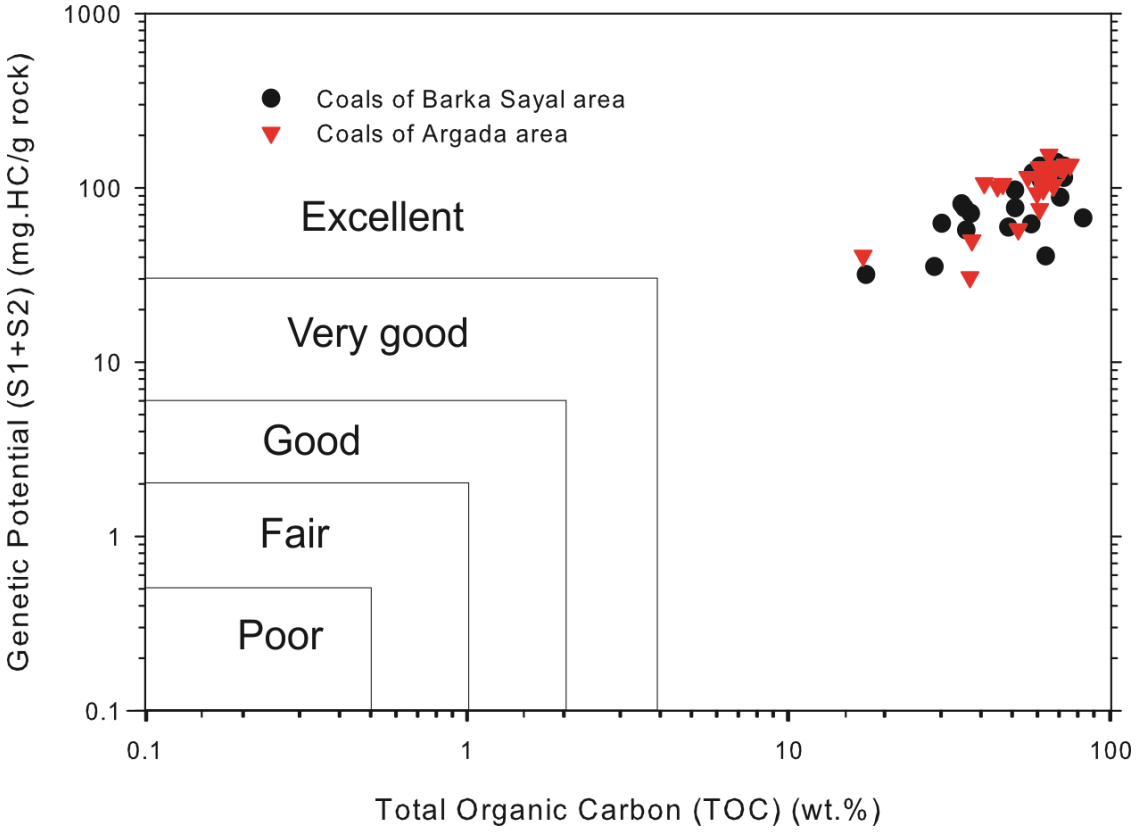


Figure 6.10 Plot of genetic potential (S1+S2) versus total organic carbon (TOC) showing the genetic potential of South Karanpura coals.

6.4.3 Source Rock Maturity

The coalification process is a combination of physical, chemical, and microbiological processes. The parameters such as vitrinite reflectance (VRo), H/C atomic ratio, reactive macerals (vitrinite + liptinite) content, and volatile matter (daf) determine the suitability of any coal for liquefaction (Cudmore 1977; Davis et al. 1976). Lignite converts more slowly and incompletely than bituminous coals, whereas high-rank coal such as anthracite remains inert during direct coal liquefaction (Kaneko et al. 2012).

Vitrinite reflectance acts as an essential parameter to determine the maturity of the organic matter or coalification trend. The mean vitrinite reflectance values of the coals of Barka Sayal area and Argada area are also plotted in the model provided by Tissot and Welte (1985), which shows that these coals had crossed the evolution stage of diagenesis and reached the catagenesis stage which may have liquid hydrocarbon generative potential

(Figure 6.11). The vitrinite reflectance value ranges between 0.5% and 0.6% for most of these coals, indicating that they are in the bituminization stage (Teichmüller and Teichmüller 1979).

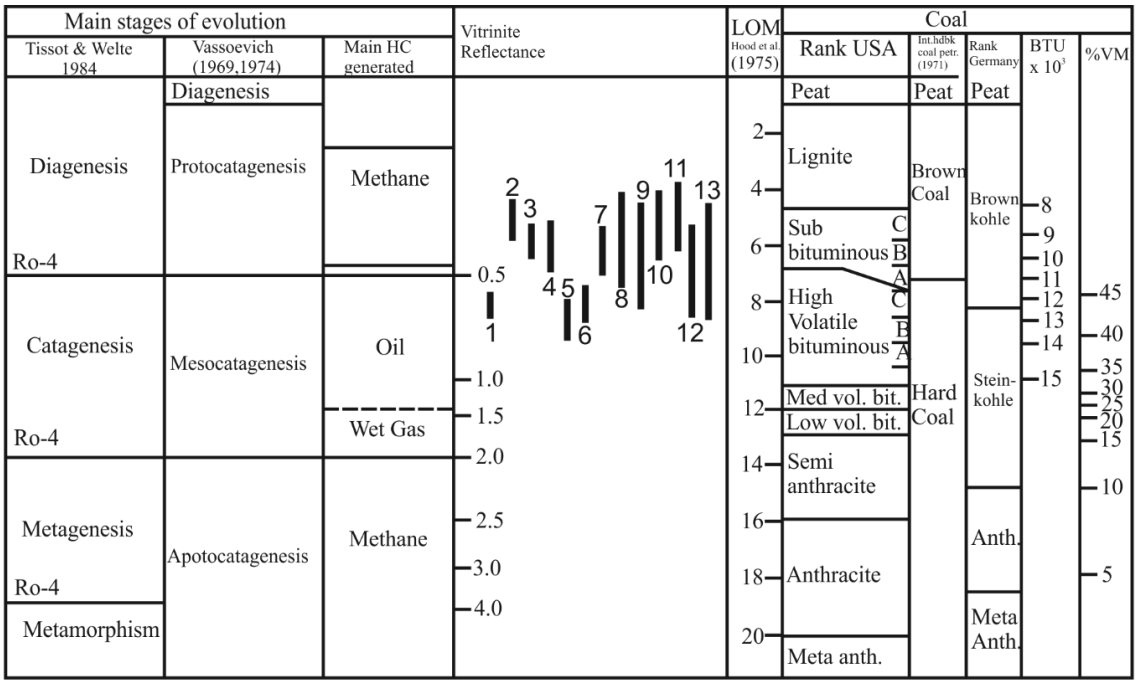


Figure 6.11 The main stage of evolution (maturation) of the organic matter and their relation with the coal rank (coalification) (after Tissot & Welte 1984).

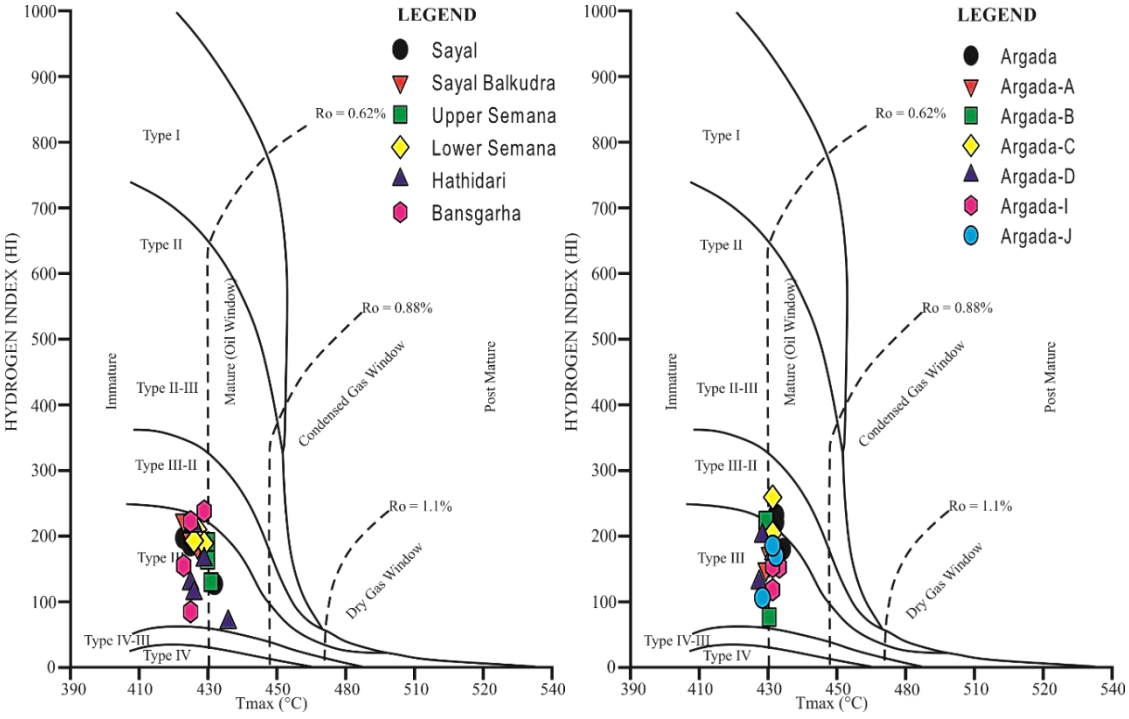


Figure 6.12 The plot of HI versus Tmax (°C) for the coal samples of South Karanpura coalfield, showing Kerogen type and thermal maturity stages (adopted after van Koeverden et al., 2011).

The plot between HI and Tmax (°C) shows that these coals are mainly Type III kerogen. However, low Tmax (422°C to 435°C), suggests that these coals have immature source rock characteristics (Van Koeverden *et al.* 2011) (Figure 6.12). A few samples have a mixed Type II-III kerogen, which is capable of generating mixed oil and gaseous hydrocarbons. However, most of the samples are Type III kerogen, which may generate gas upon pyrolysis or thermal maturation. Pyrolysis result also shows a very low production index (<0.1) of these coals, thereby making them immature (Figure 6.13) (Peters 1986). However, Peters (1986) suggested that Tmax and PI are not very reliable parameters for thermal maturity, especially for Type III kerogen because Tmax depends on several factors such as TOC content, the type of the organic matter, mineral matrix in the organic lean sediments and the sulphur content. Hence, a model based on Tmax and vitrinite reflectance was utilized which further supported the outcome due to low Tmax values (<435°C) and low vitrinite reflectance (<0.7%), which makes these coals immature

to early mature stage source rock having low grade, which is likely to yield biogenic gas and immature oil (Figure 6.14) (Peters & Cassa, 1994).

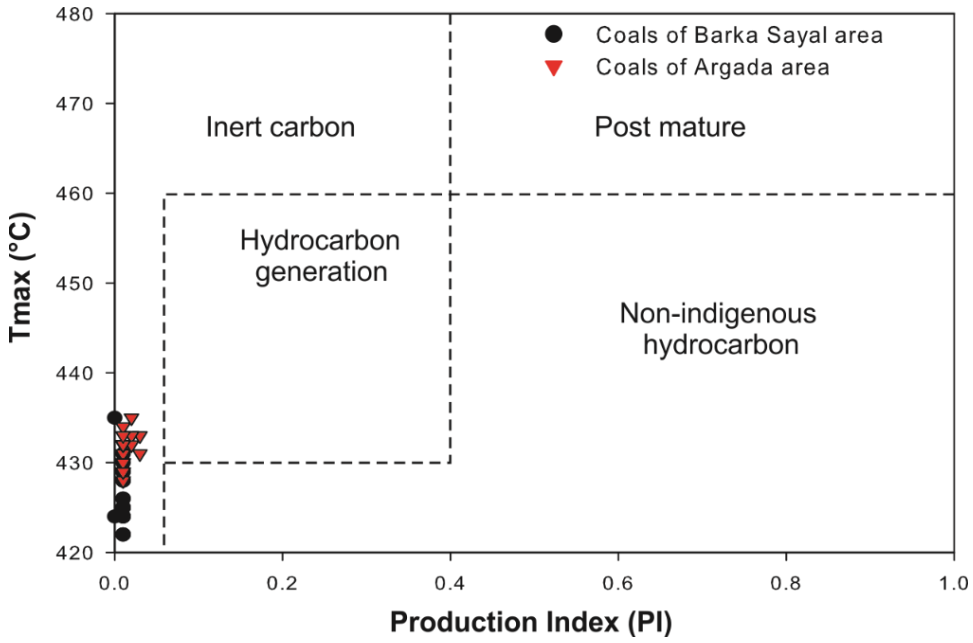


Figure 6.13 Plot of Tmax versus Production Index showing the hydrocarbon-generation zone (after Peters 1986).

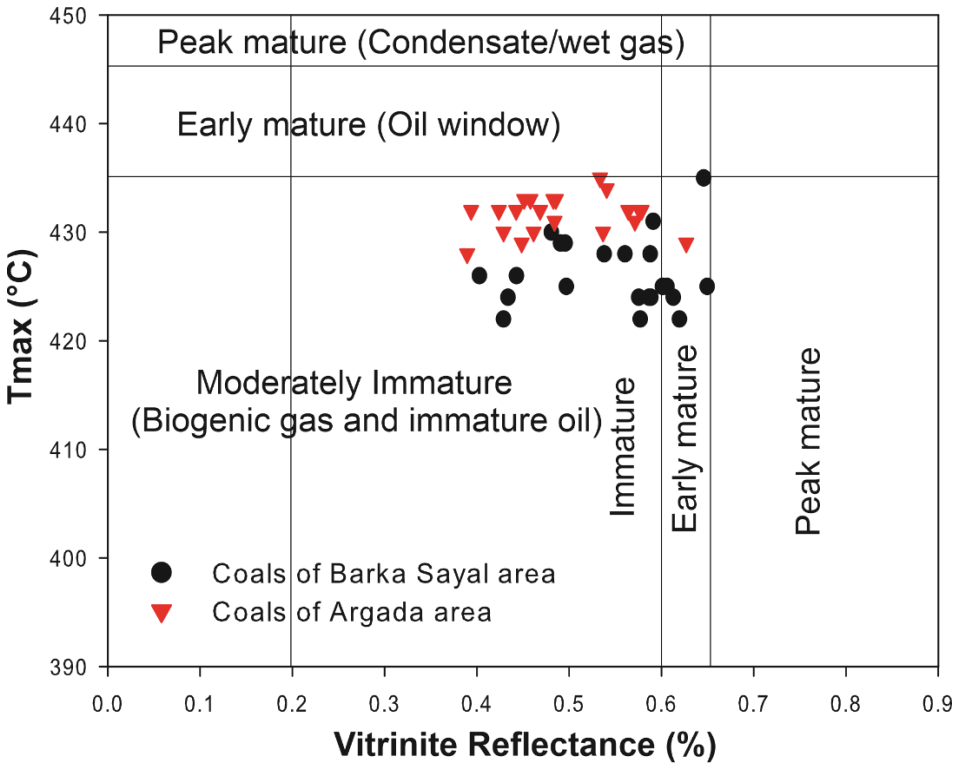


Figure 6.14 Plot of Tmax versus Vitrinite Reflectance (VRo %) showing the maturity levels (after Peters & Cassa 1994).

6.4.4 Oil yield

Cudmore (1977) has validated that coals having properties such as vitrinite reflectance less than 0.8 %, H/C atomic ratio more than 0.75, reactive macerals (vitrinite or huminite + liptinite) more than 60 % and volatile matter (daf) more than 35% are favourable for liquefaction or hydrogenation. The coal deposits of South Karanpura coalfield possess these properties, which are furnished in Table 6.8. Coals of the Argada area have less reactive macerals and a high amount of inertinite maceral, which makes those coals less favourable for hydrogenation than coals of the Barka Sayal area. Although; coals belonging to both areas have S2 values several-fold higher than S1 values, which indicates these coals are the good source rock for hydrocarbon generation. The ternary plot, based on the maceral composition of these coals, favours the generation of mainly lighter hydrocarbons (Figure 6.15).

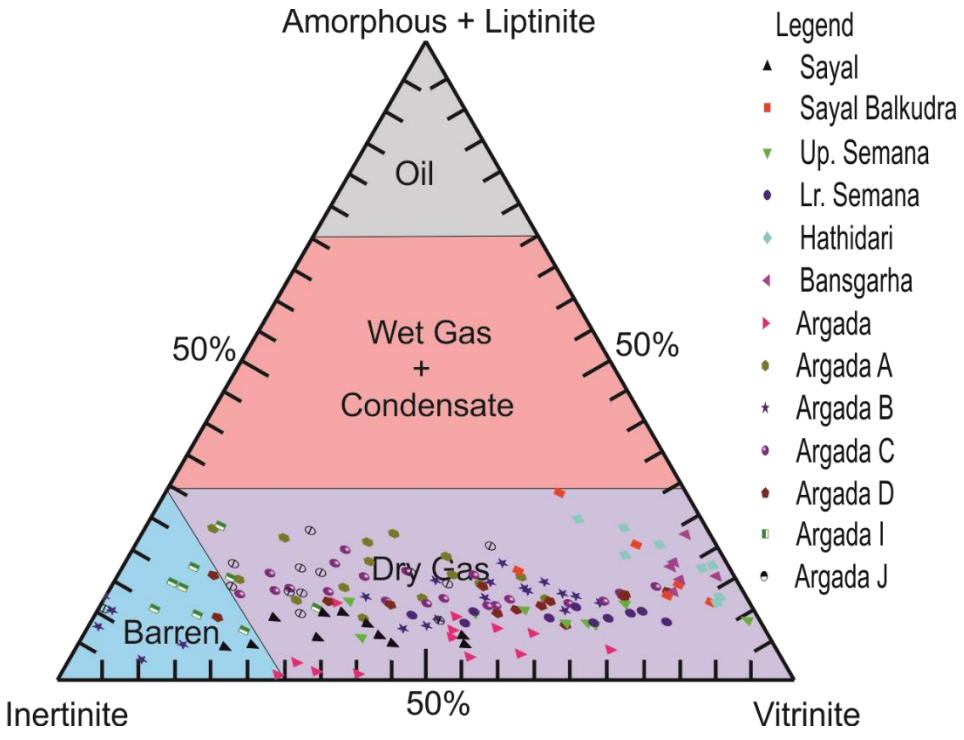


Figure 6.15 Ternary diagram based on maceral composition indicating the hydrocarbon potential of South Karanpura coals (after Tissot & Welte, 1984).

Table 6.8 Coal characteristics required for hydrogenation.

Sl No.	Properties of coal required for hydrogenation (after Cudmore, 1977)		Mean Characteristics of coals of Barka Sayal area	Mean Characteristics of coals of Argada area	Characteristics of South Karanpura coal on an average
1	Vitrinite Reflectance (VRr)	< 0.8	0.54	0.49	0.51
2	H/C atomic ratio	>0.75 %	0.80	0.75	0.77
3	Vitrinite + Liptinite content	> 60 %	76.55	51.54	64.04
4	Volatile Matter (daf)	>35 %	41.59	39.04	40.32
5	Concentration of heteroatoms	Relatively Low	Low	Low	Low

Moreover, coals of South Karanpura coalfield have presented a positive result during pyrolysis and substantiate the properties suitable for liquefaction of these coals thus an attempt was made to find out its 'conversion' into oil and its 'Oil yield' using the empirical formula given by Guyot (1978) and Jin and Shi (1997) (Table 6.9).

They introduced the following formula:

$$Petrofactor\ (RF)\ =\ 1000\ VRrmax/RM\ (Guyot, 1978).$$

$$Conversion\ (a)\ (\%) =\ 99\ -\ 0.84\ RF\ (Guyot, 1978);$$

$$Conversion\ (b)\ (\%)\ =\ 0.2\ RM + 76.6\ (Jin\ and\ Shi, 1997);$$

$$Oil\ yield\ (b)\ (\%)\ =\ 0.22\ RM + 44.8\ (Jin\ and\ Shi, 1997);$$

Where, RM= Reactive macerals (i.e. Vitrinite + Liptinite) and VRrmax= Maximum random vitrinite reflectance.

The conversion of the coals of the South Karanpura coalfield is high (72.04% to 96.06%). The oil yield of these coals lies in the range of 47.61% to 66.21% mean 58.89% (Table 6.9). The correlation graphs of macerals constituent (mmf basis) with oil yield (b) (%) clearly shows the high degree of positive correlation with vitrinite and a moderate degree

of positive correlation with liptinite and inertinite (Figure 6.16). The liptinite group of macerals are very less in these coals, among liptinites, sporinite is the most dominant maceral; they compose very less volume compared to the vitrinite macerals. The lesser volume % of liptinite is not affecting much the oil yield and most of the hydrocarbons are being derived from the vitrinite group of macerals which is also a part of reactive macerals. That is why the liptinite group of macerals indicating weak correlation with the oil yield.

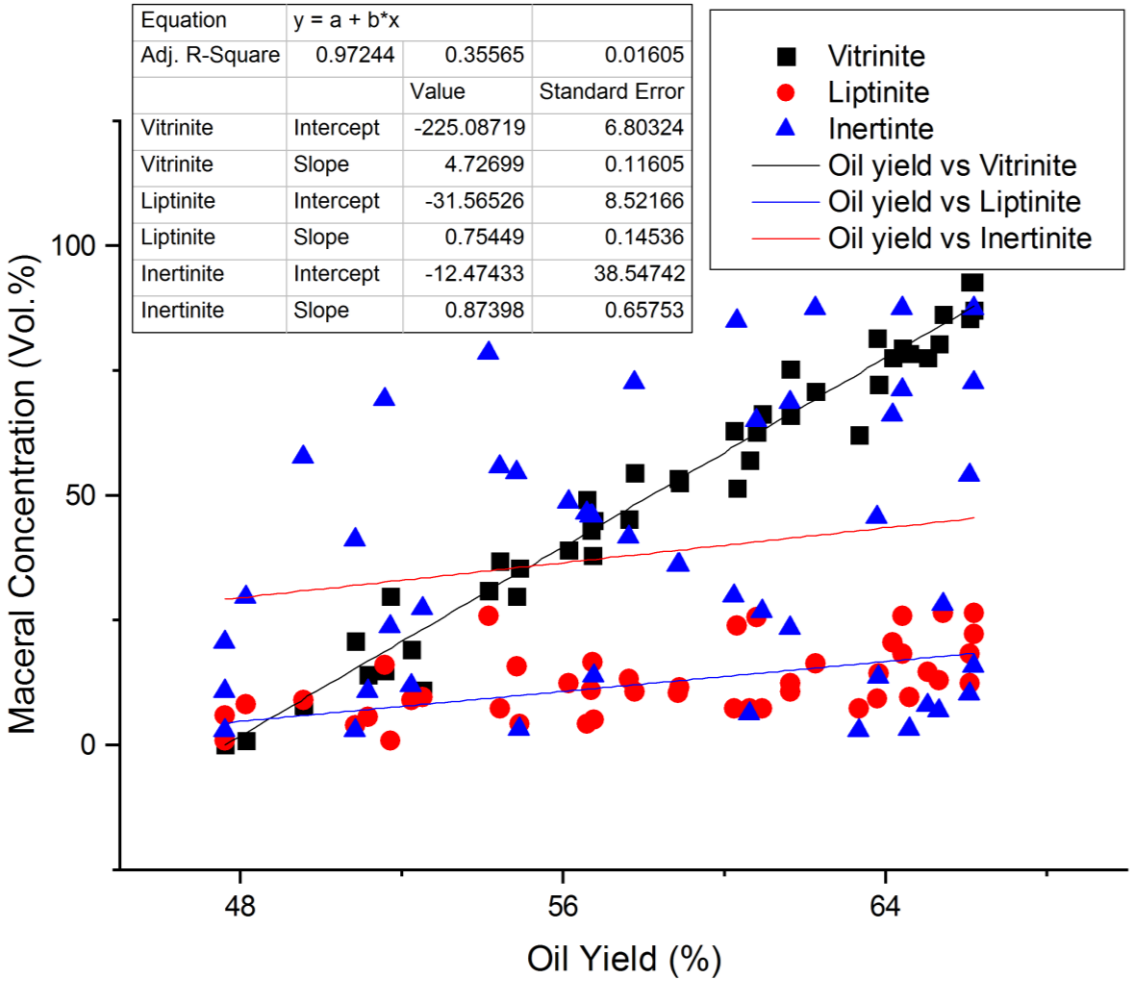


Figure 6.16 Correlation of Oil yield (b) with microscopic constituents of South Karanpura coals.

The source potential of the coal macerals increases with increasing their H/C ratio (Hunt 1995). Saxby (1980) noticed a relationship between the chemical composition of the coal

and oil yield obtained by open-system pyrolysis by testing many coal and oil shale samples and proposed the formula:

$$Oil\ wt.\%\ (dry, mineral\ free\ basis) = 66.7\ H/C - 57.0\ O/C - 33.3$$

Based on the H/C ratio and O/C ratio of the South Karanpura coals, the oil wt.% (dry, mineral-free basis) is found between 1.35% and 17.80% with an average of 9.63% (Saxby 1980).

The correlation graph of maximum random vitrinite reflectance (VRrmax) and values of H/C and O/C shows a positive correlation (Figure 6.17).

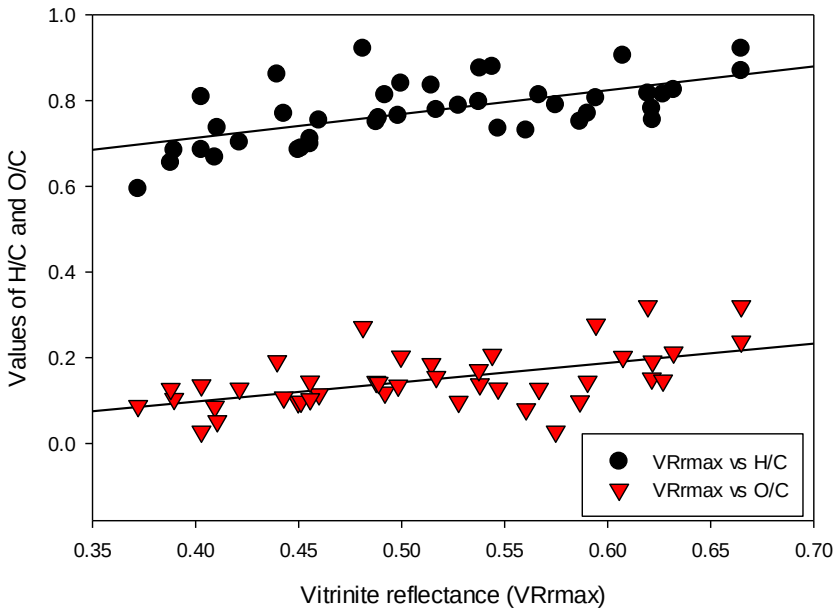


Figure 6.17 Cross plot of Vitrinite reflectance and the values of H/C and O/C for coals of South Karanpura coalfield.

The coals of South Karanpura are found rich in hydrocarbons having good source potential but thermally immature. To know the relation of reactive macerals (vitrinite + liptinite) with Oil yield (b) %, Oil wt.%, TOC, S2 and HI of the coals of South Karanpura coalfield, a multiple scatter plot with regression lines have been plotted, which shows a positive correlation of reactive macerals with all five parameters (Figure 6.18). It suggests

that with the increasing content of reactive macerals, the hydrocarbon generation potential of the coal increases. Among the correlated parameter, HI exhibit a high positive correlation with the reactive macerals, which confirms that the reactive macerals present in the coal may contribute to the generation of hydrocarbon. A positive correlation of S2 with reactive macerals suggests that the hydrocarbon released due to thermal cracking comes from the reactive macerals, which is also confirmed by the positive correlation of TOC with the reactive macerals (Figure 6.18).

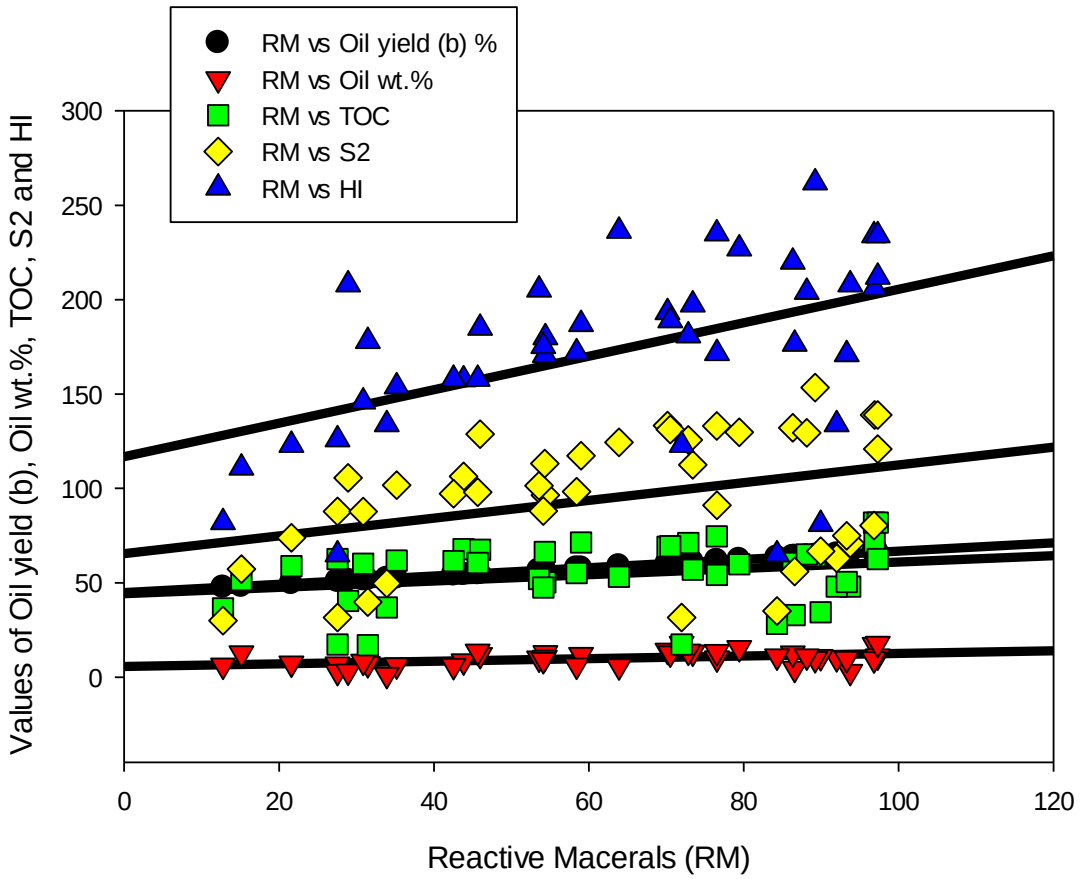


Figure 6.18 Correlation plot of total reactive macerals (RM) (vol. %) with Oil yield (b) %, Oil wt. %, TOC, S2, and HI for coals of South Karanpura coalfield.

Table 6.9 Values of Conversion, Oil yield, and Petrofactor Calculated for South Karanpura Coals Using Empirical Formula

Seam name		VRr max	Vitrinite	Liptinite	Reactive Macerals (RM)	H/C	O/C	RF (after Guyot, 1978)	Conversion (a) (after Guyot, 1978)	Conversion (b) (after Jin and Shi, 1997)	Oil yield (b) (after Jin and Shi, 1997)	Oil wt.% (after Saxby, 1980)
Sayal	Min	0.57	57.1	7.4	72.0	0.79	0.03	7.98	92.29	91.00	60.64	17.80
	Max	0.62	86.3	26.5	93.8	0.82	0.32	6.61	93.45	95.35	65.43	2.95
	Mean	0.59	72.3	14.3	86.6	0.81	0.28	6.86	93.23	93.92	63.85	4.64
Sayal	Min	0.40	45.1	5.0	54.4	0.81	0.14	7.41	92.78	87.47	56.76	12.90
Balkudra	Max	0.48	81.4	9.3	86.3	0.92	0.27	5.57	94.32	93.87	63.79	12.67
	Mean	0.44	66.2	7.2	73.4	0.86	0.19	5.99	93.97	91.29	60.95	13.20
Up. Semana	Min	0.45	20.8	4.0	27.5	0.69	0.10	16.34	85.28	82.11	50.86	6.93
	Max	0.51	54.5	10.7	59.0	0.84	0.19	8.72	91.67	88.40	57.78	11.88
	Mean	0.49	36.9	7.4	43.8	0.75	0.14	11.13	89.65	85.36	54.44	8.56
Lr. Semana	Min	0.44	35.4	4.1	45.9	0.77	0.11	9.64	90.90	85.79	54.91	11.90
	Max	0.54	92.8	12.3	96.9	0.88	0.14	5.55	94.34	95.98	66.12	17.22
	Mean	0.49	62.8	7.3	70.2	0.81	0.12	7.01	93.11	90.63	60.24	14.16
Hathidari	Min	0.59	62.2	7.3	84.3	0.75	0.10	6.96	93.15	93.46	63.35	11.18
	Max	0.66	87.2	22.1	97.3	0.87	0.24	6.83	93.26	96.06	66.21	11.11
	Mean	0.62	77.4	14.6	92.0	0.78	0.15	6.75	93.33	95.00	65.04	10.21
Bansgarha	Min	0.56	78.3	9.6	90.0	0.73	0.08	6.23	93.77	94.59	64.59	10.88
	Max	0.63	85.4	18.3	96.8	0.83	0.21	6.53	93.52	95.97	66.10	9.64
	Mean	0.59	80.3	13.0	93.3	0.77	0.14	6.33	93.69	95.26	65.33	9.85
Barka Sayal	MIN	0.40	20.8	4.0	27.5	0.69	0.03	5.55	85.28	82.11	50.86	2.95
area	MAX	0.66	92.8	26.5	97.3	0.92	0.32	16.34	94.34	96.06	66.21	17.80
	MEAN	0.54	66.0	10.7	76.6	0.80	0.17	7.35	92.83	91.91	61.64	10.10
Argada	Min	0.45	29.8	0.8	31.4	0.69	0.10	14.35	86.95	82.89	51.72	7.06
	Max	0.54	75.2	12.3	76.5	0.88	0.21	7.11	93.03	91.91	61.64	13.54
	Mean	0.50	49.2	4.4	53.6	0.76	0.13	9.31	91.18	87.31	56.58	10.02
Argada-A	Min	0.39	11.0	9.4	35.2	0.68	0.10	11.08	89.69	83.63	52.54	6.42
	Max	0.57	62.8	25.4	72.8	0.81	0.13	7.78	92.46	91.17	60.83	13.66
	Mean	0.46	37.8	16.5	54.3	0.75	0.11	8.47	91.89	87.46	56.75	10.45
Argada- B	Min	0.41	nil	5.9	12.8	0.67	0.09	32.09	72.04	79.15	47.61	6.35
	Max	0.61	70.7	16.3	79.4	0.91	0.20	7.65	92.58	92.49	62.27	15.55
	Mean	0.49	43.1	11.0	54.1	0.76	0.14	9.03	91.41	87.42	56.70	9.28
Argada- C	Min	0.39	14.1	5.7	28.9	0.66	0.13	13.42	87.73	82.38	51.16	3.15
	Max	0.52	79.6	18.1	89.2	0.78	0.16	5.79	94.13	94.44	64.43	9.78
	Mean	0.46	53.4	10.5	63.9	0.71	0.14	7.13	93.01	89.38	58.86	5.87

Seam name		VRr max	Vitrinite	Liptinite	Reactive Macerals (RM)	H/C	O/C	RF (after Guyot, 1978)	Conversion (a) (after Guyot, 1978)	Conversion (b) (after Jin and Shi, 1997)	Oil yield (b) (after Jin and Shi, 1997)	Oil wt.% (after Saxby, 1980)
Argada- D	Min	0.37	19.1	9.0	33.9	0.59	0.09	10.98	89.78	83.38	52.26	1.35
	Max	0.50	77.6	20.4	88.2	0.84	0.20	5.67	94.24	94.23	64.19	11.17
	Mean	0.42	45.1	13.3	58.4	0.70	0.13	7.21	92.94	88.28	57.65	6.28
Argada- I	Min	0.46	8.0	9.1	21.6	0.70	0.10	21.10	81.27	80.92	49.55	7.41
	Max	0.62	30.8	25.8	42.5	0.75	0.19	14.63	86.71	85.10	54.15	6.15
	Mean	0.55	14.9	16.0	30.9	0.74	0.13	17.73	84.11	82.77	51.59	8.41
Argada- J	Min	0.41	0.8	8.1	15.1	0.74	0.05	27.14	76.20	79.63	48.13	12.84
	Max	0.63	51.4	23.9	70.5	0.81	0.15	8.89	91.53	90.71	60.32	12.67
	Mean	0.53	29.8	15.9	45.6	0.79	0.10	11.56	89.29	85.73	54.84	13.74
Argada	MIN	0.37	nil	0.8	12.8	0.59	0.05	5.67	72.04	79.15	47.61	1.35
Area	MAX	0.63	79.6	25.8	89.2	0.91	0.21	32.09	94.24	94.44	64.43	15.55
	MEAN	0.49	39.0	12.5	51.5	0.75	0.13	10.06	90.55	86.91	56.14	9.15
South	MIN	0.37	nil	0.8	12.8	0.59	0.03	5.55	72.04	79.15	47.61	1.35
Karanpura	MAX	0.66	92.8	26.5	97.3	0.92	0.32	32.09	94.34	96.06	66.21	17.80
coalfield	MEAN	0.51	52.5	11.6	64.0	0.77	0.15	8.70	91.69	89.41	58.89	9.63

7 CHAPTER 7. DISCUSSION

7.1 Introduction

With the help of several petrographic and geochemical analyses such as maceral analysis; microlithotype analysis; vitrinite reflectance measurement; proximate; and ultimate analyses; and techniques like XRD, XRF, FTIR, GC-MS, and Rock-Eval pyrolysis, an extensive dataset has been generated depicting the petrographic and geochemical characteristics of the coals present in different seams of Barka Sayal as well as Argada area of South Karanpura coalfield. The study could ultimately help in the petrochemical correlation of the coals of Barka Sayal and Argada area of South Karanpura coalfield.

These data have been synthesized to present the regional scale variation and correlation of coals of different seams along with their petrochemical characteristics, kerogen type, the possibility of coal being acted as source rock, thermal maturity, and the environmental impact of major/minor elements present in these coals, etc. The evolution of these coals has also been discussed with the help of maceral and microlithotype analysis. Coal facies, along with the type of flora, depositional environment, and coalification trend, have also been discussed in the present chapter. Based on qualitative and quantitative maceral and microlithotype data generated from a large number of pillar coal samples collected from the working mines of Barka Sayal and Argada area of South Karanpura coalfield. The discussion has been made in terms of the nature of flora, development of coal facies, depositional milieux, and geothermal history (coalification trend).

7.2 Petro-chemical characterization of coals of South Karanpura coalfield

The petrographic characterization of the coals of South Karanpura coalfield includes the qualitative and quantitative analyses of maceral, microlithotype, mineral matter, and vitrinite reflectance. The geochemical characterization was done with the help of different

analytical techniques such as proximate analysis (moisture, ash, volatile matter, and fixed carbon); ultimate analysis (C, H, N, S, and O); rock-eval pyrolysis (for source rock characteristics); major/ minor/ trace element analysis; and identification of organic/inorganic constituents using XRD, FTIR, etc. Enrichment or depletion of the important petrochemical components within the seam (top to bottom) has been discussed. The variation of petrochemical components within the seam and between the coal seams provide an idea about the changes occurring in the basin during the evolution of these coals.

Paleodepositional environment, lithostatic pressure, temperature, duration of heating, and post-tectonic transformation such as igneous intrusions, have played important roles in influencing the properties of coal. These changes left imprints that are designated by the petro-chemical properties. These parameters reveal clues to the genesis of coal and also control its industrial utilization. This trend of distribution of the petrographic components infers the climatic change and fluctuation of surface water cover during the coalification process in the basin. With increasing content of vitrain, coal becomes brighter while the dull appearance of coal increases due to the presence and increment of carbonaceous shale and dirt bands (Stach *et al.* 1982). The enriched vitrinite zones indicate a tropical, humid and temperate climate with wet conditions during the development of peat, favourable for the formation of humic acid. In contrast, inertinite-enriched zones are indicative of intermittent dry conditions, oxidation, intense microbial attack, and fire activities. With the advancement in coalification, the relative percentage of carbon increases, whereas the percentages of oxygen and hydrogen decrease. Care has been taken to present the variation of initial micro constituents depicting the processing of the field samples with minimal preparation required. Petrographic components have been presented with mineral matter, while proximate constituents have been discussed and presented on an as-

received basis. The amount of hydrogen estimated by the ultimate analysis includes the organic coaly substance, the moisture and water of the constitution of the silicate mineral (Speight 2015). The moisture content present in coal also influence the oxygen content during the ultimate analysis, so the ultimate analysis discussed here is based on a dry basis.

A noticeable variation has been observed in the micro petrographic and geochemical constituents of coals of South Karanpura coalfield concerning the macroscopic bands of the coals. Generally, with increasing bright constituents in the macroscopic bands of these coals, the vitrinite, vitrinite reflectance, moisture, volatile matter, fixed carbon, carbon, hydrogen, and nitrogen content increases, while dull bands exhibit an increase in inertinite, visible mineral matter, ash yield, and oxygen content. Sulphur content usually does not show any noticeable variation in these coals, mainly due to their low occurrence (<1%).

In the coals of Sayal seam of Barka Sayal area of South Karanpura coalfield mean vitrinite reflectance (VRo %) ranges in between 0.57% to 0.62%, mean 0.59%. Vitrinite reflectance does not show much variation along with the seam profile. These coals are vitrinite rich, and its content increases towards the top. The liptinite content decreases towards the top while inertinite content first decreases, then increases from bottom to top. Visible mineral matter possesses an increasing trend from bottom to top with a discernable break in the middle portion of the seam. This suggests stable water table conditions in the basin with one flooding event in the depositional period of the middle band which increases the mineral content in the middle portion; also the ash yield is high in the middle of the seam. The moisture content first decreases, then increases, and again decreasing from bottom to top of the seam. Volatile matter is found to increase from bottom to top while the fixed carbon first decreases; and then increase towards the top,

suggesting high-quality coal towards the top portion of the Sayal seam. Carbon, hydrogen, and nitrogen content first increases then slightly decreases from bottom to top of the seam. The sulphur content decreases towards the top (Figure 7.1).

Sayal Balkudra exhibit mean values of vitrinite reflectance ranging in between 0.40% and 0.48%, mean 0.44%. The vitrinite reflectance of these coals is found to increase from bottom to top with some variations influenced by bright and dull constituents. The presence of a high amount of bright constituents slightly increases the vitrinite reflectance and *vice versa*. Because of slow response to coalification by the admixed terriginous minerals associated with the organic substances. From bottom to top, the vitrinite content is first increasing, then decreasing in this seam with a sudden decrease in the middle portion, possibly due to the high influx of terrigenous minerals because of flooding. The seam contains high mineral matter towards the top and in the middle portion of the seam, possibly due to flooding events. Inertinite and liptinite content does not show many changes along the macro petrographic section. Moisture, fixed carbon, and volatile matter exhibit an increasing trend towards the bottom while ash yield decreases towards the bottom portion, suggesting coals of higher quality are present in the bottom portion of the seam. Carbon, nitrogen, and sulphur contents first decrease, then increase towards the bottom. Hydrogen content shows a fluctuating trend mainly controlled by the lithotype of the coal and approximately coincides with the trend of liptinite macerals, which are the hydrogen-rich macerals and possibly contributed to the hydrogen content analysed. (Figure 7.2).

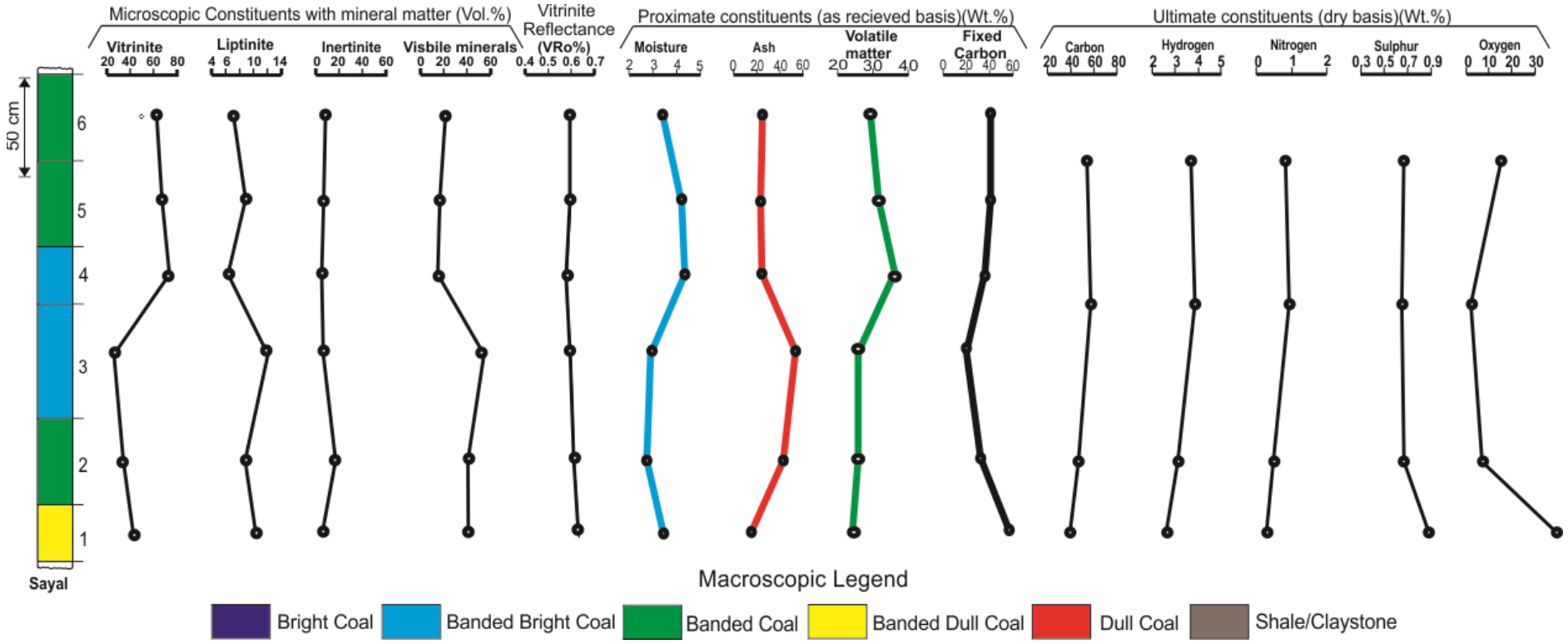


Figure 7.1 Macro-petrographic section, range of mean values of microscopic (maceral with mineral matter), vitrinite reflectance, proximate and ultimate constituents of Sayal seam, South Karanpura coalfield, India.

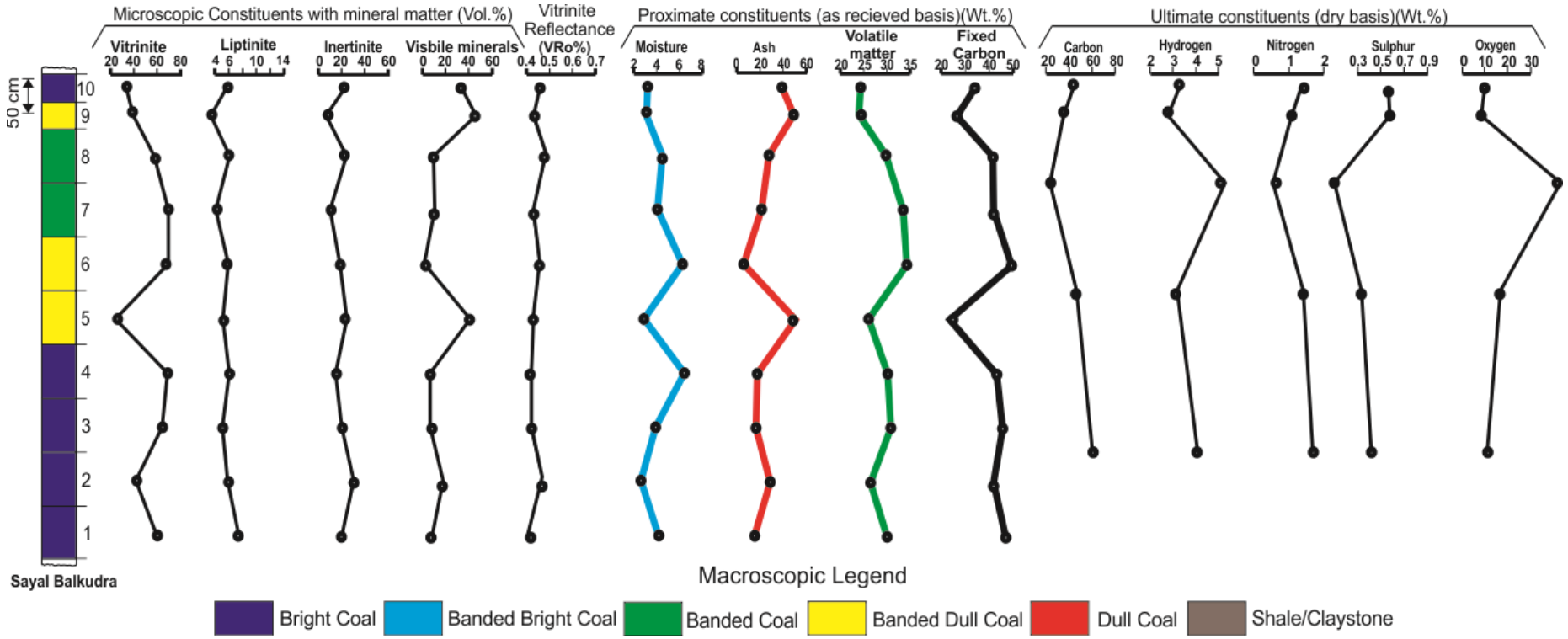


Figure 7.2Macro-petrographic section, range of mean values of microscopic (maceral with mineral matter), vitrinite reflectance, proximate and ultimate constituents of Sayal Balkudra seam, South Karanpura coalfield, India.

The vitrinite reflectance of Upper Semana varies from 0.45% to 0.51%, mean 0.49%. The variation in vitrinite reflectance and other petrographic and geochemical constituents shows two prominent episodes of variation in the depositional conditions along with the seam profile. The vitrinite reflectance exhibits an increasing trend towards the bottom, which indicates the inefficiency of syn-tectonic or post-tectonic disturbances. Vitrinite content is high in the middle portion of the seam where it reaches a maximum of 51.70 vol.% (54.47 vol.% mmf basis), while inertinite content shows a reverse trend and reaches a minimum in the middle portion of the seam. It suggests tropical, humid, and temperate climates with wet conditions prevailed during the formation of the middle portion of the seam which gradually changed to a relatively drier climate. Liptinite macerals exhibit a decreasing trend towards the bottom. Moisture and fixed carbon increase towards the bottom while ash and volatile content decrease towards the bottom portion. Carbon and hydrogen contents decrease towards the bottom while sulphur, nitrogen, and oxygen first decrease, then increase towards the bottom (Figure 7.3).

The Lower Semana coals have VRo % lying in the range of 0.44 to 0.54, mean 0.49, which is first increasing then decreasing towards the bottom of the seam. Vitrinite, moisture, volatile matter, fixed carbon, carbon (daf basis) and hydrogen (daf basis) reaches a maximum near to the bottom due to change in the megascopic band and presence of the “bright coal” band then slightly decreases towards the base, marked by the presence of again “banded coal” lithotype. Liptinite and inertinite content shows a decreasing trend up to the “bright coal” band near the bottom, further increasing towards the bottom. The Lower Semana seam exhibits a sequence of banded coal, banded bright coal, bright coal and again banded bright coal, which suggests a fluctuation of climate from wetter to drier and again wetter (Stach *et al.* 1982). Mineral matter and ash yield show a decreasing trend towards the bottom (Figure 7.4).

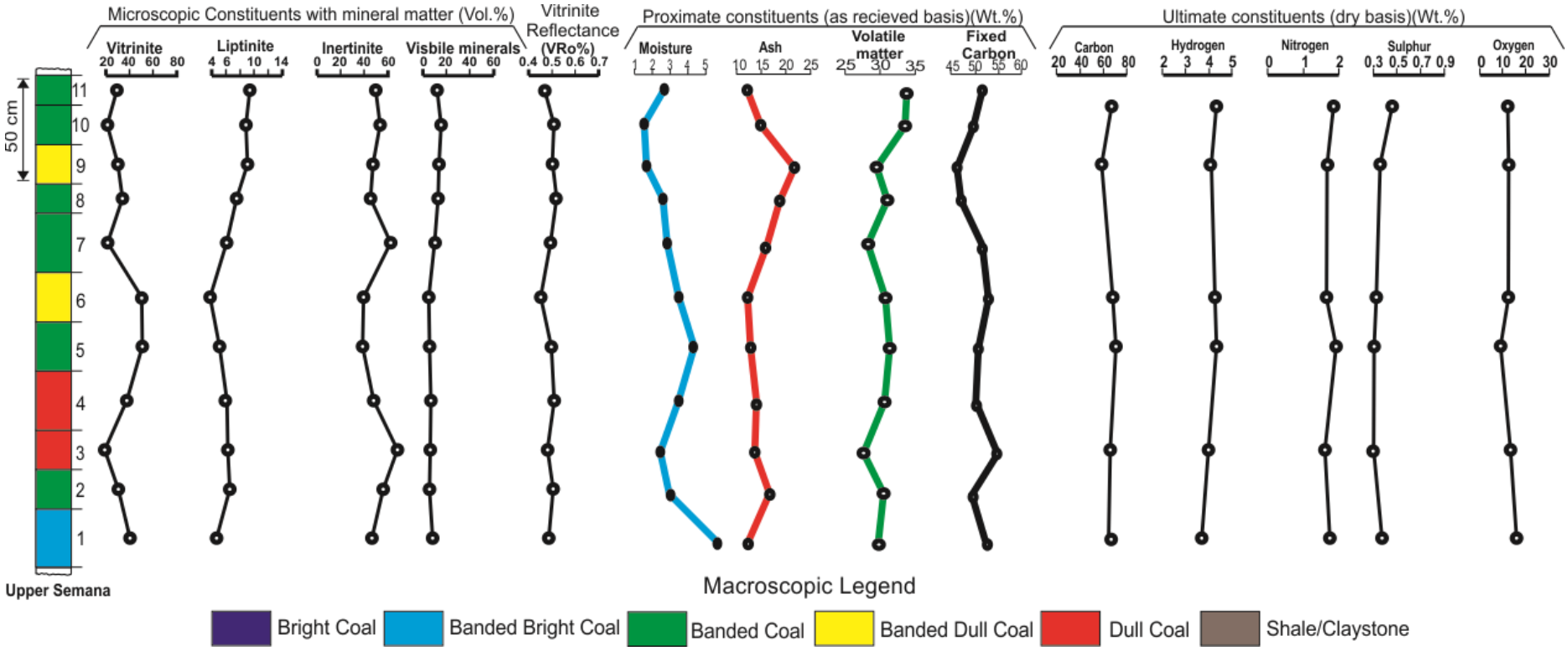


Figure 7.3 Macro-petrographic section, range of mean values of microscopic (maceral with mineral matter), vitrinite reflectance, proximate and ultimate constituents of Upper Semana seam, South Karanpura coalfield, India.

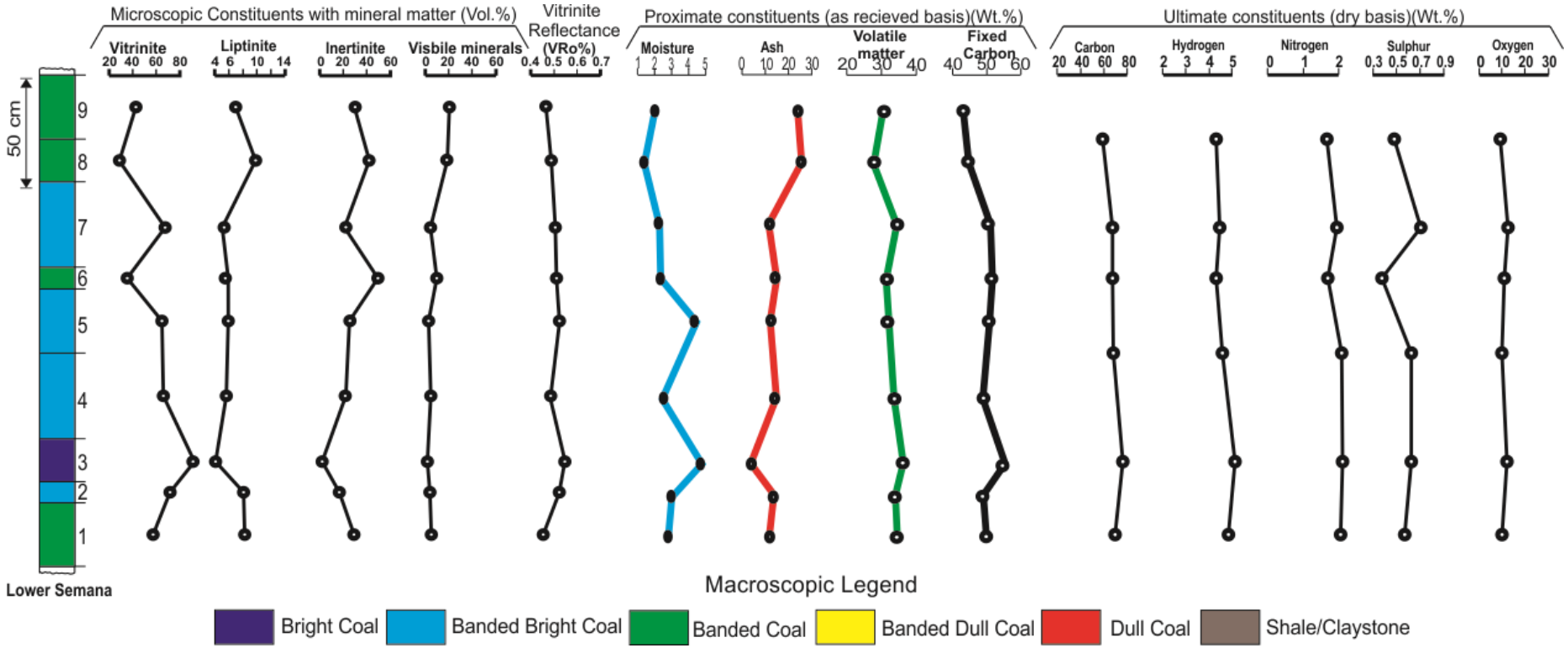


Figure 7.4 Macro-petrographic section, range of mean values of microscopic (maceral with mineral matter), vitrinite reflectance, proximate and ultimate constituents of Lower Semana seam, South Karanpura coalfield, India.

Hathidari coals have VRo % from 0.59 to 0.66, mean 0.62, the highest in the area. It shows a decreasing trend towards the bottom. The concentration of vitrinite macerals increases towards the bottom. Liptinite group shows a fluctuating trend from top to bottom, first decreases then increases till the mid-portion of the seam, and again increases towards the bottom, while inertinite macerals do not show many changes along with the seam profile. Mineral matter and ash yield increase towards the top, whereas moisture, volatile matter, and fixed carbon decreases in the top portion of the seam. The same phenomenon occurs with carbon, hydrogen and nitrogen and these contents show a decreasing trend towards the top, while sulphur first increases, then decrease and further increases towards the top (Figure 7.5).

The coals of the Bansgarha seam of the Barka Sayal area exhibit VRo% from 0.56 to 0.63, mean 0.59. In this seam, slight variation occurs in the values of vitrinite reflectance, vitrinite group, inertinite group, visible mineral matter, and volatile matter constituents because of the dominance of one type of macroscopic band, i.e. “banded coal” throughout the coal seam. Liptinite, moisture, ash yield sulphur and oxygen content shows an increasing trend towards the bottom while volatile matter, fixed carbon, carbon, hydrogen, and nitrogen content slightly decreases towards the bottom (Figure 7.6).

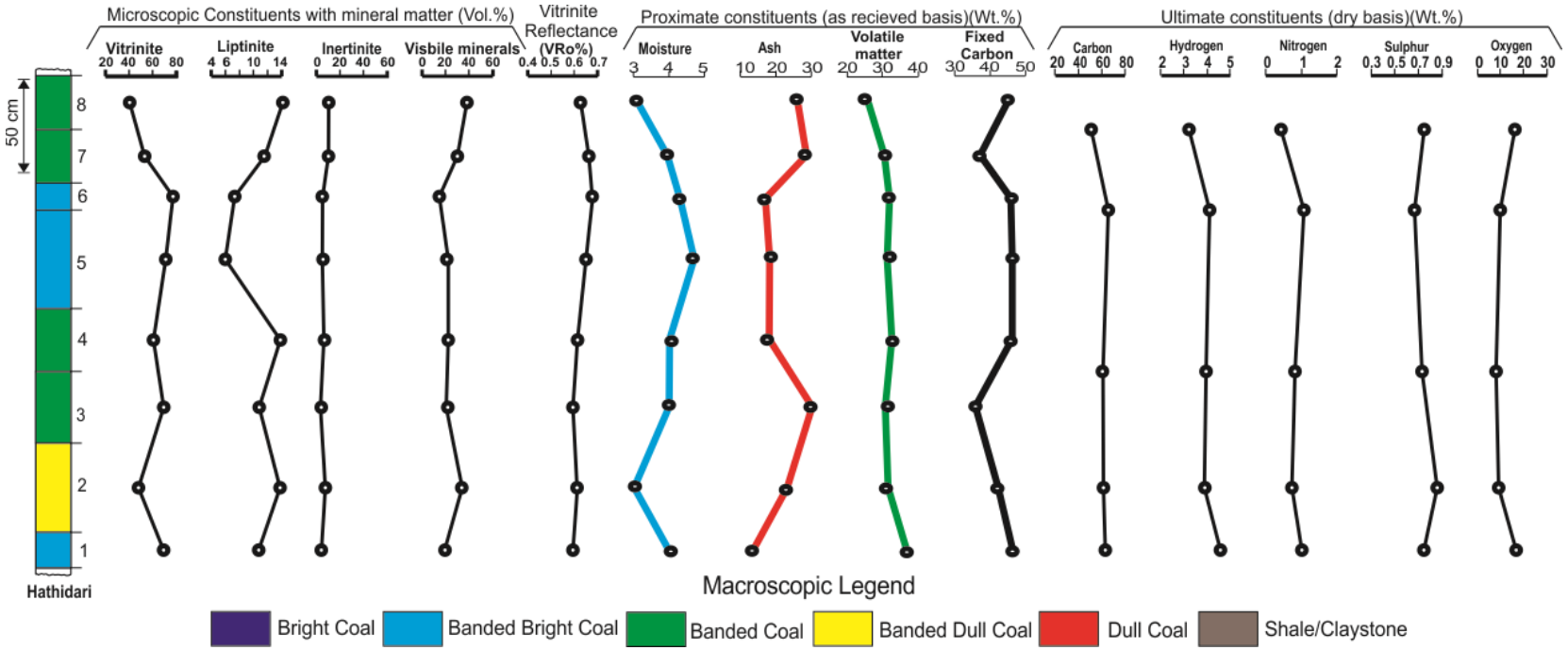


Figure 7.5 Macro-petrographic section, range of mean values of microscopic (maceral with mineral matter), vitrinite reflectance, proximate and ultimate constituents of Hathidari seam, South Karanpura coalfield, India.

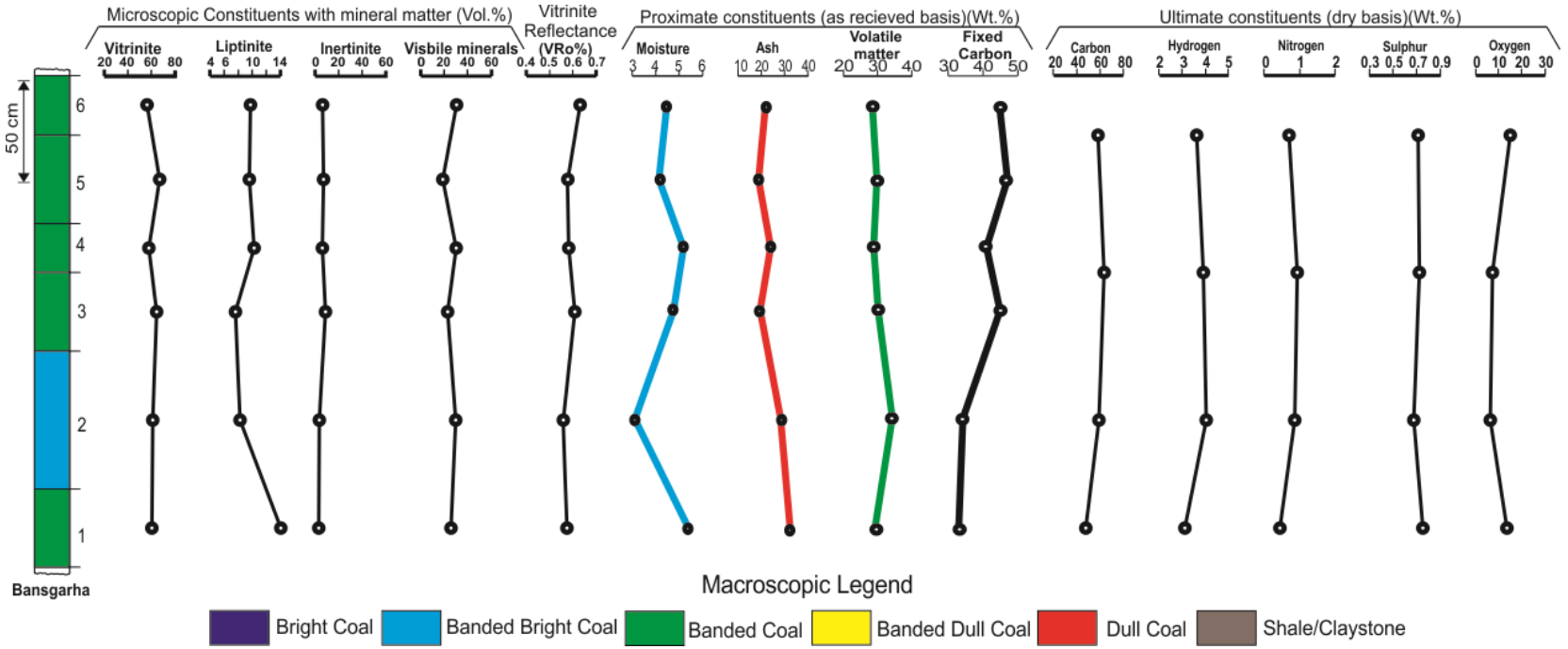


Figure 7.6 Macro-petrographic section, range of mean values of microscopic (maceral with mineral matter), vitrinite reflectance, proximate and ultimate constituents of Bansgarha seam, South Karanpura coalfield, India.

The seams of the Argada area are thicker than the seams of the Barka Sayal area. They show more variation in petrochemical constituents along with the seam profile because the deposition of thicker seams had taken sufficient geological span and exhibited more variation influenced by seasonal changes. Although the quality of these coals is comparatively poor but due to the presence of thicker bands, these seams are equally important. In the case of lithotype, coals of the Argada area are rich in “banded coal” and “banded dull coal”. The lower quality of these coals indicates less favourable depositional conditions and the high flux of terrigenous inorganic minerals in these seams.

The vitrinite reflectance of the coals of Argada seam increases towards the bottom and varies from 0.45% to 0.54%, mean 0.50% (Table 6.2). High-quality coals are present near the bottom of the seam indicated by the presence of high vitrinite, liptinite, volatile matter, and fixed carbon. Vitrinite and liptinite content further decreases towards the top portion of the seam. Moisture, carbon, hydrogen, nitrogen, and sulphur content are also high in the bottom of the seam, which decreases continuously till the middle section of the seam further increases towards the top. Visible mineral matter and ash yield exhibit fluctuation in their values according to the presence of different lithotype bands. Dull coal shows high peaks of ash yield; there it reaches a maximum of 65 wt.% near to the middle portion of the seam. The higher concentration of bright constituents near the bottom portion of the seam indicates wet and humid climate prevailed, which changed into dry climate and increased microbial activity during the formation of middle and top portion of this seam, marked by increased inertinite content (Figure 7.7).

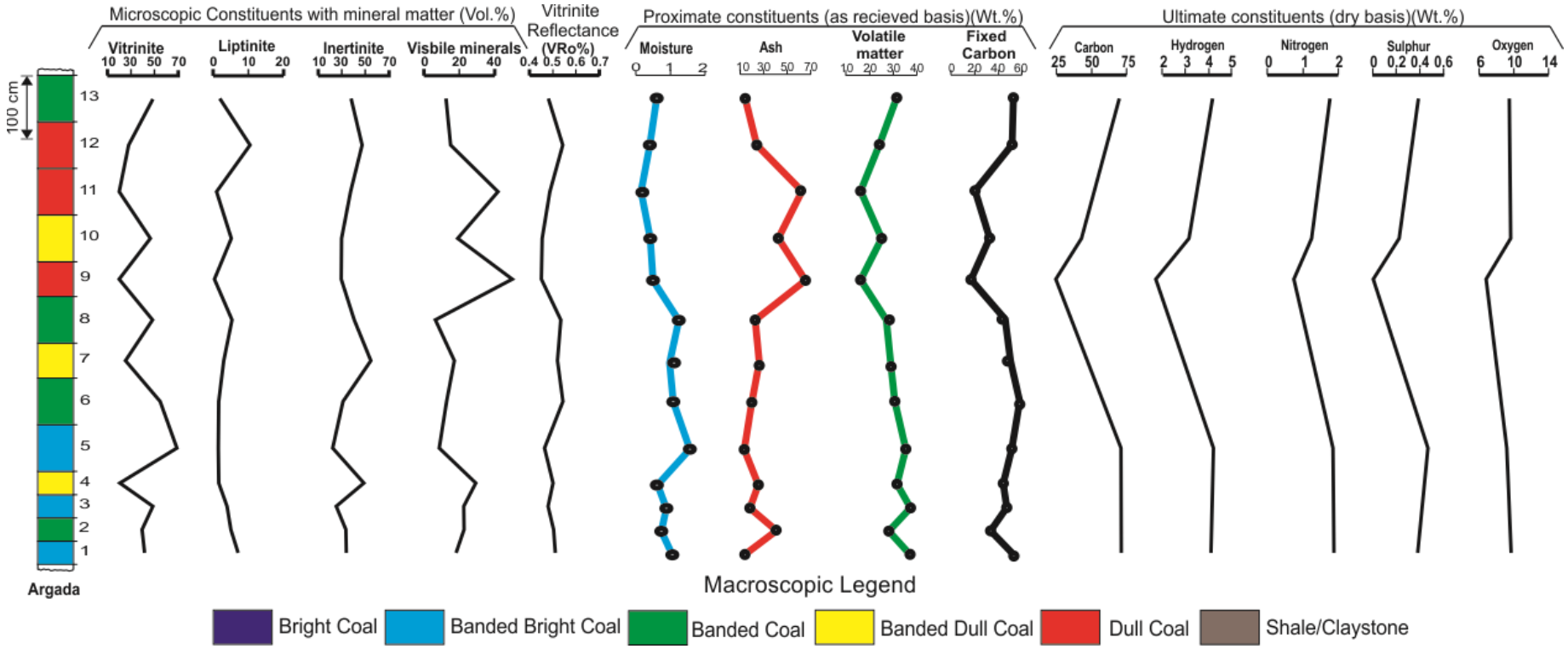


Figure 7.7 Macro-petrographic section, range of mean values of microscopic (maceral with mineral matter), vitrinite reflectance, proximate and ultimate constituents of Argada seam, South Karanpura coalfield, India.

For Argada-A, the vitrinite reflectance range lies in between 0.39% and 0.57%, mean 0.46%. This seam has high-quality coals near the bottom of the seam, indicated by high vitrinite, liptinite volatile matter and fixed carbon. The quality of the coal deteriorates towards the top. In the middle portion of the seam also a good quality of coals are present. The extreme change in depositional conditions deposited a 50 cm thick band of shale in the middle portion of this seam. Moisture content in this seam increases towards the bottom and the same with volatile matter and fixed carbon, whereas ash yield increases towards the top potion the seam. Ultimate constituents also show its variation influenced by lithotypes present. Carbon, hydrogen, and nitrogen content increase towards the bottom while sulphur and oxygen content increase, then decrease, towards the bottom (Figure 7.8). The fluctuation of megascopic bands and microscopic constituents indicate a wetter humid climate prevailed during the formation of the bottom portion of this seam, which subsequently changed into a drier season indicated by an increase in inertinite constituents and several events of flooding, which increased the ash yield.

The coals of Argada-B seam have VRo% lying in the range of 0.41 to 0.61, mean 0.49%. The bands present at the bottom portion of the seam exhibit comparatively less vitrinite reflectance than the bands present in the top portion. Vitrinite, liptinite, and inertinite content increase towards the bottom, whereas visible minerals are decreasing. Sudden change in depositional condition and the deposition of a high amount of allochthonous minerals are indicated by the presence of dull bands having a high content of visible minerals and ash yield. Moisture, volatile matter and fixed carbon exhibit an increasing trend towards the bottom. Ultimate constituents (daf basis, wt.%) such as carbon, hydrogen, sulphur and nitrogen first increases then decreases and again increases towards the top, whereas oxygen content first decreases then increases in the top portion of the seam (Figure 7.9).

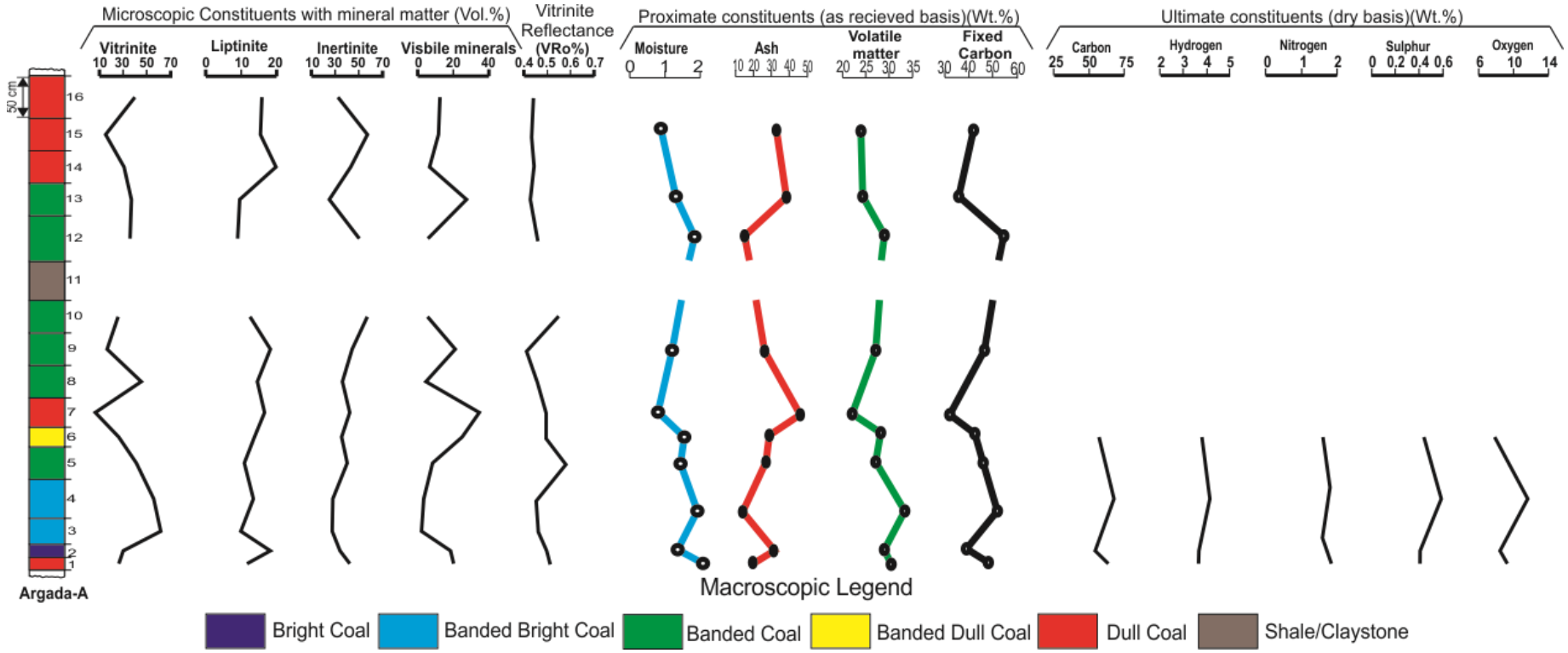


Figure 7.8 Macro-petrographic section, range of mean values of microscopic (maceral with mineral matter), vitrinite reflectance, proximate and ultimate constituents of Argada-A seam, South Karanpura coalfield, India.

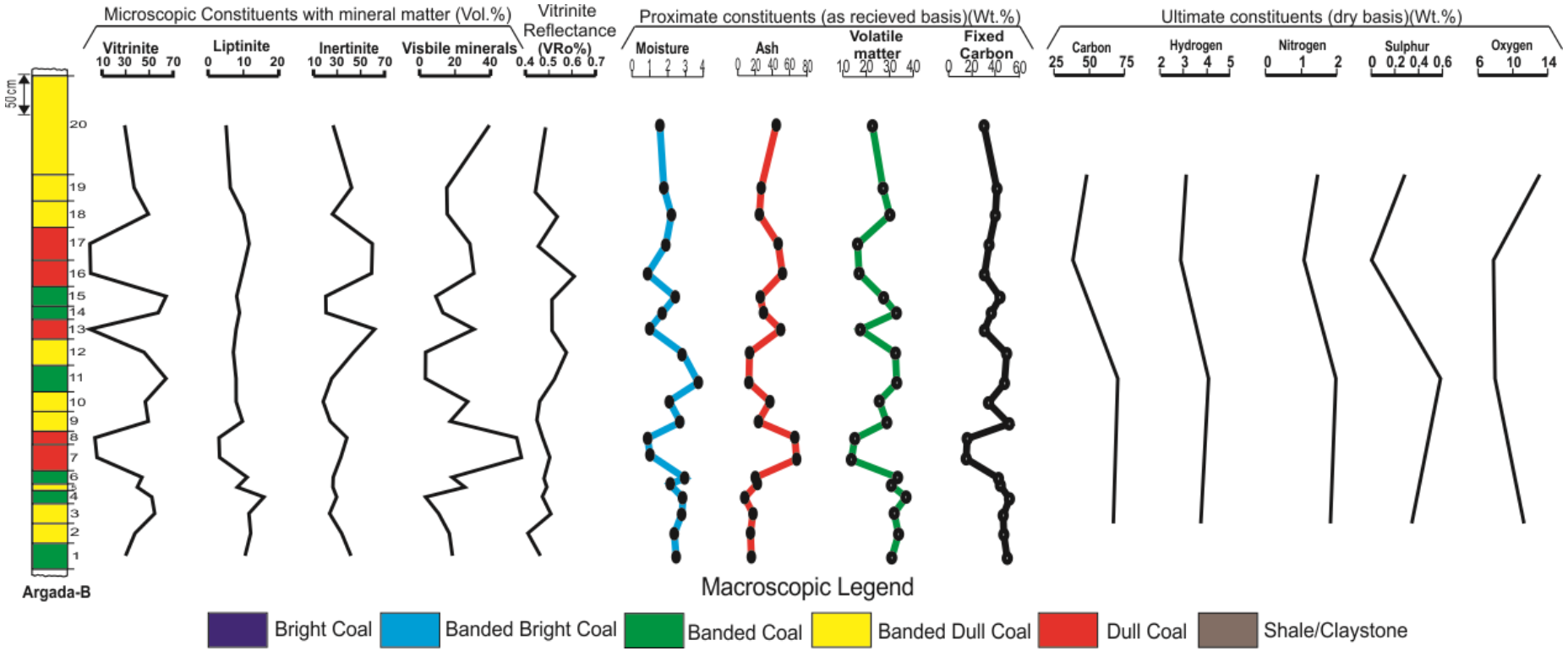


Figure 7.9 Macro-petrographic section, range of mean values of microscopic (maceral with mineral matter), vitrinite reflectance, proximate and ultimate constituents of Argada-B seam, South Karanpura coalfield, India.

VRo% of Argada-C seam is in between 0.39 and 0.52, mean 0.46. It does not show much variation along the top and bottom of the seam; only a slight variation occurs in the middle portion of the seam where the vitrinite reflectance decreases with the presence of a high amount of dull constituents. Vitrinite, liptinite macerals and visible minerals increase towards the bottom while inertinite macerals and roughly decreases towards the bottom portion of the seam. Moisture content first decreases then increases from bottom to top. Ash yield exhibits a decreasing trend towards the top, whereas fixed carbon content and volatile matter increase towards the top. Ultimate constituent such as carbon, hydrogen, nitrogen and oxygen does not show much variation in the top and bottom portion of the seam, but its quantity decreases in the middle portion. Sulphur content exhibits more variation and decreases to its minimum near to the top of the seam but further increases in the topmost part of the seam (Figure 7.10).

Coals of Argada-D seam have VRo% from 0.37 to 0.50, mean 0.42 and the seam shows a slight variation in the vitrinite reflectance. It increases towards the bottom. Vitrinite and liptinite content increases towards the bottom, whereas inertinite and visible minerals roughly decrease towards the bottom. These variations indicate coal of high-quality present near to the bottom portion of the seam. In the case of proximate constituents, moisture, volatile matter and fixed carbon decrease towards the top whereas ash yield increasing towards the top suggest good quality coals in the bottom portion of the seam and conforms the previous outcome based on microscopic constituents. Carbon, hydrogen and nitrogen content first increases but further does not show much variation towards the bottom of the seam. Sulphur content decreases towards the bottom, whereas oxygen content increases towards the bottom portion of the seam (Figure 7.11).

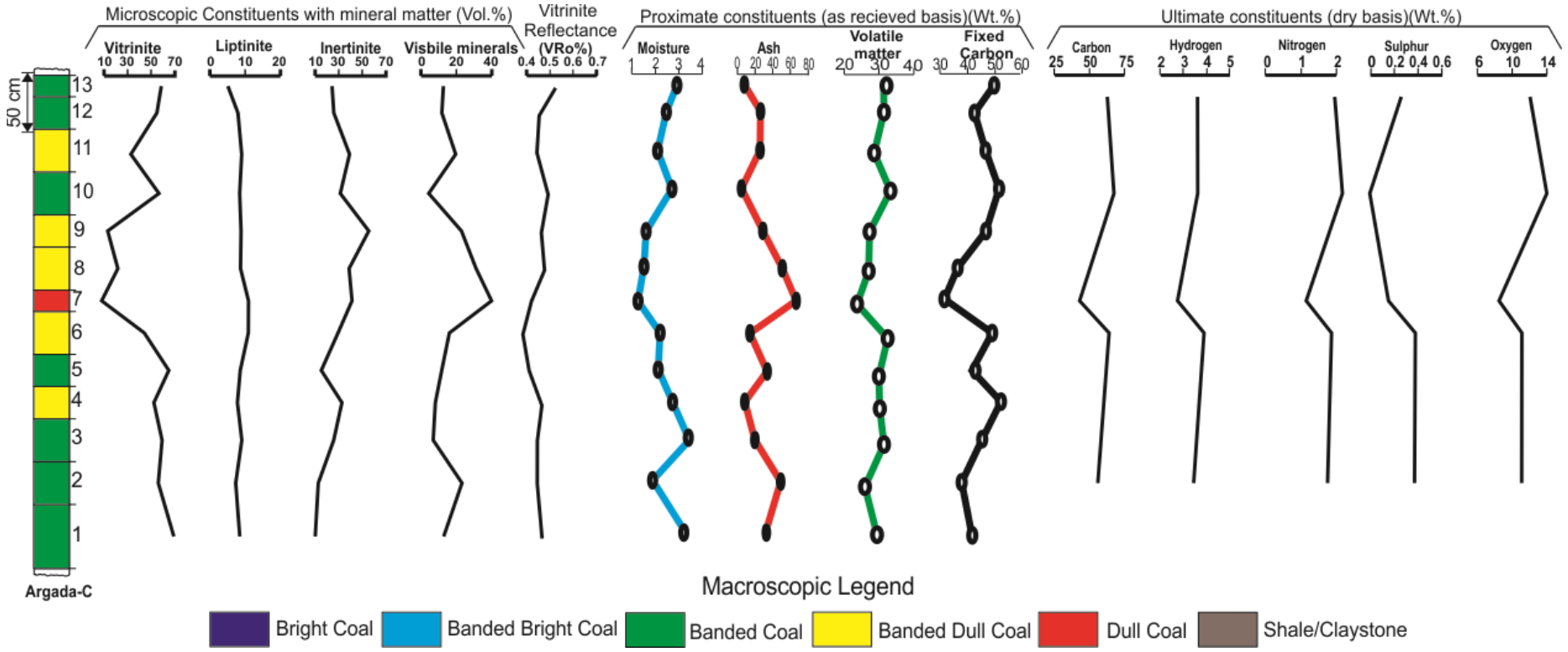


Figure 7.10 Macro-petrographic section, range of mean values of microscopic (maceral with mineral matter), vitrinite reflectance, proximate and ultimate constituents of Argada-C seam, South Karanpura coalfield, India.

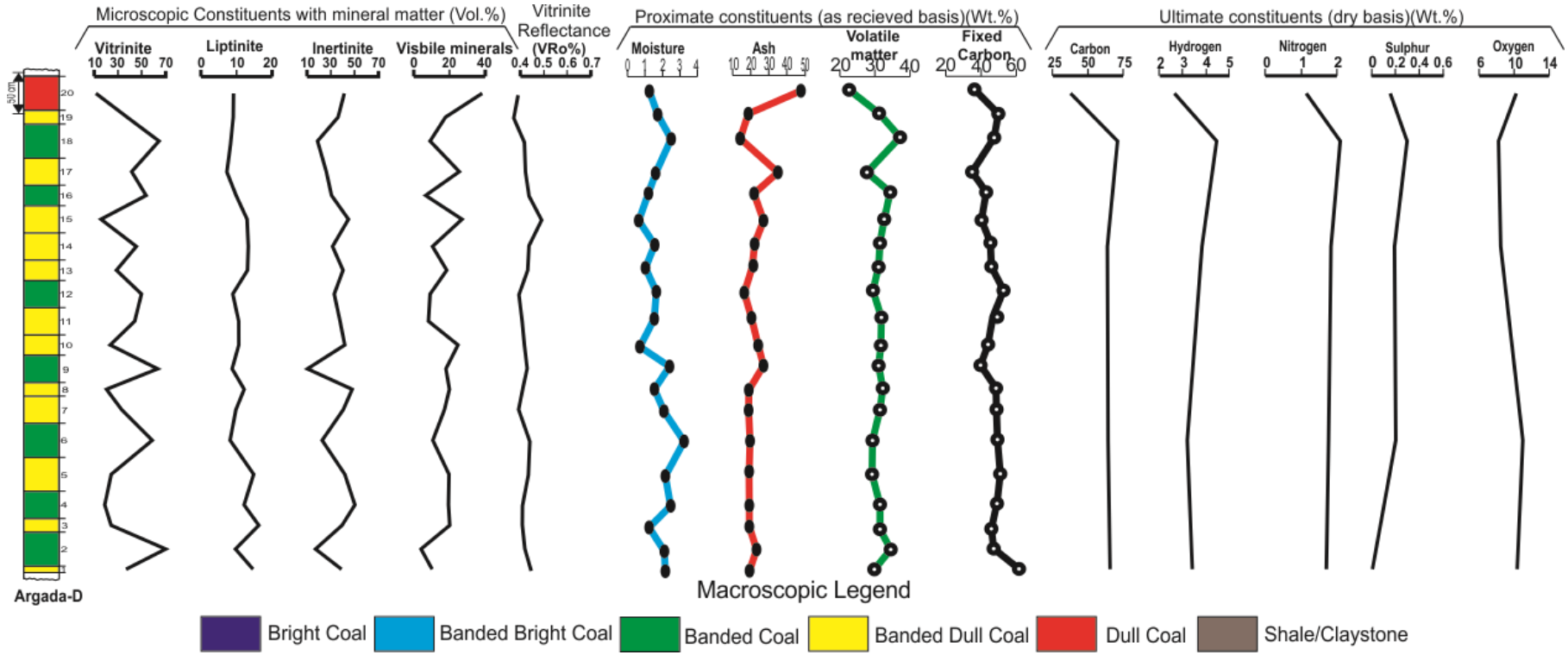


Figure 7.11 Macro-petrographic section, range of mean values of microscopic (maceral with mineral matter), vitrinite reflectance, proximate and ultimate constituents of Argada-D seam, South Karanpura coalfield, India.

Argada-I coals have vitrinite reflectance ranging in between 0.46 and 0.62, mean 0.55. The vitrinite reflectance shows an increasing trend towards the bottom of the seam. Vitrinite content also shows an increment towards the bottom, whereas liptinite and inertinite decrease towards the bottom of the seam. Moisture, volatile matter and fixed carbon increase towards the bottom of the seam whereas visible minerals and ash yield decreases towards bottom indicating high-quality coal present in the bottom portion of the seam, which conforms to the improvement in rank of the coal with depth due to coalification. The ultimate constituents also confirm the observation. Carbon and hydrogen both do not show much fluctuation till the bottom "banded coal" band and then show an increment in its values. Nitrogen and sulphur content also increases towards the bottom, whereas oxygen content first increases then decreases towards the bottom (Figure 7.12).

For the coals of Argada-J seam, the vitrinite reflectance varies from 0.41 to 0.63, mean 0.53. Vitrinite reflectance decreases towards the bottom. Vitrinite first increases, then decrease towards the bottom, while liptinite and inertinite increase towards the bottom. Visible mineral content also decreases towards the bottom, which is also supported by the ash yields decline. Moisture, volatile matter and fixed carbon show a fluctuating trend. Carbon, hydrogen, nitrogen, and sulphur first increase then do not exhibit much variation towards the bottom of the seam because of the presence of banded dull coal bands persistently towards the lower portion of the seam, whereas oxygen content decreases towards the bottom (Figure 7.13). The distribution of petrographic and chemical constituents along with the seam profile of different seams existing in both areas of South Karanpura coalfield indicates a small variation in the qualities of these coals.

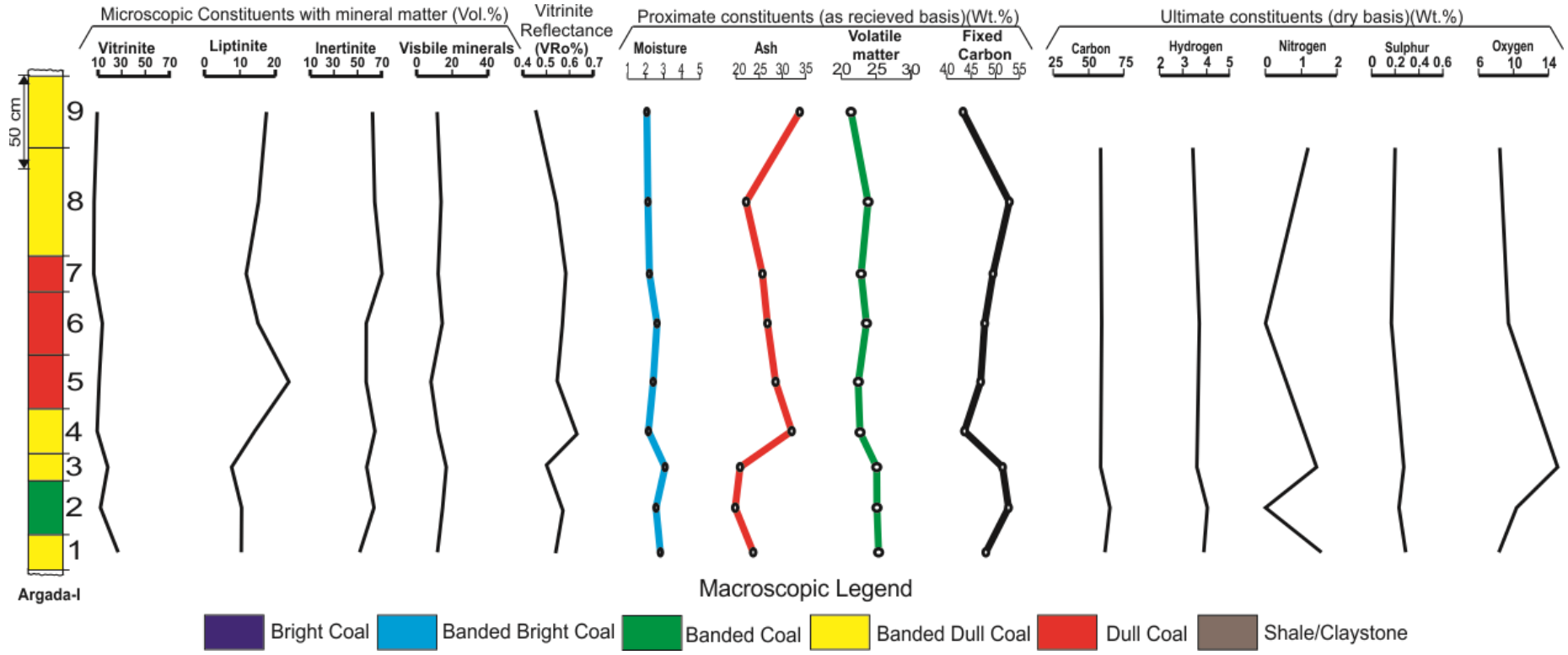


Figure 7.12 Macro-petrographic section, range of mean values of microscopic (maceral with mineral matter), vitrinite reflectance, proximate and ultimate constituents of Argada-I seam, South Karanpura coalfield, India.

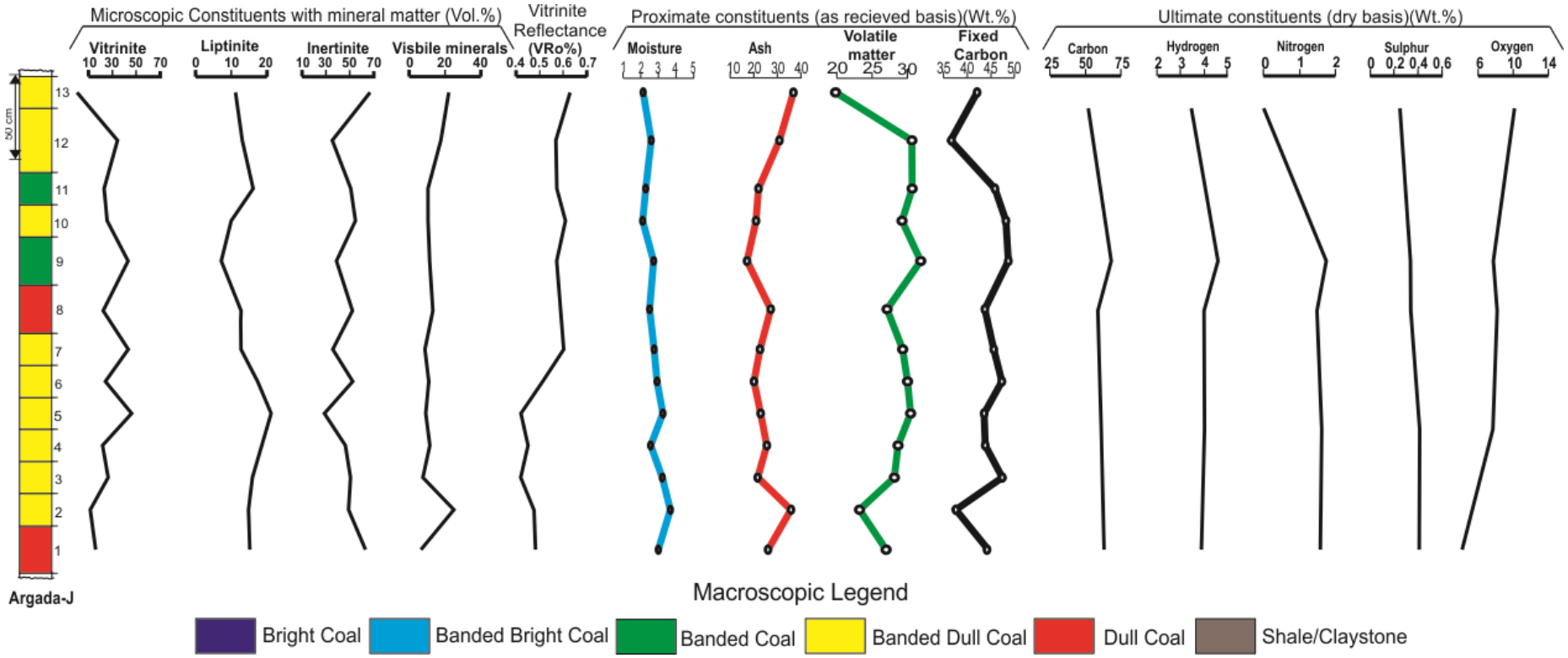


Figure 7.13 Macro-petrographic section, range of mean values of microscopic (maceral with mineral matter), vitrinite reflectance, proximate and ultimate constituents of Argada-J seam, South Karanpura coalfield, India.

It suggests that more or less similar depositional conditions have prevailed during the formation of the coals belonging to both areas. The slight variation in the petro-chemical properties may be guided by the varying nature of peat-forming plant communities, seasonal climatic fluctuations, tectonic settings, and water table conditions.

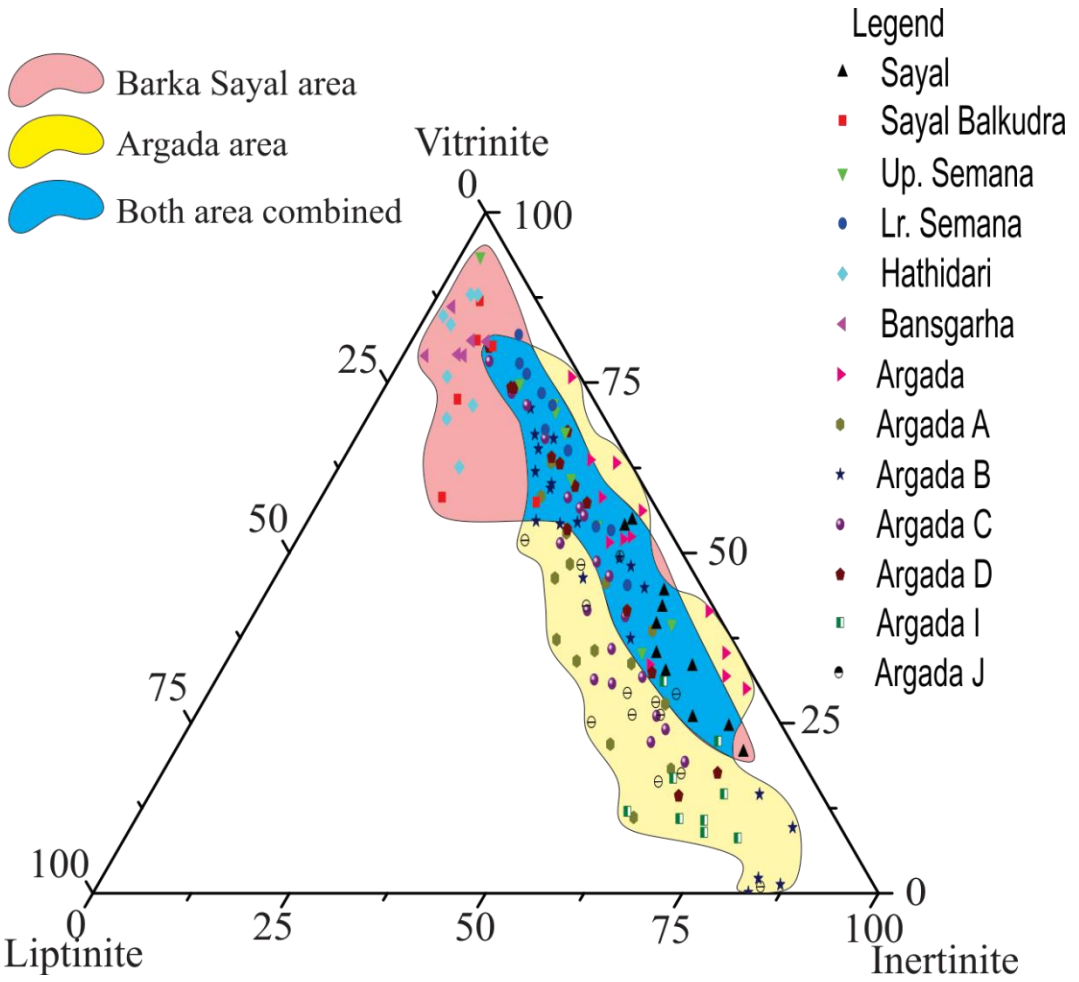


Figure 7.14 Ternary plot exhibiting the distribution of group macerals (mmf basis) in coals of South Karanpura coalfield.

For the petrographic characterization of coal deposits of South Karanpura coalfield, a ternary diagram based on the group maceral composition (mmf basis) has been applied. It clearly shows the dominance of vitrinite, followed by inertinite and liptinite in these coals. It is also clear from the plot that coals of the Baraka Sayal area comparatively rich in vitrinite, whereas coals of the Argada area are rich in inertinite (Figure 7.14). The concentration of liptinite is variable in both the area but generally, does not exceed 25 %.

The coals of Barka Sayal area exhibit liptinite concentration ranging from 3.65% to 13.97%, mean 8.08% (3.99%-26.47%, mean 10.65%, mmf basis), whereas the coals of Argada area show liptinite concentration varying in between 0.40% and 23.76%, mean 10.50% (0.81%-25.81%, mean 12.50%, mmf basis).

The ternary plot of the microlithotype composition (mmf basis) of the coals of South Karanpura coalfield shows that these coals are significantly rich in vitrinertite, which belongs to the intermediates group of microlithotype. Coals of Sayal, Sayal Balkudra, Hathidari and Bansgarha seams are rich in vitrite and clarite, whereas coals of Argada-B and Argada-I seams are durite and inertite-rich. Coal seams of Upper Semana, Lower Seaman, Argada, and Argada-A are vitrinertite rich (Figure 7.15).

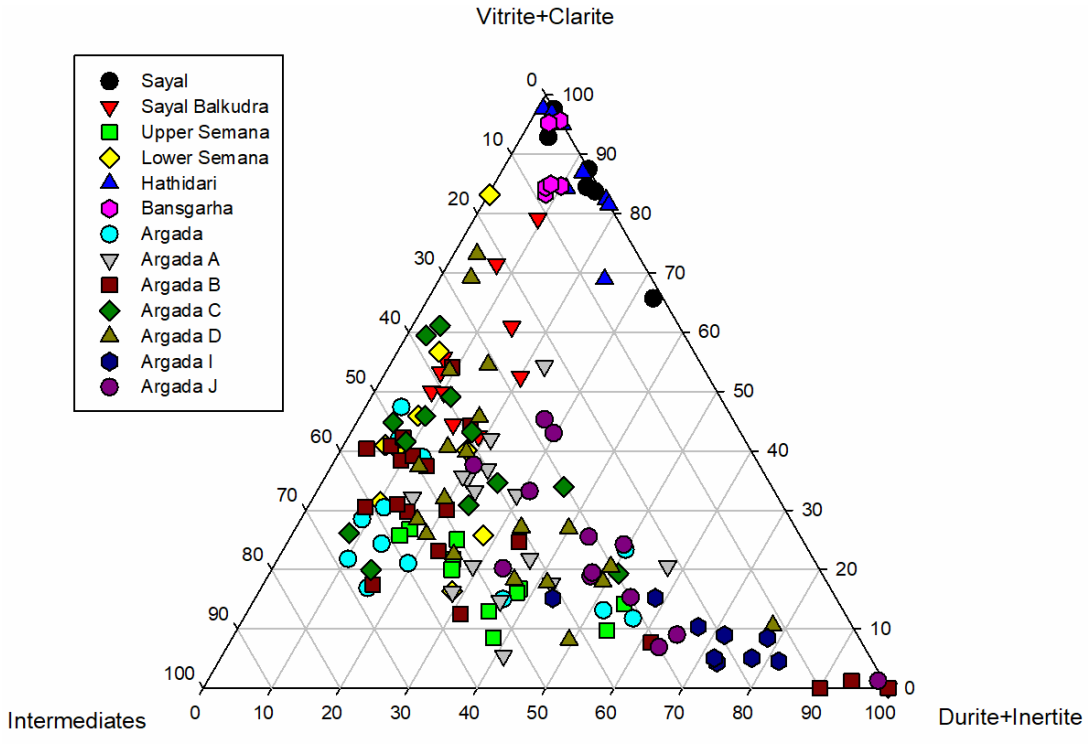


Figure 7.15 Ternary plot exhibiting the distribution of microlithotype (mmf basis) in coals of the South Karanpura coalfield.

An attempt has been made to find out the interrelation between the petrographic and chemical constituents with the help of the scatter plots. The relationship between vitrinite and liptinite (Figure 7.16A) shows that in these coals, liptinite increases with the decrease

of vitrinite. Further, the relationship between vitrinite and inertinite indicates (Figure 7.16B) a negative correlation between the vitrinite and inertinite content of these coals. Because vitrinite macerals get converted into inertinite macerals during the formation of inertinite group of macerals. All three groups of macerals show a negative correlation with the visible mineral matter, and their concentration decreases with increasing content of mineral matter (Figure 7.16C, D and E). Inertinite and liptinite are found a positive correlation with each other (Figure 7.16F).

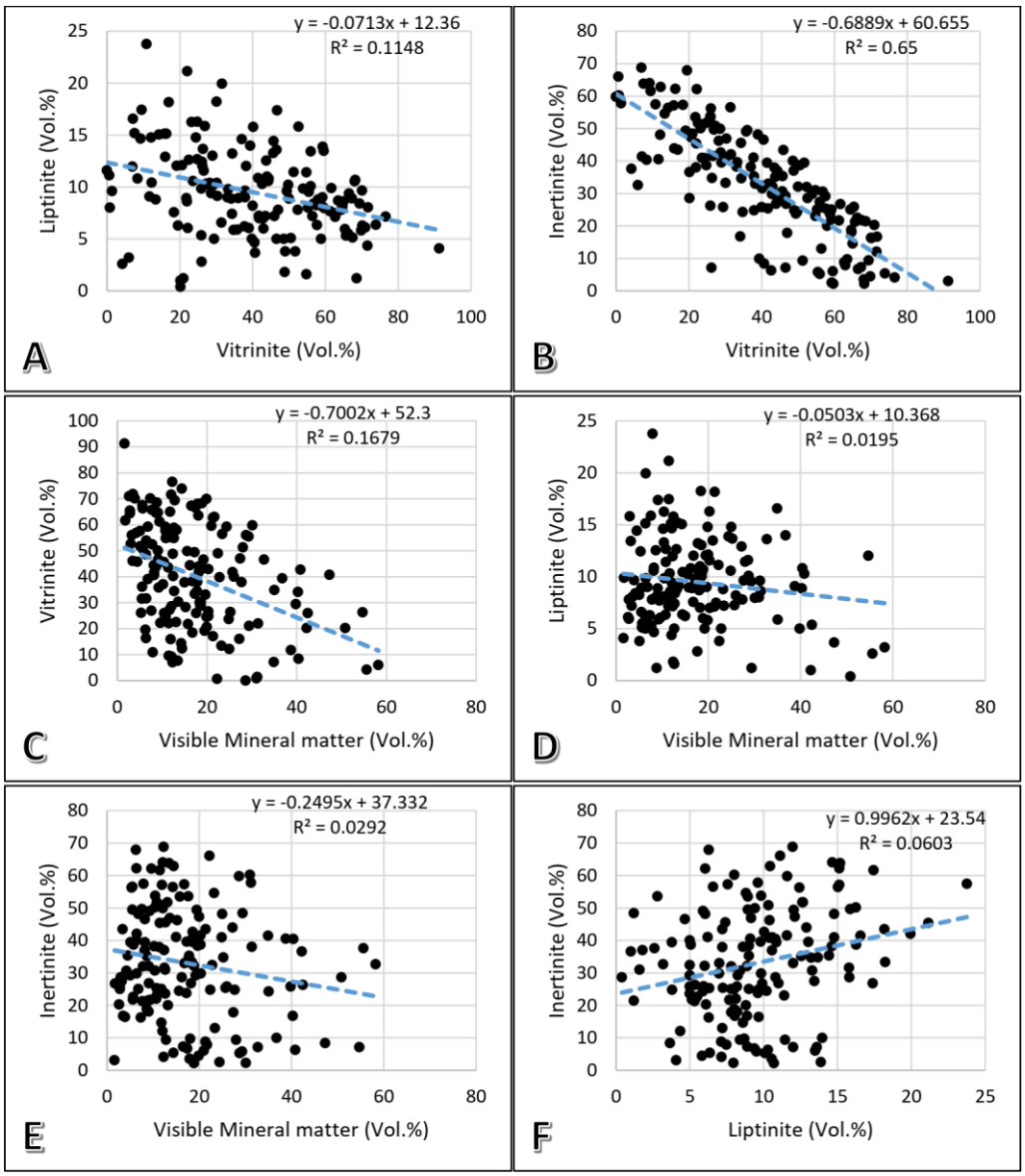


Figure 7.16 Interrelationship among micropetrographic (vitrinite, liptinite, inertinite and visible mineral matter) constituents for coals of South Karanpura coalfield.

An attempt has been made to find out the interrelationship of micropetrographic constituents (vitrinite, liptinite, inertinite, and their various combinations, mmf basis) with proximate constituent (volatile matter, daf basis). It is found that the vitrinite group of macerals have a positive correlation with the volatile matter. Those combinations in which vitrinite macerals was one of the components also found in positive correlation with the volatile matter, whereas the correlation of liptinite, inertinite, and (liptinite+inertinite) with volatile matter is found negative, which suggests that most of the volatile constituents are escaping from the vitrinite macerals (Figure 7.17A to C). Figure 7.17A exhibits a positive correlation between the vitrinite group of macerals and the volatile matter, suggesting that most of the volatile matter is coming out during the proximate analysis from the vitrinite macerals. It also suggests that the volatile matter may be in an adsorbed stage in the micropores present in the vitrinite group of macerals. Figure 7.17B shows a weak relationship between the liptinite group of macerals and volatile matter, which may be possible due to the presence of a very low concentration of liptinite macerals (<15%)` in these coals. Even at the microlithotype level, the concentration of microlithotype containing liptinite group of maceral is very low. In Figure 7.17C inertinite group of macerals is shown in a negative correlation with the volatile matter, which agrees with the general convention stating that the inertinite group of macerals generally remain inert in coal carbonisation processes. Thus they do not contain enough volatile matter. Even some of the macerals have a high concentration of semifusinite maceral, but that also seems not to produce enough volatile matter.

A scatter cross plot of volatile matter (daf basis) and fixed carbon (daf basis) with mean vitrinite reflectance for the coals of South Karanpura coalfield exhibit an insignificant correlation. The coefficient of correlation is also found very low which suggests that the rank variation of these coals is hard to distinguish with the help of proximate constituents

(Figure 7.18). The sloppiness in the correlation is a function of the influence of maceral variation on the VM in this rank range. The correlation plot of ash yield with visible mineral matter and carbominerite concentration shows a positive correlation, whereas the correlation of ash yield with volatile matter and fixed carbon is negative (Figure 7.19).

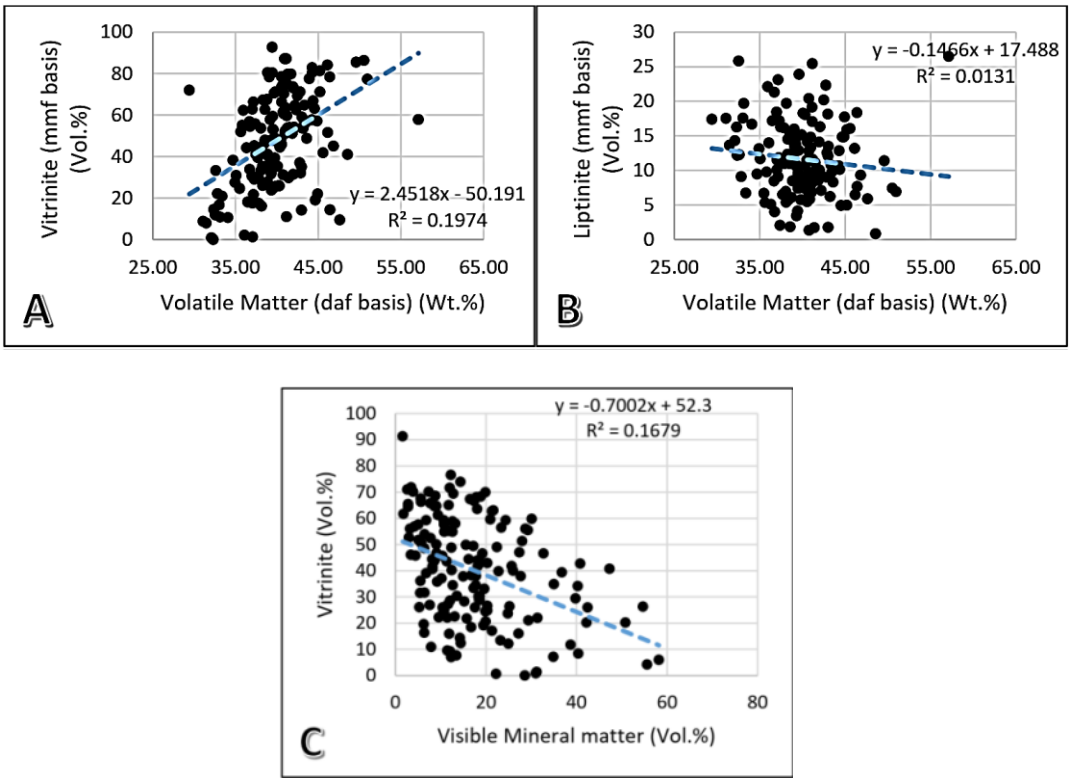


Figure 7.17 Interrelationship among micropetrographic (vitrinite, liptinite, and inertinite) and proximate (volatile matter, daf basis) constituents for coals of South Karanpura coalfield.

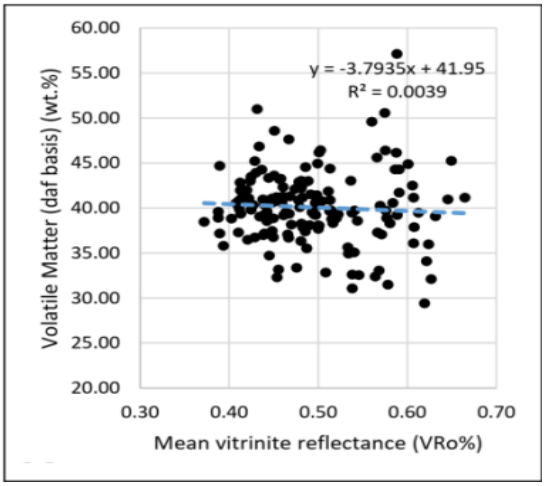


Figure 7.18 Interrelationship between vitrinite reflectance and volatile matter (daf basis) for coals of South Karanpura coalfield.

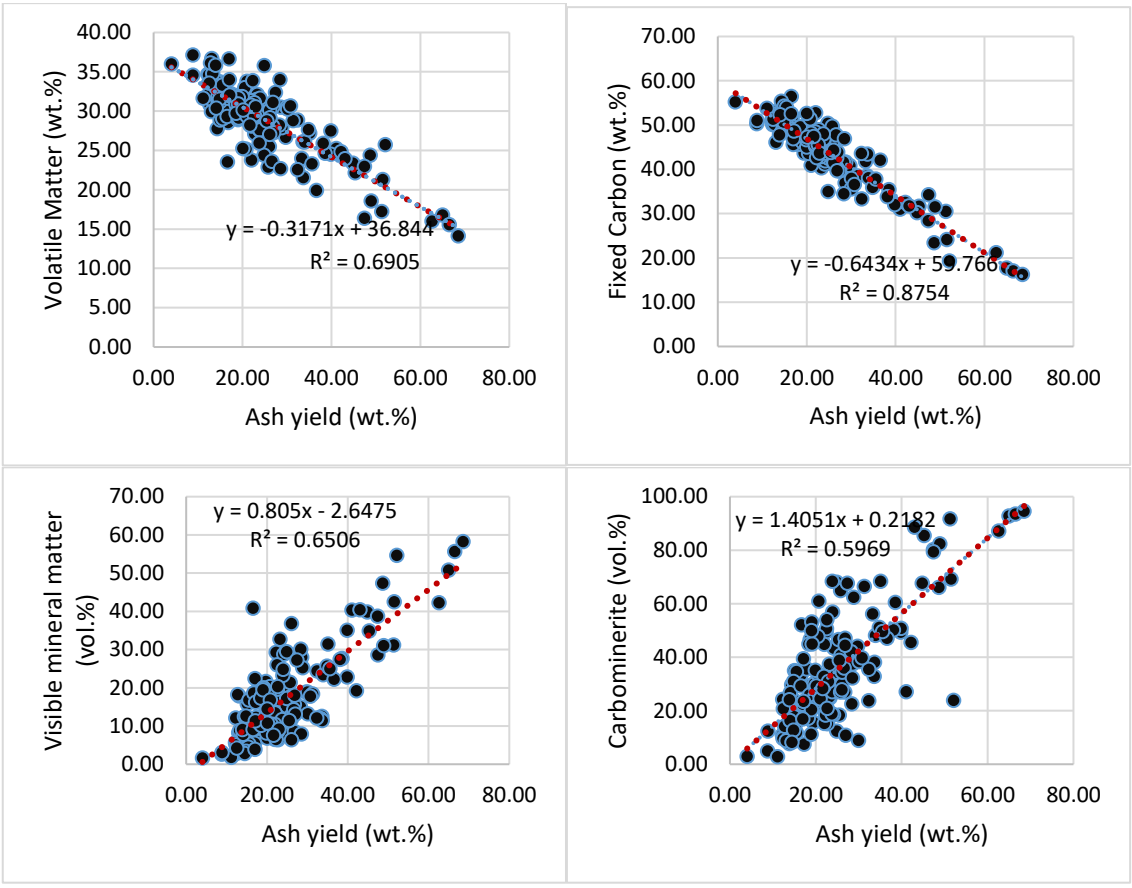


Figure 7.19 Interrelationship of ash yield with the volatile matter, fixed carbon, visible mineral matter, and carbominerite concentration (all as received basis) for coals of South Karanpura coalfield.

7.3 Kerogen Type

Kerogen is the macromolecular organic matter insoluble in aqueous alkaline solvents and common organic solvents (Tissot and Welte 1984). It is formed by the degradation of a variety of organic materials, including, pollen, algae, bacteria, plants, and structureless material and found dispersed in fine-grained sedimentary rocks. The thermal cracking of kerogen with maturation leads to the generation of liquid or gaseous hydrocarbons. With the help of analytical techniques such as proximate analysis, Rock-Eval pyrolysis, organic geochemical methods, and optical microscopy organic matter can be used to characterize as kerogen type. The determination of the quantity of organic matter can be assessed using an optical microscope. The petrographic techniques such as vitrinite reflectance also give clues about the maturity of organic matter and its hydrocarbon generation potential.

One of the most popular and widely accepted methods for kerogen characterization is that of van Krevelen (1961), based on H/C and the O/C ratio of the organic matter. According to this method, kerogens are classified into four types. Type I kerogens, with an atomic ratio of H/C > 1.25 and O/C < 0.5 are generally derived from anoxic lacustrine environment formed from protein and lipid precursors composing alginite, amorphous organic matter, cyanobacteria, algae, etc., and it is highly oil-prone. Type II kerogens, with an atomic ratio of H/C between 1 and 1.25 and O/C ratio ranging from 0.03 to 0.18, are derived from marine planktons and algae and is oil and gas prone. Type III kerogens, with a H/C ratio less than 1 and O/C ratio between 0.03 and 0.3, are derived from terrestrial plants and it is gas prone. Type IV kerogen, exhibiting a H/C ratio of less than 0.5, comprises mostly inert organic matter and it may generate dry gas only. The method of van Krevelen was further modified by several authors (McIver 1967; Welte 1969; Alpern *et al.* 1972; Jones and Edison 1978). The H/C and O/C ratios of South Karanpura coals were plotted on the modified van Krevelen diagram after Jones & Edition (1978) shows that these coals are Kerogen type III (Figure 6.7). The output is further supported by the scheme of kerogen characterization based on maceral constituents (Cornford 1979) (Figure 7.21). The high volume % of vitrinite and inertinite macerals and relatively low amount of liptinite macerals present in these coals characterizes these coals mostly as Type III, whereas inertinites rich bands are categorized as Type IV kerogen (Figure 6.2 and Figure 7.21). The cross plot of HI and OI of these coals characterizes these coals between Type II and Type III kerogen and suggests the possibility of generation of some amount of mixed liquid and gaseous hydrocarbons due to high hydrogen index of these coals (Figure 6.3). The same outcome was further supported by the scheme proposed by Petersen (2005) using vitrinite reflectance and HI (Figure 6.4) and the scheme based on HI and Tmax of these coals (Van Koeverden *et al.* 2011) (Figure 6.8). A cross plot using

S2 and TOC of these coals also supports the same belief and indicates most of these coals are gas-prone Type III kerogen while some of the bands lie in the field of mixed Type II-III kerogen capable of generation of mixed liquid and gaseous hydrocarbons (Figure 6.5).

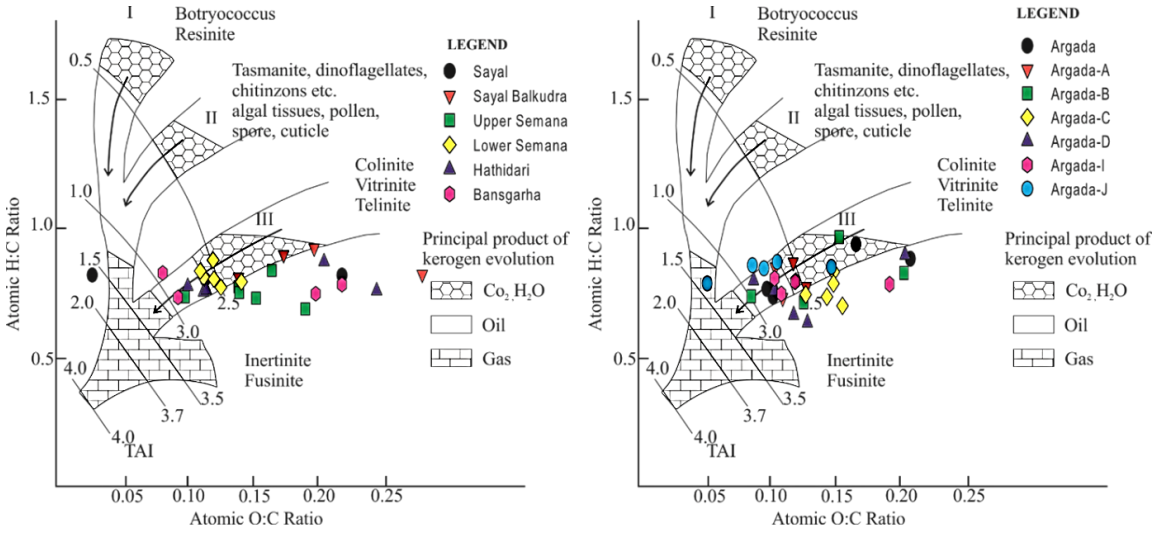


Figure 7.20 The kerogen type in coals of South Karanpura coalfield (after Jones and Edison, 1978).

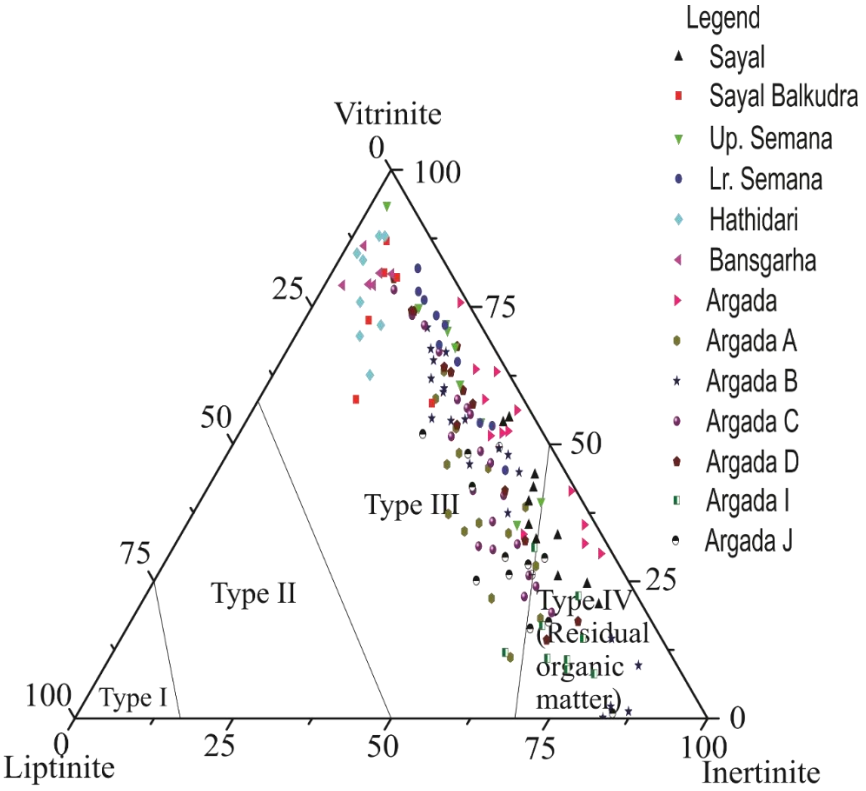


Figure 7.21 Type of kerogen present in coal seams of South Karanpura coalfield (after Cornford, 1979).

7.4 Thermal Maturity and oil potential

The average Tmax (422 °C) from Rock-Eval analyses, as well as vitrinite reflectance (0.49%-0.54%, mean 0.51%), indicate the rank of the coals of the South Karanpura coalfield lying in the range of subbituminous C to high volatile C bituminous. The immature stage of the thermal evolution of the South Karanpura coals is also evident from the molecular thermal maturity indicators from the aliphatic and aromatic fractions. Coal acting as a type of kerogen can expel hydrocarbons. Hedburg (1968) was one of the earliest researchers who established the role of terrigenous organic matter for the generation of oil. This belief was further supported by several authors (Durand and Paratte 1983; Murchison 1987a; Abdullah 1999; Callejon and Bissada 2001; Sykes and Snowdon 2002; Abbassi *et al.* 2016; Singh and Jha 2017; Takahashi *et al.* 2020). There are few coalfields reported worldwide (Khorasani 1987; Petersen *et al.* 2000) acting as the source rock for petroleum system, for example, the Surat basin in Australia (Khorasani 1987); the Ruhr Basin, northwest Germany (Littke *et al.* 1990); Barito Basin in Southeast Kalimantan, Indonesia (Witts *et al.* 2012); the Northeast Ordos Basin of China (Guoyi *et al.* 2010; Zhang *et al.* 2017) etc. Liptinite-abundant coals are rich in hydrogen and can efficiently expel hydrocarbons (Saxby 1980; Saxby and Shibaoka 1986; Erik and Sancar 2010; Dutta *et al.* 2011b). It has been observed that synthetic crude produced from coals exhibits a great similarity with the crude produced from the adjoining oilfields (Raja Rao 1981). Also, cases of coexisting of crude and coal in the same geological formations indicate a relationship between these two (Saikia and Dutta 1980; Levine 1993; Petersen *et al.* 2000; Qi 2011; Petersen and Hertle 2018). Crudes containing high wax content may find their origin from high wax containing terrigenous source material (Hunt 1991).

The guidelines for the interpretation of the source rock potential of the coal has been provided by several authors based on its petrochemical parameters. Peters (1986) has

evaluated a system for assessing the source rock potential based on the analytical result of Rock-Eval pyrolysis. Sykes & Snowdon (2002) used the parameters bitumen index (BI), defined as S1/TOC (Killops *et al.* 1978), and the quality index (QI), defined as (S1+S2)/TOC (Pepper and Corvi 1995) for the determination of the petroleum potential of coaly source rocks. The results of Rock-Eval pyrolysis of the South Karanprua coals is discussed in Chapter 7. The Total Organic Carbon (TOC) content in the coals of the South Karanpura coalfield is high, which varies from 16.97 (wt. %) to 81.93 (wt. %), mean 54.37 (wt. %). The value of S1 peak (free hydrocarbon) is low, varying from 0.14 mg HC/g rock to 2.84 mg HC/g rock, mean 0.90 mg HC/g rock. The S2 peak, which represents the number of hydrocarbons generated through thermal cracking of nonvolatile organic matter varies from 29.97 mg HC/g rock to 153.50 mg HC/g rock, mean 93.87 mg HC/g rock for coals of South Karanpura coalfield. The S3 content of the coals of South Karanpura coalfield varies from 1.07 mgCO_2/g rock to 23.74 mgCO_2/g rock, mean 7.79 mg CO_2/g rock. Tmax for these coals varies from 129 °C to 435 °C, mean 422 °C. The Hydrogen Index (HI) of the coals of South Karanpura coalfield varies from 65 mg HC/g TOC to 262 mg HC/g TOC, mean 175.02 mg HC/g TOC. The Oxygen Index (OI) for coals of South Karanpura coalfield lies in the range of 2 mg CO_2/g TOC to 67 mg CO_2/g TOC, mean 16.16 mg CO_2/g TOC. The production index of the coals of South Karanpura coalfield varies from 0 to 0.03 and do not possess any characteristic difference in both areas. As per the guidelines of source rock generative potential (Peters, 1986), the geochemical parameters obtained by rock-eval pyrolysis (S1, S2, and Tmax) indicate that the coals of South Karanpura coalfield are excellent source rock for hydrocarbon generation.

7.5 Indication of Petroleum Generation

In petroleum geology, the oil window, i.e. the maturity ranges in which a source rock expels liquid hydrocarbon ranges from 0.5- 0.6% VRo to 1.3-1.35% VRo. Humic coals can generate liquid petroleum in a three-phase complex process: (i) beginning of petroleum generation, (ii) petroleum build-up in the coal, and (iii) early oil expulsion followed by efficient oil expulsion (Petersen 2006). A high concentration of volatile matter in various seams of South Karanpura coalfield can be attributed to the presence of a higher concentration of liptinite in these particular coals. Microscopic analysis of the coals of the study area shows the presence of unstructured black or dark patches under white light; when these micro constituents were further examined under blue light irradiation, they provide fluorescence of variable intensity and colour such as brown, orange, or yellow. These microscopic constituents were identified as unstructured liptinite macerals such as bituminite, fluorinite and exsudatinite or dark vitrinite. The quantitative occurrence of these macerals is given in Chapter 4. The fluorescence of dark vitrinite macerals is caused by the adsorbed petroleum-like substance, generated during the coalification process from liptinite and lipoid substance by vitrinite macerals (Teichmüller *et al.* 1983). Sometimes oil-droplets associated with cleats in telinite and collotelinite are counted as direct evidence for liquid petroleum generation (Petersen *et al.* 2000). Coals in this study do not show these types of characteristics, suggesting the immature nature of this coal for the expulsion of liquid hydrocarbons. Exsudatinite and micrinite were observed in small concentrations in these coals, lending further support to the liquid petroleum generative capability of the coals. Exsudatinite is thought to be generated from liptinite and hydrogen-enriched vitrinite throughout maturation and possesses an orange to yellowish fluorescence (Teichmüller 1986). Micrinite is a high-reflecting maceral generated from liptinite macerals and hydrogen-enriched vitrinite

during maturation from approximately what corresponds to the late sub-bituminous stage of coalification (about 0.65% Ro), and its formation is related to the generation of petroleum (Taylor *et al.* 1998). Also, significant oil generation from liptinites produces a localized pressure, thus build-up and promote micro fracturing and migration from even thick vitrinitic bands (Saxby and Shibaoka 1986). The presence of a good amount of cleats and microfractures in the South Karanpura coals further suggests the generation and migration of the hydrocarbons from these coals.

7.6 Relation of Major and Minor Element with Mineral Matter

The elements constituting more than one weight per-cent of the coal are called major elements. Carbon, hydrogen, oxygen, nitrogen, and sulfur are the major elements present in coal. These elements form most of the organic and inorganic structures of coal. The relative percentage of carbon increases with rank, whereas the percentages of oxygen and hydrogen decrease with rank. The elements constituting 1.0 wt.% to 0.01 wt.% (whole-coal basis) of coal are called minor elements. Common elements in coal are sodium, magnesium, aluminium, silicon, phosphorus, potassium, calcium, titanium, manganese, and iron. On the whole-coal basis, the concentrations of Si, Al, and Ca, generally exceeds 1%, so these elements are reported as the major oxides, even though some of the oxides are less than 1% on the ash basis. Most of these elements exhibit their affinity with the inorganic constituents of the coal except phosphorus, which shows an association with the organic content. It is probably derived as a nutrient by the peat-forming plant communities (Valentim *et al.* 2016).

The XRF study of the coal determines the major oxides present in it, whereas the nature of the crystalline minerals in coal can be assessed using the XRD technique. The concentrations of elements may change vertically and laterally within a single coal bed

due to changes in syn- or post-depositional settings such as rate of deposition, sediment influx, precipitation from water, and bioturbation (Laban and Atkin 1999; Spears and Zheng 1999; Swaine 2013). Pyrite (FeS_2) and marcasite (FeS_2) occur in high concentrations in the coal influenced by marine conditions (Chou 2012). The coals of the South Karanpura coalfield contain a high concentration of SiO_2 (37.41 wt.% -64.02 wt.%, mean 55.33 wt.%), and the mineral quartz (35%-88%, mean 71.46%). Quartz may have a detrital origin and have been transported to the basin along with the organic debris (Dai *et al.* 2016). FTIR study of these coals also shows the presence of quartz in these coals, which may be derived through the terrigenous influx. Likewise, other major oxides also exhibit close relations with the mineralogical distribution. Their geological factors control the dispersal of trace elements in minerals in the coal. Zhang et al. (2002) found that different minerals show affinity with the certain trace elements; for example, clay minerals have high concentrations of Ba, Be, Cs, F, Ga, Nb, Rb, Rb, Th, U, and Zr; calcite has concentrations of As, Mn, and Sr while pyrite shows high concentrations of As, Cd, Hg, Mo, Sb, Se, Tl, and Zn.

Most of the trace elements are enriched in the coals of South Karanpura coalfield except strontium (Sr). Strontium (Sr) can be depleted in the coal because of its softness and nature of decomposing in water (Capo *et al.* 2014). Zirconium (Zr) is relatively higher in all the seams because of its high resistance to chemical weathering. The Sayal seam, which is the topmost seam of the area, is depleted in trace elements probably because of its higher interaction with leached surface water. All of these elements show a positive correlation with Al_2O_3 indicating the inorganic affinity of these elements, especially with aluminosilicate minerals, except Co, which exhibit a negative correlation with Al_2O_3. Sayal seam of the study area has a high concentration of clay minerals, which is also

evident from its trace elements. The relationship of major and minor elements with the ash yield of the coals of the South Karanpura coalfield is presented in Chapter 5.

7.7 Petro-chemical correlation

An attempt has been made to correlate the different coal seams of South Karanpura coalfield on the regional scale based on petrographic and geochemical constituents (Figure 7.22 to Figure 7.26). Coals seams of the Barka Sayal area have a comparatively higher concentration of vitrinite although liptinite, inertinite and mineral matter concentration is higher in the coal seams of the Argada area. The highest concentration of vitrinite is present in the Hathidari seam, whereas Argada-I seam contains the least vitrinite. The concentration of liptinite is maximum in the coals of Argada-I seam and minimum in the coals of Argada seam. Inertinite concentration is maximum in the coals of Argada-I seam and minimum in the coals of Bansgarha seam. Visible mineral matter concentration is highest in the coals of Sayal seam and lowest in the coals of Argada-J seam (Figure 7.22).

Vitrite is the dominant microlithotype in the coals of South Karanpura coalfield (Figure 7.23). Its concentration is comparatively higher in the coals of the Barka Sayal area than the coals of the Argada area. On the other hand, inertite and carbankerite are more enriched in the coals of Argada area. In the case of carbominerite, it is higher in the coals of Argada area. In the context of rank and thermal maturation, coals of Barka Sayal area exhibit a higher range of minimum, mean and maximum vitrinite reflectance compared to coals of Argada area. Coals of Bansgarha seam exhibit the maximum mean vitrinite reflectance, whereas coals of Argada-D seam exhibit the minimum vitrinite reflectance (Figure 7.24).

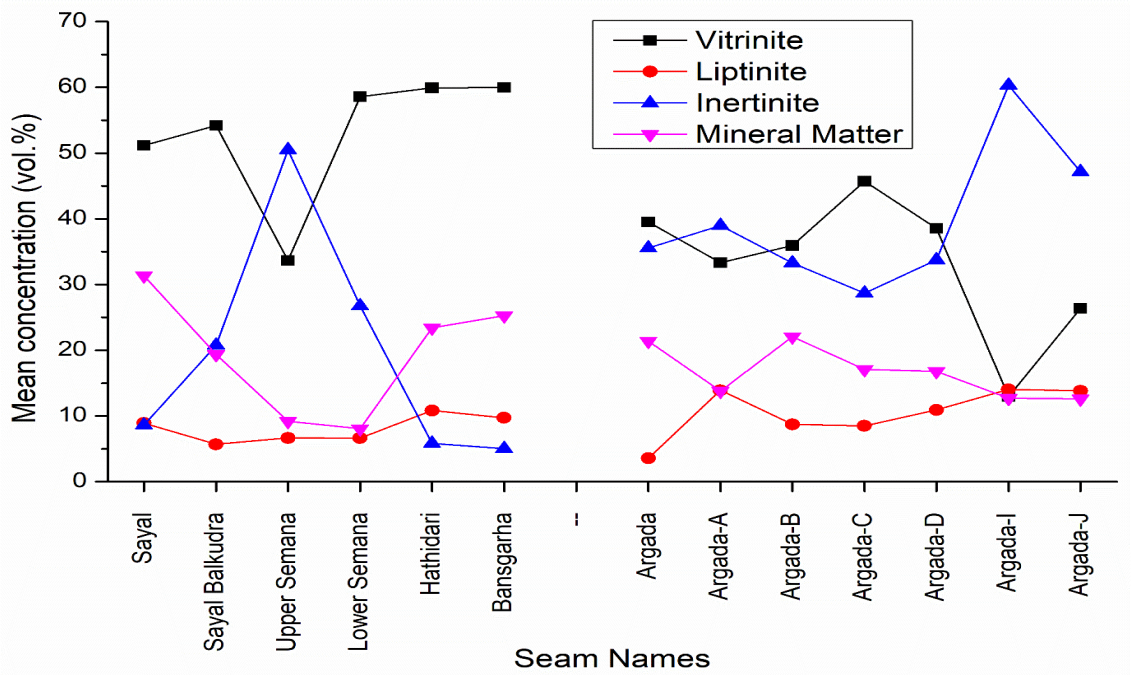


Figure 7.22 Variation of group macerals and visible minerals in the coals of different seams of South Karanpura coalfield.

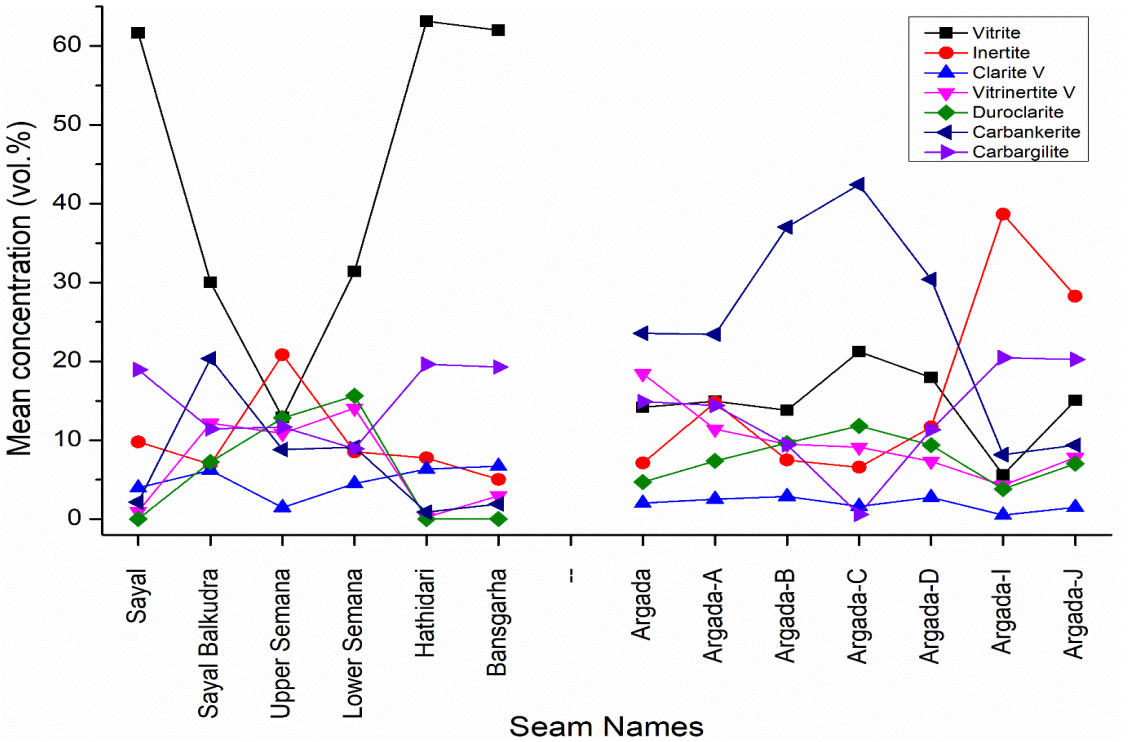


Figure 7.23 Variation of important microlithotype along different coal seams of South Karanpura coalfield.

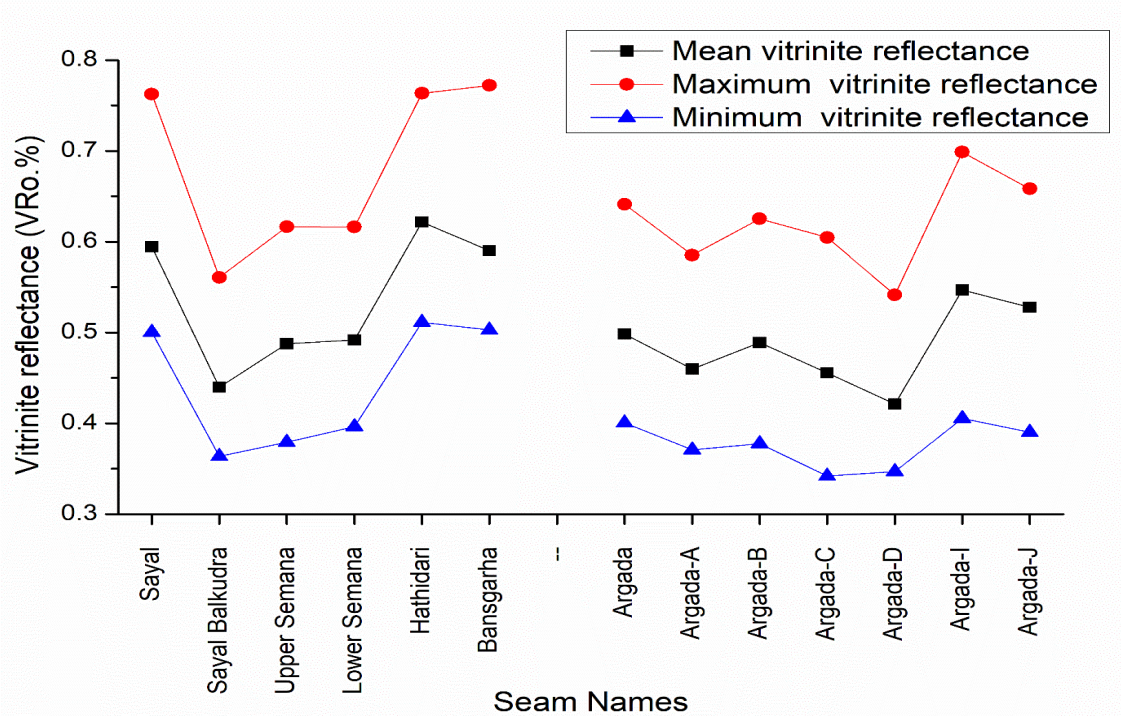


Figure 7.24 Variation of minimum, maximum and mean vitrinite reflectance along different coal seams of South Karanpura coalfield.

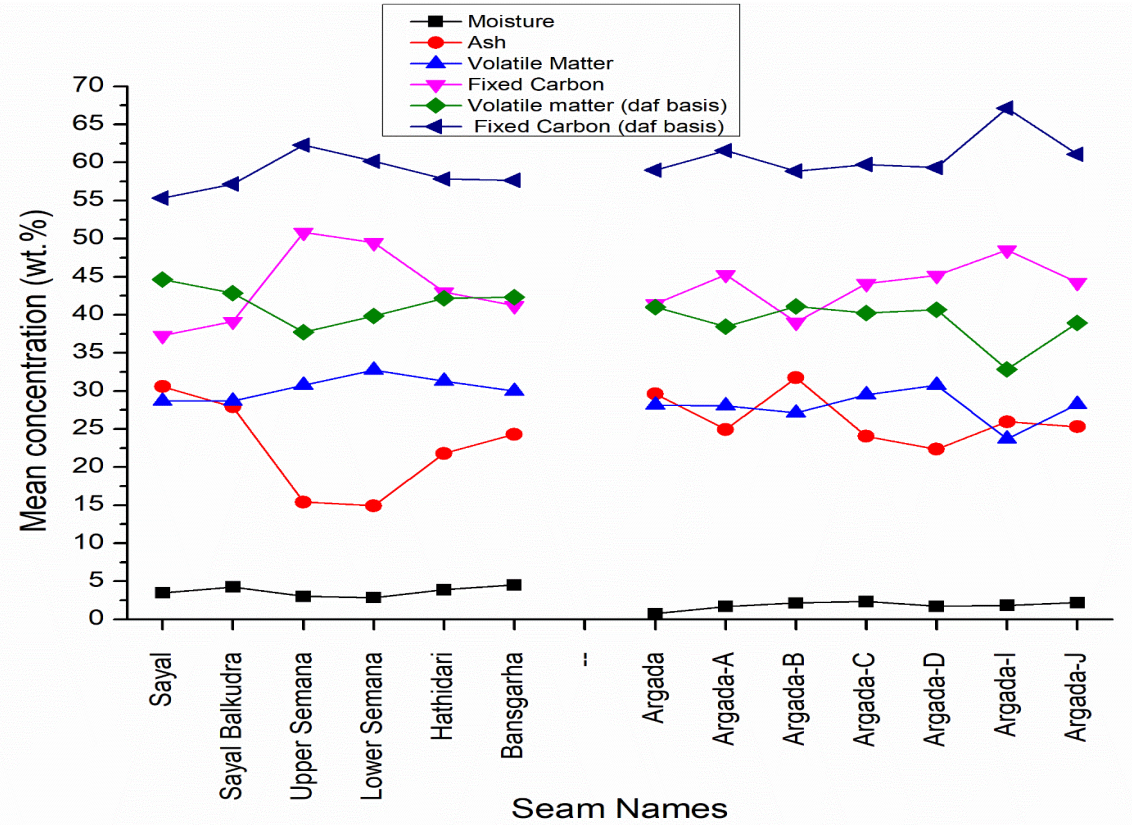


Figure 7.25 Variation of proximate constituents along different coal seams of South Karanpura coalfield.

A comparative study of the proximate constituents of the coals of South Karanpura shows that coals of Argada are exhibit comparatively lower moisture content than coals of the Barka Sayal area, but ash yield is higher in coals of Argada area. Volatile matter is higher in the coals of the Barka Sayal area, whereas there is not much variation in fixed carbon content in the coals of both the areas (Figure 7.25).

The concentrations of carbon, hydrogen, nitrogen, and sulphur are each approximately the same in both the areas of South Karanpura coalfield except slight differentiation in some seam Sayal and Sayal Balkudra which contain less carbon content, but more oxygen content compared to other seams of this coalfield (Figure 7.26). The concentration of oxygen is maximum in the Sayal Balkudra seam and minimum in Argada-J seam. Nitrogen is very less in Sayal, Hathidari, and Bansgarha seam.

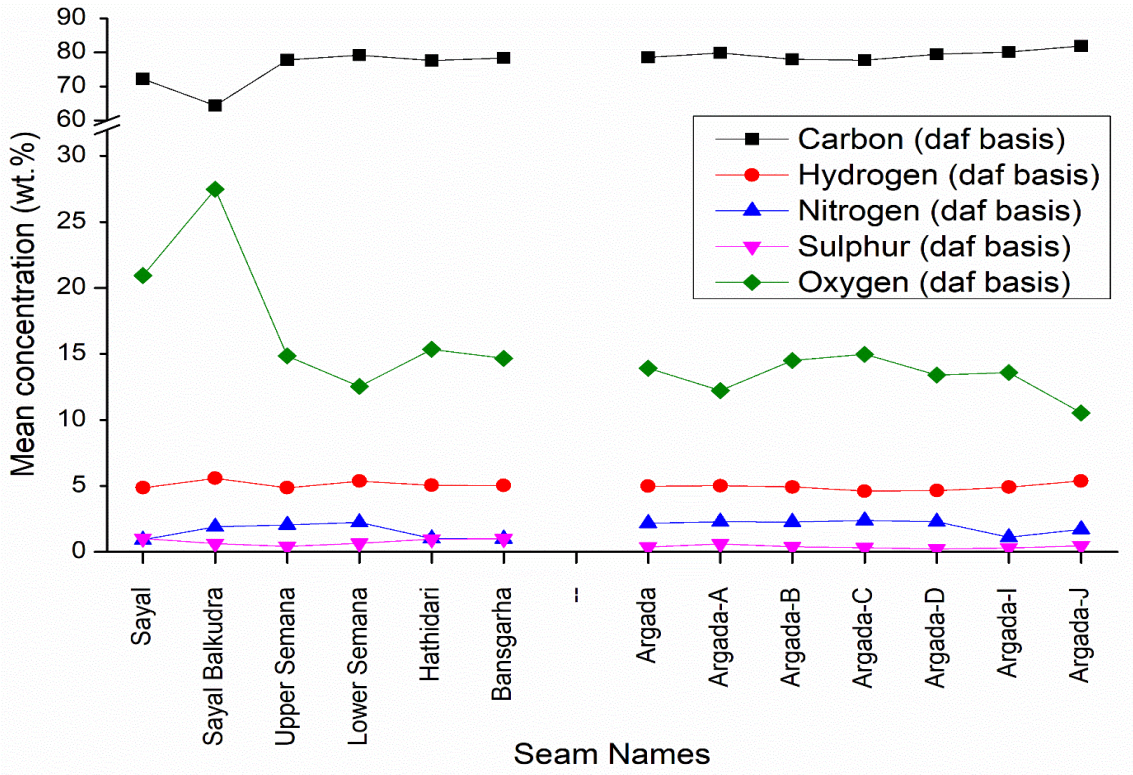


Figure 7.26 Variation of ultimate constituents along different coal seams of South Karanpura coalfield.

7.8 Occurrence and significance of major/minor and trace elements in coals of south Karanpura

Coal combustion is one of the biggest sources of trace element contamination in the environment. Several authors have discussed the adverse effect of trace elements on ecology and environment (Van Hook 1979; Finkelman and Gross 1999; Ren *et al.* 1999; Sajwan *et al.* 1999; Steinnes 2010; Pokrovsky *et al.* 2012). Arsenic (As), Lead (Pb), Cadmium (Cd), and Zinc (Zn) are environmentally sensitive elements, and their excessive intake can cause detrimental effects on human health (Sajwan *et al.* 1999; Mastalerz and Drobniak 2007). Lead (Pb) can cause mental retardation and kidney damage. Chromium inhalation may lead to lung cancer. The presence of As in the environment may also cause lung cancer or skin cancer. Copper ingestion may cause a headache. In water, a high concentration of Cu (> 1.0 mg l^{-1}) can be toxic for some fishes. Nickel and Co may be carcinogens and can cause lung or nose cancer. Intake of Zn in high concentration can produce corrosive action to the digestive mucous membranes. Vanadium toxicity may produce coughing, wheezing, and chest tightness when inhaled during respiration (Guidotti *et al.* 2008; Sajwan *et al.* 1999). Threshold limit value (TLV) for vanadium pentoxide is 0.5 mg/m^3 (dust) and 0.05 mg/m^3 (fumes) (Calabrese *et al.* 1985). The summarized toxicity and mode of occurrence of the selected trace elements are presented in Table 7.1. Cobalt, Cr, V, and Zr are among the lithophile elements and may have an affinity with aluminosilicates (Sajwan *et al.* 1999).

The concentrations of selected environmentally sensitive minor and trace elements present in these coals are also much higher than the average (arithmetic) value of world coal given by Finkelman (1999) (Table 7.1). Thus, these coals can have an intensely negative effect on the health of the people using these coals for their household activity or residing near the power plants burning these coals.

Table 7.1 Environmental significance and mode of occurrence of selected trace elements present in the Coals of South Karanpura coalfield (Gluskoter 1975).

Elements	Average (ppm) (This study)	Average (ppm) (World coal) (Finkelman 1999)	Mode of occurrence in Coal (Wei *et al.* 2018a)	Toxicity concerned (Guidotti *et al.* 2008) (Sajwan *et al.* 1999)
V	150	22	In clays and organic association	Pulmonary irritant (rare)
Cr	99	15	Organic and clay association	Digestive tract cancers
Co	110	6.1	In Pyrite, some in accessory sulfides	Pulmonary, cardiac, asthma sensitization
Ni	75	14	Unclear	Cancer risk, sensitization
Cu	83	16	Chalcopyrite	Neurotoxic
Zn	122	53	Sphalerite	Corrosion to the digestive mucous membranes
Rb	128	21	Clay minerals and Feldspar	
Sr	139	130	Clay minerals and Feldspar	
Zr	221	27	Organic association	
Pb	51	11	In Galena	Neurotoxic, renal, systemic (protean)

Paleoclimate is the most important and crucial factor affecting the deposition of sediments. Coal is deposited as organic debris along with other sediments containing different types of minerals. A proper geochemical investigation of coal ash throws light on the several depositional environmental settings and may act as a proxy for the organic petrographic models. Paleoclimate controls the weathering, erosion, alteration, compositional variation or selective elemental enrichment or depletion in the sediments (Izart *et al.* 2015). There are several proxies proposed for the determination of paleoclimate considering the weathering phenomena, such as weathering of feldspar and formation of clay minerals. Some of the indices are as follows:

i) $Chemical\ index\ of\ alteration\ (CIA) = 100 \times Al_2O_3/(Al_2O_3 + CaO* + Na_2O + K_2O)$ (Nesbitt and Young 1982)

ii) $Chemical\ index\ of\ weathering\ (CIW) = 100 \times Al_2O_3/(Al_2O_3 + CaO* + Na_2O)$ (Harnois 1988)

iii) $Index\ of\ composition\ variability\ (ICV) = (TiO_2 + Fe_2O_3 + MnO + MgO + CaO + Na_2O + K_2O)/Al_2O_3$ (Cox *et al.* 1995)

In all these equations, oxides are used in molar percentage and the CaO* is the value after removing the effect of apatite and calcite.

Chemical weathering in continents is the product of several factors such as source rock type, vegetation, tectonic and topographic settings, climate regime, soil development, and human activities as well. The high CIA values (80–100) generally reflected by muds indicates high alteration and formed under tropical conditions. On the other hand, in glacial environments, where abrasion is dominant over chemical weathering, common CIA values range from 50 to 70. The high CIA and CIW values (Table 7.2) for the coal seams of South Karanpura coalfield indicate intensive weathering of the inorganic content in these coals. The high CIA value also indicates hot and relatively humid paleoclimate prevailed during the deposition of these coals (Meunier *et al.* 2013).

Table 7.2 Calculated chemical proxies to determine the paleo depositional settings and slagging behaviour of coals of South Karanpura coalfield.

Seam and Sample No.	CIA (Nesbitt and Young 1982)	CIW (Harnois 1988)	ICV (Cox *et al.* 1995)	R_{b-a} (Scott 1999)
Sayal	73.55	77.50	1.72	0.55
Sayal Balkudra	89.19	97.54	0.37	0.09
Upper Semana	82.23	84.91	0.37	0.11
Lower Semana	86.87	91.35	0.29	0.07
Hathidari	91.50	98.94	0.24	0.06
Bansgarha	91.23	98.40	0.48	0.14
Argada	93.95	98.63	0.21	0.05
Argada-A	88.88	91.31	0.35	0.10
Argada-B	93.85	98.90	0.22	0.04
Argada-C	91.05	95.49	0.23	0.06
Argada-D	94.78	98.73	0.21	0.06
Argada-I	94.68	99.10	0.25	0.05
Argada-J	85.55	88.58	0.53	0.18

CIA- Chemical index of alteration; CIW- Chemical index of weathering; ICV- Index of compositional variability; and R_{b-a}- Ratio of basic to acidic oxides.

A high value for ICV is an indicator of minerals, high in weathering sequence. The ICV of non-clay minerals is higher than that of clay minerals, and the ICV of pyroxene is between 10 and 100. The ICV values for amphibole, K feldspar, plagioclase, and illite/muscovite are 8, 1, 0.6, and 0.3, respectively, and the range of ICV values for montmorillonite and kaolinite are only 0.15–0.3 and 0.03–0.05, respectively (Khanehbad *et al.* 2012). Mean ICV of Sayal seam is 1.72, indicating a high amount of heavy minerals prone to weathering and low amount of clay minerals. The ICV values less than 1 for other seams (Table 7.2) suggest that the inorganic content of these seams had suffered the recycling process. Quartz and clay minerals show more resistance to recycling and weathering process (Meunier *et al.* 2013). The presence of a high amount of quartz and clay minerals in the seams of South Karanpura coalfield, explain the same. Also during FTIR spectroscopy, the IR bands of these coals exhibit peaks between 1100 and 400 cm^{-1}, which are related to clay minerals such as kaolinite, illite, and montmorillonite. The IR bands from 3600-3800 cm^{-1} are associated with quartz and kaolinite.

The cross plot between SiO_2 and (Al_2O_3+K_2O+Na_2O) suggests that the coal of the South Karanpura formed under a semi-arid condition (Suttner and Dutta 1986) (Figure 7.27).

Enrichment or depletion of elements in coal depends on the ages of accumulation and its environment of deposition. The Sr/Cu ratio of sediment provides information about paleoclimate. The ratio of Sr/Cu less than 10, indicates a humid and warm climate while a ratio higher than 10 indicates arid and hot climate (McLennan 2001). The Sr/Cu ratio less than 10 for these coal seams favours the deposition of these seams under humid and warm climate condition. The high concentration of Sr is an indicator of marine facies or salty lake, while its low concentration indicates terrestrial sediments (Spears and Zheng 1999). The low sulphur content present in these coal seams is also indicative of its terrestrial origin (Spears *et al.* 1999). Vanadium (V) and Nickel (Ni) are the redox-

sensitive elements. A cross plot between V and Ni shows that coals of South Karanpura coalfield formed under a mixed type of oxic condition, where the seams formed under a transitional phase of oxic to the dysoxic condition are dominant (Figure 7.28).

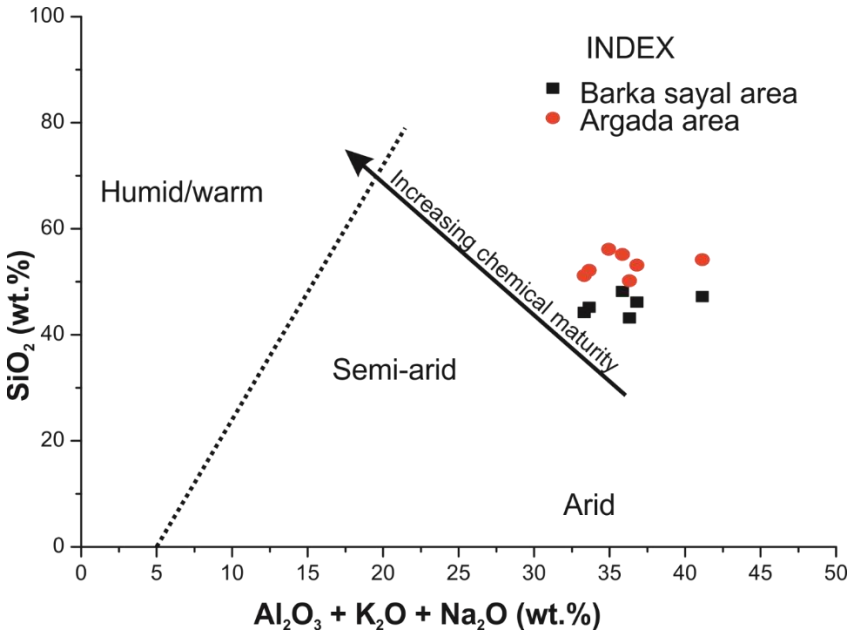


Figure 7.27 Plot of SiO2 versus (Al_2O_3+K_2O+Na_2O) showing paleoclimate condition during sedimentation (Suttner and Dutta 1986).

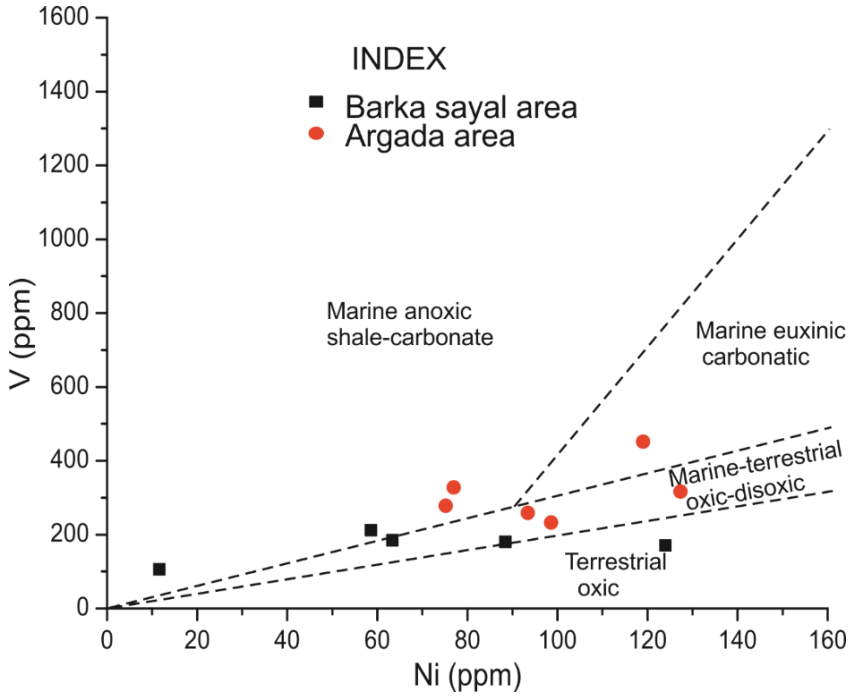


Figure 7.28 Plot of V and Ni concentration values showing depositional condition for samples of South Karanpura coalfield (after Galarraga et al., 2008).

The V/(V+Ni) ratio ranging from 0.46 to 0.6 indicates oxygen leaned condition, 0.60 to 0.84 indicates a weak anaerobic condition while a ratio higher than 0.84 indicates the anaerobic environment (Adebiyi *et al.* 2014). The mean V/(V+Ni) ratio for the inorganic content of South Karanpura coalfield indicates that coals of most of the seams formed in a weak anaerobic environment, coals of Bansgarha seam had formed under oxygen leaned environment, but coals of Sayal seam and Argad-J seam had formed under totally anaerobic condition. The relatively moderate V/(V+Ni) ratio of these seams in combination with the total sulphur contents below 1% also suggests reducing (suboxic) conditions during deposition (Figure 7.29) (Hakimi *et al.* 2017).

The Barakar Formation is the main coal-bearing sequence of the area. It is composed of coarse-grained sandstone, shales, and several economic coal seams. The Karharbari Formation underlies the Barakar Formation and contains pebbly to coarse-grained sandstones, shales, and few thin coal seams.

The Al_2O_3/TiO_2 ratio lying in the range of 8 to 21 indicates that the sediments of these seams were derived from intermediate igneous rocks (Hayashi *et al.* 1997). The cross plot of TiO_2 and Zr (Figure 7.30) is also suggestive of an intermediate source composition of the sediments associated with different seams of the area while the sediments belonging to Sayal seam were derived from slightly felsic igneous rocks (Tao et al., 2017).

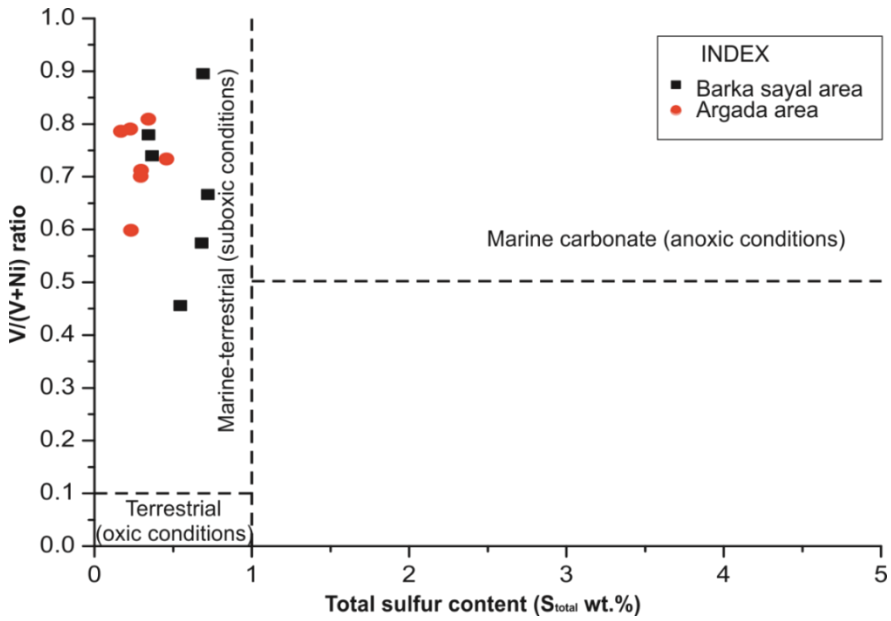


Figure 7.29 Cross-plot between the ratio of V/(V+Ni) and Total Sulphur content (S total wt.%), showing different paleoclimatic conditions (after Hail et al., 2017).

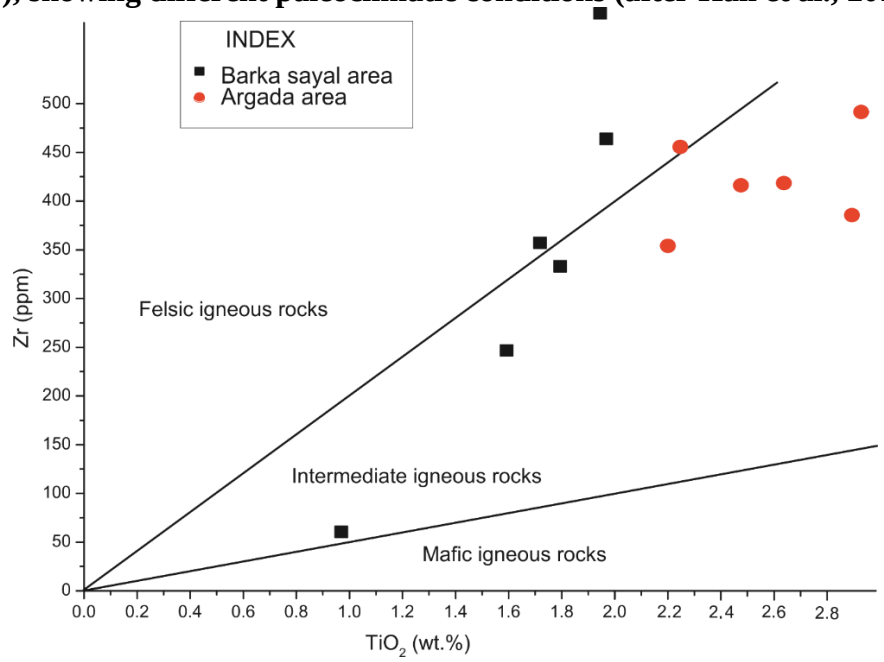


Figure 7.30 Cross-plot of Zr (ppm) and TiO_2 (wt.%), showing provenance source rock type for coal seams of Barka Sayal area (after Tao et al., 2017).

7.9 Evolution of coals of South Karanpura

The paleo-depositional conditions essentially control the behaviour of coal during its different uses. Coal-forming peat swamps were controlled and affected by several factors such as the evolutionary development of flora, paleoclimate, paleogeographical position,

and tectonic setting. Coal facies, which express the primary genetic types of coal are dependent on several factors such as the type of deposition, peat-forming plant communities, depositional environment, pH value, bacterial activity, Sulphur supply, the temperature of the peat, redox potential etc. (Stach *et al.* 1982). The petrographic constituent such as coal macerals can provide information about paleo-environment in two ways by its presence or absence and by its abundance. For example, the presence of telalginite indicates aqueous conditions because of its derivation from planktonic algal progenitors (Diessel 1982). However, the presence of a high concentration of a particular type of maceral in coal solidifies the outcome. A high rate of subsidence facilitates the large proportion of wood tissue preservation, thus a high concentration of telovitrinite. An influx of brackish water may increase the pH and lead to an increased concentration of detrovitrinite (Diessel 1992). Thus, a high degree of resolution obtained by contrasting key macerals in the form of facies ratio was used by several researchers. They used these ratios or key macerals either in cross-plot or as the apex of several diagrams for easy interpretation and visualization of conditions prevailed during peat formation. Cohen (1973) used the ratio of particle to the matrix and the ratio of non-sedimentary to sedimentary material for the characterization of peat types of the Okefenokee Swamp. Diessel (1986) introduced the gelification index (GI) and tissue preservation index (TPI) based on the gelification characteristics and fragmentation characteristics of the macerals. Several researchers used the concept of microlithotype for the determination of paleo-environment (Smyth 1979; Singh *et al.* 2013c). With the advancements in the science of organic petrology and publication of different petrography based depositional models (Hacquebard and Donaldson 1969; Smyth 1979; Marchioni 1980; Diessel 1986; Mukhopadhyay 1986; Calder *et al.* 1991; Kalkreuth *et al.* 1991; Singh and Singh 1996b, 2000; Singh *et al.* 2017a, 2010, 2013c), it became easier to decipher the peat-forming

environments. However, careful attention, as well as justification from other analytical techniques such as geochemical methods, palynological studies, sedimentological techniques etc. are also required (Bechtel *et al.* 2003, 2004; Dutta *et al.* 2011b; Singh *et al.* 2017d; Radhwani *et al.* 2018).

To find out the detailed depositional environment, generated petrographic data were plotted against several petrography based models proposed by different workers. It suggests that the coals of South Karanpura coalfield may have deposited under sufficient water level in a forest swamp quantified by the presence of more structured macerals than degraded macerals.

In the present study, a combined approach has been applied to find out the detailed petrographic and geochemical variation along the vertical section of different seams of South Karanpura Coalfield. Based on the petrographic and geochemical constituents, source vegetation and depositional conditions of the coal have been discussed. The study provides an in-depth understanding of the petrological as well as geochemical characteristics of the coals belonging to the area and will open the door for enhanced utilization and sustainable management of these coals.

7.9.1 Development of Flora

The Gondwana coals are supposed to be formed from forest swamps (Mahesh *et al.* 2015a). These coals are vitrinite rich and contain a considerable amount of liptinite and inertinite macerals, which indicates that these coals have evolved from forest type of vegetation that grew in the humid tropical climate and was subjected to a flooding event, which increased the mineral matter content of these coals. The Lower Gondwana Flora includes Pteridophytes, such as Equisetales: Schizoneura, Phyllotheca, Stellotheca; Sphenophyllales: Sphenophyllum, Raniganjia, Trizygia; Lycopodiales: Cydodendron; Filicales: Gondwanidium, Pecopteris, Sphenopteris, Angiopteridium, etc., as well as

Gymnosperms such as Glossopteridales: Gangamopteris, Glossopteris, Rubidgea, Rhabdotaenia, Vertebraria, Scutum, Ottokaria, Glossotheca, etc.; Cycadales: Pseudoctenis, Taeniopteris; Cordaitales: Noeggerathiopsis, Eury- phylum, Cardiocarpus, Samaropsis; Ginkgoales: Psygmophyllum, Ginkgophyton; Coniferales: Buriadia, Barakaria, Dadoxylon, Araucareoxylon, Agathoxylon, Damudoxylon etc. (Kulkarni 1969; Navale 1984; Tewari *et al.* 2017).

7.9.2 Development of Coal Facies

There is an inherent relationship between the original peat-forming ecosystem and specific microscopic constituents (macerals and microlithotypes). Recognition of coal facies is a challenging task because coal's observed compositional properties reflect the geological processes, influence external depositional sedimentary environments, and alteration afterwards (Dai *et al.* 2020b). The There are various models proposed by several authors, which are helpful to determine the nature of peat-forming environments (Smith 1962; Hacquebard & Donaldson 1969; Smyth 1979; Diessel 1986, 1992; Mukhopadhyay 1986; Teichmüller *et al.* 1989; Mukhopadhyay & Scotia 1989; Calder *et al.* 1991; Schneider *et al.* 1995; Singh *et al.* 2012, 2013; Singh 2016). The application of these models for coal different from the studied coals require attention and the proper provincial nature of coals should be taken into consideration. Several scientists have discussed the limitations of these models and variability in coal characters influenced by temporal and spatial variability, which restricts the applicability of models to coals of different geological age or basin (International Committee for Coal and Organic Petrology 1971; Diessel 1992; Sen *et al.* 2016a; Dai *et al.* 2020b). The determination of coal bed's original mire type and depositional setting requires integration of data on the sedimentology, stratigraphy, and sedimentary facies of associated rocks along with data on geochemistry, palynology, mineralogy, and petrology of the coal (Dai *et al.* 2020b).

Diessel (1982, 1986) emphasized the presence of diagnostic macerals as an indicator of the original plant material responsible for the formation of peat. He introduced two petrographic indices, Tissue Preservation Index (TPI) and Gelification Index (GI) based on his work on Australian Permian coals using maceral characteristics.

$$\mathrm{TPI} = \frac{\text{Telinite} + \text{Collotelinite} + \text{Semifuinite} + \text{Fusinite}}{\text{Collodetrinite} + \text{Macrinite} + \text{Inertodetrinite} + \text{Vitrodetrinite} + \text{Corpogelinite}}$$

$$\mathrm{GI} = \frac{\text{Vitrinite} + \text{Macrinite}}{\text{Semifusinite} + \text{Fusinite} + \text{Inertodetrinite}}$$

TPI contrasts between tissue-derived structured macerals to tissue-derived unstructured macerals. Thus, a high TPI value suggests the dominance of arborescent vegetation and well preservation of plant tissues in favourable circumstances such as the presence of sufficient water level, lack of bacterial activity and optimum subsidence rate. Low TPI suggests the dominance of herbaceous plants or poor preservation of woody plant tissues. The GI contrasts between macerals of the vitrinite group plus macrinite to oxidized tissues and detritus to infer the gelification degree of the organic constituents. The gelification process is primarily controlled by the water level; thus the GI value reflects the relative water level condition during peat formation, the rate of peat accumulation, the rise in relative groundwater influence table as well as periods of dryness or wetness. The GI value increases with increasing wetness. The ash yield, which also greatly influenced by the peat-forming environment was not shown on this model, but this model is suggested for low ash yield of mean values less than 10% (Ward 1984). Diessel's model was further modified by Kalkreuth et al. (1991) to show the different environmental fields in the same diagram.

Diessel's model is divided into four quadrants based on high (>1) or low (<1) TPI and GI. The high-TPI/high-GI quadrant represent peat accumulation in a forested

continuously wet raised bog if the ash yield is low or in a forested telmatic swamp if the ash yield is high. The high-GI/Low-TPI quadrant represent peat accumulation in a herbaceous dominated, continuously wet raised bog. If the ash yield is high, this quadrant is considered to represent telmatic to limnotelmatic peats derived from either herbaceous marsh vegetation or highly decomposed forest vegetation.

The low-GI/high-TPI quadrant represents peat derived from a forested raised bog if the ash is low to moderate, or a forested swamp subjected to occasional dry periods when ash is high. The low-TPI/low-GI quadrant represents peat derived from relatively dry raised bogs. Four fields representing lower delta plain, upper delta plain, back-barrier and piedmont plain settings defined based on a large number of coal samples from different depositional environments are superimposed upon these four quadrants (Diessel 1992).

Coals of the Barka Sayal area of the South Karanpura coalfield exhibit a high degree of TPI (1.18-54.75, mean 11.61) as well as GI (0.29-36.25, mean 7.92) (Figure 7.31). This suggests that coals of the Barka Sayal area were deposited under sufficient water level in a forest swamp quantified by the presence of more structured macerals than degraded macerals in these coals. Coals of Argada area of South Karanpura coalfield show moderate TPI (0.35-8.80, mean 2.63) and moderate GI (0.01-8.12, mean 1.28) (Figure 7.32). This suggests that during deposition of the coals of Argada area the climate was more variable, thus these coals formed under both forest swamp and dry forest swamp environment, which is well quantified by the presence of a high concentration of banded coal lithotype in these seams and fluctuation of vitrinite and inertinite macerals.

All of the seams of the South Karanpura coalfield exhibit a positive correlation between TPI and GI values (Figure 7.33 and Figure 7.34), which shows that the conditions in the basin were favourable for the preservation of tissues and gelification process and the

preservation of tissues was favoured by the gelification process. The presence of a high concentration of vitrinite macerals in these coals supports the same outcome.

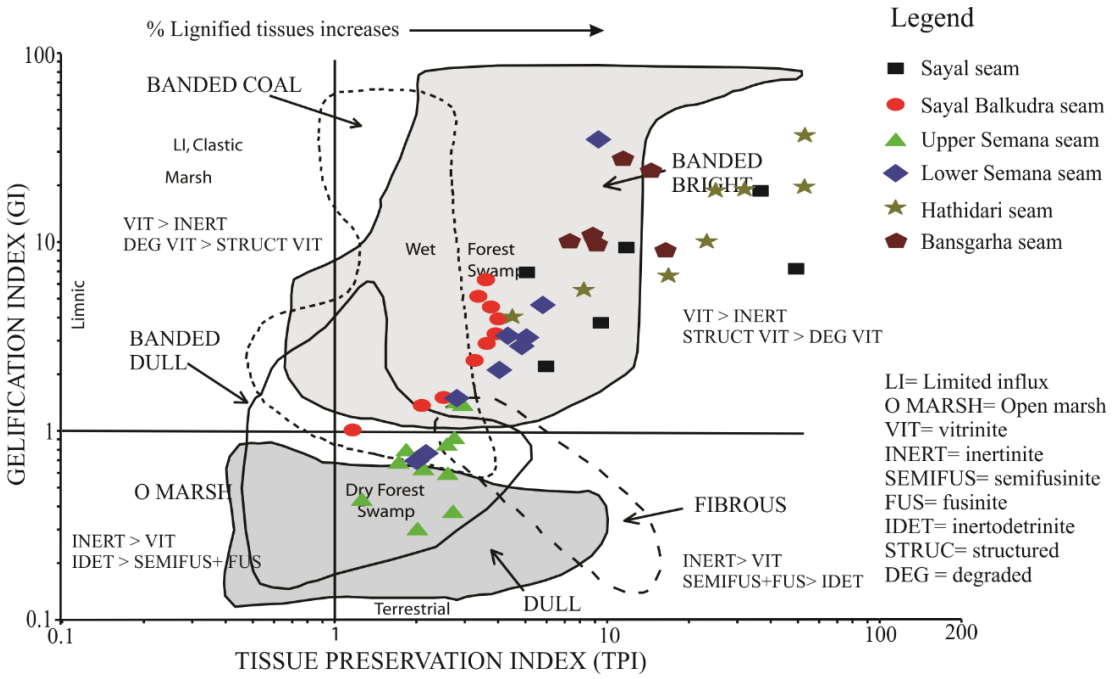


Figure 7.31 Coal facies deciphered from Gelification Index (GI) and Tissue Preservation Index (TPI) concerning depositional setting and type of mire for Coals of Barka Sayal area (after Deissel, 1986 and modified by Kalkreuth et al. 1991).

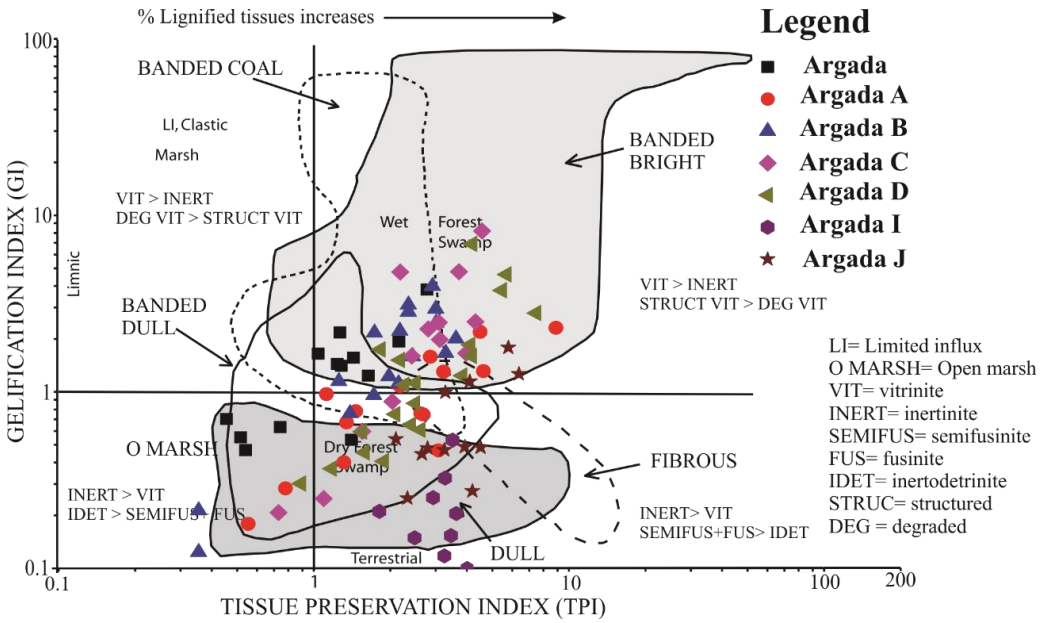


Figure 7.32 Coal facies deciphered from Gelification Index (GI) and Tissue Preservation Index (TPI) concerning depositional setting and type of mire for Coals of Argada area (after Deissel, 1986 and modified by Kalkreuth et al. 1991).

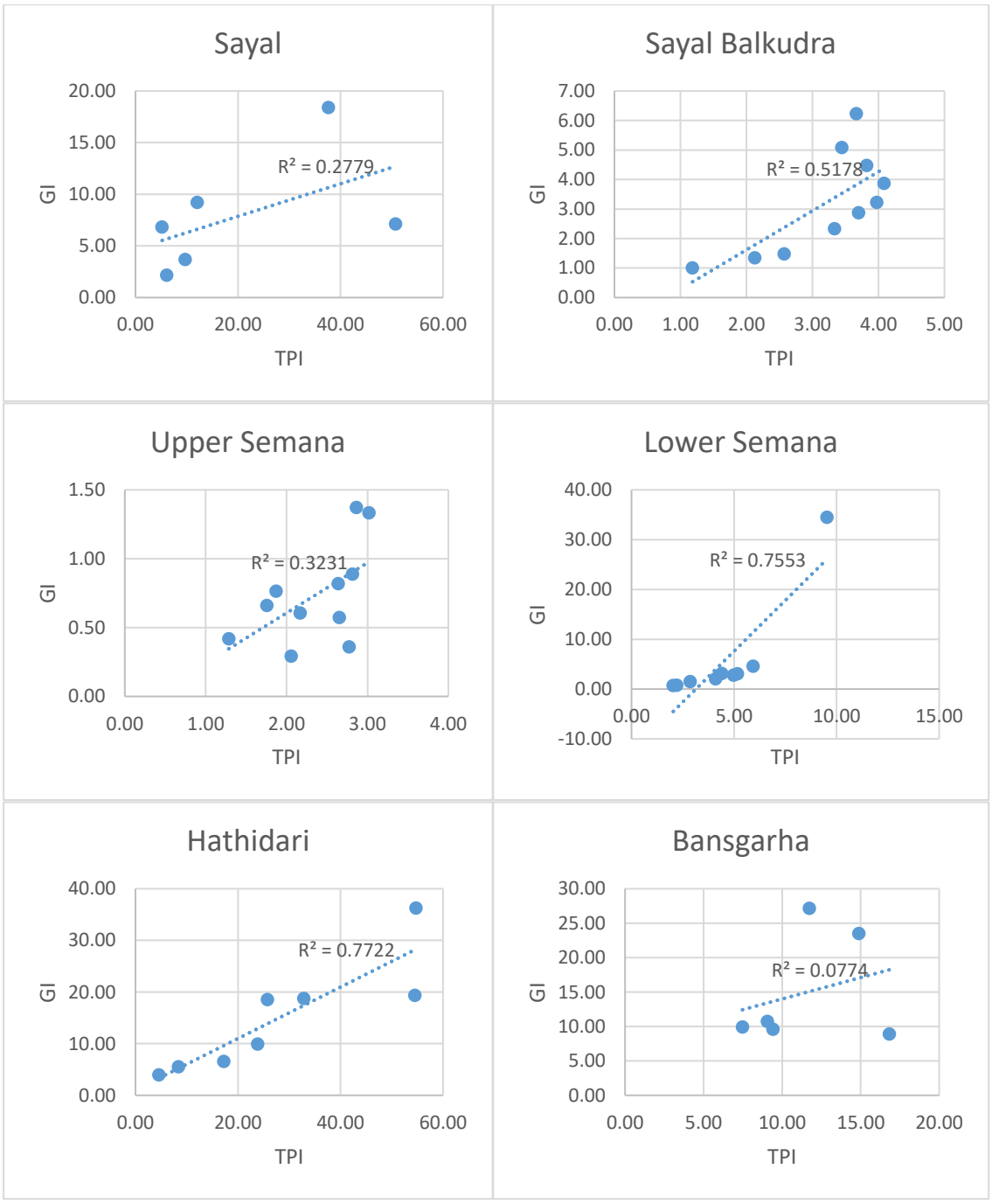


Figure 7.33 Correlation between tissue preservation index (TPI) and gelification index (GI) for different seams of Barka Sayal area, South Karanpura coalfield.

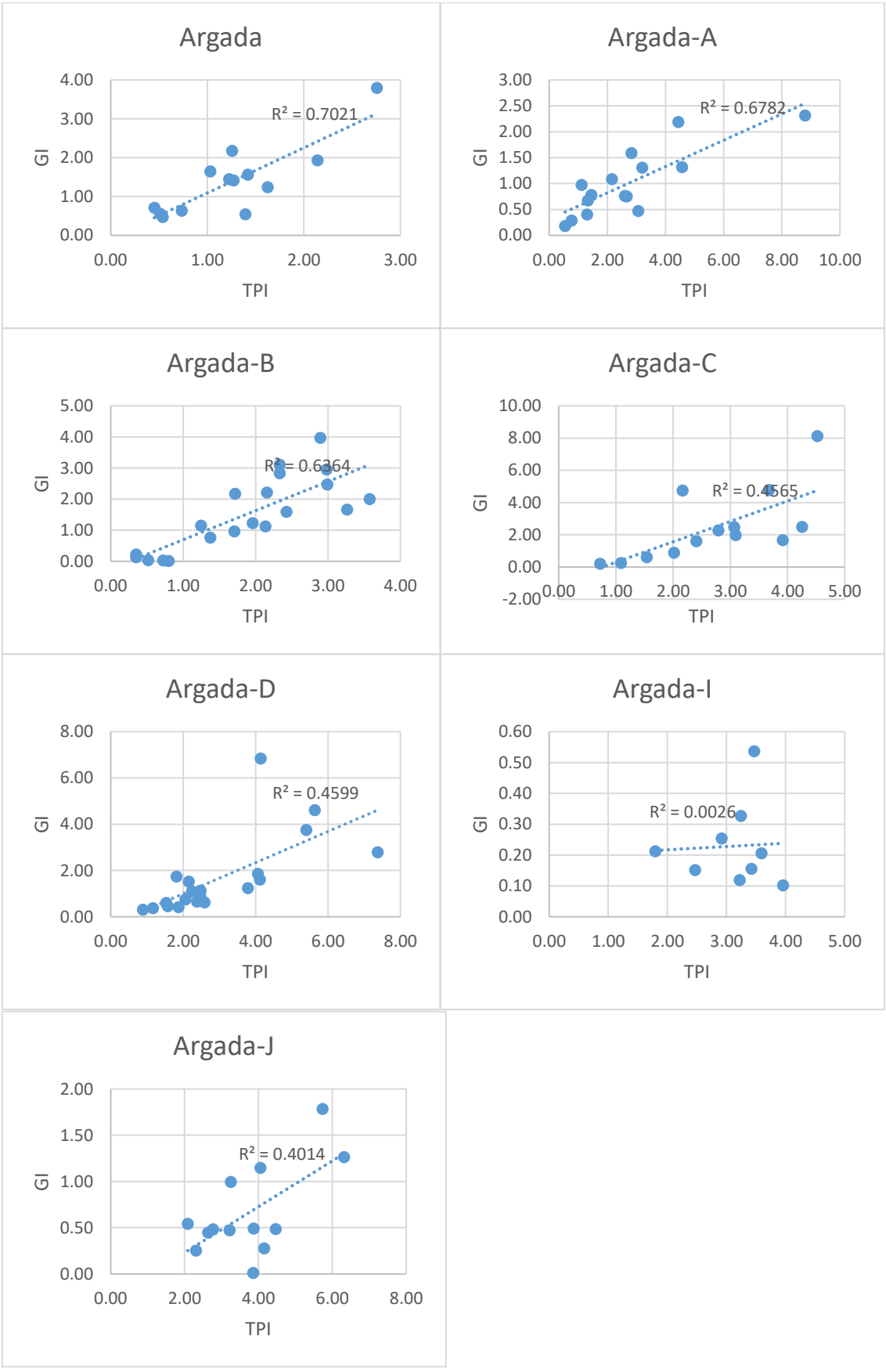


Figure 7.34 Correlation between tissue preservation index (TPI) and gelification index (GI) for different seams of Argada area, South Karanpura coalfield.

To determine the paleo-environment of coal-forming peatlands, Calder et al. (1991) introduced two petrographic indices based on their studies on Westphalian B Cumberland Basin, Nova Scotia, Canada. They modified Diessel's indices and introduced two new indices Groundwater Influence Index (GWI) and Vegetation Index (VI) emphasizing groundwater influence and vegetation type, respectively.

$$\mathrm{GWI} = \frac{\mathrm{Gelinite} + \mathrm{Corpogelinite} + \mathrm{Vitrodetrinite} + \mathrm{Mineral\ matter}}{\mathrm{Telinite} + \mathrm{Collotelinite} + \mathrm{Collodetrinite}}$$

VI

$$= \frac{\mathrm{Telinite} + \mathrm{Collotelinite} + \mathrm{Fusinite} + \mathrm{Semifusinite} + \mathrm{Funginite} + \mathrm{Secretinite} + \mathrm{Resinite}}{\mathrm{Collodetrinite} + \mathrm{Inertodetrinite} + \mathrm{Alginite} + \mathrm{Liptodetrinite} + \mathrm{Cutinite}}$$

Vegetation Index (VI) contrasts the macerals of lignin-rich derived from large terrestrial plants to the plants contributing to the detritus, gels, and liptinites that originated in the aquatic environment. Groundwater Influence Index (GWI) contrasts macerals derived from severely gelification to the macerals derived from mild or no gelification. Mineral matter is kept in the numerator part of the fraction.

The GWI and VI are plotted on a graph which is subdivided into areas representing different environments and vegetation types. A high concentration of gelified material is indicative of high groundwater influence levels (GWI>0.5) and thus implies rheotrophic conditions. A GWI between 3 and 5 are considered to represent a limnotelamtic environment, while values above 5 represent wetlands prone to siliciclastic inundation. Low GI indicates dryer conditions, suggesting a more ombrotrophic environment (GWI <0.5). Within these environments, the dominant type of vegetation is indicated by the vegetation index. High VI (VI>3) indicates high levels of structured tree-derived material as well as a more terrestrial environment. Low values (VI<3) indicate lower levels of

preserved structured material and a more limnic environment dominated by marginal aquatic or herbaceous plants.

Ground Water Index (GWI) for South Karanpura coals [GWI (nil- 38.75), mean 1.42 and VI (0.37- 29), mean 6.18] indicate that these coals had originated from ombrotrophic to a rheotrophic environmental condition having moderate to low groundwater influence (Figure 7.35 and Figure 7.36). Vegetation Index (VI) suggests that coals of these seams have been originated from forest trees of the terrestrial environment. The coals of the Barka Sayal area have GWI values ranging between 0.08 and 2.19, mean 0.57, whereas the coals of the Argada area exhibit slightly higher GWI values ranging from nil to 38.75, mean 2.27, which is because of siliciclastic inundation in some of the bands belonging to this area, especially in Argada-B and Argada-J coal seam. The VI values of the coals of Barka Sayal area varies from 1.29 to 29.00, mean 9.35, whereas coals of Argada area exhibit lower VI concentration ranging in between 0.37 and 8.71, mean 3.00, which suggests that the coals of Barka Sayal area formed with higher input of treed plants compared to the coals of Argada area (Figure 7.35 and Figure 7.36).

A dominance of structured inertinite content generally represents the oxic environment, while the presence of degraded inertinite such as inertodetrinite may deceive about the environment due to their generation from various sources such as wildfires or transportation from other parts of peatland. The coals of South Karanpura coalfield contain an appreciable amount of minerals. Minerals are directly related to the paleodepositional condition. The model proposed by Singh & Singh (1996) based on their study on Permian coal deposits of the Rajmahal basin take into account the mineral matter of coal was used for the interpretation of South Karanpura coals. Most of the coals of the area formed in alternate oxic to anoxic moor conditions, whereas coals of Bansgarha,

Hathidari, and Sayal seams of the Barka Sayal area had formed in wet mood with intermittent moderate to high flooding conditions. (Figure 7.37 and Figure 7.38).

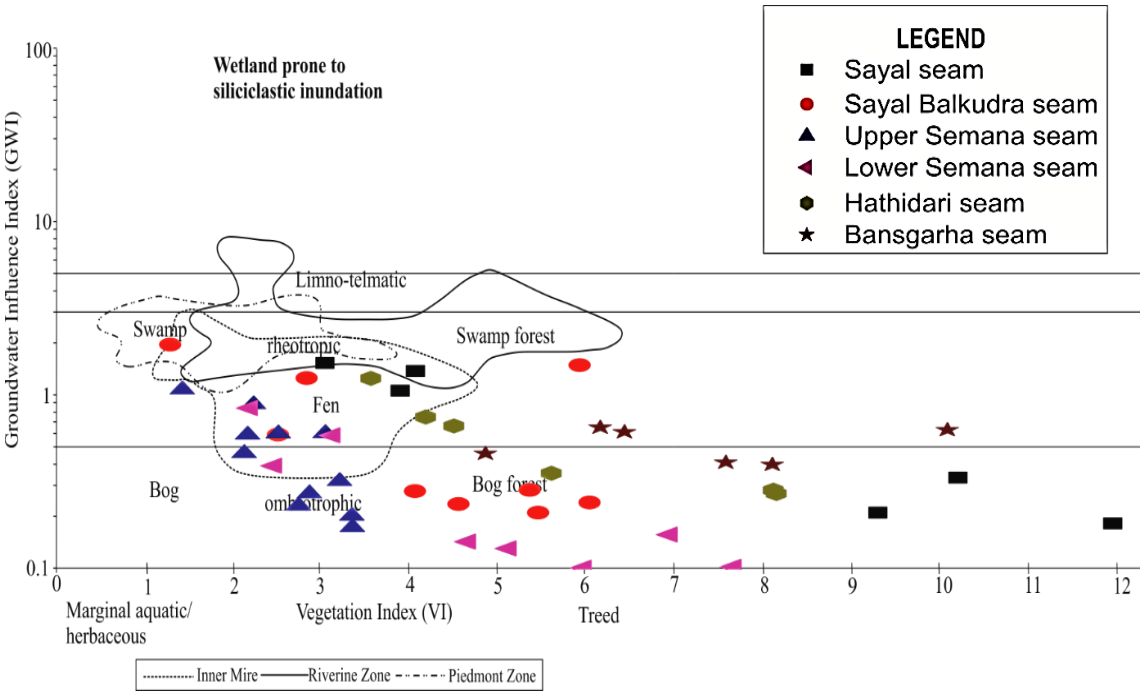


Figure 7.35 GWI vs VI Paleo-environment diagram of Barka Sayal area (modified after Calder et al., 1991).

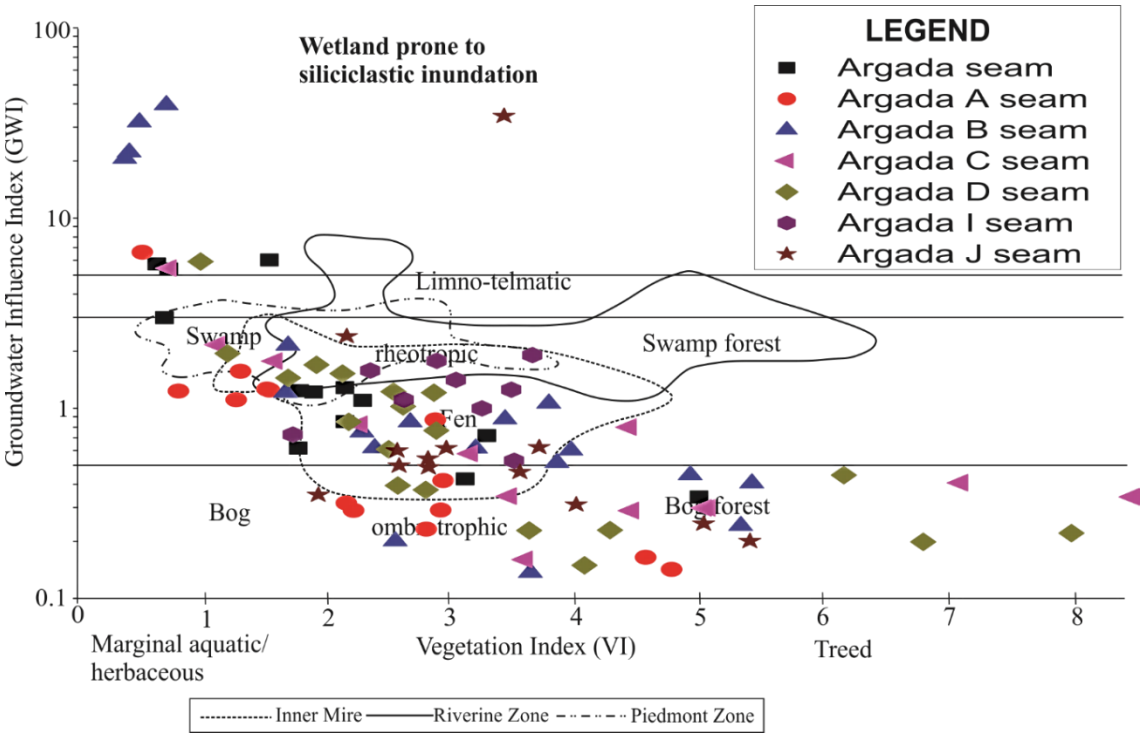


Figure 7.36 GWI vs VI Paleo-environment diagram of coals of Argada area (modified after Calder et al., 1991).

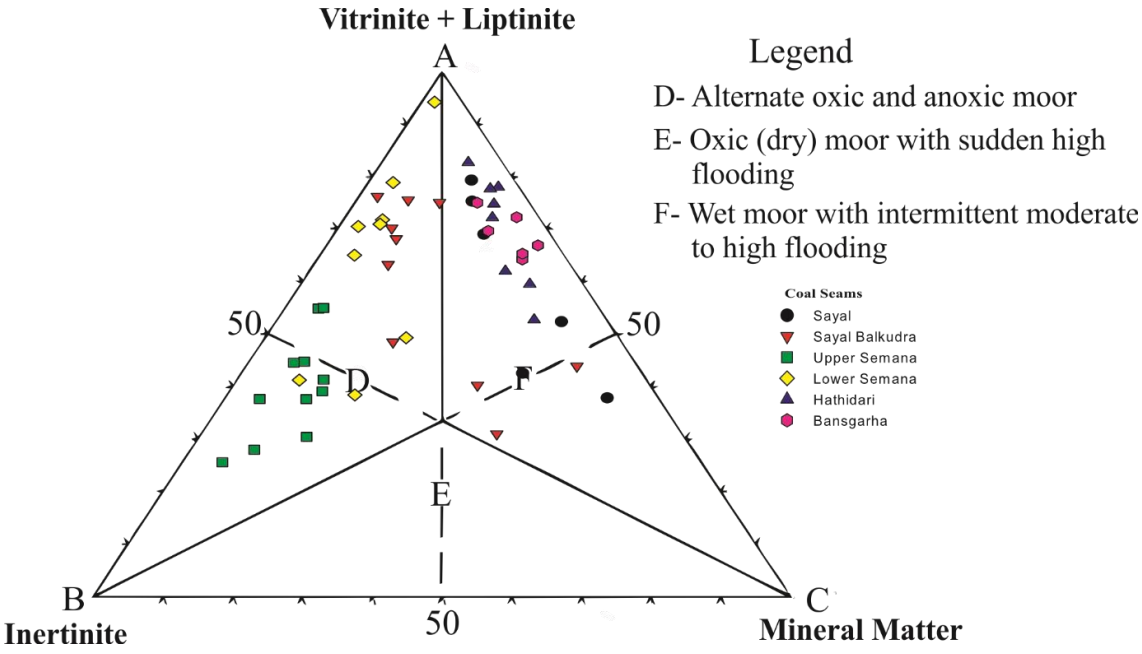


Figure 7.37 Depositional conditions of Barka Sayal coals based on maceral and mineral matter content (after Singh & Singh, 1996).

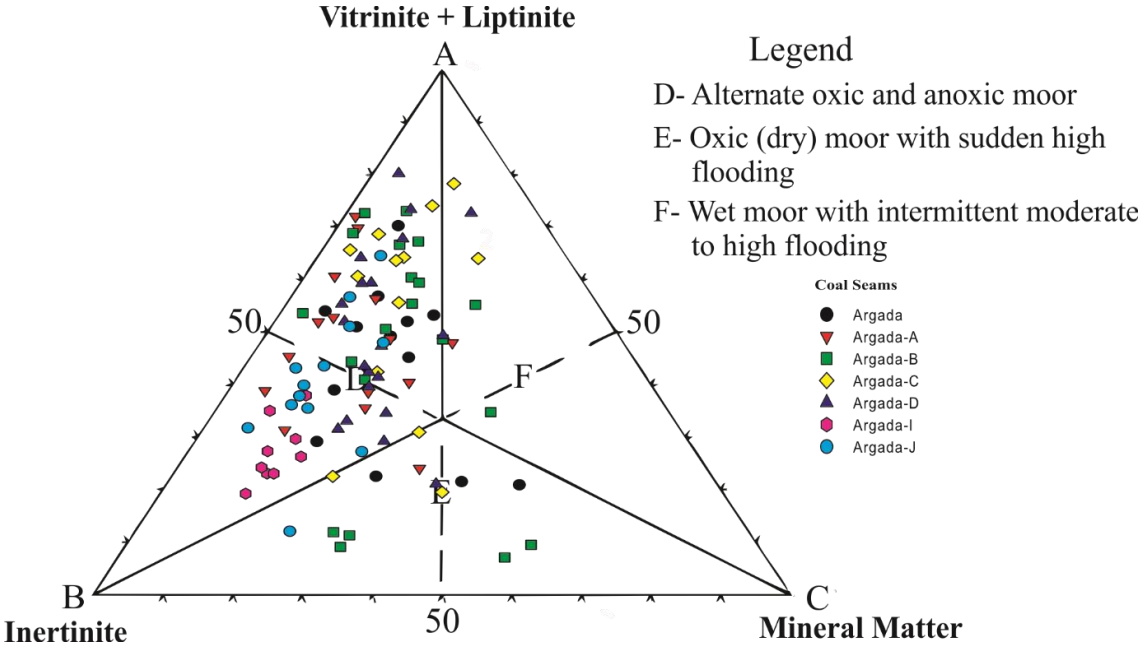


Figure 7.38 Depositional conditions of coals of Argada area based on maceral and mineral matter content (after Singh & Singh, 1996).

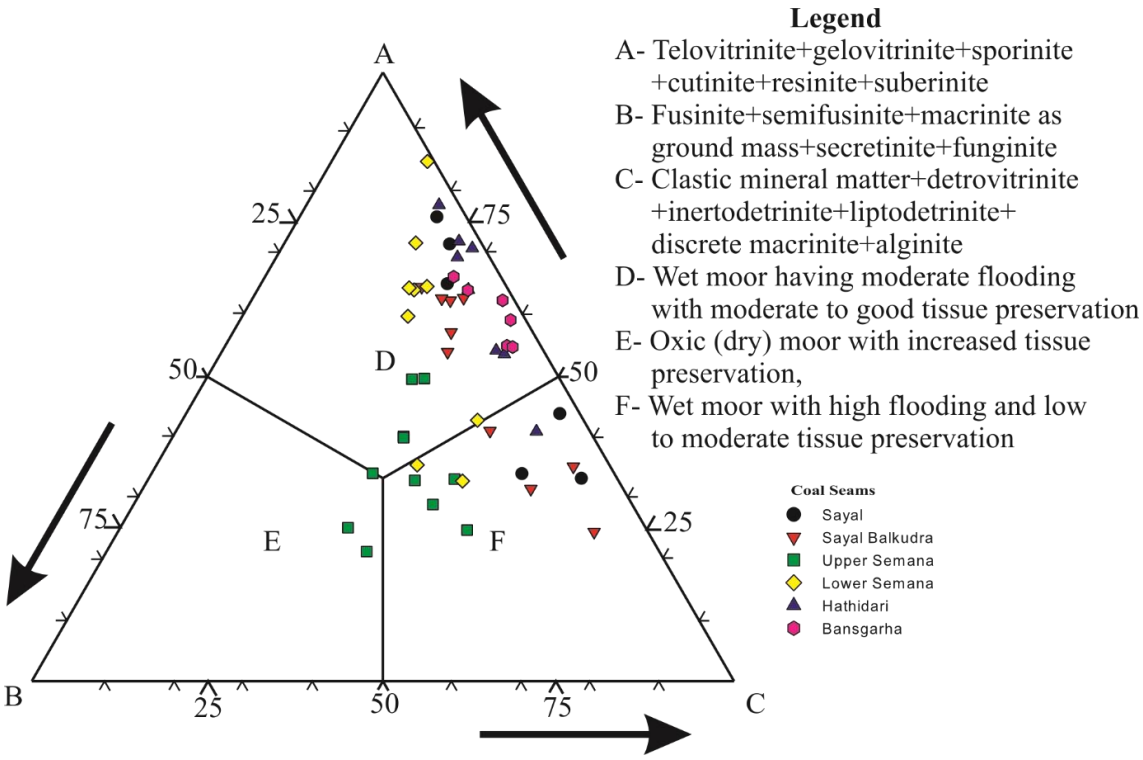


Figure 7.39 Peat-forming environment based on maceral and mineral matter contents of Barka Sayal area, South Karanpura coalfield (after Singh et al., 2012).

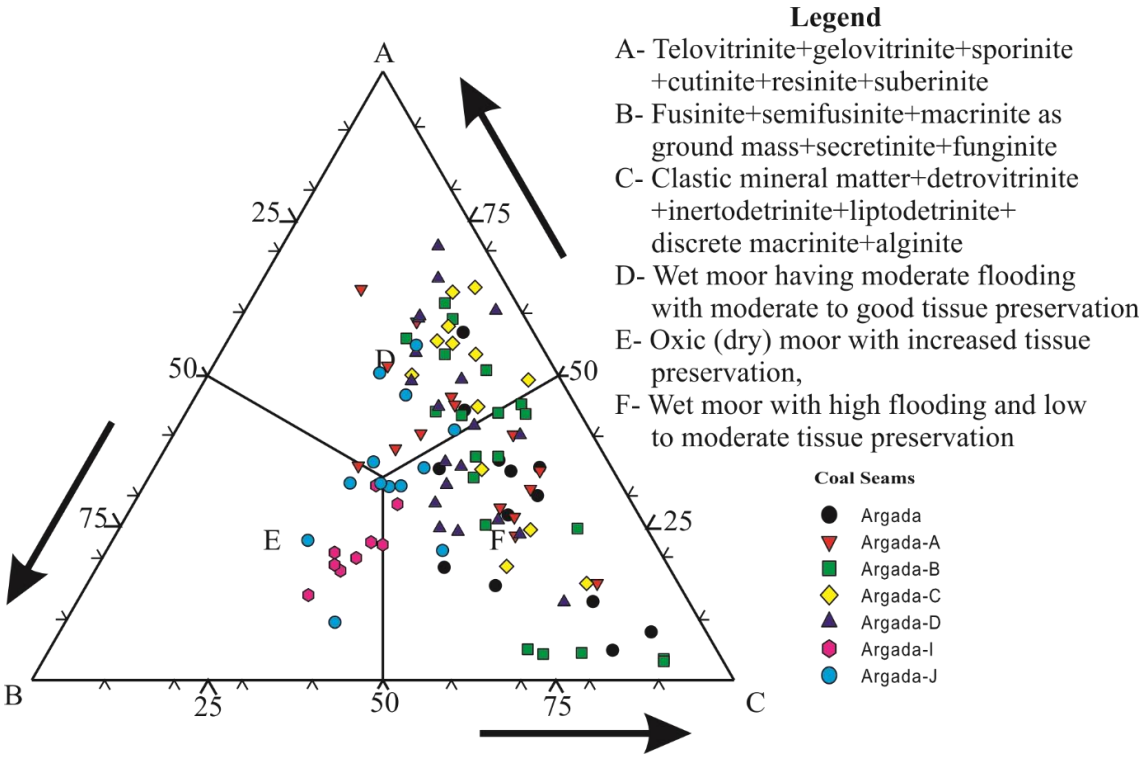


Figure 7.40 Peat-forming environment based on maceral and mineral matter contents of coals of Argada area, South Karanpura coalfield (after Singh et al., 2012).

An additional model proposed by Singh et al., (2012) considering maceral composition as parameters, primarily focuses on the flooding spells occurred during the peat formation, and conditions for tissue preservation is presented in Figure 7.39 and Figure 7.40.

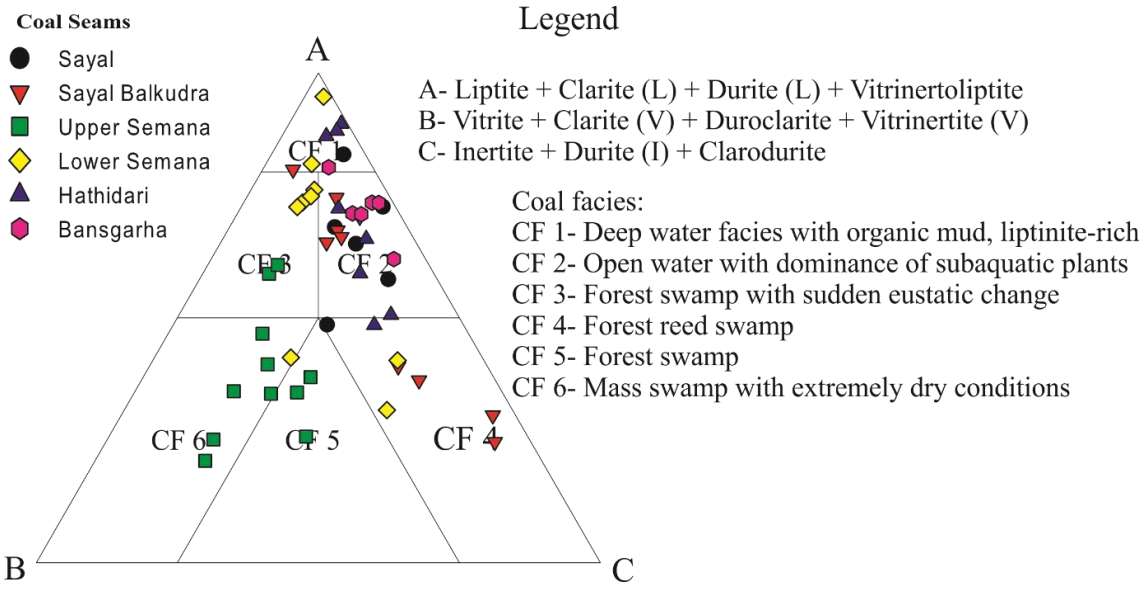


Figure 7.41 Coal facies based on the microlithotype composition of coals of Barka Sayal area, South Karanpura coalfield (after Singh et al., 2013).

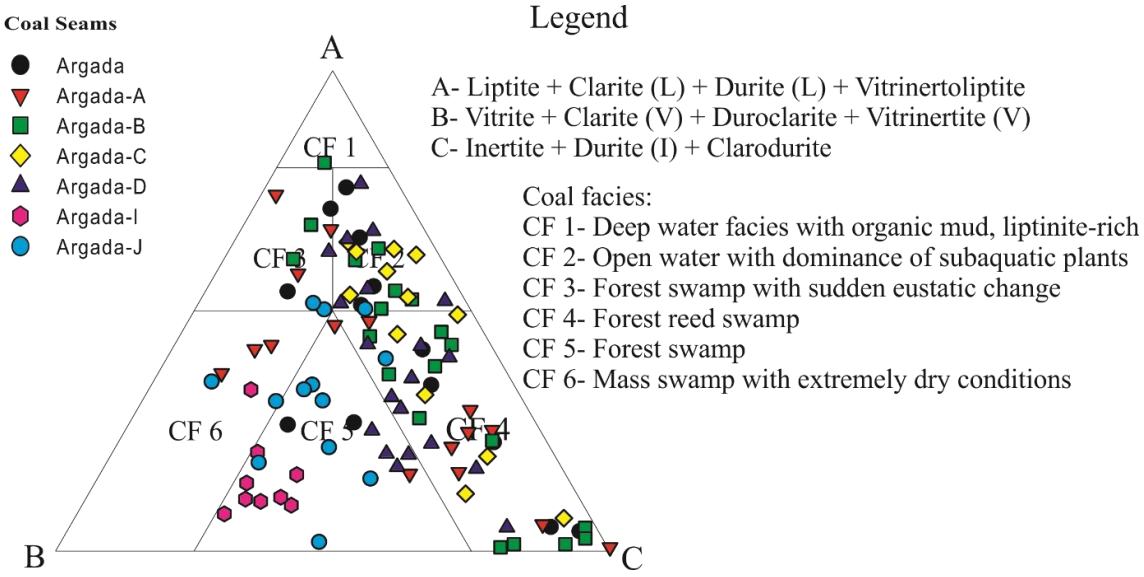


Figure 7.42 Coal facies based on the microlithotype composition of coals of Argada area, South Karanpura coalfield (after Singh et al., 2013).

The petrographic data of the present study were plotted in this model which shows most of the coal bands have evolved from a wet moor having moderate flooding with moderate to good tissue preservation characterized by the presence of the high amount of structured macerals of vitrinite and liptinite group which formed in a favourable wet moor. At the same time, some of the data denote their deposition in wet moor with high flooding event and lesser tissue preservation characterized by the presence of a high amount of clastic mineral matter and detrital macerals. The application of macerals for coal facies analysis is not sufficient because some of the macerals are very small and rarely remain present in the coal, hence models based on microlithotype may provide a good representation of the three-dimensional composition of the coal (Hower and Wagner 2012). Another facies model provided by Singh et al. (2013), based on their work on the bituminous coal of northeast India, also takes microlithotype into account (Figure 7.41 and Figure 7.42). When coals of South Karanpura coalfield were plotted in this model, its origin is denoted in an environment of forest reed swamp with high tree density and sufficient water level. Thus, inferences drawn from maceral based models are also supported by microlithotype based models.

In the context of biomarkers, the distribution pattern of *n*-alkane hydrocarbons indicates the source of organic matter. In all the samples, the predominance of mid-chain *n*-alkanes, with a maximum at *n*-C_{23} is observed. The possible biological precursors of these compounds can be aquatic flora in the case of high (ground) water levels during organic matter accumulation (Bechtel *et al.* 2007b). According to Ficken et al., (2000; 2002), the dominance of medium-chain hydrocarbons (*n*-C_{15} to *n*-C_{25}) suggests aquatic sources in which, shorter chains indicates lacustrine algae and longer chains indicate macrophytes. Vascular plants, microalgae, and cyanobacteria are also considered as the source of these compounds (Životić *et al.* 2008). Short-chain *n*-alkanes (*n*-C_{18}, *n*-C_{20}) in abundance are

indicative of organic matter input from the activity of microbial organisms (Cranwell 1977). Long-chain *n*-alkanes (*n*-C_{27}, *n*-C_{29}) in abundance are indicative of high plant wax source of the organic matter (Eglinton and Hamilton 1967). In the studied samples, short-chain *n*-alkanes are present, but long-chain hydrocarbons are relatively less abundant. This suggests the formation of these deposits in waterlogged conditions with increased organic matter input from aquatic vegetation sources.

The biomarker parameters are also used to understand the depositional conditions during the deposition of sediments. The carbon preference index (CPI) values signify the input of higher plant-derived organic matter. Values equal to 1 suggests an insignificant higher plant source (Killops and Killops 2013), while values greater than 1 suggest, significant higher plant input (Mostafa *et al.* 1998). However, CPI values can also be affected by the thermal maturity attained by the organic matter (Tissot and Welte 1984). In the studied samples, CPI values indicate higher plant-source input. The relative variation of terrestrial organic matter source against the inputs from aquatic sources is indicated by the terrigenous/aquatic ratio (TAR) values (Bourbonniere and Meyers 1996). A terrestrial source is indicated by the values greater than 1, while aquatic sources are indicated by values less than 1. Both low (<1) and high (>1) values are present and fluctuate across the section indicating variation, in the organic matter input. The relative variation in plant communities (submerged, floating or emergent aquatic and terrestrial plants) can be deduced based on the Proxy aqueous (P_{aq}) ratio (Ficken *et al.* 2000). In the studied samples, the values are between 0.4 and 1.0, corresponding to the high contribution of submerged or floating aquatic flora. The palaeo-redox conditions that existed in the depositional setting can be deciphered using the pristane/phytane (Pr/Ph) ratio (Didyk *et al.* 1978; Hughes *et al.* 1995). According to Peters et al. (2005), high Pr/Ph ratios (>3) suggests terrestrial input in the oxic environment, values ranging from 1.0-3.0 suggest an

intermediate condition; whereas values < 0.8 suggest anoxic conditions in the basin. The ratio range from 2.95 to 8.04, suggesting oxic basin conditions during the formation of these deposits. The Pr/*n*-C_{17} and Ph/*n*-C_{18} plots of these coals suggest that the deposition of this organic matter took place in a terrestrial setting under the oxic to the suboxic environment (Figure 7.43).

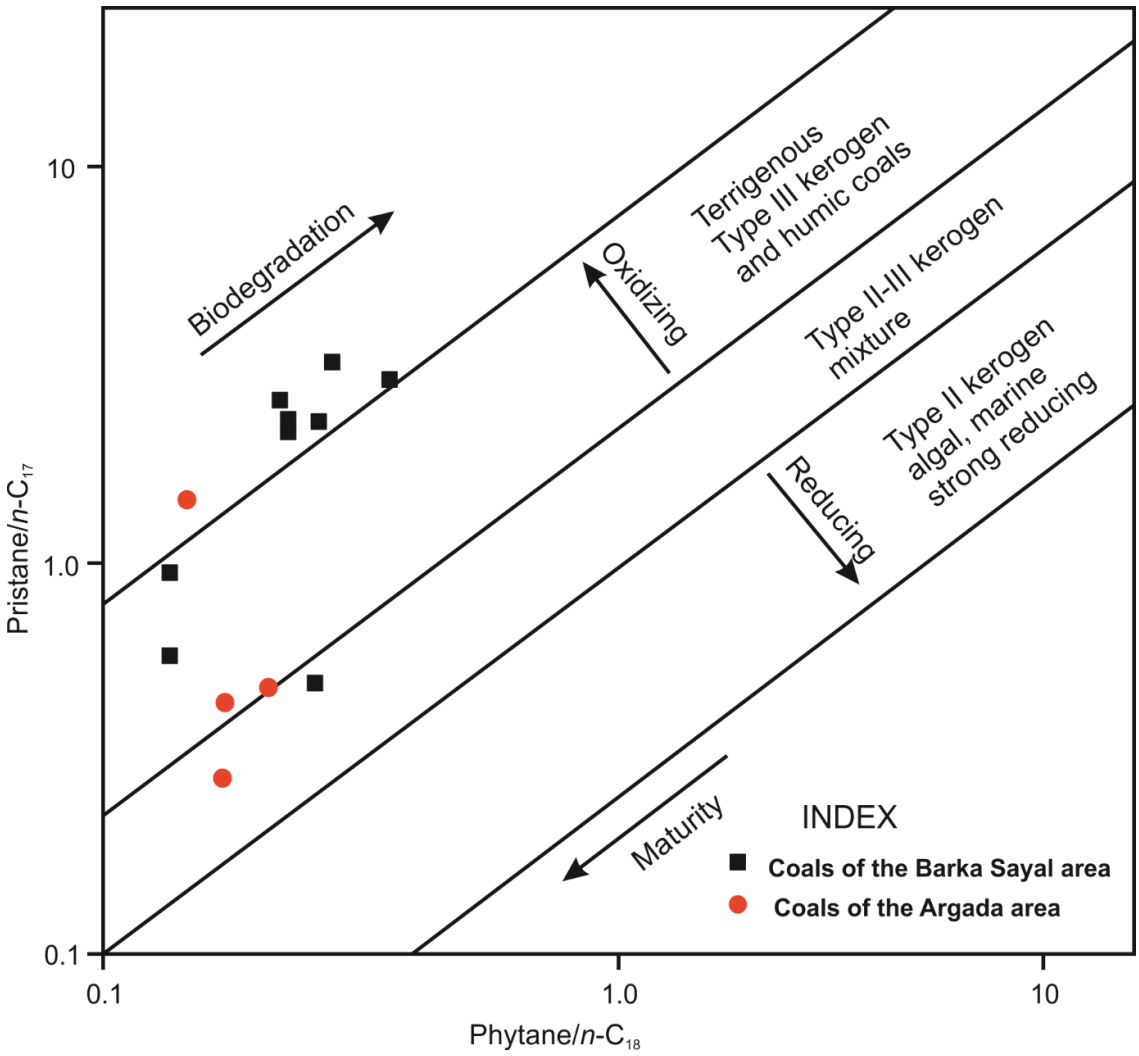


Figure 7.43 Pristane/n-C_{17} versus phytane/n-C_{18} cross-plot of the Lower Gondwana coal samples from South Karanpura coalfield, India (modified after Hunt, 1996)

The sesquiterpenoid 4β(H)-eudesmane is a land plant biomarker of a non-specific source. This compound is produced in gymnosperms and angiosperms (Noble 1986). 8β(H)-

drimane and 8β(H)-homodrimane are considered to have originated from hopanoid precursor via aerobic microbial activity during early diagenesis (Alexander *et al.* 1984). The tetracyclic compounds *ent*-beyerane and phyllocladane are known to be produced by Cupressaceae, Podocarpaceae, and Araucariaceae. However, these compounds are absent in Pinaceae (Otto and Wilde 2001). Similarly, the presence of pimarane-type diterpenoids may suggest Pinaceae, Taxodiceae and Cupressaceae sources (Noble *et al.* 1985; Dev 1989; Otto *et al.* 1997; Stefanova *et al.* 2002). These compounds are certainly produced in the extent of conifers (gymnosperms). However, these compounds were also produced by various primitive plants (Tewari *et al.* 2017). Therefore, the diterpanes in the studied Gondwana coal samples suggests a primitive conifer source of organic matter. Pentacyclic hopanoids are present in high abundance and their distributions indicate the bacterial origin of sedimentary organic matter (Peters *et al.* 2005). The biological precursor compounds of hopane derivatives are considered to be bacteriohopantetrol and to a smaller extent 3-desoxyhopanes (Ourisson *et al.* 1979; Rohmer *et al.* 1992). Aerobic bacteria, fungi, as well as cryptogams are found to contain these compounds (Bechtel *et al.* 2001). The abundance of hopanoids in the studied samples indicates a considerable contribution from bacterial sources to these sediments. ββ-hopane is the least thermodynamically stable of the hopane stereoisomeric series (Seifert and Moldowan 1980; Peters *et al.* 2005). The absence of unstable ββ-hopane and hop-17(21)-ene indicate that the samples have suffered thermal alteration. Extended hopanes up to C_{33} are present and are believed to be derived from bacteriopolyhopanol, a compound present in the prokaryotic cell membrane (Wanick 1956).

7.9.3 Depositional Environment

A model based on microlithotype composition (mmf basis), proposed by Smyth (1979) has been applied for the reconstruction of the environment. The plots of South Karnapura

coalfield in this diagram shows that most of these coals formed in fluvial, upper deltaic, lower deltaic, and lacustrine environments. Few of the bands in the Lower Semana and Argada A seams (and few other seams) also lie in the brackish water environment (Figure 7.44).

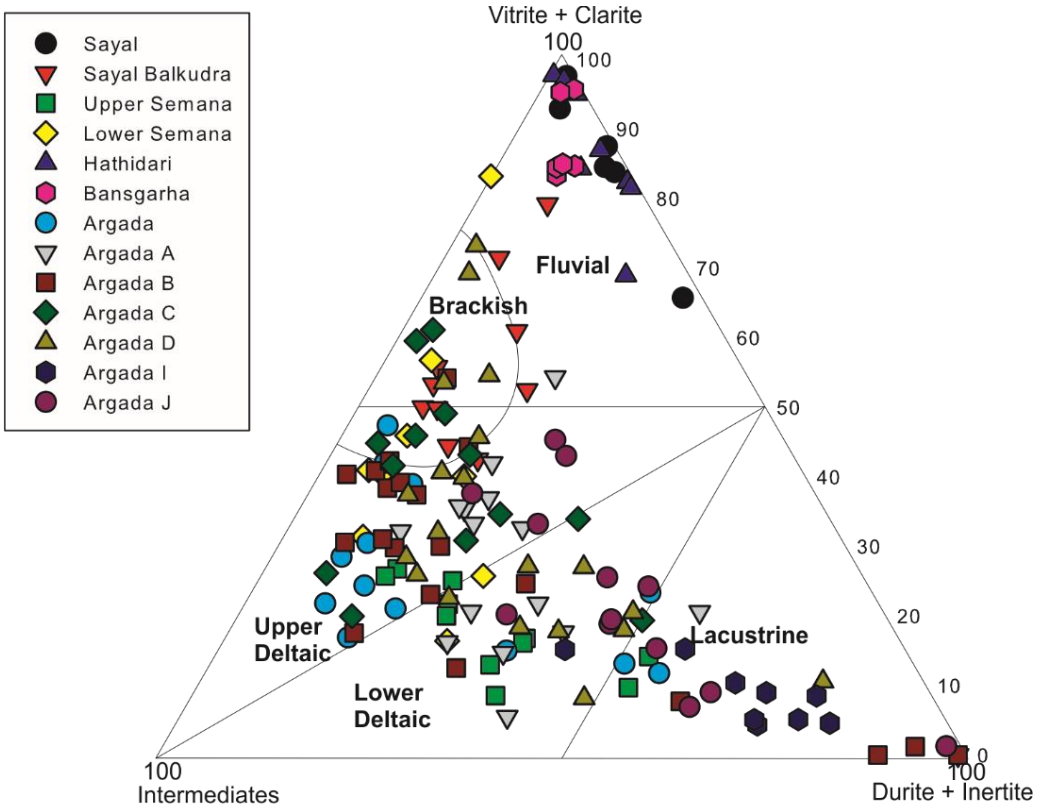


Figure 7.44 Environments of coal deposition related to microlithotype composition of coals of South Karanpura coalfield (modified after Smyth 1979).

7.10 Coalification Trend

Coalification is a very complex process, which starts with the formation of peat and ends with the further maturation/metamorphism of the peat into meta-anthracite forming sub-bituminous, bituminous, and anthracite coals in between. The coalification process is divided into two parts biochemical and geochemical (Teichmüller and Teichmüller 1979). Biochemical coalification is mainly influenced by several micro-organisms such as fungi, bacteria, etc., which helps in the formation of humic acid. Geochemical coalification is influenced by lithostatic pressure, tectonic activities, subsidence of the basin, geothermal

gradient, the effect of extraneous heat, etc. The overall coalification process is primarily governed by the rise of temperature for a prolonged duration (Stach *et al.* 1982). These processesses also include dehydration, bituminization, debituminization, and graphitization, which involve physical and chemical changes of organic matter (Flores 2014).

During the coalification process, initially, CH_4 and CO evolve from the peat in the form of biogenic methane. As the water concentration decreases, the expulsion of CH_4 and CO get retarded. In the advanced stage of coalification again CH_4 evolve in the form of catagenic methane (Kopp *et al.* 2000). With the chemical variation process of coalification, the heteroatoms cracks, hydrogen-containing alkyl side chains get degraded, and aromaticity is enhanced (Teichmüller and Teichmüller 1979; Yao *et al.* 2011). FTIR analysis of these coals also shows the peak at wavenumber (cm^{-1}) 2950, attributed to aliphatic CH_3; the peaks at 2920 and 2850 cm^{-1} can be attributed to aliphatic CH, CH_2, and CH_3 molecules; whereas the peak at 1450 cm^{-1} is for CH_2 and CH_3 aromatic ring modes. During FTIR analysis of these coals, the transmittance of aliphatic peaks is found higher compared to the peaks associated with aromatic hydrocarbons, which indicate the lower maturity of these coals (Suggate and Dickinson 2004; Presswood *et al.* 2016).

During coalification the geochemical alteration of plant debris occur due to heat and pressure over a very long period of time. The quality or rank of the coal increases with depth. Heat is the most vital variable, its availability in the basin (e.g. from nearby volcanic activity) produces coal relatively younger in age. But mostly the temperature increase that applies is the mean geothermal gradient of the earth's crust which is about 25°C/1000 m of descent. Most bituminous coal forms at temperatures of 100–150°C (Stephenson 2013). The mean maximum reflectance of vitrinite, liptinite, and inertinite

are highly correlated with the rank of the coal (Smith and Cook 1980). The reflectance of vitrinite is an important indicator of the degree of diagenesis of organic matter, maturation of hydrocarbons and coalification (Middleton 1982; Suggate 1998; Vuković *et al.* 2016). The knowledge of coal rank derived from vitrinite reflectance measurements provides the basis for estimating paleotemperatures, the amount of eroded overburden and the time of deformation concerning coalification processes (International Committee for Coal and Organic Petrology 1998). An erratic trend of vitrinite reflectance could be a function of exposure of coal to high temperature due to igneous intrusion, abrupt tectonic movement or unexpected heat flow from the basement (Chandra and Chakrabarti 1989; Jiang *et al.* 2011).

To understand the probable burial depth of South Karanpura coals, a scheme based on vitrinite reflectance has been implemented (after Teichmüller & Teichmüller 1979). Considering the geothermal gradient to be more or less the same for the Gondwana basin as 40 °C/km and heat flow of 74 mW/m^2 (Pandey and Negi 1995). The depth of burial of coals of Barka Sayal area (vitrinite reflectance 0.40 to 0.66, mean 0.54) is estimated to have been between 2000 to 2700 m, and for coals of Argada area (vitrinite reflectance 0.37 to 0.63, mean 0.49) it is estimated to have been between 1800 m and 2500 m Figure 7.45 (A). The coalification temperature of the coals of Barka Sayal area is estimated from 85 °C to 125 °C, whereas for coals of Argada area the coalification temperature lay in between 78 °C to 118 °C Figure 7.45 (B).

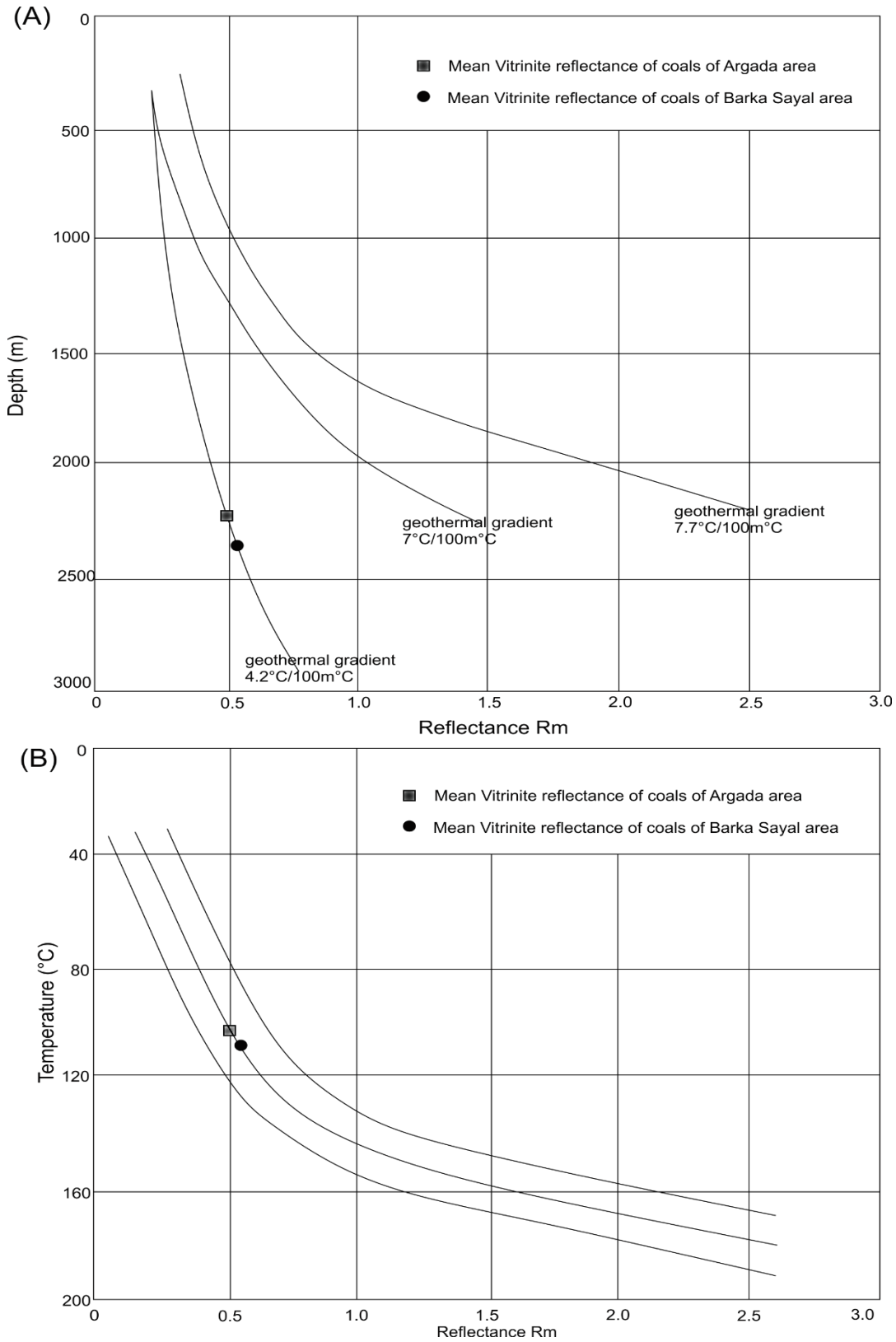


Figure 7.45 Relationship between vitrinite reflectance, depth and rock temperature for the coals of South Karanpura coalfield (after Teichmüller, 1979a) (A) Rm versus depth and (B) Rm versus temperature.

8 CHAPTER 8. CLASSIFICATION AND POTENTIAL UTILIZATION

8.1 Introduction

Coal is classified for various purposes, such as to predict the behaviour of unknown coal or for the proper selection of coal for the best utilisation in industries. Due to the heterogeneous nature of coal, there is no simple system for the classification that can provide, on a comparative basis, an indication of coal characteristics on a global scale. Several schemes have been proposed from time to time for classification, but most of them were based on the properties of coal either belonging to a particular area or a particular rank of coals. Due to these limitations, the earlier classifications were not accepted throughout the world. To overcome this problem, Alpern and Lemos de Sousa (1987) formulated a classification system which was subsequently referred by International Committee for Coal and Organic Petrology (ICCP). This classification is suitable for the Laurasian (North Atlantic) as well as Gondwana coals and is based on rank (for characterizing the degree of coalification; assessed by vitrinite reflectance), type (determined by maceral composition), and grade (determined by the mineral matter/ash).

Further, this classification applies to solid fossil fuels ranging in rank from lignite to anthracite, including coaly shale. Only a few research articles on the classification and utilization of the coals from different Indian coalfields are available. The South Karanpura coalfield, in particular, has not been much studied by workers concerned with the classification and utilization.

In the present chapter, the classification of the coals of South Karanpura coalfield is done according to the several classification schemes used worldwide, based on its petrographic and geochemical properties. Also, proper utilisation of these coals is suggested. Now, the

study provides an in-depth understanding of the detailed classification and utilisation conditions of these coals.

The earliest classification of coal was based on visual characteristics and combustion properties (Krishnan 1940). Coals are having brown to black colour, woody structure, and high moisture content was called lignites or brown coal. The coals exhibiting black colour, easy ignition with producing smoke and flame, and tendency to be agglutinated upon heating were called bituminous coal. In contrast, anthracite was recognized by its black colour, hard and lustrous appearance, difficult ignition, and burning without a flame. As per this classification, the coals of the study area can be recognized as bituminous coal.

Regnault (1810-1878) implemented the geochemical characteristics such as ultimate and proximate constituents of coal for its classification (Regnault 1840), which was further implemented and modified by several authors (Parr 1922). Fraser (1877) proposed a classification of coal, based on fuel ratio calculated from the proximate constituents using the following formula.

$$Fuel\ ratio = \frac{Fixed\ Carbon}{Volatile\ matter}$$

Fraser (1877) classified coals into four types: bituminous, semi-bituminous, semi-anthracite, and anthracite having fuel ratios from 0 to 5, 5 to 8, 8 to 12, and 12 to 100, respectively. The fuel ratio of South Karanpura coals lies between 0.75 and 2.40, indicating that these coals are bituminous. Since it was a broad classification scheme based on old literature, the data obtained from petrological and geochemical analyses were further examined using different well-known classification schemes for coal classification.

The International Organization for Standardization (ISO) classification scheme, is based on random vitrinite reflectance (VRo %), proximate constituents, and the petrographic composition [vitrinite content % by volume, mineral matter free (mmf) basis] (ISO 2005). ISO revised this classification in 2018, i.e., ISO 11760:2018, for the applicability for coals of all the ranks, but care is required concerning the classification of the same type of coal. According to this scheme the coal rank is broadly classified into Low rank coal (lignite and subbituminous coals) having bed moisture ≤ 75 % and VRo % < 0.5 %, Medium rank coal (bituminous coals) having 0.5 % ≤ VRo % < 2.0 %, and High-rank coal (anthracites) having random vitrinite reflectance in between 2.0 and 6.0 %, including the lower limit. This classification scheme also emphasizes sample quantification to provide a brief, definitive description of the sample's nature. Table 8.1 to Table 8.6 presents different conditions for the ISO classification. All the samples collected from the study area are pillar coal samples. According to this classification scheme, coals of the Barka Sayal area can be broadly classified as Medium rank D, moderately high-vitrinite, moderately high-ash coal, while coals of Argada area can be broadly classified as Low rank A, low-vitrinite, moderately high-ash coals. The detailed classification of coals of different seams is mentioned in Table 8.7.

Table 8.1 Definition of broad rank categories: low, medium and high rank

Rank	Definition
Low rank A (lignite and sub-bituminous coals)	bed moisture ≤ 75 % and *VRo%* < 0.5 %
Medium rank A (bituminous coals)	0.5 % ≤ *VRo%* < 2.0 %
High rank B (anthracites)	2.0 % ≤ *VRo%* < 6.0 % (or VRo_{max}% < 8.0 %)

Table 8.2 Subcategories of low-rank coals

Sub-category	Description
Low-rank C (lignite C)	*VRo%* < 0.4 % and bed moisture > 35 % and < 75 %, ash-free basis
Low-rank B (lignite B)	*VRo%* < 0.4 % and bed moisture ≤ 35 %, ash-free basis
Low-rank A (subbituminous coal)	0.4 % ≤ *VRo%* < 0,5 %

Table 8.3 Sub-categories for medium-rank coals

Sub-category	Description
Medium rank D (bituminous D)	0.5 % ≤ *VRo%* < 0.6 %
Medium rank C (bituminous C)	0.6 % ≤ *VRo%* < 1.0 %
Medium rank B (bituminous B)	1.0 % ≤ *VRo%* < 1.4 %
Medium rank A (bituminous A)	1.4 % ≤ *VRo%* < 2.0 %

Table 8.4 Sub-categories for high-rank coals (anthracites)

Sub-category	Description
High rank C (anthracite C)	2.0 % ≤ *VRo%* < 3.0 %
High rank B (anthracite B)	3.0 % ≤ *VRo%* < 4.0 %
High rank A (anthracite A)	4.0 % ≤ *VRo%* < 6.0 % (or VRo_{max}% < 8.0 %)

Table 8.5 Classification by the petrographic composition

Vitrinite content % by volume, mineral-free	Vitrinite class category
< 40	Low vitrinite
≥ 40 and < 60	Medium vitrinite
≥ 60 and < 80	Moderately high vitrinite
≥ 80	High vitrinite

Table 8.6 Ash yield classification

Ash yield % by mass dry basis	Ash class category
< 5	Very low ash
≥ 5 and < 10	Low ash
≥ 10 and < 20	Medium ash
≥ 20 and < 30	Moderately high ash
≥ 30 and < 50	High ash

Table 8.7 Classification of the coals of South Karanpura coalfield (seam-wise) as per the International Organization for Standardization (ISO) classification scheme (ISO, 2005).

Seam Name	Mean rank (VRo%)	Mean petrographic composition (% vitrinite by volume, mmf basis)	Ash yield %	Description term (rank, vitrinite, ash)
Sayal	0.59	72.28	30.57	Medium rank D, moderately high vitrinite, high ash
Sayal Balkudra	0.44	66.23	27.92	Low rank A, moderately high vitrinite, moderately high ash
Upper Semana	0.49	36.88	15.40	Low rank A, low vitrinite, medium ash
Lower Semana	0.49	62.82	14.93	Low rank A, moderately high vitrinite, medium ash
Hathidari	0.62	77.42	21.80	Medium rank C, moderately high vitrinite, High ash
Bansgarha	0.59	80.27	24.31	Medium rank D, high vitrinite, moderately high ash
Barka Sayal area	0.54	65.98	22.49	Medium rank D, moderately high vitrinite, moderately high ash
Argada	0.50	49.20	29.62	Medium rank D, medium vitrinite, moderately high ash
Argada-A	0.46	37.84	24.95	Low rank A, low vitrinite, moderately high ash
Argada-B	0.49	43.08	31.74	Low rank A, medium vitrinite, high ash
Argada-C	0.46	53.40	24.04	Low rank A, medium vitrinite, moderately high ash
Argada-D	0.42	45.13	22.36	Low rank A, medium vitrinite, moderately high ash
Argada-I	0.55	14.86	25.95	Medium rank D, low vitrinite, moderately high ash
Argada-J	0.53	29.78	25.30	Medium rank D, low vitrinite, moderately high ash
Argada area	0.49	39.04	26.28	Low rank A, low vitrinite, moderately high ash

8.2 South Karanpura Coals on the Seyler's Classification Chart

Another classification scheme (Seyler's coal classification) has also been used to classify these coals. It is based on carbon and hydrogen content (Parr basis) (Seyler 1931). As per this classification, the coal is categorized into four main groups based on carbon content, which is further subdivided into varieties/ genera based on hydrogen content. For the carbon content, three prefixes ortho, meta, and para have been used for typical, more, and less content of carbon, respectively. While in the case of hydrogen content, the terms are ortho, per, and sub, depicting typical, more, and less hydrogen content, respectively. Plots of Barka Sayal coals indicates the coals have variable distribution, and their species varies from ortho-lignitous to ortho-bituminous, in the case of genera some of the samples are perhydrous in nature thus they are having high hydrogen (more than 5.80%) content and may be capable of generating liquid hydrocarbons upon pyrolysis. In contrast, a good amount of the samples lie in the orthohydrous zone having a normal hydrogen range (5% to 5.80%) for coal, some of the samples also lie in the subhydrous zone having less hydrogen content (Figure 8.1). It has been attributed to the paleodepositional effects. It has also affected the vitrinite reflectance and microscopic constituents of these coals. A slight marine influence may have produced low reflecting, fluorescing perhydrous vitrinites near marine flooding surfaces. Subhydrous nature of these coals was found when oxidising conditions prevailed in the swamp. Similar conditions have also been observed in Northern Denison Trough, Bowen Basin, Australia (Kalinowski and Gurba 2020). Hydrogen-rich coals are more susceptible to produce liquid hydrocarbons, whereas poor hydrogen coals can produce gaseous hydrocarbons. In the case of coal seams of the Argada area, the species varies from ortho-lignitous to para-bituminous. However, in the case of genera, very few samples are perhydrous, a good amount of samples are ortho hydrous, but a significant number of samples belonging to Argada-B, Argada-C, and

Argada-D lie in subhydrous zone having less hydrogen content (Figure 8.1). Weathered or thermally altered coal behaves like abnormal coal and their plots do not lie on the Seyler's band because of physical, chemical, or biological processes during weathering such as exposure of coal to the air or addition of moisture by rain, etc. alter the initial geochemical constituents of the coal. It may be possible that some coals had faced the alteration processes, having plots not lying on the Seyler's band (Figure 8.1).

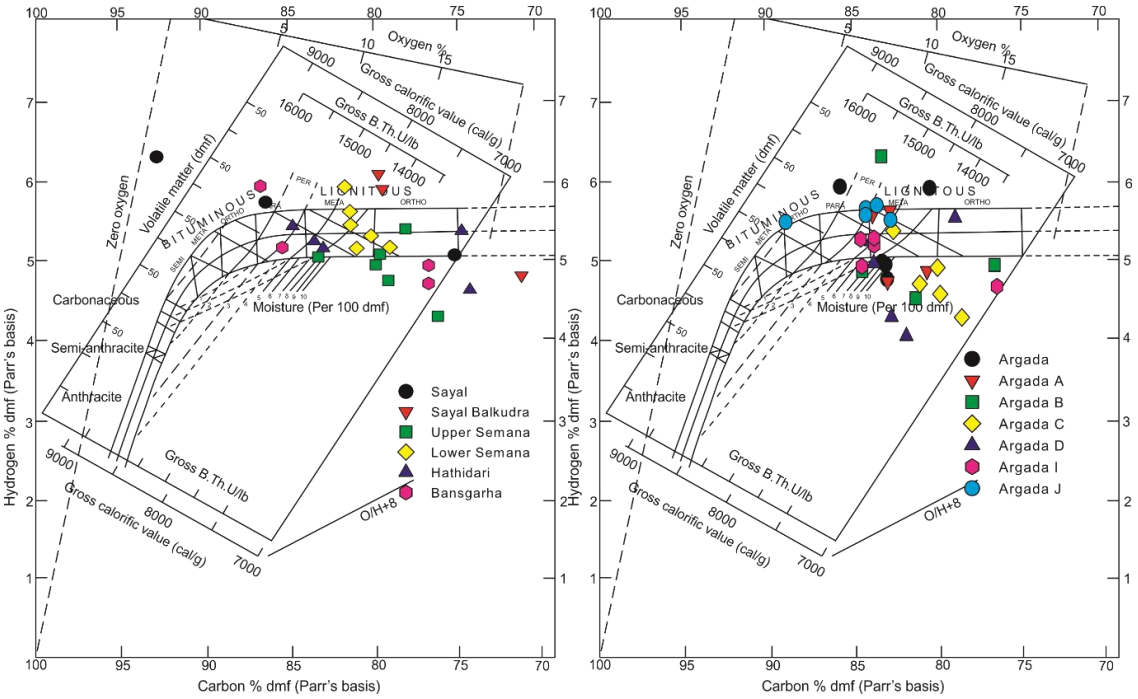
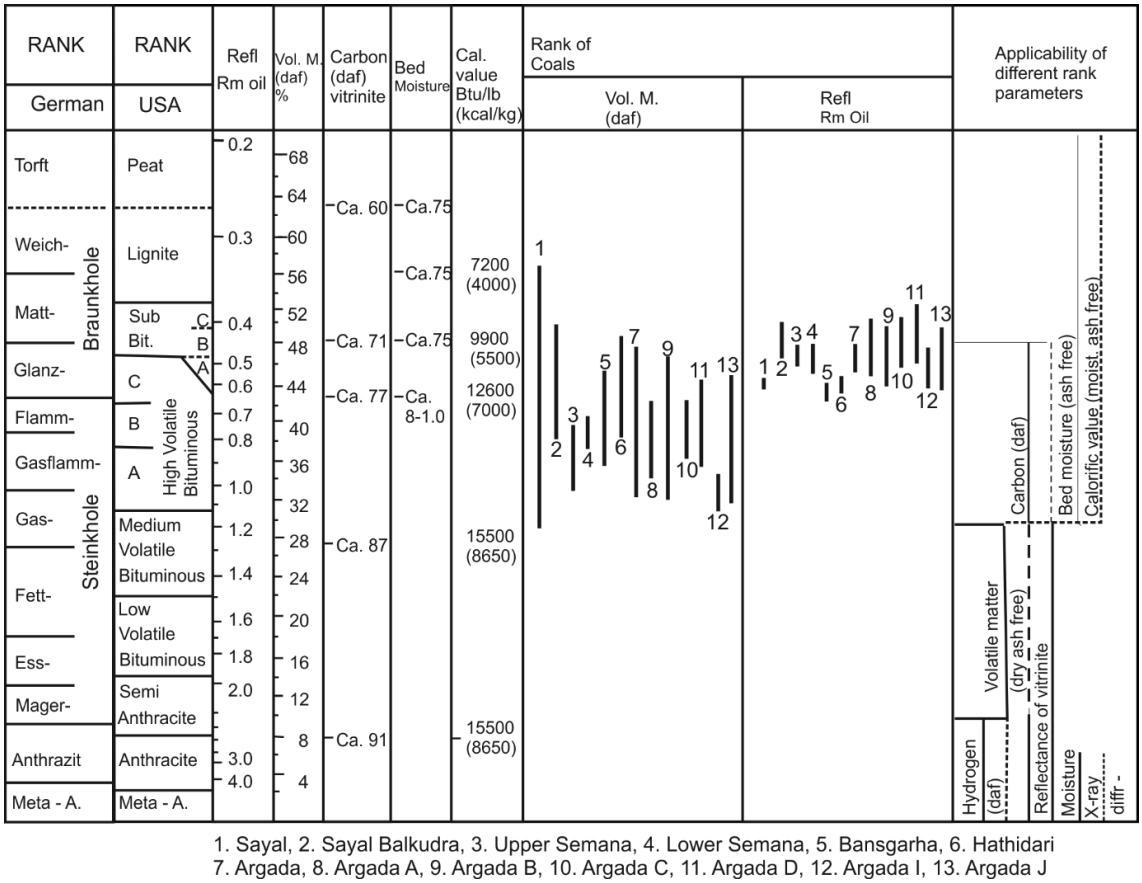


Figure 8.1 Plots of South Karanpura coals in Seyler's coal classification chart based on Carbon and Hydrogen contents (Seyler, 1938). A) Barka Sayal area, B) Argada area.

8.3 Classification according to West German (DIN) and North American (ASTM) System

West German (DIN) and the North American ASTM classification scheme (Stach *et al.* 1982) consider the volatile matter (daf basis) and vitrinite reflectance as a parameter for the classification of coals. As per the West German (DIN) classification system, the rank of the coals of South Karanpura coalfield varies from Matt-Baranukhole to Flamm-Steinkhole (Figure 8.2).

The vitrinite reflectance (VRo %) of the coals of the Barka Sayal area varies from 0.40 to 0.66, mean 0.54 (Table 6.1). The coals of Sayal seam exhibit VRo% ranging in between 0.57 to 0.62, mean 0.59. Sayal Balkudra exhibit vitrinite reflectance ranging in between 0.40 and 0.48, mean 0.44. The vitrinite reflectance of Upper Semana varies from 0.45 to 0.51, mean 0.49. The Lower Semana coals have VRo % lying in the range of 0.44 to 0.54, mean 0.49. Hathidari coals have VRo % from 0.59 to 0.66, mean 0.62, the highest in the area. The coals of the Bansgarha seam exhibit VRo% from 0.56 to 0.63, mean 0.59. The vitrinite reflectance of coals of the Barka Sayal area varies from 0.40 to 0.66, mean 0.54; hence these coals are sub-bituminous C to high volatile C bituminous in rank (Figure 8.2).



1. Sayal, 2. Sayal Balkudra, 3. Upper Semana, 4. Lower Semana, 5. Bansgarha, 6. Hathidari
7. Argada, 8. Argada A, 9. Argada B, 10. Argada C, 11. Argada D, 12. Argada I, 13. Argada J

Figure 8.2 Rank of coals of the South Karanpura Coalfield, Jharkhand, India, based on Random Vitrinite reflectance (VRo %) and V.M. (daf basis) in the scheme representing the different stages of coalification according to North American (ASTM) and West German (DIN) classification and their distinction based on different physical and chemical parameters. The last column shows the applicability of various rank parameters to different coalification stages (Stach *et al.* 1982).

The vitrinite reflectance of the coals of the Argada seam varies from 0.45 to 0.54, mean 0.50 (Table 6.2). For Argada-A, the range lies between 0.39 and 0.57, mean 0.46. The coals of Argada-B seam have VRo% lying in the range of 0.41 to 0.61, mean 0.49. in contrast, VRo% of Argada-C seam is between 0.39 and 0.52, mean 0.46. Coals of Argada-D seam have VRo% from 0.37 to 0.50, mean 0.42. Argada-I coals have vitrinite reflectance ranging in between 0.46 and 0.62, mean 0.55. For the coals of Argada-J seam, the vitrinite reflectance varies from 0.41 to 0.63, mean 0.53. Overall the coals of the Argada area exhibit vitrinite reflectance in between 0.37 and 0.63, mean 0.49. Thus these coals are a little less mature than coals of the Barka Sayal area and possess rank in between sub-bituminous C and subbituminous A.

Hence from the above discussion, it can be concluded that, according to the ASTM classification scheme, coals of the South Karanpura coalfield are subbituminous C to high volatile C bituminous in rank (Figure 8.2).

8.4 Classification of Coals according to Indian Standard (IS: 770- 1977)

According to the classification and codification of Indian coals and lignite (2nd revision of IS: 770: 2003), consider the volatile matter (dmf basis) and elemental composition (dmf basis) as the classification parameters. The coals of South Karanpura coalfield has been classified as follows (BIS 2003a).

Class-	Sub-bituminous to Bituminous
Type-	High volatile
Symbol-	SB, B2
Nature-	Non-caking

8.5 South Karanpura Coals in the International Classification System

A classification scheme proposed by Alpern (1981) and further modified by Falcon (1986) has also been used to classify the coals of South Karanpura coalfield. They have considered total reactive macerals content, reflectance, and an ash yield of the coal as

parameters for the classification. In this scheme, Alpern et al. (1989) divided coal based on their ash weight (wt.)% into, 0%-10% ash - Clean coal, 10%-50% - Ashy coal, 50%-80% - Coaly Shale (Coaly rock) and 80%-100% - Shale (Rock). Falcon (1986) has used vitrinite reflectance and the reactive macerals (vol.%) for the classification of different coals. As per Falcon's classification, the coals of the Barka Sayal and Argada area can be characterized as Meta Sub-bituminous to Hypo-bituminous in rank. Most of these coals are intermediate, while some of them are vitric and inertic types having a grade of ashy coal (Figure 8.3).

The vitrinite reflectance and vitrinite content of these coals have been plotted in Economic Commission for Europe-United Nations Classification scheme (ECE-UN 1998) (Figure 8.4), which suggests that these coals are sub-bituminous to semibituminous in rank and based on ash%, they show a range from medium ash coal to very high ash coal (Figure 8.4). A high concentration of ash% indicates that these coals are allochthones in origin.

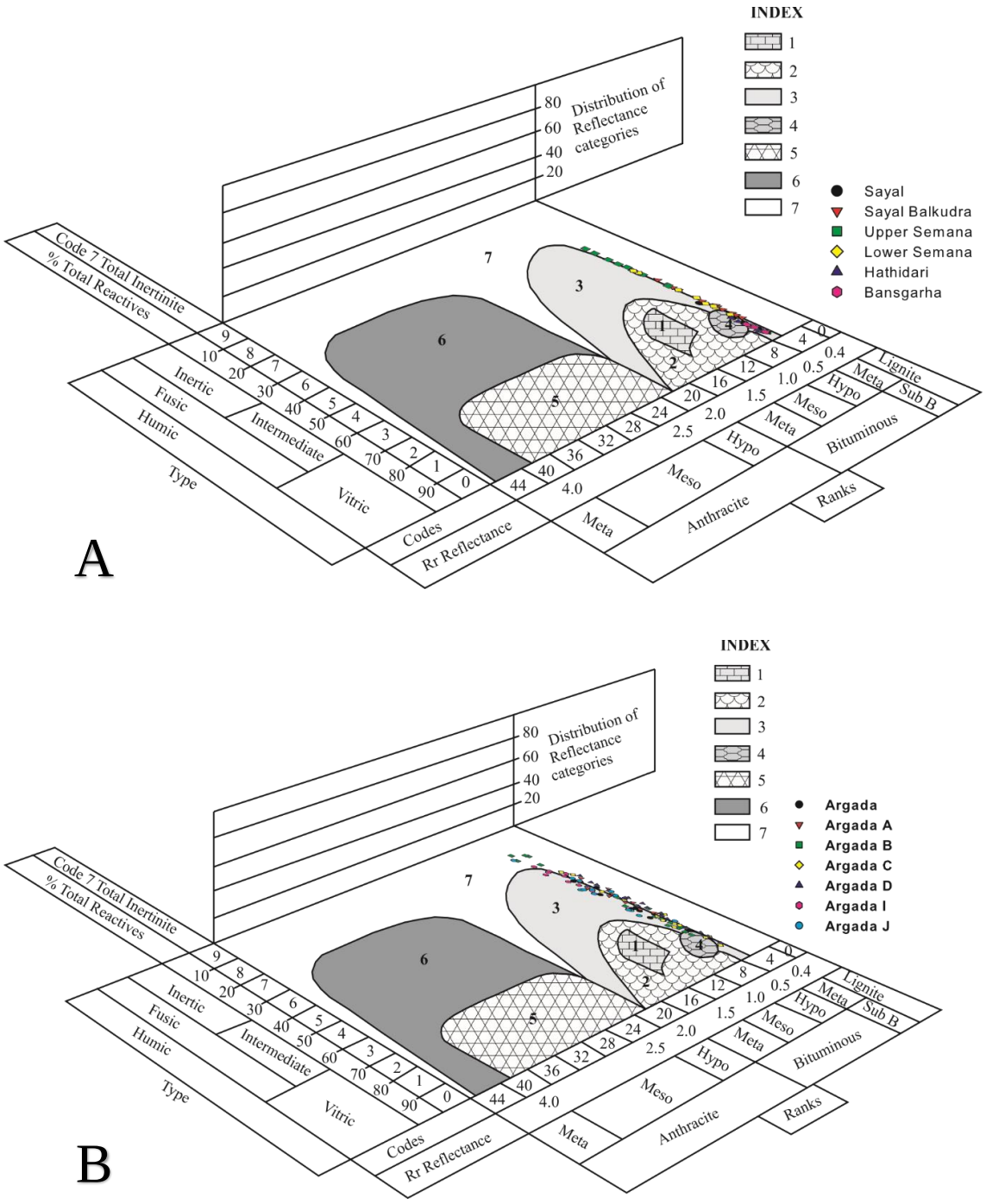


Figure 8.3 Classification and proposed potential utilisation of South Karanpura coals on the 3-D classification system of coals using rank (Vitrinite Reflectance Ro max and Ro min%) type (Vol.% of total reactive macerals) (modified after Falcon, 1986). (1. Prime coking; 2. Blend coking coals > 3 SI; 3. Blend coking coals < 3 SI; 4. Hydroliquefaction; 5. Prime anthracite for direct reduction and Sonderberg Electrode manufacture; 6. Prime anthracite for industrial and domestic combustion; 7. Less specialized utilisation- power generation, gasification, form-coke, briquette). A) Barka Sayal area, B) Argada area.

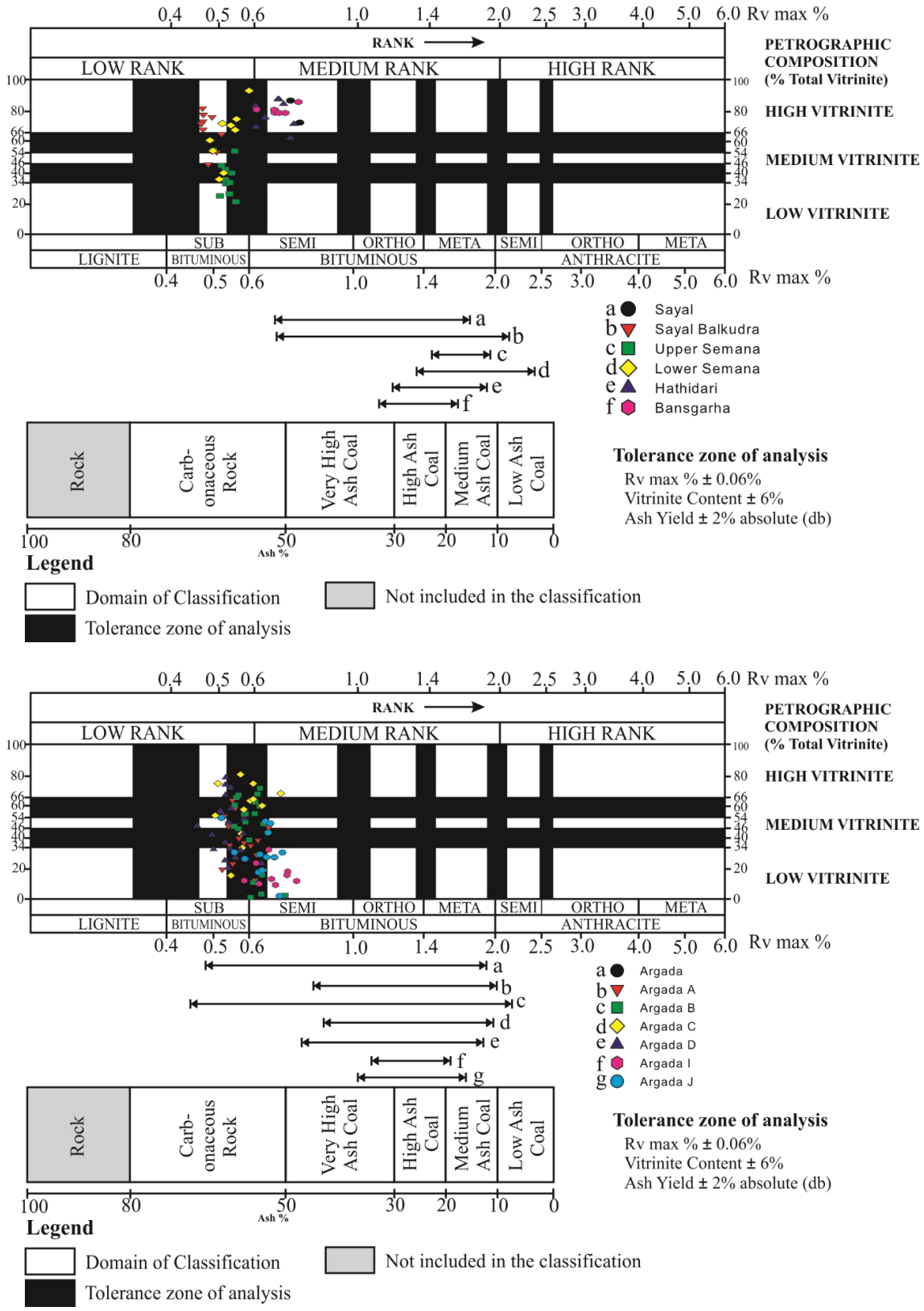


Figure 8.4 Plots of coals in ECE-UN Classification Scheme (UN-ECE classification, 1998). A) Barka Sayal area, B) Argada area.

8.6 Potential Utilisation of Coals of South Karanpura coalfield

Enhancement of scientific knowledge and introduction to the new sophisticated instruments and techniques in the field of organic petrography and geochemistry of coal has introduced the new possibilities of proper and efficient utilisation of the vast world coal reserves. There can be several possible uses of coal such as coal liquefaction, coal gasification, carbonisation, combustion, generation of coal tar, etc. (Bryers 1996; Hower *et al.* 1996; Hower 2012; Wang *et al.* 2013; Singh and Jha 2018a). India is the world's third-largest energy consumer, and its coal-fired electricity accounts for 71% of electricity generated in India (IEA 2015).

Coal is widely used as a combustion fuel for industrial as well as domestic purposes. To identify the suitability of coal, for combustion and grading, the Useful Heat Value (UHV) of the coals of South Karanpura coalfield was calculated using the following formula (Speight 2005b).

$$UHV\ in\ kcal/kg = 8900 - [138\ (ash\ content + moisture\ content)]$$

Coals of the Barka Sayal area exhibit a mean UHV of 5290 kcal/kg while coals of the Argada area have a mean UHV of 5023 kcal/kg. However, the burning of coal using conventional techniques may generate several harmful emissions and effluents that may affect the environment and ecology (Dai *et al.* 2012). Coals of South Karanpura coalfield have a range of Sulphur from nil to 0.88% (daf basis), and Nitrogen content lies in the range of nil to 2.14% (daf basis). Although the amount of Sulphur and Nitrogen is not very high in these coals as a precautionary measure to avoid the generation of oxides of sulphur and nitrogen, it requires proper attention and implementation of emission control techniques such as coal cleaning, flue gas cleaning, or Fluidized Bed Combustion (FBC), before combustion of coal (Ryberg *et al.* 2015).

Falcon (1986) provided a model to comment upon the utilisation of South Africa coals, considering the Vitrinite Reflectance and percentage of reactive macerals as a parameter. In Falcon's model, the plots show that these coals are best suited as blend coking coals because they contain a high amount of reactive macerals (mean 64.0% mmf basis) and attained sufficient maturity (mean VRo.%= 0.51) (Figure 8.3).

Coals of the Barka Sayal area have a high amount of reactive macerals lying mostly in area 3, and some bands of Sayal Balkudra, Lower Semana, and Bansgarha in area 4 and while few bands of Upper Semana in area 7 of the Falcon's diagram (Figure 8.3). This suggests that most of these coals can be utilized for blend coking coal; some are suitable for hydro-liquefaction, while few Upper Semana coal bands may have utilization options such as power generation, gasification, or for the formation of briquette (Figure 8.3). Coals of the Argada area of South Karanpura coalfield have a relatively lower amount of reactive maceral but more or less the same vitrinite reflectance range; thus, these coals are not suitable for hydroliquefaction, but they can be utilized as blend coking coal or for combustion.

Further, data of these coals were plotted in a model given by Snyman (1989), which is based on Carbon (C%) and Hydrogen (H%) obtained by ultimate analysis of coals and calculated on a dry ash-free (daf) basis. This model suggests that coals of the study area are best suited for the gasification process since they have relatively less Hydrogen% and high Carbon% than the elemental composition required for the generation of liquid fuels upon pyrolysis (Figure 8.5). These coals also can be useful for making high strength char, but the concentration of such types of coals is low.

This statement is also supported by BIS (2003) according to this, the coals of the study area can be best utilized for combustion or gasification, whereas few of the bands whose

volatile matter, carbon content, as well as hydrogen content, is high can also be utilized for hydrogenation purposes.

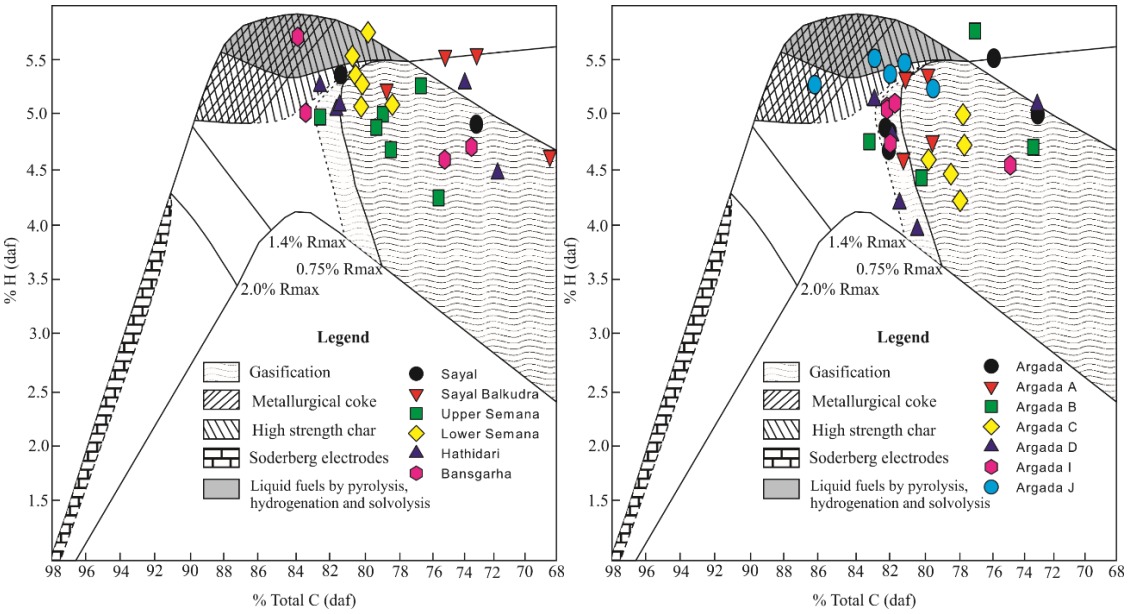


Figure 8.5 Seyler diagram modified by Snyman (1989) for South African coal has been further modified for coals of Barka Sayal area of South Karanpura Coalfield for showing their suitability for specialized fields of utilisation. A) Barka Sayal area, B) Argada area.

Although successful Underground Coal Gasification (UCG) field trials show a coal site having parameters- depth 30 to 580 m, thickness 2 to 5 m, ash 2 to 34%, moisture 7 to 35%, volatile matter 27 to 44%, and fixed carbon 12 to 38% are important for UCG (Khadse *et al.* 2007). Coals of the Barka Sayal area exhibit less moisture content, which is ranging from 2.71 to 5.42 wt.%, but other parameters lie more or less in the same range, which suggests useful utilisation of these coals for UCG too.

Vitrinite macerals possess thermoplastic properties at bituminous rank, facilitating the dissolution of the vitrinite group of macerals and lead to the success of liquefaction. Liptinite provides a relatively higher oil yield because of its greater aliphatic content. Most of the macerals of inertinite groups remain less reactive or inert during the liquefaction process, whereas most of the major mineral groups present in coal also remain unaltered during the process (Suárez-Ruiz and Crelling 2008). The coal deposits

of South Karanpura coalfield contain a significant amount of liptinite macerals and a high amount of vitrinite macerals. Hence, these coals were further analyzed for their potential for coal liquefaction. Davis et al. (1976) used the VRo%, and reactive macerals content (vitrinite + liptinite) calculated mmf basis as the parameters to predict the liquefaction behaviour of coal and suggested an area of predicted optimum liquefaction between VRo% from 0.5 to 1.0 and reactive macerals from 70 Vol.% to 100 Vol%. Most of the bands belonging to South Karanpura coalfield lies in this range. The same outcome was found to be supported by the properties given by Cudmore (1977). He estimated that the properties of coal required for hydrogenation as VRo% should be less than 0.8, H/C atomic ratio more than 0.75%, reactive macerals (vitrinite + liptinite) content should be more than 60%, volatile matter (daf) more than 35%, and the concentration of heteroatoms should be relatively low. The coals of South Karanpura coalfield have VRo 0.37% to 0.66%, H/C atomic ratio between 0.59 to 2.84, reactive macerals (vitrinite + liptinite) content 12.75 to 97.30, volatile matter daf 29.41% to 57.13% and low concentration of heteroatoms. Thus, it suggests that coals of South Karanpura coalfield are also suitable for the liquefaction process.

Coal is a critical, indigenous, and abundant fossil fuel. It is used throughout the world for electricity production. The coals of South Karanpura coalfield are mainly used for power generation and small industries nearby. Trace elements behaviour during coal combustion has been discussed by several authors (Querol *et al.* 1995, 1997a; Pires and Querol 2004). An assessment has been done for the combustion behaviour of the coals from South Karanpura coalfield to determine its behaviour during combustion processes.

The combustion efficiency of boilers depends on several factors such as air circulation within the boiler, flue gas temperature, radiation losses, fuel specification, and the temperature of ignition. Among these factors, fuel specification is the most important

factor. Larger fragments of coal are hard to burn compared to finer particles (Man and Gibbins 2011). 'Banded dull coal' is the most dominant lithotype of these coals, making it easy to break into finer fragments. Singh and Jha (2018b) found that dull coal is the most friable lithotype in South Karanpura coalfield and produce more fines. Production of fines may obstruct combustion due to its segregation behaviour; hence, coal seams having a high amount of dull bands requires conditioning with water. Since the moisture content of these coals is less; hence, it would require water from external sources.

Microscopically the dominance of reactive macerals (vitrinite and liptinite) in the Barka Sayal coals makes it suitable for the combustion process. Singh and Jha (2018a) have discussed the hydrocarbon potential of few seams of the Barka Sayal area employing petrographic and geochemical tools. It is found that these coals are immature, but they are suitable for the liquefaction process. The remaining seams of the Barka Sayal area and Argada area also exhibit the same behaviour.

Ash-deposition behaviour affects the efficiency of the boiler and limits coal utilization for combustion purposes (Barroso *et al.* 2007; Koukouzas *et al.* 2010). The effect of mineral matter present in these coals on slagging was studied using basic to acid oxides ratio (Scott 1999) mentioned below:

$$R_{b-a} = \frac{CaO + MgO + K_2O + Fe_2O_3 + Na_2O}{SiO_2 + TiO_2 + Al_2O_3}$$

The R_{b-a} value <0.2 indicates a low slagging tendency while 0.2–0.4 moderate and 0.4–0.55 indicates a very high slagging. The mean value of R_{b-a} for south Karanpura coal varies from 0.03 to 0.63, mean 0.12. This indicates that coals of South Karanpura coalfield exhibit a moderate slagging tendency. Thus, during the combustion process of these coals, appropriate steps should be taken care of, such as the blending of these coals with other high-quality coals.

9 CHAPTER 9. SUMMARY AND CONCLUSION

The present work is focused on the petrographic and geochemical characterization of the coals of the South Karanpura coalfield, which is situated in the Ramgarh district of Jharkhand state. South Karanpura coalfield is a part of the major Gondwana basin of India. A thick layer of lower Gondwana sediments is deposited here, mainly in the glacial and fluvial environment during the Permian. The basin is bounded by major faults. A thin stretch of Talchir sediments joins South Karanpura to North Karanpura coalfield. Granitic gneissic complex forms the basement, and thick sediments of Talchir, Karharbari, Barakar, Barren measure, and Raniganj formation has been spotted in the South Karanpura coalfield. Barakar formation is the main coal-bearing horizon in the study area. The coalfield comprises two areas, Barka Sayal and Argada. Upper seams such as Sayal, Sayal Balkudra, Upper Semana, Lower Semana, Hathidari and Bansgarha are exposed in the Barka Sayal area, whereas seams Argada, Argada A, Argada B, Argada C, Argada D, Argada I and Argada J are exposed in the mines of the Argada area of this coalfield.

Coal samples were collected from all the working/exposed coal seams following the pillar sampling method. The megascopic characterization of the samples was made according to Diessel's (1986) classification scheme, and based on megascopic characterization, megascopic seam profiles have been constructed. Samples having similar megascopic properties were clubbed together as one sample. The petrographic and geochemical analysis was carried out for each megascopic band of every coal seam. These data were used to understand the paleo-mires and evolution of these Gondwana coals. Source rock characteristics of these coals were also identified along with the presence of environmentally sensitive elements. Further, these coals were classified based on several widely accepted classification schemes, and their potential utilisation was also suggested. The key findings of this work are mentioned in the following sections.

- The coals of South Karanpura coalfield have originated in a faulted half-graben structure. Barakar Formation of Lower Permian comprising sediments of Lower Gondwana Group is the main coal-bearing horizon.
- South Karanpura coals are banded in nature and dominantly composed of vitrinite and inertinite groups of macerals. Liptinite occurs in low concentrations. The microlithotype analysis shows the dominance of vitrite, inertite, and clarite.
- Argillaceous and carbonaceous mineral matters are dominant in these coals, followed by sulfides and other minerals. The X-ray analysis determined the presence of quartz, kaolinite, hematite, and clay minerals in a high amount.
- The distribution of the microscopic constituents along the seam profile confirms its variability according to the type of bands. Bright bands having more vitrinite content, whereas dull bands are liptinite and inertinite rich.
- The random vitrinite reflectance (VRo%) in the coals of the Barka Sayal area is slightly higher than the coal seams of the Argada area.
- Besides having approximately similar petrochemical constituents, the coal seams of the Argada area exhibit more ash and mineral components than the coals of the Barka Sayal area, which suggests the water flooding conditions were more frequent during the deposition of coals of the Argada area.
- The genetic characterization suggests that these coals are vitric to intermediate types.
- The microscopic analysis of these coals under blue-light irradiation indicates the presence of secondary liptinite macerals such as exsudatinite, fluorinite, and bituminite, which indicate the hydrocarbon expulsion from these coals.

- Coals of South Karanpura coalfield are rich in silica followed by alumina and iron content. Other oxides are in less concentration (mean values <2%). The high concentration of oxides is mainly controlled by the nature of minerals present.
- Most of the trace elements are in high concentration. It shows seam wise variability, but overall vanadium, rubidium, strontium, and zirconium are present in comparatively higher concentrations than chromium, cobalt, nickel, copper, zinc, and lead.
- Mineral matter in these coals occurs as superficial fillings of pores and fissures, superficial mounting, massive impregnation, and cavity fillings. These modes of occurrence of minerals suggest that most of the minerals forming in these coals are syngenetic and formed during the peatification process.
- The rank of these coals has been assessed as sub-bituminous C to high volatile C bituminous as per the North American ASTM classification, taking the volatile matter (daf basis) and vitrinite reflectance into consideration.
- The high occurrence of detrital macerals such as vitrodetrinite, inertodetrinite, etc. indicates the allochthonous origin of these coals.
- The ratio of hydrogen versus carbon and carbon versus oxygen suggests that these coals are type III kerogen. This has been further supported by the data plot between H/C and vitrinite reflectance, HI versus OI, as well as Tmax versus vitrinite reflectance. Rock-Eval pyrolysis data also suggests that these coals may act like immature source rock and having the potential to generate mostly gaseous hydrocarbon.
- According to the Indian standard (IS: 770- 1977) for classification and codification of Indian coals and lignites, the coals of South Karanpura coalfield can be characterized as-

Class	-	Subbituminous to Bituminous
Type	-	High volatile
Symbol	-	SB, B2
Nature	-	Non-caking

- As per the international classification of coal, these coals can be classified as

Type	-	Intermediate
Rank	-	Meta Subbituminous to Hypo-bituminous
Grade	-	Ashy coal

- Based on the present study, it has been suggested that these coals are best suitable for gasification processes. Some of the bands can be used in the blend for coke making.

Recommendations for future works/research

- The petrographic constituents present in these coals cast a great impact on their effective utilization. The generated petrographic data could be helpful for future researchers working on the Gondwana coals in general and South Karanpura coals in specific.
- The inference drawn for the depositional environment based on coal petrographic depositional models could be helpful for Palynologists to draw a robust conclusion about the paleovegetation and paleoclimate.
- Some of the marine-influenced samples were detected in some parts of the Sayal Balkudra seam and Argada-A seam which needs more focus from future researchers to study the impact of marine incursion in these coals.
- The petrological and geochemical characteristics obtained from these coals can act like a robust tool to implement the effective utilization of these coals by mine planners and bureaucrats.

References

Abbassi, S., Edwards, D.S., George, S.C., Volk, H., Mahlstedt, N., di Primio, R. and Horsfield, B. 2016. Petroleum potential and kinetic models for hydrocarbon generation from the Upper Cretaceous to Paleogene Latrobe Group coals and shales in the Gippsland Basin, Australia. Organic Geochemistry, 91, 54–67.

Abdullah, W.H., 1999. Oil-generating potential of Tertiary coals and other organic-rich sediments of the Nyalau Formation, onshore Sarawak. Journal of Asian Earth Sciences, 17(1-2), .255–267

Acharyya, S.K. 2019. Character, Tectonism, and Rank Variation in Gondwana Coal. In: Tectonic Setting and Gondwana Basin Architecture in the Indian Shield. 111–117.

Adebiyi, F.M., Thoss, V. and Akinola, A.S. 2014. Comparative Studies of the Elements that are Associated with Petroleum Hydrocarbon Formation in Nigerian Crude oil and Bitumen Using ICP-OES. Journal of Sustainable Energy Engineering, 2, 10–18.

Ahmad, M. 1971. Petro-chemical study of coal, Laitryngew coalfield, K. & J. Hills, Assam, J. Geol. Soc. Assam, 1, 17–20.

Ahmed, M. 1996. Petrology of Oligocene coal, Makum coalfield, Assam, northeast India. International Journal of Coal Geology, 30, 319–325.

Ahmed, M. and Bharali, D. 1984. Petrographic characters of Tertiary coals, Nangalbibra, West Daranggiri coalfield, Garo Hills, Meghalaya. In: Proc. 4th Geophytol. Conf., Lucknow. 242–245.

Akande, S.O., Hoffknecht, A. and Erdtmann, B.D. 1992. Rank and petrographic composition of selected upper Cretaceous and Tertiary coals of Southern Nigeria. International Journal of Coal Geology, 20, 209–224.

Alexander, R., Kagi, R.I., Noble, R. and Volkman, J.K. 1984. Identification of some bicyclic alkanes in petroleum. Organic Geochemistry, 6, 63–72.

Ali, M., Paul, S. and Chatterjee, R. 2017. Cleat Orientation from Ground Mapping and Image Log Studies for *In Situ* Stress Analysis: Coal Bed Methane Exploration in South Karanpura Coalfield, India. Energy & Fuels, 31, 6812–6824.

Alpern, B. 1980. Petrographic du kerogene. In: Durand, B. (ed.) Kerogen, Insoluble Organic Matter from Sedimentary Rocks. 339–371.

Alpern, B. 1981. Pour une classification synthétique universelle des combustibles solides. Bull. Centres Rech. Explor.-Prod. Elf-Aquitaine, 5, 271–290.

Alpern, B. and Cheymol, D. 1978. Réflectance et fluorescence des organoclastes du Toarcien du Bassin de Paris en fonction de la profondeur et de la température. Revue de l'Institut Français du Pétrole, 33, 515–536.

Alpern, B. and Lemos de Sousa, M.J. 1987. Project of an international scientific classification of solid fossil fuels. In: Compte Rendu Congres International de Stratigraphie et de Géologie Du Carbonifere. 11e Beijing. 157–168.

Alpern, B., Durand, B., Espitalie, J. and Tissot, B. 1972. Localisation, caractérisation et classification pétrographique des substances organiques sédimentaires fossiles. Advances in Organic Geochemistry, 1971, 1–28.

Alpern, B., Lemos De Sousa, M.J. and Flores, D. 1989. A progress report on the Alpern Coal Classification. International Journal of Coal Geology, 13, 1–19.

Ammosov, I.I. 1956. New methods of coal petrography. Studies of the Laboratory of Coal Geology, 6.

Ammosov, I.I. and Ermakova, V.P. 1950. Microscopic Luminescente Des Charbons Sapropeliques.

Arbuzov, S.I., Chekryzhov, I.Y., et al. 2019. Comments on the geochemistry of rare-earth elements (La, Ce, Sm, Eu, Tb, Yb, Lu) with examples from coals of North Asia (Siberia, Russian far East, North China, Mongolia, and Kazakhstan). International Journal of Coal Geology, 206, 106–120.

ASTM Standard D388-15. 2015. Standard Classification of Coals by Rank, ASTM International, West Conshohocken, PA.

ASTM Standard D5291-16, 2016. Standard Test Methods for Instrumental Determination of Carbon, Hydrogen, and Nitrogen in Petroleum Products and Lubricants, ASTM International, West Conshohocken, PA.

ASTM Standard D5373-08. 2008. Standard Test Methods for Instrumental Determination of Carbon, Hydrogen, and Nitrogen in Laboratory Samples of Coal, ASTM International, West Conshohocken, PA.

Ayinla, H.A., Abdullah, W.H., Makeen, Y.M., Abubakar, M.B., Jauro, A., Sarki Yandoka, B.M. and Zainal Abidin, N.S. 2017. Petrographic and geochemical characterization of the Upper Cretaceous coal and mudstones of Gombe Formation, Gongola sub-basin, northern Benue trough Nigeria: Implication for organic matter preservation, paleodepositional environment and tectonic settings. International Journal of Coal Geology, 180, 67–82.

Balachandran, M. 2014. Role of Infrared Spectroscopy in Coal Analysis—An Investigation. American Journal of Analytical Chemistry, 05, 367–372.

Bandopadhyay, A.K. 2010. Determination of quartz content for Indian coals using an FTIR technique. International Journal of Coal Geology, 81, 73–78.

Banerjee, A., Mishra, P.R., Mohanty, A., Chakravarty, K., Das Biswas, R., Sahu, R. and Chakravarty, S. 2016. Distribution of mineral species in different coal seams of Talcher coalfield and its transformation behavior at varying temperatures. International Journal of Coal Science & Technology, 3, 97–103.

Banerjee, A.K. 1932. Microscopic study of some Indian coals. Geol. Surv. India, Rec, 66, 333–347.

Banerjee, I. 1960. Geology of the Area around South Karanpura Coalfield, Bihar. A Study in Stratigraphy and Petrology of the Lower Gondwana Sedimentary Rocks with Special Reference to the Barakars. University of Calcutta.

Banerjee, I. 1963. Trends of Sedimentary Differentiation in Barakar Sandstones of the South Karanpura Coalfield, India. SEPM Journal of Sedimentary Research, Vol. 33, 320–332.

Banerjee, I. 1964. Size-Roundness Relation in the Barakar Sandstones of the South Karanpura Coalfield, India. Sedimentology, 3, 22–28.

Banerjee, N.N., Ghosh, B. and Das, A. 2000. Trace Metals in Indian Coals. Allied Publishers.

Barker, C.E. and Elders, W.A. 1981. Vitrinite reflectance geothermometry and apparent heating duration in the Cerro Prieto geothermal field. Geothermics, 10, 207–223.

Barroso, J., Ballester, J. and Pina, A. 2007. Study of coal ash deposition in an entrained flow reactor: Assessment of traditional and alternative slagging indices. Fuel Processing Technology, 88, 865–876.

Baudin, F., Disnar, J.-R., Aboussou, A. and Savignac, F. 2015. Guidelines for Rock–Eval analysis of recent marine sediments. Organic Geochemistry, 86, 71–80.

Bechtel, A., Gratzer, R. and Sachsenhofer, R.. 2001. Chemical characteristics of Upper Cretaceous (Turonian) jet of the Gosau Group of Gams/Hieflau (Styria, Austria). International Journal of Coal Geology, 46, 27–49.

Bechtel, A., Gruber, W., Sachsenhofer, R.F., Gratzer, R., Lücke, A. and Püttmann, W. 2003. Depositional environment of the Late Miocene Hausruck lignite (Alpine Foreland Basin): Insights from petrography, organic geochemistry, and stable carbon isotopes. International Journal of Coal Geology, 53, 153–180.

Bechtel, A., Markic, M., Sachsenhofer, R.F., Jelen, B., Gratzer, R., Lücke, A. and Püttmann, W. 2004. Paleoenvironment of the upper Oligocene Trbovlje coal seam (Slovenia). International Journal of Coal Geology, 57, 23–48.

Bechtel, A., Reischenbacher, D., Sachsenhofer, R.F., Gratzer, R., Lücke, A. and Püttmann, W. 2007a. Relations of petrographical and geochemical parameters in the middle Miocene Lavanttal lignite (Austria). International Journal of Coal Geology, 70, 325–349.

Bechtel, A., Hámor-Vidó, M., Sachsenhofer, R.F., Reischenbacher, D., Gratzer, R. and Püttmann, W. 2007b. The middle Eocene Márkushegy subbituminous coal (Hungary): Paleoenvironmental implications from petrographical and geochemical studies. International Journal of Coal Geology, 72, 33–52.

Bharadwaj, D.C. and Tripathi, A. 1978. A palynostratigraphic study of Lower Gondwana sediments from South Karanpura Coalfield, Bihar, India. Palaeobotanist, 25, 39–61.

Bharadwaj, D.C. 1970. On the Palynostratigraphy of Argada ‘S’ seam in the South Karanpura Coalfield, Bihar. Palaeobotanist, 19, 211–213.

Bhowmick, T., Nayak, B. and Varma, A.K. 2017. Chemical and mineralogical composition of Kathara Coal, East Bokaro Coalfield, India. Fuel, 208, 91–100.

Biester, H., Hermanns, Y.-M. and Martinez Cortizas, A. 2012. The influence of organic matter decay on the distribution of major and trace elements in ombrotrophic mires – a case study from the Harz Mountains. Geochimica et Cosmochimica Acta, 84, 126–136.

BIS. 2003a. Classification and Codification of Indian Coals and Lignite (2nd Revision of IS: 770-1977), 3.1. Bureau of Indian Standards (ed.).

BIS. 2003b. Methods of Test for Coal and Coke (2nd Revision of IS: 1350). Part I, Proximate Analysis. Bureau of Indian Standards (ed.).

Blumenberg, M., Thiel, V. and Reitner, J. 2015. Organic matter preservation in the carbonate matrix of a recent microbial mat – Is there a ‘mat seal effect’? Organic Geochemistry, 87, 25–34.

Bostick, N.H. 1979. Microscopic measurement of the level of catagenesis of solid organic matter in sedimentary rocks to aid exploration for petroleum and to determine former burial temperatures - a review. SEPM Special Publication, 26, 17–43.

Bourbonniere, R.A. and Meyers, P.A. 1996. Sedimentary geolipid records of historical changes in the watersheds and productivities of Lakes Ontario and Erie. Limnology and Oceanography, 41, 352–359, https://doi.org/10.4319/lo.1996.41.2.0352.

Breeze, P. 2015. Coal Types and the Production and Trade in Coal. In: Coal-Fired Generation. 9–16., https://doi.org/10.1016/B978-0-12-804006-5.00008-3.

Bryers, R.W. 1996. Fireside slagging, fouling, and high-temperature corrosion of heat-transfer surface due to impurities in steam-raising fuels. Progress in Energy and Combustion Science, 22, 29–120, https://doi.org/10.1016/0360-1285(95)00012-7.

Bustin, R.M. 1997. Petroleum source rocks, organic maturation and thermal history of the Queen Charlotte Basin, British Columbia. Bulletin of Canadian Petroleum Geology, 45, 255–278.

Calabrese, E.J., Canada, A.T. and Sacco, C. 1985. Trace Elements and Public Health. Annual Review of Public Health, 6, 131–146.

Calder, J.H., Gibling, M.R. and Mukhopadhyay, P.K. 1991. Peat formation in a Westphalian B piedmont setting, Cumberland Basin, Nova Scotia: implications for the maceral-based interpretation of rheotrophic and raised paleomires. Bulletin - Societe Geologique de France, 162, 283–298.

Callejon, A.F. and Bissada, K.K. 2001. Role of coals and carbonaceous shales in the generation of oil in the Eastern Venezuela basin : a “petroleum system approach". In: 18th Annual TSOP Meeting. 2001.

Cameron, C.C., Esterle, J.S. and Palmer, C.A. 1989. The geology, botany and chemistry of selected peat-forming environments from temperate and tropical latitudes. International Journal of Coal Geology, 12, 105–156.

Capo, R.C., Stewart, B.W., et al. 2014. The strontium isotopic evolution of Marcellus Formation produced waters, southwestern Pennsylvania. International Journal of Coal Geology, 126, 57–63, https://doi.org/10.1016/j.coal.2013.12.010.

Casagrande, D.J., 1987, Sulphur in peat and coal, in Scott, A.C., ed., Coal and coal-bearing strata–Recent advances: Geological Society, London, Special Publications, v. 32, 1, 87–105.

Casshyap, S.M. 1970. Sedimentary Cycles and Environment of Deposition of the Barakar Coal Measures of Lower Gondwana, India. SEPM Journal of Sedimentary Research, Vol. 40, 1302–1317.

Casshyap, S.M. and Tewari, R.C. 2009. Fluvial Models of the Lower Permian Coal Measures of Son-Mahanadi and Koel-Damodar Valley Basins, India. In: Sedimentology of Coal and Coal-Bearing Sequences. 121–147.

Chabukdhara, M. and Singh, O.P. 2016. Coal mining in northeast India: an overview of environmental issues and treatment approaches. International Journal of Coal Science & Technology, 3, 87–96, https://doi.org/10.1007/s40789-016-0126-1.

Chakrabarti, N.C. 1991. Observations on surface ultra structures of vitrains from some coking and non-coking seams of lower Gondwana coal fields, India. Special Publication Series - Geological Survey of India, 16, 59–61.

Chakraborty, C. and Ghosh, S.K. 2008. Pattern of sedimentation during the Late Paleozoic, Gondwanaland glaciation: An example from the Talchir Formation, Satpura Gondwana basin, central India. Journal of Earth System Science, 117, 499–519.

Chakraborty, C., Ghosh, S.K. and Chakraborty, T. 2003a. Depositional record of tidal-flat sedimentation in the Permian coal measures of central India: Barakar Formation, Mohpani coalfield, Satpura Gondwana basin. Gondwana Research, 6, 817–827, https://doi.org/10.1016/S1342-937X(05)71027-3.

Chakraborty, C., Mandal, N. and Ghosh, S.K. 2003b. Kinematics of the Gondwana basins of peninsular India. Tectonophysics, 377, 299–324.

Chakravarty, S., Mohanty, A., Banerjee, A., Tripathy, R., Mandal, G.K., Basariya, M.R. and Sharma, M. 2015. Composition, mineral matter characteristics and ash fusion behavior of some Indian coals. Fuel, 150, 96–101.

Chandra, D. 1958. Reflectance of oxidized coals. Economic Geology, 53, 102–108.

Chandra, D. 1966. Effect of storage of coals on reflectance and petrological composition. Economic Geology, 61, 754–759, https://doi.org/10.2113/gsecongeo.61.4.754.

Chandra, D. and Chakrabarti, N.C. 1989. Coalification trends in Indian coals. International Journal of Coal Geology, 13, 413–435.

Chandra, D., Mazumdar, K. and Basumallick, S. 1983. Distribution of sulphur in the tertiary coals of Meghalaya, India. International Journal of Coal Geology, 3, 63–75, https://doi.org/10.1016/0166-5162(83)90013-7.

Chandra, S. and Chandra, A. 1988. Vegetational changes and their climatic implications in coal-bearing Gondwana. The Palaeobotanist, 36, 74–86.

Chatterjee, C.N., Ghose, S. and Chandra, D. 1990. Micropetrographic characteristics of certain Lower Permian coal seams of India with special reference to their mode of formation. International Journal of Coal Geology, 14, 295–308.

Chatterjee, N.N. 1940. A short note on the Geology of Singrimari. In: Assam, P. (ed.) Garo Hills.

Chatterjee, R. and Paul, S. 2013. Classification of coal seams for coal bed methane exploitation in central part of Jharia coalfield, India – A statistical approach. Fuel, 111, 20–29, https://doi.org/10.1016/j.fuel.2013.04.007.

Chatterjee, S. and Hotton, N. 1986. The paleoposition of India. Journal of Southeast Asian Earth Sciences, 1, 145–189, https://doi.org/10.1016/0743-9547(86)90020-6.

Cheepurupalli, N.R., Sharma, G.V.., Singh, C.. and Rao, E.N.D. 2015. Petrographic Analysis and its Relationship with Calorific Values of Non- Coking Coals, Talcher Coalfield, Orissa. International Journal of Engineering Trends and Technology, 30, 13–20, https://doi.org/10.14445/22315381/IJETT-V30P204.

Chen, J., Liu, G., et al. 2011. Geochemistry of environmentally sensitive trace elements in Permian coals from the Huainan coalfield, Anhui, China. International Journal of Coal Geology, 88, 41–54, https://doi.org/10.1016/j.coal.2011.08.002.

Chen, J., Chen, P., Yao, D., Liu, Z., Wu, Y., Liu, W. and Hu, Y. 2015a. Mineralogy and geochemistry of Late Permian coals from the Donglin Coal Mine in the Nantong coalfield in Chongqing, southwestern China. International Journal of Coal Geology, 149, 24–40, https://doi.org/10.1016/j.coal.2015.06.014.

Chen, Y., Zou, C., Mastalerz, M., Hu, S., Gasaway, C. and Tao, X. 2015b. Applications of Micro-Fourier Transform Infrared Spectroscopy (FTIR) in the Geological Sciences—A Review. International Journal of Molecular Sciences, 16, 30223–30250, https://doi.org/10.3390/ijms161226227.

Chen, Y., Qin, Y., et al. 2020. Influence of lamprophyre sills on coal metamorphism, coalbed gas composition and coalbed gas occurrence in the Tongxin Minefield, Datong Coalfield, China. International Journal of Coal Geology, 217, 103286

Chou, C.-L. 2012. Sulfur in coals: A review of geochemistry and origins. International Journal of Coal Geology, 100, 1–13, https://doi.org/10.1016/j.coal.2012.05.009.

Cohen, A.D. 1973. Petrology of Some Holocene Peat Sediments from the Okefenokee Swamp-Marsh Complex of Southern Georgia. Geological Society of America Bulletin, 84, 3867.

Cook, A.C. 1982. Organic facies in the Eromanga Basin. In: Moore, P. S. and Mount, T. J. (eds) Eromanga Basin Symposium. 234–257.

Cornford, C. 1979. Organic Deposition at a Continental Rise: Organic Geochemical Interpretation and Synthesis at DSDP Site 397, Eastern North Atlantic. In: Initial Reports of the Deep Sea Drilling Project, 47 Pt. 1. 503–510.

Cox, R., Lowe, D.R. and Cullers, R.L. 1995. The influence of sediment recycling and basement composition on evolution of mudrock chemistry in the southwestern United States. Geochimica et Cosmochimica Acta, 59, 2919–2940.

Cranwell, P.A. 1977. Organic geochemistry of Cam Loch (Sutherland) sediments. Chemical Geology, 20, 205–221, https://doi.org/10.1016/0009-2541(77)90044-4.

Cressler, W.L., Prestianni, C. and LePage, B. a. 2010. Late Devonian spermatophyte diversity and paleoecology at Red Hill, north-central Pennsylvania, USA. International Journal of Coal Geology, 83, 91–102.

Cudmore, J.F. 1977. Evaluation of Coals for Conversion To Liquid Hydrocarbons. Coal Borehole Evaluation. Proc. Australias. Min. Metall, 146–158.

D'Angelo, J.A. and Zodrow, E.L. 2015. Chemometric study of structural groups in medullosalean foliage (Carboniferous, fossil Lagerstätte, Canada): Chemotaxonomic implications. International Journal of Coal Geology, 138, 42–54.

Dai, S. and Finkelman, R.B. 2018. Coal as a promising source of critical elements: Progress and future prospects. International Journal of Coal Geology, 186, 155–164.

Dai, S., Zhao, L., et al. 2010. Abundances and distribution of minerals and elements in high-alumina coal fly ash from the Jungar Power Plant, Inner Mongolia, China. International Journal of Coal Geology, 81, 320–332.

Dai, S., Ren, D., Chou, C.-L., Finkelman, R.B., Seredin, V. V. and Zhou, Y. 2012. Geochemistry of trace elements in Chinese coals: A review of abundances, genetic types, impacts on human health, and industrial utilization. International Journal of Coal Geology, 94, 3–21, https://doi.org/10.1016/j.coal.2011.02.003.

Dai, S., Seredin, V. V., et al. 2014a. Composition and modes of occurrence of minerals and elements in coal combustion products derived from high-Ge coals. International Journal of Coal Geology, 121, 79–97, https://doi.org/10.1016/j.coal.2013.11.004.

Dai, S., Li, T., et al. 2014b. Origin of minerals and elements in the Late Permian coals, tonsteins, and host rocks of the Xinde Mine, Xuanwei, eastern Yunnan, China. International Journal of Coal Geology, 121, 53–78.

Dai, S., Liu, J., et al. 2016. Mineralogical and geochemical compositions of Late Permian coals and host rocks from the Guxu Coalfield, Sichuan Province, China, with emphasis on enrichment of rare metals. International Journal of Coal Geology, 166, 71–95, https://doi.org/10.1016/j.coal.2015.12.004.

Dai, S., Bartley, R., et al. 2017. Organic geochemistry of funginite (Miocene, Eel River, Mendocino County, California, USA) and macrinite (Cretaceous, Inner Mongolia, China). International Journal of Coal Geology, 179, 60–71.

Dai, S., Hower, J.C., et al. 2020a. Organic associations of non-mineral elements in coal: A review. International Journal of Coal Geology, 218, 103347.

Dai, S., Bechtel, A., et al. 2020b. Recognition of peat depositional environments in coal: A review. International Journal of Coal Geology, 219, 103383.

Das, S.K. and Chakrapani, G.J. 2011. Assessment of trace metal toxicity in soils of Raniganj Coalfield, India. Environmental Monitoring and Assessment, 177, 63–71.

Davis, A., Spackman, W. and Given, P.H. 1976. The influence of the properties of coals on their conversion into clean fuels. Energy Sources, 3, 55–81.

Davis, R.C., Noon, S.W. and Harrington, J. 2007. The petroleum potential of Tertiary coals from Western Indonesia: Relationship to mire type and sequence stratigraphic setting. International Journal of Coal Geology, 70, 35–52.

De, A., De, B. and Bera, S. 2003. First record of Raniganjia bengalensis (Rigby) Pant and Nautiyal from Lower Permian Beds (Barakar Formation) of South Karanpura Coalfield, Jharkhand, India. Journal of the Geological Society of India, 61, 487–490.

Dembicki, H. 2009. Three common source rock evaluation errors made by geologists during prospect or play appraisals. AAPG Bulletin, 93, 341–356.

Dev, S. 1989. Terpenoids. In: Rowe, J. W. (ed.) Natural Products of Woody Plants: Chemicals Extraneous to the Lignocellulosic Cell Wall. 691–807.

Dianshi, D., Guijian, L., Biao, F. and Cuicui, Q. 2018. Characteristics of the coal quality and elemental geochemistry in Permian coals from the Xinjier mine in the Huainan Coalfield, north China: Influence of terrigenous inputs. Journal of Geochemical Exploration, 186, 50–60, https://doi.org/10.1016/j.gexplo.2017.12.002.

Didyk, B.M., Simoneit, B.R.T., Brassell, S.C. and Eglinton, G. 1978. Organic geochemical indicators of palaeoenvironmental conditions of sedimentation. Nature, 272, 216–222, https://doi.org/10.1038/272216a0.

Diessel, C.F.K. 1965. Correlation of macro-and micropetrography of some New South Wales coals. In: Proceedings-General. 669–677.

Diessel, C.F.K. 1982. An appraisal of coal facies based on maceral characteristics. Australian Coal Geology, 4, 474–484.

Diessel, C.F.K. 1986. On The Correlation Between Coal Facies and Depositional Environments. In: Proceeding of 20th Symposium of Department of Geology, University Newcastle, NSW. 19–22.

Diessel, C.F.K. 1992. Coal-Bearing Depositional Systems. Gundermann, I. (ed.), https://doi.org/10.1007/978-3-642-75668-9.

Duan, P., Wang, W., Sang, S., Tang, Y., Ma, M., Zhang, W. and Liang, B. 2018. Geochemistry of Toxic Elements and Their Removal via the Preparation of High-Uranium Coal in Southwestern China. Minerals, 8, 83.

Durand, B. and Paratte, M. 1983. Oil Potential of Coals: A Geochemical Approach. Geological Society, London, Special Publications, 12, 255–265.

Dutcher, L.A.. and Crelling, J.C. 2000. History of applied coal petrology in the United States. International Journal of Coal Geology, 42, 93–101.

Dutta, P. 2002. Gondwana Lithostratigraphy of Peninsular India. Gondwana Research, 5, 540–553.

Dutta, P., Bhowmik, S. and Das, S. 2011a. Methane and carbon dioxide sorption on a set of coals from India. International Journal of Coal Geology, 85, 289–299.

Dutta, S., Mathews, R.P., et al. 2011b. Petrology, palynology and organic geochemistry of Eocene lignite of Matanomadh, Kutch Basin, western India: Implications to depositional environment and hydrocarbon source potential. International Journal of Coal Geology, 85, 91–102, https://doi.org/10.1016/j.coal.2010.10.003.

Dutta, S., Mallick, M., Kumar, K., Mann, U. and Greenwood, P.F. 2011c. Terpenoid composition and botanical affinity of Cretaceous resins from India and Myanmar. International Journal of Coal Geology, 85, 49–55.

ECE-UN. 1998. International Classification of In-Seam Coals. Geneva, Economic Commission for Europe-United Nations.

Eglinton, G. and Hamilton, R.J. 1967. Leaf epicuticular waxes. Science, 156, 1322–1335.

Equeenuddin, S.M., Tripathy, S., Sahoo, P.K. and Ranjan, A. 2016. Geochemical characteristics and mode of occurrence of trace elements in coal at West Bokaro coalfield. International Journal of Coal Science & Technology, 3, 399–406.

Ercegovac, M. and Kostić, A. 2006. Organic facies and palynofacies: Nomenclature, classification and applicability for petroleum source rock evaluation. International Journal of Coal Geology, 68, 70–78, https://doi.org/10.1016/j.coal.2005.11.009.

Erik, N.Y. and Sancar, S. 2010. Relationships between coal-quality and organic-geochemical parameters: A case study of the Hafik coal deposits (Sivas Basin, Turkey). International Journal of Coal Geology, 83, 396–414.

Espitalié, J., Madec, M., Tissot, B.P., Mennig, J.J. and Leplat, P. 1977. Source rock characterization method for petroleum exploration. Offshore Technology Conference, Houston, 439–444, https://doi.org/10.4043/2935-ms.

Falcon, R.M.S. 1986. Classification of coals in Southern Africa, 1899–1921. Mineral Deposits of Southern Africa, vols. I and II, Anhaeusser, CR, and Maske, S.(Eds.) Johannesburg, South Africa: Geological Society of South Africa.

Fangneng, Z. 2003. Research and development of clean coal technology in China. Energy for Sustainable Development, 7, 19–23.

Ficken, K.J., Li, B., Swain, D.L. and Eglinton, G. 2000. An n-alkane proxy for the sedimentary input of submerged/floating freshwater aquatic macrophytes. Organic Geochemistry, 31, 745–749.

Ficken, K.J., Wooller, M.J., Swain, D.L., Street-Perrott, F.A. and Eglinton, G. 2002. Reconstruction of a subalpine grass-dominated ecosystem, Lake Rutundu, Mount Kenya: A novel multi-proxy approach. Palaeogeography, Palaeoclimatology, Palaeoecology, 177, 137–149, https://doi.org/10.1016/S0031-0182(01)00356-X.

Finkelman, R.B. 1999. Trace elements in coal. Environmental and health significance. Biological Trace Element Research, 67, 197–204.

Finkelman, R.B. and Gross, P.M.K. 1999. The types of data needed for assessing the environmental and human health impacts of coal. International Journal of Coal Geology, 40, 91–101, https://doi.org/10.1016/S0166-5162(98)00061-5.

Finkelman, R.B., Dai, S. and French, D. 2019. The importance of minerals in coal as the hosts of chemical elements: A review. International Journal of Coal Geology, 212, 103251, https://doi.org/10.1016/j.coal.2019.103251.

Flores, D., Pereira, L.C.G., et al. 2010. The Buçaco Basin (Portugal): Organic petrology and geochemistry study. International Journal of Coal Geology, 81, 281–286.

Flores, R.M. 2014. Coal and Coalbed Gas, https://doi.org/10.1016/B978-0-12-396972-9.00009-4.

Flores, R.M. 2014. Coalification, Gasification, and Gas Storage. In: Coal and Coalbed Gas. 167–233.

Fowler, M.G., Gentzis, T., Goodarzi, F. and Foscolos, A.E. 1991. The petroleum potential of some Tertiary lignites from northern Greece as determined using pyrolysis and organic petrological techniques. Organic Geochemistry, 17, 805–826.

Fox, C.S. 1926. The Occurrence of Low-Phosphorus Coking Coal in the Giridih Coal-field. With analyses of mica-peridotites.] Rec. Geol. Surv. India, 59, 371–404.

Fox, C.S. 1931. The Gondwana System and Related Formations.

Fraser, P.J. 1877. Classification of Coals. Transactions of the American Institute of Mining and Metallurgical Engineers, 36, 430–451.

Friederich, M.C. and van Leeuwen, T. 2017. A review of the history of coal exploration, discovery and production in Indonesia: The interplay of legal framework, coal geology and exploration strategy. International Journal of Coal Geology, 178, 56–73, https://doi.org/10.1016/j.coal.2017.04.007.

Galarraga, F., Reategui, K., Martïnez, A., Martínez, M., Llamas, J.F. and Márquez, G. 2008. V/Ni ratio as a parameter in palaeoenvironmental characterisation of nonmature medium-crude oils from several Latin American basins. Journal of Petroleum Science and Engineering, 61, 9–14.

Ganju, P.N. 1955. Petrology of Indian Coals. Government of India Press.

Ganju, P.N. and Pant, I.D. 1963. The nature of resins in the Raniganj coals. In: Proc. Nat. Inst. Sci. Ind. 192–212.

Ganz, H. and Kalkreuth, W. 1987. Application of infrared spectroscopy to the classification of kerogen types and the evaluation of source rock and oil shale potentials. Fuel, 66, 708–711, https://doi.org/10.1016/0016-2361(87)90285-7.

Ganz, H. and Kalkreuth, W. 1991. IR classification of kerogen type, thermal maturation, hydrocarbon potential and lithological characteristics. Journal of Southeast Asian Earth Sciences, 5, 19–28, https://doi.org/10.1016/0743-9547(91)90007-K.

Gee, E. 1940. History of Coal Mining in India. Geological Survey of India, 6, 313–318.

Geological Survey of India. 2018. Indian Coal and Lignite Resources-2018.

Ghassal, B.I., Littke, R., et al. 2018. Source rock potential and depositional environment of Upper Cretaceous sedimentary rocks, Abu Gharadig Basin, Western Desert, Egypt: An integrated palynological, organic and inorganic geochemical study. International Journal of Coal Geology, 186, 14–40, https://doi.org/10.1016/j.coal.2017.11.018.

Ghosh, G., Banerjee, A. and Mazumdar, B.K. 1975. Skeletal structure of coal. Fuel, 54, 294–295.

Ghosh, T.K. 1964. On Tertiary coal from Daranggiri, Assam, Quart. QJ Geol. Soc. India, 36, 91–94.

Ghosh, T.K. 1969. Petrography and coking potentiality of Indian coals. Economic Geology, 64, 683–690.

Ghosh, T.K. 1971. Change in coal macerals. Fuel, 50, 218–221.

Gijzel, P. Van. 1971. Review of the UV-fluorescence of fresh and fossil exines and exosporia. In: Pr, A. (ed.) Brooks et Al (Eds): Sporopollenin -. 659–685.

Gluskoter, H.J. 1975. Mineral matter and trace elements in coal. In: Advances in Chemistry Series. 1–22., https://doi.org/10.1021/ba-1975-0141.ch001.

Gokul, A.R., Savanur, R. V and Ghosh, P.K. 1960. Geology and Coal Resources of Sayal-'a' Block South Karanpura Coalfield Hazaribagh District, Bihar. Geological Survey of India. https://doi.org/10.1002/14356007.a16.

Gong, B., Tian, C., Xiong, Z., Zhao, Y. and Zhang, J. 2016. Mineral changes and trace element releases during extraction of alumina from high aluminum fly ash in Inner Mongolia, China. International Journal of Coal Geology, 166, 96–107.

Gorbanenko, O.O. and Ligouis, B. 2014. Changes in optical properties of liptinite macerals from early mature to post mature stage in Posidonia Shale (Lower Toarcian, NW Germany). International Journal of Coal Geology, 133, 47–59.

Gretskaya, E. V. and Dakhnova, M. V. 2010. Hydrocarbon potential of coal-bearing deposits of south Sakhalin. Doklady Earth Sciences, 432, 825–828.

Guennel, G.K. 1952. Fossil Spores of the Alleghenian Coals in Indiana. Indiana Geological Survey.

Guidotti, T.L., McNamara, J. and Moses, M.S. 2008. The interpretation of trace element analysis in body fluids. Indian Journal of Medical Research, 128, 524–532.

Guo, Q., Fink, R., Littke, R. and Zieger, L. 2019. Methane sorption behaviour of coals altered by igneous intrusion, South Sumatra Basin. International Journal of Coal Geology, 214, 103250, https://doi.org/https://doi.org/10.1016/j.coal.2019.103250.

Guo, Y. and Bustin, R.M. 1998. Micro-FTIR spectroscopy of liptinite macerals in coal. International Journal of Coal Geology, 36, 259–275.

Guoyi, H., Jin, L., Xiuqin, S. and Zhongxi, H. 2010. The origin of natural gas and the hydrocarbon charging history of the Yulin gas field in the Ordos Basin, China. International Journal of Coal Geology, 81, 381–391.

Gupta, A. 1999. Early Permian Palaeoenvironment in Damodar Valley Coalfields, India: An Overview. Gondwana Research, 2, 149–165.

Gupta, A., Apartment, K., et al. 2000. Role of Storm in Ramgarh and West Bokaro Coalfields and Its Implication in Adjacent Peninsular Gondwana Coalfields, India. Gondwana Research, 3, 529–544.

Gupta, R. 2007. Advanced Coal Characterization: A Review. Energy & Fuels, 21, 451–460.

Gürdal, G. and Bozcu, M. 2011. Petrographic characteristics and depositional environment of Miocene Çan coals, Çanakkale-Turkey. International Journal of Coal Geology, 85, 143–160, https://doi.org/10.1016/j.coal.2010.11.001.

Guyot, R.E. 1978. Influence of Coal Characteristics on the Yields and Properties of Hydrogenation Products.

Hackley, P.C., Warwick, P.D., Hook, R.W., Alimi, H., Mastalerz, M. and Swanson, S.M. 2012. Organic geochemistry and petrology of subsurface Paleocene–Eocene Wilcox and Claiborne Group coal beds, Zavala County, Maverick Basin, Texas, USA. Organic Geochemistry, 46, 137–153.

Hacquebard, P.A. and Donaldson, J.R. 1969. Carboniferous Coal Deposition Associated with Flood-Plain and Limnic Environments in Nova Scotia. In: Geological Society of America Special Papers. 143–192., https://doi.org/10.1130/SPE114-p143.

Hakimi, M.H., Abdullah, W.H., et al. 2010. Organic geochemistry, burial history and hydrocarbon generation modelling of the upper Jurassic Madbi formation, Masila Basin, Yemen. Journal of Petroleum Geology, 33, 299–318.

Hakimi, M.H., Abdullah, W.H., Sia, S.-G. and Makeen, Y.M. 2013. Organic geochemical and petrographic characteristics of Tertiary coals in the northwest Sarawak, Malaysia: Implications for palaeoenvironmental conditions and hydrocarbon generation potential. Marine and Petroleum Geology, 48, 31–46.

Hakimi, M.H., Ahmed, A.F. and Abdullah, W.H. 2016. Organic geochemical and petrographic characteristics of the Miocene Salif organic-rich shales in the Tihama Basin, Red Sea of Yemen: Implications for paleoenvironmental conditions and oil-generation potential. International Journal of Coal Geology, 154–155, 193–204.

Hakimi, M.H., Abdullah, W.H., et al. 2017. Geochemical characterization of the Jurassic Amran deposits from Sharab area (SW Yemen): Origin of organic matter, paleoenvironmental and paleoclimate conditions during deposition. Journal of African Earth Sciences, 129, 579–595.

Harnois, L. 1988. The CIW index: A new chemical index of weathering. Sedimentary Geology, 55, 319–322, https://doi.org/10.1016/0037-0738(88)90137-6.

Hayashi, K.I., Fujisawa, H., Holland, H.D. and Ohmoto, H. 1997. Geochemistry of ~1.9 Ga sedimentary rocks from northeastern Labrador, Canada. Geochimica et Cosmochimica Acta, 61, 4115–4137.

Hayatsu, R., Botto, R.E., McBeth, R.L., Scott, R.G. and Winans, R.E. 1988. Chemical alteration of a biological polymer 'sporopollenin' during coalification: origin, formation, and transformation of the coal maceral sporinite. Energy & Fuels, 2, 843–847, https://doi.org/10.1021/ef00012a019.

Hazra, B., Varma, A.K., Bandopadhyay, A.K., Chakravarty, S., Buragohain, J., Samad, S.K. and Prasad, A.K. 2016. FTIR, XRF, XRD and SEM characteristics of Permian shales, India. Journal of Natural Gas Science and Engineering, 32, 239–255.

Hedburg, J.D. 1968. A Geological Analysis of the Cameroun Trend. Ph. D. Thesis.

Hevia Rodríguez, V. 1953. El estudio microscópico del carbón. Boletín Informativo Nacional del Carbón.

Hoffman, E. and Jenkner, A. 1932. Die inkohlung und ihre erkennung im mikrobild. Glückauf, 68, 81–88.

Holz, M., Kalkreuth, W. and Banerjee, I. 2002. Sequence stratigraphy of paralic coal-bearing strata: an overview. International Journal of Coal Geology, 48, 147–179.

Horsfield, B., Yordy, K.L.L., Crelling, J.C.C. and Company, G. 1988. Determining the petroleum-generating potential of coal using organic geochemistry and organic petrology. Organic Geochemistry, 13, 121–129.

Hower, J.C. 2012. Petrographic examination of coal-combustion fly ash. International Journal of Coal Geology, 92, 90–97, https://doi.org/10.1016/j.coal.2011.12.012.

Hower, J.C. and Wagner, N.J. 2012. Notes on the methods of the combined maceral/microlithotype determination in coal. International Journal of Coal Geology, 95, 47–53, https://doi.org/10.1016/j.coal.2012.02.011.

Hower, J.C., Esterle, J.S., Wild, G.D. and Pollock, J.D. 1990. Perspectives on coal lithotype analysis. Journal of Coal Quality, 9, 48–52.

Hower, J.C., Eble, C.F., et al. 1996. Introduction : Geology and Petrology of Appalachian Coals. International Journal of Coal Geology, 31, 1–2.

Hower, J.C., Calder, J.H., Eble, C.F., Scott, A.C., Robertson, J.D. and Blanchard, L.J. 2000. Metalliferous coals of the Westphalian A Joggins Formation, Cumberland basin, Nova Scotia, Canada: Petrology, geochemistry, and palynology. International Journal of Coal Geology, 42, 185–206.

Hower, J.C., O'Keefe, J.M.K., et al. 2009. Notes on the origin of inertinite macerals in coals: Observations on the importance of fungi in the origin of macrinite. International Journal of Coal Geology, 80, 135–143.

Hower, J.C., O'Keefe, J.M.K., Henke, K.R. and Bagherieh, A. 2011. Time series analysis of CO concentrations from an Eastern Kentucky coal fire. International Journal of Coal Geology, 88, 227–231, https://doi.org/10.1016/j.coal.2011.10.001.

Hower, J.C., O'Keefe, J.M.K., Wagner, N.J., Dai, S., Wang, X. and Xue, W. 2013a. An investigation of Wulantuga coal (Cretaceous, Inner Mongolia) macerals:

Paleopathology of faunal and fungal invasions into wood and the recognizable clues for their activity. International Journal of Coal Geology, 114, 44–53.

Hower, J.C., Misz-Keenan, M., et al. 2013b. Macrinite forms in Pennsylvanian coals. International Journal of Coal Geology, 116–117, 172–181.

Huang, S., Wang, Z., Lv, Z., Gong, D., Yu, C. and Wu, W. 2014. Geochemical identification of marine and terrigenous condensates-A case study from the Sichuan Basin, SW China. Organic Geochemistry, 74, 44–58.

Hughes, W.B., Holba, A.G. and Dzou, L.I.P. 1995. The ratios of dibenzothiophene to phenanthrene and pristane to phytane as indicators of depositional environment and lithology of petroleum source rocks. Geochimica et Cosmochimica Acta, 59, 3581–3598.

Hunt, J.M. 1991. Generation of gas and oil from coal and other terrestrial organic matter. Organic Geochemistry, 17, 673–680.

Hunt, J.M. 1995. Petroleum Geochemistry and Geology, 2nd ed.

Hutton, A.C. 1987. Petrographic classification of oil shales. International Journal of Coal Geology, 8, 203–231, https://doi.org/10.1016/0166-5162(87)90032-2.

Hutton, A.C., Kantsler, A.J., Cook, A.C. and McKirdy, D.M. 1980. Organic Matter in Oil Shales. APEA Journal, 20, 44–67, https://doi.org/10.1071/aj79005.

Hutton, W. 1833. Observation on coal: London and Edinburgh Philos. Mag. and Jl. Sci, 2, 302.

IEA. 2015. India Energy Outlook. India Energy Outlook - World Energy Outlook Special Report, 1–191.

Ikeda, K., Shimizu, T. and Taguchi, R. 2008. Targeted analysis of ganglioside and sulfatide molecular species by LC/ESI-MS/MS with theoretically expanded multiple reaction monitoring. Journal of Lipid Research, 49, 2678–2689.

Indian Bureau of Mines. 2018. Indian Minerals Yearbook 2017, 56th ed. Indian Bureau of Mines (ed.), https://doi.org/10.1007/BF03220742.

Ingram, B.L. and Sloan, D. 1992. Strontium isotopic composition of estuarine sediments as paleosalinity-paleoclimate indicator. Science, 255, 68–72.

International Committee for Coal and Organic Petrology. 1963. International Handbook of Coal Petrology, 2nd ed.

International Committee for Coal and Organic Petrology. 1971. International Handbook of Coal Petrology, 1st Supplement to 2nd Ed.

International Committee for Coal and Organic Petrology. 1975. International Handbook of Coal Petrography. 2nd Supplement to 2nd Ed.

International Committee for Coal and Organic Petrology. 1998. The new vitrinite classification (ICCP System 1994). Fuel, 77, 349–358.

International Committee for Coal and Organic Petrology. 2001. The new inertinite classification (ICCP System 1994). Fuel, 80, 459–471.

Irdi, G.A., Booher, H.B., Martello, D. V., Frommell, E.A. and Gray, R.J. 1993. The petrography and mineralogy of two Indian coals. Fuel, 72, 1093–1098.

ISO. 2005. ISO 11760: 2005(En) Classification of Coals. Standardization, I.S.O. for (ed.).

ISO 7404-5. 2009. Methods for the Petrographic Analysis of Coal—Part 5: Methods of Determining Microscopically the Reflectance of Vitrinite. 1–14.

Iyengar, M.S. and Lahiri, A. 1957. The nature of reactive groups in coal. Fuel, 36, 286–297.

Iyer, V.G. and Sundaram, N. 1955. Germanium in Coal. Indian Mining Journal, 3 (9), 182-183.

Izart, A., Suarez-Ruiz, I. and Bailey, J. 2015. Paleoclimate reconstruction from petrography and biomarker geochemistry from Permian humic coals in Sydney Coal Basin (Australia). International Journal of Coal Geology, 138, 145–157.

Jacob, H. 1952. Fortschritte quf dem Gebiet der Braunkohlen - Lumineszenz - Microskopie - Bergakademie 4. 337–347.

Jacob, H. 1964. Uber steinkohlen - Oxyhumodile aus Afghanistan, Agypten, Kolumbien und dem Iran-Kohlen-varietaten der Verwitterungszone von steinkohlenflozen. I. Die Verwitte-rung von Steinkohlen und Rolle der Oxydation. makropetrographischer befund und mikroskopische Untersuchung. brennst.-Chemie, 45, 26–29.

Jacob, H. 1974. Fluoreszenz-Mikroskopie und-Photometrie der organischen Substanz von Sedimenten und Boden. Handbuch der Mikroskopie in der Technik (H. Freund, ed.), Unschan Verlag, Frankfurt. 4 (2), 369-391.

Jaroszewicz, E., Bojanowski, M., Marynowski, L., Łoziński, M. and Wysocka, A. 2018. Paleoenvironmental conditions, source and maturation of Neogene organic matter from the siliciclastic deposits of the Orava-Nowy Targ Basin. International Journal of Coal Geology, 196, 288–301.

Jia, J., Li, X., Wu, P., Liu, Y., Han, C., Zhou, L. and Yang, L. 2015. Human health risk assessment and safety threshold of harmful trace elements in the soil environment of the wulantuga open-cast coal mine. Minerals, 5, 837–848.

Jiang, J.-Y., Cheng, Y.-P., Wang, L., Li, W. and Wang, L. 2011. Petrographic and geochemical effects of sill intrusions on coal and their implications for gas outbursts in the Wolonghu Mine, Huaibei Coalfield, China. International Journal of Coal Geology, 88, 55–66, https://doi.org/10.1016/j.coal.2011.08.007.

Jiang, R. and Yu, H. 2019. Interaction between sequestered supercritical CO_2 and minerals in deep coal seams. International Journal of Coal Geology, 202, 1–13.

Jin, J. and Shi, S. 1997. The development and prospective application of coal direct liquefaction for Chinese coals. In: Proc. Internat. Symp. on Clean Coal Technology, Xiamen, China Coal Industry Publishing House. 379.

Jing, Z., Rodrigues, S., et al. 2019. Use of FTIR, XPS, NMR to characterize oxidative effects of NaClO on coal molecular structures. International Journal of Coal Geology, 201, 1–13, https://doi.org/https://doi.org/10.1016/j.coal.2018.11.017.

Jones, J.M. and Murchison, D.G. 1963. The occurrence of resinite in bituminous coals. Economic Geology, 58, 263–273.

Jones, R.W. and Edison, T.A. 1978. Microscopic observations of kerogen related to geochemical parameters with emphasis on thermal maturation. Symposium in Geochemistry: Low Temperature Metamorphism of Kerogen and Clay Minerals, 1.

Jongmans, W.J. and Koopmans, R.G. 1933. Kohlenpetrographische Nomenclature. Geol. Bur, 49–63.

Jongmans, W.J., Koopmans, R.G. and Roos, G. 1938. Nomenclature of coal petrography - C.r.2. Congr. Intern, 1733–1737.

Jowett, A. 1925. On the Geological Structure of the Karanpura Coalfields, Bihar and Orissa.

Kalinowski, A.A. and Gurba, L.W. 2020. Interpretation of vitrinite reflectance–depth profiles in the Northern Denison Trough, Bowen Basin, Australia. International Journal of Coal Geology, https://doi.org/10.1016/j.coal.2019.103367.

Kalkreuth, W., Steller, M., Wieschenkämper, I. and Ganz, S. 1991. Petrographic and chemical characterization of Canadian and German coals in relation to utilization potential. Fuel, 70, 683–694, https://doi.org/10.1016/0016-2361(91)90063-G.

Karayigit, A. I., Gayer, R. A. and Demirel, I. H. 1998. Coal rank and petrography of Upper Carboniferous seams in the Amasra Coalfield, Turkey. International Journal of Coal Geology, 36, 277–294, https://doi.org/10.1016/S0166-5162(97)00047-5.

Karayiğit, A.I., Bircan, C., Mastalerz, M., Oskay, R.G., Querol, X., Lieberman, N.R. and Türkmen, I. 2017a. Coal characteristics, elemental composition and modes of occurrence of some elements in the İsaalan coal (Balıkesir, NW Turkey). International Journal of Coal Geology, 172, 43–59.

Karayiğit, A.İ., Littke, R., Querol, X., Jones, T., Oskay, R.G. and Christanis, K. 2017b. The Miocene coal seams in the Soma Basin (W. Turkey): Insights from coal petrography, mineralogy and geochemistry. International Journal of Coal Geology, 173, 110–128, https://doi.org/10.1016/j.coal.2017.03.004.

Karayiğit, A.İ., Mastalerz, M., Oskay, R.G. and Buzkan, İ. 2018. Bituminous coal seams from underground mines in the Zonguldak Basin (NW Turkey): Insights from mineralogy, coal petrography, Rock-Eval pyrolysis, and meso-and microporosity. International Journal of Coal Geology, 199, 91–112.

Katz, B.J. 1983. Limitations of 'Rock-Eval' pyrolysis for typing organic matter. Organic Geochemistry, 4, 195–199, https://doi.org/10.1016/0146-6380(83)90041-4.

Khadse, A., Qayyumi, M., Mahajani, S. and Ã, P.A. 2007. Underground coal gasification : A new clean coal utilization technique for India. 32, 2061–2071.

Khanehbad, M., Moussavi-Harami, R., Mahboubi, A. and Nadjafi, M. 2012. Geochemistry of Carboniferous shales of the Sardar Formation, east central Iran: Implication for provenance, paleoclimate and paleo-oxygenation conditions at a passive continental margin. Geochemistry International, 50, 777–790.

Khorasani, G.K. 1987. Oil-prone coals of the Walloon Coal Measures, Surat Basin, Australia. Coal and Coal-bearing Strata: Recent Advances, 32, 303–310.

Killops, S. and Killops, V. 2013. Anthropogenic Carbon and the Environment. In: Introduction to Organic Geochemistry. 295–321.

Killops, S.D., Funnell, R., et al. 1978. Lymphoid neoplasias I: classification categorization natural history. Recent results in cancer research. Fortschritte der Krebsforschung. Progres dans les recherches sur le cancer, 64, 1–336.

Klootwijk, C.T. 1974. Palaeomagnetic results from some Panchet clay beds, Karanpura Coalfield, northeastern India. Tectonophysics, 21, 79–92.

Kondla, D., Sanei, H., Clarkson, C.R., Ardakani, O.H., Wang, X. and Jiang, C. 2016. Effects of organic and mineral matter on reservoir quality in a Middle Triassic mudstone in the Canadian Arctic. International Journal of Coal Geology, 153, 112–126, https://doi.org/10.1016/j.coal.2015.11.012.

Kopp, O.C. and Bennett, M.E. 2001. A comparison of the loss of CO and CO_2 during coalification. International Journal of Coal Geology, 47, 63–66, https://doi.org/10.1016/s0166-5162(01)00029-5.

Kopp, O.C., Bennett, M.E. and Clark, C.E. 2000. Volatiles lost during coalification. International Journal of Coal Geology, 44, 69–84, https://doi.org/10.1016/S0166-5162(99)00069-5.

Kotter, K. 1960. Die mikroskopische Reflexions - messung mit dem Photomultiplier und ihre Anwendung auf die Kohlenuntersuchung. Brennst. - Chemie, 41, 263–272.

Koukouzas, N., Ward, C.R., Papanikolaou, D., Li, Z. and Ketikidis, C. 2009. Quantitative evaluation of minerals in fly ashes of biomass, coal and biomass-coal mixture derived from circulating fluidised bed combustion technology. Journal of Hazardous Materials, 169, 100–107, https://doi.org/10.1016/j.jhazmat.2009.03.116.

Koukouzas, N., Kalaitzidis, S.P. and Ward, C.R. 2010. Organic petrographical, mineralogical and geochemical features of the Achlada and Mavropigi lignite deposits, NW Macedonia, Greece. International Journal of Coal Geology, 83, 387–395, https://doi.org/10.1016/j.coal.2010.05.004.

Krishnan, M.S. 1940. Classification of coal. geological Survey of India, 4, 549–559.

Krook, A., Fredlund, H. and Holmberg, H. 1986. Diagnosis of pneumococcal pneumonia by detection of antigen in saliva. European Journal of Clinical Microbiology, 5, 639–642, https://doi.org/10.1007/BF02013288.

Kruszewska, K.J. 2003. Fluorescing macerals in South African coals. International Journal of Coal Geology, 54, 79–94, https://doi.org/10.1016/S0166-5162(03)00025-9.

Kulkarni, S. 1879. Glossopteris and Gangamopteris species from south Karanpura Coalfield. Palaeobotanist India, 18, 297–304.

Kulkarni, S. 1969. Studies in the Glossopteris flora of India - 40. Sphnopteris polymorpha Feistm. (1881) emend. from the barakar stage of South Karanpura coalfield, Bihar, India. Palaeobotanist, 18, 208–211.

Kumar, A. and Ahmad, T. 2007. Geochemistry of mafic dykes in part of Chotanagpur gneissic complex: Petrogenetic and tectonic implications. Geochemical Journal, 41, 173–186, https://doi.org/10.2343/geochemj.41.173.

Kumar, A. and Pandey, A.. 2013. Evaluating Impact of Coal Mining Activity on Landuse / Landcover Using Temporal Satellite Images in South Karanpura Coalfields and. International Journal of Advanced Remote Sensing and GIS, 2, 183–197.

Kumar, A., Singh, A.K., Singh, P.K., Singh, A.L. and Jha, M.K. 2018a. Demineralization Study of High-Ash Permian Coal with Pseudomonas mendocina strain B6-1: A Case Study of the South Karanpura Coalfield, Jharkhand, India. Energy & Fuels, 32, 1080–1086, https://doi.org/10.1021/acs.energyfuels.7b02562.

Kumar, A., Singh, A.K., Singh, P.K., Singh, A.L., Saikia, B.K. and Kumar, A. 2019. Desulfurization of Giral lignite of Rajasthan (Western India) using Burkholderia sp. GR 8–02. International Journal of Coal Preparation and Utilization, 1–17, https://doi.org/10.1080/19392699.2019.1651721.

Kumar, J., Mendhe, V.A., et al. 2018b. Coalbed methane reservoir characteristics of coal seams of south Karanpura coalfield, Jharkhand, India. International Journal of Coal Geology, 196, 185–200, https://doi.org/10.1016/j.coal.2018.07.011.

Kumar, M. and Patel, S.K. 2008. Characteristics of Indian non-coking coals and iron ore reduction by their chars for directly reduced iron production. Mineral Processing and Extractive Metallurgy Review, 29, 258–273, https://doi.org/10.1080/08827500801997902.

Laban, K.L. and Atkin, B.P. 1999. The determination of minor and trace element associations in coal using a sequential microwave digestion procedure. International Journal of Coal Geology, 41, 351–369, https://doi.org/10.1016/S0166-5162(99)00029-4.

Lafargue, E., Marquis, F. and Pillot, D. 1998. Rock-Eval 6 Applications in Hydrocarbon Exploration, Production, and Soil Contamination Studies. Oil & Gas Science and Technology, 53, 421–437, https://doi.org/10.2516/ogst:1998036.

Lahiri, A. 1951. Metamorphism of coal. Economic Geology, 46, 252–266, https://doi.org/10.2113/gsecongeo.46.3.252.

Lahiri, K.C. and Basu, T.N. 1952. Refractive indices of vitrain as an index of rank of coal. Journal of Scientific and Industrial Research (India), 11, 486–496.

Lahiri, K.C., Moitra, A., Sarkar, G.G. and Lahiri, A. 1968. A Petro-graphic Approach to Coal Preparation. Jour. Coal preparation, UK, 1, 225–228.

Lakshmi, P., Rao, S., Rasheed, M.A., Hasan, S.Z., Rao, P.H. and Harinarayana, T. 2014. Role of Geochemistry in Coalbed Methane -A Review. Geosciences, 4, 29–32, https://doi.org/10.5923/j.geo.20140402.01.

Langford, F.F. and Blanc-Valleron, M.M. 1990. Interpreting Rock-Eval pyrolysis data using graphs of pyrolizable hydrocarbons vs. total organic carbon. American Association of Petroleum Geologists Bulletin, 74, 799–804, https://doi.org/10.1306/0C9B238F-1710-11D7-8645000102C1865D.

Larkin, B.J. and Green, D.R. 2012. Borehole Data Standard for the Australian Coal Industry ACARP Project C21003 CoalLog Manual.

Larter, S.R. 1984. Application of Analytical Pyrolysis Techniques To Kerogen Characterization and Fossil Fuel Exploration/Exploitation. In: Voorhees, K. (ed.) Analytical Pyrolysis - Methods and Applications. 212–275., https://doi.org/10.1016/b978-0-408-01417-5.50012-3.

Lele, K.M. and Chandra, S.S. 1975. Associations of mio- and megafloras in the roof shales of some Barakar coal seams, South Karanpura coalfield, Bihar. Palaeobotanist, 24, 254–260.

Levine, J.R. 1993. Coalification: The Evolution of Coal as Source Rock and Reservoir Rock for Oil and Gas. Hydrocarbons from Coal (AAPG Studies in Geology Volume 38), 38, 39–77, https://doi.org/10.1111/j.1365-2125.2010.03794.x.

Li, B., Zhuang, X., et al. 2019. The mode of occurrence and origin of minerals in the Early Permian high-rank coals of the Jimunai depression, Xinjiang Uygur Autonomous Region, NW China. International Journal of Coal Geology, 205, 58–74, https://doi.org/https://doi.org/10.1016/j.coal.2019.03.002.

Li, C., Liang, H., Wang, S. and Liu, J. 2018. Study of harmful trace elements and rare earth elements in the Permian tectonically deformed coals from Lugou Mine, North China Coal Basin, China. Journal of Geochemical Exploration, 190, 10–25, https://doi.org/10.1016/j.gexplo.2018.02.016.

Liang, H., Xu, G., Xu, F., Yu, Q., Liang, J. and Wang, D. 2020. Paleoenvironmental evolution and organic matter accumulation in an oxygen-enriched lacustrine basin: A case study from the Laizhou Bay Sag, southern Bohai Sea (China). International Journal of Coal Geology, 217, 103318, https://doi.org/https://doi.org/10.1016/j.coal.2019.103318.

Littke, R., Leythaeuser, D., Radke, M. and Schaefer, R.G. 1990. Petroleum generation and migration in coal seams of the Carboniferous Ruhr Basin, northwest Germany.

Organic Geochemistry, 16, 247–258, https://doi.org/10.1016/0146-6380(90)90045-2.

Liu, B., Vrabec, M., Markič, M. and Püttmann, W. 2019a. Reconstruction of paleobotanical and paleoenvironmental changes in the Pliocene Velenje Basin, Slovenia, by molecular and stable isotope analysis of lignites. International Journal of Coal Geology, 206, 31–45, https://doi.org/https://doi.org/10.1016/j.coal.2019.03.006.

Liu, S., Ma, W., French, D., Tuo, K. and Mei, X. 2019b. Sequential mineral transformation during underground coal gasification with the presence of coal partings. International Journal of Coal Geology, 208, 1–11, https://doi.org/https://doi.org/10.1016/j.coal.2019.04.003.

Lomax, J. 1911. The microscopical examination of coal and its use in determining the inflammable constituent present therein. Transactions of the Institution of Mining Engineers, 42, 1–21.

López-Días, V., Urbańczyk, J., Blanco, C.G. and Borrego, Á.G. 2016. Maceral composition and molecular markers of two condensed Middle Holocene peat profiles in N Spain. International Journal of Coal Geology, 168, 55–70, https://doi.org/10.1016/j.coal.2016.09.009.

López, I.C., Ward, C.R., et al. 2008. Composition and mode of occurrence of mineral matter in some Colombian coals. International Journal of Coal Geology, 73, 3–18, https://doi.org/10.1016/j.coal.2007.03.005.

Lyons, P.C., Hatcher, P.G. and Brown, F.W. 1986. Secretinite: a proposed new maceral of the inertinite maceral group. Fuel, 65, 1094–1098, https://doi.org/10.1016/0016-2361(86)90175-4.

Macgregor, D.S. 1994. Coal-bearing strata as source rocks -- a global overview. Geological Society, London, Special Publications, 77, 107–116, https://doi.org/10.1144/GSL.SP.1994.077.01.06.

Mahesh, S., Murthy, S., Chakraborty, B. and Roy, M.D. 2015a. Fossil charcoal as Palaeofire indicators: Taphonomy and morphology of charcoal remains in sub-surface Gondwana sediments of South Karanpura coalfield. Journal of the Geological Society of India, 85, 567–576, https://doi.org/10.1007/s12594-015-0251-2.

Mahesh, S., Murthy, S., Singh, V.P. and Roy, J.S. 2015b. Thermally altered coals from bore core EBM-1, East Bokaro coal field, Damodar Valley, India: A petrographic inference. Journal of the Geological Society of India, 86, 535–546.

Małachowska, A., Mastalerz, M., Hampton, L., Hupka, J. and Drobniak, A. 2019. Origin of bitumen fractions in the Jurassic-early Cretaceous Vaca Muerta Formation in Argentina: insights from organic petrography and geochemical techniques. International Journal of Coal Geology, 205, 155–165, https://doi.org/https://doi.org/10.1016/j.coal.2018.11.013.

Man, C.K. and Gibbins, J.R. 2011. Factors affecting coal particle ignition under oxyfuel combustion atmospheres. Fuel, 90, 294–304, https://doi.org/10.1016/j.fuel.2010.09.006.

Mani, D., Patil, D.J., Dayal, A.M. and Prasad, B.N. 2015. Thermal maturity, source rock potential and kinetics of hydrocarbon generation in Permian shales from the Damodar Valley basin, Eastern India. Marine and Petroleum Geology, 66, 1056–1072, https://doi.org/10.1016/j.marpetgeo.2015.08.019.

Marchioni, D.L. 1980. Petrography and depositional environment of the Liddell seam, upper hunter valley, New South Wales. International Journal of Coal Geology, 1, 35–61, https://doi.org/10.1016/0166-5162(80)90005-1.

Mardon, S.M. and Hower, J.C. 2004. Impact of coal properties on coal combustion by-product quality : examples from a Kentucky power plant. International Journal of Coal Geology, 59, 153–169, https://doi.org/10.1016/j.coal.2004.01.004.

Mastalerz, M. 2001. Modes of occurrence of trace elements in coal. International Journal of Coal Geology, 46, 66, https://doi.org/10.1016/S0166-5162(00)00043-4.

Mastalerz, M. and Drobniak, A. 2007. Arsenic, cadmium, lead, and zinc in the Danville and Springfield coal members (Pennsylvanian) from Indiana. International Journal of Coal Geology, 71, 37–53, https://doi.org/10.1016/j.coal.2006.05.005.

Mastalerz, M., Drobniak, A., et al. 2005. Optical properties of pseudovitrinite; implications for its origin. International Journal of Coal Geology, 62, 250–258, https://doi.org/10.1016/j.coal.2005.03.019.

Mastalerz, M., Drobniak, A., Walker, R. and Morse, D. 2010. Coal lithotypes before and after saturation with CO_2; insights from micro-and mesoporosity, fluidity, and functional group distribution. International Journal of Coal Geology, 83, 467–474, https://doi.org/10.1016/j.coal.2010.06.007.

Mastalerz, M., Drobniak, A. and Stankiewicz, A.B. 2018. Origin, properties, and implications of solid bitumen in source-rock reservoirs: A review. International Journal of Coal Geology, 195, 14–36, https://doi.org/10.1016/j.coal.2018.05.013.

Mathews, R.P., Singh, B.D., et al. 2020. Organo-petrographic and geochemical characteristics of Gurha lignite deposits, Rajasthan, India: Insights into the palaeovegetation, palaeoenvironment and hydrocarbon source rock potential. Geoscience Frontiers, 11, 965–988, https://doi.org/10.1016/j.gsf.2019.10.002.

Mazumdar, B.K., Chakrabartty, S.K., Saha, M., Anand, K.S. and Lahiri, A. 1959. Further studies on the mechanism of the oxidation of coal. Fuel, 38, 469–482.

Mazumdar, B.K., Chakrabartty, S.K. and Lahiri, A. 1962. Some aspects of the constitution of coal. Fuel, 41, 129–139.

McCarthy, K., Rojas, K., et al. 2011. Basic Petroleum Geochemistry for Source Rock Evaluation. Oilfield Review, 23, 32–43.

McIver, R.D. 1967. Composition of kerogen-clue to its role in the origin of petroleum. In: World Petroleum Congress Proceedings. 25–36.

McLennan, S.M. 2001. Relationships between the trace element composition of sedimentary rocks and upper continental crust. Geochemistry, Geophysics, Geosystems, 2, 1–30, https://doi.org/10.1029/2000GC000109.

Mendhe, V.A., Kamble, A.D., Bannerjee, M., Mishra, S., Mukherjee, S. and Mishra, P. 2016. Evaluation of shale gas reservoir in Barakar and barren measures formations of north and south Karanpura Coalfields, Jharkhand. Journal of the Geological Society of India, 88, 305–316, https://doi.org/10.1007/s12594-016-0493-7.

Mendhe, V.A., Singh, P.K., Sinha, A., Mishra, S. and Bannerjee, M. 2017. Geological and Geochemical Characterization Of Lower Gondwana Shale beds of Damodar Valley For Hydrocarbon Potential and Development. In: 7th Asian Mining Congress. 8–11.

Mendhe, V.A., Kumar, V., et al. 2018. Evaluation of gas resource potentiality, geochemical and mineralogical characteristics of Permian shale beds of Latehar-

Auranga Coalfield, India. International Journal of Coal Geology, 196, 43–62, https://doi.org/10.1016/j.coal.2018.06.022.

Meunier, A., Caner, L., Hubert, F., El Albani, A. and Pret, D. 2013. The weathering intensity scale (WIS): An alternative approach of the chemical index of alteration (CIA). American Journal of Science, 313, 113–143, https://doi.org/10.2475/02.2013.03.

Middleton, M.F. 1982. Tectonic history from vitrinite reflectance. Geophysical Journal of the Royal Astronomical Society, 68, 121–132, https://doi.org/10.1111/j.1365-246X.1982.tb06965.x.

Milici, R.C. 2009. Coal-to-liquids: Potential impact on U.S. coal reserves. Natural Resources Research, 18, 85–94, https://doi.org/10.1007/s11053-009-9093-1.

Mirkowski, Z. and Jelonek, I. 2019. Petrographic composition of coals and products of coal combustion from the selected combined heat and power plants (CHP) and heating plants in Upper Silesia, Poland. International Journal of Coal Geology, 201, 102–108, https://doi.org/10.1016/j.coal.2018.11.014.

Misch, D., Riedl, F., et al. 2019. Petrographic and sorption-based characterization of bituminous organic matter in the Mandal Formation, Central Graben (Norway). International Journal of Coal Geology, 211, 103229, https://doi.org/https://doi.org/10.1016/j.coal.2019.103229.

Mishra, B.K. 1992. Tertiary coals of Makum Coalfield, Assam, India: Petrography, genesis and sedimentation. Palaeobotanist, 39, 309–326.

Mishra, H.K. and Cook, A.C. 1992. Petrology and thermal maturity of coals in the Jharia Basin: Implications for oil and gas origins. International Journal of Coal Geology, 20, 277–313, https://doi.org/10.1016/0166-5162(92)90018-R.

Mishra, H.K. and Ghosh, R.K. 1996. Geology, petrology and utilisation potential of some Tertiary coals of the northeastern region of India. International Journal of Coal Geology, 30, 65–100, https://doi.org/10.1016/0166-5162(95)00038-0.

Mishra, H.K., Chandra, T.K. and Verma, R.P. 1990. Petrology of some Permian coals of India. International Journal of Coal Geology, 16, 47–71, https://doi.org/http://dx.doi.org/10.1016/0166-5162(90)90013-O.

Mishra, M.K. and Pandey, D.P. 2011. Studies on the mineralogical characterization of coals of Jharia (District-Dhanbad) coalfield (Lodna & Bhowrah Coal), by X-Ray diffraction (XRD) and IR spectroscopic instrumental techniques. Oriental Journal of Chemistry, 27, 305–311.

Mishra, V. and Singh, K.N. 2017. Microstructural relation of macerals with mineral matter in coals from Ib valley and Umaria, Son-Mahanadi basin, India. International Journal of Coal Science and Technology, 4, 191–197, https://doi.org/10.1007/s40789-017-0169-y.

Misra, B. and Singh, B. 1993. Liptinite macerals in Singrauli coals, India: their characterization and assessment.

Misra, B.K. 1992. Optical properties of some Tertiary coals from northeastern India: their depositional environment and hydrocarbon potential. International Journal of Coal Geology, 20, 115–144, https://doi.org/10.1016/0166-5162(92)90007-J.

Misra, B.K. and Singh, B.D. 1994. Susceptibility to spontaneous combustion of Indian coals and lignites: an organic petrographic autopsy. International Journal of Coal Geology, 25, 265–286, https://doi.org/10.1016/0166-5162(94)90019-1.

Misra, B.K., Singh, B.D. and Navale, G.K.B. 1990. Resino-inertinites of Indian Permian coals - their origin, genesis and classification. International Journal of Coal Geology, 14, 277–293, https://doi.org/10.1016/0166-5162(90)90084-C.

Misra, S., Varma, A.K., Das, S.K., Mani, D. and Biswas, S. 2018. Thermal controls of lamprophyre sill on hydrocarbon generation outlook of shale beds in Raniganj basin, India. Journal of Natural Gas Science and Engineering, 56, 536–548, https://doi.org/10.1016/j.jngse.2018.06.028.

Misra, S., Varma, A.K., Hazra, B., Biswas, S. and Samad, S.K. 2019. The influence of the thermal aureole asymmetry on hydrocarbon generative potential of coal beds: Insights from Raniganj Basin, West Bengal, India. International Journal of Coal Geology, 206, 91–105, https://doi.org/https://doi.org/10.1016/j.coal.2019.03.008.

Misra, S., Das, S.K., Varma, A.K., Mani, D., Kalpana, M.S., Ekblad, A. and Biswas, S. 2020. Multi-proxy approach on the hydrocarbon generation perspective of Barjora Basin, India. Marine and Petroleum Geology, 112, 104108, https://doi.org/10.1016/j.marpetgeo.2019.104108.

Mitrović, D., Đoković, N., Životić, D., Bechtel, A., Šajnović, A. and Stojanović, K. 2016. Petrographical and organic geochemical study of the Kovin lignite deposit, Serbia. International Journal of Coal Geology, 168, 80–107, https://doi.org/10.1016/j.coal.2016.07.008.

Mostafa, A., El-Gayar, M.S. and Barakat, A.O. 1998. Relationship between petroleum composition and depositional environment of petroleum source rocks from the Gulf of Suez and the Western Desert of Egypt. Petroleum Science and Technology, 16, 191–207, https://doi.org/10.1080/10916469808949779.

Mukherjee, B. and Arabinda, G. 1969. A note on the Miospore assemblage of Bachra coal measure. North Karanpura Coalfield, Bihar and its bearing on the age of the unit. Proc. Ind. Sci. Cong, 222–223.

Mukherjee, B. and Dutta, R. 1950. A note on the constituents of the ashes of Indian coals determined spectroscopically. Fuel, 29, 190–192.

Mukherjee, K.N., Dutta, N.R., Chandra, D., Pandalai, H.S. and Singh, M.P. 1988. A statistical approach to the study of the distribution of trace elements and their organic/ inorganic affinity in lower Gondwana coals of India. International Journal of Coal Geology, 10, 99–108, https://doi.org/10.1016/0166-5162(88)90007-9.

Mukhopadhyay, G., Mukhopadhyay, S.K., et al. 2010. Stratigraphic correlation between different Gondwana Basins of India. Journal of the Geological Society of India, 76, 251–266, https://doi.org/10.1007/s12594-010-0097-6.

Mukhopadhyay, P.K. 1986. Petrography of selected Wilcox and Jackson Group lignites from the Tertiary of Texas. In: Finkelman, R. B. and Casagrande, D. J. (eds) Geology of Gulf Coast Lignites. 126–145.

Mukhopadhyay, P.K. 1989. Characterization of amorphous and other organic matter types by microscopy and pyrolysis-gas chromatography. Organic Geochemistry, 14, 269–284, https://doi.org/10.1016/0146-6380(89)90055-7.

Mukhopadhyay, P.K., Hagemann, H.W., Hollerbach, A. and Welte, D.H. 1979. The relation between organic geochemical and petrological parameters of coal in Indian coal basins. Energy Sources, 4, 313–328, https://doi.org/10.1080/00908317908908067.

Murchison, D. 2004. Aberrations in the coalification patterns of the offshore coalfields of Northumberland and Durham, United Kingdom. International Journal of Coal Geology, 58, 133–146, https://doi.org/10.1016/j.coal.2003.10.005.

Murchison, D.G. 1987a. Recent advances in organic petrology and organic geochemistry : an overview with some reference to ' oil from coal '. Geological Society, London, Special Publications, 32, 257–302, https://doi.org/10.1144/GSL.SP.1987.032.01.15.

Murchison, D.G. 1987b. Recent advances in organic petrology and organic geochemistry: an overview with some reference to 'oil from coal'. Geological Society, London, Special Publications, 32, 257–302, https://doi.org/10.1144/GSL.SP.1987.032.01.15.

Murthy, S., Tripathi, A., Chakraborti, B. and Singh, U.P. 2014. Palynostratigraphy of Permian succession from Binja Block, South Karanpura Coalfield, Jharkhand, India. Journal of Earth System Science, 123, 1895–1906, https://doi.org/10.1007/s12040-014-0505-1.

Naeth, J., Asmus, S.C. and Littke, R. 2004. Petrographic and geophysical assessment of coal quality as related to briquetting: The Miocene lignite of the Lower Rhine Basin, Germany. International Journal of Coal Geology, 60, 17–41, https://doi.org/10.1016/j.coal.2004.04.002.

Naik, A.S., Singh, M.P., Volkmann, N., Singh, P.K., Mohanty, D. and Kumar, D. 2016. Petrographic characteristics and paleomires of Mand-Raigarh coals, Mahanadi Gondwana Basin, Chhattisgarh, India. International Journal of Coal Science & Technology, 3, 165–183, https://doi.org/10.1007/s40789-016-0140-3.

Nandgaonkar, B.R. 1977. Study of the occurrence of coal at Pathakhera Coalfield, Satpura Basin of MP with special reference to their chemical and petrological characters. In: 4th Int. Gond. Symp. 320–323.

Nath, M. 2005. Geochemistry of Jarain Coal, Jaintia Hills, Meghalaya, North East India. Indian Journal of Geochemistry, 20, 19.

Navale, G.K.B. 1971. Some aspects of the physical constitution of certain lower Gondwana coal seams of India. Economic Geology, 66, 632–640, https://doi.org/10.2113/gsecongeo.66.4.632.

Navale, G.K.B. 1979. Lower Gondwana primary composite genetic coal types of India. CR (East Lansing, Mich.), 4, 62–67.

Navale, G.K.B. 1984. Lower Gondwana coals of India - Palaeobotany, Petrology and Genesis. Comunicações Geológicas Tomo 70-2, 70, 245–256.

Navale, G.K.B. and Misra, B.K. 1980. Systematic study of the organic microconstituents of the main seam of the Neyveli lignite, South India. Geophytology, 10, 2.

Navale, G.K.B. and Saxena, R. 1989. An appraisal of coal petrographic facies in Lower Gondwana (Permian) coal seams of India. International Journal of Coal Geology, 12, 553–588, https://doi.org/10.1016/0166-5162(89)90065-7.

Navale, G.K.B. and Srivastava, S.C. 1969. Petro-palynological study of the coals exposed near Gopalprasad of Talcher coalfield (Orissa), India.

Navale, G.K.B. and Tiwari, R.S. 1966. A preliminary sporological analysis of some coals from Talcher Coalfield, India. The Palaeobotanist.

Nayak, B., Singh, A.K., Upadhyay, A.K. and Bhattacharyya, K.K. 2009. A note on the characters of some Lower Gondwana coals of West Siang district in the Arunachal

Himalaya and their trace element content. Journal of the Geological Society of India, 74, 395–401, https://doi.org/10.1007/s12594-009-0138-1.

Ndip, E.A., Agyingi, C.M., Nton, M.E., Hower, J.C. and Oladunjoye, M.A. 2019. Organic petrography and petroleum source rock evaluation of the Cretaceous Mamfe Formation, Mamfe basin, southwest Cameroon. International Journal of Coal Geology, 202, 27–37, https://doi.org/https://doi.org/10.1016/j.coal.2018.11.005.

Nesbitt, H.W. and Young, G.M. 1982. Early proterozoic climates and plate motions inferred from major element chemistry of lutites. Nature, 299, 715–717, https://doi.org/10.1038/299715a0.

Niyogi, D. 1961. Pattern of Talchir sedimentation in Burhai Gondwana basin, Bihar, India. Journal of Sedimentary Research, 31, 63–72.

Niyogi, D. 1966. Lower Gondwana sedimentation in Saharjuri coalfield, Bihar, India. Journal of Sedimentary Research, 36, 960–972.

Niyogi, D. and Sanyal, S.P. 1962. Gondwana rocks of Jayanti coalfield, SP, Bihar. QJ Geol. Min. Metall. Soc. India, 34, 182–193.

Noble, R.A. 1986. A Geochemical Study of Bicyclic Alkanes and Diterpenoid Hydrocarbons in Crude Oils, Sediments and Coals.

Noble, R.A., Alexander, R., Kagi, R.I. and Knox, J. 1985. Tetracyclic diterpenoid hydrocarbons in some Australian coals, sediments and crude oils. Geochimica et Cosmochimica Acta, 49, 2141–2147, https://doi.org/10.1016/0016-7037(85)90072-9.

O'Keefe, J.M.K., Hower, J.C., Finkelman, R.F., Drew, J.W. and Stucker, J.D. 2011. Petrographic, geochemical, and mycological aspects of Miocene coals from the Nováky and Handlová mining districts, Slovakia. International Journal of Coal Geology, 87, 268–281, https://doi.org/10.1016/j.coal.2011.06.019.

O'Keefe, J.M.K., Bechtel, A., et al. 2013. On the fundamental difference between coal rank and coal type. International Journal of Coal Geology, 118, 58–87, https://doi.org/10.1016/j.coal.2013.08.007.

Ojha, K., Karmakar, B., Mandal, A. and Pathak, A.K. 2011. Coal Bed Methane in India: Difficulties and Prospects. International Journal of Chemical Engineering and Applications, 2, 256–260, https://doi.org/10.7763/IJCEA.2011.V2.113.

Orphan, V.J., House, C.H., Hinrichs, K.U., McKeegan, K.D. and DeLong, E.F. 2001. Methane-consuming archaea revealed by directly coupled isotopic and phylogenetic analysis. Science, https://doi.org/10.1126/science.1061338.

Osborne, D. 2013. The Coal Handbook: Towards Cleaner Production, https://doi.org/10.1533/9781782421177.

Ottenjann, K., Teichmuller, M. and Wolf, M. 1974. Spektrale Fluoreszenz - Messungenan Sporiniten mit Auflichit-Anregung, eine mikorskopische Methode zur Bestimmung des Inkohlungsgrades gering inmkohlter kohlen - fortschr. Geol. reinld. u. westf., 24, 1–36.

Otto, A. and Wilde, V. 2001. Sesqui-, di-, and triterpenoids as chemosystematic markers in extant conifers - A review. Botanical Review, 67, 141–238, https://doi.org/10.1007/BF02858076.

Otto, A., Walther, H. and Püttmann, W. 1997. Sesqui- and diterpenoid biomarkers preserved in Taxodium-rich Oligocene oxbow lake clays, Weisselster basin, Germany. Organic Geochemistry, 26, 105–115, https://doi.org/10.1016/S0146-6380(96)00133-7.

Ourisson, G., Albrecht, P. and Rohmer, M. 1979. The Hopanoids: palaeochemistry and biochemistry of a group of natural products. Pure and Applied Chemistry, 51, 709–729, https://doi.org/10.1351/pac197951040709.

Painter, P., Starsinic, M. and Coleman, M. 1985. Determination of Functional Groups in Coal By Fourier Transform Interferometry. In: Fourier Transform Infrared Spectra. 169–241., https://doi.org/10.1016/b978-0-12-254104-9.50011-0.

Painter, P.C., Coleman, M.M., Jenkins, R.G., Whang, P.W., Walker, P.L., Jr, P.L.W. and Walker, P.L. 1978. Fourier Transform Infrared study of mineral matter in coal. A novel method for quantitative mineralogical analysis. Fuel, 57, 337–344, https://doi.org/10.1016/0016-2361(78)90170-9.

Painter, P.C., Snyder, R.W., Starsinic, M., Coleman, M.M., Kuehn, D.W. and Davis, A. 1982. Fourier Transform IR Spectroscopy Application to the Quantitative Determination of Functional Groups in Coal Pennsylvania State University, College of Earth and Mineral Sciences, University Park, PA.

Pandey, O.P. and Negi, J.G. 1995. Geothermal fields of India: a latest update. In: Proceedings of the World Geothermal Congress. 163–171.

Papanicolaou, C., Kotis, T., Foscolos, A. and Goodarzi, F. 2004. Coals of Greece: a review of properties, uses and future perspectives. International Journal of Coal Geology, 58, 147–169, https://doi.org/10.1016/j.coal.2003.10.006.

Pareek, H.S. 1963. Petrology of Talcher coals. Economic Geology, 58, 1089–1109.

Pareek, H.S. 1964. Petrological characteristics of Barakar coal, metamorphosed by lamprophyre sill, in Jharia coalfield, India. Economic Geology, 59, 926–929, https://doi.org/10.2113/gsecongeo.59.5.926.

Pareek, H.S. 1966a. Fusinized resins in Gondwana (Permian) coals of India. Economic Geology, 61, 137–146, https://doi.org/10.2113/gsecongeo.61.1.137.

Pareek, H.S. 1966b. Petrological characteristics of Barakar coal seams, metamorphosed by lamprophyre sill in the Jharia coalfield, Bihar. In: Proceedings of the Indian Academy of Sciences-Section B. 261–270.

Pareek, H.S. 1969a. On the geology and correlation of coal seams of Pench-Kanhan-Upper Tawa valley coalfield, district Chhindwara, Madhya Pradesh.

Pareek, H.S. 1969b. Petrological study of coals from Singrauli coalfield, MP. Rec. Geol. Sur. India, 97, 87–90.

Pareek, H.S. 1970. Petrology of Coal, Burnt Coal and Para Lava from Singrauli Coalfield, MP & U. P. Geological Society of India, 11, 333–347.

Pareek, H.S. 1981. Petrology of Kalol lignite, Cambay basin, Gujarat, Symp. on Three decades of developments of Petrology, Mineralogy and Petrochemistry in India, Geol. Surv. India, Jaipur, May, 1981, 106–107.

Pareek, H.S. 1986. The role of coal petrographic characteristics in evaluating the non-coking nature of the coals of Ramagundam and Kothagudem coalfields, Godavari Valley Basin, Andhra Pradesh, India. International Journal of Coal Geology, 6, 181–198, https://doi.org/10.1016/0166-5162(86)90020-0.

Pareek, H.S. 1987. Petrographic, chemical and trace-elemental composition of the coal of Sohagpur coalfield, Madhya Pradesh, India. International Journal of Coal Geology, 9, 187–207, https://doi.org/10.1016/0166-5162(87)90045-0.

Pareek, H.S. 1988. Petrographic characteristics of the solid fuels of India with particular reference to the coking coals. International Journal of Coal Geology, 10, 285–306, https://doi.org/10.1016/0166-5162(88)90024-9.

Pareek, H.S. and Bardhan, B. 1985. Trace elements and their variation along seam profiles of certain coal seams of Middle and Upper Barakar formations (Lower Permian) in East Bokaro coalfield, district Hazaribagh, Bihar, India. International Journal of Coal Geology, 5, 281–314, https://doi.org/10.1016/0166-5162(85)90030-8.

Pareek, H.S. and Pande, B.C. 1970. On the Microscopic nature of coals from Majri Area, Wardha Valley Coalfield, Maharashtra. Palaeobotanist, 19, 76-82.

Pareek, H.S., Sanyal, S.P. and Chakrabarti, N.C. 1964. Petrographic Studies of the Coal Seams in the Pench-Kanhan Coalfield, India. XXII Int. Geol. Congr., New Delhi, 1964, IX, Proc. Section 9, Gondwanas, 1-16.

Parr, S.W. 1922. The Classification of Coal. Industrial and Engineering Chemistry, 14(10), 919-922. https://doi.org/10.1021/ie50154a019.

Pashin, J.C. 2008. Coal as a Petroleum Source Rock and Reservoir Rock. In: Applied Coal Petrology. 227–262., https://doi.org/10.1016/B978-0-08-045051-3.00009-9.

Pattanaik, D.S., Behera, P. and Singh, B. 2011. Spontaneous Combustibility Characterisation of the Chirimiri Coals, Koriya District, Chhatisgarh, India. International Journal of Geosciences, 02, 336–347, https://doi.org/10.4236/ijg.2011.23036.

Paul, S. and Chatterjee, R. 2011. Mapping of cleats and fractures as an indicator of in-situ stress orientation, Jharia coalfield, India. International Journal of Coal Geology, 88, 113–122, https://doi.org/10.1016/j.coal.2011.09.006.

Paul, S., Sharma, J., Singh, B.D., Saraswati, P.K. and Dutta, S. 2015. Early Eocene equatorial vegetation and depositional environment: Biomarker and palynological evidences from a lignite-bearing sequence of Cambay Basin, western India. International Journal of Coal Geology, 149, 77–92, https://doi.org/10.1016/j.coal.2015.06.017.

Pepper, A.S. and Corvi, P.J. 1995. Simple kinetic models of petroleum formation. Part I: oil and gas generation from kerogen. Marine and Petroleum Geology, 12, 291–319, https://doi.org/10.1016/0264-8172(95)98381-E.

Peters, K.E. 1986. Guidelines for Evaluating Petroleum Source Rock Using Programmed Pyrolysis. American Association of Petroleum Geologists Bulletin, 70, 318–329, https://doi.org/10.1306/94885688-1704-11D7-8645000102C1865D.

Peters, K.E. and Cassa, M.R. 1994. Applied Source Rock Geochemistry Magoon, L. B, and W. G. Dow, eds., 1994, The petroleum system—From source to trap. AAPG Memoirs, 60, 93–120.

Peters, K.E., Walters, C.C. and Moldowan, J.M. 2005. The Biomarker Guide.

Petersen, H.I. 2005. Oil generation from coal source rocks: the influence of depositional conditions and stratigraphic age. Geological Survey of Denmark and Greenland Bulletin, 7, 9–12.

Petersen, H.I. 2006. The petroleum generation potential and effective oil window of humic coals related to coal composition and age. International Journal of Coal Geology, 67, 221–248, https://doi.org/10.1016/j.coal.2006.01.005.

Petersen, H.I. and Hertle, M. 2018. A Review of the Coaly Source Rocks and Generated Petroleums in the Danish North Sea: an Underexplored Middle Jurassic Petroleum System? Journal of Petroleum Geology, 41, 135–154, https://doi.org/10.1111/jpg.12697.

Petersen, H.I., Andsbjerg, J., et al. 2000. Coal-generated oil: Source rock evaluation and petroleum geochemistry of the Lulita oilfield, Danish North Sea. Journal of

Petroleum Geology, 23, 55–90, https://doi.org/10.1111/j.1747-5457.2000.tb00484.x.

Phukan, S. 2002. Study of the West Daranggiri Coal Field of Garo Hills, Meghalaya. Gauhati University.

Pickel, W., Kus, J., et al. 2017. Classification of liptinite – ICCP System 1994. International Journal of Coal Geology, 169, 40–61, https://doi.org/10.1016/j.coal.2016.11.004.

Pires, M. and Querol, X. 2004. Characterization of Candiota (South Brazil) coal and combustion by-product. International Journal of Coal Geology, 60, 57–72, https://doi.org/10.1016/j.coal.2004.04.003.

Pokrovsky, O.S., Viers, J., et al. 2012. Biogeochemistry of carbon, major and trace elements in watersheds of northern Eurasia drained to the Arctic Ocean: The change of fluxes, sources and mechanisms under the climate warming prospective. Comptes Rendus - Geoscience, 344, 663–677, https://doi.org/10.1016/j.crte.2012.08.003.

Powell, T.G., Creaney, S. and Snowdon, L.R. 1982. Limitations of use of organic petrographic techniques for identification of petroleum source rocks. AAPG Bulletin, 66, 430–435.

Prachiti, P.K., Manikyamba, C., et al. 2011. Geochemical systematics and precious metal content of the sedimentary horizons of Lower Gondwanas from the Sattupalli coalfield, Godavari Valley, India. International Journal of Coal Geology, 88, 83–100, https://doi.org/10.1016/j.coal.2011.08.005.

Pradier, B., Bertrand, P., Martinez, L. and Laggoun-Defarge, F. 1991. Fluorescence of organic matter and thermal maturity assessment. Organic Geochemistry, 17, 511–524, https://doi.org/10.1016/0146-6380(91)90115-Z.

Prakash, D., Chandra Singh, P., Arima, M. and Singh, T. 2012. P-T history and geochemical characteristics of mafic granulites and charnockites from west of Periya, North Kerala, southern India. Journal of Asian Earth Sciences, 61, 102–115, https://doi.org/10.1016/j.jseaes.2012.08.023.

Presswood, S.M., Rimmer, S.M., Anderson, K.B. and Filiberto, J. 2016. Geochemical and petrographic alteration of rapidly heated coals from the Herrin (No. 6) Coal Seam, Illinois Basin. International Journal of Coal Geology, 165, 243–256, https://doi.org/10.1016/j.coal.2016.08.022.

Preuss, B. 1977. Zur Bedeutung und zum Stand mikroskopischer Fluoreszenz - Untersuchungen in der Kohlenpetrographie - Freiberger Forschungh. C, 331, 199–209.

Qi, Y. 2011. Organic geochemical characteristics of source rocks from Yiliekede Formation in the intermittent stages of volcanic activity in Mohe Basin. Acta Sedimentologica Sinica, 29, 164–172.

Qi, Y., Ju, Y., et al. 2020. Organic matter provenance and depositional environment of marine-to-continental mudstones and coals in eastern Ordos Basin, China—Evidence from molecular geochemistry and petrology. International Journal of Coal Geology, 217, 103345, https://doi.org/https://doi.org/10.1016/j.coal.2019.103345.

Qian, Y., Zhang, T., Wang, Z., Tuo, J., Zhang, M., Wu, C. and Tian, C. 2018. Organic geochemical characteristics and generating potential of source rocks from the Lower-Middle Jurassic coal-bearing strata in the East Junggar Basin, NW China.

Marine and Petroleum Geology, 93, 113–126, https://doi.org/10.1016/j.marpetgeo.2018.02.036.

Qiu, N., Li, H., Jin, Z. and Zhu, Y. 2007. Temperature and time effect on the concentrations of free radicals in coal: Evidence from laboratory pyrolysis experiments. International Journal of Coal Geology, 69, 220–228, https://doi.org/10.1016/j.coal.2006.04.002.

Querol, X., Fernández-Turiel, J. and López-Soler, A. 1995. Trace elements in coal and their behaviour during combustion in a large power station. Fuel, 74, 331–343, https://doi.org/10.1016/0016-2361(95)93464-O.

Querol, X., Alastuey, A., et al. 1997a. Geological controls on the mineral matter and trace elements of coals from the Fuxin basin, Liaoning Province, northeast China. International Journal of Coal Geology, 34, 89–109, https://doi.org/10.1016/S0166-5162(97)00014-1.

Querol, X., Whateley, M.K.G., et al. 1997b. Geological controls on the mineralogy and geochemistry of the Beypazari lignite, central Anatolia, Turkey. International Journal of Coal Geology, 33, 255–271, https://doi.org/10.1016/S0166-5162(96)00044-4.

Raask, E. 1985. The mode of occurrence and concentration of trace elements in coal. Progress in Energy and Combustion Science, 11, 97–118, https://doi.org/10.1016/0360-1285(85)90001-2.

Radhwani, M., Bechtel, A., Singh, V.P., Singh, B.D. and Mannaï-Tayech, B. 2018. Petrographic, palynofacies and geochemical characteristics of organic matter in the Saouef Formation (NE Tunisia): Origin, paleoenvironment, and economic significance. International Journal of Coal Geology, 187, 114–130, https://doi.org/https://doi.org/10.1016/j.coal.2018.01.010.

Radke, M., Leythaeuser, D., Teichmuller, M., Teichmüller, M., Teichmuller, M., Teichmüller, M. and Teichmuller, M. 1984. Relationship between rank and composition of aromatic hydrocarbons for coals of different origins. Organic Geochemistry, 6, 423–430, https://doi.org/10.1016/0146-6380(84)90065-2.

Raja Rao, C.S. 1957. Investigation by Drilling in the Gidi Block ‘A’, South Karanpura Coalfield, Hazaribagh District, Bihar. Geological Survey of India.

Raja Rao, C.S. 1981. Coalfields of India, Coalfields of North Eastern India. Bulletin of the Geological Survey of India, Series A, No. 45, I, 75.

Raja Rao, C.S. 1987. Coalfields of India: Coalfields of Bihar and West Bengal. Bulletin of the Geological Survey of India, Series A, No. 45, 4, 44.

Rajak, P.K., Singh, V.K., et al. 2018. Geochemical implications of minerals and environmentally sensitive elements of Giral lignite, Barmer Basin, Rajasthan (India). Environmental Earth Sciences, 77, 698, https://doi.org/10.1007/s12665-018-7885-5.

Rajarathnam, S., Chandra, D. and Handique, G.K. 1996. An overview of chemical properties of marine-influenced Oligocene coal from the northeastern part of the Assam-Arakan basin, India. International Journal of Coal Geology, 29, 337–361, https://doi.org/10.1016/0166-5162(95)00025-9.

Rao, B. and Rao, V. 1955. Minor elements in Indian coals. J. Ind. Geol. Sci. Assoc., 4–5.

Regnault, M. V. 1840. On a new process for determining the carbon in cast iron and steel. Journal of the Franklin Institute, 29, 327–328.

Ren, D., Zhao, F., Wang, Y. and Yang, S. 1999. Distributions of minor and trace elements in Chinese coals. International Journal of Coal Geology, 40, 109–118, https://doi.org/10.1016/S0166-5162(98)00063-9.

Ribeiro, J., Suárez-Ruiz, I., Ward, C.R. and Flores, D. 2016. Petrography and mineralogy of self-burning coal wastes from anthracite mining in the El Bierzo Coalfield (NW Spain). International Journal of Coal Geology, 154–155, 92–106, https://doi.org/10.1016/j.coal.2015.12.011.

Richardson, A.R., Eble, C.F., et al. 2012. A critical re-examination of the petrology of the No. 5 Block coal in eastern Kentucky with special attention to the origin of inertinite macerals in the splint lithotypes. International Journal of Coal Geology, 98, 41–49, https://doi.org/10.1016/j.coal.2012.04.003.

Rishi, M.K. 1970. Reflectance of sclerotioids from coals of Umaria, central India. Economic Geology, 65, 700–705, https://doi.org/10.2113/gsecongeo.65.6.700.

Robert, P. 1979. Classification des matieres organiques en fluorescence. Application aux roches - meres petrolieres. - Bull, 3, 223–263.

Robert, P. 1980. The optical evolution of kerogen and geothermal histories applied to oil and gas exploration, - In: Durand. B. : Kerogen, 385–414.

Rogers, J.J.W. and Callahan, E.J. 1987. Radioactivity, Heat Flow, and Rifting of the Indian Continental Crust. The Journal of Geology, 95, 829–836, https://doi.org/10.1086/629181.

Rohmer, M., Bisseret, P. and Neunlist, S. 1992. The hopanoids, prokaryotic triterpenoids and precursors of ubiquitous molecular fossils. Biological markers in sediments and petroleum, 54, 1–17.

Roy, P.D., Smykatz-Kloss, W. and Sinha, R. 2006. Late Holocene geochemical history inferred from Sambhar and Didwana playa sediments, Thar Desert, India: Comparison and synthesis. Quaternary International, 144, 84–98, https://doi.org/10.1016/j.quaint.2005.05.018.

Rusnak, J.A. 2017. Coal Strength Variation by Lithotype for High-Volatile A Bituminous Coal in the Central Appalachian Basin.

Ryberg, M.W., Owsianiak, M., Laurent, A. and Hauschild, M.Z. 2015. Power generation from chemically cleaned coals: do environmental benefits of firing cleaner coal outweigh environmental burden of cleaning? Energy Environ. Sci., 8, 2435–2447, https://doi.org/10.1039/C5EE01799H.

Saikia, B.K. 2009. Scanning electron microscopy of Assam coals, India. Journal of the Geological Society of India, 74, 749–752, https://doi.org/10.1007/s12594-009-0191-9.

Saikia, B.K., Boruah, R.K. and Gogoi, P.K. 2007. FT-IR and XRD analysis of coal from Makum coalfield of Assam. Journal of Earth System Science, 116, 575–579, https://doi.org/10.1007/s12040-007-0052-0.

Saikia, B.K., Ward, C.R., Oliveira, M.L.S., Hower, J.C., Baruah, B.P., Braga, M. and Silva, L.F. 2014. Geochemistry and nano-mineralogy of two medium-sulfur northeast Indian coals. International Journal of Coal Geology, 121, 26–34, https://doi.org/10.1016/j.coal.2013.11.007.

Saikia, M.M. and Dutta, T.K. 1980. Depositional environment of source beds of high-wax oils in Assam Basin, India. American Association of Petroleum Geologists Bulletin, 64, 427–430, https://doi.org/10.1306/2f91899b-16ce-11d7-8645000102c1865d.

Sajwan, K.S., Alva, A.K. and Keefer, R.F. 1999. Biogeochemistry of Trace Elements in Coal and Coal Combustion Byproducts Springer Science & Business Media. https://doi.org/10.1007/978-1-4615-4155-4.

Sarana, S. and Kar, R. 2011. Effect of igneous intrusive on coal microconstituents: Study from an Indian Gondwana coalfield. International Journal of Coal Geology, 85, 161–167, https://doi.org/10.1016/j.coal.2010.11.006.

Sarkar, P. and Singh, K.H. 2016. Petrophysical Characterization of Gondwana Shales of South Karanpura Coal Field, Jharkhand, India. ASEG Extended Abstracts, 2016, 1, https://doi.org/10.1071/ASEG2016ab248.

Saxby, J.D. 1980. Atomic H C ratios and the generation of oil from coals and kerogens. Fuel, 59, 305–307, https://doi.org/10.1016/0016-2361(80)90214-8.

Saxby, J.D. and Shibaoka, M. 1986. Coal and coal macerals as source rocks for oil and gas. Applied Geochemistry, 1, 25–36, https://doi.org/10.1016/0883-2927(86)90035-1.

Schneider, W., Braunkohlen, L., Laubag, A. and Senftenberg, D.-. 1995. Palaeohistological studies on Miocene brown coals of Central Europe. International Journal of Coal Geology, 28, 229–248, https://doi.org/10.1016/0166-5162(95)00019-4.

Schochardt, M. 1936. Zur Lumineszenz der Steinkohle. Zeiss Nachrichten, 2, 22.

Schopf, J. 1960. Field Description and Sampling of Coal Beds. In: U.S. Geological Survey Bulletin B 1111. 25–67.

Schweinfurth, S.P. 2002. Coal—A Complex Natural Resource An overview of factors affecting coal quality and use in the United States With a contribution on coal quality and public health. US Dept of the Interior, U.S. Geological Survey, 1143.

Scott, A.C. 2002. Coal petrology and the origin of coal macerals : a way ahead ? International Journal of Coal Geology, 50, 119–134, https://doi.org/10.1016/S0166-5162(02)00116-7.

Scott, D.H. 1999. Ash Behaviour During Combustion and Gasification.

Seifert, W.K. and Moldowan, J.M. 1980. The effect of thermal stress on source-rock quality as measured by hopane stereochemistry. Physics and Chemistry of the Earth, 12, 229–237, https://doi.org/10.1016/0079-1946(79)90107-1.

Sen, S. 2016. Review on coal petrographic indices and models and their applicability in paleoenvironmental interpretation. Geosciences Journal, 20, 719–729, https://doi.org/10.1007/s12303-015-0046-x.

Sen, S. and Banerjee, S. 2015. Identifying Relationship Amongst Vitrinite/Inertinite Ratio (V/I), Cleat Parameters, Vitrinite Reflectance, O/C Ratio and Permeability of Coal Seams and V/I Ratio as Exploration Tool: Study from Raniganj Coal Bed Methane Block, Essar Oil Limited, India. 205–217., https://doi.org/10.1007/978-3-319-03119-4_9.

Sen, S., Naskar, S. and Das, S. 2016a. Discussion on the concepts in paleoenvironmental reconstruction from coal macerals and petrographic indices. Marine and Petroleum Geology, 73, 371–391, https://doi.org/10.1016/j.marpetgeo.2016.03.015.

Sen, S., Das, N. and Maiti, D. 2016b. Facies analysis and depositional model of late Permian Raniganj formation: Study from Raniganj coal bed methane block. Journal of the Geological Society of India, 88, 503–516, https://doi.org/10.1007/s12594-016-0513-7.

Seyler, C.A. 1931. Petrology and the classification of coal. Proc. S. Wales Inst. Eng, 53, 254–407.

Seyler, C.A. 1943. Recent progress in the petrology of coal. J. Inst. Fuel, 16, 134–141.

Seyler, C.A. 1952. Characteristic petrological components of coal. Fuel, 31, 159–170.

Sharma, A., Saikia, A., Khare, P. and Baruah, B.P. 2014. Genesis of some tertiary Indian coals from the chemical composition of ash-a statistical approach: Part 1. Journal of Earth System Science, 123, 1705–1715, https://doi.org/10.1007/s12040-014-0479-z.

Sharma, D.K. and Wadhwa, G. 1997. Demineralization of coal by stepwise bioleaching: A comparative study of three Indian coals by Fourier Transform Infra Red and X-ray diffraction techniques. World Journal of Microbiology and Biotechnology, 13, 29–36, https://doi.org/10.1007/BF02770804.

Singh, A. 2002. On a striking fluorescing microcomponent from Indian Tertiary lignites. International Journal of Coal Geology, 51, 59–65, https://doi.org/10.1016/S0166-5162(01)00062-3.

Singh, A., Misra, B.K., Singh, B.D. and Navale, G.K.B. 1992. The Neyveli lignite deposits (Cauvery basin), India: organic composition, age and depositional pattern. International journal of coal geology, 21, 45–97.

Singh, A., Mahesh, S., Singh, H., Tripathi, S.K.M. and Singh, B.D. 2013a. Characterization of Mangrol lignite (Gujarat), India: Petrography, palynology, and palynofacies. International Journal of Coal Geology, 120, 82–94, https://doi.org/10.1016/j.coal.2013.10.001.

Singh, A.K. 2015. Petrological investigation of Eocene coals, Garo Hills, Meghalaya, India. Arabian Journal of Geosciences, 8, 10705–10714.

Singh, A.K. 2016a. Petrographic and geochemical characterization of coal from Talcher coalfield, Mahanadi Basin, India. Journal of the Geological Society of India, 87, 525–534, https://doi.org/10.1007/s12594-016-0426-5.

Singh, A.K. 2016b. Petrographic characterization and evolution of the Karharbari coals, Talcher Coalfield, Orissa, India. International Journal of Coal Science and Technology, 3, 133–147, https://doi.org/10.1007/s40789-016-0132-3.

Singh, A.K. 2018. Classification and Potential Utilization of Eocene Coals of Meghalaya, North East India. Journal of the Geological Society of India, 91, 181–187, https://doi.org/10.1007/s12594-018-0832-y.

Singh, A.K. and Banerjee, P.K. 2006. Liberation Study of Mineral Matter from the Coal : A Case Study of Seam No. VII of West Bokaro Coalfield. Mineral Processing Technology, 573–581.

Singh, A.K. and Jha, M.K. 2017. Bituminous Coal As a Potential Source Rock for Hydrocarbon Production : Study From Barka Sayal Area, South Karanpura Coalfield, Jharkhand. International Conference on ‘Challenges and Prospects of Petroleum Production and Processing Industries’, 9, https://doi.org/10.1386/eta.8.3.221_1.

Singh, A.K. and Jha, M.K. 2018a. Hydrocarbon potential of Permian coals of South Karanpura Coalfield, Jharkhand, India. Energy Sources, Part A: Recovery, Utilization and Environmental Effects, 40, 163–171, https://doi.org/10.1080/15567036.2017.1407841.

Singh, A.K. and Jha, M.K. 2018b. Petrochemical characterization of Argada seam of South Karanpura Coalfield, Jharkhand, India. Journal of Indian Association of Sedimentologists, 35, 36–46.

Singh, A.K. and Jha, M.K. 2018c. Petrochemical evaluation and classification of coal deposits of Barka Sayal area, South Karanpura Coalfield and suggestion for its proper utilisation. International Journal of Oil, Gas and Coal Technology, 18, 39–54, https://doi.org/10.1504/IJOGCT.2018.091525.

Singh, A.K. and Jha, M.K. 2020. Interrelation Between Mechanical and Petrographic Characteristics of Coals of Argada 'B' Seam: Implication To Comminution and Utilization. International Journal of Coal Preparation and Utilization, 40, 824–842, https://doi.org/10.1080/19392699.2017.1419207.

Singh, A.K. and Kumar, A. 2017. Petro-chemical characterisation and depositional paleoenvironment of lignite deposits of Nagaur, Western Rajasthan, India. Environmental Earth Sciences, 76, 692, https://doi.org/10.1007/s12665-017-7004-z.

Singh, A.K. and Kumar, A. 2018. Organic geochemical characteristics of Nagaur lignites, Rajasthan, India, and their implication on thermal maturity and paleoenvironment. Energy Sources, Part A: Recovery, Utilization and Environmental Effects, 40, 1842–1851, https://doi.org/10.1080/15567036.2018.1487480.

Singh, A.K. and Kumar, A. 2020. Assessment of Thermal Maturity, Source Rock Potential and Paleodepositional Environment of the Paleogene Lignites in Barsingsar, Bikaner–Nagaur Basin, Western Rajasthan, India. Natural Resources Research, 29, 1283–1305, https://doi.org/10.1007/s11053-019-09502-8.

Singh, A.K., Singh, M.P., Sharma, M. and Srivastava, S.K. 2007. Microstructures and microtextures of natural cokes: A case study of heat-affected coking coals from the Jharia coalfield, India. International Journal of Coal Geology, 71, 153–175, https://doi.org/10.1016/j.coal.2006.08.006.

Singh, A.K., Sharma, M. and Singh, M.P. 2008. Genesis of natural cokes: Some Indian examples. International Journal of Coal Geology, 75, 40–48, https://doi.org/10.1016/j.coal.2008.01.002.

Singh, A.K., Singh, M.P. and Singh, P.K. 2013b. Petrological Investigations of Oligocene Coals from Foreland Basin of Northeast India. Energy Exploration and Exploitation, 31, 909–936, https://doi.org/10.1260/0144-5987.31.6.909.

Singh, A.K., Singh, M.P., et al. 2013c. Petrological Investigations of Oligocene Coals from Foreland Basin of Northeast India. Energy Exploration & Exploitation, 31, 909–936, https://doi.org/10.1260/0144-5987.31.6.909.

Singh, A.K., Sharma, M. and Singh, M.P. 2013d. SEM and reflected light petrography : A case study on natural cokes from seam XIV, Jharia coalfield, India. Fuel, 112, 502–512, https://doi.org/10.1016/j.fuel.2013.02.063.

Singh, A.K., Singh, M.P. and Singh, P.K. 2015a. Microstructural Relation of Macerals with Mineral Matter in Eocene Coal. Energy Sources, Part A: Recovery, Utilization, and Environmental Effects, 37, 1089–1097, https://doi.org/10.1080/15567036.2011.603030.

Singh, A.K., Banerjee, P.K., Singh, P.K. and Das, A. 2015b. Study of washability characteristics of coals from Seam-IX of Jamadoba Colliery of the Jharia basin, India. Energy Exploration and Exploitation, 33, 181–202, https://doi.org/10.1260/0144-5987.33.2.181.

Singh, A.K., Singh, P.K., Singh, M.P. and Banerjee, P.K. 2015c. Utilization of the Permian Coal Deposits of West Bokaro, India: A Petrochemical Evaluation. Energy Sources, Part A: Recovery, Utilization, and Environmental Effects, 37, 1081–1088, https://doi.org/10.1080/15567036.2011.603029.

Singh, A.L. and Singh, P.K. 2016. Desulfurization and demineralization of coal with bacteria : An ecofriendly concept for clean coal energy. In: Bajpai, V., Sharma, P. and Gupta, V. K. (eds) Recent Trends in Microbial B. 215–231.

Singh, A.L., Singh, P.K., Kumar, A., Yadav, A. and Singh, M.P. 2014a. Experimental Study on Demineralization of Coal with Pseudomonas Mendocina Strain B6–1 Bacteria to Obtain Clean Fuel. Energy Exploration & Exploitation, 32, 831–846, https://doi.org/10.1260/0144-5987.32.5.831.

Singh, A.L., Singh, P.K., et al. 2015d. Demineralization of Rajmahal Gondwana coals by bacteria: Revelations from X-ray diffraction (XRD) and Fourier Transform Infra Red (FTIR) studies. Energy Exploration and Exploitation, 33, 755–767, https://doi.org/10.1260/0144-5987.33.5.755.

Singh, B.D. and Navale, G.K.B. 1989. Petrographic composition, maturity and depositional conditions of the Jhingurdah Seam (Raniganj Formation), Singrauli coalfield (MP). Indian Journal of Geology, 61, 50–70.

Singh, B.D. and Singh, A. 2004. Observations on Indian Permian Gondwana Coals Under Fluorescence Microscopy: An Overview. Gondwana Research, 7, 143–151, https://doi.org/10.1016/S1342-937X(05)70313-0.

Singh, B.D., Misra, B.K., Navale, G.K.B. and Singh, R.M. 1987. Organic petrological studies of Permian coal seams in Singrauli Basin, Son Valley. In: Proc. Nat. Sem. Coal Res. India. 293–323.

Singh, G.P., Singh, M.P. and Naik, A.S. 2013e. The petrology of coals from the Rampur seam-IV and the Lajkura seam, Ib River Coalfield, Mahanadi Valley, Orissa, India. Energy Sources, Part A: Recovery, Utilization and Environmental Effects, 35, 1681–1690, https://doi.org/10.1080/15567031003663158.

Singh, K.N., Singh, R.K. and Katiyar, A. 2016a. Organic Behavior of Umaria, Korba & IB-Valley Coalfields from SECL & MCL, India. Recent Advancements in Mineral and Water Resources, 43–59.

Singh, M.P. and Shukla, R.R. 2004. Petrographic characteristics and depositional conditions of Permian coals of Pench, Kanhan, and Tawa Valley Coalfields of Satpura Basin, Madhya Pradesh, India. International Journal of Coal Geology, 59, 209–243, https://doi.org/10.1016/j.coal.2004.02.002.

Singh, M.P. and Singh, A.K. 2000. Petrographic characteristics and depositional conditions of Eocene coals of platform basins, Meghalaya, India. International Journal of Coal Geology, 42, 315–356, https://doi.org/10.1016/S0166-5162(99)00045-2.

Singh, M.P. and Singh, A.K. 2001. Source rock characteristics and maturation of Palaeogene coals, Northeast India. Journal of the Geological Society of India, 57, 353–368.

Singh, M.P. and Singh, A.K. 2003. Hydrocarbon emigration through microfracturing in vitrinite: An example from the Oligocene coals of Borjan coalfield, Nagaland. Journal of the Geological Society of India, 61, 170–176.

Singh, M.P. and Singh, A.K. 2005. Evidence of pyrolysis of resinite in coal through thermal maturation vis-a-vis hydrocarbon generation: an example from the

Oligocene coals of Upper Assam. Journal of the Geological Society of India, 65, 144–738.

Singh, M.P. and Singh, G.P. 1996a. Chemical composition and classification of coals of Jammu coalfield, District Rajauri, Jammu & Kashmir., Ind. J. Geol., Vol., 68, 25–35.

Singh, M.P. and Singh, P.K. 1995. Mineral matter in the Rajmahal coals : Study through incident light microscopy and scanning electron microscopy., J. Journal of the Geological Society of India, 46, 557–564.

Singh, M.P. and Singh, P.K. 1996b. Petrographic characterization and evolution of the Permian coal deposits of the Rajmahal basin, Bihar, India. International Journal of Coal Geology, 29, 93–118, https://doi.org/10.1016/0166-5162(95)00005-4.

Singh, M.P. and Singh, P.K. 1998. Organic Maturation Study Of Permian Coal Seams, Rajmahal Basin, Bihar. Journal of the Geological Society of India, 51, 279–294.

Singh, P.K. 2004. Mineralogy and geochemistry of Lalmatia coal seams, Hura coalfield, Rajmahal Basin, Jharkhand, India. Journal of Applied Geochemistry, 6, 45–60.

Singh, P.K. 2012. Petrological and geochemical considerations to predict oil potential of Rajpardi and Vastan lignite deposits of Gujarat, western India. Journal of the Geological Society of India, 80, 759–770, https://doi.org/10.1007/s12594-012-0206-9.

Singh, P.K. and Singh, G.P. 1991. Petrographic studies of coal seams from Banki and Ghordewa areas, Korba coalfield, Bilaspur, Madhya Pradesh. Indian Minerals, 45, 189–196.

Singh, P.K. and Singh, M.P. 2011. A study on the classification and utilization of coal from Rajmahal basin, Jharkhand, India. Energy Sources, Part A: Recovery, Utilization and Environmental Effects, 34, 134–142, https://doi.org/10.1080/15567030903551216.

Singh, P.K. and Singh, M.P. 2013. Coal Resources of India in context of Recent Developments in Clean Coal Technology. In: Sharma, P. R., Yadava, R. S. and Sharma, V. N. (eds) Interdisciplinary Advances in Environmental and Earth System Studies. 460.

Singh, P.K., Singh, M.P. and Singh, A.K. 2010. Petro-chemical characterization and evolution of Vastan Lignite, Gujarat, India. International Journal of Coal Geology, 82, 1–16, https://doi.org/10.1016/j.coal.2010.01.003.

Singh, P.K., Singh, M.P.P., et al. 2012. Petrological and geochemical investigations of Rajpardi lignite deposit, Gujarat, India. Energy Exploration and Exploitation, 30, 131–152, https://doi.org/10.1260/0144-5987.30.1.131.

Singh, P.K., Singh, M.P., Volkmann, N., Naik, A.S. and Börner, K. 2014b. Petrological characteristics of Lower Gondwana coal from Singrauli coalfield, Madhya Pradesh, India. International Journal of Oil, Gas and Coal Technology, 8, 194, https://doi.org/10.1504/IJOGCT.2014.064849.

Singh, P.K., Singh, V.K., Rajak, P.K., Singh, M.P. and Naik, A.S. 2016b. Distribution and geochemistry of selected trace elements in the lignites of Cambay basin, Gujarat, western India. Journal of the Geological Society of India, 88, 131–146, https://doi.org/10.1007/s12594-016-0472-z.

Singh, P.K., Rajak, P.K., Singh, M.P., Singh, V.K. and Naik, A.S. 2016c. Geochemistry of Kasnau-Matasukh lignites, Nagaur Basin, Rajasthan (India). International

Journal of Coal Science & Technology, 3, 104–122, https://doi.org/10.1007/s40789-016-0135-0.

Singh, P.K., Rajak, P.K., Singh, M.P., Singh, V.K., Naik, A.S. and Singh, A.K. 2016d. Peat swamps at Giral lignite field of Barmer basin, Rajasthan, Western India: understanding the evolution through petrological modelling. International Journal of Coal Science and Technology, 3, 148–164, https://doi.org/10.1007/s40789-016-0137-y.

Singh, P.K., Rajak, P.K., Singh, V.K., Singh, M.P., Naik, A.S. and Raju, S. V. 2016e. Studies on thermal maturity and hydrocarbon potential of lignites of Bikaner-Nagaur basin, Rajasthan. Energy Exploration and Exploitation, 34, 140–157, https://doi.org/10.1177/0144598715623679.

Singh, P.K., Singh, V.K., Singh, M.P. and Rajak, P.K. 2017a. Petrographic characteristics and paleoenvironmental history of Eocene lignites of Cambay basin, Western India. International Journal of Coal Science and Technology, 4, 214–233, https://doi.org/10.1007/s40789-017-0173-2.

Singh, P.K., Singh, A.L., Kumar, A. and Singh, M.P. 2017b. Petrological considerations for the demineralization of Rajmahal coals with Pseudomonas mendocina B6-1. Journal of the Geological Society of India, 89, 643–652, https://doi.org/10.1007/s12594-017-0673-0.

Singh, R.M. and Dwivedi, C.S. 1994. A study of coal facies in the Korba sub-basin, Mahanadi Valley, India. International Journal of Coal Geology, 25, 113–132, https://doi.org/10.1016/0166-5162(94)90023-X.

Singh, S.M. 2000. On the genera Pantophyllum, Euryphyllum & Kawizophyllum from Karanpura and Bokaro coalfields, India. Palaeobotanist, 49, 31–42.

Singh, V.P., Singh, B.D., et al. 2017c. Depositional palaeoenvironment and economic potential of Khadsaliya lignite deposits (Saurashtra Basin), western India: Based on petrographic, palynofacies and geochemical characteristics. International Journal of Coal Geology, 171, 223–242, https://doi.org/10.1016/j.coal.2017.01.007.

Singh, V.P., Singh, B.D., et al. 2017d. Investigation on the lignite deposits of Surkha mine (Saurashtra Basin, Gujarat), western India: Their depositional history and hydrocarbon generation potential. International Journal of Coal Geology, 183, 78–99, https://doi.org/10.1016/j.coal.2017.09.016.

Smith, G.C. and Cook, A.C. 1980. Coalification paths of exinite, vitrinite and inertite. Fuel, 59, 641–646, https://doi.org/10.1016/0016-2361(80)90127-1.

Smith, A.H. V. 1962. The palaeoecology of Carboniferous peats based on the miospores and petrography of bituminous coals. In: Proceedings of the Yorkshire Geological and Polytechnic Society. 423–474.

Smyth, M. 1979. Hydrocarbon generation in the Fly Lake-Brolga area of the Cooper Basin. J. Aust. Pet. Assoc., 19, 108–114.

Snowdon, L.R. 1980. Resinite- a potential petroleum source in the Upper Cretaceous/ Tertiary of the Beaufort-MacKenzie Basin. Facts and Principles of World Petroleum Occurrence, 6, 509–521.

Snowdon, L.R. and Powell, T.G. 1982. Immature oil and condensate—modification of hydrocarbon generation model for terrestrial organic matter. AAPG Bulletin, 66, 775–788.

Sobkowiak, M. and Painter, P. 1992. Determination of the aliphatic contents of coals by FT-ir: studies of coal extracts. Fuel, 71, 1105–1125.

Song, D., He, D., Qi, X., Wang, S. and Li, D. 2015. Occurrence and composition of solid bitumens from the Bulonggoer Devonian paleo-oil reservoir, North Xinjiang, China. Organic Geochemistry, 83–84, 1–15, https://doi.org/10.1016/j.orggeochem.2015.06.003.

Soos, L. 1963. Uber das sogenannte dunkle Harz der tertiaren Kohlen insbesondere Ungarns. Ann. Univ Sci, 6, 129–151.

Spears, D.A. and Zheng, Y. 1999. Geochemistry and origin of elements in some UK coals. International Journal of Coal Geology, 38, 161–179, https://doi.org/10.1016/S0166-5162(98)00012-3.

Spears, D.A., Rippon, J.H. and Cavender, P.F. 1999. Geological controls on the sulphur distribution in British carboniferous coals: A review and reappraisal. International Journal of Coal Geology, 40, 59–81, https://doi.org/10.1016/S0166-5162(98)00057-3.

Speight, J.. 2005a. Proximate Analysis. Handbook of coal analysis, 3, 41–66, https://doi.org/10.1520/MNL11271M.

Speight, J.G. 1995. The Chemistry and Technology of Coal, Second Edition, 3rd ed. Chemical Industries, https://doi.org/10.1021/ef00050a601.

Speight, J.G. 2005b. Handbook of Coal Analysis, 2nd ed., https://doi.org/10.1002/0471718513.

Speight, J.G. 2015. Assessing fuels for gasification: Analytical and quality control techniques for coal. In: Gasification for Synthetic Fuel Production: Fundamentals, Processes and Applications. 175–198., https://doi.org/10.1016/B978-0-85709-802-3.00008-4.

Srikanth, S. and Raju, G.J.N. 2019. Quantitative Study of Trace Elements in Coal and Coal Related Ashes using PIXE. Journal of the Geological Society of India, 94, 533–537, https://doi.org/10.1007/s12594-019-1351-1.

Srivastava, A.K. and Agnihotri, D. 2013. Coal seam correlation of an Indian Gondwana coalfield: A palaeobotanical perspective. International Journal of Coal Geology, 113, 88–96, https://doi.org/10.1016/j.coal.2012.06.009.

Stach, E. 1968. Basic principles of coal petrology : macerals, microlithotypes and some effects of coalification. In: Coal and Coal Bearing Strata (Eds D. 3–17.

Stach, E. 1969. Fortschritte der Auflicht - Fluoreszenz - Mikroskopie in der Kohlenpetrographie - Freib. Forsch. - H. C, 242, 35–55.

Stach, E. and Alpern, B. 1966. Inertodetrinite. Macrinite and Micrinite. Fortschr Geol. Rheinld v. Westf., 13, 969–980.

Stach, E., Mackowsky, M.-T., Teichmüller, M., Taylor, G.H., Chandra, D. and Teichmüller, R. 1982. Stach's Textbook of Coal Petrology, 3rd ed.

Standards of Australia. 1993. AS 2519-1933: Guide to Technical Evaluation of Higher Rank Coal Deposits.

Stefanova, M., Oros, D.R., Otto, A. and Simoneit, B.R.T. 2002. Polar aromatic biomarkers in the Miocene Maritza-East lignite, Bulgaria. Organic Geochemistry, 33, 1079–1091, https://doi.org/10.1016/S0146-6380(02)00084-0.

Stefanova, M., Kortenski, J., Zdravkov, A. and Marinov, S. 2013. Paleoenvironmental settings of the Sofia lignite basin: Insights from coal petrography and molecular indicators. International Journal of Coal Geology, 107, 45–61, https://doi.org/10.1016/j.coal.2012.09.014.

Steinnes, E. 2010. Human health problems related to trace element deficiencies in soil. In: 19th World Congress of Soil Science, Soil Solutions for a Changing World. 11–14.

Steller, M., Arendt, P. and Kühl, H. 2006. Development of coal petrography applied in technical processes at the Bergbau-Forschung / DMT during the last 50 years. International Journal of Coal Geology, 67, 158–170, https://doi.org/10.1016/j.coal.2005.11.006.

Stephenson, M. 2013. The Negative Greenhouse. In: Returning Coal and Carbon to Nature. 23–44.

Stopes, M.C. 1919. On the four visible ingredients in banded bituminous coal; studies in the composition of coal, No. 1. Proceedings of the Royal Society of London. Series B, Containing Papers of a Biological Character, 90, 470–487.

Stopes, M.C. 1935. On the petrology of banded bituminous coal. Fuel, 14, 4–13.

Suárez-Ruiz, I. and Crelling, J. 2008. Applied Coal Petrology, https://doi.org/10.1016/B978-0-08-045051-3.X0001-2.

Suárez-Ruiz, I. and Crelling, J.C. 2008. Applied Coal Petrology The Role of Petrology in Coal Utilization. Suárez-Ruiz, I. and Crelling, J. C. (eds), https://doi.org/10.1016/B978-0-08-045051-3.00012-9.

Suárez-Ruiz, I., Flores, D., Filho, J.G.M. and Hackley, P.C. 2012. Review and update of the applications of organic petrology: Part 2, geological and multidisciplinary applications. International Journal of Coal Geology, 98, 73–94, https://doi.org/10.1016/j.coal.2012.03.005.

Suggate, R.P. 1998. Relations between depth of burial, vitrinite reflectance and geothermal gradient. Journal of Petroleum Geology, 22, 5–32, https://doi.org/10.1111/j.1747-5457.1999.tb00471.x.

Suggate, R.P. and Dickinson, W.W. 2004. Carbon NMR of coals : the effects of coal type and rank. International Journal of Coal Geology, 57, 1–22, https://doi.org/10.1016/S0166-5162(03)00116-2.

Sun, R., Liu, G., Zheng, L. and Chou, C.L. 2010. Geochemistry of trace elements in coals from the Zhuji Mine, Huainan Coalfield, Anhui, China. International Journal of Coal Geology, 81, 81–96, https://doi.org/10.1016/j.coal.2009.12.001.

Suttner, L.J. and Dutta, P.K. 1986. Alluvial sandstone composition and paleoclimate, I. Framework mineralogy. Journal of Sedimentary Petrology, 56, 329–345, https://doi.org/10.1306/212F8909-2B24-11D7-8648000102C1865D.

Swaine, D.J. 2013. Trace Elements in Coal.

Swanson, V.E. and Huffman, C. 1976. Guidelines for Sample Collecting and Analytical Methods Used in the U . S . Geological Survey for Determining Chemical Composition of Coal, https://doi.org/0306-4522(94)90379-4 [pii].

Sykes, R. and Snowdon, L.R. 2002. Guidelines for assessing the petroleum potential of coaly source rocks using Rock-Eval pyrolysis. Organic Geochemistry, 33, 1441–1455, https://doi.org/10.1016/S0146-6380(02)00183-3.

Sýkorová, I., Pickel, W., Christanis, K., Wolf, M., Taylor, G.H. and Flores, D. 2005. Classification of huminite—ICCP System 1994. International Journal of Coal Geology, 62, 85–106, https://doi.org/10.1016/j.coal.2004.06.006.

Takahashi, K.U., Nakajima, T., Suzuki, Y., Morita, S., Sawaki, T. and Hanamura, Y. 2020. Hydrocarbon generation potential and thermal maturity of coal and coaly mudstones from the Eocene Urahoro Group in the Kushiro Coalfield, eastern

Hokkaido, Japan. International Journal of Coal Geology, 217, 103322, https://doi.org/https://doi.org/10.1016/j.coal.2019.103322.

Tao, S., Xu, Y., et al. 2017. Geochemistry of the Shitoumei oil shale in the Santanghu Basin, Northwest China: Implications for paleoclimate conditions, weathering, provenance and tectonic setting. International Journal of Coal Geology, 184, 42–56, https://doi.org/10.1016/j.coal.2017.11.007.

Taylor, G.H., Teichmüller, M., Davis, A., Diessel, C.F.K., Littke, R. and Robert, P. 1998. Organic Petrology.

Teichmuller, M. 1974a. Enststehung und Veranderung bituminoser substazen in kohlen in Beziehung zur Entsetehung und Umwandlung des Erdols. - Fortschr. Geol. Rheinld. U. Westf., 24, 65–112.

Teichmuller, M. 1974b. Generation of petroleum-like substances in coal seams as seen under the microscope. In: Advances in Organic Geochemistry. 321–348.

Teichmuller, M. and Teichmuller, R. 1982. The geological basis of coal formation, In Stach's Textbook of coal petrology by E. Stach, M-TH Mackowsky, M.Teichmuller, G.H.Taylor, D.Chandra and R.Teichmuller, Gebruder Borntraeger, Stuttgart, pp, 5–86.

Teichmuller, M. and Wolf, M. 1977. Application of fluorescence microscopy in coal petrology and oil exploration. Journal of Microscopy, 109, 49–73, https://doi.org/10.1111/j.1365-2818.1977.tb01116.x.

Teichmüller, M. 1971. Anwendung kohlenpetrographischer Methoden bei der Erdöl-und Erdgasprospektion. Erdöl Kohle, 24, 69–76.

Teichmüller, M. 1986. Organic petrology of source rocks, history and state of the art. Organic Geochemistry, 10, 581–599, https://doi.org/10.1016/0146-63808690055-0.

Teichmüller, M. 1989. The genesis of coal from the viewpoint of coal petrology. International Journal of Coal Geology, 12, 1–87, https://doi.org/10.1016/0166-5162(89)90047-5.

Teichmüller, M. and Teichmüller, R. 1979. Diagenesis of coal (coalification). In: Developments in Sedimentology. 207–246., https://doi.org/10.1016/S0070-4571(08)71074-4.

Teichmüller, M., Durand, B., Teichmuller, M., Durand, B., Teichmüller, M. and Durand, B. 1983. Fluorescence microscopical rank studies on liptinites and vitrinites in peat and coals, and comparison with results of the Rock-Eval pyrolysis. International Journal of Coal Geology, 2, 197–230, https://doi.org/10.1016/0166-5162(83)90001-0.

Teng, J., Mastalerz, M. and Hampton, L.B. 2017. Maceral controls on porosity characteristics of lithotypes of Pennsylvanian high volatile bituminous coal: Example from the Illinois Basin. International Journal of Coal Geology, 172, 80–94, https://doi.org/10.1016/j.coal.2017.02.001.

Teot, A.S. 1982. Resins, Water Soluble. Kirk-Othmer Encylopedia of Chemical Technology, Vol. 20.

Tewari, A., Dutta, S. and Sarkar, T. 2017. Biomarker signatures of Permian Gondwana coals from India and their palaeobotanical significance. Palaeogeography, Palaeoclimatology, Palaeoecology, 468, 414–426, https://doi.org/10.1016/j.palaeo.2016.12.014.

Tewari, R.C. and Khan, Z.A. 2015. Origin of banded structure and coal lithotype cycles in Kargali coal seam of East Bokaro sub-basin, Jharkhand, India: Environmental implications. Journal of Earth System Science, 124, 643–654, https://doi.org/10.1007/s12040-015-0553-1.

Tewari, R.C. and Maejima, W. 2010. Origin of Gondwana Basins of Peninsular India. Journal of Geosciences, 53, 23.

Thiessen, R. 1920. Compilation and Composition of Bituminous Coals. The Journal of Geology, 28, 185–209, https://doi.org/10.1086/622706.

Thiessen, R. and Sprunk, G.C. 1935. Microscopic and Petrographic Studies of Certain American Coals.

Thomas, L. 2012. Coal Geology, https://doi.org/10.1002/9781118385685.

Tissot, B.P. and Welte, D.H. 1984. Petroleum Formation and Occurrence, 2nd ed., https://doi.org/10.1029/EO066i037p00643.

Tiwary, R.K. and Dhar, B.B. 1994. Environmental Pollution From Coal Mining Activities in Damodar River Basin, India. Mine, Water and the Environment, 13, 1–10.

Todd, S.P., Dunn, M.E. and Barwise, A.J.G. 1997. Characterizing petroleum charge systems in the tertiary of SE Asia. Geological Society, London, Special Publications, 126, 25–47, https://doi.org/10.1144/GSL.SP.1997.126.01.04.

Tomoaia-Cotisel, M., Chifu, E., Zsako, J., Mocanu, A., Quinn, P.J. and Kates, M. 1992. Monolayer properties of archaeol and caldarchaeol polar lipids of a methanogenic archaebacterium, Methanospirillum hungatei, at the air/water interface. Chemistry and Physics of Lipids, https://doi.org/10.1016/0009-3084(92)90029-O.

Valentim, B., Hower, J.C., O'Keefe, J.M.K., Rodrigues, S., Ribeiro, J. and Guedes, A. 2013. Notes on the origin of altered macerals in the Ragged Edge of the Pennsylvanian (Asturian) Herrin coalbed, Western Kentucky. International Journal of Coal Geology, 115, 24–40, https://doi.org/10.1016/j.coal.2013.05.001.

Valentim, B., Flores, D., Guedes, A., Guimarães, R., Shreya, N., Paul, B. and Ward, C.R. 2016. International Journal of Coal Geology Notes on the occurrence of phosphate mineral relics and spheres (phosphospheres) in coal and biomass fly ash. International Journal of Coal Geology, 154–155, 43–56, https://doi.org/10.1016/j.coal.2015.12.009.

Valentine, B.J., Morrissey, E.A., Park, A.J., Reidy, M.E. and Hackley, P.C. 2013. Development of web-based organic petrology photomicrograph atlases and internet resources for professionals and students. International Journal of Coal Geology, 111, 106–111, https://doi.org/10.1016/j.coal.2012.09.012.

Van de Wetering, N., Sanei, H., Mayer, B., Wetering, N. Van De, Sanei, H. and Mayer, B. 2016. Organic matter characterization in mixed hydrocarbon producing areas within the Duvernay Formation, Western Canada Sedimentary Basin, Alberta. International Journal of Coal Geology, 156, 1–11, https://doi.org/10.1016/j.coal.2016.01.012.

Van Hook, R.I. 1979. Potential health and environmental effects of trace elements and radionuclides from increased coal utilization. Environmental Health Perspectives, 33, 227–247, https://doi.org/10.1289/ehp.7933227.

Van Koeverden, J.H., Karlsen, D.A. and Backer-Owe, K. 2011. Carboniferous non-marine source rocks from Spitsbergen and Bjørnøya: Comparison with the western arctic. Journal of Petroleum Geology, 34, 53–66, https://doi.org/10.1111/j.1747-5457.2011.00493.x.

van Krevelen, D.W. 1961. Coal--Typology, Chemistry, Physics, Constitution. Elsevier Science & Technology.

Vandenbroucke, M. 2003. Kerogen: from Types to Models of Chemical Structure. Oil & Gas Science and Technology, 58, 243–269, https://doi.org/10.2516/ogst:2003016.

Varma, A.K., Banerjee, S.K. and Sen, D. 2013. Petrographic Characterization And Rank Evaluation Of Coal Seams Belonging To Korba Basin, Chhattisgarh, India. International Journal of Applied and Natural Sciences (IJANS), 2, 117–124.

Varma, A.K., Mishra, D.K., Samad, S.K., Prasad, A.K., Panigrahi, D.C., Mendhe, V.A. and Singh, B.D. 2018. Geochemical and organo-petrographic characterization for hydrocarbon generation from Barakar Formation in Auranga Basin, India. International Journal of Coal Geology, 186, 97–114, https://doi.org/10.1016/j.coal.2017.12.002.

Vasireddy, S., Morreale, B., Cugini, A., Song, C. and Spivey, J.J. 2011. Clean liquid fuels from direct coal liquefaction: chemistry, catalysis, technological status and challenges. Energy Environ. Sci., 4, 311–345, https://doi.org/10.1039/C0EE00097C.

Vassilev, S. V., Kitano, K. and Vassileva, C.G. 1996. Some relationships between coal rank and chemical and mineral composition. Fuel, 75, 1537–1542, https://doi.org/10.1016/0016-2361(96)00116-0.

Veevers, J.J. 2006. Updated Gondwana (Permian-Cretaceous) earth history of Australia. Gondwana Research, 9, 231–260, https://doi.org/10.1016/j.gr.2005.11.005.

Venkatachala, B. and Kar, R. 1968. Palynology of the Karanpura sedimentary basin, Bihar, India. 1. Barakar stage at Badam. Palaeobotanist, 16, 56–90.

Venkatachala, B.S. and Kar, R.K. 1964. A new pollen genus from the Permian of North Karanpura coalfield, Bihar, India. Grana Palynologica, 5, 413–424, https://doi.org/10.1080/00173136409430028.

Verma, C. and Verma, R. 2019. Leaching behaviour of fly ash: A review. Nature Environment and Pollution Technology, 18, 403–412.

Verma, R.K., Bhuin, N.C. and Mukhopadhyay, M. 1979. Geology, structure and tectonics of the Jharia coalfield, India - A three-dimensional model. Geoexploration, 17, 305–324, https://doi.org/10.1016/0016-7142(79)90025-5.

von Jacob, H. 1980. Die Anwendung der Mikrophotometrie in der organischen Petrologie. Leitz Mitteilungen fur Wissenschaft und Technik, Vll, 209–216.

Vuković, N., Životić, D., Mendonça Filho, J.G., Kravić-Stevović, T., Hámor-Vidó, M., Mendonça, J. de O. and Stojanović, K. 2016. The assessment of maturation changes of humic coal organic matter — Insights from closed-system pyrolysis experiments. International Journal of Coal Geology, 154–155, 213–239, https://doi.org/10.1016/j.coal.2016.01.007.

Walker, R. and Mastalerz, M. 2004. Functional group and individual maceral chemistry of high volatile bituminous coals from southern Indiana : controls on coking. International Journal of Coal Geology, 58, 181–191, https://doi.org/10.1016/j.coal.2003.10.008.

Wang, J., Bentley, Y. and Bentley, R. 2018. Modeling India's Coal Production with a Negatively Skewed Curve-Fitting Model. Natural Resources Research, 27, 365–378, https://doi.org/10.1007/s11053-017-9356-1.

Wang, L., Song, Z., Yin, Q. and George, S.C. 2011. Organic Geochemistry Paleosalinity significance of occurrence and distribution of methyltrimethyltridecyl chromans in

the Upper Cretaceous Nenjiang Formation, Songliao Basin, China. Organic Geochemistry, 42, 1411–1419, https://doi.org/10.1016/j.orggeochem.2011.08.012.

Wang, P., Yan, X., Guo, W., Zhang, S., Wang, Z., Xu, Y. and Wang, L. 2016. Geochemistry of trace elements in coals from the Yueliangtian mine, western Guizhou, China: abundances, modes of occurrence, and potential industrial utilization. Energy and Fuels, 30, 10268–10281.

Wang, S., Tang, Y., Schobert, H.H., Guo, Y. and Su, Y. 2013. Petrology and structural studies in liquefaction reactions of Late Permian coals from Southern China. Fuel, 107, 518–524, https://doi.org/10.1016/j.fuel.2012.11.075.

Wanick, L.R. 1956. Sôbre a histogênese do mioblastoma de células granulares do apêndice: apresentação de um caso. Memórias do Instituto Oswaldo Cruz, 54, 125–134.

Ward, C.R. 1984. Coal Geology and Coal Technology. Ward, C. R. (ed.), https://doi.org/10.1016/0166-5162(87)90056-5.

Ward, C.R. 2016. Analysis, origin and significance of mineral matter in coal: An updated review. International Journal of Coal Geology, 165, 1–27, https://doi.org/10.1016/j.coal.2016.07.014.

Ward, C.R. and Suárez-Ruiz, I. 2008. Introduction to Applied Coal Petrology. In: Applied Coal Petrology. 1–18., https://doi.org/10.1016/B978-0-08-045051-3.00001-4.

Ward, C.R. and Taylor, J.C. 1996. Quantitative mineralogical analysis of coals from the Callide Basin, Queensland, Australia using X-ray diffractometry and normative interpretation. International Journal of Coal Geology, 30, 211–229.

Ward, C.R., Spears, D.A., Booth, C.A., Staton, I. and Gurba, L.W. 1999. Mineral matter and trace elements in coals of the Gunnedah Basin, New South Wales, Australia. International Journal of Coal Geology, 40, 281–308.

Wei, Q., Dai, S., Lefticariu, L. and Costin, G. 2018a. Electron probe microanalysis of major and trace elements in coals and their low-temperature ashes from the Wulantuga and Lincang Ge ore deposits, China. Fuel, 215, 1–12, https://doi.org/10.1016/j.fuel.2017.11.012.

Wei, W., Algeo, T.J., et al. 2018b. Identifying marine incursions into the Paleogene Bohai Bay Basin lake system in northeastern China. International Journal of Coal Geology, 200, 1–17, https://doi.org/https://doi.org/10.1016/j.coal.2018.10.001.

Welte, D.H. 1969. Organic Geochemistry of Carbon. In: Handbook of Geochemistry. Heidelberg. New York, II/1. 1–6.

White, C.D. and Thiessen, R. 1913. The Origin of Coal. US Government Printing Office.

White, W.A., Radke, M., Sharp, Z. and Hall, P.P. 1998. Geochemistry. Geochemistry, 39–39, https://doi.org/10.1007/1-4020-4496-8.

Wilkins, R.W.T., Wilmshurst, J.R., Russell, N.J., Hladky, G., Ellacott, M. V. and Buckingham, C. 1992. Fluorescence alteration and the suppression of vitrinite reflectance. Organic Geochemistry, 18, 629–640.

Williams, D.H. 1852. A Geological Report on the Kymore Mountains, the Ramghur Coal Fields and on the Manufacture of Iron, edited by F. Carbery, Bengal Military Orphan Press, Calcutta

Witham, H. 1831. Observations on Fossil Vegetables: Accompanied by Representations of Their Internal Structure as Seen Through the Microscope.

Witts, D., Hall, R., Nichols, G. and Morley, R. 2012. Journal of Asian Earth Sciences A new depositional and provenance model for the Tanjung Formation, Barito Basin, SE Kalimantan, Indonesia. Journal of Asian Earth Sciences, 56, 77–104.

Wolf, M. 1966. Observations petrographiques sur les schistes beghead d'Autun (Saone-et-Loire). - Sci. dela Terre. 11, 7–18.

Yaman, S., Yavuz, R., Küçükbayrak, S. and Taptik, Y. 2001. Stepwise demineralisation and chemical isolation of the mineral matter of Göynük lignite. Energy Conversion and Management, 42, 2119–2127.

Yang, N., Tang, S., Zhang, S., Xi, Z., Li, J., Yuan, Y. and Guo, Y. 2018. In seam variation of element-oxides and trace elements in coal from the eastern Ordos Basin, China. International Journal of Coal Geology, 197, 31–41.

Yao, S., Zhang, K., Jiao, K. and Hu, W. 2011. Evolution of coal structures: FTIR analyses of experimental simulations and naturally matured coals in the Ordos Basin, China. Energy Exploration and Exploitation, 29, 1–19.

Yao, S., Cao, J., Zhang, K., Jiao, K., Ding, H. and Hu, W. 2012. Organic Geochemistry Artificial bacterial degradation and hydrous pyrolysis of suberin : Implications for hydrocarbon generation of suberinite. Organic Geochemistry, 47, 22–33.

Zhang, J., Ren, D., Zheng, C., Zeng, R., Chou, C.L. and Liu, J. 2002. Trace element abundances in major minerals of Late Permian coals from southwestern Guizhou province, China. International Journal of Coal Geology, 53, 55–64.

Zhang, W., Yang, W. and Xie, L. 2017. Controls on organic matter accumulation in the Triassic Chang 7 lacustrine shale of the Ordos Basin, central China. International Journal of Coal Geology, 183, 38–51.

Zhang, Y., Wang, J., Xue, S., Wu, J., Chang, L. and Li, Z. 2016. Kinetic study on changes in methyl and methylene groups during low-temperature oxidation of coal via in-situ FTIR. International Journal of Coal Geology, 154–155, 155–164.

Zhao, L., Sun, J., Guo, W., Wang, P. and Ji, D. 2016. Mineralogy of the Pennsylvanian coal seam in the Datanhao mine, Daqingshan Coalfield, Inner Mongolia, China: Genetic implications for mineral matter in coal deposited in an intermontane basin. International Journal of Coal Geology, 167, 201–214.

Životić, D., Wehner, H., et al. 2008. Petrological, organic geochemical and geochemical characteristics of coal from the Soko mine, Serbia. International Journal of Coal Geology, 73, 285–306, https://doi.org/10.1016/j.coal.2007.07.001.

Zodrow, E.L., D'Angelo, J.A., Helleur, R. and Šimůnek, Z. 2012. Functional groups and common pyrolysate products of Odontopteris cantabrica (index fossil for the Cantabrian Substage, Carboniferous). International Journal of Coal Geology, 100, 40–50, https://doi.org/10.1016/j.coal.2012.06.002.

Zou, J., Han, F., Li, T., Tian, H. and Li, Y. 2018. Mineralogical and Geochemical Compositions of the Lopingian Coals in the Zhongliangshan Coalfield, Southwestern China. Minerals, 8, 104, https://doi.org/10.3390/min8030104.